

# Arthritis & Rheumatology

An Official Journal of the American College of Rheumatology  
www.arthritisrheum.org and wileyonlinelibrary.com

## GENERAL INFORMATION

### TO SUBSCRIBE

#### Institutions and Non-Members

Email: wileyonlinelibrary.com  
Phone: (201) 748-6645  
Write: Wiley Periodicals LLC  
Attn: Journals Admin Dept  
UK  
111 River Street  
Hoboken, NJ 07030

Volumes 74, 2022:  
Institutional Print Only:

Institutional Online Only:  
Institutional Print and  
Online Only:

#### Arthritis & Rheumatology and Arthritis Care & Research:

\$2,603 in US, Canada, and Mexico  
\$2,603 outside North America

\$2,495 in US, Canada, Mexico, and outside North America  
\$2,802 in US, Canada, and Mexico; \$2,802 outside  
North America

For submission instructions, subscription, and all other information visit: wileyonlinelibrary.com.

Arthritis & Rheumatology accepts articles for Open Access publication. Please visit <https://authorservices.wiley.com/author-resources/Journal-Authors/open-access/hybrid-open-access.html> for further information about OnlineOpen.

Wiley's Corporate Citizenship initiative seeks to address the environmental, social, economic, and ethical challenges faced in our business and which are important to our diverse stakeholder groups. Since launching the initiative, we have focused on sharing our content with those in need, enhancing community philanthropy, reducing our carbon impact, creating global guidelines and best practices for paper use, establishing a vendor code of ethics, and engaging our colleagues and other stakeholders in our efforts. Follow our progress at [www.wiley.com/go/citizenship](http://www.wiley.com/go/citizenship).

Access to this journal is available free online within institutions in the developing world through the HINARI initiative with the WHO. For information, visit [www.healthinternetwork.org](http://www.healthinternetwork.org).

### Disclaimer

The Publisher, the American College of Rheumatology, and Editors cannot be held responsible for errors or any consequences arising from the use of information contained in this journal; the views and opinions expressed do not necessarily reflect those of the Publisher, the American College of Rheumatology and Editors, neither does the publication of advertisements constitute any endorsement by the Publisher, the American College of Rheumatology and Editors of the products advertised.

### Members:

#### American College of Rheumatology/Association of Rheumatology Professionals

For membership rates, journal subscription information, and change of address, please write:

American College of Rheumatology  
2200 Lake Boulevard  
Atlanta, GA 30319-5312  
(404) 633-3777

### ADVERTISING SALES AND COMMERCIAL REPRINTS

**Sales:** Kathleen Malseed, National Account Manager  
E-mail: [kmalseed@pmi.com](mailto:kmalseed@pmi.com)  
Phone: (215) 852-9824  
Pharmaceutical Media, Inc.  
30 East 33rd Street, New York, NY 10016

**Production:** Patti McCormack  
E-mail: [pmccormack@pmi.com](mailto:pmccormack@pmi.com)  
Phone: (212) 904-0376  
Pharmaceutical Media, Inc.  
30 East 33rd Street, New York, NY 10016

**Publisher:** Arthritis & Rheumatology is published by Wiley Periodicals LLC, 101 Station Landing, Suite 300, Medford, MA 02155

**Production Editor:** Ramona Talantor, [artprod@wiley.com](mailto:artprod@wiley.com)

ARTHRITIS & RHEUMATOLOGY (Print ISSN 2326-5191; Online ISSN 2326-5205 at Wiley Online Library, wileyonlinelibrary.com) is published monthly on behalf of the American College of Rheumatology by Wiley Periodicals LLC, a Wiley Company, 111 River Street, Hoboken, NJ 07030-5774. Periodicals postage paid at Hoboken, NJ and additional offices. POSTMASTER: Send all address changes to Arthritis & Rheumatology, Wiley Periodicals LLC, c/o The Sheridan Press, PO Box 465, Hanover, PA 17331. **Send subscription inquiries care of** Wiley Periodicals LLC, Attn: Journals Admin Dept UK, 111 River Street, Hoboken, NJ 07030, (201) 748-6645 (nonmember subscribers only; American College of Rheumatology/Association of Rheumatology Health Professionals members should contact the American College of Rheumatology). **Subscription Price:** (Volumes 74, 2022: Arthritis & Rheumatology and Arthritis Care & Research) Print only: \$2,603.00 in U.S., Canada and Mexico, \$2,603.00 rest of world. For all other prices please consult the journal's website at wileyonlinelibrary.com. All subscriptions containing a print element, shipped outside U.S., will be sent by air. Payment must be made in U.S. dollars drawn on U.S. bank. Prices are exclusive of tax. Asia-Pacific GST, Canadian GST and European VAT will be applied at the appropriate rates. For more information on current tax rates, please go to [www.wileyonlinelibrary.com/tax-vat](http://www.wileyonlinelibrary.com/tax-vat). The price includes online access to the current and all online backfiles to January 1st 2018, where available. For other pricing options including access information and terms and conditions, please visit <https://onlinelibrary.wiley.com/library-info/products/price-lists>. Terms of use can be found here: <https://onlinelibrary.wiley.com/terms-and-conditions>. **Delivery Terms and Legal Title:** Where the subscription price includes print issues and delivery is to the recipient's address, delivery terms are Delivered at Place (DAP); the recipient is responsible for paying any import duty or taxes. Title to all issues transfers Free of Board (FOB) our shipping point, freight prepaid. We will endeavor to fulfill claims for missing or damaged copies within six months of publication, within our reasonable discretion and subject to availability. **Change of Address:** Please forward to the subscriptions address listed above 6 weeks prior to move; enclose present mailing label with change of address. **Claims** for undelivered copies will be accepted only after the following issue has been received. Please enclose a copy of the mailing label or cite your subscriber reference number in order to expedite handling. Missing copies will be supplied when losses have been sustained in transit and where reserve stock permits. Send claims care of Wiley Periodicals LLC, Attn: Journals Admin Dept UK, 111 River Street, Hoboken, NJ 07030. If claims are not resolved satisfactorily, please write to Subscription Distribution c/o Wiley Periodicals LLC, 111 River Street, Hoboken, NJ 07030. **Cancellations:** Subscription cancellations will not be accepted after the first issue has been mailed. **Journal Customer Services:** For ordering information, claims and any enquiry concerning your journal subscription please go to <https://wileysupport.wiley.com/s/contactsupport?tabset-a7d10=2> or contact your nearest office. **Americas:** Email: [cs-journals@wiley.com](mailto:cs-journals@wiley.com); Tel: +1 877 762 2974. **Europe, Middle East and Africa:** Email: [cs-journals@wiley.com](mailto:cs-journals@wiley.com); Tel: +44 (0) 1865 778315; 0800 1800 536 (Germany). **Asia Pacific:** Email: [cs-journals@wiley.com](mailto:cs-journals@wiley.com); Tel: +65 6511 8000. **Japan:** For Japanese speaking support, Email: [cs-japan@wiley.com](mailto:cs-japan@wiley.com). **Visit our Online Customer Help** at <https://wileysupport.wiley.com/s/contactsupport?tabset-a7d10=2>. **Back Issues:** Single issues from current and prior year volumes are available at the current single issue price from [csjournals@wiley.com](mailto:csjournals@wiley.com). Earlier issues may be obtained from Periodicals Service Company, 351 Fairview Avenue Ste 300, Hudson, NY 12534, USA. Tel: +1 518 822-9300, Fax: +1 518 822-9305, Email: [psc@periodicals.com](mailto:psc@periodicals.com). Printed in the USA by The Sheridan Group.

# Arthritis & Rheumatology

An Official Journal of the American College of Rheumatology  
www.arthritisrheum.org and wileyonlinelibrary.com

## Editor

Daniel H. Solomon, MD, MPH, *Boston*

## Deputy Editors

Richard J. Bucala, MD, PhD, *New Haven*

Mariana J. Kaplan, MD, *Bethesda*

Peter A. Nigrovic, MD, *Boston*

## Co-Editors

Karen H. Costenbader, MD, MPH, *Boston*

David T. Felson, MD, MPH, *Boston*

Richard F. Loeser Jr., MD, *Chapel Hill*

## Social Media Editor

Paul H. Sufka, MD, *St. Paul*

## Journal Publications Committee

Amr Sawalha, MD, *Chair, Pittsburgh*

Susan Boackle, MD, *Denver*

Aileen Davis, PhD, *Toronto*

Deborah Feldman, PhD, *Montreal*

Donnamarie Krause, PhD, OTR/L, *Las Vegas*

Wilson Kuswanto, MD, PhD, *Stanford*

Michelle Ormseth, MD, *Nashville*

R. Hal Scofield, MD, *Oklahoma City*

## Editorial Staff

Kimberly M. Murphy, *Senior Director & Managing Editor, Delaware*

Lesley W. Allen, *Assistant Managing Editor, Virginia*

Ilani S. Lorber, *Assistant Managing Editor, Georgia*

Stefanie L. McKain, *Manuscript Editor, Georgia*

Rasa G. Hamilton, *Manuscript Editor, Florida*

Brian T. Robinson, *Manuscript Editor, Pennsylvania*

Christopher Reynolds, *Editorial Coordinator, Georgia*

Audra Jenson, *Assistant Editor, North Carolina*

## Associate Editors

Marta Alarcón-Riquelme, MD, PhD, *Granada*

Heather G. Allore, PhD, *New Haven*

Neal Basu, MD, PhD, *Glasgow*

Edward M. Behrens, MD, *Philadelphia*

Bryce Binstadt, MD, PhD, *Minneapolis*

Nunzio Bottini, MD, PhD, *San Diego*

John Carrino, MD, MPH, *New York*

Andrew Cope, MD, PhD, *London*

Adam P. Croft, MBChB, PhD, MRCP, *Birmingham*

Nicola Dalbeth, MD, FRACP, *Auckland*

Brian M. Feldman, MD, FRCPC, MSC, *Toronto*

Richard A. Furie, MD, *Great Neck*

J. Michelle Kahlenberg, MD, PhD, *Ann Arbor*

Benjamin Leder, MD, *Boston*

Yvonne Lee, MD, MMSc, *Chicago*

Katherine Liao, MD, MPH, *Boston*

Bing Lu, MD, DrPH, *Boston*

Stephen P. Messier, PhD, *Winston-Salem*

Rachel E. Miller, PhD, *Chicago*

Janet E. Pope, MD, MPH, *FRCPC, London, Ontario*

Lisa G. Rider, MD, *Bethesda*

Christopher T. Ritchlin, MD, MPH, *Rochester*

William Robinson, MD, PhD, *Stanford*

Carla R. Scanzello, MD, PhD, *Philadelphia*

Georg Schett, MD, *Erlangen*

Sakae Tanaka, MD, PhD, *Tokyo*

Maria Trojanowska, PhD, *Boston*

Betty P. Tsao, PhD, *Charleston*

Fredrick M. Wigley, MD, *Baltimore*

Edith M. Williams, PhD, MS, *Rochester*

## Advisory Editors

Ayaz Aghayev, MD, *Boston*

Joshua F. Baker, MD, MSCE, *Philadelphia*

Bonnie Bermas, MD, *Dallas*

Jamie Collins, PhD, *Boston*

Kristen Demoruelle, MD, PhD, *Denver*

Christopher Denton, PhD, FRCPC, *London*

Anisha Dua, MD, MPH, *Chicago*

John FitzGerald, MD, *Los Angeles*

Lauren Henderson, MD, MMSc, *Boston*

Monique Hinchcliff, MD, MS, *New Haven*

Hui-Chen Hsu, PhD, *Birmingham*

Mohit Kapoor, PhD, *Toronto*

Seoyoung Kim, MD, ScD, MSCE, *Boston*

Vasileios Kytтарыs, MD, *Boston*

Carl D. Langefeld, PhD, *Winston-Salem*

Dennis McGonagle, FRCPI, PhD, *Leeds*

Julie Paik, MD, MHS, *Baltimore*

Amr Sawalha, MD, *Pittsburgh*

Julie Zikherman, MD, *San Francisco*

## AMERICAN COLLEGE OF RHEUMATOLOGY

Kenneth G. Saag, MD, MSc, *Birmingham*, **President**

Douglas White, MD, PhD, *La Crosse*, **President-Elect**

Carol Langford, MD, MHS, *Cleveland*, **Treasurer**

Deborah Desir, MD, *New Haven*, **Secretary**

Steven Echard, IOM, CAE, *Atlanta*, **Executive Vice-President**

© 2022 American College of Rheumatology. All rights reserved. No part of this publication may be reproduced, stored or transmitted in any form or by any means without the prior permission in writing from the copyright holder. Authorization to copy items for internal and personal use is granted by the copyright holder for libraries and other users registered with their local Reproduction Rights Organization (RRO), e.g. Copyright Clearance Center (CCC), 222 Rosewood Drive, Danvers, MA 01923, USA (www.copyright.com), provided the appropriate fee is paid directly to the RRO. This consent does not extend to other kinds of copying such as copying for general distribution, for advertising or promotional purposes, for creating new collective works or for resale. Special requests should be addressed to: permissions@wiley.com.

Access Policy: Subject to restrictions on certain backfiles, access to the online version of this issue is available to all registered Wiley Online Library users 12 months after publication. Subscribers and eligible users at subscribing institutions have immediate access in accordance with the relevant subscription type. Please go to onlinelibrary.wiley.com for details.

The views and recommendations expressed in articles, letters, and other communications published in Arthritis & Rheumatology are those of the authors and do not necessarily reflect the opinions of the editors, publisher, or American College of Rheumatology. The publisher and the American College of Rheumatology do not investigate the information contained in the classified advertisements in this journal and assume no responsibility concerning them. Further, the publisher and the American College of Rheumatology do not guarantee, warrant, or endorse any product or service advertised in this journal.

Cover design: Todd Machen

©This journal is printed on acid-free paper.

# Arthritis & Rheumatology

An Official Journal of the American College of Rheumatology  
www.arthritisrheum.org and wileyonlinelibrary.com

**VOLUME 74 • December 2022 • NO. 12**

<b>In This Issue</b> .....	A15
<b>Journal Club</b> .....	A16
<b>Clinical Connections</b> .....	A17
<b>ACR Announcements</b> .....	A25
<b>Special Articles</b>	
Notes from the Field: Overturning Roe v. Wade: Toppling the Practice of Rheumatology <i>Bonnie L. Bermas, Irene Blanco, Ashira D. Blazer, Megan EB Clowse, Cuoghi Edens, Rosalind Ramsey-Goldman, and Mehret Birru Talabi</i> .....	1865
Notes from the Field: The Evolving Role of the Rheumatology Practitioner in the Care of Immunocompromised Patients in the COVID-19 Era <i>Leonard H. Calabrese, Cassandra M. Calabrese, Elizabeth Kirchner, and Kevin Winthrop</i> .....	1868
2022 American College of Rheumatology/EULAR Classification Criteria for Takayasu Arteritis <i>Peter C. Grayson, Cristina Ponte, Ravi Suppiah, Joanna C. Robson, Katherine Bates Gribbons, Andrew Judge, Anthea Craven, Sara Khalid, Andrew Hutchings, Debashish Danda, Raashid A. Luqmani, Richard A. Watts, and Peter A. Merkel, for the DCVAS Study Group</i> .....	1872
2022 American College of Rheumatology/EULAR Classification Criteria for Giant Cell Arteritis <i>Cristina Ponte, Peter C. Grayson, Joanna C. Robson, Ravi Suppiah, Katherine Bates Gribbons, Andrew Judge, Anthea Craven, Sara Khalid, Andrew Hutchings, Richard A. Watts, Peter A. Merkel, and Raashid A. Luqmani, for the DCVAS Study Group</i> .....	1881
Editorial: Disentangling the Causal Effect of Telomere Length in Systemic Lupus Erythematosus Using Genetic Variants as Instruments <i>Yiqiang Zhan and Xiaoying Kang</i> .....	1890
Review: Artificial Intelligence and Deep Learning for Rheumatologists <i>Christopher McMaster, Alix Bird, David F. L. Liew, Russell R. Buchanan, Claire E. Owen, Wendy W. Chapman, and Douglas E. V. Pires</i> .....	1893
<b>COVID-19</b>	
Breakthrough SARS-CoV-2 Infections in Patients With Immune-Mediated Disease Undergoing B Cell-Depleting Therapy: A Retrospective Cohort Analysis <i>Cassandra M. Calabrese, Elizabeth Kirchner, Elaine M. Husni, Brandon P. Moss, Anthony P. Fernandez, Yuxuan Jin, and Leonard H. Calabrese</i> .....	1906
<b>Rheumatoid Arthritis</b>	
Synovial Inflammatory Pathways Characterize Anti-TNF-Responsive Rheumatoid Arthritis Patients <i>Jing Wang, Donna Conlon, Felice Rivellese, Alessandra Nerviani, Myles J. Lewis, William Housley, Marc C. Levesque, Xiaohong Cao, Carolyn Cuff, Andrew Long, Costantino Pitzalis, and Melanie C. Ruzek</i> .....	1916
<b>Clinical Images</b>	
Clinical Images: Giant Intraosseous Synovial Cyst With Intraarticular Connection at the Elbow in Rheumatoid Arthritis <i>Can M. Sungur and Jonathan C. Baker</i> .....	1927
<b>Osteoarthritis</b>	
Contribution of MicroRNA-27b-3p to Synovial Fibrotic Responses in Knee Osteoarthritis <i>Ghazaleh Tavallae, Starlee Lively, Jason S. Rockel, Shabana Amanda Ali, Michelle Im, Clementine Sarda, Greniqueca M. Mitchell, Evgeny Rossomacha, Sayaka Nakamura, Pratibha Potla, Sarah Gabriel, John Matelski, Anusha Ratneswaran, Kim Perry, Boris Hinz, Rajiv Gandhi, Igor Jurisica, and Mohit Kapoor</i> .....	1928
<b>Spondyloarthritis</b>	
Safety and Efficacy of Bimekizumab in Patients With Active Ankylosing Spondylitis: Three-Year Results From a Phase IIb Randomized Controlled Trial and Its Open-Label Extension Study <i>Xenofon Baraliakos, Atul Deodhar, Maxime Dougados, Lianne S. Gensler, Anna Molto, Sofia Ramiro, Alan J. Kivitz, Denis Poddubnyy, Marga Oortgiesen, Thomas Vaux, Carmen Fleurinck, Julie Shepherd-Smith, Christine de la Loge, Natasha de Peyrecave, and Désirée van der Heijde</i> .....	1943
<b>Psoriatic Arthritis</b>	
Safety and Efficacy of Bimekizumab in Patients With Active Psoriatic Arthritis: Three-Year Results From a Phase IIb Randomized Controlled Trial and Its Open-Label Extension Study <i>Laura C. Coates, Iain B. McInnes, Joseph F. Merola, Richard B. Warren, Arthur Kavanaugh, Alice B. Gottlieb, Laure Gossec, Deepak Assudani, Rajan Bajracharya, Jason Coarse, Barbara Ink, and Christopher T. Ritchlin</i> .....	1959

## Systemic Lupus Erythematosus

### Modulation of the Itaconate Pathway Attenuates Murine Lupus

Luz P. Blanco, Eduardo Patino-Martinez, Shuichiro Nakabo, Mingzeng Zhang, Hege L. Pedersen, Xinghao Wang, Carmelo Carmona-Rivera, Dillon Claybaugh, Zu-Xi Yu, Equar Desta, and Mariana J. Kaplan .....1971

### Brief Report: Telomere Length and Development of Systemic Lupus Erythematosus: A Mendelian Randomization Study

Xu-Fan Wang, Wen-Jing Xu, Fei-Fei Wang, Rui Leng, Xiao-Ke Yang, Hua-Zhi Ling, Yin-Guang Fan, Jin-Hui Tao, Zong-Wen Shuai, Li Zhang, Dong-Qing Ye, and Rui-Xue Leng .....1984

## Sjögren's Syndrome

### Variability of Primary Sjögren's Syndrome Is Driven by Interferon- $\alpha$ and Interferon- $\alpha$ Blood Levels Are Associated

#### With the Class II HLA-DQ Locus

Diana Trutschel, Pierre Bost, Xavier Mariette, Vincent Bondet, Alba Llibre, Celine Posseme, Bruno Charbit, Christian W. Thorball, Roland Jonsson, Christopher J. Lessard, Renaud Felten, Wan Fai Ng, Lucienne Chatenoud, Hélène Dumortier, Jean Sibilia, Jacques Fellay, Karl A. Brokstad, Silke Appel, Jessica R. Tarn, Lluís Quintana-Murci, Michael Mingueneau, Nicolas Meyer, Darragh Duffy, Benno Schwikowski, and Jacques Eric Gottenberg, On behalf of The Milieu Intérieur Consortium, ASSESS study investigators, and NECESSITY Consortium .....1991

## Systemic Sclerosis

### Epigenetic Regulation of Profibrotic Macrophages in Systemic Sclerosis–Associated Interstitial Lung Disease

Anna Papazoglou, Mengqi Huang, Melissa Bulik, Annika Lafyatis, Tracy Tabib, Christina Morse, John Sembrat, Mauricio Rojas, Eleanor Valenzi, and Robert Lafyatis .....2003

## Gout

### Superiority of Low-Dose Benzbromarone to Low-Dose Febuxostat in a Prospective, Randomized Comparative

#### Effectiveness Trial in Gout Patients With Renal Uric Acid Underexcretion

Fei Yan, Xiaomei Xue, Jie Lu, Nicola Dalbeth, Han Qi, Qing Yu, Can Wang, Mingshu Sun, Lingling Cui, Zhen Liu, Yuwei He, Xuan Yuan, Ying Chen, Xiaoyu Cheng, Lidan Ma, Hailong Li, Aichang Ji, Shuhui Hu, Zijiang Ran, Robert Terkeltaub, and Changgui Li .....2015

## Pediatric Rheumatology

### Brief Report: Imaging Mass Cytometry Reveals Predominant Innate Immune Signature and Endothelial–Immune Cell Interaction in Juvenile Myositis Compared to Lupus Skin

Jessica L. Turnier, Christine M. Yee, Jacqueline A. Madison, Syed M. Rizvi, Celine C. Berthier, Fei Wen, and J. Michelle Kahlenberg .....2024

## Autoimmune Disease

### Increasing Prevalence of Antinuclear Antibodies in the United States

Gregg E. Dinse, Christine G. Parks, Clarice R. Weinberg, Carroll A. Co, Jesse Wilkerson, Darryl C. Zeldin, Edward K. L. Chan, and Frederick W. Miller .....2032

## Letters

### Systemic Glucocorticoids Confound SARS–CoV-2 Acquisition or Even Clinical Outcomes in Patients With Autoimmune Disease Treated With Biologics: Comment on the Article by Simon et al

Man-Man Niu, Qi Jiang, Yan-Fang Zhang, Dao-Ting Li, Qian Yang, and Peng Hu .....2042

#### Reply

Georg Schett, David Simon, Filippo Fagni, and Korey Tascilar .....2043

### Optimal Bridging Strategy in Active Early Rheumatoid Arthritis: A Bridge Falling Short? Comment on the Article by Krause et al

Joydeep Samanta, Alekhya Amudalapalli, Ashlesha Shukla, BV Harish, Sudhish Gadde, Rasmi R. Sahoo, and Pradeepta S. Patro .....2044

#### Reply

Dietmar Krause and Juergen Braun .....2045

### Characterization of Mucosal-Associated Invariant T Cells in Blood of Patients With Axial Spondyloarthritis and in Axial Entheses of Healthy Controls: Comment on the Article by Rosine et al

Eric Toussiot, Caroline Laheurte, and Philippe Saas .....2045

#### Reply

Nicolas Rosine, Lars Rogge, Dennis McGonagle, and Corinne Miceli-Richard .....2046

## Reviewers .....2048

## Volume 74 Table of Contents .....2052

**Cover image:** The illustration on the cover (accompanying Bermas et al, page 1865–1867) highlights the significance of the decision to overturn the Roe v. Wade decision as it pertains to the impact on patient care, specifically for pregnant women with rheumatic diseases, and the significance of the patient–provider relationship and decision-making. Illustration courtesy of Jennifer E. Fairman, CMI, FAMI.



# VOLUME 74 TABLE OF CONTENTS

## VOLUME 74 • January 2022 • NO.1

<b>In This Issue</b> .....	A5
<b>Journal Club</b> .....	A6
<b>Clinical Connections</b> .....	A7
<b>Special Articles</b>	
Notes from the Field: Global Rheumatology Research: Frontiers, Challenges, and Opportunities <i>Joshua B. Bilsborrow, Ingris Peláez-Ballestas, Bernardo Pons-Estel, Christiaan Scott, Xinping Tian, Graciela S. Alarcon, Richard Bucala, Laura B. Lewandowski, and Evelyn Hsieh</i> .....	1
Editorial: Reexamining Remission Definitions in Rheumatoid Arthritis: Considering the Twenty-Eight-Joint Disease Activity Score, C-Reactive Protein Level, and Patient Global Assessment <i>David T. Felson, Diane Lacaille, Michael P. LaValley, and Daniel Aletaha</i> .....	5
Editorial: Lung Inflammation, NETosis, and the Pulmonary Initiation of Anti-Citrullinated Protein Antibody Response: What Came First, the Chicken or the Egg? <i>Jeremy Sokolove</i> .....	10
Review: Systemic Sclerosis–Associated Interstitial Lung Disease: How to Incorporate Two Food and Drug Administration–Approved Therapies in Clinical Practice <i>Dinesh Khanna, Alain Lescoat, David Roofeh, Elana J. Bernstein, Ella A. Kazerooni, Michael D. Roth, Fernando Martinez, Kevin R. Flaherty, and Christopher P. Denton</i> .....	13
<b>COVID-19</b>	
Disease Flare and Reactogenicity in Patients With Rheumatic and Musculoskeletal Diseases Following Two-Dose SARS–CoV-2 Messenger RNA Vaccination <i>Caoilfhionn M. Connolly, Jake A. Ruddy, Brian J. Boyarsky, Iulia Barbur, William A. Werbel, Duvuru Geetha, Jacqueline M. Garonzik-Wang, Dorry L. Segev, Lisa Christopher-Stine, and Julie J. Paik</i> .....	28
Humoral and Cellular Immune Responses to SARS–CoV-2 Infection and Vaccination in Autoimmune Disease Patients With B Cell Depletion <i>David Simon, Koray Tascilar, Katja Schmidt, Bernhard Manger, Leonie Weckwerth, Maria Sokolova, Laura Bucci, Filippo Fagni, Karin Manger, Florian Schuch, Monika Ronneberger, Axel Hueber, Ulrike Steffen, Dirk Mielenz, Martin Herrmann, Thomas Harrer, Arnd Kleyer, Gerhard Krönke, and Georg Schett</i> .....	33
<b>Rheumatoid Arthritis</b>	
Association of Sputum Neutrophil Extracellular Trap Subsets With IgA Anti-Citrullinated Protein Antibodies in Subjects at Risk for Rheumatoid Arthritis <i>Yuko Okamoto, Stephanie Devoe, Nickie Seto, Valerie Minarchick, Timothy Wilson, Heather M. Rothfuss, Michael P. Mohning, Jaron Arbet, Miranda Kroehl, Ashley Visser, Justin August, Stacey M. Thomas, Laura Lenis Charry, Chelsie Fleischer, Marie L. Feser, Ashley A. Frazer-Abel, Jill M. Norris, Brian D. Cherrington, William J. Janssen, Mariana J. Kaplan, Kevin D. Deane, V. Michael Holers, and M. Kristen Demoruelle</i> .....	38
<b>Osteoarthritis</b>	
Role of Ciliary Protein Intraflagellar Transport Protein 88 in the Regulation of Cartilage Thickness and Osteoarthritis Development in Mice <i>Clarissa R. Coveney, Linyi Zhu, Jadwiga Miotla-Zarebska, Bryony Stott, Ida Parisi, Vicky Batchelor, Claudia Duarte, Emer Chang, Eleanor McSorley, Tonia L. Vincent, and Angus K. T. Wann</i> .....	49
Magnetic Resonance Imaging–Assessed Subchondral Cysts and Incident Knee Pain and Knee Osteoarthritis: Data From the Multicenter Osteoarthritis Study <i>Thomas A. Perry, Terence W. O'Neill, Irina Tolstykh, John Lynch, David T. Felson, Nigel K. Arden, and Michael C. Nevitt</i> .....	60
<b>Spondyloarthritis</b>	
Safety and Efficacy of Upadacitinib in Patients With Active Ankylosing Spondylitis and an Inadequate Response to Nonsteroidal Antiinflammatory Drug Therapy: One-Year Results of a Double-Blind, Placebo-Controlled Study and Open-Label Extension <i>Atul Deodhar, Désirée van der Heijde, Joachim Sieper, Filip Van den Bosch, Walter P. Maksymowych, Tae-Hwan Kim, Mitsumasa Kishimoto, Andrew Ostor, Bernard Combe, Yunxia Sui, Alvina D. Chu, and In-Ho Song</i> .....	70
<b>Psoriatic Arthritis</b>	
Identification and Evaluation of Serum Protein Biomarkers That Differentiate Psoriatic Arthritis From Rheumatoid Arthritis <i>Angela Mc Ardle, Anna Kwasnik, Agnes Szentpetery, Belinda Hernandez, Andrew Parnell, Wilco de Jager, Sytze de Roock, Oliver Fitzgerald, and Stephen R. Pennington</i> .....	81

## Systemic Lupus Erythematosus

Induction of Interferon- $\gamma$  and Tissue Inflammation by Overexpression of Eosinophil Cationic Protein in T Cells and Exosomes

*Huai-Chia Chuang, Ming-Han Chen, Yi-Ming Chen, Yi-Ru Ciou, Chia-Hsin Hsueh, Ching-Yi Tsai, and Tse-Hua Tan* . . . . . 92

Brief Report: Anti-Double-Stranded DNA Antibodies Recognize DNA Presented on HLA Class II Molecules of Systemic Lupus Erythematosus Risk Alleles

*Hideaki Tsuji, Koichiro Ohmura, Hui Jin, Ryota Naito, Noriko Arase, Masako Kohyama, Tadahiro Suenaga, Shuhei Sakakibara, Yuta Kochi, Yukinori Okada, Kazuhiko Yamamoto, Hitoshi Kikutani, Akio Morinobu, Tsuneyo Mimori, and Hisashi Arase* . . . . . 105

Phase III/IV, Randomized, Fifty-Two-Week Study of the Efficacy and Safety of Belimumab in Patients of Black African Ancestry With Systemic Lupus Erythematosus

*Ellen Ginzler, Luiz Sergio Guedes Barbosa, David D'Cruz, Richard Furie, Kathleen Maksimowicz-McKinnon, James Oates, Mittermayer Barreto Santiago, Amit Saxena, Saira Sheikh, Damon L. Bass, Susan W. Burriss, Jennifer A. Gilbride, James G. Groark, Michelle Miller, Amy Pierce, David A. Roth, and Beulah Ji* . . . . . 112

## Vasculitis

Phase IIa Global Study Evaluating Rituximab for the Treatment of Pediatric Patients With Granulomatosis With Polyangiitis or Microscopic Polyangiitis

*Paul Brogan, Rae S. M. Yeung, Gavin Cleary, Satyapal Rangaraj, Ozgur Kasapcopur, Aimee O. Hersh, Suzanne Li, Dusan Paripovic, Kenneth Schikler, Andrew Zeff, Claudia Bracaglia, Despina Eleftheriou, Pooneh Pordeli, Simone Melega, Candice Jamois, Jacques Gaudreault, Margaret Michalska, Paul Brunetta, Jennifer C. Cooper, Patricia B. Lehane, and the PePRS Study Group* . . . . . 124

A Worldwide Pharmacoepidemiologic Update on Drug-Induced Antineutrophil Cytoplasmic Antibody-Associated Vasculitis in the Era of Targeted Therapies

*Samuel Deshayes, Charles Dolladille, Anaël Dumont, Nicolas Martin Silva, Basile Chretien, Hubert De Boysson, Joachim Alexandre, and Achille Aouba* . . . . . 134

## Myositis

Time-Dependent Analysis of Risk of New-Onset Heart Failure Among Patients With Polymyositis and Dermatomyositis

*Chun-Yu Lin, Hung-An Chen, Tsai-Ching Hsu, Chun-Hsin Wu, Yu-Jih Su, and Chung-Yuan Hsu* . . . . . 140

## Pediatric Rheumatology

Effect of Clonally Expanded PD-1<sup>high</sup>CXCR5-CD4<sup>+</sup> Peripheral T Helper Cells on B Cell Differentiation in the Joints of Patients With Antinuclear Antibody-Positive Juvenile Idiopathic Arthritis

*Jonas Fischer, Johannes Dirks, Julia Klaussner, Gabriele Haase, Annette Holl-Wieden, Christine Hofmann, Stephan Hackenberg, Hermann Girschick, and Henner Morbach* . . . . . 150

## Autoimmune Disease

Variants on the *UBE2L3/YDJC* Autoimmune Disease Risk Haplotype Increase *UBE2L3* Expression by Modulating CCCTC-Binding Factor and YY1 Binding

*Jaanam Gopalakrishnan, Kandice L. Tessneer, Yao Fu, Satish Pasula, Richard C. Pelikan, Jennifer A. Kelly, Graham B. Wiley, and Patrick M. Gaffney* . . . . . 163

## Letters

Hypogammaglobulinemia in Rheumatoid Arthritis Patients Treated With Rituximab: Should We Switch Biologics?

Comment on the Article by Fraenkel et al

*Gerasimos Evangelatos, Melina Moschopoulou, Alexios Iliopoulos, and George E. Fragoulis* . . . . . 174

Reply

*Liana Fraenkel, Joan M. Bathon, Bryant R. England, E. William St.Clair, and Elie A. Akl, on behalf of the ACR RA Guideline Author Group* . . . . . 175

Importance of Internal and External Validity in Clinical Research: Comment on the Article by Fatima et al

*Yusuke Matsuo, Yoshie Yamada, Jun Miyata, Tetsuro Aita, and Takashi Yoshioka* . . . . . 175

Considerations for a Study Using the Health Assessment Questionnaire to Predict All-Cause Mortality in Early Rheumatoid Arthritis: Comment on the Article by Fatima et al

*Po-Yun Ko, Da-Ming Yeh, and James Cheng-Chung Wei* . . . . . 176

Functional Capacity at 1 Year Predicts All-Cause Mortality in Patients With Rheumatoid Arthritis: Comment on the Article by Fatima et al

*Richard K. Jacoby and Johannes J. Rasker* . . . . . 177

Reply

*Safoora Fatima, O. Schieir, E. C. Keystone, M. F. Valois, S. J. Bartlett, L. Bessette, G. Boire, G. Hazlewood, C. Hitchon, D. Tin, C. Thorne, V. P. Bykerk, and J. E. Pope, on behalf of the CATCH Investigators* . . . . . 178

## VOLUME 74 • February 2022 • NO.2

<b>In This Issue</b> .....	A11
<b>Journal Club</b> .....	A12
<b>Clinical Connections</b> .....	A13
<b>Special Articles</b>	
Editorial: Are Intraarticular Glucocorticoids Safe in Osteoarthritis?	
<i>Joel A. Block</i> .....	181
Review: Myocardial Dysfunction and Heart Failure in Rheumatoid Arthritis	
<i>Elizabeth Park, Jan Griffin, and Joan M. Bathon</i> .....	184
<b>Rheumatoid Arthritis</b>	
Activated Peripheral Blood B Cells in Rheumatoid Arthritis and Their Relationship to Anti-Tumor Necrosis Factor Treatment and Response: A Randomized Clinical Trial of the Effects of Anti-Tumor Necrosis Factor on B Cells	
<i>Nida Meednu, Jennifer Barnard, Kelly Callahan, Andreea Coca, Bethany Marston, Ralf Thiele, Darren Tabechian, Marcy Bolster, Jeffrey Curtis, Meggan Mackay, Jonathan Graf, Richard Keating, Edwin Smith, Karen Boyle, Lynette Keyes-Elstein, Beverly Welch, Ellen Goldmuntz, and Jennifer H. Anolik</i> .....	200
Activation of Hypothalamic AMP-Activated Protein Kinase Ameliorates Metabolic Complications of Experimental Arthritis	
<i>Patricia Seoane-Collazo, Eva Rial-Pensado, Ánxela Estévez-Salguero, Edward Milbank, Lucía García-Caballero, Marcos Ríos, Laura Liñares-Pose, Morena Scotece, Rosalía Gallego, José Manuel Fernández-Real, Rubén Nogueiras, Carlos Diéguez, Oreste Gualillo, and Miguel López</i> .....	212
<b>Clinical Images</b>	
The Appearance of Scurvy on Magnetic Resonance Imaging	
<i>Sami Giryès, Daniela Militianu, and Yolanda Braun-Moscovici</i> .....	222
<b>Osteoarthritis</b>	
Brief Report: Progression of Knee Osteoarthritis With Use of Intraarticular Glucocorticoids Versus Hyaluronic Acid	
<i>Justin Bucci, Xiaoyang Chen, Michael LaValley, Michael Nevitt, James Torner, Cora E. Lewis, and David T. Felson</i> .....	223
Association of Increased Serum Lipopolysaccharide, But Not Microbial Dysbiosis, With Obesity-Related Osteoarthritis	
<i>Richard F. Loeser, Liubov Arbeeva, Kathryn Kelley, Anthony A. Fodor, Shan Sun, Veronica Ulici, Lara Longobardi, Yang Cui, Delisha A. Stewart, Susan J. Sumner, M. Andrea Azcarate-Peril, R. Balfour Sartor, Ian M. Carroll, Jordan B. Renner, Joanne M. Jordan, and Amanda E. Nelson</i> .....	227
<b>Psoriatic Arthritis</b>	
Incidence of Psoriatic Arthritis Among Patients Receiving Biologic Treatments for Psoriasis: A Nested Case-Control Study	
<i>Yael Shalev Rosenthal, Naama Schwartz, Iftach Sagy, and Lev Pavlovsky</i> .....	237
Risk of Inflammatory Bowel Disease in Patients With Psoriasis and Psoriatic Arthritis/Ankylosing Spondylitis Initiating Interleukin-17 Inhibitors: A Nationwide Population-Based Study Using the French National Health Data System	
<i>Laetitia Penso, Christina Bergqvist, Antoine Meyer, Philippe Herlemont, Alain Weill, Mahmoud Zureik, Rosemary Dray-Spira, and Emilie Sbidian</i> .....	244
Association of Structural Enthesal Lesions With an Increased Risk of Progression From Psoriasis to Psoriatic Arthritis	
<i>David Simon, Koray Tascilar, Arnd Kleyer, Sara Bayat, Eleni Kampylafka, Maria V. Sokolova, Ana Zekovic, Axel J. Hueber, Jürgen Rech, Louis Schuster, Klaus Engel, Michael Sticherling, and Georg Schett</i> .....	253
<b>Clinical Images</b>	
Diffuse Systemic Sclerosis, Skin Bleaching, and Telangiectasia	
<i>Cindy Flower</i> .....	262
<b>Systemic Lupus Erythematosus</b>	
International Consensus for the Dosing of Corticosteroids in Childhood-Onset Systemic Lupus Erythematosus With Proliferative Lupus Nephritis	
<i>Nathalie E. Chalhoub, Scott E. Wenderfer, Deborah M. Levy, Kelly Rouster-Stevens, Amita Aggarwal, Sonia I. Savani, Natasha M. Ruth, Thaschawee Arkachaisri, Tingting Qiu, Angela Merritt, Karen Onel, Beatrice Goilav, Raju P. Khubchandani, Jianghong Deng, Adriana R. Fonseca, Stacy P. Ardoin, Coziana Ciurtin, Ozgur Kasapcopur, Marija Jelusic, Adam M. Huber, Seza Ozen, Marisa S. Klein-Gitelman, Simone Appenzeller, André Cavalcanti, Lampros Fotis, Sern Chin Lim, Rodrigo M. Silva, Julia Ramírez-Miramontes, Natalie L. Rosenwasser, Claudia Saad-Magalhaes, Dieneke Schonenberg-Meinema, Christiaan Scott, Clovis A. Silva, Sandra Enciso, Maria T. Terreri, Alfonso-Ragnar Torres-Jimenez, Maria Trachana, Sulaiman M. Al-Mayouf, Prasad Devarajan, Bin Huang, and Hermine I. Brunner</i> .....	263

Association of a Combination of Healthy Lifestyle Behaviors With Reduced Risk of Incident Systemic Lupus Erythematosus <i>May Y. Choi, Jill Hahn, Susan Malspeis, Emma F. Stevens, Elizabeth W. Karlson, Jeffrey A. Sparks, Kazuki Yoshida, Laura Kubzansky, and Karen H. Costenbader</i> . . . . .	274
Evaluation of Immune Response and Disease Status in Systemic Lupus Erythematosus Patients Following SARS-CoV-2 Vaccination <i>Peter M. Izmirly, Mimi Y. Kim, Marie Samanovic, Ruth Fernandez-Ruiz, Sharon Ohana, Kristina K. Deonaraine, Alexis J. Engel, Mala Masson, Xianhong Xie, Amber R. Cornelius, Ramin S. Herati, Rebecca H. Haberman, Jose U. Scher, Allison Guttmann, Rebecca B. Blank, Benjamin Plotz, Mayce Haj-Ali, Brittany Banbury, Sara Stream, Ghadeer Hasan, Gary Ho, Paula Rackoff, Ashira D. Blazer, Chung-E Tseng, H. Michael Belmont, Amit Saxena, Mark J. Mulligan, Robert M. Clancy, and Jill P. Buyon</i> . . . . .	284
<b>Vasculitis</b>	
Mepolizumab for Eosinophilic Granulomatosis With Polyangiitis: A European Multicenter Observational Study <i>Alessandra Bettiol, Maria Letizia Urban, Lorenzo Dagna, Vincent Cottin, Franco Franceschini, Stefano Del Giacco, Franco Schiavon, Thomas Neumann, Giuseppe Lopalco, Pavel Novikov, Chiara Baldini, Carlo Lombardi, Alvise Berti, Federico Alberici, Marco Folci, Simone Negrini, Renato Alberto Sinico, Luca Quartuccio, Claudio Lunardi, Paola Parronchi, Frank Moosig, Georgina Espígal-Frigolé, Jan Schroeder, Anna Luise Kernder, Sara Monti, Ettore Silvagni, Claudia Crimi, Francesco Cinetto, Paolo Fraticelli, Dario Roccatello, Angelo Vacca, Aladdin J. Mohammad, Bernhard Hellmich, Maxime Samson, Elena Bargagli, Jan Willem Cohen Tervaert, Camillo Ribi, Davide Fiori, Federica Bello, Filippo Fagni, Luca Moroni, Giuseppe Alvise Ramirez, Mouhamad Nasser, Chiara Marvisi, Paola Toniati, Davide Firinu, Roberto Padoan, Allyson Egan, Benjamin Seeliger, Florenzo Iannone, Carlo Salvarani, David Jayne, Domenico Prisco, Augusto Vaglio, and Giacomo Emmi, On behalf of the European EGPA Study Group</i> . . . . .	295
<b>Systemic Sclerosis</b>	
Defective Early B Cell Tolerance Checkpoints in Patients With Systemic Sclerosis Allow the Production of Self Antigen-Specific Clones <i>Salome Glauzy, Brennan Olson, Christopher K. May, Daniele Parisi, Christopher Massad, James E. Hansen, Changwan Ryu, Erica L. Herzog, and Eric Meffre</i> . . . . .	307
Platelet Phagocytosis via P-selectin Glycoprotein Ligand 1 and Accumulation of Microparticles in Systemic Sclerosis <i>Angelo A. Manfredi, Giuseppe A. Ramirez, Cosmo Godino, Annalisa Capobianco, Antonella Monno, Stefano Franchini, Enrico Tombetti, Sara Corradetti, Jörg H. W. Distler, Marco E. Bianchi, Patrizia Rovere-Querini, and Norma Maugeri</i> . . . . .	318
Expansion of Fcγ Receptor IIIa-Positive Macrophages, Ficolin 1-Positive Monocyte-Derived Dendritic Cells, and Plasmacytoid Dendritic Cells Associated With Severe Skin Disease in Systemic Sclerosis <i>Dan Xue, Tracy Tabib, Christina Morse, Yi Yang, Robyn T. Domsic, Dinesh Khanna, and Robert Lafyatis</i> . . . . .	329
<b>Myositis</b>	
Contribution of Rare Genetic Variation to Disease Susceptibility in a Large Scandinavian Myositis Cohort <i>Matteo Bianchi, Sergey V. Kozyrev, Antonella Notarnicola, Lina Hultin Rosenberg, Åsa Karlsson, Pascal Pucholt, Simon Rothwell, Andrei Alexsson, Johanna K. Sandling, Helena Andersson, Robert G. Cooper, Leonid Padyukov, Anna Tjärnlund, Maryam Dastmalchi, The ImmunoArray Development Consortium, The DISSECT Consortium, Jennifer R. S. Meadows, Louise Pyndt Diederichsen, Øyvind Molberg, Hector Chinoy, Janine A. Lamb, Lars Rönnblom, Kerstin Lindblad-Toh, and Ingrid E. Lundberg</i> . . . . .	342
<b>Autoinflammatory Disease</b>	
Brief Report: Excess Serum Interleukin-18 Distinguishes Patients With Pathogenic Mutations in <i>PSTPIP1</i> <i>Deborah L. Stone, Amanda Ombrello, Juan I. Arostegui, Corinne Schneider, Vinh Dang, Adriana de Jesus, Charlotte Girard-Guyonvarc'h, Cem Gabay, Wonyong Lee, Jae Jin Chae, Ivona Aksentijevich, Raphaela T. Goldbach-Mansky, Daniel L. Kastner, and Scott W. Canna</i> . . . . .	353
<b>Pediatric Rheumatology</b>	
Brief Report: Anti-Cortactin Autoantibodies Are Associated With Key Clinical Features in Adult Myositis But Are Rarely Present in Juvenile Myositis <i>Iago Pinal-Fernandez, Katherine Pak, Albert Gil-Vila, Andres Baucells, Benjamin Plotz, Maria Casal-Dominguez, Assia Derfoul, Maria Angeles Martinez-Carretero, Albert Selva-O'Callaghan, Sara Sabbagh, Livia Casciola-Rosen, Jemima Albayda, Julie Paik, Eleni Tiniakou, Sonye K. Danoff, Thomas E. Lloyd, Frederick W. Miller, Lisa G. Rider, Lisa Christopher-Stine, and Andrew L. Mammen, On behalf of the Childhood Myositis Heterogeneity Collaborative Study Group</i> . . . . .	358

## Letters

Safety and Tolerability of the COVID-19 Messenger RNA Vaccine in Adolescents With Juvenile Idiopathic Arthritis Treated With Tumor Necrosis Factor Inhibitors <i>Dimitra Dimopoulou, Nikos Spyridis, George Vartzelis, Maria N. Tsolia, and Despoina N. Maritsi</i> . . . . .	365
Sjögren Disease, Not Sjögren's: Comment on the Article by Baer and Hammitt <i>Vincent Cottin</i> . . . . .	366
Reply <i>Alan N. Baer and Katherine M. Hammitt</i> . . . . .	367
Long-Term Risk of Cancer Development Among Anti-Th/To Antibody-Positive Systemic Sclerosis Patients: Comment on the Article by Mecoli et al <i>Yuta Yamashita, Yoshinao Muro, Haruka Koizumi, Takuya Takeichi, Yasuhiko Yamano, Yasuhiro Kondoh, and Masashi Akiyama</i> . . . . .	368
VEXAS Syndrome With Systemic Lupus Erythematosus: Expanding the Spectrum of Associated Conditions <i>Aman Sharma, Gsrnk Naidu, Prateek Deo, and David B. Beck</i> . . . . .	369
Long-Term Extension Study of Tofacitinib in Refractory Dermatomyositis <i>Julie J. Paik, Matthew Shneyderman, Laura Gutierrez-Alamillo, Jemima Albayda, Eleni Tiniakou, Jamie Perin, Grazyna Purwin, Sherry Leung, Doris Leung, Livia Casciola-Rosen, Andrew S. Koenig, and Lisa Christopher-Stine</i> . . . . .	371

## VOLUME 74 • March 2022 • NO. 3

<b>In This Issue</b> . . . . .	A17
<b>Journal Club</b> . . . . .	A18
<b>Clinical Connections</b> . . . . .	A19
<b>Special Articles</b>	
Winner of the 2021 American College of Rheumatology Annual Image Competition <i>American College of Rheumatology Image Library Diversity Task Force</i> . . . . .	373
Rheumatology Is Amazing <i>David R. Karp</i> . . . . .	375
Editorial: New Classification Criteria for Small-Vessel Vasculitis: Is Antineutrophil Cytoplasmic Antibody Inclusion Their Major Advance? <i>Christian Dejaco and Loïc Guillevin</i> . . . . .	383
2022 American College of Rheumatology/European Alliance of Associations for Rheumatology Classification Criteria for Eosinophilic Granulomatosis With Polyangiitis <i>Peter C. Grayson, Cristina Ponte, Ravi Suppiah, Joanna C. Robson, Anthea Craven, Andrew Judge, Sara Khalid, Andrew Hutchings, Raashid A. Luqmani, Richard A. Watts, and Peter A. Merkel</i> . . . . .	386
2022 American College of Rheumatology/European Alliance of Associations for Rheumatology Classification Criteria for Granulomatosis With Polyangiitis <i>Joanna C. Robson, Peter C. Grayson, Cristina Ponte, Ravi Suppiah, Anthea Craven, Andrew Judge, Sara Khalid, Andrew Hutchings, Richard A. Watts, Peter A. Merkel, and Raashid A. Luqmani</i> . . . . .	393
2022 American College of Rheumatology/European Alliance of Associations for Rheumatology Classification Criteria for Microscopic Polyangiitis <i>Ravi Suppiah, Joanna C. Robson, Peter C. Grayson, Cristina Ponte, Anthea Craven, Sara Khalid, Andrew Judge, Andrew Hutchings, Peter A. Merkel, Raashid A. Luqmani, and Richard A. Watts</i> . . . . .	400
<b>Rheumatoid Arthritis</b>	
Association of Bone Erosions and Osteophytes With Systemic Bone Involvement on High-Resolution Peripheral Quantitative Computed Tomography in Premenopausal Women With Longstanding Rheumatoid Arthritis <i>Mariana O. Perez, Camille P. Figueiredo, Lucas P. Sales, Ana Cristina Medeiros-Ribeiro, Liliam Takayama, Diogo S. Domiciano, Karina Bonfiglioli, Valeria F. Caparbo, and Rosa M. R. Pereira</i> . . . . .	407
Microstructural Bone Changes Are Associated With Broad-Spectrum Autoimmunity and Predict the Onset of Rheumatoid Arthritis <i>David Simon, Arnd Kleyer, Duy Bui Cong, Axel Hueber, Holger Bang, Andreas Ramming, Juergen Rech, and Georg Schett</i> . . . . .	418



Attenuation of Rheumatoid Arthritis Through the Inhibition of Tumor Necrosis Factor–Induced Caspase 3/Gasdermin E–Mediated Pyroptosis <i>Zeqing Zhai, Fangyuan Yang, Wenchao Xu, Jiaochan Han, Guihu Luo, Yehao Li, Jian Zhuang, Hongyu Jie, Xing Li, Xingliang Shi, Xinai Han, Xiaoqing Luo, Rui Song, Yonghong Chen, Jianheng Liang, Shufan Wu, Yi He, and Erwei Sun.</i> . . . . .	427
Effect of JAK Inhibition on the Induction of Proinflammatory HLA–DR+CD90+ Rheumatoid Arthritis Synovial Fibroblasts by Interferon- $\gamma$ <i>Shuyang Zhao, Ricardo Grieshaber-Bouyer, Deepak A. Rao, Philipp Kolb, Haizhang Chen, Ivana Andreeva, Theresa Tretter, Hanns-Martin Lorenz, Carsten Watzl, Guido Wabnitz, Lars-Oliver Tykocinski, and Wolfgang Merkt.</i> . . . .	441
<b>Osteoarthritis</b>	
Association Between Race and Radiographic, Symptomatic, and Clinical Hand Osteoarthritis: A Propensity Score–Matched Study Using Osteoarthritis Initiative Data <i>Farhad Pishgar, Robert M. Kwee, Arya Haj-Mirzaian, Ali Guermazi, Ida K. Haugen, and Shadpour Demehri</i> . . . . .	453
SH2 Domain–Containing Phosphatase 2 Inhibition Attenuates Osteoarthritis by Maintaining Homeostasis of Cartilage Metabolism via the Docking Protein 1/Uridine Phosphorylase 1/Uridine Cascade <i>Qianqian Liu, Linhui Zhai, Mingrui Han, Dongquan Shi, Ziyang Sun, Shuang Peng, Meijing Wang, Chenyang Zhang, Jian Gao, Wenjin Yan, Qing Jiang, Dijun Chen, Qiang Xu, Minjia Tan, and Yang Sun</i> . . . . .	462
<b>Clinical Images</b>	
Extranodal Natural Killer/T Cell Lymphoma As a Rare Mimicker of Granulomatosis With Polyangiitis <i>Jennifer Strouse, Anand Rajan, He B. Chang, Mohamad D. Dimachkie, Christopher Halbur, and Brittany Bettendorf.</i> . . . .	474
<b>Psoriatic Arthritis</b>	
Long-Term Efficacy and Safety of Guselkumab, a Monoclonal Antibody Specific to the p19 Subunit of Interleukin-23, Through Two Years: Results From a Phase III, Randomized, Double-Blind, Placebo-Controlled Study Conducted in Biologic-Naive Patients With Active Psoriatic Arthritis <i>Iain B. McInnes, Proton Rahman, Alice B. Gottlieb, Elizabeth C. Hsia, Alexa P. Kollmeier, Xie L. Xu, Yusang Jiang, Shihong Sheng, May Shawi, Soumya D. Chakravarty, Désirée van der Heijde, and Philip J. Mease</i> . . . . .	475
Pregnancy Outcomes in Women With Psoriatic Arthritis in Relation to Presence and Timing of Antirheumatic Treatment <i>Katarina Remaeus, Kari Johansson, Fredrik Granath, Olof Stephansson, and Karin Hellgren</i> . . . . .	486
<b>Systemic Lupus Erythematosus</b>	
Up-Regulated Interleukin-10 Induced by E2F Transcription Factor 2–MicroRNA-17-5p Circuitry in Extrafollicular Effector B Cells Contributes to Autoantibody Production in Systemic Lupus Erythematosus <i>Lingxiao Xu, Lei Wang, Yumeng Shi, Yun Deng, Jim C. Oates, Diane L. Kamen, Gary S. Gilkeson, Fang Wang, Miaojia Zhang, Wenfeng Tan, and Betty P. Tsao</i> . . . . .	496
<b>Myositis</b>	
Performance of the 2017 European Alliance of Associations for Rheumatology/American College of Rheumatology Classification Criteria for Idiopathic Inflammatory Myopathies in Patients With Myositis-Specific Autoantibodies <i>Maria Casal-Dominguez, Iago Pinal-Fernandez, Katherine Pak, Wilson Huang, Albert Selva-O'Callaghan, Jemima Albayda, Livia Casciola-Rosen, Julie J. Paik, Eleni Tiniakou, Christopher A. Mecoli, Thomas E. Lloyd, Sonye K. Danoff, Lisa Christopher-Stine, and Andrew L. Mammen.</i> . . . .	508
<b>Systemic Sclerosis</b>	
Nintedanib in Patients With Systemic Sclerosis–Associated Interstitial Lung Disease: Subgroup Analyses by Autoantibody Status and Modified Rodnan Skin Thickness Score <i>Masataka Kuwana, Yannick Allanore, Christopher P. Denton, Jörg H. W. Distler, Virginia Steen, Dinesh Khanna, Marco Matucci-Cerinic, Maureen D. Mayes, Elizabeth R. Volkman, Corinna Miede, Martina Gahlemane, Manuel Quaresma, Margarida Alves, and Oliver Distler</i> . . . . .	518
<b>Immune-Related Adverse Events</b>	
Predictors of Rheumatic Immune-Related Adverse Events and De Novo Inflammatory Arthritis After Immune Checkpoint Inhibitor Treatment for Cancer <i>Amy Cunningham-Bussell, Jiaqi Wang, Lauren C. Prisco, Lily W. Martin, Kathleen M. M. Vanni, Alessandra Zaccardelli, Mazen Nasrallah, Lydia Gedmintas, Lindsey A. MacFarlane, Nancy A. Shadick, Mark M. Awad, Osama Rahma, Nicole R. LeBoeuf, Ellen M. Gravallese, and Jeffrey A. Sparks</i> . . . . .	527

## Letters

Effective Viral Vector Response to SARS-CoV-2 Booster Vaccination in a Patient With Rheumatoid Arthritis After Initial Ineffective Response to Messenger RNA Vaccine <i>Matthew C. Baker, Vamsee Mallajosyula, Mark M. Davis, Scott D. Boyd, Kari C. Nadeau, and William H. Robinson</i> . . . . .	541
Potential Residual Confounders in an Analysis of Lifestyle Factors and Risk of Incident Systemic Lupus Erythematosus: Comment on the Article by Choi et al <i>Pei-En Kao, Amy Ker, Cheng-Ruei Yang, and James Cheng-Chung Wei</i> . . . . .	542
Reply <i>May Y. Choi, Jill Hahn, Susan Malspeis, Emma F. Stevens, Elizabeth W. Karlson, Jeffrey A. Sparks, Kazuki Yoshida, Laura Kubzansky, and Karen H. Costenbader</i> . . . . .	543
Rituximab Versus Cyclophosphamide for Remission Induction in Active, Severe Antineutrophil Cytoplasmic Antibody-Associated Vasculitis: Comment on the Article by Chung et al <i>Siddharth Jain, G. S. R. S. N. K. Naidu, and Aman Sharma</i> . . . . .	544
Reply <i>Sharon A. Chung, Philip Seo, Peter A. Merkel, and Carol A. Langford</i> . . . . .	545
Consideration of Confounders, Accuracy of Diagnosis, and Disease Severity in Assessing the Risk of Inflammatory Bowel Disease in Patients With Psoriasis and Psoriatic Arthritis/Ankylosing Spondylitis Beginning Interleukin-7 Inhibitor Treatment: Comment on the Article by Penso et al <i>Cheng-Ruei Yang, Amy Ker, Pei-En Kao, and James Cheng-Chung Wei</i> . . . . .	546
Reply <i>Emilie Sbidian, Laëtitia Penso, and Antoine Meyer</i> . . . . .	547

## VOLUME 74 • April 2022 • NO. 4

In This Issue . . . . .	A13
Journal Club . . . . .	A14
Clinical Connections . . . . .	A15

## Online-Only Special Article

American College of Rheumatology Clinical Guidance for Multisystem Inflammatory Syndrome in Children Associated With SARS-CoV-2 and Hyperinflammation in Pediatric COVID-19: Version 3 <i>Lauren A. Henderson, Scott W. Canna, Kevin G. Friedman, Mark Gorelik, Sivia K. Lapidus, Hamid Bassiri, Edward M. Behrens, Kate F. Kernan, Grant S. Schuler, Philip Seo, Mary Beth F. Son, Adriana H. Tremoulet, Christina VanderPluym, Rae S. M. Yeung, Amy S. Mudano, Amy S. Turner, David R. Karp, and Jay J. Mehta</i> . . . . .	e1
--	----

## Special Articles

Editorial: Fanning the Flames of Autoimmunity: The Microbiome in Rheumatic Disease <i>Renuka R. Nayak</i> . . . . .	549
2021 American College of Rheumatology Guideline for the Treatment of Juvenile Idiopathic Arthritis: Therapeutic Approaches for Oligoarthritis, Temporomandibular Joint Arthritis, and Systemic Juvenile Idiopathic Arthritis <i>Karen B. Onel, Daniel B. Horton, Daniel J. Lovell, Susan Shenoi, Carlos A. Cuello, Sheila T. Angeles-Han, Mara L. Becker, Randy Q. Cron, Brian M. Feldman, Polly J. Ferguson, Harry Gewanter, Jaime Guzman, Yukiko Kimura, Tzielan Lee, Katherine Murphy, Peter A. Nigrovic, Michael J. Ombrello, C. Eglia Rabinovich, Melissa Teshler, Marinka Twilt, Marisa Klein-Gitelman, Fatima Barbar-Smiley, Ashley M. Cooper, Barbara Edelheit, Miriah Gillispie-Taylor, Kimberly Hays, Melissa L. Mannion, Rosemary Peterson, Elaine Flanagan, Nadine Saad, Nancy Sullivan, Ann Marie Szymanski, Rebecca Trachtman, Marat Turgunbaev, Keila Veiga, Amy S. Turner, and James T. Reston</i> . . . . .	553
2021 American College of Rheumatology Guideline for the Treatment of Juvenile Idiopathic Arthritis: Recommendations for Nonpharmacologic Therapies, Medication Monitoring, Immunizations, and Imaging <i>Karen B. Onel, Daniel B. Horton, Daniel J. Lovell, Susan Shenoi, Carlos A. Cuello, Sheila T. Angeles-Han, Mara L. Becker, Randy Q. Cron, Brian M. Feldman, Polly J. Ferguson, Harry Gewanter, Jaime Guzman, Yukiko Kimura, Tzielan Lee, Katherine Murphy, Peter A. Nigrovic, Michael J. Ombrello, C. Eglia Rabinovich, Melissa Teshler, Marinka Twilt, Marisa Klein-Gitelman, Fatima Barbar-Smiley, Ashley M. Cooper, Barbara Edelheit, Miriah Gillispie-Taylor, Kimberly Hays, Melissa L. Mannion, Rosemary Peterson, Elaine Flanagan, Nadine Saad, Nancy Sullivan, Ann Marie Szymanski, Rebecca Trachtman, Marat Turgunbaev, Keila Veiga, Amy S. Turner, and James T. Reston</i> . . . . .	570

2021 American College of Rheumatology/Vasculitis Foundation Guideline for the Management of Kawasaki Disease <i>Mark Gorelik, Sharon A. Chung, Kaveh Ardalan, Bryce A. Binstadt, Kevin Friedman, Kristen Hayward, Lisa F. Imundo, Sivia K. Lapidus, Susan Kim, Mary Beth Son, Sangeeta Sule, Adriana H. Tremoulet, Heather Van Mater, Cagri Yildirim-Toruner, Carol A. Langford, Mehrdad Maz, Andy Abril, Gordon Guyatt, Amy M. Archer, Doyt L. Conn, Kathy A. Full, Peter C. Grayson, Maria F. Ibarra, Peter A. Merkel, Rennie L. Rhee, Philip Seo, John H. Stone, Robert P. Sundel, Omar I. Vitobaldi, Ann Warner, Kevin Byram, Anisha B. Dua, Nedaa Husainat, Karen E. James, Mohamad Kalot, Yih Chang Lin, Jason M. Springer, Marat Turgunbaev, Alexandra Villa-Forte, Amy S. Turner, and Reem A. Mustafa</i> . . . . .	586
<b>Rheumatoid Arthritis</b>	
Brief Report: Antibody Responses to Epstein-Barr Virus in the Preclinical Period of Rheumatoid Arthritis Suggest the Presence of Increased Viral Reactivation Cycles <i>Sabrina Fechtner, Heather Berens, Elizabeth Bemis, Rachel L. Johnson, Carla J. Guthridge, Nichole E. Carlson, M. Kristen Demoruelle, John B. Harley, Jess D. Edison, Jill A. Norris, William H. Robinson, Kevin D. Deane, Judith A. James, and V. Michael Holers</i> . . . . .	597
The Effect of Discontinuing Denosumab in Patients With Rheumatoid Arthritis Treated With Glucocorticoids <i>Kenneth G. Saag, Michele T. McDermott, Jonathan Adachi, Willem Lems, Nancy E. Lane, Piet Geusens, Robert Kees Stad, Li Chen, Shuang Huang, Robin Dore, and Stanley Cohen</i> . . . . .	604
<b>Osteoarthritis</b>	
Recreational Physical Activity and Risk of Incident Knee Osteoarthritis: An International Meta-Analysis of Individual Participant-Level Data <i>Lucy S. Gates, Thomas A. Perry, Yvonne M. Golightly, Amanda E. Nelson, Leigh F. Callahan, David Felson, Michael Nevitt, Graeme Jones, Cyrus Cooper, Mark E. Batt, Maria T. Sanchez-Santos, and Nigel K. Arden</i> . . . . .	612
Clinical and Preclinical Evidence for Roles of Soluble Epoxide Hydrolase in Osteoarthritis Knee Pain <i>Peter R. W. Gowler, James Turnbull, Mohsen Shahtaheri, Sameer Gohir, Tony Kelly, Cindy McReynolds, Jun Yang, Rakesh R. Jha, Gwen S. Fernandes, Weiya Zhang, Michael Doherty, David A. Walsh, Bruce D. Hammock, Ana M. Valdes, David A. Barrett, and Victoria Chapman</i> . . . . .	623
<b>Clinical Images</b>	
Clinical Images: Two Distinct Magnetic Resonance Imaging Findings in Polyarteritis Nodosa <i>Ken Yoshida, Taro Ukichi, and Daitaro Kurosaka</i> . . . . .	633
<b>Systemic Lupus Erythematosus</b>	
Brief Report: Host Genetics But Not Commensal Microbiota Determines the Initial Development of Systemic Autoimmune Disease in BXD2 Mice <i>Huixian Hong, Fatima Alduraibi, David Ponder, Wayne L. Duck, Casey D. Morrow, Jeremy B. Foote, Trenton R. Schoeb, Huma Fatima, Charles O. Elson III, Hui-Chen Hsu, and John D. Mountz</i> . . . . .	634
Effect of Impaired T Cell Receptor Signaling on the Gut Microbiota in a Mouse Model of Systemic Autoimmunity <i>Mirei Shirakashi, Mikako Maruya, Keiji Hirota, Tatsuaki Tsuruyama, Takashi Matsuo, Ryu Watanabe, Koichi Murata, Masao Tanaka, Hiromu Ito, Hajime Yoshifuji, Koichiro Ohmura, Dirk Elewaut, Shimon Sakaguchi, Sidonia Fagarasan, Tsuneyo Mimori, and Motomu Hashimoto</i> . . . . .	641
<b>Sjögren's Syndrome</b>	
Maladaptive Autophagy in the Pathogenesis of Autoimmune Epithelitis in Sjögren's Syndrome <i>Serena Colafrancesco, Cristiana Barbat, Roberta Priori, Erisa Putro, Federico Giardina, Angelica Gattamelata, Benedetta Monosi, Tania Colasanti, Alessandra Ida Celia, Bruna Cerbelli, Carla Giordano, Susanna Scarpa, Massimo Fusconi, Giulio Cavalli, Onorina Berardicurti, Saviana Gandolfo, Saba Nayar, Francesca Barone, Roberto Giacomelli, Salvatore De Vita, Cristiano Alessandri, and Fabrizio Conti</i> . . . . .	654
<b>Vasculitis</b>	
Brief Report: VEXAS Syndrome: A Case Series From a Single-Center Cohort of Italian Patients With Vasculitis <i>Francesco Muratore, Chiara Marvisi, Paola Castrignanò, Davide Nicoli, Enrico Farnetti, Orsola Bonanno, Rosina Longo, Piera Zaldini, Elena Galli, Nicholas Balanda, David B. Beck, Peter C. Grayson, Nicolò Pipitone, Luigi Boiardi, and Carlo Salvarani</i> . . . . .	665

## Behçet's Disease

Identification of Novel Risk Loci for Behçet's Disease-Related Uveitis in a Chinese Population in a Genome-Wide Association Study

Guannan Su, Zhenyu Zhong, Qingyun Zhou, Liping Du, Zi Ye, Fuzhen Li, Wenjuan Zhuang, Chaokui Wang, Liang Liang, Yan Ji, Qingfeng Cao, Qingfeng Wang, Rui Chang, Handan Tan, Shenglan Yi, Yujing Li, Xiaojie Feng, Weiting Liao, Wanyun Zhang, Jia Shu, Shiyao Tan, Jing Xu, Su Pan, Hongxi Li, Jing Shi, Zhijun Chen, Ying Zhu, Xingsheng Ye, Xiao Tan, Jun Zhang, Zhangluxi Liu, Fanfan Huang, Gangxiang Yuan, Tingting Pang, Yizong Liu, Jiadong Ding, Yingnan Gao, Meifen Zhang, Wei Chi, Xiaoli Liu, Yuqin Wang, Ling Chen, Akira Meguro, Masaki Takeuchi, Nobuhisa Mizuki, Shigeaki Ohno, Xianbo Zuo, Aize Kijlstra, and Peizeng Yang . . . . . 671

## Gout

Association Between Gut Microbiota and Elevated Serum Urate in Two Independent Cohorts

Jie Wei, Yuqing Zhang, Nicola Dalbeth, Robert Terkeltaub, Tuo Yang, Yilun Wang, Zidan Yang, Jiatian Li, Ziyang Wu, Chao Zeng, and Guanghua Lei . . . . . 682

## Autoinflammatory Disease

Brief Report: First Description of Late-Onset Autoinflammatory Disease Due to Somatic *NLR4* Mosaicism

Daniela Ionescu, Alejandro Peñín-Franch, Anna Mensa-Vilaró, Paola Castillo, Laura Hurtado-Navarro, Cristina Molina-López, Silvia Romero-Chala, Susana Plaza, Virginia Fabregat, Segundo Buján, Joana Marques, Ferran Casals, Jordi Yagüe, Balamero Oliva, Luis Miguel Fernández-Pereira, Pablo Pelegrín, and Juan I. Aróstegui . . . . . 692

## Fibromyalgia

Dynamic Functional Brain Connectivity Underlying Temporal Summation of Pain in Fibromyalgia

Joshua C. Cheng, Alessandra Anzolin, Michael Berry, Hamed Honari, Myrella Paschali, Asimina Lazaridou, Jeungchan Lee, Dan-Mikael Ellingsen, Marco L. Loggia, Arvina Grahl, Martin A. Lindquist, Robert R. Edwards, and Vitaly Napadow . . . . . 700

## Autoimmunity

Birth Outcomes in Women Who Have Taken Hydroxychloroquine During Pregnancy: A Prospective Cohort Study

Christina D. Chambers, Diana L. Johnson, Ronghui Xu, Yunjun Luo, Robert Felix, Minh Fine, Chloe Lessard, Margaret P. Adam, Stephen R. Braddock, Luther K. Robinson, Leah Burke, Kenneth Lyons Jones, and the OTIS Collaborative Research Group . . . . . 711

## Letters

Factors Influencing Severe COVID-19 in Systemic Vasculitis Patients: Comment on the Article by Rutherford et al

Rıza Can Kardaş and Hamit Küçük . . . . . 725

Reply

Matthew A. Rutherford and Neil Basu . . . . . 725

Rapid Attenuation of Anti-SARS-CoV-2 Antibodies in Patients With Musculoskeletal Diseases in Whom Intensive Immunosuppressive Therapies Were Reinitiated After COVID-19: Comment on the Article by Curtis et al

Masashi Okamoto, Shoji Kawada, Hiroshi Shimagami, Naoko Fujii, Kazuki Matsukawa, Nachi Ishikawa, Keisuke Kawamoto, Shinji Higa, Yutaka Ishida, Atsushi Ogata, Yuta Yamaguchi, Takayoshi Morita, Yasuhiro Kato, and Atsushi Kumanogoh . . . . . 726

Risk of Nonserious Infections in Rheumatoid Arthritis: Comment on the Article by Bechman et al

Olli Ruuskanen and Matti Waris . . . . . 728

Reply

Katie Bechman and James B. Galloway . . . . . 729

Possible Confounding Factors Explaining Data on Heart Failure Risk in Patients With Polymyositis/Dermatomyositis: Comment on the Article by Lin et al

Shih-Yu Yang, Chi-Ya Yang, and James Cheng-Chung Wei . . . . . 729

Heart Failure Among Patients With Polymyositis/Dermatomyositis: Comment on the Article by Lin et al

Renin Chang, Yao-Min Hung, and James Cheng-Chung Wei . . . . . 730

Reply

Chun-Yu Lin and Chung-Yuan Hsu . . . . . 730

Are Salivary Gland Epithelial Cells the Main Source of Increased Interleukin-7 Levels in Primary Sjögren's Syndrome?

Comment on the Article by Rivière et al

Caiqun Chen, Yan Liang, and Zaixing Yang . . . . . 731

## Reply

<i>Elodie Rivière, Juliette Pascaud, Xavier Mariette, and Gaetane Nocturne</i> . . . . .	732
Additional Points to Consider Before Incorporating the Food and Drug Administration–Approved Therapies for Systemic Sclerosis–Associated Interstitial Lung Disease: Comment on the Article by Khanna et al <i>Markus Bredemeier</i> . . . . .	733

## VOLUME 74 • May 2022 • NO. 5

<b>In This Issue</b> . . . . .	A17
--------------------------------	-----

<b>Journal Club</b> . . . . .	A18
-------------------------------	-----

<b>Clinical Connections</b> . . . . .	A19
---------------------------------------	-----

**Online-Only Special Article**

American College of Rheumatology Guidance for COVID-19 Vaccination in Patients With Rheumatic and Musculoskeletal Diseases: Version 4 <i>Jeffrey R. Curtis, Sindhu R. Johnson, Donald D. Anthony, Reuben J. Arasaratnam, Lindsey R. Baden, Anne R. Bass, Cassandra Calabrese, Ellen M. Gravalles, Rafael Harpaz, Andrew Kroger, Rebecca E. Sadun, Amy S. Turner, Eleanor Anderson Williams, and Ted R. Mikuls</i> . . . . .	e21
--	-----

**Special Articles**

The 2021 European Alliance of Associations for Rheumatology/American College of Rheumatology Points to Consider for Diagnosis and Management of Autoinflammatory Type I Interferonopathies: CANDLE/PRAAS, SAVI, and AGS <i>Kader Cetin Gedik, Lovro Lamot, Micol Romano, Erkan Demirkaya, David Piskin, Sofia Torreggiani, Laura A. Adang, Thais Armangue, Kathe Barchus, Devon R. Cordova, Yanick J. Crow, Russell C. Dale, Karen L. Durrant, Despina Eleftheriou, Elisa M. Fazzi, Marco Gattorno, Francesco Gavazzi, Eric P. Hanson, Min Ae Lee-Kirsch, Gina A. Montealegre Sanchez, Bénédicte Neven, Simona Orcesi, Seza Ozen, M. Cecilia Poli, Elliot Schumacher, Davide Tonduti, Katsiaryna Uss, Daniel Aletaha, Brian M. Feldman, Adeline Vanderver, Paul A. Brogan, and Raphaela Goldbach-Mansky</i> . . . . .	735
Review: Safety and Efficacy of Mesenchymal Stromal Cells and Other Cellular Therapeutics in Rheumatic Diseases in 2022: A Review of What We Know So Far <i>Gary S. Gilkeson</i> . . . . .	752

**COVID-19**

SARS–CoV-2 Infection and COVID-19 Outcomes in Rheumatic Diseases: A Systematic Literature Review and Meta-Analysis <i>Richard Conway, Alyssa A. Grimshaw, Maximilian F. Konig, Michael Putman, Alí Duarte-García, Leslie Yingzhijie Tseng, Diego M. Cabrera, Yu Pei Eugenia Chock, Huseyin Berk Degirmenci, Eimear Duff, Bugra Han Egeli, Elizabeth R. Graef, Akash Gupta, Patricia Harkins, Bimba F. Hoyer, Arundathi Jayatilleke, Shangyi Jin, Christopher Kasia, Aneka Khilnani, Adam Kilian, Alfred H. J. Kim, Chung Mun Alice Lin, Candice Low, Laurie Proulx, Sebastian E. Sattui, Namrata Singh, Jeffrey A. Sparks, Herman Tam, Manuel F. Ugarte-Gil, Natasha Ung, Kaicheng Wang, Leanna M. Wise, Ziyi Yang, Kristen J. Young, Jean W. Liew, Rebecca Grainger, Zachary S. Wallace, and Evelyn Hsieh, on behalf of the COVID-19 Global Rheumatology Alliance</i> . . . . .	766
Brief Report: B Cell Reconstitution Is Strongly Associated With COVID-19 Vaccine Responsiveness in Rheumatic Disease Patients Who Received Treatment With Rituximab <i>Sarah Jinich, Kaitlin Schultz, Deanna Jannat-Khah, and Robert Spiera</i> . . . . .	776
Brief Report: Impact of Cytokine Inhibitor Therapy on the Prevalence, Seroconversion Rate, and Longevity of the Humoral Immune Response Against SARS–CoV-2 in an Unvaccinated Cohort <i>David Simon, Koray Tascilar, Arnd Kleyer, Filippo Fagni, Gerhard Krönke, Christine Meder, Peter Dietrich, Till Orlemann, Thorsten Kliem, Johanna Mößner, Anna-Maria Liphardt, Verena Schöna, Daniela Bohr, Louis Schuster, Fabian Hartmann, Moritz Leppkes, Andreas Ramming, Milena Pachowsky, Florian Schuch, Monika Ronneberger, Stefan Kleinert, Axel J. Hueber, Karin Manger, Bernhard Manger, Raja Atreya, Carola Berking, Michael Sticherling, Markus F. Neurath, and Georg Schett</i> . . . . .	783

**Rheumatoid Arthritis**

Association of Polygenic Risk Scores With Radiographic Progression in Patients With Rheumatoid Arthritis <i>Suguru Honda, Katsunori Ikari, Koichiro Yano, Chikashi Terao, Eiichi Tanaka, Masayoshi Harigai, and Yuta Kochi</i> . . . . .	791
Extramucosal Formation and Prognostic Value of Secretory Antibodies in Rheumatoid Arthritis <i>Klara Martinsson, Lovisa Lyttbacka Kling, Karin Roos-Ljungberg, Irina Griaeva, Marina Samoylovich, Stephane Paul, Johan Rönnelid, Tomas Weitoft, Jonas Wetterö, and Alf Kastbom</i> . . . . .	801



## Clinical Images

- Clinical Images: Giant Cell Arteritis With Positive Temporal Artery Biopsy Findings But Without Ultrasound Halo Sign  
*Takeshi Suzuki, Sumiyo Ando, Miho Ohshima, and Akitake Suzuki* ..... 809

## Osteoarthritis

- Associations of Body Mass Index With Pain and the Mediating Role of Inflammatory Biomarkers in People With Hand Osteoarthritis  
*Marthe Gløersen, Pernille Steen Pettersen, Tuhina Neogi, S. Reza Jafarzadeh, Maria Vistnes, Christian S. Thudium, Anne-Christine Bay-Jensen, Joe Sexton, Tore K. Kvien, Hilde B. Hammer, and Ida K. Haugen* ..... 810
- No Added Value of Duloxetine in Patients With Chronic Pain due to Hip or Knee Osteoarthritis: A Cluster-Randomized Trial  
*Jacoline J. van den Driest, Dieuwke Schiphof, Aafke R. Koffeman, Marc A. Koopmanschap, Patrick J. E. Bindels, and Sita M. A. Bierma-Zeinstra* ..... 818

## Systemic Lupus Erythematosus

- Urine Proteomics and Renal Single-Cell Transcriptomics Implicate Interleukin-16 in Lupus Nephritis  
*Andrea Fava, Deepak A. Rao, Chandra Mohan, Ting Zhang, Avi Rosenberg, Paride Fenaroli, H. Michael Belmont, Peter Izmirly, Robert Clancy, Jose Monroy Trujillo, Derek Fine, Arnon Arazi, Celine C. Berthier, Anne Davidson, Judith A. James, Betty Diamond, Nir Hacohen, David Wofsy, Soumya Raychaudhuri, William Apruzzese, the Accelerating Medicines Partnership in Rheumatoid Arthritis and Systemic Lupus Erythematosus Network, Jill Buyon, and Michelle Petri* ..... 829
- Identification of Shared and Asian-Specific Loci for Systemic Lupus Erythematosus and Evidence for Roles of Type III Interferon Signaling and Lysosomal Function in the Disease: A Multi-Ancestral Genome-Wide Association Study  
*Yong-Fei Wang, Wei Wei, Pattarin Tangtanatakul, Lichuan Zheng, Yao Lei, Zhiming Lin, Chengmin Qian, Xiao Qin, Fei Hou, Xinyu Zhang, Li Shao, Nusara Satproedprai, Surakameth Mahasirimongkol, Prapaporn Pisitkun, Qin Song, Yu Lung Lau, Yan Zhang, Nattiya Hirankarn, and Wanling Yang* ..... 840

## Systemic Sclerosis

- Diastolic Dysfunction in Systemic Sclerosis: Risk Factors and Impact on Mortality  
*Alicia M. Hinze, Jamie Perin, Adrienne Woods, Laura K. Hummers, Fredrick M. Wigley, Monica Mukherjee, and Ami A. Shah* ..... 849
- Therapeutic Effect of Cyclin-Dependent Kinase 4/6 Inhibitor on Dermal Fibrosis in Murine Models of Systemic Sclerosis  
*Akio Yamamoto, Tetsuya Saito, Tadashi Hosoya, Kimito Kawahata, Yoshihide Asano, Shinichi Sato, Fumitaka Mizoguchi, Shinsuke Yasuda, and Hitoshi Kohsaka* ..... 860
- Impaired Mitochondrial Transcription Factor A Expression Promotes Mitochondrial Damage to Drive Fibroblast Activation and Fibrosis in Systemic Sclerosis  
*Xiang Zhou, Thuong Trinh-Minh, Cuong Tran-Manh, Andreas Gießl, Christina Bergmann, Andrea-Hermina Györfi, Georg Schett, and Jörg H. W. Distler* ..... 871

## Dermatomyositis

- Identification of Similarities Between Skin Lesions in Patients With Antisynthetase Syndrome and Skin Lesions in Patients With Dermatomyositis by Highly Multiplexed Imaging Mass Cytometry  
*Jay Patel, Adarsh Ravishankar, Spandana Maddukuri, Thomas Vazquez, Madison Grinnell, and Victoria P. Werth* ..... 882

## IgG4-Related Disease

- CD163+ M2 Macrophages Promote Fibrosis in IgG4-Related Disease Via Toll-like Receptor 7/Interleukin-1 Receptor-Associated Kinase 4/NF- $\kappa$ B Signaling  
*Akira Chinju, Masafumi Moriyama, Noriko Kakizoe-Ishiguro, Hu Chen, Yuka Miyahara, A. S. M. Rafiul Haque, Katsuhiro Furusho, Mizuki Sakamoto, Kazuki Kai, Kotono Kibe, Sachiko Hatakeyama-Furukawa, Miho Ito-Ohta, Takashi Maehara, and Seiji Nakamura* ..... 892

## Antiphospholipid Syndrome

- Brief Report: Defibrotide Inhibits Antiphospholipid Antibody-Mediated Neutrophil Extracellular Trap Formation and Venous Thrombosis  
*Ramadan A. Ali, Shanea K. Estes, Alex A. Gandhi, Srilakshmi Yalavarthi, Claire K. Hoy, Hui Shi, Yu Zuo, Doruk Erkan, and Jason S. Knight* ..... 902

## Letters

- Low Levels of Anti-SARS-CoV-2 Antibodies After Vaccination in Rituximab-Treated Patients: Comment on the Article by Simon et al  
*Gerasimos Evangelatos, Konstantina Kouna, George E. Fragoulis, Melina Moschopoulou, Maria Triantafylli, Antigoni Lekka, and Alexios Iliopoulos* ..... 908

Reply	
<i>David Simon, Filippo Fagni, Koray Tascilar, and Georg Schett</i> . . . . .	909
Extensive Bone Marrow Capillary Network Masquerading as Fungal Hyphae in a Patient With Systemic Lupus Erythematosus	
<i>Dominic Seet, Shir Ying Lee, Melissa Ooi, Ju Ee Seet, Jiakai Cho, and Anselm Mak</i> . . . . .	910
Conflicting Reports of Anti-Cytosolic 5'-Nucleotidase 1A Autoantibodies in Juvenile Dermatomyositis: Comment on the Article by Rietveld et al	
<i>Andrew L. Mammen, Iago Pinal-Fernandez, and Lisa G. Rider</i> . . . . .	911
The Importance of Rigorous Methods in Observational Comparative Effectiveness Studies of Rare Diseases: Comment on the Article by Ruperto et al	
<i>Yukiko Kimura, Mei-Sing Ong, George Tomlinson, Sarah Ringold, Laura E. Schanberg, Brian M. Feldman, Anne Dennos, Vincent Del Gaizo, Katherine L. Murphy, and Marc Natter</i> . . . . .	912
Reply	
<i>Nicolino Ruperto, Alberto Martini, and Angela Pistorio, for the Paediatric Rheumatology International Trials Organisation</i> . .	913

## VOLUME 74 • June 2022 • NO. 6

<b>In This Issue</b> . . . . .	A13
<b>Journal Club</b> . . . . .	A14
<b>Clinical Connections</b> . . . . .	A15
<b>Special Articles</b>	
Expert Perspective: An Approach to Refractory Lupus Nephritis	
<i>Swati Arora and Brad H. Rovin</i> . . . . .	915
<b>COVID-19</b>	
Rituximab Impairs B Cell Response But Not T Cell Response to COVID-19 Vaccine in Autoimmune Diseases	
<i>Samuel Bitoun, Julien Henry, Delphine Desjardins, Christelle Vauloup-Fellous, Nicolas Dib, Rakiba Belkhir, Lina Mouna, Candie Joly, Marie Bitu, Bineta Ly, Juliette Pascaud, Raphaële Seror, Anne-Marie Roque Afonso, Roger Le Grand, and Xavier Mariette</i> . . . . .	927
B Cell Numbers Predict Humoral and Cellular Response Upon SARS-CoV-2 Vaccination Among Patients Treated With Rituximab	
<i>Ana-Luisa Stefanski, Hector Rincon-Arevalo, Eva Schrezenmeier, Kirsten Karberg, Franziska Szelinski, Jacob Ritter, Bernd Jahrsdörfer, Hubert Schrezenmeier, Carolin Ludwig, Arne Sattler, Katja Kotsch, Yidan Chen, Anne Claußnitzer, Hildrun Haibel, Fabian Proft, Gabriela Guerra, Pawel Durek, Frederik Heinrich, Marta Ferreira-Gomes, Gerd R. Burmester, Andreas Radbruch, Mir-Farzin Mashreghi, Andreia C. Lino, and Thomas Dörner</i> . . . . .	934
<b>Rheumatoid Arthritis</b>	
Role of Lysine-Specific Demethylase 1 in Metabolically Integrating Osteoclast Differentiation and Inflammatory Bone Resorption Through Hypoxia-Inducible Factor 1 $\alpha$ and E2F1	
<i>Kohei Doi, Koichi Murata, Shuji Ito, Akari Suzuki, Chikashi Terao, Shinichiro Ishie, Akio Umemoto, Yoshiki Murotani, Kohei Nishitani, Hiroyuki Yoshitomi, Takayuki Fujii, Ryu Watanabe, Motomu Hashimoto, Kosaku Murakami, Masao Tanaka, Hiromu Ito, Kyung-Hyun Park-Min, Lionel B. Ivashkiv, Akio Morinobu, and Shuichi Matsuda</i> . . . . .	948
Antibodies to Cartilage Oligomeric Matrix Protein Are Pathogenic in Mice and May Be Clinically Relevant in Rheumatoid Arthritis	
<i>Changrong Ge, Dongmei Tong, Erik Lönnblom, Bibo Liang, Weiwei Cai, Cecilia Fahlquist-Hagert, Taotao Li, Alf Kastbom, Inger Gjertsson, Doreen Dobritzsch, and Rikard Holmdahl</i> . . . . .	961
Central Role of Semaphorin 3B in a Serum-Induced Arthritis Model and Reduced Levels in Patients With Rheumatoid Arthritis	
<i>Ana Igea, Tiago Carvalheiro, Beatriz Malvar-Fernández, Sara Martinez-Ramos, Carlos Rafael-Vidal, Ellis Niemantsverdriet, Jezabel Varadé, Andrea Fernández-Carrera, Norman Jimenez, Trudy McGarry, Angela Rodriguez-Trillo, Douglas Veale, Ursula Fearon, Carmen Conde, Jose M. Pego-Reigosa, África González-Fernández, Kris A. Reedquist, Timothy R. D. J. Radstake, Annette van der Helm-Van Mil, and Samuel García</i> . . . . .	972
Rheumatoid Factor and Anti-Modified Protein Antibody Reactivities Converge on IgG Epitopes	
<i>Aisha M. Mergaert, Zihao Zheng, Michael F. Denny, Maya F. Amjadi, S. Janna Bashar, Michael A. Newton, Vivianne Malmström, Caroline Grönwall, Sara S. McCoy, and Miriam A. Shelef</i> . . . . .	984

## Osteoarthritis

Prevalence, Incidence, and Progression of Radiographic and Symptomatic Hand Osteoarthritis: The Osteoarthritis Initiative

*Charles B. Eaton, Lena F. Schaefer, Jeff Duryea, Jeff B. Driban, Grace H. Lo, Mary B. Roberts, Ida K. Haugen, Bing Lu, Michael C. Nevitt, Marc C. Hochberg, Rebecca D. Jackson, C. K. Kwok, and Timothy McAlindon* . . . . . 992

## Antiphospholipid Syndrome

Antiphospholipid Antibodies Increase Endometrial Stromal Cell Decidualization, Senescence, and Inflammation via Toll-like Receptor 4, Reactive Oxygen Species, and p38 MAPK Signaling

*Mancy Tong, Teimur Kayani, Deidre M. Jones, Jane E. Salmon, Shannon Whirledge, Lawrence W. Chamley, and Vikki M. Abrahams* . . . . . 1001

## Systemic Sclerosis

Interleukin-1 $\beta$ -Activated Microvascular Endothelial Cells Promote DC-SIGN-Positive Alternatively Activated Macrophages as a Mechanism of Skin Fibrosis in Systemic Sclerosis

*Paoline Laurent, Joelle Lapoirie, Damien Leleu, Emeline Levionnois, Cyrielle Grenier, Blanca Jurado-Mestre, Estibaliz Lazaro, Pierre Duffau, Christophe Richez, Julien Seneschal, Jean-Luc Pellegrin, Joel Constans, Thierry Schaefferbeke, Isabelle Douchet, Dorothée Duluc, Thomas Pradeu, Carlo Chizzolini, Patrick Blanco, Marie-Elise Truchetet, and Cécile Contin-Bordes, on behalf of the Fédération Hospitalo-Universitaire ACRONIM and the Centre National de Référence des Maladies Auto-Immunes Systémiques Rares de l'Est et du Sud-Ouest (RESO)* . . . . . 1013

Involvement of Multiple Variants of Soluble CD146 in Systemic Sclerosis: Identification of a Novel Profibrotic Factor

*Marie Nollet, Richard Bachelier, Ahmad Joshkon, Wael Traboulsi, Amandine Mahieux, Anais Moyon, Alexandre Muller, Indumathi Somasundaram, Stéphanie Simoncini, Franck Peiretti, Aurélie S. Leroyer, Benjamin Guillet, Brigitte Granel, Françoise Dignat-George, Nathalie Bardin, Alexandrine Foucault-Bertaud, and Marcel Blot-Chabaud* . . . . . 1027

Nintedanib in Patients With Autoimmune Disease-Related Progressive Fibrosing Interstitial Lung Diseases: Subgroup Analysis of the INBUILD Trial

*Eric L. Matteson, Clive Kelly, Jörg H. W. Distler, Anna-Maria Hoffmann-Vold, James R. Seibold, Shikha Mittoo, Paul F. Dellaripa, Martin Aringer, Janet Pope, Oliver Distler, Alexandra James, Rozsa Schlenker-Herceg, Susanne Stowasser, Manuel Quaresma, and Kevin R. Flaherty, on behalf of the INBUILD Trial Investigators.* . . . . 1039

## Myositis

Contribution of Necroptosis to Myofiber Death in Idiopathic Inflammatory Myopathies

*Qing-Lin Peng, Ya-Mei Zhang, Yan-Chun Liu, Lin Liang, Wen-Li Li, Xiao-Lan Tian, Lu Zhang, Hong-Xia Yang, Xin Lu, and Guo-Chun Wang* . . . . . 1048

## Gout

Intensive Serum Urate Lowering With Oral Urate-Lowering Therapy for Erosive Gout: A Randomized Double-Blind Controlled Trial

*Nicola Dalbeth, Anthony J. Doyle, Karen Billington, Greg D. Gamble, Paul Tan, Kieran Latta, Thrishila Parshu Ram, Ravi Narang, Rachel Murdoch, David Bursill, Borislav Mihov, Lisa K. Stamp, and Anne Horne* . . . . . 1059

## Clinical Images

Clinical Images: Detection of Titanium Dioxide Particles by Raman Spectroscopy in Synovial Fluid from a Swollen Ankle

*Tom Niessink, Jasper Ringoot, Cees Otto, Matthijs Janssen, and Tim L. Jansen* . . . . . 1069

## IgG4-Related Disease

Contribution of Interleukin-4-Induced Epithelial Cell Senescence to Glandular Fibrosis in IgG4-Related Sialadenitis

*Sai-Nan Min, Meng-Qi Zhu, Xiang-Di Mao, Wei Li, Tai Wei, Mei Mei, Yan Zhang, Li-Ling Wu, Guang-Yan Yu, and Xin Cong* . . . . . 1070

## Autoinflammatory Disease

Brief Report: Haploinsufficiency of PSMD12 Causes Proteasome Dysfunction and Subclinical Autoinflammation

*Kai Yan, Jiahui Zhang, Pui Y. Lee, Panfeng Tao, Jun Wang, Shihao Wang, Qing Zhou, and Minyue Dong* . . . . . 1083

## Letters

COVID-19 Vaccine Uptake and Vaccine Hesitancy in Rheumatic Disease Patients Receiving Immunomodulatory Therapies in Community Practice Settings

*Stephanie S. Ledbetter, Fenglong Xie, Gary Cutter, Kenneth G. Saag, Lesley Jackson, Maria I. Danila, Patrick Stewart, Michael George, William Benjamin Nowell, Ted Mikuls, Kevin Winthrop, and Jeffrey R. Curtis* . . . . . 1091

A Clinician's Perspective on Why the Trial Did Not Work: Comment on the Editorial by Merrill <i>Michael R. Bubb</i> .....	1092
Reply <i>Joan T. Merrill</i> .....	1093
Absent in Melanoma 2 Protein in Systemic Lupus Erythematosus: Friend or Foe? Comment on the Article by Lu et al <i>Wang-Dong Xu and An-Fang Huang</i> .....	1093
Reply <i>Ailing Lu and Guangxun Meng</i> .....	1094
Airway Obstruction as a Pulmonary Manifestation of Rheumatoid Arthritis: Comment on the Article by Prisco et al <i>Sheng-Yuan Wang, Chih-Wei Chen, and James Cheng-Chung Wei</i> .....	1095
Reply <i>Lauren Prisco, Matthew Moll, Tracey J. Doyle, Michael H. Cho, and Jeffrey A. Sparks</i> .....	1096

## VOLUME 74 • July 2022 • NO. 7

<b>In This Issue</b> .....	A19
<b>Journal Club</b> .....	A20
<b>Clinical Connections</b> .....	A21

### Editorial

Arthritis & Rheumatology: "Mid-Term" Report <i>Daniel H. Solomon, Richard Bucala, Mariana J. Kaplan, and Peter A. Nigrovic</i> .....	1099
---	------

### Special

The 2021 EULAR/American College of Rheumatology Points to Consider for Diagnosis, Management and Monitoring of the Interleukin-1 Mediated Autoinflammatory Diseases: Cryopyrin-Associated Periodic Syndromes, Tumour Necrosis Factor Receptor-Associated Periodic Syndrome, Mevalonate Kinase Deficiency, and Deficiency of the Interleukin-1 Receptor Antagonist <i>Micol Romano, Z. Serap Arici, David Piskin, Sara Alehashemi, Daniel Aletaha, Karyl Barron, Susanne Benseler, Roberta A. Berard, Lori Broderick, Fatma Dedeoglu, Michelle Diebold, Karen Durrant, Polly Ferguson, Dirk Foell, Jonathan S. Hausmann, Olcay Y. Jones, Daniel Kastner, Helen J. Lachmann, Ronald M. Laxer, Dorelia Rivera, Nicola Ruperto, Anna Simon, Marinka Twilt, Joost Frenkel, Hal M. Hoffman, Adriana A. de Jesus, Jasmin B. Kuemmerle-Deschner, Seza Ozen, Marco Gattorno, Raphaela Goldbach-Mansky, and Erkan Demirkaya</i> .....	1102
--	------

### Review

The Conundrum of Lung Disease and Drug Hypersensitivity-like Reactions in Systemic Juvenile Idiopathic Arthritis <i>Bryce A. Binstadt and Peter A. Nigrovic</i> .....	1122
--	------

### COVID-19

Endothelial Cell-Activating Antibodies in COVID-19 <i>Hui Shi, Yu Zuo, Sherwin Navaz, Alyssa Harbaugh, Claire K. Hoy, Alex A. Gandhi, Gautam Sule, Srilakshmi Yalavarthi, Kelsey Gockman, Jacqueline A. Madison, Jintao Wang, Melanie Zuo, Yue Shi, Michael D. Maile, Jason S. Knight, and Yogendra Kanthi</i> .....	1132
---	------

### Clinical Images

Clinical Images: Motor Deficiency and Radicular Pain Secondary to Sarcoidosis <i>Coralie Humann, Caroline Raymond, Daniel Wendling, and Frank Verhoeven</i> .....	1138
--	------

### Rheumatoid Arthritis

Brief Report: The Prominent Role of Hematopoietic Peptidyl Arginine Deiminase 4 in Arthritis: Collagen- and Granulocyte Colony-Stimulating Factor-Induced Arthritis Model in C57BL/6 Mice <i>Shoichi Fukui, Sarah Gutch, Saeko Fukui, Deya Cherpokova, Karen Aymonnier, Casey E. Sheehy, Long Chu, and Denisa D. Wagner</i> .....	1139
IgG Anti-Citrullinated Protein Antibody Variable Domain Glycosylation Increases Before the Onset of Rheumatoid Arthritis and Stabilizes Thereafter: A Cross-Sectional Study Encompassing ~1,500 Samples <i>Theresa Kissel, Lise Hafkenscheid, Tineke J. Wesemael, Mami Tamai, Shin-ya Kawashiri, Atsushi Kawakami, Hani S. El-Gabalawy, Dirkjan van Schaardenburg, Solbritt Rantapää-Dahlqvist, Manfred Wuhrer, Annette H. M. van der Helm-van Mil, Cornelia F. Allaart, Diane van der Woude, Hans U. Scherer, Rene E. M. Toes, and Tom W. J. Huizinga</i> .....	1147

Epigenetic Regulation of Nutrient Transporters in Rheumatoid Arthritis Fibroblast-like Synoviocytes <i>Alyssa Torres, Brian Pedersen, Isidoro Cobo, Rizi Ai, Roxana Coras, Jessica Murillo-Saich, Gyrid Nygaard, Elsa Sanchez-Lopez, Anne Murphy, Wei Wang, Gary S. Firestein, and Monica Guma</i> . . . . .	1159
<b>Osteoarthritis</b>	
Prevalence Trends of Site-Specific Osteoarthritis From 1990 to 2019: Findings From the Global Burden of Disease Study 2019 <i>Huibin Long, Qiang Liu, Heyong Yin, Kai Wang, Naicheng Diao, Yuqing Zhang, Jianhao Lin, and Ai Guo</i> . . . . .	1172
<b>Clinical Images</b>	
Clinical Images: Voriconazole-Induced Synovitis, Enthesitis, and Periostitis <i>Larissa Valor-Méndez, Jochen Wacker, Georg Schett, Bernhard Manger, Julia Fürst, Richard Strauß, and Arnd Kleyer</i> . . . . .	1183
<b>Psoriatic Arthritis</b>	
Association of Cardiac Biomarkers With Cardiovascular Outcomes in Patients With Psoriatic Arthritis and Psoriasis: A Longitudinal Cohort Study <i>Keith Colaco, Ker-Ai Lee, Shadi Akhtari, Raz Winer, Paul Welsh, Naveed Sattar, Iain B. McInnes, Vinod Chandran, Paula Harvey, Richard J. Cook, Dafna D. Gladman, Vincent Piguët, and Lihi Eder</i> . . . . .	1184
<b>Systemic Lupus Erythematosus</b>	
Identification of Mitofusin 1 and Complement Component 1q Subcomponent Binding Protein as Mitochondrial Targets in Systemic Lupus Erythematosus <i>Yann L. C. Becker, Jean-Philippe Gagné, Anne-Sophie Julien, Tania Lévesque, Isabelle Allaeys, Nadine Gougéard, Vicente Rubio, François-Michel Boisvert, Dominique Jean, Eric Wagner, Guy G. Poirier, Paul R. Fortin, and Éric Boilard</i> . . . . .	1193
Brief Report: Role of Glutaminase 2 in Promoting CD4+ T Cell Production of Interleukin-2 by Supporting Antioxidant Defense in Systemic Lupus Erythematosus <i>Ryo Hisada, Nobuya Yoshida, Seo Yeon K. Orite, Masataka Umeda, Catalina Burbano, Marc Scherlinger, Michihito Kono, Suzanne Krishfield, and George C. Tsokos</i> . . . . .	1204
B Cell-Specific Deletion of CR6-Interacting Factor 1 Drives Lupus-like Autoimmunity by Activation of Interleukin-17, Interleukin-6, and Pathogenic Follicular Helper T Cells in a Mouse Model <i>Jin-Sil Park, SeungCheon Yang, Sun-Hee Hwang, JeongWon Choi, Seung-Ki Kwok, Young-Yun Kong, Jeehee Youn, Mi-La Cho, and Sung-Hwan Park</i> . . . . .	1211
Aptamer-Based Screen of Neuropsychiatric Lupus Cerebrospinal Fluid Reveals Potential Biomarkers That Overlap With the Choroid Plexus Transcriptome <i>Kamala Vanarsa, Prashanth Sasidharan, Valeria Duran, Sirisha Gokaraju, Malavika Nidhi, Anto Sam Crosslee Louis Sam Titus, Sanam Soomro, Ariel D. Stock, Evan Der, Chaim Putterman, Benjamin Greenberg, Chi Chiu Mok, John G. Hanly, and Chandra Mohan</i> . . . . .	1223
<b>Vasculitis</b>	
Critical Role of Notch-1 in Mechanistic Target of Rapamycin Hyperactivity and Vascular Inflammation in Patients With Takayasu Arteritis <i>Wanwan Jiang, Mengyao Sun, Ying Wang, Ming Zheng, Zixin Yuan, Shixiong Mai, Xin Zhang, Longhai Tang, Xiyu Liu, Chunhong Wang, and Zhenke Wen</i> . . . . .	1235
<b>Systemic Sclerosis</b>	
Self-Assembled Human Skin Equivalents Model Macrophage Activation of Cutaneous Fibrogenesis in Systemic Sclerosis <i>Mengqi Huang, Avi Smith, Matthew Watson, Rajan Bhandari, Lauren M. Baugh, Irena Ivanovska, Trishawna Watkins, Irene Lang, Maria Trojanowska, Lauren D. Black III, Patricia A. Pioli, Jonathan Garlick, and Michael L. Whitfield</i> . . . . .	1245
<b>Pediatric Rheumatology</b>	
Role for Granulocyte Colony-Stimulating Factor in Neutrophilic Extramedullary Myelopoiesis in a Murine Model of Systemic Juvenile Idiopathic Arthritis <i>Bert Malengier-Devlies, Eline Bernaerts, Kourosh Ahmadzadeh, Jessica Filtjens, Jessica Vandenhaute, Bram Boeckx, Oliver Burton, Amber De Visscher, Tania Mitera, Nele Berghmans, Geert Verbeke, Adrian Liston, Diether Lambrechts, Paul Proost, Carine Wouters, and Patrick Matthys</i> . . . . .	1257
Identification of Distinct Inflammatory Programs and Biomarkers in Systemic Juvenile Idiopathic Arthritis and Related Lung Disease by Serum Proteome Analysis <i>Guangbo Chen, Gail H. Deutsch, Grant S. Schulert, Hong Zheng, SoRi Jang, Bruce Trapnell, Pui Y. Lee, Claudia Macaubas, Katherine Ho, Corinne Schneider, Vivian E. Saper, Adriana Almeida de Jesus, Mark A. Krasnow, Alexei Grom, Raphaela Goldbach-Mansky, Purvesh Khatri, Elizabeth D. Mellins, and Scott W. Canna</i> . . . . .	1271



Brain Structural Changes During Juvenile Fibromyalgia: Relationships With Pain, Fatigue, and Functional Disability <i>Maria Suñol, Michael F. Payne, Han Tong, Thomas C. Maloney, Tracy V. Ting, Susmita Kashikar-Zuck, Robert C. Coghill, and Marina López-Solà</i> .....	1284
<b>Letters</b>	
Vascular Deposition of Monosodium Urate Crystals in Gout: Analysis of Cadaveric Tissue by Dual-Energy Computed tomography and Compensated Polarizing Light Microscopy <i>Nicola Dalbeth, Mariam Alhilali, Peter Riordan, Ravi Narang, Ashika Chhana, Sue McGlashan, Anthony Doyle, and Mariano Andres</i> .....	1295
Sequencing of the 16S Ribosomal DNA Gene and Virulence of the Oral Microbiome in Patients With Rheumatoid Arthritis: Comment on the Article by Kroese et al <i>Yu-Ze Luan, Brian Shiian Chen, and Kevin Sheng-Kai Ma</i> .....	1296
Reply <i>Johanna M. Kroese, Bernd W. Brandt, Mark J. Buijs, Wim Crielaard, Frank Lobbezoo, Bruno G. Loos, Egija Zaura, Laurette van Boheemen, Dirkjan van Schaardenburg, and Catherine M. C. Volgenant</i> .....	1297
Increased Cadmium Inhalation as a Possible Explanation for an Increased Risk of Rheumatoid Arthritis Development: Comment on the Article by Okamoto et al <i>David G. Hutchinson</i> .....	1299
Reply <i>Yuko Okamoto and M. Kristen Demoruelle</i> .....	1299
Suggested Additions to Future Directions: Comment on the ACR White Paper on Antimalarials and Cardiac Toxicity by Desmarais et al <i>Daniel J. Wallace</i> .....	1300
Reply <i>Julianna Desmarais, Nicole Fett, James T. Rosenbaum, Karen H. Costenbader, Ellen M. Ginzler, Susan Goodman, James O'Dell, Christian A. Pineau, Gabriela Schmajuk, Victoria P. Werth, Mark S. Link, and Richard Kovacs</i> .....	1301
Successful Use of Cyclosporin A and Interleukin-1 Blocker Combination Therapy in VEXAS Syndrome: A Single-Center Case Series <i>Corrado Campochiaro, Alessandro Tomelleri, Giulio Cavalli, Giacomo De Luca, Greta Grassini, Maria G. Cangì, and Lorenzo Dagna</i> .....	1302

## VOLUME 74 • August 2022 • NO. 8

<b>In This Issue</b> .....	A11
<b>Journal Club</b> .....	A12
<b>Clinical Connections</b> .....	A13
<b>Special Articles</b>	
Expert Perspectives on Clinical Challenges: Expert Perspective: Management of Antineutrophil Cytoplasmic Antibody–Associated Vasculitis <i>Naomi J. Patel and John H. Stone</i> .....	1305
Editorial: Complement C4, the Major Histocompatibility Complex, and Autoimmunity <i>Timothy J. Vyse and Betty P. Tsao</i> .....	1318
<b>COVID-19</b>	
Immunogenicity and Safety of Standard and Third-Dose SARS–CoV-2 Vaccination in Patients Receiving Immunosuppressive Therapy <i>Silje W. Syversen, Ingrid Jysum, Anne T. Tveter, Trung T. Tran, Joseph Sexton, Sella A. Provan, Siri Mjaaland, David J. Warren, Tore K. Kvien, Gunnveig Grødeland, Lise S. H. Nissen-Meyer, Petr Ríčanek, Adity Chopra, Ane M. Andersson, Grete B. Kro, Jørgen Jahnsen, Ludvig A. Munthe, Espen A. Haavardsholm, John T. Vaage, Fridtjof Lund-Johansen, Kristin K. Jørgensen, and Guro L. Goll</i> .....	1321
<b>Clinical Images</b>	
Clinical Images: Hydroxyurea-Induced Dermatomyositis-Like Rash <i>Sweta Subhadarshani, Susie Min, Kathryn Holloway, and Matthew Steadmon</i> .....	1332

## Osteoarthritis

Five-Year Structural Changes in the Knee Among Patients With Meniscal Tear and Osteoarthritis:

Data From a Randomized Controlled Trial of Arthroscopic Partial Meniscectomy Versus Physical Therapy

*Jamie E. Collins, Swastina Shrestha, Elena Losina, Robert G. Marx, Ali Guermazi, Mohamed Jarraya, Morgan H. Jones, Bruce A. Levy, Lisa A. Mandl, Emma E. Williams, Rick W. Wright, Kurt P. Spindler, and Jeffrey N. Katz, on behalf of the METEOR Investigator Group* ..... 1333

Do Glucocorticoid Injections Increase the Risk of Knee Osteoarthritis Progression Over 5 Years?

*Augustin Latourte, Anne-Christine Rat, Abdou Omorou, Willy Ngueyon-Sime, Florent Eymard, Jérémie Sellam, Christian Roux, Hang-Korng Ea, Martine Cohen-Solal, Thomas Bardin, Johann Beaudreuil, Francis Guillemin, and Pascal Richette* ..... 1343

## Clinical Images

Clinical Images: Intraosseous Calcification Migration: Journey to the Center of the Bone

*Clément Cholet, Justine Mugnier, Anne Miquel, Juliette Petit, Jérémie Sellam, and Lionel Arrivé* ..... 1351

## Spondyloarthritis

Vertebral Bone Mineral Density, Vertebral Strength, and Syndesmophyte Growth in Ankylosing Spondylitis:

The Importance of Bridging

*Sovira Tan, Hadi Bagheri, David Lee, Ahmad Shafiei, Tony M. Keaveny, Lawrence Yao, and Michael M. Ward* ..... 1352

## Erratum

Addition of Corresponding Author's Email Address to the Letter by Wang et al (Arthritis Rheumatol, June 2022) ..... 1362

## Systemic Lupus Erythematosus

Small Molecule Inhibitors of Nuclear Export and the Amelioration of Lupus by Modulation of Plasma Cell

Generation and Survival

*Javier Rangel-Moreno, Maria de la Luz Garcia-Hernandez, Teresa Owen, Jennifer Barnard, Enrique Becerril-Villanueva, Trinayan Kashyap, Christian Argueta, Armando Gamboa-Dominguez, Sharon Tamir, Yosef Landesman, Bruce I. Goldman, Christopher T. Ritchlin, and Jennifer H. Anolik* ..... 1363

## Vasculitis

Global Transcriptomic Profiling Identifies Differential Gene Expression Signatures Between Inflammatory and

Noninflammatory Aortic Aneurysms

*Benjamin Hur, Matthew J. Koster, Jin Sung Jang, Cornelia M. Weyand, Kenneth J. Warrington, and Jaeyun Sung* ..... 1376

## Systemic Sclerosis

Driving Role of Interleukin-2-Related Regulatory CD4<sup>+</sup> T Cell Deficiency in the Development of Lung Fibrosis and Vascular Remodeling in a Mouse Model of Systemic Sclerosis

*Camelia Frantz, Anne Cauvet, Aurélie Durand, Virginie Gonzalez, Rémi Pierre, Marcio Do Cruzeiro, Karine Bailly, Muriel Andrieu, Cindy Orvain, Jérôme Avouac, Mina Ottaviani, Raphaël Thuillet, Ly Tu, Christophe Guignabert, Bruno Lucas, Cédric Auffray, and Yannick Allanore* ..... 1387

Adipose-Derived Regenerative Cell Transplantation for the Treatment of Hand Dysfunction in Systemic Sclerosis:

A Randomized Clinical Trial

*Dinesh Khanna, Paul Caldron, Richard W. Martin, Suzanne Kafaja, Robert Spiera, Shadi Shahouri, Ankoor Shah, Vivien Hsu, John Ervin, Robert Simms, Robyn T. Domsic, Virginia Steen, Laura K. Hummers, Chris Derk, Maureen Mayes, Soumya Chatterjee, John Varga, Steven Kesten, John K. Fraser, and Daniel E. Furst* ..... 1399

## Pediatric Rheumatology

A Comparison of International League of Associations for Rheumatology and Pediatric Rheumatology International Trials Organization Classification Systems for Juvenile Idiopathic Arthritis Among Children in a Canadian

Arthritis Cohort

*Jennifer J. Y. Lee, Simon W. M. Eng, Jaime Guzman, Ciáran M. Duffy, Lori B. Tucker, Kiem Oen, Rae S. M. Yeung, and Brian M. Feldman, on behalf of the ReACCh-Out Investigators* ..... 1409

Identification of Novel Loci Shared by Juvenile Idiopathic Arthritis Subtypes Through Integrative Genetic Analysis

*Jin Li, Yun R. Li, Joseph T. Glessner, Jie Yang, Michael E. March, Charly Kao, Courtney N. Vaccaro, Jonathan P. Bradfield, Junyi Li, Frank D. Mentch, Hui-Qi Qu, Xiaohui Qi, Xiao Chang, Cuiping Hou, Debra J. Abrams, Haijun Qiu, Zhi Wei, John J. Connolly, Fengxiang Wang, James Snyder, Berit Flatø, Susan D. Thompson, Carl D. Langefeld, Benedicte A. Lie, Jane E. Munro, Carol Wise, Patrick M. A. Sleiman, and Hakon Hakonarson* ..... 1420

Racial Disparities in Renal Outcomes Over Time Among Hospitalized Children With Systemic Lupus Erythematosus

*Joyce C. Chang, Cora Sears, Veronica Torres, and Mary Beth F. Son* ..... 1430

## Autoimmune Disease

Complement C4 Copy Number Variation is Linked to SSA/Ro and SSB/La Autoantibodies in Systemic Inflammatory Autoimmune Diseases

*Christian Lundtoft, Pascal Pucholt, Myriam Martin, Matteo Bianchi, Emeli Lundström, Maija-Leena Eloranta, Johanna K. Sandling, Christopher Sjöwall, Andreas Jönsen, Iva Gunnarsson, Solbritt Rantapää-Dahlqvist, Anders A. Bengtsson, Dag Leonard, Eva Baecklund, Roland Jonsson, Daniel Hammenfors, Helena Forsblad-d'Elia, Per Eriksson, Thomas Mandl, Sara Magnusson Bucher, Katrine B. Norheim, Svein Joar Auglænd Johnsen, Roald Omdal, Marika Kvarnström, Marie Wahren-Herlenius, Antonella Notarnicola, Helena Andersson, Øyvind Molberg, Louise Pyndt Diederichsen, Jonas Almlöf, Ann-Christine Syvänen, Sergey V. Kozyrev, Kerstin Lindblad-Toh, the DISSECT Consortium, the ImmunoArray Development Consortium, Bo Nilsson, Anna M. Blom, Ingrid E. Lundberg, Gunnel Nordmark, Lina Marcela Diaz-Gallo, Elisabet Svenungsson, and Lars Rönnblom* ..... 1440

## Letters

On the Perils of Peeking Into the Future: Comment on the Article by Rosenthal et al

*Melek Yalcin Mutlu and Koray Tascilar* ..... 1451

Reply

*Yael Shalev Rosenthal, Naama Schwartz, Iftach Sagy, and Lev Pavlovsky* ..... 1451

No Evidence of Leptin Mediating the Effect of Body Mass Index on Hand Pain and Its Duration in the Chingford

1000 Women Study: Original Research Supplementing the Study by Gløersen et al

*Romain S. Perera, Malvika Gulati, Karishma Shah, Deborah J. Hart, Tim D. Spector, Nigel K. Arden, and Maja R. Radojčić* . . 1452

Reply

*Marthe Gløersen, Tuhina Neogi, S. Reza Jafarzadeh, Joe Sexton, and Ida K. Haugen* ..... 1454

Very Limited Data in the Global Burden of Disease Study 2019 to Estimate the Prevalence of Osteoarthritis in

204 Countries Over 30 years: Comment on the Article by Long et al

*Qiuzhe Chen, Christopher G. Maher, and Gustavo C. Machado* ..... 1455

Reply

*Huibin Long, Ai Guo, Yuqing Zhang, Qiang Liu, and Jianhao Lin* ..... 1456

Report of the American College of Rheumatology Fellows-in-Training Subcommittee: Experiences of Rheumatology

Fellows Early in the COVID-19 Pandemic

*ACR Fellows-in-Training Subcommittee, Didem Saygin, Jean Lin, Noelle A. Rolle, and Mary Mamut* ..... 1457

## VOLUME 74 • September 2022 • NO. 9

**In This Issue** ..... A13

**Journal Club** ..... A14

**Clinical Connections** ..... A15

## Special Articles

Notes from the Field: Recognizing Racial Bias and Promoting Diversity in the Rheumatology Workforce

*Siobhan M. Case, Gail S. Kerr, Mia Chandler, Valerie E. Stone, Irene Blanco, and Candace H. Feldman* ..... 1459

2022 American College of Rheumatology/American Association of Hip and Knee Surgeons Guideline for the Perioperative Management of Antirheumatic Medication in Patients With Rheumatic Diseases Undergoing Elective Total Hip or Total Knee Arthroplasty

*Susan M. Goodman, Bryan D. Springer, Antonia F. Chen, Marshall Davis, David R. Fernandez, Mark Figgie, Heather Finlayson, Michael D. George, Jon T. Giles, Jeremy Gililland, Brian Klatt, Ronald MacKenzie, Kaleb Michaud, Andy Miller, Linda Russell, Alexander Sah, Matthew P. Abdel, Beverly Johnson, Lisa A. Mandl, Peter Sculco, Marat Turgunbaev, Amy S. Turner, Adolph Yates Jr., and Jasvinder A. Singh* ..... 1464

Editorial: Sacroiliac Bone Marrow Edema: Innocent Until Proven Guilty?

*Michael M. Ward and Lawrence Yao* ..... 1474

Editorial: Toward Precision Medicine—Is Genetic Risk Prediction Ready for Prime Time in Osteoarthritis?

*Michelle S. Yau and John Loughlin* ..... 1477

## Osteoarthritis

Genomic Risk Score for Advanced Osteoarthritis in Older Adults

*Paul Lacaze, Yuanyuan Wang, Galina Polekhina, Andrew Bakshi, Moeen Riaz, Alice Owen, Angus Franks, Jawad Abidi, Jane Tiller, John McNeil, and Flavia Cicuttini* ..... 1480

## Clinical Images

### Clinical Images: Gout of the Spine

*Guojie Wang* ..... 1487

## Osteoarthritis

### Risk Assessment for Hip and Knee Osteoarthritis Using Polygenic Risk Scores

*Bahar Sedaghati-Khayat, Cindy G. Boer, Jos Runhaar, Sita M. A. Bierma-Zeinstra, Linda Broer, M. Arfan Ikram, Eleftheria Zeggini, André G. Uitterlinden, Jeroen G. J. van Rooij, and Joyce B. J. van Meurs* ..... 1488

## Spondyloarthritis

### Effects of Anti-Tumor Necrosis Factor Therapy on Osteoblastic Activity at Sites of Inflammatory and Structural Lesions in Radiographic Axial Spondyloarthritis: A Prospective Proof-of-Concept Study Using Positron Emission Tomography/Magnetic Resonance Imaging of the Sacroiliac Joints and Spine

*Nils Martin Bruckmann, Christoph Rischpler, Styliani Tsiami, Julian Kirchner, Daniel B. Abrar, Timo Bartel, Jens Theysohn, Lale Umutlu, Ken Herrmann, Wolfgang P. Fendler, Christian Buchbender, Gerald Antoch, Lino M. Sawicki, Athanasios Tsobanelis, Juergen Braun, and Xenofon Baraliakos* ..... 1497

### Progressive Increase in Sacroiliac Joint and Spinal Lesions Detected on Magnetic Resonance Imaging in Healthy Individuals in Relation to Age

*Thomas Renson, Manouk de Hooge, Ann-Sophie De Craemer, Liselotte Deroo, Zuzanna Lukasik, Philippe Carron, Nele Herregods, Lennart Jans, Roos Colman, Filip Van den Bosch, and Dirk Elewaut* ..... 1506

### Treatment With Tumor Necrosis Factor Inhibitors Is Associated With a Time-Shifted Retardation of Radiographic Sacroiliitis Progression in Patients With Axial Spondyloarthritis: 10-Year Results From the German Spondyloarthritis Inception Cohort

*Murat Torgutalp, Valeria Rios Rodriguez, Fabian Proft, Mikhail Protopopov, Maryna Verba, Judith Rademacher, Hildrun Haibel, Joachim Sieper, Martin Rudwaleit, and Denis Poddubnyy* ..... 1515

## Psoriatic Arthritis

### Peripheral $\gamma\delta$ T Cells Regulate Neutrophil Expansion and Recruitment in Experimental Psoriatic Arthritis

*Cuong Thach Nguyen, Hiroki Furuya, Dayasagar Das, Alina I. Marusina, Alexander A. Merleev, Resmi Ravindran, Zahra Jalali, Imran H. Khan, Emanuel Maverakis, and Iannis E. Adamopoulos* ..... 1524

### Comparative Genetic Analysis of Psoriatic Arthritis and Psoriasis for the Discovery of Genetic Risk Factors and Risk Prediction Modeling

*Mehreen Soomro, Michael Stadler, Nick Dand, James Bluett, Deepak Jadon, Farideh Jalali-najafabadi, Michael Duckworth, Pauline Ho, Helena Marzo-Ortega, Philip S. Helliwell, Anthony W. Ryan, David Kane, Eleanor Korendowych, Michael A. Simpson, Jonathan Packham, Ross McManus, Cem Gabay, Céline Lamacchia, Michael J. Nissen, Matthew A. Brown, Suzanne M. M. Verstappen, Tjeerd Van Staa, Jonathan N. Barker, Catherine H. Smith, the BADBIR Study Group, the BSTOP Study Group, Oliver FitzGerald, Neil McHugh, Richard B. Warren, John Bowes, and Anne Barton* ..... 1535

## Systemic Lupus Erythematosus

### Interleukin-13 Receptor $\alpha 1$ -Mediated Signaling Regulates Age-Associated/Autoimmune B Cell Expansion and Lupus Pathogenesis

*Zhu Chen, Danny Flores Castro, Sanjay Gupta, Swati Phalke, Michela Manni, Juan Rivera-Correa, Rolf Jessberger, Habib Zaghouani, Eugenia Giannopoulou, Tania Pannellini, and Alessandra B. Pernis* ..... 1544

### Plasmablast-like Phenotype Among Antigen-Experienced CXCR5-CD19<sup>low</sup> B Cells in Systemic Lupus Erythematosus

*Franziska Szelinski, Ana Luisa Stefanski, Eva Schrezenmeier, Hector Rincon-Arevalo, Annika Wiedemann, Karin Reiter, Jacob Ritter, Marie Lettau, Van Duc Dang, Sebastian Fuchs, Andreas P. Frei, Tobias Alexander, Andreia C. Lino, and Thomas Dörner* ..... 1556

## Sjögren's Syndrome

### Symptom-Based Cluster Analysis Categorizes Sjögren's Disease Subtypes: An International Cohort Study Highlighting Disease Severity and Treatment Discordance

*Sara S. McCoy, Miguel Woodham, Christie M. Bartels, Ian J. Saldanha, Vatinée Y. Bunya, Noah Maerz, Esen K. Akpek, Matthew A. Makara, and Alan N. Baer* ..... 1569

## Systemic Sclerosis

### Development of Pulmonary Hypertension in Over One-Third of Patients With Th/To Antibody-Positive Scleroderma in Long-Term Follow-Up

*Shashank Suresh, Devon Charlton, Erin K. Snell, Maureen Laffoon, Thomas A. Medsger Jr, Lei Zhu, and Robyn T. Domsic* . . . 1580

## Dermatomyositis

Brief Report: Performance of the 2017 European Alliance of Associations for Rheumatology/American College of Rheumatology Classification Criteria in Patients With Idiopathic Inflammatory Myopathy and Anti-Melanoma Differentiation-Associated Protein 5 Positivity

*Ho So, Jacqueline So, Tommy Tsz-On Lam, Victor Tak-Lung Wong, Roy Ho, Wai Ling Li, Chi Chiu Mok, Chak Sing Lau, and Lai-Shan Tam* ..... 1588

## Gout

Evaluation of the Relationship Between Serum Urate Levels, Clinical Manifestations of Gout, and Death From Cardiovascular Causes in Patients Receiving Febuxostat or Allopurinol in an Outcomes Trial

*Kenneth G. Saag, Michael A. Becker, William B. White, Andrew Whelton, Jeffrey S. Borer, Philip B. Gorelick, Barbara Hunt, Majin Castillo, and Lhanoo Gunawardhana, on behalf of the CARES Investigators* ..... 1593

## Letters

Increased Risk of Statin-Associated Autoimmune Myopathy Among American Indians

*Jennie Wei, Elizabeth Ketner, and Andrew L. Mammen* ..... 1602

von Willebrand Factor as an Indicator of Endothelial Injury in COVID-19: Comment on the Article by Shi et al

*Darryl E. Palmer-Toy, Timothy M. Cotter, Hedyeh Shafi, Su-Jau T. Yang, and Alexander H. Cotter* ..... 1603

Reply

*Hui Shi, Jason S. Knight, and Yogendra Kanthi* ..... 1603

Addressing Readability of Online Patient Materials: Comment on the American College of Rheumatology Online Information Pages for Patients and Caregivers

*Ahmad AlAbdulkareem* ..... 1604

Reply

*Mohammad A. Ursani* ..... 1605

Criteria for the Pathogenicity of Anticentromere (Anti-CENP-B) Autoantibodies in Systemic Sclerosis:

Comment on the Article by van Leeuwen et al

*Jean-Luc Senécal, Martial Koenig, Gabriel Archambault, and Sabrina Hoa* ..... 1606

Reply

*Nina M. van Leeuwen, Sophie I. E. Liem, Hans U. Scherer, and Jeska K. de Vries-Bouwstra* ..... 1607

## VOLUME 74 • October 2022 • NO. 10

**In This Issue** ..... A11

**Journal Club** ..... A12

**Clinical Connections** ..... A13

## Special Articles

Editorial: Three Months of Glucocorticoids in Rheumatoid Arthritis: A Bridge Too Short?

*Maarten Boers* ..... 1609

Editorial: Is Rheumatoid Arthritis a Causal Factor in Cardiovascular Disease?

*S. Louis Bridges Jr, Timothy B. Niewold, and Tony R. Merriman* ..... 1612

Review: Intracellular Sensing of DNA in Autoinflammation and Autoimmunity

*Susan MacLauchlan, Katherine A. Fitzgerald, and Ellen M. Gravallese* ..... 1615

Notes from the Field: The Transition From Residency to Fellowship: Enhancing Training by Increasing Transparency

*Eli M. Miloslavsky and Anisha B. Dua* ..... 1625

## Rheumatoid Arthritis

The Efficacy of Short-Term Bridging Strategies With High- and Low-Dose Prednisolone on Radiographic and Clinical Outcomes in Active Early Rheumatoid Arthritis: A Double-Blind, Randomized, Placebo-Controlled Trial

*Dietmar Krause, Anna Mai, Renate Klaassen-Mielke, Nina Timmesfeld, Ulrike Trampisch, Henrik Rudolf, Xenofon Baraliakos, Elmar Schmitz, Claas Fendler, Claudia Klink, Stephanie Boeddeker, Ertan Saracbası-Zender, Hans-Joachim Christoph, Manfred Igelmann, Hans-Juergen Menne, Albert Schmid, Rolf Rau, Siegfried Wassenberg, Nilüfer Sonuc, Claudia Ose, Carmen Schade-Brittinger, Hans J. Trampisch, and Juergen Braun* ..... 1628

## Clinical Images

Clinical Images: Granulomatosis with Polyangiitis and Transthyretin-Related Amyloidosis

*Justas Grimalauskas-Suchina, Frank Behrendt, Corina Schuster-Amft, Katrin Parmar, Leo Bonati, and Hans U. Gerth* ..... 1637



## Rheumatoid Arthritis

- Genetic Liability to Rheumatoid Arthritis in Relation to Coronary Artery Disease and Stroke Risk  
*Shuai Yuan, Paul Carter, Amy M. Mason, Fangkun Yang, Stephen Burgess, and Susanna C. Larsson* ..... 1638
- Tofacitinib and Risk of Malignancy: Results From the Safety of Tofacitinib in Routine Care Patients With Rheumatoid Arthritis (STAR-RA) Study  
*Farzin Khosrow-Khavar, Rishi J. Desai, Hemin Lee, Su Been Lee, and Seoyoung C. Kim* ..... 1648

## Osteoarthritis

- Association Between Walking for Exercise and Symptomatic and Structural Progression in Individuals With Knee Osteoarthritis: Data From the Osteoarthritis Initiative Cohort  
*Grace H. Lo, Surabhi Vinod, Michael J. Richard, Matthew S. Harkey, Timothy E. McAlindon, Andrea M. Kriska, Bonny Rockette-Wagner, Charles B. Eaton, Marc C. Hochberg, Rebecca D. Jackson, C. Kent Kwoh, Michael C. Nevitt, and Jeffrey B. Driban* ..... 1660
- The Relationship of Pain Reduction With Prevention of Knee Replacement Under Dynamic Intervention Strategies  
*S. Reza Jafarzadeh, Tuhina Neogi, Daniel K. White, and David T. Felson* ..... 1668

## Clinical Images

- Clinical Images: Huriez Syndrome, a Rare Scleroderma Mimic  
*Sayan Mukherjee, Mukesh K. Maurya, and Puneet Kumar* ..... 1675

## Systemic Lupus Erythematosus

- Dynamics of Methylation of CpG Sites Associated With Systemic Lupus Erythematosus Subtypes in a Longitudinal Cohort  
*Cristina M. Lanata, Joanne Nititham, Kimberly E. Taylor, Olivia Solomon, Sharon A. Chung, Ashira Blazer, Laura Trupin, Patricia Katz, Maria Dall'Era, Jinoos Yazdany, Marina Sirota, Lisa F. Barcellos, and Lindsey A. Criswell* ..... 1676
- Multidimensional Immune Profiling of Cutaneous Lupus Erythematosus In Vivo Stratified by Patient Response to Antimalarials  
*Jay Patel, Thomas Vazquez, Felix Chin, Emily Keyes, Daisy Yan, DeAnna Diaz, Madison Grinnell, Meena Sharma, Yubin Li, Rui Feng, Grant Sprow, Josh Dan, and Victoria P. Werth* ..... 1687

## Sjögren's Syndrome

- Brief Report: In Vivo Generation of SSA/Ro Antigen-Specific Regulatory T Cells Improves Experimental Sjögren's Syndrome in Mice  
*Junji Xu, Ousheng Liu, Dandan Wang, Fu Wang, Dunfang Zhang, Wenwen Jin, Alexander Cain, Andrew Bynum, Na Liu, Yichen Han, and WanJun Chen* ..... 1699

## Corrigendum

- Correction of Figure 2C in the Article by Chen et al (Arthritis Rheumatol, September 2015) ..... 1705

## Autoimmunity

- Machine Learning for the Identification of a Common Signature for Anti-SSA/Ro 60 Antibody Expression Across Autoimmune Diseases  
*Nathan Foulquier, Christelle Le Dantec, Eleonore Bettacchioli, Christophe Jamin, Marta E. Alarcón-Riquelme, and Jacques-Olivier Pers* ..... 1706

## Letters

- Pregnancy Outcomes in Women with Psoriatic Arthritis: Comment on the Article by Remaeus et al  
*Aine Gorman, Sonia Sundanum, Louise Moore, Celine O'Brien, Fionnula McAuliffe, and Douglas J. Veale* ..... 1720
- Reply  
*Katarina Remaeus, Kari Johansson, Fredrik Granath, Olof Stephansson, and Karin Hellgren* ..... 1720
- Revisiting the Disease Specificity and Nomenclature of Ficolin-1-Positive Monocyte-Derived Dendritic Cells in Diffuse Cutaneous Systemic Sclerosis: Comment on the Article by Xue et al  
*Marika Sarfati, Laurence Chapuy, and Heena Mehta* ..... 1721
- Reply  
*Robert Lafyatis and Tracy Tabib* ..... 1722
- Concerns Regarding the Title and Abstract Conclusion in a Recent Genome-Wide Association Study on Behçet's Disease: Comment on the Article by Su et al  
*Muhammed Abdulkarim Sahin and Sinem Nihal Esatoglu* ..... 1723

Reply	
<i>Guannan Su and Peizeng Yang</i> . . . . .	1724
A Methodologic Problem and a Conceptual Issue Related to the New 2022 Antineutrophil Cytoplasmic Antibody-Related Vasculitis Criteria Sets: Comment on Criteria Sets Approved by the American College of Rheumatology Board of Directors and the European Alliance of Associations for Rheumatology Executive Committee	
<i>Hasan Yazici and Yusuf Yazici</i> . . . . .	1724
Reply	
<i>Peter C. Grayson, Cristina Ponte, Joanna C. Robson, Ravi Suppiah, Andrew Judge, Andrew Hutchings, Anthea Craven, Sara Khalid, Raashid A. Luqmani, Richard A. Watts, and Peter A. Merkel</i> . . . . .	1725

## VOLUME 74 • November 2022 • NO. 11

<b>In This Issue</b> . . . . .	A15
<b>Journal Club</b> . . . . .	A16
<b>Clinical Connections</b> . . . . .	A17
<b>Special Articles</b>	
Editorial: Immune Cell Signatures to Stratify Patients With Systemic Autoimmune Diseases: A Step Toward Individualized Medicine?	
<i>Takahisa Gono and Divi Cornec</i> . . . . .	1727
Editorial: Transforming Rheumatology Practice With Technology: Products, Processes, People, and Purpose	
<i>Rebecca Grainger</i> . . . . .	1730
Notes from the Field: VEXAS Syndrome and Disease Taxonomy in Rheumatology	
<i>Peter C. Grayson, David B. Beck, Marcela A. Ferrada, Peter A. Nigrovic, and Daniel L. Kastner</i> . . . . .	1733
<b>Rheumatoid Arthritis</b>	
Smartphone-Assisted Patient-Initiated Care Versus Usual Care in Patients With Rheumatoid Arthritis and Low Disease Activity: A Randomized Controlled Trial	
<i>Bart Seppen, Jimmy Wiegel, Marieke M. ter Wee, Dirkjan van Schaardenburg, Leo D. Roorda, Michael T. Nurmohamed, Maarten Boers, and Wouter H. Bos</i> . . . . .	1737
Heavy Chain Constant Region Usage in Antibodies to Peptidylarginine Deiminase 4 as a Marker of Disease Subsets in Rheumatoid Arthritis	
<i>E. Gómez-Bañuelos, J. Shi, H. Wang, M. I. Danila, S. L. Bridges Jr., J. T. Giles, G. P. Sims, F. Andrade, and E. Darrah</i> . . . . .	1746
A Risk Score to Detect Subclinical Rheumatoid Arthritis-Associated Interstitial Lung Disease	
<i>Pierre-Antoine Juge, Benjamin Granger, Marie-Pierre Debray, Esther Ebstein, Fabienne Louis-Sidney, Joanna Kedra, Tracy J. Doyle, Raphaël Borie, Arnaud Constantin, Bernard Combe, René-Marc Flipo, Xavier Mariette, Olivier Vittecoq, Alain Saraux, Guillermo Carvajal-Alegria, Jean Sibilia, Francis Berenbaum, Caroline Kannengiesser, Catherine Boileau, Jeffrey A. Sparks, Bruno Crestani, Bruno Fautrel, and Philippe Dieudé</i> . . . . .	1755
Serologic Biomarkers of Progression Toward Diagnosis of Rheumatoid Arthritis in Active Component Military Personnel	
<i>Matthew J. Loza, Sunil Nagpal, Suzanne Cole, Renee M. Laird, Ashley Alcala, Navin L. Rao, Mark S. Riddle, and Chad K. Porter</i> . . . . .	1766
Phase II/III Results of a Trial of Anti-Tumor Necrosis Factor Multivalent NANOBODY Compound Ozoralizumab in Patients With Rheumatoid Arthritis	
<i>Tsutomu Takeuchi, Masafumi Kawanishi, Megumi Nakanishi, Hironori Yamasaki, and Yoshiya Tanaka</i> . . . . .	1776
<b>Spondyloarthritis</b>	
Characterization of Blood Mucosal-Associated Invariant T Cells in Patients With Axial Spondyloarthritis and of Resident Mucosal-Associated Invariant T Cells From the Axial Entheses of Non-Axial Spondyloarthritis Control Patients	
<i>Nicolas Rosine, Hannah Rowe, Surya Koturan, Hanane Yahia-Cherbal, Claire Leloup, Abdulla Watad, Francis Berenbaum, Jeremie Sellam, Maxime Dougados, Vishukumar Aimaniananda, Richard Cuthbert, Charlie Bridgewood, Darren Newton, Elisabetta Bianchi, Lars Rogge, Dennis McGonagle, and Corinne Miceli-Richard</i> . . . . .	1786

## Systemic Lupus Erythematosus

- Choroid Plexus-Infiltrating T Cells as Drivers of Murine Neuropsychiatric Lupus  
*Erica Moore, Michelle W. Huang, Cara A. Reynolds, Fernando Macian, and Chaim Putterman* ..... 1796
- Longitudinal Immune Cell Profiling in Patients With Early Systemic Lupus Erythematosus  
*Takanori Sasaki, Sabrina Bracero, Joshua Keegan, Lin Chen, Ye Cao, Emma Stevens, Yujie Qu, Guoxing Wang, Jennifer Nguyen, Jeffrey A. Sparks, V. Michael Holers, Stephen E. Alves, James A. Lederer, Karen H. Costenbader, and Deepak A. Rao* ..... 1808

## Dermatomyositis

- Two Distinct Immune Cell Signatures Predict the Clinical Outcomes in Patients With Amyopathic Dermatomyositis With Interstitial Lung Disease  
*Yan Ye, Xueliang Zhang, Teng Li, Jiaqiang Ma, Ran Wang, Chunmei Wu, Runci Wang, Chunde Bao, Shuang Ye, Nan Shen, Qiang Guo, Qiong Fu, and Xiaoming Zhang* ..... 1822

## Autoimmune Disease

- Recombinant Zoster Vaccine Uptake and Risk of Flares Among Older Adults With Immune-Mediated Inflammatory Diseases in the US  
*Jessica Leung, Tara C. Anderson, Kathleen Dooling, Fenglong Xie, and Jeffrey R. Curtis* ..... 1833

## Sjögren's Syndrome

- Strong Association of Combined Genetic Deficiencies in the Classical Complement Pathway With Risk of Systemic Lupus Erythematosus and Primary Sjögren's Syndrome  
*Christian Lundtoft, Christopher Sjöwall, Solbritt Rantapää-Dahlqvist, Anders A. Bengtsson, Andreas Jönsen, Pascal Pucholt, Yee Ling Wu, Emeli Lundström, Maija-Leena Eloranta, Iva Gunnarsson, Eva Baecklund, Roland Jonsson, Daniel Hammenfors, Helena Forsblad-d'Elia, Per Eriksson, Thomas Mandl, Sara Bucher, Katrine B. Norheim, Svein Joar Auglaend Johnsen, Roald Omdal, Marika Kvarnström, Marie Wahren-Herlenius, Lennart Truedsson, Bo Nilsson, Sergey V. Kozyrev, Matteo Bianchi, Kerstin Lindblad-Toh, the DISSECT consortium, the ImmunoArray consortium, Chack-Yung Yu, Gunnel Nordmark, Johanna K. Sandling, Elisabet Svenungsson, Dag Leonard, and Lars Rönnblom* ..... 1842

## Pediatric Rheumatology

- Joint-Specific Memory and Sustained Risk for New Joint Accumulation in Autoimmune Arthritis  
*Margaret H. Chang, Alexandra V. Bocharnikov, Siobhan M. Case, Marc Todd, Jessica Laird-Gion, Maura Alvarez-Baumgartner, and Peter A. Nigrovic* ..... 1851

## Letters

- Duloxetine and Osteoarthritis, a Herd of Elephants in the Room: Comment on the Article by van den Driest et al  
*Alain Braillon* ..... 1859
- Duloxetine May Have Clinical Value: Comment on the Article by van den Driest et al  
*Joel A. Block and Theodore Pincus* ..... 1859
- Reply  
*Jacoline J. van den Driest, Dieuwke Schiphof, Patrick J. E. Bindels, Aafke R. Koffeman, Marc A. Koopmanschap, and Sita M. A. Bierma-Zeinstra* ..... 1860
- Differences in Definitions and Prevalence of Hand Osteoarthritis: Comment on the Article by Eaton et al  
*Amanda E. Nelson, Todd A. Schwartz, Carolina Alvarez, and Yvonne M. Golightly* ..... 1861
- Reply  
*Charles B. Eaton, Tim McAlindon, and Jeffrey Driban* ..... 1862

## Clinical Images

- Clinical Images: VEXAS Syndrome Presenting as Treatment-Refractory Polyarteritis Nodosa  
*Masaki Itagane, Hiroyuki Teruya, Tomohiro Kato, Naomi Tsuchida, Ayaka Maeda, Yohei Kirino, Yuri Uchiyama, Naomichi Matsumoto, and Mitsuyo Kinjo* ..... 1863

## VOLUME 74 • December 2022 • NO. 12

- In This Issue ..... A15
- Journal Club ..... A16
- Clinical Connections ..... A17
- ACR Announcements ..... A25

## Special Articles

- Notes from the Field: Overturning *Roe v. Wade*: Toppling the Practice of Rheumatology  
*Bonnie L. Bermas, Irene Blanco, Ashira D. Blazer, Megan EB Clowse, Cuoghi Edens, Rosalind Ramsey-Goldman, and Mehret Birru Talabi* ..... 1865
- Notes from the Field: The Evolving Role of the Rheumatology Practitioner in the Care of Immunocompromised Patients in the COVID-19 Era  
*Leonard H. Calabrese, Cassandra M. Calabrese, Elizabeth Kirchner, and Kevin Winthrop* ..... 1868
- 2022 American College of Rheumatology/EULAR Classification Criteria for Takayasu Arteritis  
*Peter C. Grayson, Cristina Ponte, Ravi Suppiah, Joanna C. Robson, Katherine Bates Gribbons, Andrew Judge, Anthea Craven, Sara Khalid, Andrew Hutchings, Debashish Danda, Raashid A. Luqmani, Richard A. Watts, and Peter A. Merkel, for the DCVAS Study Group* ..... 1872
- 2022 American College of Rheumatology/EULAR Classification Criteria for Giant Cell Arteritis  
*Cristina Ponte, Peter C. Grayson, Joanna C. Robson, Ravi Suppiah, Katherine Bates Gribbons, Andrew Judge, Anthea Craven, Sara Khalid, Andrew Hutchings, Richard A. Watts, Peter A. Merkel, and Raashid A. Luqmani, for the DCVAS Study Group* . . . 1881
- Editorial: Disentangling the Causal Effect of Telomere Length in Systemic Lupus Erythematosus Using Genetic Variants as Instruments  
*Yiqiang Zhan and Xiaoying Kang* ..... 1890
- Review: Artificial Intelligence and Deep Learning for Rheumatologists  
*Christopher McMaster, Alix Bird, David F. L. Liew, Russell R. Buchanan, Claire E. Owen, Wendy W. Chapman, and Douglas E. V. Pires* ..... 1893

## COVID-19

- Breakthrough SARS-CoV-2 Infections in Patients With Immune-Mediated Disease Undergoing B Cell-Depleting Therapy: A Retrospective Cohort Analysis  
*Cassandra M. Calabrese, Elizabeth Kirchner, Elaine M. Husni, Brandon P. Moss, Anthony P. Fernandez, Yuxuan Jin, and Leonard H. Calabrese* ..... 1906

## Rheumatoid Arthritis

- Synovial Inflammatory Pathways Characterize Anti-TNF-Responsive Rheumatoid Arthritis Patients  
*Jing Wang, Donna Conlon, Felice Rivellese, Alessandra Nerviani, Myles J. Lewis, William Housley, Marc C. Levesque, Xiaohong Cao, Carolyn Cuff, Andrew Long, Costantino Pitzalis, and Melanie C. Ruzek* ..... 1916

## Clinical Images

- Clinical Images: Giant Intraosseous Synovial Cyst With Intraarticular Connection at the Elbow in Rheumatoid Arthritis  
*Can M. Sungur and Jonathan C. Baker* ..... 1927

## Osteoarthritis

- Contribution of MicroRNA-27b-3p to Synovial Fibrotic Responses in Knee Osteoarthritis  
*Ghazaleh Tavallaei, Starlee Lively, Jason S. Rockel, Shabana Amanda Ali, Michelle Im, Clementine Sarda, Greniqueca M. Mitchell, Evgeny Rossomacha, Sayaka Nakamura, Pratibha Potla, Sarah Gabriel, John Matelski, Anusha Ratneswaran, Kim Perry, Boris Hinz, Rajiv Gandhi, Igor Jurisica, and Mohit Kapoor* ..... 1928

## Spondyloarthritis

- Safety and Efficacy of Bimekizumab in Patients With Active Ankylosing Spondylitis: Three-Year Results From a Phase IIb Randomized Controlled Trial and Its Open-Label Extension Study  
*Xenofon Baraliakos, Atul Deodhar, Maxime Dougados, Lianne S. Gensler, Anna Molto, Sofia Ramiro, Alan J. Kivitz, Denis Poddubnyy, Marga Oortgiesen, Thomas Vaux, Carmen Fleurinck, Julie Shepherd-Smith, Christine de la Loge, Natasha de Peyrecave, and Désirée van der Heijde* ..... 1943

## Psoriatic Arthritis

- Safety and Efficacy of Bimekizumab in Patients With Active Psoriatic Arthritis: Three-Year Results From a Phase IIb Randomized Controlled Trial and Its Open-Label Extension Study  
*Laura C. Coates, Iain B. McInnes, Joseph F. Merola, Richard B. Warren, Arthur Kavanaugh, Alice B. Gottlieb, Laure Gossec, Deepak Assudani, Rajan Bajracharya, Jason Coarse, Barbara Ink, and Christopher T. Ritchlin* ..... 1959

## Systemic Lupus Erythematosus

- Modulation of the Itaconate Pathway Attenuates Murine Lupus  
*Luz P. Blanco, Eduardo Patino-Martinez, Shuichiro Nakabo, Mingzeng Zhang, Hege L. Pedersen, Xinghao Wang, Carmelo Carmona-Rivera, Dillon Claybaugh, Zu-Xi Yu, Equar Desta, and Mariana J. Kaplan* ..... 1971
- Brief Report: Telomere Length and Development of Systemic Lupus Erythematosus: A Mendelian Randomization Study  
*Xu-Fan Wang, Wen-Jing Xu, Fei-Fei Wang, Rui Leng, Xiao-Ke Yang, Hua-Zhi Ling, Yin-Guang Fan, Jin-Hui Tao, Zong-Wen Shuai, Li Zhang, Dong-Qing Ye, and Rui-Xue Leng* ..... 1984

## Sjögren's Syndrome

Variability of Primary Sjögren's Syndrome Is Driven by Interferon- $\alpha$  and Interferon- $\alpha$  Blood Levels Are Associated With the Class II HLA-DQ Locus

*Diana Trutschel, Pierre Bost, Xavier Mariette, Vincent Bondet, Alba Llibre, Celine Posseme, Bruno Charbit, Christian W. Thorball, Roland Jonsson, Christopher J. Lessard, Renaud Felten, Wan Fai Ng, Lucienne Chatenoud, Hélène Dumortier, Jean Sibilia, Jacques Fellay, Karl A. Brokstad, Silke Appel, Jessica R. Tarn, Lluis Quintana-Murci, Michael Mingueneau, Nicolas Meyer, Darragh Duffy, Benno Schwikowski, and Jacques Eric Gottenberg, On behalf of The Milieu Intérieur Consortium, ASSESS study investigators, and NECESSITY Consortium* ..... 1991

## Systemic Sclerosis

Epigenetic Regulation of Profibrotic Macrophages in Systemic Sclerosis-Associated Interstitial Lung Disease

*Anna Papazoglou, Mengqi Huang, Melissa Bulik, Annika Lafyatis, Tracy Tabib, Christina Morse, John Sembrat, Mauricio Rojas, Eleanor Valenzi, and Robert Lafyatis* ..... 2003

## Gout

Superiority of Low-Dose Benzbromarone to Low-Dose Febuxostat in a Prospective, Randomized Comparative Effectiveness Trial in Gout Patients With Renal Uric Acid Underexcretion

*Fei Yan, Xiaomei Xue, Jie Lu, Nicola Dalbeth, Han Qi, Qing Yu, Can Wang, Mingshu Sun, Lingling Cui, Zhen Liu, Yuwei He, Xuan Yuan, Ying Chen, Xiaoyu Cheng, Lidan Ma, Hailong Li, Aichang Ji, Shuhui Hu, Zijing Ran, Robert Terkeltaub, and Changgui Li* ..... 2015

## Pediatric Rheumatology

Brief Report: Imaging Mass Cytometry Reveals Predominant Innate Immune Signature and Endothelial-Immune Cell Interaction in Juvenile Myositis Compared to Lupus Skin

*Jessica L. Turnier, Christine M. Yee, Jacqueline A. Madison, Syed M. Rizvi, Celine C. Berthier, Fei Wen, and J. Michelle Kahlenberg* ..... 2024

## Autoimmune Disease

Increasing Prevalence of Antinuclear Antibodies in the United States

*Gregg E. Dinse, Christine G. Parks, Clarice R. Weinberg, Carol A. Co, Jesse Wilkerson, Darryl C. Zeldin, Edward K. L. Chan, and Frederick W. Miller* ..... 2032

## Letters

Systemic Glucocorticoids Confound SARS-CoV-2 Acquisition or Even Clinical Outcomes in Patients With Autoimmune Disease Treated With Biologics: Comment on the Article by Simon et al

*Man-Man Niu, Qi Jiang, Yan-Fang Zhang, Dao-Ting Li, Qian Yang, and Peng Hu* ..... 2042

## Reply

*Georg Schett, David Simon, Filippo Fagni, and Korey Tascilar* ..... 2043

Optimal Bridging Strategy in Active Early Rheumatoid Arthritis: A Bridge Falling Short? Comment on the Article by Krause et al

*Joydeep Samanta, Alekhya Amudalapalli, Ashlesha Shukla, BV Harish, Sudhish Gadde, Rasmi R. Sahoo, and Pradeepta S. Patro* ..... 2044

## Reply

*Dietmar Krause and Juergen Braun* ..... 2045

Characterization of Mucosal-Associated Invariant T Cells in Blood of Patients With Axial Spondyloarthritis and in Axial Entheses of Healthy Controls: Comment on the Article by Rosine et al

*Eric Toussiot, Caroline Laheurte, and Philippe Saas* ..... 2045

## Reply

*Nicolas Rosine, Lars Rogge, Dennis McGonagle, and Corinne Miceli-Richard* ..... 2046

**Reviewers** ..... 2048

**Volume 74 Table of Contents** ..... 2052



# In this Issue

Highlights from this issue of *A&R* | By Lara C. Pullen, PhD

## 4-OI Treatment Attenuates Murine Lupus

A recent murine study found that intranasal treatment with 4-octyl itaconate (OI) reduced dendritic cell priming activity and attenuated a specific allergic inflammatory response.

p. 1971

Additional studies have suggested that 4-OI modulates JAK1-mediated pathways. Building upon that work, Blanco et al (p. 1971) report their results to be consistent, supporting the idea that targeting immunometabolism is a viable approach to the treatment of autoimmune disease. In particular, the investigators found that 4-OI displayed a beneficial role in attenuating immune dysregulation and organ damage in lupus.

Using female (NZW × NZB)F<sub>1</sub> lupus-prone mice, the researchers found that subcutaneous administration of 4-OI after the animals developed lupus improved features of clinical disease relative to the vehicle group. Treatment also reduced the levels of various antinuclear antibodies, including anti-RNP autoantibodies relative to controls. Moreover, the investigators found that 4-OI-treated mice had decreased splenomegaly compared to vehicle-treated mice and that this decrease was associated with decreases in activation markers in

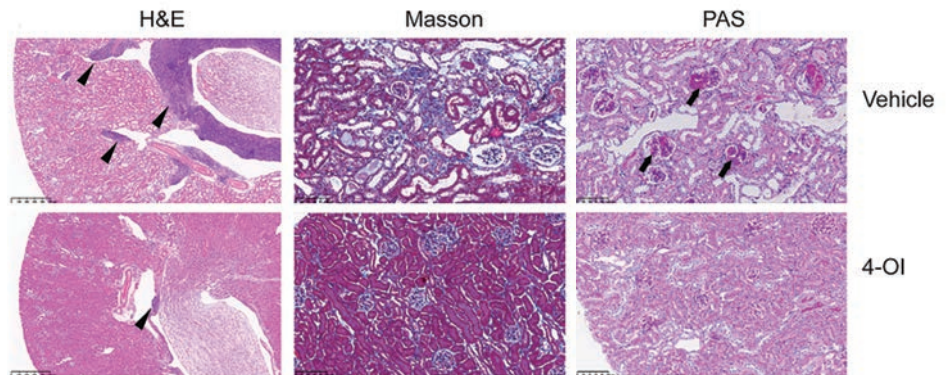


**Figure 1.** Representative kidney tissue images stained with hematoxylin and eosin (H&E), Masson's trichrome, and periodic acid–Schiff (PAS). In H&E–stained images, **arrowheads** show inflammation. In PAS–stained images, **arrows** show glomerulosclerosis.

innate and adaptive immune cells, increases in CD8+ T cell numbers, and inhibition of JAK1 activation. When the team examined human control and lupus myeloid cells, they found that 4-OI in vitro treatment decreased proinflammatory responses.

The team next performed gene expression analysis of murine splenocytes and found that 4-OI improved type I interferon (IFN) pathway dysregulation as evidenced by significant

decreases in type I IFN and proinflammatory cytokine genes. Gene expression analysis also revealed increased Treg cell–associated markers in the 4-OI group compared to the vehicle group. Treatment did not, however, transcriptionally regulate FoxP3 levels. The authors call for future studies to assess whether survival of memory CD8 T cells and CD8-specific FoxP3 expression or Treg cell suppressor function are affected by the treatment.

## IFN $\alpha$ as a Driver of Variability in Primary SS

In the case of primary Sjögren's syndrome (SS), both genetic predisposition to disease and pathogenic cell populations point to type I and type II IFNs as playing a critical role

p. 1991

in disease. Trutschel et al (p. 1991) identify IFN $\alpha$  as a driver of primary SS variability, and report that IFN $\alpha$  demonstrates an association with HLA gene polymorphism. The authors state that, since most of the genes induced by IFN $\alpha$  are also induced by IFN $\gamma$ , the IFN $\alpha$  signature may be a broader marker of both IFN $\alpha$  and IFN $\gamma$  activity. Their results also reveal the potential of circulating IFN $\alpha$

to be used as a biomarker in primary SS.

The investigators applied their unsupervised gene expression analytic pipeline to blood transcriptome data first from 351 patients with primary SS who were participants in a multicenter prospective clinical cohort and then from 3 independent cohorts, for a total of 813 patients. The authors note that the unsupervised clustering method has only been previously reported for single cell analysis, and so its use to analyze the transcriptome data across different primary SS cohorts is novel. The multiomic study allowed the researchers to analyze the

relationship between IFN protein concentrations and patient genotypes, whole-blood transcriptome results, and clinical phenotypes. They identified strong transcriptomic stratification of patients with primary SS, a finding that supported their observation that SS was driven by IFN $\alpha$  rather than IFN $\gamma$ . The authors propose that, in patients with primary SS, HLA may predispose to IFN $\alpha$  secretion indirectly by favoring classic presentation by conventional dendritic cells of SSA peptides to T cells. This, in turn, could lead to anti-SSA antibodies and immune complexes, which further stimulate IFN $\alpha$  secretion.

# IMID Patients With BCDT Susceptible to Breakthrough COVID-19

Rheumatologists recognize that patients with immune-mediated inflammatory diseases (IMIDs) receiving B cell depletion therapy (BCDT) are vulnerable to severe COVID-19

**p. 1906** infections. However, few studies address risks for, and outcomes of, breakthrough infections. Calabrese et al (p. 1906) report that IMID patients receiving BCDT appear to be vulnerable to SARS-CoV-2 regardless of vaccine status, and the use of BCDT was frequently associated with severe outcomes in infected patients. In contrast, outpatient use of anti-SARS-CoV-2 monoclonal antibody (mAb) therapy seems to be associated with enhanced clinical outcomes.

The study examined a large cohort of IMID patients (n = 1,696) exposed to BCDT in 2020 and compared the results to

previous findings. The investigators focused on patients receiving any 1 of several classes of immunosuppressant treatments, including conventional, synthetic, or targeted disease-modifying therapies and/or glucocorticoids. They calculated a time-adjusted incidence of breakthrough infection rate of 5.19 cases per 1,000 person-months, with most of the cases identified during the Delta surge. Given that breakthrough infection in patients receiving BCDT appears to be associated with poor outcomes, the investigators conducted an additional exploratory analysis in unvaccinated patients with the same diagnoses and use of BCDTs over the same time. They found that the incidence of infection was similar but numerically lower in the unvaccinated patients (3.9% versus 4.4%).

Although breakthrough patients receiving

anti-SARS-CoV-2 mAb did extremely well, the authors report that only 21 of 74 breakthrough patients (28.4%) received anti-SARS-CoV-2 mAb therapy. Use of mAb therapy was even lower in the unvaccinated cohort, leading the authors to question whether the findings reflect disparities in health care access and/or belief in health care resources. They note that these findings of severe outcomes of COVID-19 in breakthrough infections in patients receiving treatment with BCDTs are important for understanding the implications of the evolving picture of vaccine responsiveness in this population. They also state that their study has identified an important segment of the immunocompromised patient population who are likely to face ongoing and formidable risks despite aggressive vaccination.

## Journal Club

*A monthly feature designed to facilitate discussion on research methods in rheumatology.*

### Telomere Length and Development of SLE: A Mendelian Randomization Study

Wang et al, *Arthritis Rheumatol.* 2022;74:1984–1990

The involvement of accelerated immune senescence in autoimmune disorders has drawn a substantial amount of interest in the investigation of telomere length as a putative cause of the initiation and progression of SLE. Previous observational studies and meta-analyses compared telomere length between SLE patients and healthy controls. Given the presence of potential unadjusted confounding factors and reverse causation, achieving a reasonable conclusion can be challenging in traditional case-control or cross-sectional studies. More robust methods should be employed to determine causality. Wang et al examined whether leukocyte telomere length is causally associated with risk of SLE based on genetic data. They also estimated the effects of SLE on telomere length.

Two-sample Mendelian randomization (MR) analysis was first conducted to estimate causality of leukocyte telomere length on SLE in samples of European ancestry. Given the random allocation of genetic variants at conception, the MR estimates are usually not biased. The 2-sample MR design can be performed using results from genome-wide association studies, bypassing the need for individual-level data. This has a tremendous advantage in that causal inference can be made between the 2 traits even if they are

not measured in the same set of samples. The MR method was applied following a rigorous framework that included obtaining SNPs that reliably associate with the exposure, extracting SNP effects on the outcome, harmonizing exposure and outcome SNP effects, performing MR analysis, and conducting diagnostics and sensitivity analyses. A replication 2-sample MR study was also conducted using genetic data from those with Asian ancestry. Following similar procedures, a reverse MR analysis was then performed to test the effects of SLE on telomere length using European genetic data.

#### Questions

1. What is currently known about telomere length with susceptibility of SLE in different populations?
2. Why use the 2-sample MR analysis instead of the traditional case-control studies? Why were the bidirectional MR methods used to estimate causality?
3. Did the MR methods influence findings?
4. Are there other MR methods capable of determining causality based on individual-level data?

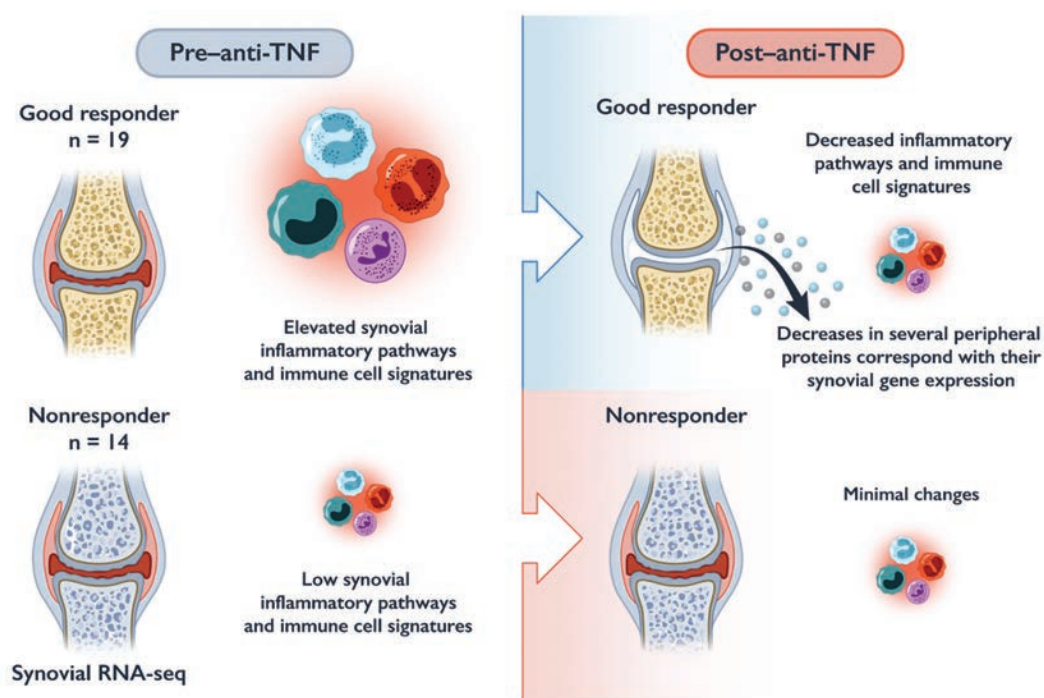
# Clinical Connections

## Synovial Inflammatory Pathways Characterize Anti-TNF-Responsive RA Patients

Wang et al, *Arthritis Rheumatol.* 2022;74:1916–1927

### CORRESPONDENCE

Melanie Ruzek, PhD: melanie.ruzek@abbvie.com



### KEY POINTS

- RA patients show varying levels of synovial inflammation.
- Baseline synovial inflammation is higher in patients showing good responses to anti-TNF therapy.
- Patients not responding to anti-TNF therapy have lower synovial inflammation.
- Following anti-TNF treatment, good responder patients show decreases in both synovial inflammation and inflammatory proteins in blood.

### SUMMARY

Rheumatoid arthritis (RA) is an inflammatory autoimmune disease localized to the synovium in the joints. While anti-tumor necrosis factor (anti-TNF) is a commonly used therapy for RA, only a portion of patients show a good response, and the mechanistic basis has been difficult to discern. Using molecular analysis of synovial biopsy tissue pre- and post-anti-TNF treatment in good and poor responder patients, Wang et al demonstrated that inflammatory pathways within the synovium are elevated in good responders compared to poor responders. Cell gene signatures similarly suggested elevations in inflammatory cells within the synovium prior to anti-TNF therapy in good, but not poor, responders. After anti-TNF treatment, these synovial inflammatory pathways and cell signatures were reduced only in good responders. Additionally, several corresponding peripheral blood inflammatory proteins were similarly decreased in good responder patients. These data demonstrate that patients with greater synovial inflammation are more likely to respond to anti-TNF therapy. These findings could lead to the identification of predictive markers and earlier treatment options for RA patients.

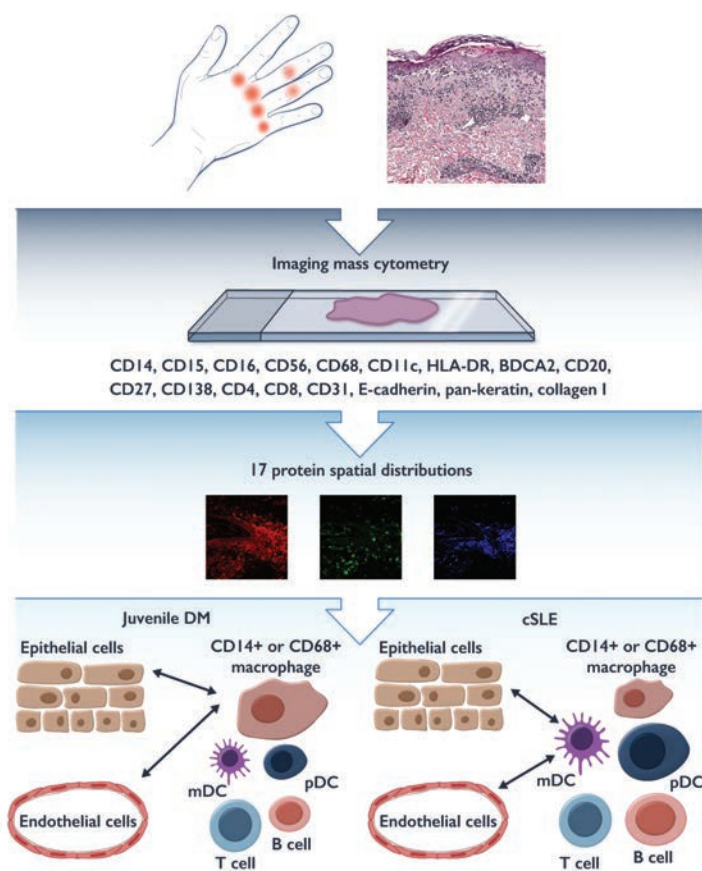


# Differences in Immune Cell Populations and Interactions Between JDM and cSLE Skin

Turnier et al, *Arthritis Rheumatol.* 2022;74:2024–2031

## CORRESPONDENCE

Jessica Turnier, MD: [turnierj@med.umich.edu](mailto:turnierj@med.umich.edu)



## KEY POINTS

- cSLE skin lesions demonstrated a denser inflammatory cell infiltrate, notably with a higher absolute number of CD14<sup>+</sup> macrophages, pDCs, and CD8<sup>+</sup> T cells and an overall higher number of cell–cell interactions as compared to juvenile DM.
- A more prominent innate immune signature was identified in juvenile DM compared to cSLE skin.
- As compared to cSLE, juvenile DM patients did not display a prominent epithelial–immune cell interaction.

## SUMMARY

Juvenile dermatomyositis (DM) and childhood-onset systemic lupus erythematosus (cSLE) are rare childhood autoimmune diseases that frequently first present with rash and progress to multiorgan inflammation. The appearance of the rashes in juvenile DM and cSLE appear visually similar to the eye and under the microscope with standard testing. Turnier et al used imaging mass cytometry to characterize the similarities and differences in immune cell types and interactions in skin rashes of juvenile DM and cSLE patients. Overall, cSLE patients were identified to have a higher total number of immune cells in skin and higher numbers of CD14<sup>+</sup> macrophages, plasmacytoid dendritic cells (pDCs), and CD8<sup>+</sup> T cells. The composition of immune cell types within the rashes of the 2 diseases differed, and juvenile DM patients had a predominance of the innate immune cells CD14<sup>+</sup> and CD68<sup>+</sup> macrophages in the skin, with macrophages composing >60% of the identified immune cell types. While cSLE patients also had a high percentage of CD14<sup>+</sup> macrophages in the skin, the relative composition of the adaptive immune cells (B cells and CD8<sup>+</sup> T cells) was higher. Interestingly, immune cells in juvenile DM skin appeared to interact more closely with endothelial cells within blood vessels, whereas in cSLE, immune cells interacted more equally with both epithelial cells composing the skin barrier layers and the endothelial cells. The identified differences in immune cell populations and interactions between juvenile DM and cSLE skin holds the potential to lead to targeted, cell-based treatments for each disease and also to advance understanding of what causes differences in organ inflammation and clinical presentations between the 2 diseases.

## ACR Announcements



**Douglas W. White, MD, PhD, ACR President**

### Eighty-Sixth President of the ACR

At the annual business meeting of the American College of Rheumatology on November 14, 2022, Douglas W. White, MD, PhD, was installed as the eighty-sixth President of the College.

Dr. White is the Chair of Rheumatology at Gundersen Health System in La Crosse, Wisconsin, where he also served as the head of the Rheumatology Research Laboratory. He holds adjunct faculty positions in the Department of Medicine at the University of Wisconsin School of Medicine and Public Health in Madison and the Department of Microbiology at the University of Wisconsin in La Crosse. He sees rheumatology patients four and a half days per week, and supervises nurse practitioners, a physician assistant, residents, and medical students rotating in clinic and on the inpatient rheumatology service.

Dr. White grew up in Milwaukee and graduated with a degree in biochemistry from the University of Wisconsin-Madison following a year abroad in Madrid. He then worked briefly on the campus of Genentech in South San Francisco before enrolling in the Medical Scientist Training Program at the University of Iowa, where he studied medicine and immunology. Dr. White completed internal medicine residency training at the University of Texas Southwestern in Dallas, followed by fellowship training in rheumatology at Washington University in St. Louis. He completed postdoctoral training and joined the faculty as an instructor at

Washington University in St. Louis prior to taking his current position in La Crosse.

Many important mentors and colleagues have provided inspiration and opportunities over the years that have allowed Dr. White to follow this path. One of the first was Lloyd Smith, PhD, in the Department of Chemistry at University of Wisconsin-Madison, who introduced Dr. White to basic science research. The Human Genome Project was getting under way and the focus of Dr. Smith's laboratory was the development of high-throughput sequencing technologies. Hands-on experience with capillary electrophoresis in Dr. Smith's laboratory led to Dr. White's next opportunity – a job at a start-up firm called Genomix, where mass spectrometry was used in tandem with high-speed electrophoresis to sequence DNA.

John Harty, PhD, in the Department of Microbiology at the University of Iowa, was another important mentor and supervised Dr. White's PhD thesis on the effector functions of CD8+ T cells in murine listeriosis. While CD4+ "helper" T cells were known to produce cytokines, perforin- and granzyme-mediated cytotoxicity of infected target cells had recently been established as an important mechanism by which CD8+ "killer" T cells mediated immunity. Dr. White's work expanded on this model by demonstrating that CD8+ T cells need not have cytolytic capacity to provide protection and that perforin-independent mechanisms, some of which require tumor necrosis factor (TNF), were sufficient for antilisterial immunity in vivo.

Herbert "Skip" Virgin, MD, PhD, in the Department of Pathology at Washington University in St. Louis, supervised Dr. White's postdoctoral research and provided fertile ground for studies of the interactions between latent herpesviruses and the host immune system. In Dr. Virgin's laboratory, Dr. White had the good fortune to secure K08 funding and to work with outstanding collaborators on projects demonstrating that latent infection with murine gammaherpesvirus (analogous to Epstein-Barr virus and Kaposi sarcoma-associated herpesvirus) shapes the host cytokine milieu, macrophage activation, and arming of natural killer cells with profound effects on host susceptibility to heterologous infection.

Dr. White was fortunate to have outstanding clinical mentors at every stage of his training, including Joel Gordon, MD, and Peter Densen, MD, in Iowa, L. David Hillis, MD, Daniel Foster, MD, Pat Cook, MD, and David Karp, MD, in Dallas, and Richard Brasington, MD, Leslie Kahl, MD, Prabha Ranganathan, MD, John Atkinson, MD, and Wayne Yokoyama, MD, in St. Louis. Indeed, it was Drs. Brasington and Yokoyama, when TNF inhibitors were emerging as new therapeutic options for rheumatology patients and the need for basic immunology training among clinicians was becoming acute, who encouraged Dr. White and his colleague, Deborah Lenschow, MD, PhD, to expand the didactic offerings for fellows at Washington University and create a new basic immunology course.

In 2009 Dr. White moved back to Wisconsin and started the Rheumatology Research Laboratory, where he established a viral recombineering program, underwritten by the Gundersen Research Foundation, that has contributed to productive collaborations across the US for over a decade. Darby Oldenburg, PhD, Dr. White's long-time collaborator, took over supervision of the laboratory in 2021.

Dr. White first volunteered at the American College of Rheumatology in 2011 when he became a member of the Committee on Rheumatologic Care (CORC). He has served in a number of roles since then, including as the chair of CORC, chair of the Alternative Payment Model Workgroup, and chair of the newly formed Membership and Awards Committee. He joined the Board of Directors in 2017, joined the Executive Committee



in 2019, and served as the Executive Committee Liaison to the COVID-19 Practice and Advocacy Task Force from 2020 to 2021. He was Treasurer from 2019 to 2021, and President-Elect from 2021 to 2022.

Dr. White was inducted into Phi Beta Kappa at the University of Wisconsin, and received the Titus Volunteer Scholarship from the Free Medical Clinic, the Edward Heath Award for Medical Research, and the William R. Wilson Award at the University of Iowa. He received 2 teaching awards at University of Texas-Southwestern, was an Abbott Scholar while at Washington University, and has received 7 teaching awards at Gundersen. He has delivered invited presentations across the US and internationally and his works have been published in more than a dozen journals, including *Nature*, *Blood*, *Annual Review of Immunology*, the *Journal of Virology*, and *Arthritis & Rheumatology*.

He lives in Onalaska, Wisconsin with his wife Theresa. Their children, Harrison and Alexandra, attend the University of Wisconsin.

## ACR Board of Directors, 2022–2023

### *Executive Committee*

President: Douglas W. White, MD, PhD, Chair, Department of Rheumatology, Gundersen Health System, Gundersen Medical Foundation, La Crosse, Wisconsin; Clinical Adjunct Assistant Professor, Department of Medicine, University of Wisconsin School of Medicine and Public Health, Madison, Wisconsin; and Clinical Adjunct Assistant Professor, Department of Microbiology, University of Wisconsin, La Crosse, Wisconsin.

President-Elect: Deborah D. Desir, MD, Associate Professor of Clinical Medicine, Department of Medicine, Section of Rheumatology, Allergy & Immunology, Yale School of Medicine, New Haven, Connecticut; and Medical Director, YM Rheumatology, Hamden Site, Hamden, Connecticut.

Secretary/Treasurer: Carol Langford, MD, MHS, Professor of Medicine, Harold C. Schott Endowed Chair in Rheumatic and Immunologic Diseases, and Director, Center for Vasculitis Care and Research, Cleveland Clinic, Cleveland, Ohio.

Foundation President: V. Michael Holers, MD, Smyth Professor of Rheumatology, Professor of Medicine and Immunology, and Director of Faculty Ventures within CU Innovations, University of Colorado School of Medicine, Aurora, Colorado.

ARP President: Kori Dewing, DNP, ARNP, University of Washington, School of Nursing and Seattle Arthritis Clinic, University of Washington, Seattle, Washington.

### *Members*

Marcy Bolster, MD  
Deborah Desir, MD  
Kori Dewing, ARNP, DNP  
Sean Fahey, MD  
V. Michael Holers, MD  
Maura Iversen, BSc, DPT, DSc, MPH, PT  
Jane Kang, MD, MS  
Carol Langford, MD, MHS  
Andrew Laster, MD  
Sam Lim, MD, MPH  
Amanda Myers, CCD, MD  
Deborah Parks, MD  
Tamar Rubinstein, MD, MS  
Eric Ruderman, FACR, MD  
Saira Sheikh, MD  
Nehad Soloman, MD  
Blair Solow, MD  
Swamy Venuturupalli, MD  
Douglas White, MD, PhD

## NOTES FROM THE FIELD

# Overturing Roe v. Wade: Toppling the Practice of Rheumatology

Bonnie L. Bermas,<sup>1</sup> Irene Blanco,<sup>2</sup> Ashira D. Blazer,<sup>3</sup> Megan EB Clowse,<sup>4</sup> Cuoghi Edens,<sup>5</sup> Rosalind Ramsey-Goldman,<sup>2</sup> and Mehret Birru Talabi<sup>6</sup>

## Introduction

On June 24, 2022, the US Supreme Court overturned the landmark Roe v. Wade decision that has guaranteed the right to abortion across the US since 1973. As a result, abortion, per the Court, will be legislated at the state level. Abortion bans drafted by more than half of the states can now be implemented; many more restrictive reproductive legislative efforts are in development. These regulations undermine the autonomy of all persons with gestational capacity. For patients with rheumatic diseases, family planning choices will be limited, thereby severely restricting options for the medical treatment of their rheumatic disorder. The Supreme Court's decision portends grave consequences for the practice of rheumatology as providers weigh delivering evidence-based clinical recommendations against the personal, professional, and legal risks of violating constraints on reproductive rights.

## Pregnancy and rheumatic diseases

Rheumatic diseases disproportionately occur during women's reproductive years. Pregnancies in this population are often high-risk, precipitating disease flares that can cause organ- and life-threatening complications with catastrophic outcomes. For example, systemic lupus erythematosus (SLE) pregnancies have significantly more early-onset and severe preeclampsia with maternal mortality in women with SLE, 20-fold greater than in the healthy population (1). Women with a variety of rheumatic diseases have an increased risk of miscarriage, stillbirth, preeclampsia, preterm delivery, cesarean delivery, and maternal death. Their infants are more likely to be small for their gestational age and

need neonatal intensive care. Pregnancy outcomes are worse when the pregnancy is unplanned or occurs in the midst of organ-threatening disease, such as active lupus nephritis, systemic vasculitis, myositis, or systemic sclerosis.

Patients with rheumatoid arthritis (RA) and other inflammatory arthropathies, including ankylosing spondylitis, psoriatic arthritis, and juvenile idiopathic arthritis (JIA), were historically thought to fare better during pregnancy; nevertheless, recent evidence suggests that these pregnancies are accompanied by high rates of pregnancy-induced hypertension, preeclampsia, cesarean delivery, preterm birth, and preterm premature rupture of the membranes (2). Abortion restrictions will limit options for the management of complicated life-threatening pregnancies and will ultimately have a detrimental effect on maternal and fetal mortality in patients with rheumatic diseases.

## Fetotoxic medications

Evidence-based standard of care for the most common rheumatic conditions includes fetotoxic medications (3). The American College of Rheumatology (ACR) treatment guidelines strongly recommend methotrexate as first-line therapy for several of the most common rheumatic diseases including RA and JIA (4,5). However, methotrexate is teratogenic, and in doses higher than prescribed for rheumatic disease, embryotoxic (6). The medications used for managing the most severe manifestations of SLE are also teratogenic. Mycophenolate (MMF) causes congenital anomalies in up to 25% of fetuses exposed (7). Cyclophosphamide has substantial teratogenic and abortogenic potential (3). Actual numbers of teratogen-exposed pregnancies in rheumatology patients are

The content of this article is solely the responsibility of the authors and does not necessarily represent the official view of any of the authors' funding sources.

All authors contributed equally to this work.

<sup>1</sup>Bonnie L. Bermas, MD: UT Southwestern Medical Center, Dallas, Texas; <sup>2</sup>Irene Blanco, MD, MS, Rosalind Ramsey-Goldman, MD, DrPH: Northwestern University Feinberg School of Medicine, Chicago, Illinois; <sup>3</sup>Ashira D. Blazer, MD, MSCI: Weill Cornell Medicine, Hospital for Special Surgery, New York, New York; <sup>4</sup>Megan EB Clowse, MD, MPH: Duke University School of Medicine, Durham, North Carolina; <sup>5</sup>Cuoghi Edens, MD:

University of Chicago Medicine, Chicago, Illinois; <sup>6</sup>Mehret Birru Talabi, MD, PHD: University of Pittsburgh Department of Medicine, Pittsburgh, Pennsylvania.

Author disclosures are available at <https://onlinelibrary.wiley.com/action/downloadSupplement?doi=10.1002%2Fart.42336&file=art42336-sup-0001-Disclosureform.pdf>.

Address correspondence via email to Bonnie L. Bermas, MD, at [Bonnie.Bermas@UTSouthwestern.edu](mailto:Bonnie.Bermas@UTSouthwestern.edu).

Submitted for publication July 14, 2022; accepted in revised form August 19, 2022.

unknown; however, many of us have encountered this clinical dilemma, almost exclusively after the 6-week timeframe defined by “heartbeat laws.” In the new era of abortion restrictions, many patients who become pregnant while receiving fetotoxic medications will be forced to continue their pregnancies despite the risk of fetal compromise. Thus, the very individuals who are personally impacted by a chronic, disabling, and at times life-threatening diagnosis may be forced to grapple with caring for a medically complex child with congenital anomalies and/or neurodevelopmental delays.

### Abortion in rheumatic disease patients

Annually in the US, the abortion rate is 11.4 per 1,000 women ages 15–44 years. Abortion-related deaths occur in 0.4 per 100,000 procedures, few in comparison to the 17.4 per 100,000 pregnancy-related deaths. Ninety-three percent of abortions are performed earlier than 13 weeks, with fewer than 1% of abortions being performed at gestations of >21 weeks (8). Abortions can be performed medically with a combination of mifepristone and misoprostol, or surgically by uterine aspiration and dilatation and curettage or evacuation (9). In patients with rheumatic diseases, there are no worrisome safety signals for pregnancy termination (10).

### Other proposed contraceptive restrictions

While abortion restriction is concerning enough for rheumatology patients, some anti-abortion activists are introducing legislation to criminalize the use of intrauterine devices (IUDs) and emergency contraception (EC) pills. IUDs are highly effective methods of contraception, reversible, and safe to use among people with rheumatic diseases. IUDs prevent pregnancy through various mechanisms of action: thinning of the uterine lining, damage to spermatozoa, preventing ovulation, and thickening of the cervical mucus that impedes fertilization. EC pills prevent ovulation and halt transport of both sperm and egg, preventing fertilization. Neither of these methods induce an abortion (11).

Currently, the ACR Guideline for the Management of Reproductive Health in Rheumatic and Musculoskeletal Diseases lists IUDs as one of the preferred contraceptives for women with active SLE and/or antiphospholipid antibody syndrome (3). EC pills are deemed medically safe and are recommended by the American College of Obstetrics and Gynecology and the ACR, without restriction, to women with rheumatic and thrombotic conditions (12). Restricting access to IUDs and/or EC leaves our highest-risk patients, who have the greatest need for highly effective contraception, few choices.

### Potential impact of abortion legislation on the practice of rheumatology

A worrisome consequence of abortion restriction is that real or anticipated clinician liability may lead to more conservative prescribing practices. Providers may become unwilling to prescribe evidence-based and appropriate therapies for fear of fetotoxicity. This anxiety will limit access to the most appropriate medications in our patients with childbearing capacity, regardless of medical evidence, effectiveness, or the patient’s individual health needs. For example, if providers avoid guideline-recommended first-line therapy for lupus nephritis, such as cyclophosphamide or MMF, in nonpregnant women with reproductive potential, this will lead to progression of SLE nephritis culminating in higher rates of end-stage renal disease, need for dialysis or renal transplant, and death. Similarly, providers may forego prescribing methotrexate, the foundational treatment for inflammatory arthritis, thereby increasing disability and decreasing quality of life for our patients. In a specialty whose patient population is largely female, restricting specific medical treatments based on one’s potential to become pregnant is clearly medical sexism and prohibited by the Affordable Care Act.

### Vulnerable populations

The burden of rheumatic diseases falls heavily on racial and ethnic minority women, who face both greater morbidity and mortality due to their illness and are also at greatest risk for this assault on reproductive rights. Our patients often carry multiple minoritized identities at the intersection of race, language, gender, disability, and socioeconomic status, and they experience disparities in all aspects of reproductive healthcare. Structural racism inhibits reproductive freedom through coercive counseling and limited contraception access particularly among Black and Indigenous women. Moreover, these women have higher rates of unintended pregnancy and are more likely to have pregnancy-complicating comorbidities. These marginalized groups are often concentrated in states with the most restrictive abortion laws and rheumatology workforce shortages. This, together with biases held by the medical workforce, has led to unacceptably high maternal and infant mortality rates for minority women (13).

Rheumatic disease patients face job loss and disability at higher rates, leading to financial hardship and lack of insurance coverage. Indeed, ~50% of women with SLE will experience work loss within 13 years of diagnosis (14). Women with disabilities are twice as likely to experience sexual violence than nondisabled women, highlighting their need for abortion access. Yet these women will be unable to access abortion services if they do not have the resources required to travel to another state. Being denied the right to abortion further compounds economic distress, propelling patients with severe disease deeper into poverty. Denying safe and often lifesaving abortions to the most vulnerable

among us will undoubtedly drive larger divides between those who can and cannot live well with rheumatic disease.

## Call to action

While the full ramifications of the reversal of *Roe v. Wade* is uncertain, as a rheumatology community, we must prepare for the multitude of ways in which abortion restriction will affect our patients and our practices. Several states have pending legislation that threaten criminal proceedings against patients who obtain abortions, providers who perform these procedures, as well as anyone who “aids or abets” an abortion. While the legal interpretation of the latter is unclear, one could imagine extension of the aid and abet concept to a provider who presents abortion as an option for a pregnant patient even in life-threatening situations. In light of this, we as providers must be vigilant about addressing contraception and family planning with our patients with empathy and knowledge, using tools that our organization has already endorsed such as the Reproductive Health Guidelines (3) and the Reproductive Health Initiative contraception handouts.

The looming nationwide restrictions around abortion, with their anticipated implementation of contraception limitations, will undermine the health and treatment options for the millions of rheumatic disease patients who have childbearing potential, and will leave a lasting impact on the practice of rheumatology and health care in this country. When the early restrictive abortion law was passed in Georgia, prior ACR presidents and members of the Board of Directors were prescient in their reminder to their colleagues that rheumatologists have the “responsibility to practice evidence-based medicine in their [patients’] best interests, and the freedom to do so without political interference” (15). On behalf of our patients, we are compelled to criticize and protest the Supreme Court’s decision to overturn *Roe v. Wade*.

## AUTHOR CONTRIBUTIONS

All authors drafted the article, revised it critically for important intellectual content, and approved the final version to be published.

## REFERENCES

1. Clowse ME, Jamison M, Myers E, et al. A national study of the complications of lupus in pregnancy. *Am J Obstet Gynecol* 2008;199:127.e1–6.
2. Chakravarty EF. Rheumatoid arthritis and pregnancy: beyond smaller and preterm babies [editorial]. *Arthritis Rheum* 2011;63:1469–71.
3. Sammaritano LR, Bermas BL, Chakravarty EE, et al. 2020 American College of Rheumatology guideline for the management of reproductive health in rheumatic and musculoskeletal diseases. *Arthritis Rheumatol* 2020;72:529–56.
4. Fraenkel L, Bathon JM, England BR, et al. 2021 American College of Rheumatology guideline for the treatment of rheumatoid arthritis. *Arthritis Care Res (Hoboken)* 2021;73:924–39.
5. Onel KB, Horton DB, Lovell DJ, et al. 2021 American College of Rheumatology guideline for the treatment of juvenile idiopathic arthritis: therapeutic approaches for oligoarthritis, temporomandibular joint arthritis, and systemic juvenile idiopathic arthritis. *Arthritis Rheumatol* 2022;74:553–69.
6. Hyoun SC, Običan SG, Scialli AR. Teratogen update: methotrexate. *Birth Defects Res A Clin Mol Teratol* 2012;94:187–207.
7. Coscia LA, Armenti DP, King RW, et al. Update on the teratogenicity of maternal mycophenolate mofetil. *J Pediatr Genet* 2015;4:42–55.
8. Kortsmit K, Mandel MG, Reeves JA, et al. Abortion Surveillance—United States, 2019. *MMWR Surveill Summ* 2021;70:1–29.
9. Kapp N, Lohr PA. Modern methods to induce abortion: safety, efficacy and choice. *Best Pract Res Clin Obstet Gynaecol* 2020;63:37–44.
10. Lockshin MD, Guerra M, Salmon JE. Elective termination of pregnancy in autoimmune rheumatic diseases: experience from two databases. *Arthritis Rheumatol* 2020;72:1325–9.
11. Rivera R, Yacobson I, Grimes D. The mechanism of action of hormonal contraceptives and intrauterine contraceptive devices. *Am J Obstet Gynecol* 1999;181:1263–9.
12. Practice Bulletin No. 152. *Obstet Gynecol* 2015;126:e1–11.
13. Greenwood BN, Hardeman RR, Huang L, et al. Physician-patient racial concordance and disparities in birthing mortality for newborns. *Proc Natl Acad Sci U S A* 2020;117:21194–200.
14. Drenkard C, Bao G, Dennis G, et al. Burden of systemic lupus erythematosus on employment and work productivity: data from a large cohort in the southeastern United States. *Arthritis Care Res (Hoboken)* 2014;66:878–87.
15. Craft JE, Crow MK, Lockshin MD, et al. Georgia abortion law and our commitment to patients [letter]. *Arthritis Rheumatol* 2020;72:377–8.

## NOTES FROM THE FIELD

# The Evolving Role of the Rheumatology Practitioner in the Care of Immunocompromised Patients in the COVID-19 Era

Leonard H. Calabrese,<sup>1</sup>  Cassandra M. Calabrese,<sup>1</sup> Elizabeth Kirchner,<sup>1</sup> and Kevin Winthrop<sup>2</sup> 

## Introduction

The impact of the global COVID-19 pandemic on the field of rheumatology has been dramatic and broad-ranging. These effects include the pandemic's ongoing influence on models of care delivery, the intermittent impact on drug availability to our patients, and the output of research our field has contributed to increasing our understanding of the disease's epidemiology, basic and clinical immunology, clinical outcomes, and vaccinology in immunocompromised hosts. The next phase of the pandemic cannot be totally predicted, but there is broad agreement that SARS-CoV-2 as a global pathogen is unlikely to disappear quietly; the virus appears to be becoming endemic, and it is likely we will face continued emerging variants of unpredictable pathogenicity.

If this prediction comes to fruition, SARS-CoV-2 infections will likely impact the population along 2 different paths. The first and most common scenario will be new or recurrent infection among healthy, previously exposed, or vaccinated individuals whose disease course will, in the vast majority of cases, be of lesser severity and low mortality. The second more troubling scenario will occur with infections in our immunocompromised patients who, even if vaccinated, are more likely to experience severe outcomes from the disease (1,2). We, as rheumatologists, must prepare for the latter scenario even though it is yet to be determined what will constitute best practice models for both prevention and care for our immunocompromised patients. There is clearly no one-size-fits-all approach, as rheumatologists practice in many different models of care, ranging from solo practices to small- and large-group practices, multispecialty, and hospital-based practices; in each of these settings, practitioners have access to varying levels of resources. The goals, however, are the same for all of us: protecting our most vulnerable patients from infection wherever possible and contributing to providing or

directing those who become infected to the best possible care. While these goals seem unassailable, they raise important questions about the boundaries of rheumatologic care. These questions are similar, in some ways, to the controversies surrounding our role in the care of other non-rheumatologic problems: cardiovascular risk management, diagnosis and treatment of infections, providing vaccinations, and management of other medical problems in patients with complex conditions.

One could easily ask whether COVID-19 should be considered different from any other medical problem we may either treat ourselves or refer to others. We believe it is different, and accordingly, we would like to start a discussion within the rheumatology profession in this call to action by posing a series of questions and possible answers regarding how these goals may be achieved.

## Which of our immunocompromised patients are of highest concern?

Defining and determining precisely who is immunocompromised is surprisingly difficult and a work continually in progress. Definitions put forth by the Centers for Disease Control and Prevention (CDC) (3) are inadequate and note that such determination may be best arrived at in consultation with a specialist. Data from numerous studies including the COVID-19 Global Rheumatology Alliance (4) and others (5) have provided insights into epidemiologic factors imparting risk, including comorbidities, disease activity, and the use of certain immunomodulatory drugs, especially rituximab and glucocorticoids. While the utility of measuring serologic response to vaccine has also been discouraged by the CDC (6) and is not currently recommended by the American College of Rheumatology (ACR) COVID-19 Vaccine Task Force due to lack of supportive data at the time of last guidance release,

<sup>1</sup>Leonard H. Calabrese, DO, Cassandra M. Calabrese, DO, Elizabeth Kirchner, DNP: Department of Rheumatologic and Immunologic Disease, Cleveland Clinic, Cleveland, Ohio; <sup>2</sup>Kevin Winthrop, MD, MPH: Division of Infectious Diseases, Oregon Health & Science University, Portland.

Author disclosures are available at <https://onlinelibrary.wiley.com/action/downloadSupplement?doi=10.1002%2Fart.42334&file=art42334-sup-0001-Disclosureform.pdf>.

Address correspondence via email to Leonard H. Calabrese, DO, at [calabrl@ccf.org](mailto:calabrl@ccf.org).

Submitted for publication July 19, 2022; accepted in revised form August 17, 2022.



other groups such as the transplantation community (7) have advocated for such testing to identify the most vulnerable among their patients. The status quo of such a nonspecific definition is not acceptable, and we urgently need to develop more quantitative biomarkers, both clinical and laboratory-based, to identify those among our community who are most at risk and need prioritization of resources.

### **What role can rheumatologists play in prevention of COVID-19?**

While prevention of infection is clearly the most desirable strategy for limiting the effects of COVID-19 on our immunocompromised patients, our capacity to achieve this with continued viral evolutionary escape has become challenging, and we have more realistically moved to preventing severe outcomes, including death from primary or breakthrough infection, as our highest priority. The most powerful preventive measure currently available against severe clinical outcomes is vaccination; however, both patients and practitioners are often confused by the rapidly changing guidelines for immunocompromised individuals, as well as the general community, and thus need to be continually educated. Despite strong evidence of benefit from vaccination, additional dosing, and boosting, it is unfortunate that not all of our patients are willing or able to be vaccinated (8). Furthermore, and implicit in the definition of the immunocompromised state, those most heavily immunocompromised are unlikely to fully respond, both immunologically and clinically, to vaccinations; this includes those receiving rituximab as well as other immunosuppressive therapies (2,9).

Providing clear education to our most immunocompromised patients regarding the continued use of some level of nonpharmacologic measures of infection, including masking in public and social distancing when appropriate, is also important (10). Most important for the most severely immunocompromised patients, however, is preexposure prophylaxis with tixagevimab and cilgavimab, which have been demonstrated to significantly reduce the likelihood and severity of COVID-19 (11). Often unclear is exactly who on the health care team should initiate such discussions and referrals, which may lead to lapses in administration to those who would benefit most. Consideration of individual practices and groups should be given to system-based screening of patient treatment records to identify those at the highest risk, such as those undergoing B cell-depletion therapy, and proactively contact those patients to ensure that preexposure prophylaxis has been offered and encouraged. It is our belief that the rheumatologist should take the lead in preexposure prophylaxis and accordingly must commit to both learning about the therapy and becoming familiar with how and where it can be accessed in their area.

### **What is our role in outpatient treatment of COVID-19?**

Rheumatologists in general will have a limited role in managing patients hospitalized with COVID-19, but they will be confronted with determining what their role is in diagnosing and managing outpatients. The armamentarium of COVID-19 outpatient treatments is rapidly growing (12) and includes monoclonal antibodies (a constantly changing option due to viral escape), which need to be administered within a specific timeline (generally 7–10 days) (13), as well as both a single parenteral and several oral antiviral agents, which must also be given within a critical time window (i.e., 0–5 days after symptom onset for oral therapies, 0–7 days for parenteral therapy) (12). With this in mind, we believe that rheumatology practitioners must educate our immunocompromised patients on how to be rapidly diagnosed and treated, in the event that they do become infected (Figure 1). Such education includes an understanding of the time urgency of available therapies, vigilance for early signs or symptoms of COVID-19, and encouraging access to rapid testing (preferably at home). Another critical step in optimal COVID-19 outpatient care is clear awareness of who to call once an immunocompromised patient is diagnosed or strongly suspected of having COVID-19; such a resource (i.e., physician, advanced practitioner, consultant) can then direct the patient to the appropriate outpatient treatment without delay. Each practice setting, whether solo, small- or large-group, or academic center should have its own network of consultants to refer patients to or commit to take it upon themselves to initiate such therapies.

Finally, it is unknown whether our immunocompromised patients will have more severe or more frequent sequelae from COVID-19 (post-acute sequelae of COVID-19, or long COVID), but early research demonstrates that prolonged symptom duration is common in our patients (14). Given the current lack of firm diagnostic criteria or biomarkers and no evidence-based therapies, the profession will have to remain engaged in active research to answer these questions; our future role in diagnosis and management for now is far from clear.

### **What educational resources are available to rheumatologists?**

Defining our role in this rapidly changing landscape of care will continue to be challenging, and we propose that, at minimum, rheumatologists should maintain declarative knowledge of COVID-19, allowing them to educate their immunocompromised patients, critically appraise the data on preventative and therapeutic options, and be able to prescribe or at least direct immunocompromised patients to the most current and effective care pathway in the event of infection. Given the explosion of peer-

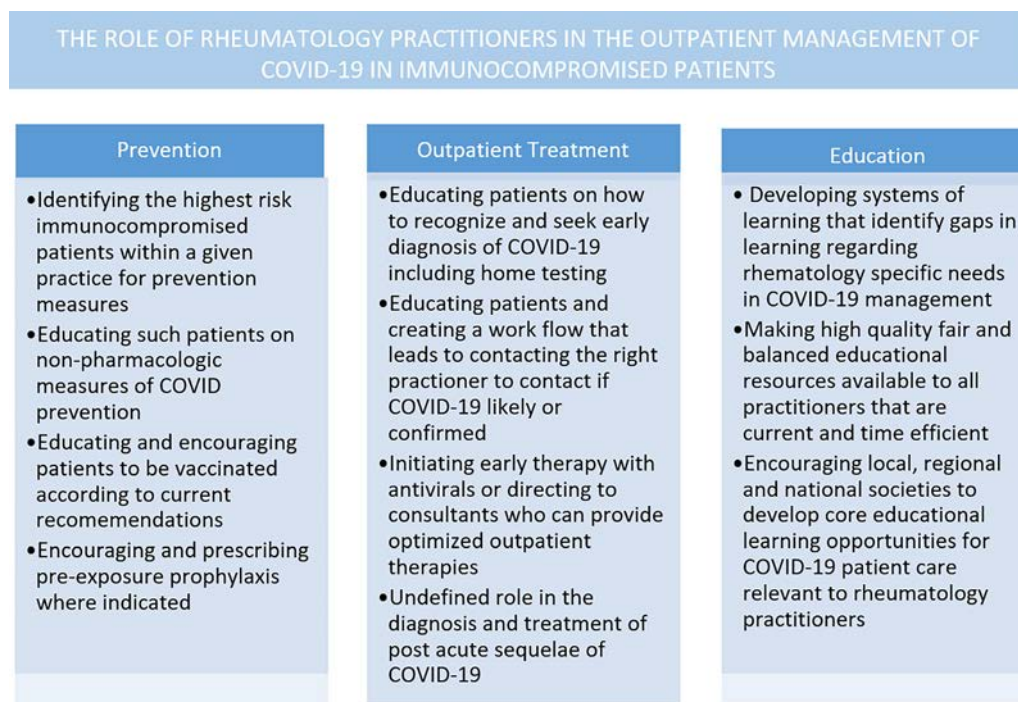


**Figure 1.** Considerations for the role of rheumatology practitioners in COVID-19 outpatient management in immunocompromised patients, including prevention, treatment, and practitioner education.

reviewed publications, pre-peer review publications, and online sources of unfiltered data often referred to as gray literature (e.g., as of July 1, 2022, there are >11 billion citations on COVID-19), it is more challenging than ever to be confident in our knowledge base regarding the changing practice standards for COVID-19 prevention and management. As a result, most practitioners must rely on real-time or living guidelines on disease management from organizations invested in providing such guidance. Examples of such information include the National Institutes of Health, CDC, Infectious Disease Society of America, and the ongoing efforts by the ACR (15), which summarize and provide the best available evidence, including vaccine recommendations, nonpharmacologic and pharmacologic preventive measures, and outpatient therapeutic options. Rheumatology meetings and educational venues must also step in to address clinical needs surrounding prevention and management for the practitioner in addition to presenting the latest basic and clinical science on the disease. The road ahead unfortunately appears to be a long one, and we as professionals who manage immunocompromised patients have an additional formidable challenge to address through education, prevention, and management (12).

## AUTHOR CONTRIBUTIONS










All authors drafted the article, revised it critically for important intellectual content, and approved the final version to be published.

## REFERENCES

1. Singson JR, Kirley PD, Pham H, et al. Factors associated with severe outcomes among immunocompromised adults hospitalized for COVID-19—COVID-NET, 10 States, March 2020–February 2022. *MMWR Morb Mortal Wkly Rep* 2022;71:878–84.
2. Calabrese CM, Kirchner E, Husni EM, et al. Breakthrough SARS-CoV-2 infections in immune mediated disease patients undergoing B cell depleting therapy: a retrospective cohort analysis. *Arthritis Rheumatol* 2022;74:1906–15.
3. Centers for Disease Control and Prevention. COVID-19 vaccines for people who are moderately or severely immunocompromised, 2022. URL: <https://www.cdc.gov/coronavirus/2019-ncov/vaccines/recommendations/immuno.html>.
4. Sparks JA, Wallace ZS, Seet AM, et al. Associations of baseline use of biologic or targeted synthetic DMARDs with COVID-19 severity in rheumatoid arthritis: Results from the COVID-19 Global Rheumatology Alliance physician registry. *Ann Rheum Dis* 2021;80:1137–46.
5. Conway R, Grimshaw AA, König MF, et al. SARS-CoV-2 infection and COVID-19 outcomes in rheumatic disease: a systematic literature review and meta-analysis. *Arthritis Rheumatol* 2021;74:766–75.
6. Centers for Disease Control and Prevention. Interim guidelines for COVID-19 antibody testing, 2022. URL: <https://www.cdc.gov/coronavirus/2019-ncov/lab/resources/antibody-tests-guidelines.html>.
7. Werbel WA, Segev DL. SARS-CoV-2 antibody testing for transplant recipients: a tool to personalize protection versus COVID-19. *Am J Transplant* 2022;22:1316–20.
8. Boekel L, Hooijberg F, van Kempen ZL, et al. Perspective of patients with autoimmune diseases on COVID-19 vaccination. *Lancet Rheumatol* 2021;3:e241–3.

9. Deepak P, Kim W, Paley MA, et al. Effect of immunosuppression on the immunogenicity of mRNA vaccines to SARS-CoV-2 : a prospective cohort study. *Ann Intern Med* 2021;174:1572–85.
10. Centers for Disease Control and Prevention. How to protect yourself & others, 2022. URL: <https://www.cdc.gov/coronavirus/2019-ncov/lab/resources/antibody-tests-guidelines.html>.
11. Levin MJ, Ustianowski A, De Wit S, et al. Intramuscular AZD7442 (tixagevimab-cilgavimab) for prevention of Covid-19. *N Engl J Med* 2022; 386:2188–2200.
12. Bhimraj A, Morgan RL, Shumaker AH, et al. IDSA guidelines on the treatment and management of patients with COVID-19. *Clin Infect Dis* 2020. Doi: <https://doi.org/10.1093/cid/ciaa478>. E-pub ahead of print.
13. Focosi D, McConnell S, Casadevall A, et al. Monoclonal antibody therapies against SARS-CoV-2 [review]. *Lancet Infect Dis* 2022. Doi: <https://doi.org/10.1016/s1473-309900311-5>. E-pub ahead of print.
14. Di Iorio M, Cook CE, Vanni KM, et al. DMARD disruption, rheumatic disease flare, and prolonged COVID-19 symptom duration after acute COVID-19 among patients with rheumatic disease: a prospective study. *Semin Arthritis Rheum* 2022;55:152025.
15. Curtis JR, Johnson SR, Anthony DD, et al. American College of Rheumatology guidance for COVID-19 vaccination in patients with rheumatic and musculoskeletal diseases: version 4. *Arthritis Rheumatol* 2022;74:e21–36.

# 2022 American College of Rheumatology/EULAR Classification Criteria for Takayasu Arteritis

Peter C. Grayson,<sup>1</sup>  Cristina Ponte,<sup>2</sup>  Ravi Suppiah,<sup>3</sup> Joanna C. Robson,<sup>4</sup>  Katherine Bates Gribbons,<sup>1</sup> Andrew Judge,<sup>5</sup>  Anthea Craven,<sup>6</sup>  Sara Khalid,<sup>6</sup> Andrew Hutchings,<sup>7</sup>  Debashish Danda,<sup>8</sup>  Raashid A. Luqmani,<sup>6</sup>  Richard A. Watts,<sup>9</sup> and Peter A. Merkel<sup>10</sup> , for the DCVAS Study Group

*This criteria set has been approved by the American College of Rheumatology (ACR) Board of Directors and the EULAR Executive Committee. This signifies that the criteria set has been quantitatively validated using patient data, and it has undergone validation based on an independent data set. All ACR/EULAR-approved criteria sets are expected to undergo intermittent updates.*

*The ACR is an independent, professional, medical and scientific society that does not guarantee, warrant, or endorse any commercial product or service.*

**Objective.** To develop and validate new classification criteria for Takayasu arteritis (TAK).

**Methods.** Patients with vasculitis or comparator diseases were recruited into an international cohort. The study proceeded in 6 phases: 1) identification of candidate criteria items, 2) collection of candidate items present at diagnosis, 3) expert panel review of cases, 4) data-driven reduction of candidate items, 5) derivation of a points-based classification score in a development data set, and 6) validation in an independent data set.

**Results.** The development data set consisted of 316 cases of TAK and 323 comparators. The validation data set consisted of an additional 146 cases of TAK and 127 comparators. Age  $\leq 60$  years at diagnosis and imaging evidence of large-vessel vasculitis were absolute requirements to classify a patient as having TAK. The final criteria items and weights were as follows: female sex (+1), angina (+2), limb claudication (+2), arterial bruit (+2), reduced upper extremity pulse (+2), reduced pulse or tenderness of a carotid artery (+2), blood pressure difference between arms of  $\geq 20$  mm Hg (+1), number of affected arterial territories (+1 to +3), paired artery involvement (+1), and abdominal aorta plus renal or mesenteric involvement (+3). A patient could be classified as having TAK with a cumulative score of  $\geq 5$  points. When these criteria were tested in the validation data set, the model area under the curve was 0.97 (95% confidence interval [95% CI] 0.94–0.99) with a sensitivity of 93.8% (95% CI 88.6–97.1%) and specificity of 99.2% (95% CI 96.7–100.0%).

**Conclusion.** The 2022 American College of Rheumatology/EULAR classification criteria for TAK are now validated for use in research.

This article is published simultaneously in *Annals of the Rheumatic Diseases*.

The Diagnostic and Classification Criteria in Vasculitis (DCVAS) study, which included the development of this classification criteria, was funded by grants from the American College of Rheumatology (ACR), EULAR, the Vasculitis Foundation, and the University of Pennsylvania Vasculitis Center. This study was also supported by the Intramural Research Program of the National Institute of Arthritis and Musculoskeletal and Skin Diseases, NIH.

<sup>1</sup>Peter C. Grayson, MD, MSc, Katherine Bates Gribbons, BS: Systemic Autoimmunity Branch, National Institute of Arthritis and Musculoskeletal and Skin Diseases, NIH, Bethesda, Maryland; <sup>2</sup>Cristina Ponte, MD, PhD: Department of Rheumatology, Centro Hospitalar Universitário Lisboa Norte, Centro Académico de Medicina de Lisboa, Lisbon, Portugal, and Rheumatology Research

Unit, Instituto de Medicina Molecular, Faculdade de Medicina, Universidade de Lisboa, Centro Académico de Medicina de Lisboa, Lisbon, Portugal; <sup>3</sup>Ravi Suppiah, MBChB, MD, FRACP: Te Whatu Ora - Health New Zealand, Auckland, New Zealand; <sup>4</sup>Joanna C. Robson, MBBS, PhD: Centre for Health and Clinical Research, University of the West of England, and Rheumatology Department, University Hospitals Bristol and Weston NHS Foundation Trust, Bristol, UK; <sup>5</sup>Andrew Judge, PhD: Nuffield Department of Orthopaedics Rheumatology and Musculoskeletal Sciences, Oxford NIHR Biomedical Research Centre, University of Oxford, Oxford, UK, Musculoskeletal Research Unit, Translational Health Sciences, Bristol Medical School, University of Bristol, Bristol, UK, and National Institute for Health Research Bristol Biomedical Research Centre, University Hospitals Bristol and Weston NHS Foundation Trust and University of Bristol, Bristol, UK; <sup>6</sup>Anthea Craven, BSc, Sara Khalid, DPhil, Raashid A.

## INTRODUCTION

Takayasu arteritis (TAK) is one of the major forms of large-vessel vasculitis (LVV) (1). TAK is a chronic disease defined by granulomatous inflammation affecting the aorta and its primary branches. Complications from vascular damage can result in substantial morbidity including stroke, myocardial infarction, mesenteric ischemia, and limb claudication.

Unlike diagnostic criteria, the purpose of classification criteria is to ensure that a homogenous population is selected for inclusion into clinical trials and other research studies (2). In 1990, the American College of Rheumatology (ACR) endorsed classification criteria for TAK (3). These criteria were developed using data from only 63 patients with TAK and have never been independently validated. Additionally, these criteria were derived using data from patients exclusively from North America without representation from Europe or Asia, where clinical patterns of disease may differ (4), limiting the generalizability of results. Given these constraints, the 1990 ACR criteria for TAK no longer satisfy accepted current standards (5) for classification criteria development, and updated criteria are warranted. Further highlighting a need for uniform, revised criteria in TAK is the use of divergent eligibility criteria to define study populations in 2 recent randomized clinical trials conducted in North America and Japan, making comparisons between the trial findings difficult (6,7).

Advancements in imaging techniques and the ongoing adoption of noninvasive vascular imaging approaches in clinical practice have broadened understanding of the clinical heterogeneity in LVV (8). Disease of the extracranial arteries is increasingly recognized in patients with giant cell arteritis (GCA), making the distinction between TAK and GCA more challenging (9). Age is typically used as a primary classifier to differentiate between TAK and GCA; however, specific age thresholds to define each disease have not been standardized. Therefore, in addition to incorporating data from a larger patient population from a wider geographic spectrum, the updated TAK classification criteria should reflect modern clinical practice, including current imaging techniques, and also define specific age thresholds.

This article outlines the development and validation of the new ACR/EULAR-endorsed classification criteria for TAK.

## METHODS

An international Steering Committee comprising clinician investigators with expertise in vasculitis, statisticians, and data

managers was established to oversee the overall development of classification criteria for primary vasculitis (10). A detailed and complete description of the methods involved in the development and validation of the classification criteria for TAK is located in Supplementary Appendix 1 (<http://onlinelibrary.wiley.com/doi/10.1002/art.42324>). Briefly, the Steering Committee implemented a 6-stage plan using data-driven and consensus methodology to develop the following criteria.

**Stage 1: generation of candidate classification items for the systemic vasculitides.** Candidate classification items were generated by expert opinion and reviewed by a group of vasculitis experts across a range of specialties using nominal group technique.

**Stage 2: Diagnostic and Classification Criteria for Vasculitis (DCVAS) prospective observational study.** A prospective, international, multisite observational study was conducted (see Appendix A for study investigators and sites). Ethical approval was obtained from local ethics committees. Consecutive patients representing the full spectrum of vasculitides were recruited from academic and community practices. Patients were included if they were 18 years or older and had a diagnosis of vasculitis or a condition that mimics vasculitis (e.g., infection, malignancy, atherosclerosis). Patients with TAK could only be enrolled within 5 years of diagnosis. Only data present at diagnosis were used to develop the classification criteria.

**Stage 3: expert review to derive a gold standard-defined set of cases of LVV.** Experts in vasculitis from a wide range of geographic locations and specialties (see Appendix A) reviewed all submitted cases of vasculitis and a random selection of vasculitis mimics. Each reviewer was asked to review ~50 submitted cases to confirm the diagnosis and to specify the degree of certainty of their diagnosis as follows: very certain, moderately certain, uncertain, or very uncertain. Only cases agreed upon with at least moderate certainty by 2 reviewers were retained for further analysis.

**Stage 4: refinement of candidate items specifically for LVV.** The Steering Committee conducted a data-driven process to reduce the number of candidate items of relevance to cases

Luqmani, DM, FRCP: Nuffield Department of Orthopaedics Rheumatology and Musculoskeletal Sciences, Oxford NIHR Biomedical Research Centre, University of Oxford, Oxford, UK; <sup>7</sup>Andrew Hutchings, MSc: Department of Health Services Research and Policy, London School of Hygiene and Tropical Medicine, London, UK; <sup>8</sup>Debashish Danda, MD, DM, FRCP: Department of Clinical Immunology and Rheumatology, Christian Medical College, Vellore, Tamil Nadu, India; <sup>9</sup>Richard A. Watts, MD: Nuffield Department of Orthopaedics, Rheumatology and Musculoskeletal Sciences, Oxford NIHR Biomedical Research Centre, University of Oxford, Oxford, UK, and Norwich Medical School, University of East Anglia, Norwich, UK; <sup>10</sup>Peter A. Merkel, MD, MPH:

Division of Rheumatology, Department of Medicine, and Division of Epidemiology, Department of Biostatistics, Epidemiology, and Informatics, University of Pennsylvania, Philadelphia.

Author disclosures are available at <https://onlinelibrary.wiley.com/action/downloadSupplement?doi=10.1002%2Fart.42324&file=art42324-sup-0001-Disclosureform.pdf>.

Address correspondence via email to Peter A. Merkel, MD, MPH, at [pmerkel@upenn.edu](mailto:pmerkel@upenn.edu).

Submitted for publication February 14, 2022; accepted in revised form July 30, 2022.



and comparators for LVV. Density plots were assessed to study age distribution at diagnosis and symptom onset for TAK and GCA. Absolute age requirements versus incorporation of age as a candidate criteria item were considered. Items related to the vascular physical examination, vascular imaging, arterial biopsy, and laboratory values were combined or eliminated based on consensus review. Items were selected for exclusion if they had a prevalence of <5% within the data set, and/or they were not clinically relevant for classification criteria (e.g., related to infection, malignancy, or demography). Low-frequency items of clinical importance could be combined, when appropriate. Patterns of vascular imaging findings detected by vascular ultrasound, angiography, or positron emission tomography were defined by K-means clustering (11).

**Stage 5: derivation of the final classification criteria for TAK.** The DCVAS data set was split into development (70%) and validation (30%) sets. Comparisons were performed between cases of TAK and a randomly selected comparator group in the following proportions: GCA, 33.6%; other vasculitides that mimic GCA and TAK (isolated aortitis, primary central nervous system vasculitis, polyarteritis nodosa, Behçet's disease, and other LVV), 33.1%; a comparator mimic of LVV (e.g., headache syndrome or atherosclerosis), 33.3%. Least absolute shrinkage and selection operator (lasso) logistic regression was used to identify predictors from the data set and create a parsimonious model including only the most important predictors. The final items in the model were formulated into a clinical risk-scoring tool, with each factor assigned a weight based on its respective regression coefficient. A threshold that best balanced sensitivity and specificity was identified for classification.

**Stage 6: validation of the final classification criteria for TAK.** Performance of the new criteria was validated in an independent set of cases and comparators. Performance of the final classification criteria was examined in specific subsets of patients with TAK using data from the combined development and validation sets, to maximize sample sizes for the subgroups. Patients were studied according to different intervals of age at diagnosis to determine if the criteria performed well across the age spectrum of TAK. Performance characteristics of the new criteria were also tested in patients recruited into the DCVAS study from different regions of the world where prevalence of TAK and clinical assessment approaches may differ. Comparison was made between the measurement properties of the new 2022 ACR/EULAR classification criteria for TAK and the 1990 ACR classification criteria.

## RESULTS

**Generation of candidate classification items for the systemic vasculitides.** The Steering Committee identified >1,000 candidate items for the DCVAS Case Report Form

(Supplementary Appendix 2, <http://onlinelibrary.wiley.com/doi/10.1002/art.42324>).

**DCVAS prospective observational study.** Between January 2011 and December 2017, the DCVAS study recruited 6,991 participants from 136 sites in 32 countries. Information on the DCVAS sites, investigators, and study participants is listed in Supplementary Appendices 3, 4, and 5 (<http://onlinelibrary.wiley.com/doi/10.1002/art.42324>).

**Expert review methodology to derive a gold standard-defined final set of cases of LVV.** The LVV expert panel review process included 56 experts who reviewed vignettes derived from the Case Report Forms for 2,131 cases submitted with a diagnosis of LVV (1,608 [75.5% of Case Report Forms]), another type of vasculitis (118 [5.5% of Case Report Forms]), or a mimic of vasculitis (405 [19.0% of Case Report Forms]). Characteristics and the list of expert reviewers are shown in Supplementary Appendices 6 and 7 (<http://onlinelibrary.wiley.com/doi/10.1002/art.42324>). A sample vignette and the LVV expert panel review flow chart are shown in Supplementary Appendices 8 and 9. A total of 1,695 cases (80%) passed the main LVV process. An additional 373 cases of LVV and comparators, confirmed during a previous review process to derive the classification criteria for antineutrophil cytoplasmic antibody-associated vasculitis, were also included. In total, after both review processes, 2,068 cases were available for the stages 4 and 5 analyses.

The submitting physician diagnosis of TAK was confirmed in 500 of 610 cases (82.0%) after both expert panel reviews. The reasons for exclusion were diagnosis of TAK categorized as “uncertain” or “very uncertain” during panel review ( $n = 95$ ) or change in diagnosis during panel review to another type of vasculitis (e.g., GCA, isolated aortitis, LVV that could not be subtyped) ( $n = 10$ ) or to a comparator disease ( $n = 5$ ). An additional 9 patients who were not initially diagnosed as having TAK by the submitting physician were diagnosed as having TAK after panel review and DCVAS Steering Committee member adjudication. Per Steering Committee consensus, imaging evidence of LVV was considered an absolute requirement to classify TAK. Of 509 cases confirmed by expert panel review, 47 patients with TAK did not have documented disease according to a vascular imaging study and were excluded from further analysis, leaving a total of 462 patients with TAK for subsequent analysis.

### Refinement of candidate items specifically for TAK.

Patients with TAK were diagnosed in the following age groups: 18–39 years ( $n = 355$ ; 77%); 40–60 years ( $n = 104$ ; 23%); and >60 years ( $n = 3$ ; <1%) (see Supplementary Appendix 10 for the distribution of “age at diagnosis” in patients with LVV, and the similar distribution of “age at symptom onset,” <http://onlinelibrary.wiley.com/doi/10.1002/art.42324>). Therefore, an age

of  $\leq 60$  years at diagnosis was considered an absolute requirement to classify a patient as having TAK.

Prevalence of arterial damage (stenosis, occlusion, or aneurysm) was greater in TAK compared to GCA in the following 9 arterial territories: thoracic aorta, abdominal aorta, left and right carotid, left and right subclavian, mesenteric, and left and right renal arteries (Supplementary Appendix 11, <http://onlinelibrary.wiley.com/doi/10.1002/art.42324>). Therefore, a composite variable representing the number of affected arteries was created based upon luminal damage in those 9 territories. As previously reported, cluster analyses identified vascular damage in the abdominal aorta and the renal or mesenteric arteries as a specific imaging pattern for TAK in the DCVAS cohort (11); thus, this arterial pattern was tested as a potential classifier of TAK (Supplementary Appendix 12, <http://onlinelibrary.wiley.com/doi/10.1002/art.42324>). Symmetric disease in branch arteries (carotid, subclavian, and renal arteries) was seen in 30.3% patients with TAK compared to 2.7% of the comparators ( $P < 0.01$ ) and, therefore, was included as a potential classifier. A systolic blood pressure difference of  $\geq 20$  mm Hg between upper extremities optimized specificity to differentiate TAK from other forms of LVV.

Following a data-driven and expert consensus process, 72 items from the DCVAS Case Report Form were retained for lasso regression analysis, including 32 demographic and clinical items, 14 laboratory items (including values of C-reactive protein level and erythrocyte sedimentation rate, each divided into 5 categories), 14 imaging items (13 composite), 11 vascular examination items (5 composite, and upper extremity blood pressure

divided into 6 categories), and 1 arterial biopsy item (Supplementary Appendix 13, <http://onlinelibrary.wiley.com/doi/10.1002/art.42324>). Criteria for TAK and GCA were independently derived from this common set of 72 items.

### Derivation of the final classification criteria for TAK.

Table 1 lists the demographic and disease features of the 462 patients with TAK and 450 comparators used to develop and validate the criteria, of which 316 patients with TAK and 323 comparators were in the development data set and 146 patients with TAK and 127 comparators were in the validation data set. The patients with TAK were recruited from Asia ( $n = 298$ ), Europe ( $n = 130$ ), North America ( $n = 28$ ), Africa ( $n = 3$ ), and Oceania ( $n = 3$ ). Clinical diagnoses assigned to patients in the comparator group are detailed in Supplementary Appendix 14 (<http://onlinelibrary.wiley.com/doi/10.1002/art.42324>).

Lasso logistic regression analysis using all 72 items resulted in a model of 9 independent items (Supplementary Appendix 15B, <http://onlinelibrary.wiley.com/doi/10.1002/art.42324>). Weighting of individual criterion was based on logistic regression fitted to the 9 selected predictors. The number of affected arterial territories functioned as an almost perfect classifier (Supplementary Appendix 16B) and was thus also included in the final model, with criterion weighting determined by consensus of the Steering Committee (Supplementary Appendix 17B).

### Validation of the final classification criteria for TAK.

Using a cutoff of  $\geq 5$  in total risk score in the validation data set (see Supplementary Appendix 18B for cutoff points), the sensitivity was

**Table 1.** Demographic and disease features of the patients with Takayasu arteritis and the comparators\*

	TAK (n = 462)	Comparators (n = 450)†	P
Age, mean $\pm$ SD years	32.3 $\pm$ 10.4	58.6 $\pm$ 18.0	<0.001
Female sex	391 (84.6)	246 (54.7)	<0.001
Clinical features			
Angina	56 (12.1)	7 (1.6)	<0.001
Arm claudication	233 (50.4)	11 (2.4)	<0.001
Leg claudication	88 (19.0)	17 (3.8)	<0.001
Vascular examination findings			
Arterial bruit	263 (56.9)	32 (7.1)	<0.001
Reduced or absent pulse in upper extremity	309 (66.9)	16 (3.6)	<0.001
Carotid artery with reduced pulse or tenderness	171 (37.0)	16 (3.6)	<0.001
Difference in systolic blood pressure $\geq 20$ mm Hg between arms	190 (41.1)	16 (3.6)	<0.001
Imaging findings			
1 affected arterial territory	76 (16.5)	36 (8.0)	<0.001
2 affected arterial territories	114 (24.7)	12 (2.7)	<0.001
$\geq 3$ affected arterial territories	89 (19.2)	5 (1.1)	<0.001
Vasculitis affecting paired branch arteries	140 (30.3)	12 (2.7)	<0.001
Abdominal aorta involvement with renal or mesenteric artery involvement	83 (18.0)	5 (1.1)	<0.001

\* Except where indicated otherwise, values are the number (%).

† Diagnoses of comparators for the classification criteria for Takayasu arteritis (TAK) included giant cell arteritis ( $n = 151$ ), Behçet's disease ( $n = 80$ ), polyarteritis nodosa ( $n = 39$ ), clinically isolated aortitis ( $n = 12$ ), primary central nervous system vasculitis ( $n = 11$ ), large-vessel vasculitis (LVV) that could not be subtyped ( $n = 7$ ), and other diseases that mimic LVV ( $n = 150$ ).

93.8% (95% confidence interval [95% CI] 88.6–97.1%), and the specificity was 99.2% (95% CI 96.7–100.0%). The area under the curve for the model was 0.97 (95% CI 0.94–0.99) (Supplementary Appendix 19B, <http://onlinelibrary.wiley.com/doi/10.1002/art.42324>).

The final classification criteria for TAK are shown in Figure 1 (for the slide presentation versions, see Supplementary Figure 1, <http://onlinelibrary.wiley.com/doi/10.1002/art.42324>).

## 2022 AMERICAN COLLEGE OF RHEUMATOLOGY / EULAR

### CLASSIFICATION CRITERIA FOR **TAKAYASU ARTERITIS**

#### CONSIDERATIONS WHEN APPLYING THESE CRITERIA

- These classification criteria should be applied to classify the patient as having Takayasu arteritis when a diagnosis of medium-vessel or large-vessel vasculitis has been made
- Alternate diagnoses mimicking vasculitis should be excluded prior to applying the criteria

#### ABSOLUTE REQUIREMENTS

Age ≤ 60 years at time of diagnosis

Evidence of vasculitis on imaging<sup>1</sup>

#### ADDITIONAL CLINICAL CRITERIA

Female sex	+1
Angina or ischemic cardiac pain	+2
Arm or leg claudication	+2
Vascular bruit <sup>2</sup>	+2
Reduced pulse in upper extremity <sup>3</sup>	+2
Carotid artery abnormality <sup>4</sup>	+2
Systolic blood pressure difference in arms ≥ 20 mm Hg	+1

#### ADDITIONAL IMAGING CRITERIA

Number of affected arterial territories (select one) <sup>5</sup>	
One arterial territory	+1
Two arterial territories	+2
Three or more arterial territories	+3
Symmetric involvement of paired arteries <sup>6</sup>	+1
Abdominal aorta involvement with renal or mesenteric involvement <sup>7</sup>	+3

**Sum the scores for 10 items, if present. A score of ≥ 5 points is needed for the classification of **TAKAYASU ARTERITIS**.**

1. Evidence of vasculitis in the aorta or branch arteries must be confirmed by vascular imaging (e.g., computed tomographic/catheter-based/magnetic resonance angiography, ultrasound, positron emission tomography).
2. Bruit detected by auscultation of a large artery, including the aorta, carotid, subclavian, axillary, brachial, renal, or iliofemoral arteries.
3. Reduction or absence of pulse by physical examination of the axillary, brachial, or radial arteries.
4. Reduction or absence of pulse of the carotid artery or tenderness of the carotid artery.

5. Number of arterial territories with luminal damage (e.g., stenosis, occlusion, or aneurysm) detected by angiography or ultrasonography from the following nine territories: thoracic aorta, abdominal aorta, mesenteric, left or right carotid, left or right subclavian, left or right renal arteries.
6. Bilateral luminal damage (stenosis, occlusion, or aneurysm) detected by angiography or ultrasonography in any of the following paired vascular territories: carotid, subclavian, or renal arteries.
7. Luminal damage (stenosis, occlusion, aneurysm) detected by angiography or ultrasonography involving the abdominal aorta and either the renal or mesenteric arteries.

**Figure 1.** The final 2022 American College of Rheumatology/EULAR Classification Criteria for Takayasu arteritis.

**Table 2.** Performance characteristics of the 2022 ACR/EULAR classification criteria for Takayasu arteritis\*

Patient subset	Total no. patients (no. TAK patients)	Sensitivity (95% CI)	Specificity (95% CI)	AUC (95% CI)
Development data set	639 (316)	89.9 (86.0–93.0)	96.6 (94.0–98.3)	0.93 (0.91–0.95)
Validation data set	273 (146)	93.8 (88.6–97.1)	99.2 (96.7–100.0)	0.97 (0.94–0.99)
Age intervals				
18–39 years	437 (351)	94.0 (91.0–96.3)	97.7 (91.9–99.7)	0.96 (0.94–0.98)
40–60 years	226 (104)	83.7 (75.1–90.2)	91.8 (85.4–96.0)	0.88 (0.83–0.92)
World regions				
North America	127 (28)	85.7 (67.3–96.0)	92.9 (86.0–97.1)	0.89 (0.82–0.96)
Europe	422 (130)	91.5 (85.4–95.7)	94.9 (91.7–97.1)	0.93 (0.90–0.96)
North America/Europe combined	549 (158)	90.5 (84.8–94.6)	94.4 (91.6–96.4)	0.92 (0.90–0.95)
Asia	357 (298)	92.0 (88.3–94.8)	93.2 (83.5–98.1)	0.94 (0.89–0.96)

\* Performance characteristics for the age and regional subsets were reported using data from the combined development and validation data sets to maximize sample size. ACR = American College of Rheumatology; TAK = Takayasu arteritis; 95% CI = 95% confidence interval; AUC = area under the curve.

The performance characteristics of the criteria in different subsets of patients with TAK are shown in Table 2 and Supplementary Appendix 20B. For patients who were diagnosed between 18 and 39 years of age, the sensitivity of the criteria was 94.0% (95% CI 91.0–96.3%), and the specificity was 97.7% (95% CI 91.9–99.7%). For patients who were diagnosed between 40 and 60 years of age, the sensitivity of the criteria was 83.7% (95% CI 75.1–90.2%), and the specificity was 91.8% (95% CI 85.4–96.0%). Because age restrictions are absolute requirements for the 2022 ACR/EULAR classification criteria for TAK ( $\leq 60$  years at diagnosis) and GCA ( $\geq 50$  years at diagnosis), patients with LVV between the ages of 50 and 60 years are potentially eligible to fulfill criteria for TAK and GCA. Of the 26 patients with TAK diagnosed between the ages of 50 and 60 years, 23 (88.5%) were classified correctly as having TAK, 1 (3.9%) was incorrectly classified as having GCA, and 1 (3.9%) fulfilled criteria for both TAK and GCA (Supplementary Appendix 21, <http://onlinelibrary.wiley.com/doi/10.1002/art.42324>). The criteria performed well in both Asia (sensitivity 92.0%, specificity 93.2%) and Europe/North America (sensitivity 90.5%, specificity 94.4%).

When the 1990 ACR classification criteria for TAK were applied to the DCVAS validation data set, the criteria performed poorly due to low sensitivity (84.3% [95% CI 77.3–89.7%]) but retained excellent specificity (99.2% [95% CI 95.7–100.0%]). In particular, the 1990 criteria had poor sensitivity for patients who were diagnosed as having TAK between 40 and 60 years of age (62.5% [95% CI 52.5–71.8%]).

## DISCUSSION

Presented here are the final 2022 ACR/EULAR TAK classification criteria. A 6-stage approach was used, underpinned by data from the multinational, prospective DCVAS study and informed by expert review and consensus at each stage. The comparator group for developing and validating the criteria were other vasculitides and conditions that mimic TAK, where

discrimination from TAK is difficult but important. In the validation data set, the new criteria had a sensitivity of 93.8% (95% CI 88.6–97.1%) and a specificity of 99.2% (95% CI 96.7–100.0%). These are the official final values that should be quoted when referring to the criteria. The sensitivity and specificity values calculated in the development data set were very similar, providing reassurance that the statistical methods avoided overfitting of models. Calculations of sensitivity and specificity for patient subgroups were made in the combined development and validation data sets to maximize sample sizes for the subgroups. Reassuringly, the new criteria for TAK have excellent sensitivity and specificity across different regions of the world. The criteria also incorporate modern imaging techniques, which are useful both to diagnose LVV and to differentiate among different types of vasculitis. The criteria were designed to have face and content validity for use in clinical trials and other research studies.

These criteria are validated and intended for the purpose of *classification* of vasculitis and are not appropriate for use to establish a *diagnosis* of vasculitis (2). The aim of the classification criteria is to differentiate cases of TAK from similar types of vasculitis in research settings (5). Therefore, *the criteria should only be applied when a diagnosis of large- or medium-vessel vasculitis has been made and all potential “vasculitis mimics” have been excluded*. For example, the criteria were not developed to differentiate patients with TAK from patients with atherosclerosis or noninflammatory genetic diseases that damage the large arteries. The 1990 ACR classification criteria for vasculitis perform poorly when used for diagnosis (i.e., when used to differentiate between cases of vasculitis versus mimics without vasculitis), and it is expected that the 2022 criteria would also perform poorly if used inappropriately as diagnostic criteria (12).

The 2022 ACR/EULAR TAK classification criteria reflect the collaborative effort of the international vasculitis community to delineate the salient clinical features that differentiate TAK from

other forms of vasculitis, most notably GCA. The final criteria include 10 clinical items that are routinely assessed during clinical evaluation of patients with TAK. The criteria highlight the importance of clinical symptoms, vascular physical examination, and vascular imaging as important disease classifiers. Features of TAK may differ in patients from different parts of the world (13). The 2022 ACR/EULAR TAK classification criteria retained excellent performance characteristics when tested in patients from different regions, including Asia where the disease is most prevalent (14). While TAK is often considered a disease of the young, 25% of the patients with TAK in the DCVAS cohort were older than 40 years at the time of diagnosis. Therefore, an age at diagnosis of  $\leq 60$  years, rather than a lower age threshold, was set as an absolute requirement for disease classification. The 2022 ACR/EULAR TAK classification criteria performed well when applied to patients ages 18–60 years and outperformed the 1990 ACR Classification Criteria for TAK in the subset of patients diagnosed as having TAK ages 40–60 years.

There are several strengths of the new 2022 ACR/EULAR TAK classification criteria. The criteria were developed by a large group of international experts in systemic vasculitis, with guidance from the ACR regarding modern methods of classification criteria development. The criteria represent several important methodologic advancements compared to the original 1990 ACR classification criteria for TAK. First, expert review rather than submitting physician diagnosis was used as the diagnostic reference standard to minimize investigator bias. Second, while the 1990 ACR criteria were entirely derived using data from 63 North American patients with TAK and not validated in a separate data set, the new criteria were developed in 316 patients with TAK and validated in an independent data set which contained an additional 146 patients with TAK from an international cohort. Third, unlike the 1990 ACR criteria, the new ACR/EULAR TAK criteria are weighted to reflect the relative importance of specific items (e.g., number of affected arterial territories). Finally, when both criteria sets were tested within the DCVAS cohort, the performance characteristics of the 2022 ACR/EULAR TAK criteria outperformed the 1990 ACR criteria.

There are some study limitations to consider. Acquisition of clinical and imaging data among patients with LVV and comparators was not standardized (e.g., not all pulses were recorded by the investigators; patients with suspected diagnosis of TAK rarely underwent investigation of the cranial arteries; temporal artery biopsy was not performed in all patients with suspected GCA). However, this limitation reflects the existing differences in how these diseases are assessed in routine clinical practice. Most patients were recruited from Europe, Asia, and North America, with fewer patients from Africa and Oceania. The performance characteristics of the criteria should be further tested in populations that were underrepresented in the DCVAS cohort and may have different clinical presentations of TAK. These criteria were

developed using data collected from adult patients with vasculitis and should be tested in children with TAK (15).

The 2022 ACR/EULAR classification criteria for TAK are the product of a rigorous methodologic process that utilized an extensive data set generated by the work of a remarkable international group of collaborators. These criteria have been endorsed by the ACR and EULAR and are now ready for use in research.

## ACKNOWLEDGMENTS

We acknowledge the patients and clinicians who provided data to the DCVAS project.

## AUTHOR CONTRIBUTIONS

All authors were involved in drafting the article or revising it critically for important intellectual content, and all authors approved the final version to be published. Dr. Merkel had full access to all of the data in the study and takes responsibility for the integrity of the data and the accuracy of the data analysis.

**Study conception and design.** Grayson, Ponte, Suppiah, Robson, Judge, Craven, Hutchings, Luqmani, Watts, Merkel.

**Acquisition of data.** Grayson, Ponte, Suppiah, Robson, Craven, Danda, Luqmani, Watts, Merkel.

**Analysis and interpretation of data.** Grayson, Ponte, Suppiah, Robson, Gribbons, Judge, Craven, Khalid, Hutchings, Luqmani, Watts, Merkel.

## REFERENCES

- Jennette JC, Falk RJ, Bacon PA, et al. 2012 revised International Chapel Hill Consensus Conference nomenclature of vasculitides. *Arthritis Rheum* 2013;65:1–11.
- Aggarwal R, Ringold S, Khanna D, et al. Distinctions between diagnostic and classification criteria? [review]. *Arthritis Care Res (Hoboken)* 2015;67:891–7.
- Arend WP, Michel BA, Bloch DA, et al. The American College of Rheumatology 1990 criteria for the classification of Takayasu arteritis. *Arthritis Rheum* 1990;33:1129–34.
- Maksimowicz-McKinnon K, Clark TM, Hoffman GS. Limitations of therapy and a guarded prognosis in an American cohort of Takayasu arteritis patients. *Arthritis Rheum* 2007;56:1000–9.
- Singh JA, Solomon DH, Dougados M, et al. Development of classification and response criteria for rheumatic diseases [editorial]. *Arthritis Rheum* 2006;55:348–52.
- Langford CA, Cuthbertson D, Ytterberg SR, et al. A randomized, double-blind trial of Abatacept (CTLA-4Ig) for the treatment of Takayasu arteritis. *Arthritis Rheumatol* 2017;69:846–53.
- Nakaoka Y, Isobe M, Takei S, et al. Efficacy and safety of tocilizumab in patients with refractory Takayasu arteritis: results from a randomised, double-blind, placebo-controlled, phase 3 trial in Japan (the TAKT study). *Ann Rheum Dis* 2018;77:348–54.
- Dejaco C, Ramiro S, Duftner C, et al. EULAR recommendations for the use of imaging in large vessel vasculitis in clinical practice. *Ann Rheum Dis* 2018;77:636–43.
- Koster MJ, Matteson EL, Warrington KJ. Large-vessel giant cell arteritis: diagnosis, monitoring and management. *Rheumatology (Oxford)* 2018;57 Suppl:ii32–42.
- Craven A, Robson J, Ponte C, et al. ACR/EULAR-endorsed study to develop Diagnostic and Classification Criteria for Vasculitis (DCVAS). *Clin Exp Nephrol* 2013;17:619–21.



11. Gribbons KB, Ponte C, Carette S, et al. Patterns of arterial disease in Takayasu arteritis and giant cell arteritis. *Arthritis Care Res (Hoboken)* 2020;72:1615–24.
12. Rao JK, Allen NB, Pincus T. Limitations of the 1990 American College of Rheumatology classification criteria in the diagnosis of vasculitis. *Ann Intern Med* 1998;129:345–52.
13. Goel R, Gribbons KB, Carette S, et al. Derivation of an angiographically based classification system in Takayasu's arteritis: an observational study from India and North America. *Rheumatology (Oxford)* 2020;59:1118–27.
14. Onen F, Akkoc N. Epidemiology of Takayasu arteritis. *Presse Med* 2017;46:e197–203.
15. Danda D, Goel R, Joseph G, et al. Clinical course of 602 patients with Takayasu's arteritis: comparison between Childhood-onset versus adult onset disease. *Rheumatology (Oxford)* 2021;60:2246–55.

## APPENDIX A: THE DCVAS INVESTIGATORS

The DCVAS study investigators are as follows: Paul Gatenby (ANU Medical Centre, Canberra, Australia); Catherine Hill (Central Adelaide Local Health Network: The Queen Elizabeth Hospital, Australia); Dwarakanathan Ranganathan (Royal Brisbane and Women's Hospital, Australia); Andreas Kronbichler (Medical University Innsbruck, Austria); Daniel Blockmans (University Hospitals Leuven, Belgium); Lillian Barra (Lawson Health Research Institute, London, Ontario, Canada); Simon Carette, Christian Pagnoux (Mount Sinai Hospital, Toronto, Canada); Navjot Dhindsa (University of Manitoba, Winnipeg, Canada); Aurore Fifi-Mah (University of Calgary, Alberta, Canada); Nader Khalidi (St Joseph's Healthcare, Hamilton, Ontario, Canada); Patrick Liang (Sherbrooke University Hospital Centre, Canada); Nataliya Milman (University of Ottawa, Canada); Christian Pineau (McGill University, Canada); Xinping Tian (Peking Union Medical College Hospital, Beijing, China); Guochun Wang (China-Japan Friendship Hospital, Beijing, China); Tian Wang (Anzhen Hospital, Capital Medical University, China); Ming-hui Zhao (Peking University First Hospital, China); Vladimir Tesar (General University Hospital, Prague, Czech Republic); Bo Baslund (University Hospital, Copenhagen [Rigshospitalet], Denmark); Nevin Hammam (Assiut University, Egypt); Amira Shahin (Cairo University, Egypt); Laura Pirla (Turku University Hospital, Finland); Jukka Putaala (Helsinki University Central Hospital, Finland); Bernhard Hellmich (Kreiskliniken Esslingen, Germany); Jörg Henes (Universitätsklinikum Tübingen, Germany); Julia Holle, Frank Moosig (Klinikum Bad Bramstedt, Germany); Peter Lamprecht (University of Lübeck, Germany); Thomas Neumann (Universitätsklinikum Jena, Germany); Wolfgang Schmidt (Immanuel Krankenhaus Berlin, Germany); Cord Sunderkoetter (Universitätsklinikum Münster, Germany); Zoltan Szekanez (University of Debrecen Medical and Health Science Center, Hungary); Debashish Danda (Christian Medical College & Hospital, Vellore, India); Siddharth Das (Chatrapathi Shahuji Maharaj Medical Center, Lucknow [IP], India); Rajiva Gupta (Medanta, Delhi, India); Liza Rajasekhar (NIMS, Hyderabad, India); Aman Sharma (Postgraduate Institute of Medical Education and Research, Chandigarh, India); Shrikant Wagh (Jehangir Clinical Development Centre, Pune [IP], India); Michael Clarkson (Cork University Hospital, Ireland); Eamonn Molloy (St. Vincent's University Hospital, Dublin, Ireland); Carlo Salvarani (Santa Maria Nuova Hospital, Reggio Emilia, Italy); Franco Schiavon (L'Azienda Ospedaliera di University of Padua, Italy); Enrico Tombetti (Università Vita-Salute San Raffaele Milano, Italy); Augusto Vaglio (University of Parma, Italy); Koichi Amano (Saitama Medical University, Japan); Yoshihiro Arimura (Kyorin University Hospital, Japan); Hiroaki Dobashi (Kagawa University Hospital, Japan); Shouichi Fujimoto (Miyazaki University Hospital [HUB], Japan); Masayoshi Harigai, Fumio Hirano (Tokyo Medical and Dental University Hospital, Japan); Junichi Hirahashi (University Tokyo Hospital, Japan); Sakae Honma (Toho University Hospital, Japan); Tamihiro Kawakami (St. Marianna University Hospital Dermatology, Japan); Shigeto

Kobayashi (Juntendo University Koshigaya Hospital, Japan); Hajime Kono (Teikyo University, Japan); Hirofumi Makino (Okayama University Hospital, Japan); Kazuo Matsui (Kameda Medical Centre, Kamogawa, Japan); Eri Muso (Kitano Hospital, Japan); Kazuo Suzuki, Kei Ikeda (Chiba University Hospital, Japan); Tsutomu Takeuchi (Keio University Hospital, Japan); Tatsuo Tsukamoto (Kyoto University Hospital, Japan); Shunya Uchida (Teikyo University Hospital, Japan); Takashi Wada (Kanazawa University Hospital, Japan); Hidehiro Yamada (St. Marianna University Hospital Internal Medicine, Japan); Kunihiro Yamagata (Tsukuba University Hospital, Japan); Wako Yumura (IUHW Hospital [Jichi Medical University Hospital], Japan); Kan Sow Lai (Penang General Hospital, Malaysia); Luis Felipe Flores-Suarez (Instituto Nacional de Enfermedades Respiratorias, Mexico City, Mexico); Andrea Hinojosa-Azaola (Instituto Nacional de Ciencias Médicas y Nutrición Salvador Zubirán, Mexico City, Mexico); Bram Rutgers (University Hospital Groningen, Netherlands); Paul-Peter Tak (Academic Medical Centre, University of Amsterdam, Netherlands); Rebecca Grainger (Wellington, Otago, New Zealand); Vicki Quincey (Waikato District Health Board, New Zealand); Lisa Stamp (University of Otago, Christchurch, New Zealand); Ravi Suppiah (Auckland District Health Board, New Zealand); Emilio Besada (Tromsø, Northern Norway, Norway); Andreas Diamantopoulos (Hospital of Southern Norway, Kristiansand, Norway); Jan Sznajd (University of Jagiellonian, Poland); Elsa Azevedo (Centro Hospitalar de São João, Porto, Portugal); Ruth Geraldès (Hospital de Santa Maria, Lisbon, Portugal); Miguel Rodrigues (Hospital Garcia de Orta, Almada, Portugal); Ernestina Santos (Hospital Santo Antonio, Porto, Portugal); Yeong-Wook Song (Seoul National University Hospital, Republic of Korea); Sergey Moiseev (First Moscow State Medical University, Russia); Alojzija Hočevar (University Medical Centre Ljubljana, Slovenia); Maria Cinta Cid (Hospital Clinic de Barcelona, Spain); Xavier Solanich Moreno (Hospital de Bellvitge-Idibell, Spain); Inoshi Atukorala (University of Colombo, Sri Lanka); Ewa Berglin (Umeå University Hospital, Sweden); Aladdin Mohammed (Lund-Malmö University, Sweden); Mårten Segelmark (Linköping University, Sweden); Thomas Daikeler (University Hospital Basel, Switzerland); Haner Direskeneli (Marmara University Medical School, Turkey); Gulen Hatemi (Istanbul University, Cerrahpasa Medical School, Turkey); Sevil Kamali (Istanbul University, Istanbul Medical School, Turkey); Ömer Karadağ (Hacettepe University, Turkey); Seval Pehlevan (Fatih University Medical Faculty, Turkey); Matthew Adler (Frimley Health NHS Foundation Trust, Wexham Park Hospital, UK); Neil Basu (NHS Grampian, Aberdeen Royal Infirmary, UK); Iain Bruce (Manchester University Hospitals NHS Foundation Trust, UK); Kuntal Chakravarty (Barking, Havering and Redbridge University Hospitals NHS Trust, UK); Bhaskar Dasgupta (Southend University Hospital NHS Foundation Trust, UK); Oliver Flossmann (Royal Berkshire NHS Foundation Trust, UK); Nagui Gendi (Basildon and Thurrock University Hospitals NHS Foundation Trust, UK); Alaa Hassan (North Cumbria University Hospitals, UK); Rachel Hoyles (Oxford University Hospitals NHS Foundation Trust, UK); David Jayne (Cambridge University Hospitals NHS Foundation Trust, UK); Colin Jones (York Teaching Hospitals NHS Foundation Trust, UK); Rainer Klocke (The Dudley Group NHS Foundation Trust, UK); Peter Lanyon (Nottingham University Hospitals NHS Trust, UK); Cathy Laversuch (Taunton & Somerset NHS Foundation Trust, Musgrove Park Hospital, UK); Raashid Luqmani, Joanna Robson (Nuffield Orthopaedic Centre, Oxford, UK); Malgorzata Magliano (Buckinghamshire Healthcare NHS Trust, UK); Justin Mason (Imperial College Healthcare NHS Trust, UK); Win Win Maw (Mid Essex Hospital Services NHS Trust, UK); Iain McInnes (NHS Greater Glasgow & Clyde, Gartnavel Hospital & GRI, UK); John McLaren (NHS Fife, Whyteman's Brae Hospital, UK); Matthew Morgan (University Hospitals Birmingham NHS Foundation Trust, Queen Elizabeth Hospital, UK); Ann Morgan (Leeds Teaching Hospitals NHS Trust, UK); Chetan Mukhtyar (Norfolk and Norwich University Hospitals NHS Foundation Trust, UK); Edmond O'Riordan (Salford Royal NHS Foundation Trust, UK); Sanjeev Patel (Epsom and St Helier University Hospitals NHS Trust, UK); Adrian Peall (Wye Valley NHS Trust, Hereford County Hospital, UK); Joanna Robson (University Hospitals Bristol NHS Foundation

Trust, UK); Srinivasan Venkatachalam (The Royal Wolverhampton NHS Trust, UK); Erin Vermaak, Ajit Menon (Staffordshire & Stoke on Trent Partnership NHS Trust, Haywood Hospital, UK); Richard Watts (East Suffolk and North Essex NHS Foundation Trust, UK); Chee-Seng Yee (Doncaster and Bassetlaw Hospitals NHS Foundation Trust, UK); Daniel Albert (Dartmouth-Hitchcock Medical Center, US); Leonard Calabrese (Cleveland Clinic Foundation, US); Sharon Chung (University of California, San Francisco, US); Lindsay

Forbess (Cedars-Sinai Medical Center, US); Angelo Gaffo (University of Alabama at Birmingham, US); Ora Gewurz-Singer (University of Michigan, US); Peter Grayson (Boston University School of Medicine, US); Kimberly Liang (University of Pittsburgh, US); Eric Matteson (Mayo Clinic, US); Peter A. Merkel, Rennie Rhee (University of Pennsylvania, US); Jason Springer (University of Kansas Medical Center Research Institute, US); and Antoine Sreih (Rush University Medical Center, US).

# 2022 American College of Rheumatology/EULAR Classification Criteria for Giant Cell Arteritis

Cristina Ponte,<sup>1</sup> Peter C. Grayson,<sup>2</sup> Joanna C. Robson,<sup>3</sup> Ravi Suppiah,<sup>4</sup> Katherine Bates Gribbons,<sup>2</sup> Andrew Judge,<sup>5</sup> Anthea Craven,<sup>6</sup> Sara Khalid,<sup>6</sup> Andrew Hutchings,<sup>7</sup> Richard A. Watts,<sup>8</sup> Peter A. Merkel,<sup>9</sup> and Raashid A. Luqmani,<sup>6</sup> for the DCVAS Study Group

*This criteria set has been approved by the American College of Rheumatology (ACR) Board of Directors and the EULAR Executive Committee. This signifies that the criteria set has been quantitatively validated using patient data, and it has undergone validation based on an independent data set. All ACR/EULAR-approved criteria sets are expected to undergo intermittent updates.*

*The ACR is an independent, professional, medical and scientific society that does not guarantee, warrant, or endorse any commercial product or service.*

**Objective.** To develop and validate updated classification criteria for giant cell arteritis (GCA).

**Methods.** Patients with vasculitis or comparator diseases were recruited into an international cohort. The study proceeded in 6 phases: 1) identification of candidate items, 2) prospective collection of candidate items present at the time of diagnosis, 3) expert panel review of cases, 4) data-driven reduction of candidate items, 5) derivation of a points-based risk classification score in a development data set, and 6) validation in an independent data set.

**Results.** The development data set consisted of 518 cases of GCA and 536 comparators. The validation data set consisted of 238 cases of GCA and 213 comparators. Age  $\geq 50$  years at diagnosis was an absolute requirement for classification. The final criteria items and weights were as follows: positive temporal artery biopsy or temporal artery halo sign on ultrasound (+5); erythrocyte sedimentation rate  $\geq 50$  mm/hour or C-reactive protein  $\geq 10$  mg/liter (+3); sudden visual loss (+3); morning stiffness in shoulders or neck, jaw or tongue claudication, new temporal headache, scalp tenderness, temporal artery abnormality on vascular examination, bilateral axillary involvement on imaging, and fluorodeoxyglucose–positron emission tomography activity throughout the aorta (+2 each). A patient could be classified as having GCA with a cumulative score of  $\geq 6$  points. When these criteria were tested in the validation data set, the model area under the curve was 0.91 (95% confidence interval [95% CI] 0.88–0.94) with a sensitivity of 87.0% (95% CI 82.0–91.0%) and specificity of 94.8% (95% CI 91.0–97.4%).

**Conclusion.** The 2022 American College of Rheumatology/EULAR GCA classification criteria are now validated for use in clinical research.

This article is published simultaneously in *Annals of the Rheumatic Diseases*.

The Diagnostic and Classification Criteria in Vasculitis (DCVAS) study, which included the development of this classification criteria, was funded by grants from the American College of Rheumatology (ACR), EULAR, the Vasculitis Foundation, and the University of Pennsylvania Vasculitis Center. This study was also supported by the Intramural Research Program of the National Institute of Arthritis and Musculoskeletal and Skin Diseases, NIH.

<sup>1</sup>Cristina Ponte, MD, PhD: Department of Rheumatology, Centro Hospitalar Universitário Lisboa Norte, Centro Académico de Medicina de Lisboa, Lisbon, Portugal, and Rheumatology Research Unit, Instituto de Medicina Molecular, Faculdade de Medicina, Universidade de Lisboa, Centro Académico de Medicina de Lisboa, Lisbon, Portugal; <sup>2</sup>Peter C. Grayson, MD, MSc, Katherine Bates Gribbons, BS: Systemic Autoimmunity Branch, National Institute of Arthritis and Musculoskeletal and Skin Diseases, NIH, Bethesda, Maryland; <sup>3</sup>Joanna C. Robson, MBBS, PhD:

Centre for Health and Clinical Research, University of the West of England, and Rheumatology Department, University Hospitals Bristol and Weston NHS Foundation Trust, Bristol, UK; <sup>4</sup>Ravi Suppiah, MBChB, MD, FRACP: Te Whatu Ora - Health New Zealand, Auckland, New Zealand; <sup>5</sup>Andrew Judge, PhD: Nuffield Department of Orthopaedics Rheumatology and Musculoskeletal Sciences, Oxford NIHR Biomedical Research Centre, University of Oxford, Oxford, UK, Musculoskeletal Research Unit, Translational Health Sciences, Bristol Medical School, University of Bristol, Bristol, UK, and National Institute for Health Research Bristol Biomedical Research Centre, University Hospitals Bristol and Weston NHS Foundation Trust and University of Bristol, Bristol, UK; <sup>6</sup>Anthea Craven, BSc, Sara Khalid, DPhil, Raashid A. Luqmani, DM, FRCP: Nuffield Department of Orthopaedics Rheumatology and Musculoskeletal Sciences, Oxford NIHR Biomedical Research Centre, University of Oxford, Oxford, UK; <sup>7</sup>Andrew Hutchings, MSc: Department of Health Services Research and Policy, London School

## INTRODUCTION

Giant cell arteritis (GCA), formerly known as temporal arteritis, is the most common form of systemic vasculitis in patients aged  $\geq 50$  years (1). GCA is defined by granulomatous arteritis that affects large- and medium-sized blood vessels with a predisposition to affect the cranial arteries (2). Common presenting features of the disease include headache, constitutional symptoms, jaw claudication, scalp tenderness, visual disturbances, and elevated inflammatory markers (3).

In 1990, the American College of Rheumatology (ACR) endorsed classification criteria for GCA (4). These criteria were established before the widespread use of noninvasive and advanced vascular imaging modalities, which have become increasingly incorporated in the clinical assessment of GCA. Vascular ultrasound can be used to diagnose GCA, and depending on the clinical setting, a noncompressible “halo” sign of a temporal  $\pm$  axillary artery may replace the need for temporal artery biopsy (TAB) (5–8). Moreover, vascular imaging has demonstrated that arterial involvement in GCA is not exclusively confined to the cranial arteries (9,10) and can commonly affect the aorta and primary branches in a pattern similar to Takayasu arteritis (TAK) (11,12).

The limitations of the ACR 1990 criteria for GCA have become more apparent in the conduct of recent clinical trials and other research studies, in which investigators typically modify the 1990 ACR criteria to reflect modern practice (6,13,14). Notably, the 1990 ACR criteria focus mostly on cranial features of GCA and do not perform well in classifying patients with disease predominantly affecting the larger arteries. The 1990 ACR criteria were derived using comparator populations which included many patients with small-vessel vasculitis, a form of vasculitis that is not typically difficult to differentiate from GCA. In addition, the 1990 ACR criteria for GCA followed the “number of criteria” rule, which considered each criterion to have equal weight as a classifier for the disease. Since then, methodologic advances in classification criteria have allowed movement toward weighted criteria with threshold scores that improve performance characteristics (15,16).

This article outlines the development and validation of the revised ACR/EULAR–endorsed classification criteria for GCA.

## METHODS

An international Steering Committee comprising clinician investigators with expertise in vasculitis, statisticians, and data

managers was assembled to oversee the overall development of classification criteria for primary vasculitis (17). A detailed and complete description of the methods involved in the development and validation of the classification criteria for GCA is located in the Supplementary Appendix 1 (<http://onlinelibrary.wiley.com/doi/10.1002/art.42325>). Briefly, the Steering Committee implemented a 6-stage plan using data-driven and consensus methodology to develop the following criteria.

**Stage 1: generation of candidate classification items for the systemic vasculitides.** Candidate classification items were generated by expert opinion and reviewed by a group of vasculitis experts across a range of specialties using nominal group technique.

**Stage 2: Diagnostic and Classification Criteria for Vasculitis (DCVAS) prospective observational study.** A prospective, international, multisite observational study was conducted (see Appendix A for study investigators and sites). Ethical approval was obtained from local ethics committees. Consecutive patients representing the full spectrum of vasculitides were recruited from academic and community practices. Patients were included if they were 18 years or older and had a diagnosis of vasculitis or a condition that mimics vasculitis (e.g., infection, malignancy, atherosclerosis). Patients with GCA could only be enrolled within 2 years of diagnosis. Only data present at diagnosis were used to develop the classification criteria.

**Stage 3: expert review to derive a gold standard-defined set of cases of large-vessel vasculitis (LVV).** Experts in vasculitis from a wide range of geographic locations and specialties (see Appendix A) reviewed all submitted cases of vasculitis and a random selection of vasculitis mimics. Each reviewer was asked to review ~50 submitted cases to confirm the diagnosis and to specify the degree of certainty of their diagnosis as follows: very certain, moderately certain, uncertain, or very uncertain. Only cases agreed upon with at least moderate certainty by 2 reviewers were retained for further analysis.

**Stage 4: refinement of candidate items specifically for LVV.** The Steering Committee conducted a data-driven process to reduce the number of candidate items of relevance to cases and comparators for LVV. Density plots were assessed to study age distribution at diagnosis and symptom onset for GCA

of Hygiene and Tropical Medicine, UK; <sup>8</sup>Richard A. Watts, MD: Nuffield Department of Orthopaedics Rheumatology and Musculoskeletal Sciences, Oxford NIHR Biomedical Research Centre, University of Oxford, UK, and Norwich Medical School, University of East Anglia, Norwich, UK; <sup>9</sup>Peter A. Merkel, MD, MPH: Division of Rheumatology, Department of Medicine, and Division of Epidemiology, Department of Biostatistics, Epidemiology, and Informatics, University of Pennsylvania, Philadelphia.

Author disclosures are available at <https://onlinelibrary.wiley.com/action/downloadSupplement?doi=10.1002%2Fart.42325&file=art42325-sup-0001-Disclosureform.pdf>.

Address correspondence via email to Peter A. Merkel, MD, MPH, at [pmerkel@upenn.edu](mailto:pmerkel@upenn.edu).

Submitted for publication February 14, 2022; accepted in revised form July 30, 2022.

and TAK. Absolute age requirements versus incorporation of age as a candidate criteria item was considered. Items related to the vascular physical examination, vascular imaging, arterial biopsy, and laboratory values were combined or eliminated based on consensus review. Items were selected for exclusion if they had a prevalence of <5% within the data set, and/or they were not clinically relevant for classification criteria (e.g., related to infection, malignancy, or demography). Low-frequency items of clinical importance could be combined, when appropriate. Patterns of vascular imaging findings detected by vascular ultrasound, angiography, or positron emission tomography (PET) were defined by K-means clustering (18).

**Stage 5: derivation of the final classification criteria for GCA.** The DCVAS data set was split into development (70%) and validation (30%) sets. Comparisons were performed between cases of GCA and a randomly selected comparator group in the following proportions: TAK, 33.5%; other vasculitides that mimic GCA and TAK (isolated aortitis, primary central nervous system vasculitis, polyarteritis nodosa, Behçet's disease, and other LVV), 33.4%; and other diagnoses that mimic LVV (e.g., atherosclerosis, unspecific headache), 33.1%. Least absolute shrinkage and selection operator (lasso) logistic regression was used to identify predictors from the data set and create a parsimonious model including only the most important predictors (19). The final items in the model were formulated into a clinical risk-scoring tool, with each factor assigned a weight based on its respective regression coefficient. A threshold that best balanced sensitivity and specificity was identified for classification.

**Stage 6: validation of the final classification criteria for GCA.** Performance of the new criteria was validated in an independent set of cases and comparators. Performance of the final classification criteria was examined in specific subsets of patients with GCA using data from the combined development and validation sets to maximize sample sizes for the subgroups. Patients were studied according to different disease subtypes (biopsy-proven GCA and large-vessel GCA) and regions of the world (North America, Europe) where clinical strategies to assess GCA are known to differ (20). Biopsy-proven GCA was defined as definite vasculitis on TAB reported by the submitting physician, and large-vessel GCA was defined as vasculitic involvement of the aorta or its branch arteries on either angiography (computed tomography, magnetic resonance imaging, or catheter-based angiography), ultrasound, or PET, without vasculitis on TAB. Comparison was made between the measurement properties of the new classification criteria for GCA and the 1990 ACR classification criteria in the validation data set. Performance characteristics of the criteria were also tested in patients with TAK and compared to those with GCA diagnosed between the ages of 50 and 60 years.

## RESULTS

**Generation of candidate classification items for the systemic vasculitides.** The Steering Committee identified >1,000 candidate items for the DCVAS Case Report Form (see Supplementary Appendix 2, <http://onlinelibrary.wiley.com/doi/10.1002/art.42325>).

**DCVAS prospective observational study.** Between January 2011 and December 2017, the DCVAS study recruited 6,991 participants from 136 sites in 32 countries. Information on the DCVAS sites, investigators, and study participants is listed in Supplementary Appendices 3, 4, and 5 (<http://onlinelibrary.wiley.com/doi/10.1002/art.42325>).

**Expert review methodology to derive a gold standard-defined final set of cases of LVV.** The LVV expert panel review process included 56 experts who reviewed vignettes derived from the Case Report Forms for 2,131 cases submitted with a diagnosis of LVV (1,608 [75.5% of Case Report Forms]), another type of vasculitis (118 [5.5% of Case Report Forms]), or a mimic of vasculitis (405 [19.0% of Case Report Forms]). Characteristics and the list of expert reviewers are shown in Supplementary Appendices 6 and 7 (<http://onlinelibrary.wiley.com/doi/10.1002/art.42325>). A sample vignette and the LVV expert panel review flow chart are shown in Supplementary Appendices 8 and 9 (<http://onlinelibrary.wiley.com/doi/10.1002/art.42325>). A total of 1,695 cases (80%) passed the main LVV process. An additional 373 cases of LVV and comparators, confirmed during a previous review process to derive the classification criteria for antineutrophil cytoplasmic antibody-associated vasculitis, were also included. In total, after both review processes, 2,068 cases were available for the stages 4 and 5 analyses.

The submitting physician diagnosis of GCA was confirmed in 913 of 1,137 cases (80.3%) after both expert panel reviews. The reasons for exclusion were diagnosis of GCA categorized as "uncertain" or "very uncertain" during panel review ( $n = 187$ ) or change in diagnosis during panel review to another type of vasculitis (isolated aortitis, TAK, other vasculitides) ( $n = 11$ ) or to a comparator disease ( $n = 26$ ). An additional 29 patients who were not initially diagnosed as having GCA by the submitting physician were diagnosed as having GCA after panel review and DCVAS Steering Committee member adjudication. In total, 942 cases of confirmed GCA were available for analysis. To balance the number of cases of GCA with the number of available comparators, 756 cases of GCA were randomly selected for subsequent analysis.

### Refinement of candidate items specifically for GCA.

Only 7 of 942 patients with GCA (<1%) were diagnosed at age <50 years (see Supplementary Appendix 10 for the distribution of "age at diagnosis" in patients with LVV, and the similar



distribution of “age at symptom onset,” <http://onlinelibrary.wiley.com/doi/10.1002/art.42325>). Therefore, an age of  $\geq 50$  years at diagnosis was considered an absolute requirement to classify GCA. Cluster analyses of vascular imaging data identified bilateral axillary involvement and diffuse fluorodeoxyglucose uptake throughout the aorta on PET as specific imaging patterns for GCA (see Supplementary Appendices 11 and 12, <http://onlinelibrary.wiley.com/doi/10.1002/art.42325>). These imaging patterns were tested as potential classifiers.

Following a data-driven and expert consensus process, 72 items of the DCVAS Case Report Form were retained for regression analysis, including 32 demographic and clinical items, 14 laboratory items (including values of C-reactive protein [CRP] level and erythrocyte sedimentation rate [ESR], each divided into 5 categories), 14 imaging items (13 composite), 11 vascular examination items (5 composite, and upper extremity blood pressure divided into 6 categories), and 1 biopsy item (Supplementary Appendix 13, <http://onlinelibrary.wiley.com/doi/10.1002/art.42325>).

**Derivation of the final classification criteria for GCA.** A total of 1,505 patients were selected for analysis (756 GCA and 749 comparators), of which 1,054 (70%) were in the development data set (518 GCA and 536 comparators) and 451 (30%) in the validation data set (238 GCA and 213 comparators). Table 1 describes the demographic and clinical features of the patients with GCA and the comparators. The patients with GCA were recruited from Europe ( $n = 796$ ), North America ( $n = 112$ ), Oceania ( $n = 18$ ),

and Asia ( $n = 16$ ). Clinical diagnoses assigned to patients in the comparator group are detailed in Supplementary Appendix 14 (<http://onlinelibrary.wiley.com/doi/10.1002/art.42325>).

Lasso regression of the previously selected 72 items yielded 27 independent predictor variables for GCA (Supplementary Appendix 15A, <http://onlinelibrary.wiley.com/doi/10.1002/art.42325>). Each predictor variable was then reviewed for inclusion by the DCVAS Steering Committee, based on their odds ratios and specificity to GCA, to ensure face validity. The variables “definitive vasculitis on TAB” and “halo sign on temporal artery ultrasound” were found to dominate the model as quite strong predictors of GCA (see Supplementary Appendix 16A for cluster plots showing almost a perfect overlap between the diagnosis of GCA and positive TAB or halo sign on temporal artery ultrasound, <http://onlinelibrary.wiley.com/doi/10.1002/art.42325>). Therefore, for the remaining variables to have discriminatory value, both of these items were removed from the model, combined into one composite item “vasculitis on TAB or halo sign on temporal artery ultrasound” and given a risk score of one point below the final threshold set to classify GCA to maintain face validity. The variables “jaw claudication” and “tongue claudication” were combined into 1 item, as were the variables “maximum ESR ( $>50$  mm/hour)” and “maximum CRP ( $>10$  mg/liter).” Although the variable “new persistent headache, occipital or cervical” showed important statistical significance, it decreased the overall specificity of the model when testing their final performance characteristics (patients versus comparators) and was, therefore, also removed. Weighting of the individual criterion

**Table 1.** Demographic and disease features of the patients with giant cell arteritis and the comparators\*

	GCA ( $n = 756$ )	Comparators ( $n = 749$ )†	<i>P</i>
Age, mean $\pm$ SD years	72.2 $\pm$ 8.5	44.6 $\pm$ 18.0	<0.001
Female sex	511 (67.6)	447 (59.7)	0.001
Clinical features			
Morning stiffness, neck/torso	88 (11.6)	15 (2.0)	<0.001
Morning stiffness, shoulders/arms	174 (23.0)	23 (3.1)	<0.001
Sudden visual loss	102 (13.5)	29 (3.9)	<0.001
Jaw claudication	356 (47.1)	19 (2.5)	<0.001
Tongue claudication	21 (2.8)	1 (0.1)	<0.001
New persistent temporal headache	475 (62.8)	90 (12.0)	<0.001
Scalp tenderness	260 (34.4)	25 (3.3)	<0.001
Temporal artery abnormality on vascular examination‡	354 (46.8)	35 (4.7)	<0.001
Investigations			
Maximum ESR $\geq 50$ mm/hour	558 (73.8)	291 (38.9)	<0.001
Maximum CRP $\geq 10$ mg/liter	683 (90.3)	445 (59.4)	<0.001
Definitive vasculitis on temporal artery biopsy	335 (44.3)	1 (0.1)	<0.001
Halo sign on temporal artery ultrasound	211 (27.9)	1 (0.1)	<0.001
Bilateral axillary involvement on imaging§	57 (7.5)	12 (1.6)	<0.001
FDG-PET activity throughout aorta¶	52 (6.9)	9 (1.2)	<0.001

\* Except where indicated otherwise, values are the number (%). ESR = erythrocyte sedimentation rate; CRP = C-reactive protein; FDG-PET =  $^{18}$ F-fluorodeoxyglucose–positron emission tomography.

† Diagnoses of comparators for the classification criteria for giant cell arteritis (GCA) included Takayasu arteritis ( $n = 251$ ), Behçet’s disease ( $n = 133$ ), polyarteritis nodosa ( $n = 74$ ), isolated aortitis ( $n = 16$ ), primary central nervous system vasculitis ( $n = 16$ ), large-vessel vasculitis (LVV) that could not be subtyped ( $n = 9$ ), other diseases that mimic LVV ( $n = 250$ ).

‡ Absent or diminished pulse, tenderness, or hard ‘cord like’ appearance.

§ Defined as damage (i.e., stenosis, occlusion, or aneurysm) on angiography (computed tomography, magnetic resonance, or catheter-based) or ultrasound, halo sign on ultrasound, or abnormal FDG uptake on PET.

¶ Descending thoracic and abdominal aorta.

included in the model was based on logistic regression fitted to the remaining 9 selected predictors (Supplementary Appendix 17A, <http://onlinelibrary.wiley.com/doi/10.1002/art.42325>).

### Validation of the final classification criteria for GCA.

Using a cutoff of  $\geq 6$  in total risk score in the validation data set (see Supplementary Appendix 18A at <https://onlinelibrary.wiley.com/doi/10.1002/art.42325> for different cutoff points), the sensitivity

was 87.0% (95% confidence interval [95% CI] 82.0–91.0%) and specificity was 94.8% (95% CI 91.0–97.4%). The area under the curve for the model was 0.91 (95% CI 0.88–0.94) (Supplementary Appendix 19A, <http://onlinelibrary.wiley.com/doi/10.1002/art.42325>). The final 2022 ACR/EULAR classification criteria for GCA are presented in Figure 1 (for the slide presentation versions, see Supplementary Figure 1, <http://onlinelibrary.wiley.com/doi/10.1002/art.42325>).

## 2022 AMERICAN COLLEGE OF RHEUMATOLOGY / EULAR

## CLASSIFICATION CRITERIA FOR **GIANT CELL ARTERITIS**

### CONSIDERATIONS WHEN APPLYING THESE CRITERIA

- These classification criteria should be applied to classify the patient as having giant cell arteritis when a diagnosis of medium-vessel or large-vessel vasculitis has been made
- Alternate diagnoses mimicking vasculitis should be excluded prior to applying the criteria

### ABSOLUTE REQUIREMENT

Age  $\geq 50$  years at time of diagnosis

### ADDITIONAL CLINICAL CRITERIA

Morning stiffness in shoulders/neck	+2
Sudden visual loss	+3
Jaw or tongue claudication	+2
New temporal headache	+2
Scalp tenderness	+2
Abnormal examination of the temporal artery <sup>1</sup>	+2

### LABORATORY, IMAGING, AND BIOPSY CRITERIA

Maximum ESR $\geq 50$ mm/hour or maximum CRP $\geq 10$ mg/liter <sup>2</sup>	+3
Positive temporal artery biopsy or halo sign on temporal artery ultrasound <sup>3</sup>	+5
Bilateral axillary involvement <sup>4</sup>	+2
FDG-PET activity throughout aorta <sup>5</sup>	+2

**Sum the scores for 10 items, if present. A score of  $\geq 6$  points is needed for the classification of **GIANT CELL ARTERITIS**.**

1. Examination of the temporal artery showing absent or diminished pulse, tenderness, or hard 'cord-like' appearance.
2. Maximum erythrocyte sedimentation rate (ESR) or C-reactive protein (CRP) values prior to initiation of treatment for vasculitis.
3. Presence of either definitive vasculitis on temporal artery biopsy or halo sign on temporal artery ultrasound. There are no specific histopathologic criteria to define definitive vasculitis on temporal artery biopsy. Presence of giant cells, mononuclear leukocyte infiltration, and fragmentation of the internal elastic lamina were independently associated with histopathologic interpretation of definite vasculitis in the DCVAS cohort<sup>[24]</sup>. Halo sign is defined by the presence of an homogenous, hypoechoic wall thickening on ultrasound<sup>[25]</sup>.

4. Bilateral axillary involvement is defined as luminal damage (stenosis, occlusion, or aneurysm) on angiography (computed tomography, magnetic resonance, or catheter-based) or ultrasound, halo sign on ultrasound, or fluorodeoxyglucose uptake on positron emission tomography.
5. Abnormal fluorodeoxyglucose (FDG) uptake in the arterial wall (e.g., greater than liver uptake by visual inspection) throughout the descending thoracic and abdominal aorta on positron emission tomography (PET).

**Figure 1.** The final 2022 American College of Rheumatology/EULAR Classification Criteria for Giant Cell Arteritis.

**Table 2.** Performance characteristics of the 2022 ACR/EULAR classification criteria for giant cell arteritis\*

Patient subset	Total no. patients (no. GCA patients)	Sensitivity (95% CI)	Specificity (95% CI)	AUC (95% CI)
Development data set	1,054 (518)	84.8 (81.4–87.7)	95.0 (92.8–96.7)	0.90 (0.88–0.92)
Validation data set	451 (238)	87.0 (82.0–91.0)	94.8 (91.0–97.4)	0.91 (0.88–0.94)
Biopsy-proven GCA†	1,104 (355)	100.0 (99.0–100.0)	94.9 (93.1–96.4)	0.97 (0.97–0.98)
Large-vessel GCA‡	873 (124)	55.7 (46.5–64.6)	94.9 (93.1–96.4)	0.75 (0.71–0.80)

\* Performance characteristics were tested in the subsets using the combined development and validation data sets to maximize sample size. ACR = American College of Rheumatology; GCA = giant cell arteritis; 95% CI = 95% confidence interval; AUC = area under the curve.

† Definite vasculitis on temporal artery biopsy (TAB).

‡ Involvement of the aorta or its branch arteries on imaging, without vasculitis on TAB.

The performance characteristics of the criteria in different subsets of patients with GCA are shown in Table 2 and Supplementary Appendix 20A (<https://onlinelibrary.wiley.com/doi/10.1002/art.42325>). Biopsy-proven GCA showed a sensitivity of 100% (95% CI 99.0–100.0%) and a specificity of 94.9% (95% CI 93.1–96.4%), and large-vessel GCA showed a sensitivity of 55.7% (95% CI 46.5–64.6%) and a specificity of 94.9% (93.1–96.4%). Sensitivity of the criteria in North America was 77.8% (95% CI 67.8–85.9%) and in Europe was 87.2% (95% CI 84.4–89.7%). Specificity in North America was 95.6% (95% CI 90.6–98.4%) and in Europe was 88.8% (95% CI 84.9–92.0%).

When the 1990 ACR classification criteria for GCA were applied to the DCVAS validation data set, the criteria performed poorly due to low sensitivity (80.3% [95% CI 74.6–85.1%]) but retained good specificity (92.5% [95% CI 88.1–95.7%]). In particular, the 1990 ACR criteria had poor sensitivity for patients with large-vessel GCA (37.1% [95% CI 28.6–46.2%]).

Age restrictions are absolute requirements for the 2022 ACR/EULAR classification criteria for GCA ( $\geq 50$  years at diagnosis) and TAK ( $\leq 60$  years at diagnosis). However, of the 70 patients with GCA diagnosed between the ages of 50 and 60 years, 44 (62.9%) met the new GCA classification criteria, 9 (12.9%) met the new TAK classification criteria, and only 2 (2.9%) met both the new GCA and TAK classification criteria (Supplementary Appendix 21, <http://onlinelibrary.wiley.com/doi/10.1002/art.42325>).

## DISCUSSION

Presented here are the final 2022 ACR/EULAR GCA classification criteria. A 6-stage approach was used, underpinned by data from the multinational, prospective DCVAS study and informed by expert review and consensus at each stage. The comparator group for developing and validating the criteria were other vasculitides and conditions that mimic GCA, where discrimination from GCA is difficult but important. In the validation set, the new criteria had a sensitivity of 87.0% (95% CI 82.0–91.0%) and a specificity of 94.8% (95% CI 91.0–97.4%). These are the official final values that should be quoted when referring to the criteria. The sensitivity and specificity values calculated in the development set were very similar, providing reassurance that the

statistical methods avoided overfitting of models. The new criteria incorporate modern imaging techniques and have excellent specificity and sensitivity within a large, international cohort of patients with GCA. The criteria were designed to have face and content validity for use in clinical trials and other research studies.

These criteria are validated and intended for the purpose of *classification* of vasculitis and are not appropriate for use to establish a *diagnosis* of vasculitis. The aim of the classification criteria is to differentiate cases of GCA from similar types of vasculitis in research settings (21). *Therefore, the criteria should only be applied when a diagnosis of large- or medium-vessel vasculitis has been made and all potential “vasculitis mimics” have been excluded.* The exclusion of mimics is a key aspect of many classification criteria including those for Sjögren’s syndrome (22) and rheumatoid arthritis (16). The 1990 ACR classification criteria for vasculitis perform poorly when used for diagnosis (i.e., when used to differentiate between cases of vasculitis versus mimics without vasculitis) (23), and it is expected that the 2022 criteria would also perform poorly if used inappropriately as diagnostic criteria in people for whom alternative diagnoses, such as infection or other non-vasculitis inflammatory diseases, are still being considered.

The 2022 ACR/EULAR GCA classification criteria are the result of an incredibly large worldwide effort, in which an extensive set of data was collected from >1,000 patients with the submitted diagnosis of GCA. These criteria reflect current clinical practice, integrating different investigative methods (e.g., TAB, ultrasound, angiography, PET) from various countries and medical specialties. Real cases of GCA and comparators were reviewed by a wide range of experts in vasculitis to establish an unbiased diagnostic reference to derive the criteria. Advanced statistical methods including lasso logistic regression and cluster analyses were applied, which facilitated testing for different covariates of interest, namely specific patterns of vasculitic involvement in imaging. Modern classification techniques with weighted criterion with threshold scores were used, allowing for more discriminatory items to factor more heavily in disease classification.

When compared to the original 1990 ACR classification criteria for GCA, the 2022 ACR/EULAR GCA classification criteria

demonstrated greater sensitivity while maintaining similar specificity to the 1990 criteria. In particular, the new criteria were able to correctly classify more patients with the large-vessel GCA subtype, in whom the sensitivity of the 1990 ACR criteria was only 37.1%. Unlike the 1990 ACR criteria, an age of  $\geq 50$  years at diagnosis is a mandatory requirement to classify GCA in the 2022 ACR/EULAR criteria. This age threshold included >99% of patients with the reference diagnosis of GCA. The new criteria maintain good discriminative ability for patients diagnosed between the ages of 50 and 60 years, the interval where the absolute age requirements for the 2022 ACR/EULAR criteria for GCA and for TAK can overlap.

A potential limitation of these criteria was the nonstandardized acquisition of clinical and imaging data among patients with LVV and comparators (e.g., not all patients underwent vascular examination of the temporal arteries, PET was not available in many centers treating patients with LVV, and TAB and/or ultrasound was not performed in all patients with suspected GCA, etc.). However, this reflects existing differences in clinical practice, and the 11 items included in the criteria allow for a feasible evaluation of patients in any clinical setting. These criteria also provide flexibility for classifying a patient, regardless of the diagnostic assessment strategy employed by physicians. Definite vasculitis on TAB was defined by the submitting physician and did not undergo central review; ~20% of cases did not have specific histopathologic findings but were reported as “definitive vasculitis on TAB” alone. Most patients were recruited from Europe and North America, with fewer patients from Asia and Oceania. The performance characteristics of the criteria should be further tested in other populations that were underrepresented in the DCVAS cohort and may have different clinical presentations of GCA.

The 2022 ACR/EULAR classification criteria for GCA are the product of a rigorous methodologic process that utilized an extensive data set generated by the work of a remarkable international group of collaborators. These criteria have been endorsed by the ACR and EULAR and are now ready for use in clinical research.

## ACKNOWLEDGMENTS

We acknowledge the patients and clinicians who provided data to the DCVAS project.

## AUTHOR CONTRIBUTIONS

All authors were involved in drafting the article or revising it critically for important intellectual content, and all authors approved the final version to be published. Dr. Merkel had full access to all of the data in the study and takes responsibility for the integrity of the data and the accuracy of the data analysis.

**Study conception and design.** Ponte, Grayson, Robson, Suppiah, Judge, Craven, Hutchings, Watts, Merkel, Luqmani.

**Acquisition of data.** Ponte, Grayson, Robson, Suppiah, Craven, Watts, Merkel, Luqmani.

**Analysis and interpretation of data.** Ponte, Grayson, Robson, Suppiah, Gribbons, Judge, Craven, Khalid, Hutchings, Watts, Merkel, Luqmani.

## REFERENCES

- Watts RA, Robson J. Introduction, epidemiology and classification of vasculitis [review]. *Best Pract Res Clin Rheumatol* 2018; 32:3–20.
- Jennette JC, Falk RJ, Bacon PA, et al. 2012 revised International Chapel Hill Consensus Conference nomenclature of vasculitides. *Arthritis Rheum* 2013;65:1–11.
- Ponte C, Águeda AF, Luqmani RA. Clinical features and structured clinical evaluation of vasculitis. *Best Pract Res Clin Rheumatol* 2018; 32:31–51.
- Hunder GG, Bloch DA, Michel BA, et al. The American College of Rheumatology 1990 criteria for the classification of giant cell arteritis. *Arthritis Rheum* 1990;33:1122–8.
- Dejaco C, Ramiro S, Duftner C, et al. EULAR recommendations for the use of imaging in large vessel vasculitis in clinical practice. *Ann Rheum Dis* 2018;77:636–43.
- Luqmani R, Lee E, Singh S, et al. The role of ultrasound compared to biopsy of temporal arteries in the diagnosis and treatment of giant cell arteritis (TABUL): a diagnostic accuracy and cost-effectiveness study. *Health Technol Assess* 2016;20:1–238.
- Hellmich B, Agueda A, Monti S, et al. 2018 Update of the EULAR recommendations for the management of large vessel vasculitis. *Ann Rheum Dis* 2020;79:19–30.
- Mackie SL, Dejaco C, Appenzeller S, et al. British Society for Rheumatology guideline on diagnosis and treatment of giant cell arteritis. *Rheumatology (Oxford)* 2020;59:e1–23.
- Blockmans D, de Ceuninck L, Vanderschueren S, et al. Repetitive  $^{18}\text{F}$ -fluorodeoxyglucose positron emission tomography in giant cell arteritis: a prospective study of 35 patients. *Arthritis Rheum* 2006;55:131–7.
- Prieto-González S, Argüis P, García-Martínez A, et al. Large vessel involvement in biopsy-proven giant cell arteritis: prospective study in 40 newly diagnosed patients using CT angiography. *Ann Rheum Dis* 2012;71:1170–6.
- Grayson PC, Maksimowicz-McKinnon K, Clark TM, et al. Distribution of arterial lesions in Takayasu's arteritis and giant cell arteritis. *Ann Rheum Dis* 2012;71:1329–34.
- Furuta S, Cousins C, Chaudhry A, et al. Clinical features and radiological findings in large vessel vasculitis: are Takayasu arteritis and giant cell arteritis 2 different diseases or a single entity? *J Rheumatol* 2015;42:300–8.
- Stone JH, Tuckwell K, Dimonaco S, et al. Trial of tocilizumab in giant-cell arteritis. *N Engl J Med* 2017;377:317–28.
- Langford CA, Cuthbertson D, Ytterberg SR, et al. A randomized, double-blind trial of abatacept (CTLA-4Ig) for the treatment of takayasu arteritis. *Arthritis Rheumatol* 2017;69:846–53.
- Sanchez ML, Alarcón GS, McGwin G, et al. Can the weighted criteria improve our ability to capture a larger number of lupus patients into observational and interventional studies? A comparison with the American College of Rheumatology criteria. *Lupus* 2003;12:468–70.
- Aletaha D, Neogi T, Silman AJ, et al. 2010 Rheumatoid arthritis classification criteria: an American College of Rheumatology/European League Against Rheumatism collaborative initiative. *Arthritis Rheum* 2010;62:2569–81.
- Craven A, Robson J, Ponte C, et al. ACR/EULAR-endorsed study to develop Diagnostic and Classification Criteria for Vasculitis (DCVAS). *Clin Exp Nephrol* 2013;17:619–21.

18. Gribbons KB, Ponte C, Carette S, et al. Patterns of arterial disease in Takayasu's arteritis and giant cell arteritis. *Arthritis Care Res (Hoboken)* 2020;72:1615–24.
19. Pavlou M, Ambler G, Seaman SR, et al. How to develop a more accurate risk prediction model when there are few events. *BMJ* 2015;351:h3868.
20. Gribbons KB, Ponte C, Craven A, et al. Diagnostic assessment strategies and disease subsets in giant cell arteritis: data from an international observational cohort. *Arthritis Rheumatol* 2020;72:667–76.
21. Aggarwal R, Ringold S, Khanna D, et al. Distinctions between diagnostic and classification criteria? [review] *Arthritis Care Res (Hoboken)* 2015;67:891–7.
22. Shiboski CH, Shiboski SC, Seror R, et al. 2016 American College of Rheumatology/European League Against Rheumatism classification criteria for primary Sjögren's syndrome: a consensus and data-driven methodology involving three international patient cohorts. *Arthritis Rheumatol* 2017;69:35–45.
23. Rao JK, Allen NB, Pincus T. Limitations of the 1990 American College of Rheumatology classification criteria in the diagnosis of vasculitis. *Ann Intern Med* 1998;129:345–52.
24. Putman MS, Gribbons KB, Ponte C, et al. Clinicopathologic associations in a large international cohort of patients with giant cell arteritis. *Arthritis Care Res (Hoboken)* 2020;74:1013–8.
25. Chrysidi S, Duftner C, Dejaco C, Schäfer VS, Ramiro S, Carrara G, et al. Definitions and reliability assessment of elementary ultrasound lesions in giant cell arteritis: a study from the OMERACT Large Vessel Vasculitis Ultrasound Working Group. *RMD Open* 2018;4:e000598.

## APPENDIX A: THE DCVAS INVESTIGATORS

The DCVAS study investigators are as follows: Paul Gatenby (ANU Medical Centre, Canberra, Australia); Catherine Hill (Central Adelaide Local Health Network: The Queen Elizabeth Hospital, Australia); Dwarkanathan Ranganathan (Royal Brisbane and Women's Hospital, Australia); Andreas Kronbichler (Medical University Innsbruck, Austria); Daniel Blockmans (University Hospitals Leuven, Belgium); Lillian Barra (Lawson Health Research Institute, London, Ontario, Canada); Simon Carette, Christian Pagnoux (Mount Sinai Hospital, Toronto, Canada); Navot Dhindsa (University of Manitoba, Winnipeg, Canada); Aurore Fifi-Mah (University of Calgary, Alberta, Canada); Nader Khalidi (St Joseph's Healthcare, Hamilton, Ontario, Canada); Patrick Liang (Sherbrooke University Hospital Centre, Canada); Nataliya Milman (University of Ottawa, Canada); Christian Pineau (McGill University, Canada); Xiping Tian (Peking Union Medical College Hospital, Beijing, China); Guochun Wang (China-Japan Friendship Hospital, Beijing, China); Tian Wang (Anzhen Hospital, Capital Medical University, China); Ming-hui Zhao (Peking University First Hospital, China); Vladimir Tesar (General University Hospital, Prague, Czech Republic); Bo Baslund (University Hospital, Copenhagen [Rigshospitalet], Denmark); Nevin Hammam (Assiut University, Egypt); Amira Shahin (Cairo University, Egypt); Laura Pirila (Turku University Hospital, Finland); Jukka Putaala (Helsinki University Central Hospital, Finland); Bernhard Hellmich (Kreiskliniken Esslingen, Germany); Jörg Henes (Universitätsklinikum Tübingen, Germany); Julia Holle, Frank Moosig (Klinikum Bad Bramstedt, Germany); Peter Lamprecht (University of Lübeck, Germany); Thomas Neumann (Universitätsklinikum Jena, Germany); Wolfgang Schmidt (Immanuel Krankenhaus Berlin, Germany); Cord Sunderkoetter (Universitätsklinikum Münster, Germany); Zoltan Szekanez (University of Debrecen Medical and Health Science Center, Hungary); Debashish Danda (Christian Medical College & Hospital, Vellore, India); Siddharth Das (Chatrapathi Shahuji Maharaj Medical Center, Lucknow [IP], India); Rajiva Gupta (Medanta, Delhi, India); Liza Rajasekhar (NIMS, Hyderabad, India); Aman Sharma (Postgraduate Institute of Medical Education and Research, Chandigarh, India); Shrikant Wagh (Jehangir Clinical Development Centre, Pune [IP],

India); Michael Clarkson (Cork University Hospital, Ireland); Eamonn Molloy (St. Vincent's University Hospital, Dublin, Ireland); Carlo Salvarani (Santa Maria Nuova Hospital, Reggio Emilia, Italy); Franco Schiavon (L'Azienda Ospedaliera of University of Padua, Italy); Enrico Tombetti (Università Vita-Salute San Raffaele Milano, Italy); Augusto Vaglio (University of Parma, Italy); Koichi Amano (Saitama Medical University, Japan); Yoshihiro Arimura (Kyorin University Hospital, Japan); Hiroaki Dobashi (Kagawa University Hospital, Japan); Shouichi Fujimoto (Miyazaki University Hospital [HUB], Japan); Masayoshi Harigai, Fumio Hirano (Tokyo Medical and Dental University Hospital, Japan); Junichi Hirahashi (University Tokyo Hospital, Japan); Sakae Honma (Toho University Hospital, Japan); Tamihiko Kawakami (St. Marianna University Hospital Dermatology, Japan); Shigeto Kobayashi (Juntendo University Koshigaya Hospital, Japan); Hajime Kono (Teikyo University, Japan); Hirofumi Makino (Okayama University Hospital, Japan); Kazuo Matsui (Kameda Medical Centre, Kamogawa, Japan); Eri Muso (Kitano Hospital, Japan); Kazuo Suzuki, Kei Ikeda (Chiba University Hospital, Japan); Tsutomu Takeuchi (Keio University Hospital, Japan); Tatsuo Tsukamoto (Kyoto University Hospital, Japan); Shunya Uchida (Teikyo University Hospital, Japan); Takashi Wada (Kanazawa University Hospital, Japan); Hidehiro Yamada (St. Marianna University Hospital Internal Medicine, Japan); Kunihiro Yamagata (Tsukuba University Hospital, Japan); Wako Yumura (IUHW Hospital [Jichi Medical University Hospital], Japan); Kan Sow Lai (Penang General Hospital, Malaysia); Luis Felipe Flores-Suarez (Instituto Nacional de Enfermedades Respiratorias, Mexico City, Mexico); Andrea Hinojosa-Azaola (Instituto Nacional de Ciencias Médicas y Nutrición Salvador Zubirán, Mexico City, Mexico); Bram Rutgers (University Hospital Groningen, Netherlands); Paul-Peter Tak (Academic Medical Centre, University of Amsterdam, Netherlands); Rebecca Grainger (Wellington, Otago, New Zealand); Vicki Quincey (Waikato District Health Board, New Zealand); Lisa Stamp (University of Otago, Christchurch, New Zealand); Ravi Suppiah (Auckland District Health Board, New Zealand); Emilio Besada (Tromsø, Northern Norway, Norway); Andreas Diamantopoulos (Hospital of Southern Norway, Kristiansand, Norway); Jan Sznajd (University of Jagiellonian, Poland); Elsa Azevedo (Centro Hospitalar de São João, Porto, Portugal); Ruth Gerales (Hospital de Santa Maria, Lisbon, Portugal); Miguel Rodrigues (Hospital Garcia de Orta, Almada, Portugal); Ernestina Santos (Hospital Santo Antonio, Porto, Portugal); Yeong-Wook Song (Seoul National University Hospital, Republic of Korea); Sergey Moiseev (First Moscow State Medical University, Russia); Alojzija Hočevar (University Medical Centre Ljubljana, Slovenia); Maria Cinta Cid (Hospital Clinic de Barcelona, Spain); Xavier Solanich Moreno (Hospital de Bellvitge-Idibell, Spain); Inoshi Atukorala (University of Colombo, Sri Lanka); Ewa Berglin (Umeå University Hospital, Sweden); Aladdin Mohammed (Lund-Malmö University, Sweden); Mårten Segelmark (Linköping University, Sweden); Thomas Däikeler (University Hospital Basel, Switzerland); Haner Direskeneli (Marmara University Medical School, Turkey); Gulen Hatemi (Istanbul University, Cerrahpasa Medical School, Turkey); Sevil Kamali (Istanbul University, Istanbul Medical School, Turkey); Ömer Karadağ (Hacettepe University, Turkey); Seval Pehlevan (Fatih University Medical Faculty, Turkey); Matthew Adler (Frimley Health NHS Foundation Trust, Wexham Park Hospital, UK); Neil Basu (NHS Grampian, Aberdeen Royal Infirmary, UK); Iain Bruce (Manchester University Hospitals NHS Foundation Trust, UK); Kuntal Chakravarty (Barking, Havering and Redbridge University Hospitals NHS Trust, UK); Bhaskar Dasgupta (Southend University Hospital NHS Foundation Trust, UK); Oliver Flossmann (Royal Berkshire NHS Foundation Trust, UK); Nagui Gendi (Basildon and Thurrock University Hospitals NHS Foundation Trust, UK); Alaa Hassan (North Cumbria University Hospitals, UK); Rachel Hoyles (Oxford University Hospitals NHS Foundation Trust, UK); David Jayne (Cambridge University Hospitals NHS Foundation Trust, UK); Colin Jones (York Teaching Hospitals NHS Foundation Trust, UK); Rainer Klocke (The Dudley Group NHS Foundation Trust, UK); Peter Lanyon (Nottingham University Hospitals NHS Trust, UK); Cathy Laversuch (Taunton & Somerset NHS Foundation Trust, Musgrove Park Hospital, UK); Raashid Luqmani, Joanna Robson (Nuffield Orthopaedic Centre, Oxford, UK); Malgorzata Magliano (Buckinghamshire Healthcare NHS Trust, UK); Justin Mason (Imperial College Healthcare NHS Trust, UK); Win Win Maw (Mid Essex Hospital Services NHS Trust, UK); Iain McInnes (NHS Greater Glasgow &



Clyde, Gartnavel Hospital & GRI, UK); John McLaren (NHS Fife, Whyteman's Brae Hospital, UK); Matthew Morgan (University Hospitals Birmingham NHS Foundation Trust, Queen Elizabeth Hospital, UK); Ann Morgan (Leeds Teaching Hospitals NHS Trust, UK); Chetan Mukhtyar (Norfolk and Norwich University Hospitals NHS Foundation Trust, UK); Edmond O'Riordan (Salford Royal NHS Foundation Trust, UK); Sanjeev Patel (Epsom and St Helier University Hospitals NHS Trust, UK); Adrian Peall (Wye Valley NHS Trust, Hereford County Hospital, UK); Joanna Robson (University Hospitals Bristol NHS Foundation Trust, UK); Srinivasan Venkatachalam (The Royal Wolverhampton NHS Trust, UK); Erin Vermaak, Ajit Menon (Staffordshire & Stoke on Trent Partnership NHS Trust, Haywood Hospital, UK); Richard Watts (East Suffolk and North

Essex NHS Foundation Trust, UK); Chee-Seng Yee (Doncaster and Bassetlaw Hospitals NHS Foundation Trust, UK); Daniel Albert (Dartmouth-Hitchcock Medical Center, US); Leonard Calabrese (Cleveland Clinic Foundation, US); Sharon Chung (University of California, San Francisco, US); Lindsay Forbess (Cedars-Sinai Medical Center, US); Angelo Gaffo (University of Alabama at Birmingham, US); Ora Gewurz-Singer (University of Michigan, US); Peter Grayson (Boston University School of Medicine, US); Kimberly Liang (University of Pittsburgh, US); Eric Matteson (Mayo Clinic, US); Peter A. Merkel, Rennie Rhee (University of Pennsylvania, US); Jason Springer (University of Kansas Medical Center Research Institute, US); and Antoine Sreih (Rush University Medical Center, US).

**EDITORIAL**

# Disentangling the Causal Effect of Telomere Length in Systemic Lupus Erythematosus Using Genetic Variants as Instruments

Yiqiang Zhan<sup>1</sup>  and Xiaoying Kang<sup>2</sup>

Telomeres, the repeated DNA sequences surrounded by protein complexes at the end of our chromosomes, are the key structures that protect against chromosomal fusion and instability (1). Over the life course, telomere shortening occurs as a consequence of several cellular events including cell division and inflammation, which negatively affects the structural and functional integrity of chromosomes and may further lead to cell senescence and apoptosis. Consistent with this, development of several age-related health problems, such as cardiovascular diseases, cognitive impairment, and Alzheimer's disease, have also been causally linked to shorter telomeres, supporting the implicated role of telomere length as a biologic clock or biomarker of aging.

The involvement of accelerated immune aging in autoimmune dysfunction has drawn a substantial amount of interest in the investigation of telomere length, an indicator of immune senescence, as a putative cause of the initiation and progression of various autoimmune disorders. Although this hypothesis has been supported by mounting evidence, it is important to note that most of the findings to date came from case-control studies, which are prone to biases (e.g., confounding and reverse causation) and are thus methodologically inadequate for causal inference. Meanwhile, lack of a consensus on environmental risk factors for autoimmune diseases, such as systemic lupus erythematosus (SLE), often results in the inconsistent adjustment for confounding variables in different epidemiologic studies, restricting the comparability of results.

In this issue of *Arthritis & Rheumatology*, Wang et al harnessed the 2-sample Mendelian randomization (MR) design and examined the causal effect of telomere length shortening on SLE using 2 independent samples of European and Chinese ancestries (2,3). With an objective to evaluate nongenetic

environmental risk factors as potential causes of a disease phenotype (e.g., SLE), the MR design is a research approach gaining popularity for its theoretical advantages in addressing confounding and reverse causation. The concept behind the MR design in medical research stems from Dr. Katan (4), a Dutch nutritionist who proposed assessing whether the empirical relationship between cholesterol and cancer was causal by examining the effect of genetic determinants of cholesterol, rather than the effect of cholesterol itself, on cancer. This is because, according to Dr. Katan, if cholesterol indeed causes cancer, its genetic determinants must be an upstream cause of cancer as well.

Following this rationale, the MR design takes advantage of genetic variants as instrumental variables to infer causality in the presence of both measured and unmeasured confounding. By testing the associations of the genetic instruments with outcome, a qualitative conclusion regarding the causal role of the exposure of interest on the outcome can be made. The strength of the causality could then be further quantified as effect size and confidence interval via different MR estimators. However, caution is also needed when implementing this exciting technique in practice. Two review articles about MR design emphasized that MR results should be interpreted critically because the assumptions underlying MR estimators are rarely satisfied. This is of particular concern for the exclusion restriction assumption, also known as the “no pleiotropy” assumption, which assumes that the genetic instruments may only affect the outcome through the exposure of interest. Despite the available statistical methods, this assumption is empirically impossible to statistically test.

The majority of MR studies to date have been based on data and samples from subjects of European ancestry. Limited by issues like data availability and sample size, MR results derived

<sup>1</sup>Yiqiang Zhan, MD, PhD: Department of Epidemiology, School of Public Health (Shenzhen), Sun Yat-Sen University, Shenzhen, China, and Institute of Environmental Medicine, Karolinska Institutet, Stockholm, Sweden; <sup>2</sup>Xiaoying Kang, PhD, MPH: Department of Medical Epidemiology and Biostatistics, Karolinska Institutet, Stockholm, Sweden, and Brigham and Women's Hospital, Harvard Medical School, Boston, Massachusetts.

Author disclosures are available at <https://onlinelibrary.wiley.com/action/downloadSupplement?doi=10.1002%2Fart.42313&file=art42313-sup-0001-Disclosureform.pdf>.

Address correspondence via email to Yiqiang Zhan, MD, PhD, at [zhanyq8@mail.sysu.edu.cn](mailto:zhanyq8@mail.sysu.edu.cn).

Submitted for publication June 29, 2022; accepted in revised form July 20, 2022.

from other ethnic groups remain scarce. In this article, Wang et al, for the first time, examined the causal effect of telomere length on SLE in a Chinese-only population. Importantly, the authors selected the instrumental variables (10 single-nucleotide polymorphisms [SNPs]) for telomere length from the Singaporean Chinese study to ensure that the samples for exposure and outcome came from the same ethnic population. Such instrument selection effectively minimized bias due to population stratification in MR estimation and is critical in MR design. In a second MR analysis, the authors also used 7 SNPs as instrumental variables selected from the Telomere European Network for Genetic and Genomic Epidemiology Consortium, a collaborative work of telomere research teams in a European population. The outcome data, SLE genome-wide association study (GWAS), were then derived from a previously published study in patients of European ancestry to account for ethnic background. After data harmonization, the authors performed the MR analyses using the inverse variance-weighted estimators as the primary approach and several other estimators, including MR-Egger regression, MR pleiotropy residual sum and outlier method, median- and mode-based approaches, and Cochrane's Q statistic, for the purpose of sensitivity analysis. Interestingly, results from both analyses of Chinese data and European data demonstrate a robust causal association of longer telomere length with a higher risk of SLE.

While Wang et al reported longer telomeres as a risk factor for SLE, observational findings published to date appear to contradictorily support an inverse association between telomere length and SLE (5). One possible explanation for such discrepancy is that the observational findings are biased. Indeed, almost all of these observational studies were conducted in case-control designs, and it is unclear whether the SLE patients were selected as prevalent or incident cases (Table 1) (6–13). Besides, only age and sex were adjusted for, whereas adjustment for other potential confounders (e.g., smoking, inflammatory status, obesity, and comorbidities) was poorly described or not included in these analyses. Similarly, a significant reduction in telomere length has been associated with glucocorticoid treatment in SLE in previous studies of both animal models and human subjects; however, no

consideration was given to any medical therapies for SLE in the included observational studies. Last, it should also be noted that prior studies might be biased due to reverse causation. However, the hypothetical influence of SLE on telomere length is refuted by the reverse MR analysis using SLE as exposure and telomere length as outcome, as reported by Wang et al.

Although this study has a particular strength in that it utilizes the novel and robust MR design to assess the causal role of telomere length in SLE, it has a few limitations. First, telomere length was only measured in blood leukocytes without considering other cells or tissue. These measurements can only be viewed as a proxy or surrogate for telomere length in general. Second, all analyses were based on GWAS summary statistics using a linear assumption. Without additional modelling of individual-level data, it is unclear whether the relationship between telomere length and SLE may be nonlinear. Lastly, a more careful interpretation of results in comparison to other epidemiologic evidence is needed. Since GWAS summary statistics are typically derived from large-scale studies among individuals who have survived to a certain age, results from such summary statistics-based MR analysis are prone to selection bias or survival bias. Therefore, there remains a scarcity of longitudinal studies leveraging both traditional epidemiologic designs and MR framework in future research.

To conclude, novel and powerful epidemiologic designs such as MR hold great promise for disentangling the cause-and-effect relationship in SLE research. In the absence of other gold standards of causal inference, triangulation is critically needed to compare and cross-validate scientific evidence collected from multiple sources before randomized controlled trials become feasible (14), as each approach has different potential biases that might be related or unrelated to each other. When several results of various approaches all point to the same conclusion, this would surely strengthen our confidence in these findings and causal inference. When there are inconsistencies, and results from several approaches differ, understanding the key sources of bias in each approach could greatly help to determine what further research is required to address key causal questions.

AUTHOR CONTRIBUTIONS

Dr. Zhan drafted the article, Dr. Kang revised it critically for important intellectual content, and both authors approved the final version to be published.

REFERENCES

1. Blackburn EH, Epel ES, Lin J. Human telomere biology: a contributory and interactive factor in aging, disease risks, and protection. *Science* 2015;350:1193–8.

2. Wang X, Xu W, Wang F, et al. Telomere length and development of systemic lupus erythematosus: a Mendelian randomization study. *Arthritis Rheumatol* 2022;74:1984–90.

**Table 1.** Characteristics of published case-control studies on telomere length and SLE\*

Author, year (ref.)	No. of SLE cases	No. of healthy controls
Skamra et al, 2013 (6)	154	152
Haque et al, 2013 (7)	63	63
Hoffecker et al, 2013 (8)	59	59
Wu et al, 2007 (9)	60	26
Beier et al, 2007 (13)	22	20
Kurosaka et al, 2006 (10)	34	17
Kurosaka et al, 2003 (11)	30	45
Honda et al, 2001 (12)	90	64

\* SLE = systemic lupus erythematosus.

3. Smith GD, Ebrahim S. 'Mendelian randomization': can genetic epidemiology contribute to understanding environmental determinants of disease? *Int J Epidemiol* 2003;32:1–22.
4. Katan MB. Commentary: mendelian randomization, 18 years on. *Int J Epidemiol* 2004;33:10–1.
5. Lee YH, Jung JH, Seo YH, et al. Association between shortened telomere length and systemic lupus erythematosus: a meta-analysis. *Lupus* 2017;26:282–8.
6. Skamra C, Romero-Diaz J, Sandhu A, et al. Telomere length in patients with systemic lupus erythematosus and its associations with carotid plaque. *Rheumatology (Oxford)* 2013;52:1101–8.
7. Haque S, Rakieh C, Marriage F, et al. Shortened telomere length in patients with systemic lupus erythematosus. *Arthritis Rheum* 2013;65:1319–23.
8. Hoffecker BM, Raffield LM, Kamen DL, et al. Systemic lupus erythematosus and vitamin D deficiency are associated with shorter telomere length among African Americans: a case-control study. *PLoS One* 2013;8:e63725.
9. Wu CH, Hsieh SC, Li KJ, et al. Premature telomere shortening in polymorphonuclear neutrophils from patients with systemic lupus erythematosus is related to the lupus disease activity. *Lupus* 2007;16:265–72.
10. Kurosaka D, Yasuda J, Yoshida K, et al. Abnormal telomerase activity and telomere length in T and B cells from patients with systemic lupus erythematosus. *J Rheumatol* 2006;33:1102–7.
11. Kurosaka D, Yasuda J, Yoshida K, et al. Telomerase activity and telomere length of peripheral blood mononuclear cells in SLE patients. *Lupus* 2003;12:591–9.
12. Honda M, Mengesha E, Albano S, et al. Telomere shortening and decreased replicative potential, contrasted by continued proliferation of telomerase-positive CD8+CD28(lo) T cells in patients with systemic lupus erythematosus. *Clin Immunol* 2001;99:211–21.
13. Beier F, Balabanov S, Amberger CC, et al. Telomere length analysis in monocytes and lymphocytes from patients with systemic lupus erythematosus using multi-color flow-FISH. *Lupus* 2007;16:955–62.
14. Lawlor DA, Tilling K, Smith GD. Triangulation in aetiological epidemiology. *Int J Epidemiol* 2016;45:1866–86.

## REVIEW

# Artificial Intelligence and Deep Learning for Rheumatologists

Christopher McMaster,<sup>1</sup>  Alix Bird,<sup>2</sup>  David F. L. Liew,<sup>3</sup>  Russell R. Buchanan,<sup>4</sup>  Claire E. Owen,<sup>4</sup>  Wendy W. Chapman,<sup>5</sup>  and Douglas E. V. Pires<sup>6</sup> 

Deep learning has emerged as the leading method in machine learning, spawning a rapidly growing field of academic research and commercial applications across medicine. Deep learning could have particular relevance to rheumatology if correctly utilized. The greatest benefits of deep learning methods are seen with unstructured data frequently found in rheumatology, such as images and text, where traditional machine learning methods have struggled to unlock the trove of information held within these data formats. The basis for this success comes from the ability of deep learning to learn the structure of the underlying data. It is no surprise that the first areas of medicine that have started to experience impact from deep learning heavily rely on interpreting visual data, such as triaging radiology workflows and computer-assisted colonoscopy. Applications in rheumatology are beginning to emerge, with recent successes in areas as diverse as detecting joint erosions on plain radiography, predicting future rheumatoid arthritis disease activity, and identifying halo sign on temporal artery ultrasound. Given the important role deep learning methods are likely to play in the future of rheumatology, it is imperative that rheumatologists understand the methods and assumptions that underlie the deep learning algorithms in widespread use today, their limitations and the landscape of deep learning research that will inform algorithm development, and clinical decision support tools of the future. The best applications of deep learning in rheumatology must be informed by the clinical experience of rheumatologists, so that algorithms can be developed to tackle the most relevant clinical problems.

## Introduction

Deep learning refers to a group of algorithms that use artificial neural networks and an optimization algorithm called backpropagation (with gradient descent) to model complex problems by learning complex functions that describe them (see Figure 1) (1). While deep learning methods have been designed and applied for many decades, it is only in the last 10 years that computer hardware has been able to train these increasingly complex models to such a level that they now dominate the machine learning landscape, both in terms of publications and performance. In recent years, the applications of deep learning in medicine have

not only gained prominence but have started entering clinical practice. At the time of writing, the American College of Radiology lists 201 US Food and Drug Administration (FDA)-approved machine learning algorithms to support radiology (2), many of which use deep learning approaches. Deep learning methods power computers that beat grandmasters in Chess and Go (3), summarize documents as diverse as patents and academic papers (4), control autonomous cars (5), and predict and design macromolecules (6). Although still in its infancy, applications of deep learning in rheumatology are increasing across a broad range of areas (see Table 1). There are several ways to classify

<sup>1</sup>Christopher McMaster, FRACP, MBBS: Department of Rheumatology and Department of Clinical Pharmacology and Therapeutics, Austin Health, Victoria, Melbourne, Australia, and Centre for Digital Transformation of Health and School of Computing and Information Systems, University of Melbourne, Victoria, Melbourne, Australia; <sup>2</sup>Alix Bird, MBBS: Australian Institute for Machine Learning, University of Adelaide, Adelaide, South Australia, Australia; <sup>3</sup>David F. L. Liew, FRACP, MBBS: Department of Rheumatology and Department of Clinical Pharmacology and Therapeutics, Austin Health, Department of Clinical Pharmacology and Therapeutics, Austin Health, and Department of Medicine, University of Melbourne, Victoria, Melbourne, Australia; <sup>4</sup>Russell R. Buchanan, FRACP, MD, MBBS, Claire E. Owen, FRACP, PhD, MBBS: Department of Rheumatology, Austin Health, and Department

of Medicine, University of Melbourne, Victoria, Melbourne, Australia; <sup>5</sup>Wendy W. Chapman, PhD: Centre for Digital Transformation of Health, University of Melbourne, Victoria, Melbourne, Australia; <sup>6</sup>Douglas E. V. Pires, PhD: Centre for Digital Transformation of Health and School of Computing and Information Systems, University of Melbourne, Victoria, Melbourne, Australia.

Author disclosures are available at <https://onlinelibrary.wiley.com/action/downloadSupplement?doi=10.1002%2Fart.42296&file=art42296-sup-0001-Disclosureform.pdf>.

Address correspondence via email to Christopher McMaster, FRACP, MBBS, at [christopher.mcmaster@austin.org.au](mailto:christopher.mcmaster@austin.org.au).

Submitted for publication March 6, 2022; accepted in revised form July 7, 2022.



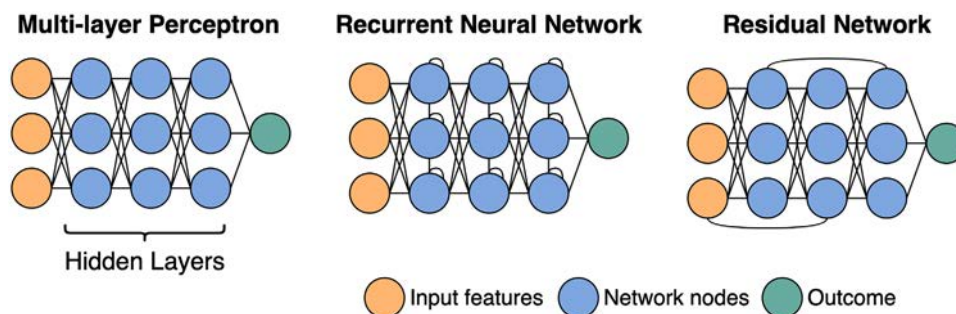


**Figure 1.** Neural network architectures. The first layer of a neural network consists of the data. These data are then passed to the first “hidden layer.” Each node, represented by a circle, is a weighted linear combination of all the nodes in the layer before. It is the weights that the model “learns.” Apart from a classic neural network where all nodes from 1 layer are connected to the next (otherwise known as a multilayer perceptron), other common architectures include recurrent networks with connections between nodes within a layer, usually used for sequence data (e.g., time-series or text), and residual networks, where information from 1 layer can “skip” the next layer, giving the network a way to bypass inefficient layers.

these various applications; however, one logical way to categorize deep learning algorithms is based on the input data type. Time-series data are used for prediction tasks, written text is used for natural language processing, and images are used for computer vision. Here we explore rheumatic applications of deep learning across these 3 categories.

## Learning from text

Natural language processing (NLP) is an interdisciplinary field of study with the main aim of having computers “perform useful

tasks involving human language” (7). Traditionally, NLP has heavily relied on linguistic models of syntax and grammar, complemented by statistical analysis. In contrast, deep learning approaches in contemporary NLP rely less on assumptions about rules of natural language, including expertly curated words and phrases, building models capable of inferring those rules by learning from large bodies of text (8). Most recently, deep learning models for NLP have moved toward attention-based models, in particular a group of models collectively referred to as “Transformers” (9). While previous state-of-the-art NLP algorithms relied on modeling text as a sequence of words read one-by-one directionally (left-to-right for

**Table 1.** Current applications of deep learning in rheumatology\*

Problem (source ref.)	Data type	Model	Implications
Identifying GCA features from temporal artery biopsy reports (13)	Text	Transformer	Accurate auditing of temporal artery biopsy reports can be performed using deep learning; however, this performance dropped when tested across centers.
Classifying HEp-2 cells based on ANA IIF patterns (29)	Images	CNN	Automated ANA classification based on HEp-2 cells is approaching expert human performance.
OESS from synovial ultrasound (44)	Images	CNN	Deep learning can identify synovitis on ultrasound with a high degree of accuracy.
SHS scoring using hand and foot radiographs (51)	Images	CNN	Radiographic scoring for RA is improving but still requires work for clinical implementation.
Predicting progression (any increase in K/L score) of knee OA based on baseline knee radiographs plus other clinical features (58)	Images	CNN	Radiographic progression in knee OA can be predicted with a combination of clinical features and baseline radiography using deep learning; however, there are unmeasured factors missing in these models.
Identifying halo sign on temporal artery ultrasound images (68)	Images	CNN	Deep learning has significant potential for automated identification of the halo sign; however, ensuring standardized image acquisition is a major barrier to implementation.
Predicting future RA disease activity (controlled versus uncontrolled) using clinical data from previous encounters (19)	EHRs	RNN	Deep learning can predict future disease activity from past disease activity and baseline factors; however, performance significantly dropped when the model was tested at a second center, suggesting that there is substantial heterogeneity between centers that must be accounted for in future models.

\* GCA = giant cell arteritis; ANA = antinuclear antibody; IIF = immunofluorescence; CNN = convolutional neural network; OESS = EULAR Outcome Measures in Rheumatology synovitis scoring; SHS = modified Sharp/van der Heijde; RA = rheumatoid arthritis; K/L = Kellgren/Lawrence; OA = osteoarthritis; EHRs = electronic health records; RNN = recurrent neural network.

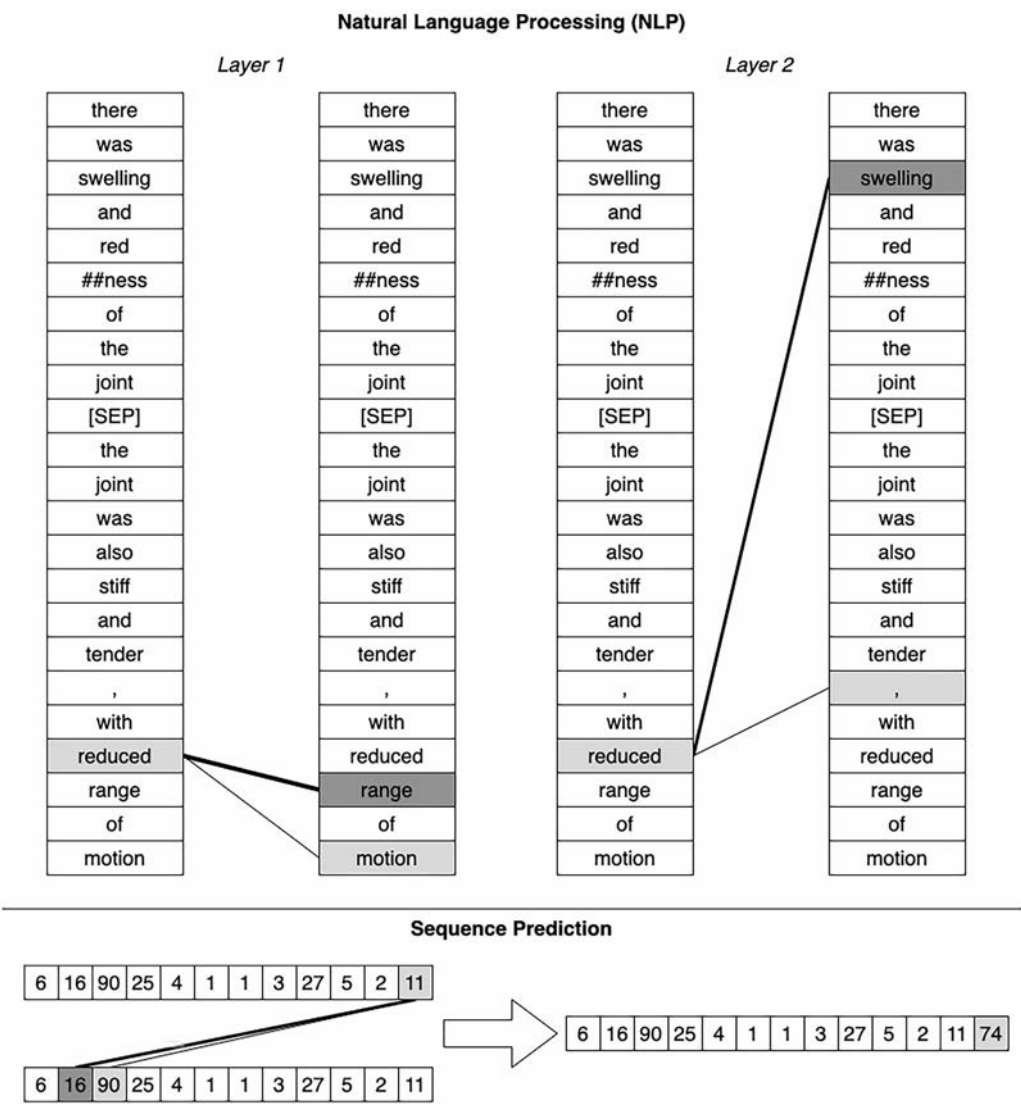


**Figure 2.** Visualization of attention model (ref. 94). Two attention layers are shown with text input for NLP (top). The original input text reads, “There was swelling and redness of the joint. The joint was also stiff and tender, with reduced range of motion.” This text is converted into tokens, sometimes splitting words into more than one token (here “redness” is split into “red” and “##ness”—the “##” signifying that this token belongs with the preceding token). On the left, a lower layer of the attention-based model relied on the words “range” and “motion” to interpret the word “reduced.” On the right, at a higher layer, the word “reduced” also depends strongly on the word “swelling” in the previous sentence. An attention model can be used for any sequence data (bottom). Here, these numbers could be laboratory values, with the task of predicting the next value in the sequence. The attention layer used the values “16” and “90” to predict the next value in the sequence. In this instance, attention is used to focus on a similar pattern to anticipate a future value.

English text), Transformers allow the algorithm to view all the text at once and pick out the important words that provide context (see Figure 2). Attention-based models, combined with pretraining on very large bodies of text (see section on transfer learning below), have allowed deep learning NLP algorithms to achieve state-of-the-art performance on many language tasks.

*Classifying temporal artery biopsy reports.* Classic NLP techniques have successfully been used for identifying patients with rheumatic diseases using electronic health records (EHRs) (10–12). These methods generally rely on the cultivation of a set of words and phrases strongly associated with the disease of

interest. Given the wide phenotypic variability of rheumatic diseases, accurate identification and classification of patients based on clinical notes lends itself to deep learning techniques.

Presently, deep learning on text has only been applied in a single conference abstract, using Transformer models to classify temporal artery biopsy reports based on the presence of 3 histopathologic features (adventitial inflammation, giant cells, intimal hyperplasia) and overall conclusion (giant cell arteritis [GCA] or not) (13). This study used a model called DistilBERT (14), training on 161 biopsy reports from 1 center and testing both within that center and on 220 biopsy reports from a second center.

The authors achieved excellent performance, particularly on the report conclusion (area under receiver operating characteristic curve [AUC] 0.99) and the presence of giant cells (AUC 0.99), with performance reducing slightly in the second center (AUC 0.93 and 0.97, respectively). Pooling data between the 2 centers and training a new model resulted in significant improvements (AUC 0.99 and 0.99, respectively) when tested on reports across both sites, suggesting that a diverse data set drawing on the language of multiple institutions will result in more generalizable models. It remains to be seen whether this model can generalize beyond 2 centers, particularly given the fact that both were within the same city in Australia—it is likely that variability in documentation practices, vocabulary, and idiomatic expressions results in reduced performance.

## Learning from EHRs

Deep learning algorithms used for predicting future events are varied in design, but often rely on the use of time-series data modeled as sequences. In this respect, predictive algorithms often use similar architectures to those used when learning from texts, which are also modeled as sequences. Many EHR prediction algorithms have been developed, most notably and commonly for inpatient outcomes such as length of stay and inpatient mortality rate (15). The nature of EHR data produces unique challenges, reflecting the bias of clinical decisions as much as patient physiology. Which data are missing and the presence of noise often reflects systematic decision making, rather than a random process (e.g., the absence of invasive blood pressure data in a critically ill patient may reflect a decision about the goals of care, rather than the lack of critical illness). Additionally, care must be taken to ensure data set leakage (16) does not occur, where the training data set is inadvertently informed by the testing data set (e.g., the same patient appears in both, but for different inpatient visits).

*Predicting future diagnoses using EHRs.* The Transformer architecture that has been successfully applied to NLP has demonstrated similar success in sequence models. Such models may use time-sequence data to predict future events, drawing on the power of self-attention, efficiently learning to recognize long-range relationships between past events and future events (9). Li et al developed a Transformer model trained on 1.6 million primary care patients with at least 5 EHR encounters (17). For each individual, they created a sequence of EHR encounters, with the diagnoses and patient age at the time of the encounter forming the components of the sequence. The authors assessed predictive performance for a number of diseases, including rheumatic diseases. Most notably, the model was able to predict the future development of polymyalgia rheumatica (PMR) with very high accuracy (AUC 0.96). This result may partially reflect data quality issues, with PMR diagnosis in primary care frequently occurring without exclusion of alternative diagnoses (18); thus, the model is likely predicting the onset of a polymyalgic syndrome, rather

than the specific diagnosis of PMR. Additionally, this algorithm may simply be identifying a pattern of clinical coding, rather than a sequence of clinical events—any model that uses clinical interpretation rather than patient physiology is prone to modeling not just patient outcomes, but also physician behavior.

*Predicting disease activity using EHRs.* Rheumatology, as a specialty dealing with chronic, relapsing–remitting disease, has maintained a strong interest in the task of predicting future disease activity. Frequent outpatient follow-up with clinical and laboratory testing is used to detect changes in disease state and allow for interventions to treat any disease relapse or deterioration; yet precisely predicting who will experience relapse or deterioration remains a difficult task. Apart from the Transformer architecture mentioned above, for a long time, deep learning has approached the analysis of sequence data and prediction using recurrent neural networks (RNNs).

Norgeot et al (19) developed a model to predict whether patients with rheumatoid arthritis (RA) would have controlled or uncontrolled disease at their next clinic visit, based on data from the EHR. Their definition of disease control was based on a threshold cutoff of the Clinical Disease Activity Index (CDAI) (20). The input data included baseline measures (demographic characteristics, rheumatoid factor, citrullinated peptide antibody) and time-dependent variables (laboratory values, medication, CDAI) from each visit. The time-dependent variables were used to train an RNN—designed to identify periodicity and trend—to account for long-range influences that might affect future disease states. The model was trained and tested on data from one hospital, before being further assessed on data from a different hospital. Predictably, the performance on data from the second hospital was inferior; however, the authors were able to improve the performance with a small amount of training on data from the new hospital, in a process known as transfer learning.

*Learning from images.* Computer vision is a field of image processing interested in automating tasks of visual perception. Since the groundbreaking AlexNet architecture won the ImageNet competition in 2012 (21), computer vision has been dominated by deep learning algorithms. The basis for its success to date has been one specific neural network architecture: the convolutional neural network (CNN). The CNN has had several inventors without reference to each other with slight variations; however, the precursor to modern CNN models is most frequently attributed to a 1999 paper by LeCun et al on object detection (22).

The building block of CNNs is a convolution kernel, a grid or matrix of numbers. The convolution passes over an image (a grid of numbers representing the individual pixels of an image), transforming the image in particular ways. Hard-coded convolutions, like the one in Figure 3, may perform tasks like vertical edge detection. While convolutions have existed as an image processing technique for many decades, the innovation in deep learning is that the convolutions are not hard coded, they are learned. The layering of many convolutions allows a model to progressively

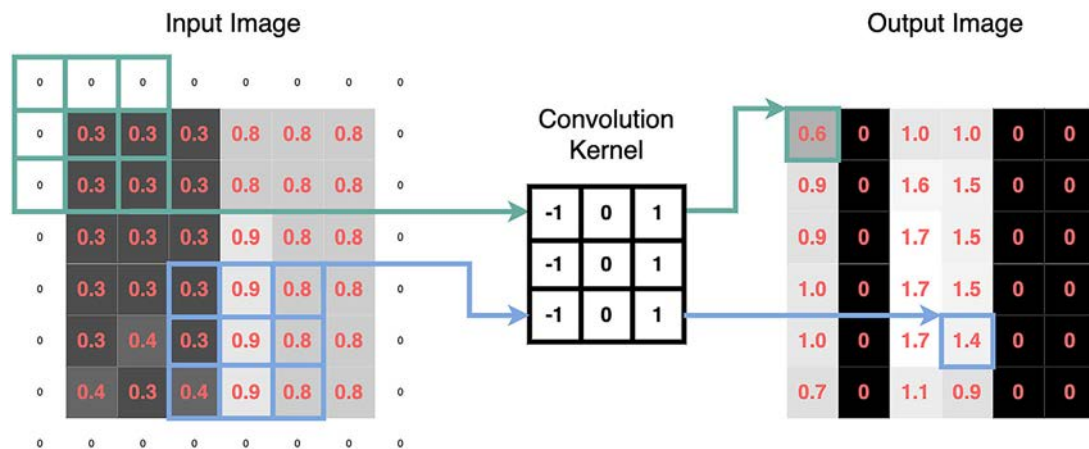


**Figure 3.** A vertical edge detector convolution kernel. Edges that transition from dark to light (as shown in the input image) will be light in the output image. The pixel values (representing light intensity) are shown as pink numbers. No values in the output image are  $<0$ . This is because all values  $<0$  are turned into 0 by a function known as a rectified linear unit (ref. 95)—this is known as an activation function and is a common technique in deep learning. The rim of zeroes around the input image—known as “padding”—allows the output image to retain the same dimensions as the input image. Color figure can be viewed in the online issue, which is available at <http://onlinelibrary.wiley.com/doi/10.1002/art.42296/abstract>.

build complex features. While early layers might learn convolutions for simple tasks like edge detection, later layers may join different edge detectors together to make object detectors, face detectors, and eventually solve complex tasks like facial expression detection.

**HEp-2 image classification.** Testing for antinuclear antibodies (ANAs) using indirect immunofluorescence (IIF) assays has been a cornerstone of the diagnostic evaluation of systemic autoimmunity for many decades (23). These methods rely on the visual inspection of HEp-2 cells, mixed with fluorescence-labeled antibodies from patient sera. Because different antigens are distributed differently within the HEp-2 cells, the staining pattern produced by the fluorescence-labeled antibodies can provide important diagnostic information about the antigen target and associated disease (24).

Automated analysis of HEp-2 images has arisen as a field of research interest, motivated by concerns that the visual assessment of IIF patterns is subjective and time consuming (25). Recently, deep learning techniques have been applied to this task, with increasing success. Broadly, these techniques attempt to classify either individual HEp-2 cells or specimens (containing many cells), by applying deep learning to coarsely labeled images. Rahman et al reviewed the application of deep learning techniques to these tasks, identifying 24 published methods for the classification of individual HEp-2 cells and 7 methods for the classification of specimens (26).

A wide variety of deep learning techniques have been applied to cell classification. Broadly, deep learning has been applied in 2 ways to this task by 1) automatically extracting features and classifying cells or 2) automatically extracting features, which are then passed to an alternative model for classification. State-of-the-art models using either technique have achieved accuracies

exceeding 97% (26,27), which favorably compare to human accuracy (73.3%) (28). However, this comparison has been criticized, as the task of classifying a single HEp-2 cell, isolated from the broader context of the specimen, is not representative of how IIF tests for ANAs are performed in real clinical practice (29). Moreover, these methods are developed, tested, and validated using limited data sets (30–33). These data sets lack consistency, both in terms of whether the images contain single cells or specimens, and the number of different staining categories classified.

In response to these data issues, Wu et al (29) curated a large data set of 51,694 HEp-2 cell slides that more closely reflect clinical practice. These slides contain multiple cells per image, with up to 4 different patterns present in a single image. They tested multiple CNN architectures, ultimately finding that the Inception-ResNet v2 architecture (34) had the best performance. In their testing data set, they found interobserver agreement—as measured using Cohen’s kappa coefficient (35)—was similar between expert readers (0.85) and between expert readers and the final model (0.84).

**Synovial ultrasound.** Synovial ultrasound is an important and emerging technology in the diagnosis (36) and assessment (37) of inflammatory arthritis. Recently, the EULAR Outcome Measures in Rheumatology (EULAR-OMERACT) ultrasound taskforce developed a scoring system, sometimes referred to as the EULAR-OMERACT Synovitis Scoring (OESS) system, designed to be used as an outcome measure in clinical trials (37). While there is ongoing effort to validate and refine its use (38), the standardized application of an ultrasound synovitis scoring system is amenable to deep learning methods. Andersen et al (39) first applied 2 well-studied CNN architectures to this problem (VGG-16 [40] and Inception v3 [41]), after first performing pretraining on the popular ImageNet data set (42). They found overall good performance

(AUC 0.93) for the task of discriminating healthy joints (OESS score 0–1) from unhealthy joints (OESS score 2–3); however, precise scoring on the ordinal scale did not appear to match human performance (43). A follow-up method from the same group, this

time using a so-called “cascade” CNN (Figure 4A), showed similar performance compared to expert rheumatologists (44). In this algorithm, a CNN is given the task of classifying a power Doppler ultrasound image as either being at or above a given OESS grade.

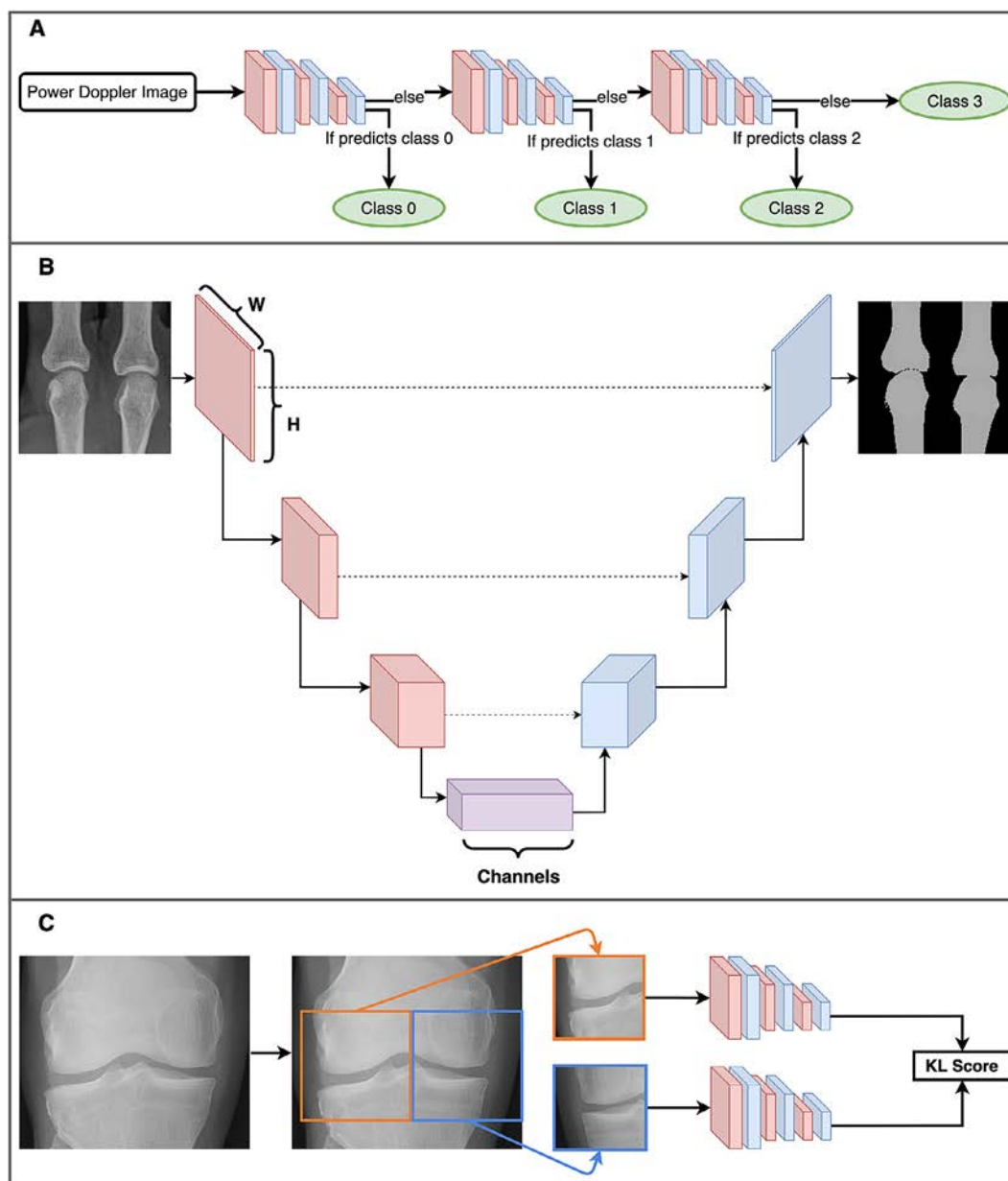


**Figure 4.** Three unique deep learning methods used in rheumatology. **A**, A cascade of convolutional neural networks (CNNs) used to classify power Doppler images. At each step, the CNN classifies the image as either a certain EULAR Outcome Measures in Rheumatology synovitis scoring class or any higher class (e.g., the first step classifies to either a class of 0 or >0). If the CNN determines that it belongs to a higher class, it is passed along to the next CNN, which performs the same task for the next highest class. Eventually, the final CNN simply classifies images as either class 2 or class 3. **B**, A simplified diagram of the U-Net architecture (49). An image begins as an “ $N \times N \times C$ ” shape, where “ $N \times N$ ” is the image size (e.g.,  $224 \times 224$  pixels) and “ $C$ ” is the number of channels (typically 3 channels of red/green/blue for a color image). The model gradually reduces the size, while increasing the number of channels, until the bottom of the architecture is reached, and then the reverse occurs. Connections across the architecture (dashed lines) act as a “memory.” The image recovered at the end is a segmented image, partitioning the original into the relevant parts. In this example, the bones of 2 metacarpal joints are segmented from the plain radiograph. **C**, A single coronal radiograph of the knee joint split into 2 images: the right half of the knee and the horizontally flipped left half. Both images are passed through the same CNN before joining up to produce a Kellgren/Lawrence (K/L) composite score as the model output. Color figure can be viewed in the online issue, which is available at <http://onlinelibrary.wiley.com/doi/10.1002/art.42296/abstract>.



Each image that is classified as being of a higher grade is then passed to the next CNN, which performs an identical task for the next highest grade. These algorithms may be further enhanced with larger, multicenter data sets and further refinement of the CNN architecture. As in many medical applications, the laborious task of manually labeling images could be augmented by semisupervised learning and potentially by synthetic data from methods such as generative adversarial networks (45).

*Joint damage in inflammatory arthritis.* Progressive joint erosion early in the course of RA is one of the major predictors of future physical function (46). The prevention of progressive joint erosions is an important outcome measure in establishing the efficacy of any disease-modifying agent in RA and other inflammatory arthritides. It is therefore important that erosive disease is measured consistently and with high sensitivity. The modified total van der Heijde Sharp Score (mTSS) (47) is commonly used in clinical trials to assess progressive joint erosions, consisting of both an erosion score and joint space narrowing score (JSN). The process of grading these components is a visual task performed by trained radiologists and rheumatologists, making it a good application for neural network models.

Hirano et al developed a neural network model to grade hand joints according to mTSS scores using hand radiographs (48). To perform joint-level scoring, their model first had to perform a task called image segmentation to create bounding boxes around individual joints so they could be assessed. Rather than utilizing a deep learning model for this task, such as the popular U-Net model (Figure 4B) first developed for biomedical image segmentation (49), the authors used hard-coded convolutions known as Haar-like features, in a method first described by Viola et al (50). After image segmentation, the authors built JSN and erosion score models with 2 convolutional layers and 3 fully connected layers. The JSN and erosion score models had similar performance compared to clinician assessment (correlation coefficients 0.72–0.88 and 0.54–0.75, respectively); however, overall sensitivity to detect erosions was low (34.8–42.4%). The major limitation of this algorithm was a relatively small data set (186 radiographs). With larger data sets, deeper models with more sophisticated architectures will perhaps make this a clinically applicable scenario for deep learning.

Recently, deep learning methods using a combination of CNNs and attention mechanisms (51) have been used for mTSS scoring in RA. The authors also used a 2-stage approach, first using a CNN architecture called RetinaNet (52) to detect joint groups, followed by another CNN architecture called EfficientNet (53) to score individual joints. Additionally, the authors applied an attention layer (Figure 2) after the convolutional layers. The attention layer effectively constrains the area of interest to only those pixels in the image that provide a substantial contribution to the final prediction—the attention to all other pixels becomes negligible. By interrogating this attention layer, the authors generated heatmaps to demonstrate which regions contribute to the scoring

of a joint, although interpreting these as an explanation of how the model works should be treated with great caution (see section on explainability below) (54,55).

*Plain films in knee osteoarthritis (OA).* Current EULAR recommendations for the diagnosis of OA only support imaging as a diagnostic tool in atypical presentations of suspected OA (56); however, this recommendation is not supported by high-level evidence and the role of routine imaging remains a topic of debate (57). Outside of diagnosis, there is also debate about the prognostic role of imaging features to predict symptom severity and progression. The current EULAR recommendations do not support the use of imaging for prognostication; however, this is on the basis of older studies using hand-crafted imaging features, not the systematic discovery of prognostic features from deep learning algorithms.

Tiulpin et al developed deep learning models for diagnosis and prognosis of knee OA using plain radiographs (58–61). For diagnosis, the authors utilized CNN architectures to train 2 models to grade images according to OA severity. In their first model, they used a Siamese network to grade knee radiographs according to the Kellgren/Lawrence (K/L) composite score (62), a global rating system for knee OA (scale 0–4). The Siamese Network, as first proposed by Baldi and Chauvin (63), trains 2 identical neural networks simultaneously, with the task of determining whether 2 images meet some similarity threshold—in the original paper, the models compare 2 fingerprints to determine whether they come from the same finger. In the present study, the input image pairs were automatically segmented from the original plain radiographs, consisting of the right half of the tibiofemoral joint and the horizontally flipped left half. Because the tibiofemoral joint has horizontal symmetry with respect to the features that predict K/L score (Figure 4C), a single model can identify salient features from both sides (provided one half is horizontally flipped). These left- and right-sided predictions are then joined to provide an overall K/L score. Overall, they found good agreement between model and clinician scores, with a Cohen's kappa coefficient of 0.83.

The second diagnostic model from Tiulpin et al used a conventional ResNet architecture with transfer learning from ImageNet to grade both individual OA features using the Osteoarthritis Research Society International (OARSI) atlas of OA radiographic features (64) and K/L score. The model was able to achieve state-of-the-art results on OARSI scoring, exceeding human accuracy on this task.

For the task of prognostication, the authors trained a CNN on baseline knee radiographs to predict whether repeat radiography would show an increase in K/L score (58). They compared this model to a model that used tabular data: age, sex, body mass index, K/L grade, Western Ontario and McMaster Universities Osteoarthritis Index, injury, and surgery history. Additionally, they combined these 2 models to test whether there was any additional benefit from a so-called “multimodal” approach.

Their CNN model outperformed the tabular data model, while the multimodal approach outperformed the individual models, demonstrating that knee radiographs contain prognostic features not present in structured patient data, even reported K/L grade. Despite accurate radiographic scoring, applicability will ultimately be limited given the poor correlation between radiographic scoring and clinical outcomes such as pain scores (65). Predicting progressive disease may only be helpful if the definition of progressive disease is a clinical, rather than radiographic outcome.

## Temporal artery ultrasound

The diagnosis of GCA is a vexing problem for rheumatologists, in no small part due to the lack of an accurate noninvasive diagnostic test. Temporal artery ultrasound is one emerging solution to this problem, with EULAR guidelines recommending ultrasound as the first-line imaging modality for the evaluation of suspected GCA (66). Despite its relatively good performance as a diagnostic test, temporal artery ultrasound suffers from only moderate interrater agreement, with significant training requirements that pose a barrier to the widespread adoption of this test (67). Deep learning therefore appears attractive as a tool to reduce the variability in interpretation and perhaps even lower the barrier to the adoption of this test.

Roncato et al (68) developed a CNN model, specifically to identify 1 common feature in positive temporal artery ultrasounds: the halo sign (69). The first step in their algorithm was to perform semantic segmentation of transverse and longitudinal color Doppler or power Doppler images of temporal arteries. This process involved drawing boxes around arteries and adjacent tissue, with individual pixels in these boxes labeled as either halo sign–positive or halo sign–negative. The authors used a U-Net model, designed specifically for biomedical image segmentation (49). The final classification of each image as either positive or negative was based on the percentage of pixels within the bounding box classified as halo sign–positive—a higher percentage of halo sign pixels means a higher probability that the image truly contains a halo sign. The accuracy of the model was compared using 2 groups of images: group 1 obtained by a single operator, using a standardized protocol; and group 2 obtained by multiple different operators using a variety of parameters. The performance on group 1 was significantly higher than group 2 (AUC 0.95 versus 0.82). Although training on more nonstandard images may improve performance, deep learning can also be used for computer-assisted image acquisition to assist clinicians and sonographers in acquiring standardized views at the time of ultrasound.

## The future

*Learning with limited data.* One of the main features of deep learning is the ability to capitalize on the wealth of large data sets, with improvements in computer vision models seen even beyond

massive data sets composed of 300 million images (70). Despite this, there are 3 established and emerging technical solutions to the problem of learning with limited data (See Figure 5).

*Transfer learning.* The first method, now well-established in deep learning research and applications, is a concept known as transfer learning. Transfer learning is the process whereby a model is trained on a large data set (pretraining), and then only partially retrained on a small data set, even from a different domain (e.g., a model trained on photographs is retrained on radiographs). The motivation for this process is that, in training a large data set, the model will have learned generalizable properties. These generalizable properties are believed to be learned in the early layers, and so it is only the final layers that are retrained on the new, smaller data set of interest. This has the effect of “specializing” a pretrained model for a downstream task. The pretraining process is generally performed using a process called self-supervised learning, which does not require any hand-labeled data, but instead learns by predicting missing words, the next word in a sentence or similar tasks. In certain circumstances, these pretrained models can be used in a few- or zero-shot setting, meaning they are fine-tuned on few or even no examples of the downstream task. This is particularly the case for NLP, where the task can be distinguished by a text prompt (e.g., a clinical question)—if the pretrained model can interpret the prompt, then it may not necessarily need to see any examples in order to perform the task.

*Self-supervised learning.* Recently, self-supervised learning has emerged as a method to learn from large, unlabeled data sets (71). Self-supervision is achieved by creating tasks that allow models to learn generalizable features. For example, in NLP, learning to predict the next word in a sentence requires learning common linguistic features, such as sentence structure and word meaning. In computer vision, learning to pair original and distorted versions of the same image requires learning invariant features, such as the rounded shape of the metacarpal head. Self-supervised models can then be used in a transfer learning process to train on smaller, labeled data sets. Given the relatively small data sets in rheumatology, it is highly likely that new applications for deep learning will be powered by self-supervised learning and transfer learning.

*Methods of increasing data set size.* While single institutions might generate only relatively small data sets, pooling data across many institutions can result in large data sets. Large data sets may be necessary, particularly where outcomes are rare. In rheumatology, the Rheumatology Informatics System for Effectiveness registry has begun pooling EHR data to further our understanding of rheumatic diseases (72); however, further barriers exist where text and image data are needed. Concerns about data privacy can be a barrier to sharing data across institutional, regional, and international borders—aside from specific data sharing agreements, much effort has been made in producing technical solutions to this problem.

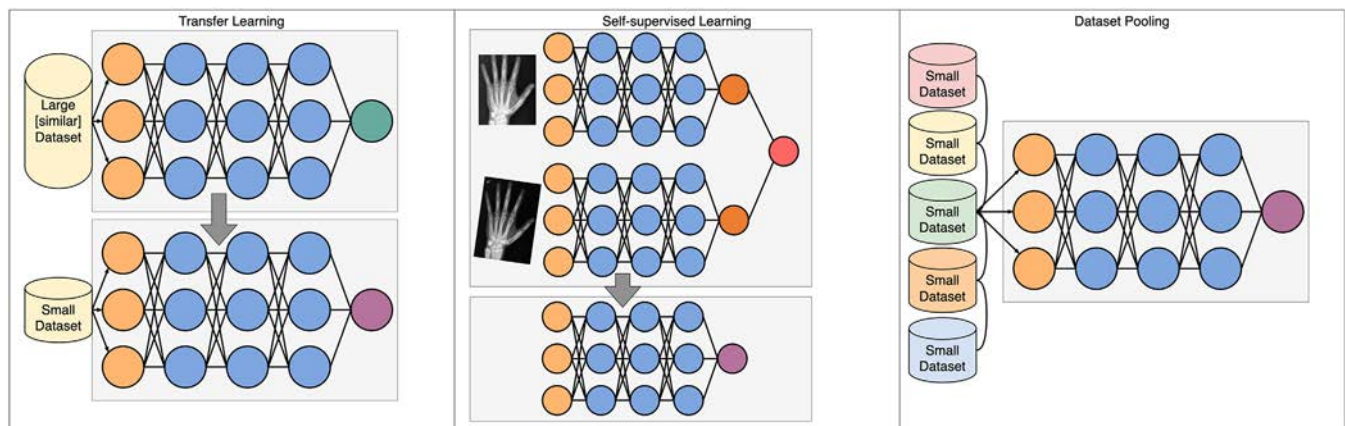


**Figure 5.** Three methods to overcome the complications of limited data sets. Transfer learning takes a model trained on a large data set and repurposes it for a new task, replacing only the final layer. Self-supervised learning is a type of transfer learning; however, the data set used in pre-training does not need to have labels—here the task is simply to recognize that 2 versions of the same image are indeed the same image, and in doing so the model learns to recognize invariant features. Increasing data set size can be done in a number of ways; however, pooling data across institutions has technical, logistical, and privacy issues that must be overcome. Circles represent individual nodes. Color figure can be viewed in the online issue, which is available at <http://onlinelibrary.wiley.com/doi/10.1002/art.42296/abstract>.

Recently, federated learning has emerged as a powerful tool to allow multiple sites to contribute training data without ever sharing raw data (73). Several federated learning techniques exist; however, recent work has focused on methods whereby individual sites train small models on local data, with the coefficients of these models sent to a central site that uses these to train a multicenter model (74,75). Federated learning is not without significant challenges, including the high cost of setting up a central server and communication between sites, black box models (particularly if only model weights are shared and not raw data), and no clear best way to aggregate data from heterogeneous sites (76). In addition to these concerns, federated learning does not fully solve the data privacy problem; all models can “memorize” training data and therefore if privacy is a significant concern, models have to be trained using a special technique called differential privacy to prevent data memorization (77).

When there is not even enough data to pool, or data pooling is impractical, an alternative practice is to generate synthetic data. Generating artificial samples has been an area of intense research in deep learning, particularly after the development of Generative Adversarial Networks (GANs) (45) by Goodfellow et al in 2014. GANs train 2 networks simultaneously: a generator network to generate new data and a discriminator network to discriminate real data from synthetic data. Although these models can be difficult to train, as it becomes harder and harder for the discriminator to distinguish between real and synthetic data, the quality of synthetic data increases.

**Data integrity, bias, and ethics.** Although deep learning has a long history in computer science research, it has only been the relatively recent development of computers capable of training these algorithms that has resulted in an explosion of applications in medicine. In rheumatology, these methods have only now begun to show promise—although not without potential impediments.

As deep learning methods gain more prominence, issues of data integrity and standardization will become more important. As we saw above, the standardized acquisition of temporal artery ultrasound images poses a potential barrier to the effective deployment of deep learning algorithms to diagnose GCA. Outside of rheumatology, a similar problem in echocardiography has led to several FDA-approved ultrasound machines that not only interpret images, but guide the user on how to adjust the probe to obtain enhanced views (78). As rheumatologists and machine learning engineers begin applying deep learning techniques to clinical problems, we will need an even greater focus on data integrity and quality. Beyond simply ensuring high quality data, careful collection and curation of data sets is required when considering how data may reflect the systematic biases against marginalized and underrepresented minorities in our communities, making resultant algorithms unsafe and inaccurate for many.

New guidelines for reporting clinical trials of artificial intelligence interventions provide a guide for the steps required to demonstrate safety and efficacy of these algorithms (79). Like clinical trials of conventional medical interventions, careful trial design is paramount in testing clinical algorithms. Unlike conventional trials, the risk of bias extends beyond the study design and into the algorithm design itself. The data set or sets used to train deep learning algorithms can introduce substantial bias that may not only invalidate the results, but also introduce racial, sex-based, or other forms of discrimination if applied systematically. Promising methods to identify and minimize such bias include report cards for evaluating performance in particular groups (80); however, static model checks are not enough in production, and the predictions of any model should be periodically examined to ensure they are not introducing or perpetuating unacceptable bias. For more detail on bias in clinical machine learning, Chen et al (81) provide a detailed overview of how bias is

introduced at each step of the algorithm development process, while Gianfrancesco et al (82) detail the sources of bias in EHR-based models.

New technologies like wearable devices, assisted by automatic deep learning algorithms, have the potential to diagnose a myriad of conditions under circumstances never seen before at such scale (e.g., asymptomatic atrial fibrillation in young people), with the resulting risk of widespread overdiagnosis. In rheumatology, for example, the unsolved problem of treatment for clinically suspect arthralgia may be compounded should automated diagnostic tools become available, identifying subclinical reductions in morning mobility leading to a tidal wave of very early arthritis diagnoses. While coordinated data collection will be needed to quantify the risks associated with these new diagnostic paradigms (83), this also presents a new opportunity to further our understanding of rheumatic diseases by studying longitudinal cohorts from very early disease stages. Compounding this, access to these devices is contingent on affordability (84)—one way in which technologically enhanced medicine widens the socioeconomic disparities in the provision of health care.

## Explainability in rheumatology

*Definition of explainability.* Neural networks are often described as black boxes, in that their internal processes are inscrutable to humans. Many have argued that we need ways to explain why a model reaches a decision so that doctors are able to interpret it and apply it clinically (85). The most common methods for explainability in conventional machine learning—in particular Shapley Additive Explanations and Local Interpretable Model-Agnostic Explanations (86)—are broadly classified as post hoc perturbation methods. These algorithms perturb the input data and measure how these perturbations in the input alter the model output. Although post hoc explainability methods have shortcomings, including susceptibility to hide model bias (86), even inadequate model explanations provide interpretable outputs when the input variables are themselves simple and interpretable (e.g., how does cardiovascular risk change if the patient has hypertension). Compared to conventional machine learning methods, explainability methods for deep learning are more difficult to interpret. In medical imaging, the most common method of explainability is saliency maps, which visually show the parts of the input image that most contributed to the final prediction (87).

*Strengths.* Explainability methods may have a role in evaluating models. As previously discussed, a 2019 article predicted future Clinical Disease Activity Index (CDAI) and used permutation importance scores to determine feature importance. The authors concluded that disease activity, laboratory test values, and medications were the best predictors of future CDAI (19). With simple input data, this method provides useful information regarding

how the model operates, but when dealing with complex data (e.g., text, images), interpretation is unclear.

*Weaknesses.* In a model diagnosing knee OA, saliency maps were used to show that the model was identifying relevant radiologic features (60). The authors found that osteophytes were highlighted and concluded that attention maps would “build better trust in the clinical community.” However, they also acknowledge that the reason these anatomically relevant areas were highlighted was because they constrained the model to only assess these regions. Additionally, a model developed to predict RA radiographic scores used saliency maps to determine which joints were predictive of the scores (51). While these images show some focus over bone and joint space, they also highlight parts of the image that are empty.

In both of these cases, the meaning of these explanations is unclear. In the first, it was inevitable that these regions would be highlighted, while in the second case, the model uses areas that have no anatomical relevance in its prediction. Both papers use this as evidence that their model is performing reliably. Even more problematically, it has been shown that in models where the input image is modified to result in an incorrect prediction, the saliency map can still highlight clinically relevant regions of the image (88). This is falsely reassuring that the model is behaving appropriately, while still providing the wrong answer. A recent paper highlighted these concerns about the danger of relying on such methods to engender trust in a system and suggests we ought to depend on rigorous evaluation instead (54). Whether or not saliency maps produce sensible explanations, they should not be what we rely on to trust the behavior of neural networks.

*Evaluation.* Although explainability techniques can tell us something about model behavior, they cannot tell us how to interpret the predictions. Three steps are needed for safe implementation: testing on external data sets is needed to ensure models generalize to different population, performance should be evaluated in subgroups to eliminate bias (89), and, ultimately, models should be tested in randomized control trials. It is vital to understand how models affect patient outcomes in clinical settings and it is this, not explainability techniques, that rheumatologists should be demanding before a model reaches clinical implementation.

*Translation into practice.* Deep learning is transforming many industries and at an ever-increasing pace. For example, Google's language translation (90), Uber's expected arrival time (ETA) prediction (91), and Microsoft's code completion tool (92) are all deep learning algorithms that many people rely on daily. Uber switched their ETA algorithm to deep learning because of its ability to easily scale up with larger data sets and larger models. However, the same cost/benefit tradeoff is not always clear in medicine, where the scale may not be so large and financial barriers, such as the cost of regulatory approval, may be a substantial impediment. The barriers to widespread adoption are necessarily set high, with minimum standards of safety and efficacy set not only by the



regulatory authorities, but also the clinicians who must “buy in” to this new technology. Nevertheless, the deep learning revolution has been largely driven by falling costs in computing power (93), with no clear indication that this will significantly plateau. We can therefore expect further improvements, shifting the cost/benefit tradeoff and encouraging even greater investment in research. Who takes advantage of this, whether it be academic or industry, is an open question.

## Conclusion

Deep learning is an important method in medical machine learning applications and will likely become the dominant method in the future. Several applications of deep learning in rheumatology have been reported, with the promise of many more to come. Importantly, although deep learning methods offer the opportunity to improve the efficiency of some clinical tasks, they also provide a powerful technique for generating new knowledge and insights, particularly in the previously impenetrable analysis of unstructured data such as text and images. To date, much of the published work applying deep learning in rheumatology has occurred on small, homogeneous public data sets that do not reflect the diversity of real data, including the interactions between different data modalities (e.g., EHRs plus imaging). Further collaboration and interaction between machine learning researchers and rheumatology researchers will likely result in more clinically applicable algorithms, with translation into clinical practice being the next great hurdle to overcome. Researchers should therefore be familiar with the potential applications and limitations of these methods in their own research, and clinicians should be familiar with some of the potential benefits and pitfalls as these methods make their way into clinical practice.

## Acknowledgment

Open access publishing was facilitated by The University of Melbourne, as part of the Wiley - The University of Melbourne agreement via the Council of Australian University Librarians.

## Author Contributions

All authors were involved in drafting the article or revising it critically for important intellectual content, and all authors approved the final version to be published.

## References




1. LeCun Y, Bengio Y, Hinton G. Deep learning. *Nature* 2015;521:436–44.
2. American College of Radiology. AI Central. URL: <https://aicentral.acrdsi.org/>.
3. Silver D, Hubert T, Schrittwieser J, et al. Mastering chess and shogi by self-play with a general reinforcement learning algorithm. *arXiv [cs.AI]* 2017. URL: <http://arxiv.org/abs/1712.01815>.
4. Zhang J, Zhao Y, Saleh M, et al. PEGASUS: Pre-training with Extracted Gap-sentences for Abstractive Summarization. *arXiv [cs.CL]* 2019. URL: <http://arxiv.org/abs/1912.08777>.
5. Chen K, Oldja R, Smolyanskiy N, et al. MVLidarNet: Real-time multi-class scene understanding for autonomous driving using multiple views. *arXiv [cs.CV]* 2020. URL: <http://arxiv.org/abs/2006.05518>.
6. Jumper J, Evans R, Pritzel A, et al. Highly accurate protein structure prediction with AlphaFold. *Nature* 2021;596:583–9.
7. Jurafsky D, Martin JH. *Speech and language processing: an introduction to natural language processing, computational linguistics, and speech recognition*. Prentice Hall: Hoboken; 2009.
8. Young T, Hazarika D, Poria S, et al. Recent trends in deep learning based natural language processing [review]. *IEEE Comput Intell Mag* 2018;13:55–75.
9. Vaswani A, Shazeer N, Parmar N, et al. Attention is all you need. In: Guyon I, Luxburg UV, Bengio S, et al, editors. *Advances in neural information processing systems* 30. Curran Associates, Inc: Red Hook (New York); 2017. p. 5998–6008.
10. Liao KP, Cai T, Gainer V, et al. Electronic medical records for discovery research in rheumatoid arthritis. *Arthritis Care Res (Hoboken)* 2010;62:1120–7.
11. Zhao SS, Hong C, Cai T, et al. Incorporating natural language processing to improve classification of axial spondyloarthritis using electronic health records. *Rheumatology (Oxford)* 2020;59:1059–65.
12. Tedeschi SK, Cai T, He Z, et al. Classifying pseudogout using machine learning approaches with electronic health record data. *Arthritis Care Res (Hoboken)* 2021;3:442–8.
13. McMaster C, Yang V, Sutu B, et al. Temporal artery biopsy reports can be accurately classified by artificial intelligence [abstract]. *Arthritis Rheumatol* 2021;73 Suppl. URL: <https://acrabstracts.org/abstract/temporal-artery-biopsy-reports-can-be-accurately-classified-by-artificial-intelligence/>.
14. Sanh V, Debut L, Chaumond J, et al. DistilBERT, a distilled version of BERT: smaller, faster, cheaper and lighter. *arXiv [cs.CL]* 2019. URL: <http://arxiv.org/abs/1910.01108>.
15. Rajkomar A, Oren E, Chen K, et al. Scalable and accurate deep learning with electronic health records. *NPJ Digit Med* 2018;1:18.
16. Elangovan A, He J, Verspoor K. Memorization vs. generalization: quantifying data leakage in NLP performance evaluation. *arXiv [cs.CL]* 2021. URL: <http://arxiv.org/abs/2102.01818>.
17. Li Y, Rao S, Solares JR, et al. BEHRT: transformer for electronic health records. *Sci Rep* 2020;10:7155.
18. Helliwell T, Hider SL, Mallen CD. Polymyalgia rheumatica: diagnosis, prescribing, and monitoring in general practice. *Br J Gen Pract* 2013;63:e361–6.
19. Norgeot B, Glicksberg BS, Trupin L, et al. Assessment of a deep learning model based on electronic health record data to forecast clinical outcomes in patients with rheumatoid arthritis. *JAMA Netw Open* 2019;2:e190606.
20. Aletaha D, Nell VP, Stamm T, et al. Acute phase reactants add little to composite disease activity indices for rheumatoid arthritis: validation of a clinical activity score. *Arthritis Res Ther* 2005;7:R796–806.
21. Krizhevsky A, Sutskever I, Hinton GE. ImageNet classification with deep convolutional neural networks. In: Pereira F, Burges CJ, Bottou L, et al, editors. *Advances in neural information processing systems* 25. Curran Associates, Inc: New York; 2012. p. 1097–105.
22. LeCun Y, Haffner P, Bottou L, et al. Object recognition with gradient-based learning. In: Forsyth DA, Mundy JL, di Gesù V, et al, editors. *Shape, contour and grouping in computer vision*. Springer Berlin Heidelberg; 1999. p. 319–45.
23. Mahler M, Meroni PL, Bossuyt X, et al. Current concepts and future directions for the assessment of autoantibodies to cellular antigens



- referred to as anti-nuclear antibodies. *J Immunol Res* 2014;2014: 315179.
24. Damoiseaux J, Andrade LE, Carballo OG, et al. Clinical relevance of HEp-2 indirect immunofluorescent patterns: the International Consensus on ANA patterns (ICAP) perspective. *Ann Rheum Dis* 2019;78: 879–89.
  25. Infantino M, Meacci F, Grossi V, et al. The burden of the variability introduced by the HEp-2 assay kit and the CAD system in ANA indirect immunofluorescence test. *Immunol Res* 2017;65:345–54.
  26. Rahman S, Wang L, Sun C, et al. Deep learning based HEp-2 image classification: a comprehensive review. *arXiv [cs.CV]* 2019. URL: <http://arxiv.org/abs/1911.08916>.
  27. Vununu C, Lee SH, Kwon KR. A strictly unsupervised deep learning method for HEp-2 cell image classification. *Sensors* 2020;20:2717.
  28. Foggia P, Percannella G, Soda P, et al. Benchmarking HEp-2 cells classification methods. *IEEE Trans Med Imaging* 2013;32:1878–89.
  29. Wu YD, Sheu RK, Chung CW, et al. Application of supervised machine learning to recognize competent level and mixed antinuclear antibody patterns based on ICAP International Consensus. *Diagnos-tics (Basel)* 2021;11:642.
  30. Benammar Elgaied A, Cascio D, Bruno S, et al. Computer-assisted classification patterns in autoimmune diagnostics: the AIDA Project. *Biomed Res Int* 2016;2016:2073076.
  31. Heo-2 Benchmarking. Datasets & Tools: HEp-2 contest @ ICPR 2016. URL: <https://hep2.unisa.it/dbtools.html>.
  32. Mivia. ICPR 2012–Contest on HEp-2 cells classification. URL: <https://mivia.unisa.it/contest-hep-2/>.
  33. Wiliem A, Wong Y, Sanderson C, et al. Classification of human epithelial type 2 cell indirect immunofluorescence images via codebook based descriptors. URL: <http://staff.itee.uq.edu.au/lovell/snphep2/>.
  34. Kassani SH, Kassani PH, Khazaeinezhad R, et al. Diabetic retinopathy classification using a modified Xception architecture. In: 2019 IEEE International Symposium on Signal Processing and Information Technology (ISSPIT); 2019. p. 1–6.
  35. Cohen J. A coefficient of agreement for nominal scales. *Educ Psychol Meas* 1960;20:37–46.
  36. Kaeley GS, Bakewell C, Deodhar A. The importance of ultrasound in identifying and differentiating patients with early inflammatory arthritis: a narrative review. *Arthritis Res Ther* 2020;22:1.
  37. D'Agostino MA, Terslev L, Aegerter P, et al. Scoring ultrasound synovitis in rheumatoid arthritis: a EULAR-OMERACT ultrasound taskforce-Part 1: definition and development of a standardised, consensus-based scoring system. *RMD Open* 2017;3:e000428.
  38. Terslev L, Christensen R, Aga AB, et al. Assessing synovitis in the hands in patients with rheumatoid arthritis by ultrasound: an agreement study exploring the most inflammatory active side from two Norwegian trials. *Arthritis Res Ther* 2019;21:166.
  39. Andersen JK, Pedersen JS, Laursen MS, et al. Neural networks for automatic scoring of arthritis disease activity on ultrasound images. *RMD Open* 2019;5:e000891.
  40. Simonyan K, Zisserman A. Very deep convolutional networks for large-scale image recognition. *arXiv [cs.CV]* 2014. URL: <http://arxiv.org/abs/1409.1556>.
  41. Szegedy C, Vanhoucke V, Ioffe S, et al. Rethinking the inception architecture for computer vision. *arXiv [cs.CV]* 2015. URL: <http://arxiv.org/abs/1512.00567>.
  42. Russakovsky O, Deng J, Su H, et al. ImageNet large scale visual recognition challenge. *Int J Comput Vis* 2015;115:211–52.
  43. Terslev L, Naredo E, Aegerter P, et al. Scoring ultrasound synovitis in rheumatoid arthritis: a EULAR-OMERACT ultrasound taskforce-Part 2: reliability and application to multiple joints of a standardised consensus-based scoring system. *RMD Open* 2017;3:e000427.
  44. Christensen AB, Just SA, Andersen JK, et al. Applying cascaded convolutional neural network design further enhances automatic scoring of arthritis disease activity on ultrasound images from rheumatoid arthritis patients. *Ann Rheum Dis* 2020;79:1189–93.
  45. Goodfellow IJ, Pouget-Abadie J, Mirza M, et al. Generative adversarial networks. *arXiv [stat.ML]* 2014. URL: <http://arxiv.org/abs/1406.2661>.
  46. Ødegård S, Landewé R, van der HD, et al. Association of early radiographic damage with impaired physical function in rheumatoid arthritis: a ten-year, longitudinal observational study in 238 patients. *Arthritis Rheum* 2006;54:68–75.
  47. Van der Heijde D. How to read radiographs according to the Sharp/van der Heijde method. *J Rheumatol* 2000;27:261–3.
  48. Hirano T, Nishide M, Nonaka N, et al. Development and validation of a deep-learning model for scoring of radiographic finger joint destruction in rheumatoid arthritis. *Rheumatol Adv Pract* 2019;3:rkz047.
  49. Ronneberger O, Fischer P, Brox T. U-Net: convolutional networks for biomedical image segmentation. In: Medical image computing and computer-assisted intervention–MICCAI 2015. Springer International Publishing: New York; 2015. p. 234–41.
  50. Viola P, Jones M. Rapid object detection using a boosted cascade of simple features. In: Proceedings of the 2001 IEEE Computer Society Conference on Computer Vision and Pattern Recognition CVPR 2001. 2001. p. I.
  51. Chaturvedi N. DeepRA: predicting joint damage from radiographs using CNN with attention. *arXiv [cs.CV]* 2021. URL: <http://arxiv.org/abs/2102.06982>.
  52. Lin TY, Goyal P, Girshick R, et al. Focal loss for dense object detection. *arXiv [cs.CV]* 2017. URL: <http://arxiv.org/abs/1708.02002>.
  53. Tan M, Le QV. EfficientNet: rethinking model scaling for convolutional neural networks. *arXiv [cs.LG]* 2019. URL: <http://arxiv.org/abs/1905.11946>.
  54. Ghassemi M, Oakden-Rayner L, Beam AL. The false hope of current approaches to explainable artificial intelligence in health care. *Lancet Digit Health* 2021;3:e745–50.
  55. Lipton ZC. The mythos of model interpretability. *arXiv [cs.LG]* 2016. URL: <http://arxiv.org/abs/1606.03490>.
  56. Sakellariou G, Conaghan PG, Zhang W, et al. EULAR recommendations for the use of imaging in the clinical management of peripheral joint osteoarthritis. *Ann Rheum Dis* 2017;76:1484–94.
  57. Wang X, Oo WM, Linklater JM. What is the role of imaging in the clinical diagnosis of osteoarthritis and disease management? *Rheumatology (Oxford)* 2018;57 Suppl:iv51–60.
  58. Tulpin A, Klein S, Bierma-Zeinstra SM, et al. Multimodal machine learning-based knee osteoarthritis progression prediction from plain radiographs and clinical data. *Sci Rep* 2019;9:20038.
  59. Tulpin A, Saarakkala S. Automatic grading of individual knee osteoarthritis features in plain radiographs using deep convolutional neural networks. *arXiv [eess.IV]* 2019. URL: <http://arxiv.org/abs/1907.08020>.
  60. Tulpin A, Thevenot J, Rahtu E, et al. Automatic knee osteoarthritis diagnosis from plain radiographs: a deep learning-based approach. *Sci Rep* 2018;8:1727.
  61. Tulpin A, Klein S, Bierma-Zeinstra S, et al. Deep learning predicts knee osteoarthritis progression from plain radiographs. *Osteoarthritis Cartilage* 2019;27:S397–8.
  62. Kellgren JH, Lawrence JS. Radiological assessment of osteoarthrosis. *Ann Rheum Dis* 1957;16:494–502.
  63. Baldi P, Chauvin Y. Neural networks for fingerprint recognition. *Neural Comput* 1993;5:402–18.
  64. Altman RD, Gold GE. Atlas of individual radiographic features in osteoarthritis, revised. *Osteoarthritis Cartilage* 2007;15 Suppl:A1–56.
  65. Finan PH, Buenaver LF, Bounds SC, et al. Discordance between pain and radiographic severity in knee osteoarthritis: findings from

- quantitative sensory testing of central sensitization. *Arthritis Rheum* 2013;65:363–72.
66. DeJaco C, Ramiro S, Duftner C, et al. EULAR recommendations for the use of imaging in large vessel vasculitis in clinical practice. *Ann Rheum Dis* 2018;77:636–43.
  67. Luqmani R, Lee E, Singh S, et al. The role of ultrasound compared to biopsy of temporal arteries in the diagnosis and treatment of giant cell arteritis (TABUL): a diagnostic accuracy and cost-effectiveness study. *Health Technol Assess* 2016;20:1–238.
  68. Roncato C, Perez L, Brochet-Guégan A, et al. Colour Doppler ultrasound of temporal arteries for the diagnosis of giant cell arteritis: a multicentre deep learning study. *Clin Exp Rheumatol* 2020;38:120–5.
  69. Schmidt WA, Kraft HE, Völker L, et al. Colour Doppler sonography to diagnose temporal arteritis. *Lancet* 1995;345:866.
  70. Zhai X, Kolesnikov A, Hounsby N, et al. Scaling vision transformers. *arXiv [cs.CV]* 2021. URL: <http://arxiv.org/abs/2106.04560>.
  71. Zbontar J, Jing L, Misra I. Barlow twins: self-supervised learning via redundancy reduction. *arXiv [cs.CV]* 2021. URL: <https://arxiv.org/abs/2103.03230>.
  72. Yazdany J, Bansback N, Clowse M, et al. Rheumatology informatics system for effectiveness: a national informatics-enabled registry for quality improvement. *Arthritis Care Res (Hoboken)* 2016;68:1866–73.
  73. Yang Q, Liu Y, Chen T, et al. Federated machine learning: concept and applications. *ACM Trans Intell Syst Technol* 2019;10:1–19.
  74. Dayan I, Roth HR, Zhong A, et al. Federated learning for predicting clinical outcomes in patients with COVID-19. *Nat Med* 2021;27:1735–43.
  75. McMahan B, Moore E, Ramage D, et al. Communication-efficient learning of deep networks from decentralized data. In: Singh A, Zhu J, editors. *PMLR* 2017;54:1273–82.
  76. Rieke N, Hancox J, Li W, et al. The future of digital health with federated learning. *NPJ Digit Med* 2020 14;3:119.
  77. Abadi M, Chu A, Goodfellow I, et al. Deep learning with differential privacy. *arXiv [stat.ML]* 2016. URL: <http://arxiv.org/abs/1607.00133>.
  78. U.S. Food and Drug Administration Office of the Commissioner. FDA authorizes marketing of first cardiac ultrasound software that uses artificial intelligence to guide user; 2020. URL: <https://www.fda.gov/news-events/press-announcements/fda-authorizes-marketing-first-cardiac-ultrasound-software-uses-artificial-intelligence-guide-user>.
  79. Liu X, Rivera SC, Moher D, et al, on behalf of the SPIRIT-AI and CONSORT-AI Working Group. Reporting guidelines for clinical trial reports for interventions involving artificial intelligence: the CONSORT-AI extension. *Nat Med* 2020;26:1364–74.
  80. Mitchell M, Wu S, Zaldivar A, et al. Model cards for model reporting. *arXiv [cs.LG]* 2018. URL: <http://arxiv.org/abs/1810.03993>.
  81. Chen IY, Pierson E, Rose S, et al. Ethical machine learning in health care. *arXiv [cs.CY]* 2020. URL: <http://arxiv.org/abs/2009.10576>.
  82. Gianfrancesco MA, Tamang S, Yazdany J, et al. Potential biases in machine learning algorithms using electronic health record data. *JAMA Intern Med* 2018;178:1544–7.
  83. Capurro D, Coghlan S, Pires DE. Preventing digital overdiagnosis. *JAMA* 2022;327:525–6.
  84. Smuck M, Odonkor CA, Wilt JK, et al. The emerging clinical role of wearables: factors for successful implementation in healthcare. *NPJ Digit Med* 2021;4:45.
  85. Holzinger A, Biemann C, Pattichis CS, et al. What do we need to build explainable AI systems for the medical domain? *arXiv [cs.AI]* 2017. URL: <http://arxiv.org/abs/1712.09923>.
  86. Slack D, Hilgard S, Jia E, et al. Fooling LIME and SHAP: adversarial attacks on post hoc explanation methods. In: *Proceedings of the AAAI/ACM Conference on AI, Ethics, and Society*. New York: Association for Computing Machinery; 2020. p. 180–6.
  87. Simonyan K, Vedaldi A, Zisserman A. Deep inside convolutional networks: visualising image classification models and saliency maps. *arXiv [cs.CV]* 2013. URL: <http://arxiv.org/abs/1312.6034>.
  88. Adebayo J, Gilmer J, Muelly M, et al. Sanity checks for saliency maps. *arXiv [cs.CV]* 2018. URL: <http://arxiv.org/abs/1810.03292>.
  89. Oakden-Rayner L, Dunnmon J, Carneiro G, et al. Hidden stratification causes clinically meaningful failures in machine learning for medical imaging. *Proc ACM Conf Health Inference Learn* 2020;2020:151–9.
  90. Caswell I, Liang B. Recent advances in google translate. *Google AI Blog*. URL: <https://ai.googleblog.com/2020/06/recent-advances-in-google-translate.html>.
  91. Hu X, Cirit O, Binaykiya T, et al. DeepETA: how uber predicts arrival times using deep learning. *Uber Engineering*. URL: <https://eng.uber.com/deepeta-how-uber-predicts-arrival-times/>.
  92. Chen M, Tworek J, Jun H, et al. Evaluating large language models trained on code. *arXiv [cs.LG]* 2021. URL: <http://arxiv.org/abs/2107.03374>.
  93. Slominski A, Muthusamy V, Ishakian V. Future of computing is boring (and that is exciting!) or how to get to computing nirvana in 20 years or less. *arXiv [cs.CY]* 2019. URL: <http://arxiv.org/abs/1906.10398>.
  94. Vig J. A multiscale visualization of attention in the transformer model. *arXiv [cs.HC]* 2019. URL: <https://arxiv.org/abs/1906.05714>.
  95. Nair V, Hinton GE. Rectified linear units improve restricted Boltzmann machines. In: *Proceedings of the 27th International Conference on International Conference on Machine Learning*. Omnipress: Madison (Wisconsin); 2010. p. 807–14.

# Breakthrough SARS-CoV-2 Infections in Patients With Immune-Mediated Disease Undergoing B Cell-Depleting Therapy: A Retrospective Cohort Analysis

Cassandra M. Calabrese,<sup>1</sup> Elizabeth Kirchner,<sup>1</sup> Elaine M. Husni,<sup>1</sup>  Brandon P. Moss,<sup>2</sup> Anthony P. Fernandez,<sup>3</sup>   
Yuxuan Jin,<sup>4</sup> and Leonard H. Calabrese<sup>1</sup> 

**Objective.** Patients with immune-mediated inflammatory diseases (IMIDs) receiving B cell-depleting therapy (BCDT) are among the most vulnerable to severe COVID-19, as well as the most likely to suboptimally respond to SARS-CoV-2 vaccines. However, little is known about the frequency or severity of breakthrough infection in this population. We retrospectively analyzed a large group of vaccinated IMID patients undergoing BCDT in order to identify breakthrough COVID-19 infections and assess their outcomes.

**Methods.** In this retrospective cohort study, the pharmacy records and COVID-19 registry at the Cleveland Clinic were searched using specific International Statistical Classification of Diseases and Related Health Problems, Tenth Revision codes to identify IMIDs patients who 1) received treatment with BCDT, 2) were vaccinated against SARS-CoV-2, and 3) experienced breakthrough infections. Each electronic medical record was reviewed to extract clinical data and outcomes. Univariate and multivariable logistic/proportional odds regression models were used to examine the risk factors for severe outcomes.

**Results.** Of 1,696 IMID patients receiving BCDT, 74 developed breakthrough COVID-19 prior to December 16, 2021. Outcomes were severe, with 29 patients hospitalized (39.2%), 11 patients requiring critical care (14.9%), and 6 deaths (8.1%). Outpatient anti-SARS-CoV-2 monoclonal antibodies were used to treat 21 patients, with 1 hospitalization and no deaths. A comparator analysis examining 1,437 unvaccinated IMID patients receiving BCDT over the same time period identified 57 COVID-19 cases (4.0%), with 28 requiring hospitalization (49.1%), including 7 deaths (12.3%).

**Conclusion.** IMID patients receiving BCDT regardless of vaccine status appear to be vulnerable to infection with SARS-CoV-2, and use of BCDT is frequently associated with severe outcomes. Outpatient use of anti-SARS-CoV-2 monoclonal antibody therapy appears to be associated with enhanced clinical outcomes.

## INTRODUCTION

The deployment of vaccines to both prevent infection with SARS-CoV-2 as well as limit the severity of COVID-19 has proven efficacious in the general population. However, data regarding patients with underlying immunocompromising conditions, including those with immune-mediated inflammatory diseases (IMIDs), suggest both an increased likelihood of developing breakthrough infections and of experiencing more severe outcomes despite full vaccination status (1–3).

While there is significant heterogeneity in the capacity of specific immunosuppressive agents to limit the integrated immune response to both natural infection and vaccines, of particular concern is the class of B cell-depleting therapies (BCDTs) widely used to treat an array of IMIDs. Before the introduction of SARS-CoV-2 vaccines, treatment of both rheumatic and neurologic IMIDs with such BCDTs was associated with more severe COVID-19 (4–10). Furthermore, numerous studies have shown the capacity for certain BCDTs to profoundly impair humoral response to vaccines, including the vaccine against

Supported by the R. J. Fasanmyer Center for Clinical Immunology, Cleveland Clinic.

<sup>1</sup>Cassandra M. Calabrese, DO, Elizabeth Kirchner, DNP, Elaine M. Husni, MD, Leonard H. Calabrese, DO: Department of Rheumatic and Immunologic Diseases, Cleveland Clinic, Cleveland, Ohio; <sup>2</sup>Brandon P. Moss, MD: Mellen Center for Multiple Sclerosis Treatment and Research, Cleveland Clinic, Cleveland, Ohio; <sup>3</sup>Anthony P. Fernandez, MD, PhD: Department of Dermatology, Cleveland Clinic, Cleveland, Ohio; <sup>4</sup>Yuxuan Jin, MS: Quantitative Health Sciences, Cleveland Clinic, Cleveland, Ohio.

Author disclosures are available at <https://onlinelibrary.wiley.com/action/downloadSupplement?doi=10.1002%2Fart.42287&file=art42287-sup-0001-Disclosureform.pdf>.

Address correspondence via email to Leonard H. Calabrese, DO, at [calabrl@ccf.org](mailto:calabrl@ccf.org).

Submitted for publication February 22, 2022; accepted in revised form June 26, 2022.

SARS-CoV-2 (11–14). More recently, however, several studies (15,16) have demonstrated a dichotomy in vaccine responses in IMiD patients receiving BCDTs, demonstrating suppression of the humoral response while showing a preserved and robust cell-mediated immune response—providing hope that such a pattern of immunity will afford adequate protection. To date, there have been only limited investigations of IMiD patients receiving BCDTs examining the frequency and outcomes of breakthrough infections. Using pharmacologic records and the COVID-19 registry at the Cleveland Clinic, we systematically examined a large population of IMiD patients who received BCDTs and were vaccinated against SARS-CoV-2 to describe the frequency of breakthrough infections and their outcomes.

## PATIENTS AND METHODS

**Patient identification and data extraction.** This study was a retrospective cohort analysis. Pharmacy records from the Cleveland Clinic were electronically searched for patients undergoing BCDT (rituximab [RTX], ocrelizumab, ofatumumab) in the year 2020, prior to receipt of SARS-CoV-2 vaccine. Records with ICD-10 codes for IMiDs were identified; those who also had ICD-10 codes for malignancies were excluded (see Supplementary Table 1, available on the *Arthritis & Rheumatology* website at <http://onlinelibrary.wiley.com/doi/10.1002/art.42287>). Using the Cleveland Clinic COVID-19 Research Registry, which tracks vaccine and COVID-19 data across our system, we cross-referenced these patients to identify those who were vaccinated at least once and developed breakthrough COVID-19. Only infections confirmed by polymerase chain reaction or rapid test at any time after the first vaccination were included. In addition, patients identified through routine care who fulfilled the above criteria were included. This strategy allowed for the identification of breakthrough patients who may have received BCDT and/or were diagnosed outside our health care system but who were nevertheless under the care of our providers. Patients who received BCDT during the same time period for the same International Statistical Classification of Diseases and Related Health Problems, Tenth Revision (ICD-10) codes, but who were never vaccinated, were also identified, using the same search strategy.

In the primary analysis cohort of patients with breakthrough COVID-19, additional data on demographic characteristics (age, gender, race), weight, comorbidities (heart disease, pulmonary disease, chronic kidney disease, malignancy, smoking history), associated immunosuppressive medications, prednisone use and dosage, timing and duration of BCDT, vaccine type and number of doses, whether or not the patient received outpatient anti-SARS-CoV-2 monoclonal antibody (mAb) treatment, and clinical outcomes were extracted by individual chart review from patient electronic medical records. Each breakthrough infection was classified as complete (i.e.,  $\geq 14$  days following the second messenger RNA [mRNA] vaccine [or first Johnson & Johnson

vaccine]) or incomplete. For an additional exploratory analysis of unvaccinated patients receiving BCDTs who contracted COVID-19 over the same time period, data were gathered utilizing the same strategy.

**Outcome assessment.** Our primary outcome was disease severity; each patient was classified using the 8-point National Institutes of Health (NIH) COVID-19 ordinal scale (17) (Supplementary Table 2, <http://onlinelibrary.wiley.com/doi/10.1002/art.42287>). Patients were classified to their highest level of disease severity and grouped as mild (groups 1–3) or severe (groups 4–8).

**Influence of the Delta variant on infection incidence and classification of vaccination status.** To account for changes in COVID-19 breakthrough infection rates attributable to the Delta variant, we used June 20, 2021 as the date by which to stratify the follow-up period into pre- or post-Delta phases. The date was based on the Centers for Disease Control and Prevention (CDC) report of the Delta variant being the dominant SARS-CoV-2 strain ( $>50\%$ ) in the US (18). The end date of the study was December 15, 2021, selected based on the date that the Cleveland Clinic microbiology laboratory monitoring SARS-CoV-2 variants in northeastern Ohio identified as when Omicron became and persisted as the dominant variant.

Because of the timing of Emergency Use Authorization (EUA) and EUA amendments for primary vaccination and boosters (see Supplementary Table 3, <http://onlinelibrary.wiley.com/doi/10.1002/art.42287>), the most doses any patient in our cohort could have received by our cutoff date of December 15, 2021, was 3—all considered part of the primary series. For the purposes of our analysis, “incomplete” vaccination refers to the receipt of 1 dose of the mRNA vaccine. “Complete” vaccination refers to either the receipt of 1 dose of the Johnson & Johnson vaccine or 2 doses of either mRNA vaccine. “Additionally dosed” patients are those who received either 3 doses of mRNA vaccines or 1 dose of Johnson & Johnson plus 1 dose of either mRNA vaccine.

The Cleveland Clinic Institutional Review Board approved this study.

**Statistical analysis.** Continuous variables were summarized using the mean  $\pm$  SD or the median (interquartile range) when appropriate. Categorical variables were summarized using counts and frequencies. For patients who received anti-SARS-CoV-2 mAb treatment compared to those who did not, 2-sample *t*-tests (or Wilcoxon tests) and Pearson's chi-square tests (or Fisher's exact tests) were performed. Person-time (at risk) was accrued from the date of the first dose of the vaccine to the date of breakthrough infection or December 15, 2021, whichever occurred first. Unadjusted Poisson regression was used to calculate the overall incidence rate, and the



incidence rates of pre- and post-Delta periods. We then investigated the association between each risk factor and COVID-19 severity outcome using univariate logistic regression. Additionally, we built multivariable logistic regression models to examine the effect of potential risk factors on severity outcomes after controlling for confounding variables. The exploratory analysis of outcomes and epidemiologic risk factors in patients receiving BCDTs who were not vaccinated against SARS-CoV-2 and tested positive for the virus were compared descriptively. Data management and analysis were conducted using R package (version 4.0), with a 2-sided alpha level of 0.05 for all tests.

## RESULTS

**Clinical features of the primary cohort.** The results of our search revealed 3,220 patients with IMIDs (as identified via specific ICD-10 codes) receiving  $\geq 1$  dose of approved BCDT in the year 2020. Of these patients, 1,696 received  $\geq 1$  dose of vaccine against SARS-CoV-2. From this vaccinated group, 74 were found to have had breakthrough infection from the time of their first vaccine through December 15, 2021. The demographic and clinical characteristics of these patients are shown in Table 1. The number of patients was nearly equally distributed between rheumatic disease and neuroinflammatory disease, with multiple sclerosis as the single most common diagnosis. A total of 34 patients (45.9%) were receiving additional immunosuppressive medications, with prednisone being the most common (35.1%). A total of 13 patients (17.6%) were receiving  $\geq 1$  additional disease-modifying antirheumatic drug, including 6 patients receiving methotrexate, 4 patients receiving azathioprine, and 4 patients receiving mycophenolate. Half of the patients with breakthrough infection (37 [50.0%]) had  $\geq 1$  comorbidity.

In terms of vaccination history and status, 45 patients received the Pfizer mRNA vaccine: 2 patients received only 1 dose before breakthrough, 39 patients received 2 doses, and 4 patients received an additional third dose. A total of 23 patients received the Moderna mRNA vaccine, with only 1 patient receiving a single vaccination before breakthrough, 17 patients having received 2 doses, and 5 patients having received an additional third dose before infection. Six patients received a single Johnson & Johnson vaccination before breakthrough. Overall, of those experiencing breakthrough infections, defined as 14 days past the second vaccination (or single Johnson & Johnson vaccine), 6 of 74 had a vaccination status classified as incomplete, while 68 were either completely vaccinated or completely vaccinated and additionally dosed.

**Incidence.** Of 1,696 patients with any form of vaccination, 74 had breakthrough infection, for a raw incidence rate of 4.4%; 68 breakthrough infection cases (91.9%) occurred after complete vaccination (i.e., 14 days after the final administration). We also examined the crude incidence rate of COVID-19 breakthrough as a function of the pre- and post-Delta periods in 2021. Prior to

**Table 1.** Demographic and clinical characteristics of vaccinated breakthrough COVID-19 patients and breakthrough COVID-19 patients who were unvaccinated\*

	Vaccinated (n = 74)	Unvaccinated (n = 57)
Median age, years	53	50.3
Female sex	46 (62.2)	42 (73.7)
White race	62 (83.8)	41 (71.9)
Diagnosis		
Inflammatory CNS disease	34 (45.9)	33 (57.9)
Vasculitis	20 (27.0)	4 (7.0)
RA	9 (12.2)	12 (21.1)
Other	11 (14.9) <sup>†</sup>	11 (19.3) <sup>‡</sup>
Comorbidities		
BMI $\geq 30$	35 (47.3)	30 (52.6)
Heart disease <sup>§</sup>	36 (48.6)	24 (42.1)
Pulmonary <sup>¶</sup>	13 (17.6)	17 (29.9)
CKD	8 (10.8)	3 (5.3)
Malignancy	6 (8.1)	3 (5.3)
No. of comorbidities		
0	23 (31.1)	22 (38.6)
1	24 (32.4)	18 (31.6)
2	9 (12.2)	13 (22.8)
$\geq 3$	18 (24.3)	4 (7.0)
Vaccine		
Pfizer	45 (60.8)	
Moderna	23 (31.1)	
Johnson & Johnson	6 (8.1)	
Duration of BCDT		
<1 year	20 (27.0)	9 (16.1) <sup>#</sup>
1–3 years	20 (27.0)	27 (48.2) <sup>#</sup>
$\geq 3$ years	34 (45.9)	20 (35.7) <sup>#</sup>
Immunosuppression		
Glucocorticoids		
<10 mg/day	20 (27.0)	2 (3.5)
$\geq 10$ mg/day	6 (8.1)	4 (7.0)
DMARD <sup>**</sup>		
1 DMARD	12 (16.2)	9 (15.8)
2 DMARDs	1 (1.3)	3 (5.3)
Time between BCDT and first vaccine		
<3 months	22 (32.8)	
3–6 months	36 (53.7)	
>6 months	9 (13.4)	
Time between BCDT and COVID-19 diagnosis		
<3 months	36 (48.6)	
3–6 months	21 (28.4)	
>6 months	17 (22.9)	
Received anti-SARS-CoV-2 mAb therapy	21 (31.3)	7 (12.3)

\* Except where indicated otherwise, values are the number (%) of patients. CNS = central nervous system; RA = rheumatoid arthritis; BMI = body mass index; CKD = chronic kidney disease; BCDT = B cell-depleting therapy; mAb = monoclonal antibody.

<sup>†</sup> Includes 2 patients with systemic lupus erythematosus, 2 with sarcoidosis, 2 who had a solid organ transplant, 2 with myositis, 1 with interstitial lung disease (ILD), and 2 with hematologic disease.

<sup>‡</sup> Includes 3 patients with systemic sclerosis, 2 with pemphigus, 2 with Sjögren's syndrome, and 1 each with autoimmune encephalitis, myasthenia gravis, sarcoidosis, or mixed connective tissue disease.

<sup>§</sup> Heart disease indicates hypertension, coronary artery disease, or congestive heart failure.

<sup>¶</sup> Pulmonary indicates chronic obstructive pulmonary disease, asthma, or ILD.

<sup>#</sup> Data were missing for one patient.

<sup>\*\*</sup> Disease-modifying antirheumatic drugs (DMARDs) included hydroxychloroquine, methotrexate, azathioprine, and mycophenolate.



June 20, (the date CDC identified as the onset of the Delta surge) 12 of 74 cases were identified, while after June 20 there were 62, supporting a seeming acceleration of breakthrough infections with the Delta variant. The total person-time of vaccine exposure in this cohort (1,696 patients who received at least 1 vaccine) was 14,302.67 months. As a result, the time-adjusted incidence rate of breakthrough infection in the entire group was 5.19 cases per 1,000 person-months (95% confidence interval [95% CI] 4.13–6.52). The time-adjusted incidence rate of breakthrough infection in the pre-Delta period was 2.48 cases per 1,000 person-months (95% CI 1.41–4.36). The incidence rate in the post-Delta period was 6.59 cases per 1,000 person-months (95% CI 5.14–8.45).

**Outcomes.** Clinical outcomes for the entire group revealed that 45 patients had outpatient-managed disease, with 30 patients in group 1 (40.5%) and 15 patients in group 2 (20.3%). The remaining 29 patients (39.2%) were hospitalized, with 6 patients (8.1%) not requiring supplemental oxygen (groups 3 and 4) and the remaining requiring some level of oxygen support (12 patients [16.2%] [group 5] required any oxygen, and 5 patients [6.8%] [groups 6 or 7] required high-flow oxygen or mechanical ventilation). There were 6 (8.1%) deaths. In terms of risk factors for severe outcomes, we examined the groups based on clinical grade by ordinal scale, separating the patients into 2 groups: those with mild disease (groups 1–3) and those with more severe disease (groups 4–8). Univariate and multivariate analyses (Table 2) comparing mild disease (ordinal

**Table 2.** Univariate and multivariate analysis of clinical variables with a potential impact on COVID-19 severity in patients with breakthrough COVID-19 \*

	NIH COVID-19 ordinal scale		P†	Multivariable logistic regression	
	Score 1–3 (n = 47)	Score 4–8 (n = 27)		OR (95% CI)	P†
Age at first vaccination, median (25th percentile, 75th percentile)	52.3 (40.3, 61.9)	60.7 (49.0, 71.7)	0.088	–	–
Sex				–	–
Female	30 (63.8)	16 (59.3)	Referent		
Male	17 (36.2)	11 (40.7)	0.696		
Diagnosis				–	–
Neuroinflammatory disease or other	25 (53.2)	15 (55.6)	Referent		
Rheumatic disease	22 (46.8)	12 (44.4)	0.844		
Comorbidities (binary)					
0–1	40 (85.1)	13 (48.1)	Referent	–	–
≥2	7 (14.9)	14 (51.9)	0.001	5.9 (1.56–22.27)	0.009
Vaccination status				–	–
Complete	29 (61.7)	16 (59.3)	Referent		
Boosted	14 (29.8)	9 (33.3)	0.772		
Incomplete	4 (8.51)	2 (7.41)	0.915		
Duration of therapy with BCDT				–	–
<1 year	13 (27.7)	7 (25.9)	Referent		
1–3 years	11 (23.4)	9 (33.3)	0.519		
>3 years	23 (48.9)	11 (40.7)	0.842		
Most recent BCDT at time of first vaccination					
<3 months	13 (31.7)	8 (32.0)	Referent	–	–
3–6 months	25 (61.0)	11 (44.0)	0.561	0.8 (0.21–3.07)	0.744
>6 months	3 (7.32)	6 (24.0)	0.159	1.75 (0.28–10.94)	0.55
Concomitant therapies				–	–
Glucocorticoids					
<10 mg/day	13 (27.7)	7 (25.9)	Referent		
>10 mg/day	2 (4.26)	4 (14.8)	0.183		
Other concomitant therapy	32 (68.1)	16 (59.3)	0.895		
Prior COVID history				–	–
No	45 (97.8)	24 (88.9)	Referent		
Yes	1 (2.17)	3 (11.1)	0.144		
SARS-CoV-2 mAb treatment					
No	27 (57.4)	26 (96.3)	Referent	–	–
Yes	20 (42.6)	1 (3.70)	0.005	0.06 (0.01–0.57)	0.006

\* Except where indicated otherwise, values are the number (%) of patients. NIH = National Institutes of Health; OR = odds ratio; 95% CI = 95% confidence interval; BCDT = B cell-depleting therapy; mAb = monoclonal antibody.

† P values less than 0.05 were considered statistically significant.

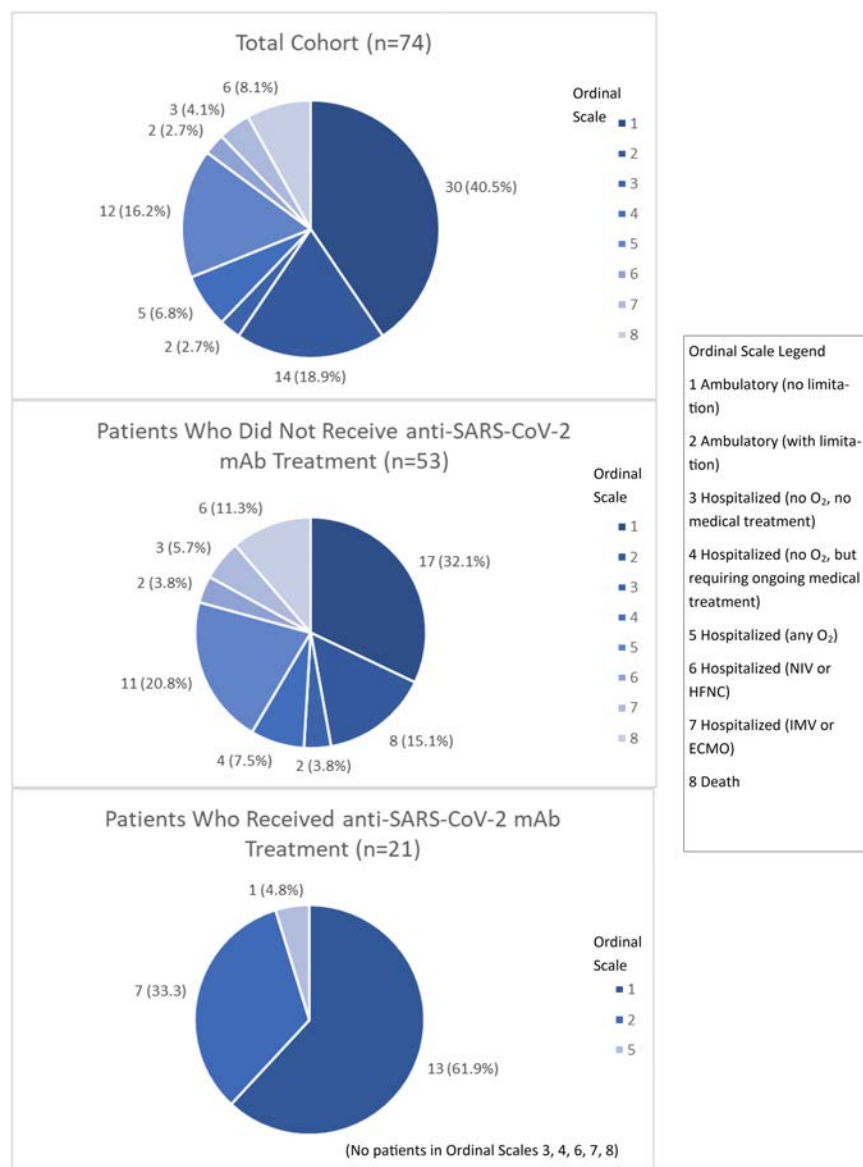


**Figure 1.** COVID-19 outcomes according to National Institutes of Health (NIH) COVID-19 ordinal scale. Pie chart showing clinical outcomes in 74 cases of COVID-19 breakthrough infection among 1,776 vaccinated patients receiving B cell-depleting therapies. Top, Clinical status among all patients according to an 8-point ordinal scale. Middle, Clinical outcomes in the subset of 53 patients who did not receive outpatient monoclonal antibody (mAb) therapy. Bottom, Clinical outcomes in the subset of 21 patients who received outpatient mAb therapy. NIV = noninvasive ventilation; HFNC = high-flow nasal cannula; IMV = intermittent mandatory ventilation; ECMO = extracorporeal membrane oxygenation.

scale groups 1–3) to severe disease (ordinal scale groups 4–8) revealed that only the presence of  $\geq 2$  comorbidities (present in 21 of the 74 breakthrough patients) was associated with disease severity ( $P = 0.001$  and  $P = 0.009$ , respectively).

Vaccine-associated variables (i.e., complete, incomplete, additionally dosed) had no association with severe outcomes, nor did the concomitant use of immunosuppressive therapies. Analysis of BCDT-associated variables, including duration of therapy and the time interval from most recent BCDT treatment to vaccination, demonstrated no statistical effect on the risk of severe outcomes in either the univariate or multivariate analysis. Four breakthrough patients experienced a single prior episode

of COVID-19 before receiving their first vaccine, which had no association with severe outcomes in the univariate analysis (Table 2).

**Incidence and severity of COVID-19 among unvaccinated patients.** An additional exploratory analysis was performed examining the incidence and severity of COVID-19 in 1,437 unvaccinated patients identified using the same search strategy as a comparator group. Among these, 57 patients were diagnosed as having COVID-19 for a crude incidence of 4.0%, with 27 patients diagnosed before June 20 (47.4%) and 30 patients diagnosed after June 20 (52.6%).

In terms of severity as measured using the NIH ordinal scale, 29 patients (50.9%) fit the criteria for groups 1–3 and 28 patients were in groups 4–8 (49.1%); 7 patients died (12.3%). Summaries of the clinical and epidemiologic features of this group are shown in Table 1.

### Effects of outpatient therapy with anti-SARS-CoV-2 mAb.

Anti-SARS-CoV-2 mAb therapy (casirivimab and imdevimab) was employed in 21 patients within 10 days of symptom onset as outpatient therapy for COVID-19. No patients in our cohort received any other type of anti-SARS-CoV-2 mAb treatment. In the multivariate model, after controlling for both the number of comorbidities and time of first vaccination administration, this therapy was associated with more favorable outcomes, with only 1 of 21 patients requiring hospitalization (with oxygen support; ordinal scale 5) and no deaths occurring ( $P = 0.006$ ) (Table 2). The results of this intervention and effects on the highest level of ordinal scale severity is shown in Figure 1. To explore the possibility that those who received treatment with anti-SARS-CoV-2 mAb differed in some manner that could potentially contribute to their markedly different clinical outcomes, we compared a select number of clinical characteristics (age, number of comorbidities, concomitant use of immunosuppressive therapies, duration of BCDT) between those who received anti-SARS-CoV-2 mAb therapy and the entire breakthrough cohort; none were statistically significant (Table 3). In the exploratory analysis of COVID-19 outcomes in the unvaccinated cohort, 7 of 57 patients received anti-SARS-CoV-2 mAb therapy, with 3 of these 7 patients requiring hospitalization and no deaths occurring (Supplementary Table 4, <http://onlinelibrary.wiley.com/doi/10.1002/art.42287>).

## DISCUSSION

The current study examines a large cohort of patients exposed to BCDT in 2020, a timeframe that began nearly 12 months before the introduction of the SARS-CoV-2 vaccine, all of whom received  $\geq 1$  vaccination for COVID-19 and developed breakthrough infection. Breakthrough occurred in 74 patients (4.4 %) or nearly 1 in 20 patients. Our data clearly show that breakthrough infection in this population is associated with severe outcomes, as 39.2% of patients required hospitalization, 14.9% of patients required critical care, and 8.1% of patients died. Thus we confirm that IMiD patients receiving BCDTs appear vulnerable to breakthrough infections and, most importantly, have severe outcomes.

While patients with IMiDs receiving BCDTs are recognized to be vulnerable to severe COVID-19 infections (5,7,8,19), relatively little data exist regarding their risks for and outcomes of breakthrough infection (20,21). The current cohort of breakthrough patients consisted of nearly equal numbers of patients with rheumatic disease and neuroinflammatory disease, and most were either fully vaccinated or additionally dosed (91.9%), with only 6 with incomplete vaccination status (8.1%). Of note is that the group as a whole was heavily exposed to BCDTs, with 27.0% receiving therapy for 1–3 years and 45.9% receiving therapy for  $>3$  years. More importantly, 86.3% of patients received their last BCDT  $<6$  months before their first vaccine, a time point that several studies have demonstrated is critical for any reasonable chance of developing a humoral response (11,13,15).

Although our study lacked comparator groups of healthy patients or immunocompromised patients not receiving BCDTs to appraise breakthrough frequency and severity, indirect

**Table 3.** Comparisons of clinical features between patients with breakthrough COVID-19 receiving anti-SARS-CoV-2 mAb therapy and those with breakthrough COVID-19 not receiving anti-SARS-CoV-2 mAb therapy\*

	Total (n = 74)	Anti-SARS-CoV-2 mAb-positive patients (n = 53)	Anti-SARS-CoV-2 mAb-negative patients (n = 21)	P
Age at first vaccination, median (25th percentile, 75th percentile)	55.2 (41.7, 65.4)	54.9 (44.0, 65.5)	55.5 (37.6, 65.1)	
Sex				
Female	46 (62.2)	34 (64.2)	12 (57.1)	0.679
Male	28 (37.8)	19 (35.8)	9 (42.9)	0.768
Concomitant therapies				
Glucocorticoids				
<10 mg/day	20 (27.0)	11 (20.8)	9 (42.9)	0.129
>10 mg/day	6 (8.11)	4 (7.55)	2 (9.52)	
Others	48 (64.9)	38 (71.7)	10 (47.6)	
No. of comorbidities (binary)				
0–1	53 (71.6)	35 (66.0)	18 (85.7)	0.160
$\geq 2$	21 (28.4)	18 (34.0)	3 (14.3)	
Duration of BCDT				
<1 year	20 (27.0)	15 (28.3)	5 (23.8)	0.783
1–3 years	20 (27.0)	15 (28.3)	5 (23.8)	
>3 years	34 (45.9)	23 (43.4)	11 (52.4)	

\* Except where indicated otherwise, values are the number (%) of patients. mAb = monoclonal antibody; BCDT = B cell-depleting therapy.

comparisons to previously reported studies provide some perspective for interpreting our findings. In terms of severity of breakthrough infections, Sun et al (1) retrospectively examined 664,772 patients in the National COVID Cohort Collaborative with a variety of disorders sharing varying degrees of immune dysfunction but not broken down by therapies. This study reported an overall rate of serious disease (as determined by need for hospitalization) of 20.7%, far less than the 39.2% observed in our cohort. Another study by Shen et al (22) examined a large population of immunocompromised patients over a similar timeframe as our investigation in a single health system.

Patients were identified as taking any 1 of a number of classes of immunosuppressant treatments including conventional, synthetic, or targeted disease-modifying therapies and/or glucocorticoids; only 0.35% of patients required hospitalization. A study by Di Fusco et al (3) utilizing the HealthVerity national database examined breakthrough infections from December 2020 through July 2021 among a broad spectrum of immunocompromised patients ( $n = 1,277,747$ ). This cohort consisted of patients with malignancies, solid organ transplants, HIV infection, and rheumatic/autoimmune disease; among 950 breakthrough patients only 12.7% required hospitalization, and inpatient deaths occurred in 0.2%—far below the severity observed in our study. In a post hoc analysis, a recent study from the Netherlands by Boekel et al (23) examining breakthrough infections during the Delta epoch in a large cohort of 3,207 IMiD patients receiving various immunosuppressant treatments demonstrated that severe outcomes appeared to be more frequent in the subset of patients receiving BCDTs, with 3 of 16 patients receiving BCDTs requiring hospitalization (19%) compared to only 5 of 132 receiving other immunosuppressive agents (4%). Based on these published studies, vaccinated patients receiving BCDTs for immune-mediated diseases appear to have particularly severe outcomes within the spectrum of immunosuppressed patients.

As opposed to breakthrough infection severity (which can be determined by hospitalizations and death), it is more difficult to examine breakthrough infection frequency via indirect comparisons given differences in study durations, epochs of investigation and thus the influence of viral variants, as well as differences in detection vigilance. In terms of the overall rate of breakthrough infection, a study conducted by the CDC in the general population estimated a breakthrough rate of 2.8% per 6-month period on September 30, 2021, which is somewhat lower than our observed crude rate of 4.4% over nearly 12 months of observation (24). Our time-adjusted incidence rate of 5.19 cases per 1,000 person-months appears comparable to the overall rate of 5.0 cases per 1,000 person-months (95% CI 2.9–2.9) found in immunocompromised patients in the study by Sun et al (1). Another study of breakthrough infections by Ahmed et al (25), conducted in India from March to October 2021, found an overall rate of breakthrough infection of 7.5%. This rate is higher than noted in our study, but included 2 vaccines not used in the US,

limiting comparability. A study by Shen et al (22), which was conducted over the same time period as our study in a heterogeneous population receiving a wide range of immunosuppressive drugs, found a breakthrough rate of 1.3% among immunocompetent subjects and 2.8% in immunocompromised subjects. Thus it appears that breakthrough infection rates in patients receiving BCDTs may be higher than rates in immunocompetent individuals and are the range of other studies examining immunocompromised patients; again, direct comparator studies are needed.

Our study also examined the potential impact of the Delta variant on breakthrough incidence and found that the majority of cases were identified during the period of the Delta surge, with 62 of 74 cases diagnosed between June 20, 2021 (the date determined to be the onset of the Delta surge by the CDC [1]) and December 15, 2021 (the end of our study and the end of the Delta surge in northeastern Ohio). This observation is consistent with the study by Sun et al (1), who described a tripling of incidence in the period following June 20 until the end of their study period of September 16, 2021. While all of these studies demonstrated an increase in incidence of breakthrough within the time period of the Delta surge, the reasons for this remain unclear. Indeed the increased transmissibility of the Delta strain may be one explanation for this rise in incidence; another consideration could be waning vaccine effectiveness as the time since vaccine administration increased. This possibility of waning vaccine effectiveness would seem to be supported by our exploratory analysis of the unvaccinated cohort, which over the same time periods demonstrated little change in crude incidence, with nearly equal numbers of patients infected over both time periods (i.e., pre-Delta and Delta phases). Further studies examining biomarker correlates of infection as well as the impact of new variants and the effectiveness of additional doses are needed to increase our understanding of this phenomenon.

Our findings indicating severe outcomes of COVID-19 in breakthrough infections in patients receiving treatment with BCDTs are important for understanding the implications of the evolving picture of vaccine responsiveness in this population. From early on it has been understood that patients receiving agents such as RTX and ocrelizumab have severe deficits in their capacity to mount humoral responses to a variety of vaccines and more recently to vaccination against SARS-CoV-2 (11). Our data also helps understand the implications and clinical limitations of the surprisingly robust T cell response following mRNA vaccination in patients receiving BCDTs, which has been documented in a number of recent studies (15,16,26). Further work carefully studying breakthrough infection, paired with detailed examinations of biomarkers for humoral- and cell-mediated immunity, is urgently needed.

Given our data indicating that breakthrough infection in patients receiving BCDT appears to be associated with poor outcomes, we conducted an additional exploratory analysis in

unvaccinated patients with the same diagnoses and use of BCDTs over the same time period to gain insight as to what degree of protection may be afforded by vaccinating such patients. From this analysis we found that the incidence of infection was similar but numerically less in the unvaccinated patients (4.0% versus 4.4%). In terms of severity, both groups had poor outcomes, with the distribution of mild and severe cases in the unvaccinated cohort (ordinal scale categories 1–3 versus 4–8) of 57.9% and 42.1% with 12.3% fatality, compared to 63.5% and 36.5% with 8.1% fatality in the breakthrough group. Given that the assignment to these 2 groups (i.e., no vaccination versus vaccination) was nonrandom and may indicate differences in health disparities as well as risk behaviors, these small differences should be viewed with caution. At the minimum, we must conclude that patients receiving BCDTs, regardless of vaccine status, are at risk of serious and fatal COVID-19.

Our observation that breakthrough patients receiving anti-SARS-CoV-2 mAb did extremely well is important (supported by the fact that only 1 vaccinated patient who received anti-SARS-CoV-2 mAb treatment required hospitalization) yet is limited by the nonrandom use of the therapy and the risk of confounding by indication. While anti-SARS-CoV-2 mAb have been used extensively, their utility at reducing the need for acute care and death is based on clinical trials in patients largely at increased risk based on age and concomitant diseases, as opposed to a small minority of immunocompromised patients, and none that we are aware of explicitly recruited patients receiving BCDTs, such as in our study (27). We examined the groups divided into those who received treatment with anti-SARS-CoV-2 mAb and those who did not, looking for select clinical characteristics with the potential to influence clinical outcomes. We found that the groups were well-matched for traditional risk factors for COVID-19 progression (i.e., age, comorbidities) as well as concomitant immunosuppression and duration of BCDT. Only 7 patients (12.3%) in the unvaccinated cohort received anti-SARS-CoV-2 mAb (12.3%); 3 of these patients required hospitalization and none died. While intriguing, we would caution against any strong conclusions regarding the efficacy of anti-SARS-CoV-2 mAb in this population due to limitations including nonrandom allocation and likely residual confounding effects.

A more practical question perhaps should be posed: why only 21 of 74 breakthrough patients (28.4%) received anti-SARS-CoV-2 mAb therapy. The seeming underutilization of these treatments in our patients is both important and disappointing. There are a number of possible explanations for this underutilization of early and aggressive outpatient therapy. First, during various surges of COVID-19, there were periods of time when these therapies had limited availability. However, upon individual examination of medical records, this was not explicitly noted as a limitation in any case. A more likely cause of lack of outpatient therapy was patients failing to connect with their providers within the 10-day window of eligibility (23). Numerous reasons could

cause such a delay, including failure of the provider to educate patients on the urgency to seek care if they suspected COVID-19 infection. This education must include how to recognize the often subtle symptoms of breakthrough infection (28) as well as how to promptly self-test or obtain testing within the important time window for the given treatment.

Also plausible and anecdotally noted in our chart review were uncertainties regarding the patients who were diagnosed promptly as to which provider to contact (i.e., primary care or specialist), at times leading to delays caused by caregivers who were unfamiliar with rapidly changing care pathways. The even lower use of anti-SARS-CoV-2 mAb in the unvaccinated cohort is of great concern and may reflect disparities in health care access and/or belief in health care resources. Moving ahead, practitioners caring for immunocompromised patients will need to stay knowledgeable about the standards of care and fill any outstanding deficits in declarative or procedural knowledge on how to manage COVID-19 in their patients.

Our study has several important limitations. First, we have no direct comparator group of immunocompromised patients based on therapy; it would be of interest to compare severity and outcomes to other patients receiving different immunosuppressive therapies. For now, unfortunately, large studies such as these have not been reported. Second, it is likely that unknown cases of mild or even asymptomatic infection may have been unreported or missed, and certain data fields extracted from the chart review may have been missing, especially from patients receiving their BCDT outside of our health care system. Third, while we chose to examine patients who received BCDTs in the year 2020, we did not account for ongoing BCDT through the end of the study, which may have further contributed to immunosuppression. A recent study of RTX in vasculitis patients demonstrated that antibody levels to S protein fell by >50% within 4 weeks of drug administration (29). Finally, it would clearly be of interest to examine breakthrough infections in concert with the status of patients' integrated immune responses by assessing serologic responses, especially anti-spike antibody titers, which have been associated with breakthrough infection in IMiD patients (23,25), as well as B cell numbers and cell-mediated immune responses. Unfortunately this was not possible in this retrospective study, where such data were not gathered or were missing for the vast majority of patients.

In terms of practical implications, our study should serve to highlight the plight of this important segment of the immunocompromised patient population who are likely to face ongoing and formidable risks despite aggressive vaccination if, as many observers predict, an ensuing endemic phase of the pandemic lies ahead with future variants of unknown pathogenicity. For now, enhanced nonpharmacologic measures (masking, social distancing, etc.) will remain important; expanded access to preexposure prophylaxis with anti-SARS-CoV-2 mAb effective against prevalent variants and access to emerging antiviral therapies will



be vital (28,30,31). Enhanced education of both patients and the providers who care for them to increase their awareness and utilization of current and future outpatient therapies is urgently needed.

## AUTHOR CONTRIBUTIONS

All authors were involved in drafting the article or revising it critically for important intellectual content, and all authors approved the final version to be published. Dr. L. Calabrese had full access to all of the data in the study and takes responsibility for the integrity of the data and the accuracy of the data analysis.

**Study conception and design.** C. Calabrese, Kirchner, Husni, Moss, L. Calabrese.

**Acquisition of data.** C. Calabrese, Kirchner, Husni, Jin, L. Calabrese.




**Analysis and interpretation of data.** C. Calabrese, Kirchner, Husni, Moss, Fernandez, Jin, L. Calabrese.

## REFERENCES

- Sun J, Zheng Q, Madhira V, et al. Association between immune dysfunction and COVID-19 breakthrough infection after SARS-CoV-2 vaccination in the US. *JAMA Intern Med* 2022;182:153–162.
- Cook C, Patel NJ, D'Silva KM, et al. Clinical characteristics and outcomes of COVID-19 breakthrough infections among vaccinated patients with systemic autoimmune rheumatic diseases. *Ann Rheum Dis* 2022;81:289–91.
- Di Fusco M, Moran MM, Cane A, et al. Evaluation of COVID-19 vaccine breakthrough infections among immunocompromised patients fully vaccinated with BNT162b2. *J Med Econ* 2021;24:1248–60.
- Jones JM, Faruqi AJ, Sullivan JK, et al. COVID-19 outcomes in patients undergoing B cell depletion therapy and those with humoral immunodeficiency states: a scoping review. *Pathog Immun* 2021;6:76–103.
- Sparks JA, Wallace ZS, Seet AM, et al. Associations of baseline use of biologic or targeted synthetic DMARDs with COVID-19 severity in rheumatoid arthritis: results from the COVID-19 Global Rheumatology Alliance physician registry. *Ann Rheum Dis* 2021;80:1137–46.
- Andersen KM, Bates BA, Rashidi ES, et al. Long-term use of immunosuppressive medicines and in-hospital COVID-19 outcomes: a retrospective cohort study using data from the National COVID Cohort Collaborative. *Lancet Rheumatol* 2022;4:e33–41.
- Strangfeld A, Schäfer M, Gianfrancesco MA, et al. Factors associated with COVID-19-related death in people with rheumatic diseases: results from the COVID-19 Global Rheumatology Alliance physician-reported registry. *Ann Rheum Dis* 2021;80:930–42.
- Patel NJ, D'Silva KM, Hsu TY, et al. COVID-19 outcomes among users of CD20 inhibitors for immune-mediated diseases: a comparative cohort study [preprint]. *medRxiv* 2021. E-pub ahead of print.
- Conway R, Grimshaw AA, König MF, et al. SARS-CoV-2 infection and COVID-19 outcomes in rheumatic disease: a systematic literature review and meta-analysis. *Arthritis Rheumatol* 2022;74:766–75.
- Patel NJ, D'Silva KM, Hsu TY, et al. Coronavirus disease 2019 outcomes among recipients of anti-CD20 monoclonal antibodies for immune-mediated diseases: a comparative cohort study. *ACR Open Rheumatol* 2022;4:238–46.
- Friedman MA, Curtis JR, Winthrop KL. Impact of disease-modifying antirheumatic drugs on vaccine immunogenicity in patients with inflammatory rheumatic and musculoskeletal diseases. *Ann Rheum Dis* 2021;80:1255–65.
- Jena A, Mishra S, Deepak P, et al. Response to SARS-CoV-2 vaccination in immune mediated inflammatory diseases: systematic review and meta-analysis. *Autoimmun Rev* 2022;21:102927.
- Spiera R, Jinich S, Jannat-Khah D. Rituximab, but not other antirheumatic therapies, is associated with impaired serological response to SARS-CoV-2 vaccination in patients with rheumatic diseases. *Ann Rheum Dis* 2021;80:1357–9.
- Moor MB, Suter-Riniker F, Horn MP, et al. Humoral and cellular responses to mRNA vaccines against SARS-CoV-2 in patients with a history of CD20 B-cell-depleting therapy (RituxiVac): an investigator-initiated, single-centre, open-label study. *Lancet Rheumatol* 2021;3:e789–97.
- Bitoun S, Henry J, Desjardins D, et al. Rituximab impairs B cell response but not T cell response to COVID-19 vaccine in autoimmune diseases. *Arthritis Rheumatol* 2022;74:927–33.
- Madelon N, Lauper K, Breville G, et al. Patients treated with anti-CD20 therapy can mount robust T cell responses to mRNA-based COVID-19 vaccines. *Clin Infect Dis* 2021. DOI: <https://doi.org/10.1093/cid/ciab954>. E-pub ahead of print.
- Desai A, Gyawali B. Endpoints used in phase III randomized controlled trials of treatment options for COVID-19. *EClinicalMedicine* 2020;23:100403.
- Centers for Disease Control and Prevention. COVID data tracker: monitoring variant proportions 2021. URL: <https://covid.cdc.gov/covid-data-tracker/#variant-proportions>.
- Jones J, Aiman F, Sullivan J, et al. COVID-19 outcomes in patients undergoing B cell depletion therapy and those with humoral immunodeficiency states: a scoping review. *Pathog Immun* 2021;6:76–103.
- Lawson-Tovey S, Hyrich KL, Gossec L, et al. SARS-CoV-2 infection after vaccination in patients with inflammatory rheumatic and musculoskeletal diseases. *Ann Rheum Dis* 2022;81:145–50.
- Cook C, Patel NJ, D'Silva KM, et al. Clinical characteristics and outcomes of COVID-19 breakthrough infections among vaccinated patients with systemic autoimmune rheumatic diseases. *Ann Rheum Dis* 2022;81:289–91.
- Shen C, Risk M, Schiopu E, et al. Efficacy of COVID-19 vaccines in patients taking immunosuppressants. *Ann Rheum Dis* 2022;81:875–80.
- Boekel L, Stalman EW, Wieske L, et al. Breakthrough SARS-CoV-2 infections with the  $\delta$  (B.1.617.2) variant in vaccinated patients with immune-mediated inflammatory diseases using immunosuppressants: a substudy of two prospective cohort studies. *Lancet Rheumatol* 2022;4:e417–29.
- Centers for Disease Control and Prevention. COVID-19 vaccine breakthrough case investigation and reporting, 2021. URL: <https://www.cdc.gov/vaccines/covid-19/health-departments/breakthrough-cases.html>.
- Ahmed S, Mehta P, Paul A, et al. Postvaccination antibody titres predict protection against COVID-19 in patients with autoimmune diseases: survival analysis in a prospective cohort. *Ann Rheum Dis* 2022;81:868–74.
- Apostolidis SA, Kakara M, Painter MM, et al. Cellular and humoral immune responses following SARS-CoV-2 mRNA vaccination in patients with multiple sclerosis on anti-CD20 therapy. *Nat Med* 2021;27:1990–2001.
- Lin WT, Hung SH, Lai CC, et al. The impact of neutralizing monoclonal antibodies on the outcomes of COVID-19 outpatients: a systematic review and meta-analysis of randomized controlled trials. *J Med Virol* 2022;94:2222–9.
- Cohen MS, Wohl DA, Fischer WA, et al. Outpatient treatment of severe acute respiratory syndrome coronavirus 2 infection to prevent

- coronavirus disease 2019 progression. Clin Infect Dis 2021;73:1717–21.
29. Kant S, Azar A, Geetha D. Antibody response to COVID-19 booster vaccine in rituximab-treated patients with anti-neutrophil cytoplasmic antibody-associated vasculitis. Kidney Int 2022;101:414–5.
30. Rubin R. Questions remain about who will get monoclonal antibodies for COVID-19 preexposure prophylaxis. JAMA 2022;327:207–8.
31. NIH. NIH COVID-19 treatment guidelines: management of nonhospitalized patients with acute covid-19, 2022. URL: <https://www.covid19treatmentguidelines.nih.gov/management/clinical-management/nonhospitalized-patients--general-management/General>.

# Synovial Inflammatory Pathways Characterize Anti-TNF-Responsive Rheumatoid Arthritis Patients

Jing Wang,<sup>1</sup> Donna Conlon,<sup>2</sup> Felice Rivellesse,<sup>3</sup> Alessandra Nerviani,<sup>3</sup> Myles J. Lewis,<sup>3</sup>  William Housley,<sup>2</sup> Marc C. Levesque,<sup>4</sup> Xiaohong Cao,<sup>1</sup> Carolyn Cuff,<sup>2</sup> Andrew Long,<sup>2</sup> Costantino Pitzalis,<sup>3</sup>  and Melanie C. Ruzek<sup>2</sup> 

**Objective.** This study was undertaken to understand the mechanistic basis of response to anti-tumor necrosis factor (anti-TNF) therapies and to determine whether transcriptomic changes in the synovium are reflected in peripheral protein markers.

**Methods.** Synovial tissue from 46 rheumatoid arthritis (RA) patients was profiled with RNA sequencing before and 12 weeks after treatment with anti-TNF therapies. Pathway and gene signature analyses were performed on RNA expression profiles of synovial biopsies to identify mechanisms that could discriminate among patients with a good response, a moderate response, or no response, according to the American College of Rheumatology (ACR)/EULAR response criteria. Serum proteins encoded by synovial genes that were differentially expressed between ACR/EULAR response groups were measured in the same patients.

**Results.** Gene signatures predicted which patients would have good responses, and pathway analysis identified elevated immune pathways, including chemokine signaling, Th1/Th2 cell differentiation, and Toll-like receptor signaling, uniquely in good responders. These inflammatory pathways were correspondingly down-modulated by anti-TNF therapy only in good responders. Based on cell signature analysis, lymphocyte, myeloid, and fibroblast cell populations were elevated in good responders relative to nonresponders, consistent with the increased inflammatory pathways. Cell signatures that decreased following anti-TNF treatment were predominately associated with lymphocytes, and fewer were associated with myeloid and fibroblast populations. Following anti-TNF treatment, and only in good responders, several peripheral inflammatory proteins decreased in a manner that was consistent with corresponding synovial gene changes.

**Conclusion.** Collectively, these data suggest that RA patients with robust responses to anti-TNF therapies are characterized at baseline by immune pathway activation, which decreases following anti-TNF treatment. Understanding mechanisms that define patient responsiveness to anti-TNF treatment may assist in development of predictive markers of patient response and earlier treatment options.

## INTRODUCTION

Rheumatoid arthritis (RA) is a debilitating joint disease characterized by progressive cartilage and bone destruction (1). Among the biologic agents, anti-tumor necrosis factor (anti-TNF) therapies are the most commonly used to treat RA patients, but many patients remain unresponsive to these treatments (2,3). Understanding the mechanisms that drive clinical efficacy and predict response/nonresponse to anti-TNF would benefit patients.

Several studies have profiled peripheral blood and synovial tissue with transcriptomics, proteomics, and clinical disease measures in an attempt to understand the patient anti-TNF therapy response (4–7). There is a reported discordance between synovial tissue and peripheral gene expression profiles (8), and synovial tissue analysis is more relevant to the disease compared to blood analysis (5,9,10). However, because synovial tissue collection requires specialized procedures such as ultrasound-guided biopsy, studies on synovial profiling are limited. Furthermore, the

Supported by AbbVie.

<sup>1</sup>Jing Wang, PhD, Xiaohong Cao, PhD: Immunology Systems Computational Biology, Genomic Research Center, AbbVie, Cambridge, Massachusetts; <sup>2</sup>Donna Conlon, BA, William Housley, PhD, Carolyn Cuff, PhD, Andrew Long, PhD, Melanie C. Ruzek, PhD: Immunology Discovery, AbbVie Research Center, Worcester, Massachusetts; <sup>3</sup>Felice Rivellesse, MD, Alessandra Nerviani, MD, PhD, Myles J. Lewis, PhD, Costantino Pitzalis, MD, PhD: Centre for Experimental Medicine & Rheumatology, William Harvey Research Institute and Barts and The London School of Medicine and Dentistry, Queen Mary

University of London, London, UK; <sup>4</sup>Marc C. Levesque, MD, PhD: Immunology Discovery, Cambridge Research Center, Cambridge, Massachusetts.

Author disclosures are available at <https://onlinelibrary.wiley.com/action/downloadSupplement?doi=10.1002%2Fart.42295&file=art42295-sup-0001-Disclosureform.pdf>.

Address correspondence via email to Melanie Ruzek, PhD, at [melanie.ruzek@abbvie.com](mailto:melanie.ruzek@abbvie.com).

Submitted for publication September 27, 2021; accepted in revised form June 30, 2022.

studies exploring synovial biopsies in RA patients have evaluated few subjects and only baseline data; there are even fewer studies that have measured the impact of anti-TNF therapies on synovial pathways and mechanisms following treatment (11,12). In addition, while more advanced techniques are being used to profile RA synovial tissues, such as single-cell RNA sequencing, studies often focus on a single cell type, such as synovial macrophages (13), but lack treatment effects and assessment of impact of the collective cell populations and intercellular pathways that contribute to disease. Thus, many studies have used cell signatures from single-cell RNA sequencing data to portray the cellular heterogeneity in bulk data and then linked the cell types with clinical features from bulk data (14–16).

In the present study, to characterize disease mechanisms differentiating anti-TNF response from nonresponse in RA patients, we profiled synovial tissue both pre- and post-anti-TNF treatment from RA patients who were either good responders, moderate responders, or nonresponders; we used bulk RNA sequencing transcriptome profiling and overlaid cellular signatures identified from RA patient single-cell RNA-Seq. To the best of our knowledge, this is the first bulk RNA-Seq analysis of RA synovial tissue before and after treatment with anti-TNF therapies and the largest sample size within the last 10 years (Supplementary Table 1, available on the *Arthritis & Rheumatology* website at <https://onlinelibrary.wiley.com/doi/10.1002/art.42295>). We also extended evaluation to peripheral secreted proteins based on synovial gene expression.

## PATIENTS AND METHODS

### Patient clinical assessments and synovial biopsies.

Forty-six RA patients fulfilling the 2010 American College of Rheumatology (ACR)/EULAR RA classification criteria (17) were enrolled at the Centre for Experimental Medicine and Rheumatology, Barts and The London School of Medicine, Queen Mary University of London, UK. The study received ethical approval from the local UK Health Research Authority (no. 10/H0801/47), and all patients provided written informed consent. Patients had clinically defined synovitis and were eligible to start anti-TNF treatment according to UK National Institute for Health and Care Excellence guidelines (failure of  $\geq 2$  conventional synthetic disease-modifying antirheumatic drugs [DMARDs] and a Disease Activity Score in 28 joints [DAS28] [18] of  $\geq 5.1$ ). Upon enrollment and acquisition of demographic characteristics, current medications, and clinical disease parameters (including C-reactive protein, erythrocyte sedimentation rate, rheumatoid factor/anti-citrullinated protein antibody positivity titer, and DAS28), patients underwent minimally invasive ultrasound-guided synovial biopsy of the most inflamed joint (ultrasound synovial thickening score  $\geq 2$ ) (19) at baseline and 12 weeks after treatment with anti-TNF therapy ( $n = 19$  receiving etanercept,  $n = 27$  receiving certolizumab pegol). Duration of treatment was ensured up to

the primary end point, and there were no treatment interruptions. Blood was also collected for plasma and serum.

Responses to therapy were evaluated using ACR/EULAR DAS28 response criteria defined as good response (DAS28 change [DAS28 at baseline – DAS28 at 12 weeks after treatment]  $> 1.2$  with DAS28 at 12 weeks  $\leq 3.2$ ), moderate response (DAS28 change  $> 1.2$  with DAS28 at 12 weeks  $> 3.2$ , or DAS28 change  $0.6$ – $1.2$  with DAS28 at 12 weeks  $\leq 5.1$ ), or nonresponse (DAS28 change  $\leq 0.6$ , or DAS28 change  $0.6$ – $1.2$  with DAS28 at 12 weeks  $> 5.1$ ) (20). There was no significant difference between the number of good responders, moderate responders, and nonresponders for etanercept and certolizumab ( $P = 0.69$ ) (Supplementary Table 2, <https://onlinelibrary.wiley.com/doi/10.1002/art.42295>).

**RNA-Seq and data analyses.** Total RNA was extracted from synovial tissue using TRIzol and chloroform (ThermoFisher Scientific), as previously described (9), and sequenced on an Illumina HiSeq-3000 using single reads extending 50 bases. RNA-Seq reads were aligned to the Ensembl release 76 top-level assembly with STAR version 2.0.4b (21). Quality control reports can be found in Supplementary Methods (<https://onlinelibrary.wiley.com/doi/10.1002/art.42295>). Gene counts were derived from the number of uniquely aligned unambiguous reads by Subread:featureCount version 1.4.5 (22). Sequencing performance was assessed for the total number of aligned reads, total number of uniquely aligned reads, genes and transcripts detected, ribosomal fraction, known junction saturation, and read distribution over known gene models with RSeQC version 2.3 (23). The data have been deposited in Gene Expression Omnibus (GEO) (24) and are accessible through GEO series accession number GSE198520 (<https://www.ncbi.nlm.nih.gov/geo/query/acc.cgi?acc=GSE198520>).

In the count matrix, genes with counts per million of  $> 1$  in at most 50% of all samples were removed for further analyses. The trimmed mean of M values method (25) and Limma/Voom method (26) were applied to normalize the data and identify differentially expressed genes (DEGs) based on a fold change of  $> 1.5$  and a  $P$  value of  $< 0.05$ . Pathway enrichment analysis for DEGs was performed based on the WebGestalt web tool (27,28) using KEGG database (29) based on a false discovery rate (FDR) of  $< 0.1$ . The gene set variation analysis (GSVA) method (30) was used to calculate the pathway signature score by comparing the ranking of DEGs annotated to each pathway with other genes based on expression in each sample.

To identify cell types related to anti-TNF treatment, cell signatures were downloaded from Zhang et al and Stephenson et al, which identified 18 and 13 cell clusters, respectively, from RA synovial single-cell data (31,32). Each signature included the top 20 most significant genes for each cell type, and there were few overlapping genes between each pair of signatures in each of 2 data sets (Supplementary Figure 1, <https://onlinelibrary.wiley.com/doi/10.1002/art.42295>).

[com/doi/10.1002/art.42295](https://doi.org/10.1002/art.42295)). Cell signature scores were also calculated using the GSVA method (30) based on cell signature.

**Peripheral protein measurements.** The following proteins were measured in serum or plasma at baseline and at 12 weeks in patients at the time synovial tissue was collected: growth-related oncogene  $\alpha$  (GRO $\alpha$ ; CXCL1), calprotectin (S100A8/A9), interleukin-10 (IL-10), interferon- $\gamma$ -inducible 10-kd protein (IP10; CXCL10), monocyte chemotactic protein 1 (MCP1; CCL2), monokine induced by interferon- $\gamma$  (MIG; CXCL9), BRAK (CXCL14), CXCL16, high mobility group box chromosomal protein 1 (HMGB1), IL-32, YKL40 (CHI3L1), 6Ckine (CCL21), MCP2 (CCL8), B cell-attracting chemokine 1 (BCA1; CXCL13), MCP4 (CCL13), IL-16, and TRAIL (TNFSF10). Protein levels for all except calprotectin were assessed using multiplex magnetic bead-based Milliplex MAP Human Cytokine/Chemokine immunoassay kits according to instructions of the manufacturer (Millipore).

Briefly, plasma (25  $\mu$ l/well) was incubated with antibody-conjugated magnetic beads at 4°C overnight in 96-well assay plates with agitation, followed by washing with assay buffer and incubation for 1 hour with a biotinylated detection antibody cocktail, followed by streptavidin/phycoerythrin. After additional washes, beads were resuspended in sheath fluid, and samples were analyzed on a Luminex 200 instrument. All samples were run in duplicate. Unknown concentrations of each analyte were determined based on regression curves (5-parameter logistic) from the standard curve of each analyte using xPONENT software (Luminex). For calprotectin, plasma samples were evaluated using a MRP8/14 enzyme-linked immunosorbent assay kit according to instructions of the manufacturer (Buhlmann Laboratories AG). Briefly, diluted plasma samples were incubated on the antibody-coated microplate at 4°C overnight, followed by washing and incubation with an enzyme-linked monoclonal antibody at room temperature for 1 hour, and a final wash before substrate solution addition prior to obtaining optical density at 450 nm. Concentrations of calprotectin were determined by regression analysis (4- or 5-parameter) based on the standard curve.

**Public RA synovial microarray data.** Three RA synovial microarray data sets with anti-TNF treatment information (GSE15602 [11], GSE21537 [33], and GSE47726 [34]) were downloaded from GEO. All data sets were normalized by the authors of the original publications. If gene IDs were not mapped to a Human Genome Organisation (HUGO) gene symbol, we mapped these gene IDs to HUGO gene symbols using the mapping table from GEO. The DEGs were identified based on Limma using a fold change of  $>1.5$  and a  $P$  value of  $<0.05$ , and KEGG enriched pathways were identified based on WebGestalt using an FDR of  $<0.1$ .

**Statistical analysis.** The comparisons of binary or categorical demographics (e.g., gender and ethnicity) among the 3 ACR/EULAR response groups were performed using Fisher's exact

test, while the comparisons of continuous demographics (e.g., age) were calculated using analysis of variance (ANOVA). The comparison of principle component 1 (PC1) between each pair of response groups was performed using Wilcoxon's rank sum test. Variables related to PC1 were identified using Pearson's correlation (continuous variable), Wilcoxon's rank sum test (binary variable), and ANOVA (categorical variable). Pathway signature score (or cell signature score) comparisons between pre- and posttreatment were performed using paired Wilcoxon's rank sum tests, while pairwise pretreatment comparisons between good, moderate, and nonresponders were performed using standard Wilcoxon's rank sum tests.

**Data availability.** Data are available upon reasonable request. The transcriptomics data are uploaded to the GEO database.

## RESULTS

**Patient demographic characteristics, disease characteristics, and clinical responses.** We compared baseline patient demographics between ACR/EULAR good responders, moderate responders, and nonresponders (Table 1). At baseline, good responders had significantly lower scores of the patient global assessment of disease activity, the patient global assessment of pain, and the Health Assessment Questionnaire (HAQ) disability index (DI) when compared to moderate responders or nonresponders. Good responders also had significantly lower DAS28 scores at baseline when compared to both moderate responders and nonresponders. These results indicate that good responders in this study had reduced disease activity prior to anti-TNF treatment. Lower baseline disease activity in those with a good response to anti-TNF treatment has been observed in other studies (7,35). Consistent with the defined response groups, we found that the mean  $\pm$  SD change in DAS28 was  $-3.1 \pm 0.9$  for good responders,  $-2.4 \pm 1.0$  for moderate responders, and  $-0.6 \pm 0.5$  for nonresponders. Most baseline biopsy specimens were from the wrist, and only 3 patients changed biopsy location for posttreatment samples (Supplementary Table 3, <https://onlinelibrary.wiley.com/doi/10.1002/art.42295>).

**Good responders distinguished from moderate responders and nonresponders at baseline via global synovial molecular phenotypes.** To understand global gene expression differences between patients responding and those not responding to anti-TNF treatment, principal component analysis (PCA) of the synovial RNA sequencing was compared before and after treatment (Figure 1). At baseline, good responders were distinct from the majority of moderate and nonresponders along PC1 ( $P = 5.2 \times 10^{-3}$  versus moderate responders, and  $P = 6.5 \times 10^{-6}$  versus nonresponders), indicating that good responders demonstrated a different gene expression pattern compared to other patient groups before treatment. Variables related to PC1 at baseline were tender joint count, HAQ DI, and



**Table 1.** Demographic and clinical characteristics of the rheumatoid arthritis patients (n = 46)\*

	Good responders (n = 19)	Moderate responders (n = 13)	Nonresponders (n = 14)
Female sex	13 (68)	10 (77)	12 (86)
Ethnicity†			
Asian	3 (16)	6 (46)	6 (43)
Caucasian	14 (74)	4 (31)	7 (50)
Other	2 (10)	3 (23.0)	1 (7)
Age, mean ± SD years	56.6 ± 12.2	49.9 ± 13.8	54.6 ± 12.1
Joint involvement			
Wrist	16 (84)	9 (70)	10 (71)
MCP	2 (11)	2 (15)	3 (22)
Other (elbow, knee, MTP)	1 (5)	2 (15)	1 (7)
Disease duration, mean ± SD years	5.7 ± 5.9	6.9 ± 5.3	7.8 ± 8.3
Previous smoker	9 (47)	3 (23)	4 (29)
Current smoker	3 (16)	3 (23)	4 (29)
Type of DMARD			
MTX	4 (21)	5 (39)	3 (22)
MTX + HCQ	7 (37)	4 (30)	8 (57)
MTX + SSZ	7 (37)	1 (8)	2 (14)
Leflunomide	0 (0)	1 (8)	0 (0)
MTX + SSZ + HCQ	1 (5)	2 (15)	1 (7)
Current steroid use	6 (32)	5 (39)	5 (36)
Disease status			
SJC, mean ± SD	9.8 ± 3.8	10.4 ± 7.3	9.7 ± 2.7
TJC, mean ± SD	13.4 ± 6.3	18.2 ± 7.7	15.5 ± 7.1
PtGA of pain, mean ± SD‡	49.0 ± 25.8	63.5 ± 16.3	72.1 ± 21.1
PtGA of disease activity, mean ± SD†	67.8 ± 18.7	83.7 ± 10.0	80.4 ± 15.4
PGA of disease activity, mean ± SD	66.1 ± 15.9	76.2 ± 11.3	67.7 ± 13.5
HAQ DI score, mean ± SD‡	1.2 ± 0.59	1.7 ± 0.8	1.9 ± 0.57
RF positive, %	68.4	61.5	71.4
ACPA positive, %	78.9	76.9	78.6
CRP, mean ± SD	7.2 ± 9.5	16.2 ± 33.1	11.1 ± 15.0
ESR, mean ± SD	19.5 ± 16.4	32.2 ± 22.7	23.9 ± 13.3
DAS28, mean ± SD‡	5.7 ± 0.54	6.6 ± 0.89	6.3 ± 0.95

\* Except where indicated otherwise, values are the number (%). MCP = metacarpophalangeal; MTP = metatarsophalangeal; DMARD = disease-modifying antirheumatic drug; MTX = methotrexate; HCQ = hydroxychloroquine; SSZ = sulfasalazine; SJC = swollen joint count; TJC = tender joint count; PtGA = patient global assessment; PGA = physician global assessment; HAQ = Health Assessment Questionnaire; DI = disability index; RF = rheumatoid factor; ACPA = anti-citrullinated protein antibody; CRP = C-reactive protein; ESR = erythrocyte sedimentation rate; DAS28 = Disease Activity Score in 28 joints.

†  $P < 0.05$  for good responders versus moderate responders.

‡  $P < 0.05$  for good responders versus nonresponders.

DAS28 (Supplementary Table 4, <https://onlinelibrary.wiley.com/doi/10.1002/art.42295>). Differences between good responders and moderate responders/nonresponders were less marked after treatment ( $P = 0.022$  versus moderate responders, and  $P = 0.046$  versus nonresponders), indicating that pretreatment differences were most pronounced.

#### Elevation of several immune/inflammatory pathways in good responders prior to treatment.

To identify the genes and pathways driving the differences observed at baseline in good responders compared to moderate responders and nonresponders, DEGs were identified between each pair of groups at baseline. Consistent with the PCA results, 5,857 DEGs were observed between good responders and nonresponders at baseline (Supplementary Tables 5 and 6, [https://](https://onlinelibrary.wiley.com/doi/10.1002/art.42295)

[onlinelibrary.wiley.com/doi/10.1002/art.42295](https://onlinelibrary.wiley.com/doi/10.1002/art.42295)), and there were 2,515 DEGs between good responders and moderate responders at baseline, using a fold change of  $>1.5$  and a  $P$  value of  $<0.05$  (Supplementary Tables 7 and 8). In contrast, there were only 312 DEGs between moderate responders and nonresponders at baseline (Supplementary Tables 9 and 10), suggesting greater similarity between moderate responders and nonresponders (Figure 2A). We were also able to predict those who would be good responders (versus nonresponders) pretreatment, based on our RNA-Seq data as assessed by a 16-gene random forest model showing the highest accuracy of 0.92 (Supplementary Figure 2 and Supplementary Table 11).

There were 93 differential pathways between good responders and nonresponders at baseline, with 72 up-regulated and 21 down-regulated pathways in good responders (Supplementary Tables 12

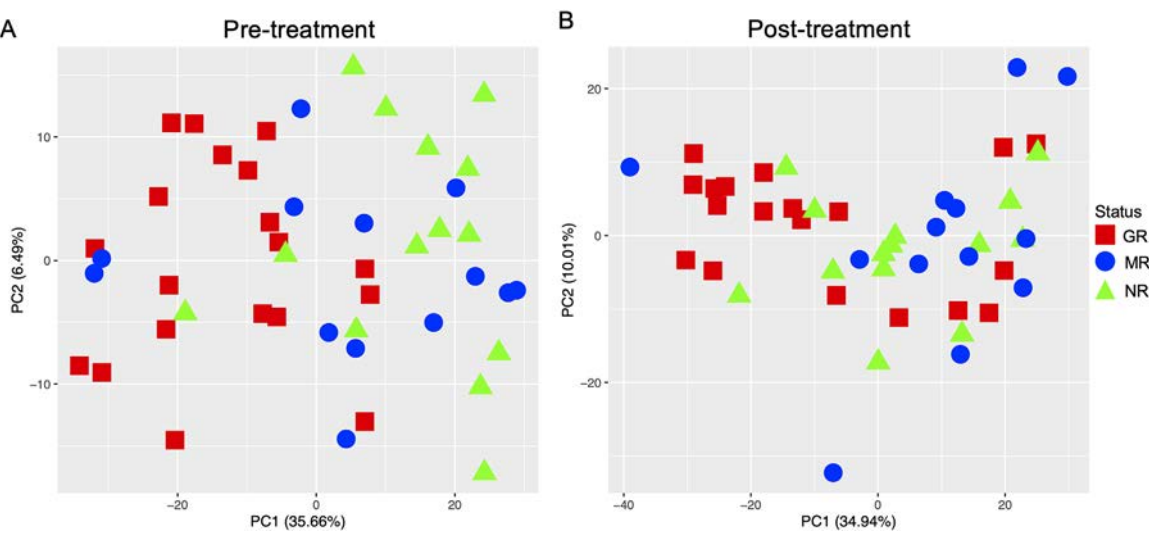


**Figure 1.** Principal components (PC) analysis plots showing the distribution of pretreatment (A) and posttreatment samples (B) from rheumatoid arthritis patients classified as good responders (GR; n = 19), moderate responders (MR; n = 13), or nonresponders (NR; n = 14) to anti-tumor necrosis factor therapy.

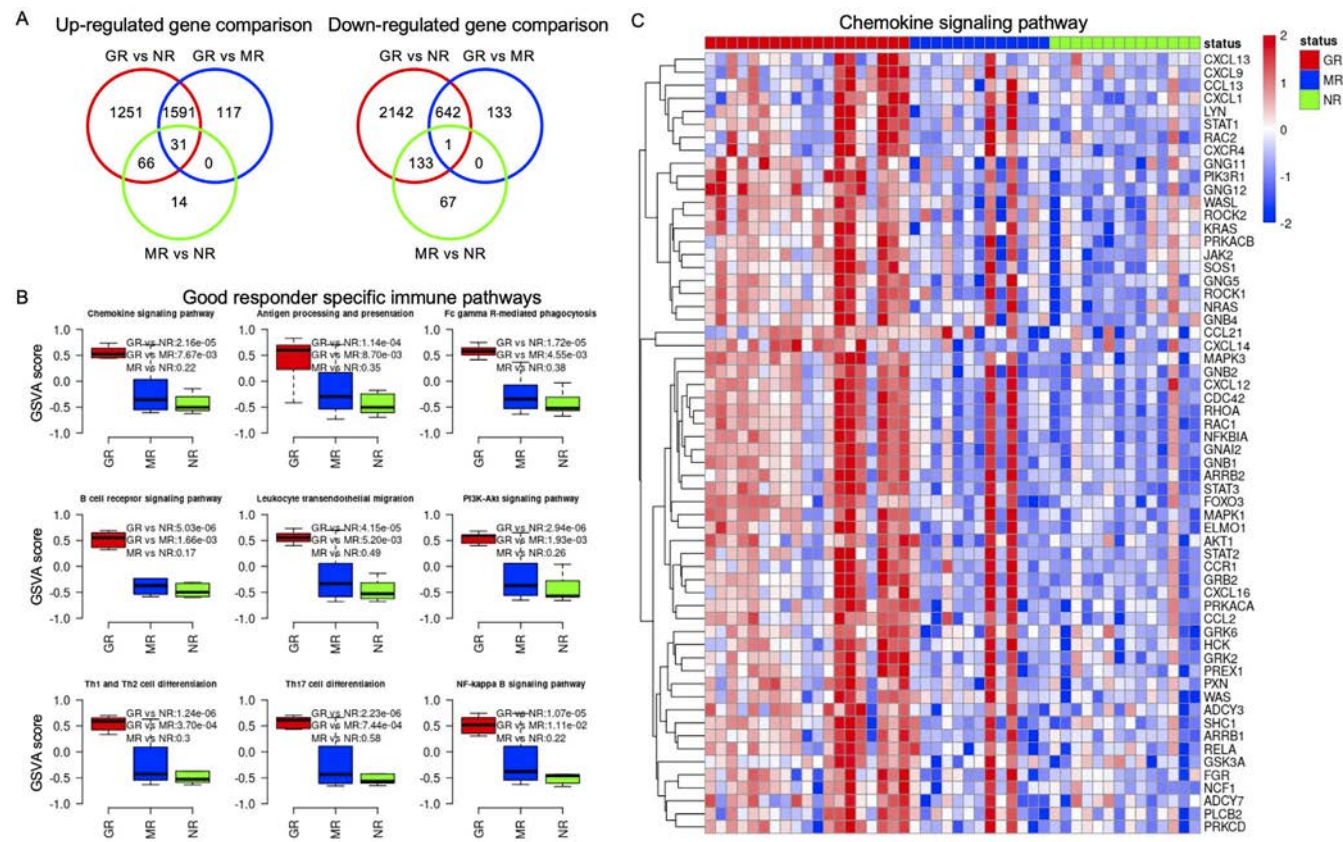


**Figure 2.** Pretreatment comparisons of gene expression in good responders (GR), moderate responders (MR), and nonresponders (NR) to anti-tumor necrosis factor therapy, showing greater differential gene expression in good responders, mapping to several inflammatory pathways. **A**, Pair-wise comparisons of up-regulated and down-regulated genes between good responders, moderate responders, and nonresponders. **B**, Signature score comparison of responder-specific immune pathways in each responder group of samples. Data are shown as box plots, where each box represents the upper and lower interquartile range (IQR). Lines inside the boxes represent the median, and whiskers represent 1.5 times the upper and lower IQRs. *P* values were calculated based on Wilcoxon's rank sum tests. **C**, Expression patterns of the chemokine signaling pathway for up-regulated genes in good responders compared to nonresponders. GSEA = gene set variation analysis; PI3K = phosphatidylinositol 3-kinase.

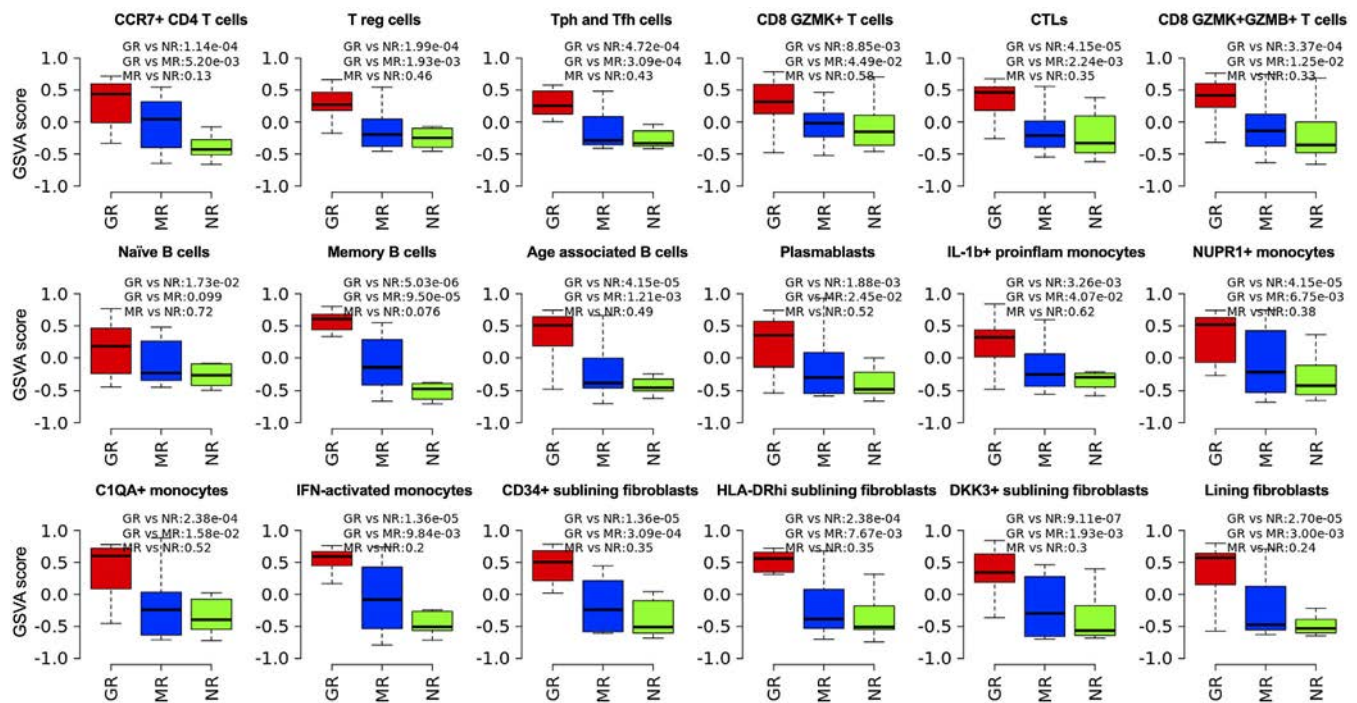


**Figure 3.** Pretreatment comparisons of gene-derived cell signatures in good responders, moderate responders, and nonresponders to anti-tumor necrosis factor therapy. Signature scores were plotted for synovial cell populations previously identified by single-cell RNA sequencing (ref. 28), including T cell populations (CCR7+, regulatory, peripheral helper [Tph]/follicular helper [Tfh], granzyme K-positive [GZMK+], cytotoxic T lymphocyte [CTL], and GZMK+/GZMB+), B cell populations (naïve, memory, age-associated, plasmablasts), myeloid cells (C1qA+, proinflammatory [proinflam], NUPR1+, interferon [IFN]-activated), and fibroblasts (HLA-DR<sup>high</sup>, CD34+ sublining, DKK3+ sublining). Data are shown as box plots, where each box represents the upper and lower IQR. Lines inside the boxes represent the median, and whiskers represent 1.5 times the upper and lower IQRs. *P* values were calculated based on Wilcoxon's rank sum tests. IL-1b = interleukin-1β (see Figure 2 for other definitions).

and 13, <https://onlinelibrary.wiley.com/doi/10.1002/art.42295>). The 21 down-regulated pathways (elevated in nonresponders) were largely sensory and metabolic pathways, with the top 3 pathways being neuroactive ligand–receptor interaction, olfactory transduction, and taste transduction. Of the 72 up-regulated pathways in good responders compared to nonresponders at baseline, ~60% were related to immune responses, inflammation, or infection, including innate pathways (e.g., leukocyte transmigration, Fc gamma receptor phagocytosis) and adaptive immune pathways (e.g., B cell receptor signaling and Th1 versus Th2 cell differentiation) as shown in Figure 2B. The chemokine signaling pathway, involved in cell recruitment and inflammatory responses, demonstrated a high differential expression of several inflammatory genes between good responders and moderate responders/nonresponders at baseline (Figure 2C). The heatmap of other significant pathways in Figure 2B can be found in Supplementary Figures 3–10. However, we did not observe similar results based on 3 published data sets (Supplementary Figure 11 and Supplementary Tables 14–16).

In an effort to determine which specific cell populations might be contributing to the up-regulated immune pathways, cell signatures defined by Zhang et al (31) describing 18 synovial cell populations were overlaid onto this data set. This analysis showed higher signature scores for all immune and fibroblast populations in good responders compared to nonresponders at baseline (Figure 3).

A permutation test proved that these results were not due to data bias (Supplementary Figure 12 and Supplementary Table 17, <https://onlinelibrary.wiley.com/doi/10.1002/art.42295>). We obtained similar results based on the cell signatures defined in another synovial single-cell data set (32) (Supplementary Figure 13). While these data further supported an increased immune activation status in good responders compared to moderate responders/nonresponders, they suggested that most synovial cell types were contributing to the immune activation signature in good responders. Collectively, these results identified several inflammatory pathways elevated at baseline in synovium of patients who responded well to anti-TNF therapy compared to patients showing moderate or no response.

**Reduction of inflammatory pathways in good responders by anti-TNF treatment.** To identify which pathways were modulated by anti-TNF therapy after treatment in the RA patient response groups, we identified 451, 215, and 180 DEGs up-regulated pretreatment compared to posttreatment in good responders, moderate responders, and nonresponders, respectively (Figure 4A, Supplementary Figure 14, and Supplementary Tables 18–20, <https://onlinelibrary.wiley.com/doi/10.1002/art.42295>). There was minimal overlap among the 3 pre- versus posttreatment DEG lists, indicating that anti-TNF therapy affected the treatment response patient populations



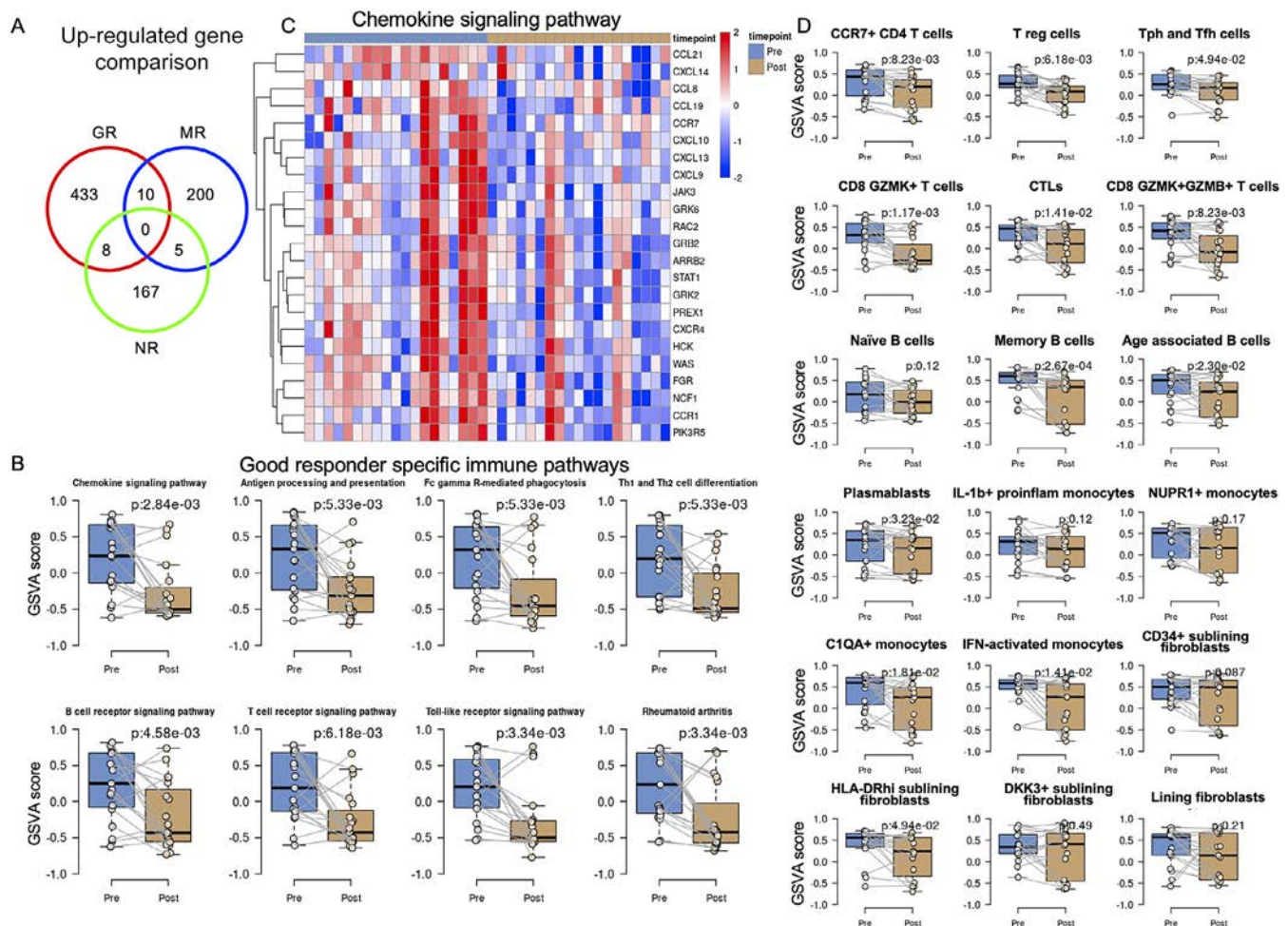


**Figure 4.** Effects of anti-tumor necrosis factor therapy on gene expression profiles, pathways, and cell signatures when comparing pre- and posttreatment in good responders, moderate responders, and nonresponders. **A**, Comparison of up-regulated genes in pretreatment compared to posttreatment in each responder group. **B**, Signature score comparison of good responder-specific immune pathways between pre- and posttreatment samples. **C**, Expression patterns of the chemokine signaling pathway for up-regulated genes in pretreatment compared to posttreatment for good responders. **D**, Cell signature scores for synovial cell populations identified previously by single-cell RNA sequencing (ref. 28) (see Figure 3 for list of cell populations). In **B** and **D**, data are shown as box plots, where each box represents the upper and lower IQR. Lines inside the boxes represent the median, and whiskers represent 1.5 times the upper and lower IQRs. *P* values were calculated based on paired Wilcoxon's rank sum tests. See Figure 2 for other definitions.

differently. Pathway enrichment analysis of these DEGs in each of the anti-TNF treatment response groups revealed that 28 pathways decreased in good responders, 5 decreased in moderate responders, and none were significantly decreased in nonresponders (Supplementary Tables 21–23). Among the pathways decreasing after anti-TNF treatment in good responders, >80% were the same pathways elevated at baseline relative to nonresponders (Figure 4B). For example, messenger RNA expression of many genes in the chemokine signaling pathway that were elevated in good responders at baseline (Figure 2C) decreased following anti-TNF treatment, including the following: *CXCL13*, *CCR1*, *GRK2*, *FGR*, *GRK6*, *GRB2*, *HCK*, *ARRB2*, *CXCL9*, *PREX1*, *RAC2*, *CCL21*, *NCF1*, *STAT1*, *WAS*, *CXCR4*, and *CXCL14* (Figure 4C). Only 2 of the inflammatory pathways that were elevated at baseline in good responders, Th17

differentiation and leukocyte transendothelial migration, were not significantly changed by anti-TNF treatment. None of these immune pathways that decreased in good responders were significantly impacted in moderate responders or nonresponders, suggesting that pathways that decreased after anti-TNF treatment were unique to good responders. Heatmaps of other pathways in Figure 4B can be found in Supplementary Figures 15–21.

We again overlaid synovial immune and fibroblasts cell signatures obtained from the work of Zhang et al (31) onto this data set to determine if specific cell populations may be responding to the anti-TNF treatment. Cell population signatures decreased following anti-TNF treatment in all T cell populations (CCR7+, regulatory, peripheral helper/follicular helper, granzyme K+, cytotoxic T lymphocyte, and granzyme K+/granzyme B+) in good responders (Figure 4D), while most of them were not significantly decreased in

moderate responders and nonresponders (Supplementary Figures 22–23, <https://onlinelibrary.wiley.com/doi/10.1002/art.42295>). Other specific cell signatures that decreased following anti-TNF treatment in good responders, but not in moderate responders/nonresponders, included memory B cells, age-associated B cells, plasmablasts, as well as C1qA+ and interferon-activated myeloid subpopulations and HLA-DR<sup>high</sup> fibroblasts. Naive B cells, proinflammatory macrophages, and CD34+ sublining fibroblasts were unchanged following anti-TNF treatment in all patients. DKK3+ sublining fibroblasts and lining fibroblasts were significantly increased in nonresponders but not in good and moderate responders. We obtained similar results based on Stephenson's signatures (32) (Supplementary Figures 24–26). Collectively, these data suggest that in addition to showing higher inflammatory signatures at baseline, following treatment with anti-TNF, good responders show decreases in many of these inflammatory pathways as well as decreases in certain cell population signatures, including lymphocytes and specific myeloid populations.

**Changes observed over time in synovial inflammatory genes in good responders after anti-TNF treatment corresponding to protein changes in matched peripheral blood.** In an effort to connect synovial changes to changes observed in the blood, we selected several inflammatory genes encoding soluble proteins that showed either differential expression at baseline and/or were decreased following anti-TNF treatment to measure at the protein level in the periphery. These proteins included the following: GRO $\alpha$  (CXCL1), calprotectin (S100A8/A9), IL-10, IP10 (CXCL10),

MCP1 (CCL2), MIG (CXCL9), BRAK (CXCL14), CXCL16, HMGB1, IL-32, YKL40 (CHI3L1), 6Ckine (CCL21), MCP2 (CCL8), BCA1 (CXCL13), MCP4 (CCL13), IL-16, and TRAIL (TNFSF10). None of the proteins tested showed a significant differential between good responders and nonresponders at baseline (Supplementary Table 24, <https://onlinelibrary.wiley.com/doi/10.1002/art.42295>), even with multivariate analysis (data not shown). However, all proteins that had been selected based on decreased synovial gene expression following anti-TNF treatment showed a similar significant reduction in the periphery posttreatment (e.g., calprotectin, IP10, MIG, BCA1, and YKL40; IL-10 and IL-32 were excluded due to a majority of values below the limit of detection) (Figure 5 and Supplementary Table 25).

Also consistent with the gene expression data, there was no significant difference between pre- and posttreatment levels of these proteins for moderate responders and nonresponders (Supplementary Figures 27 and 28 and Supplementary Table 25, <https://onlinelibrary.wiley.com/doi/10.1002/art.42295>). While corresponding peripheral proteins were unable to predict a good response inhibition at baseline, there was a link between several synovial and peripheral biomarkers when observed within the same patient longitudinally.

## DISCUSSION

The current study of synovial tissue biopsies from RA patients pre- and posttreatment with anti-TNF therapy yielded 3 key findings: 1) increased baseline inflammatory pathways in

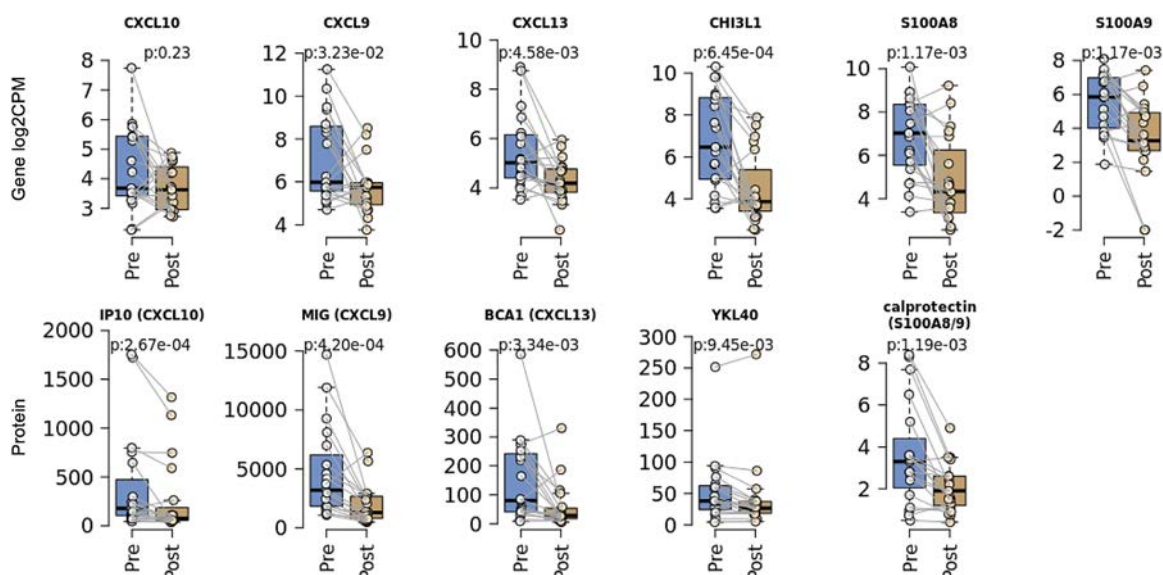


**Figure 5.** Comparison of synovial gene expression and circulating protein changes following anti-tumor necrosis factor treatment. Relative synovial gene levels and circulating protein levels are shown. Data are shown as box plots, where each box represents the upper and lower interquartile range (IQR). Lines inside the boxes represent the median, and whiskers represent 1.5 times the upper and lower IQRs. *P* values were calculated based on paired Wilcoxon's rank sum tests. CPM = counts per million; IP10 = interferon- $\gamma$ -inducible 10-kd protein; MIG = monokine induced by interferon- $\gamma$ ; BCA1 = B cell-attracting chemokine 1.



good responders were consistently reduced by anti-TNF treatment; 2) cell signatures similarly reflected elevated inflammation in good responders at baseline, and lymphocyte populations were the most responsive to anti-TNF therapy; and 3) a high concordance of inpatient peripheral protein changes and synovial gene expression changes following anti-TNF therapy were observed. Collectively, our findings demonstrate that patients responding to anti-TNF therapy show synovial elevations of genes reflecting diverse inflammatory mechanisms, including several inflammatory cell types.

The elevations in synovial inflammatory genes and pathways pretreatment are consistent with prior studies that showed an association of histologic response to infliximab based on changes in lymphoid aggregates in the synovium (36,37). However, results from synovial gene array profiling were inconsistent, and good response was not associated with elevated inflammatory pathways. For example, Badot et al found that synovial inflammatory genes were elevated in nonresponders instead of good responders (11), and Lindberg et al were unable to find any significant gene differences between good responders and nonresponders with an FDR of  $<0.05$  and only obtained similar results to our study when considering genes with weaker signals (33).

We reanalyzed publicly available synovial tissue data based on the criteria used in our study and could not identify immune-related pathway elevations in good responders from any other data set. For example, although 886 up-regulated genes in good responders compared to nonresponders pretreatment were identified in the data set from Badot et al (11), only 1 KEGG pathway was enriched in these genes (Supplementary Table 14, <https://onlinelibrary.wiley.com/doi/10.1002/art.42295>). The lack of DEGs with consistent functions in these prior studies could be due to small patient numbers and/or the use of microarrays. The analysis of larger patient numbers and the use of RNA sequencing in the present study may have been able to identify the presence of greater synovial inflammation as an indicator of a greater likelihood of response to anti-TNF and demonstrate decreases in these pathways following treatment. Because of the inconsistency between published data sets and our data set, the model we built cannot predict the status for the 3 previously published data sets. However, we will need to further validate the above results based on other large RNA-Seq data sets.

We also evaluated differential genes and pathways in nonresponders and found that pathways up-regulated in nonresponders compared to good responders were largely sensory and metabolic pathways; top pathways included neuroactive ligand–receptor interaction, olfactory transduction, and taste transduction. These are intriguing observations given the significantly greater scores of patient global assessment of pain in nonresponders and the reported expression of olfactory and taste receptor expression in tissues (38). The functional role of these pathways in disease is not entirely clear but may have functions unrelated to olfaction, as these receptors are found expressed in a variety of tissues

(39,40). Therefore, additional investigation will be required to fully understand the implications of their expression in the synovium.

We found certain inflammatory pathways at baseline that diverge between good responders and nonresponders and were not significantly changed following anti-TNF treatment in good responders. These included Th17 differentiation and leukocyte transendothelial cell migration. These pathways may require more time to be impacted by the TNF neutralizing therapy or potentially reflect the emergence of plastic resistance following blockade of the TNF pathway, as reported for IL-17 (41–43). We did not find any significant differential pathways in the nonresponder group when comparing pre- and posttreatment, further confirming that TNF inhibition in these patients has minimal effects. These data support the concept that disease in responders is driven by inflammatory pathways that are normalized following anti-TNF treatment, whereas nonresponder disease is driven by an alternative inflammatory mechanism, perhaps a sensory or metabolic pathway, which is TNF-independent and thus is not changed by anti-TNF therapy. We are currently exploring these potential alternative inflammatory mechanisms identified in nonresponders.

We were unable in this cohort of patients with established RA to find a significant relationship between response status and Krenn score (Supplementary Figure 29A, <https://onlinelibrary.wiley.com/doi/10.1002/art.42295>) or synovial pathotype, assessed either by histology (Supplementary Figure 29B) or based on the molecular signatures described by Lewis et al (9) (Supplementary Figure 29C). While this could be due to low patient numbers upon stratification into individual pathotypes, it is also important to note that the patients included in that study were at a different disease stage (i.e., early RA, average disease duration 6.8 months) and had a different treatment exposure (synthetic DMARD-naïve). Therefore, the reported baseline pathotype association with therapy response to DMARDs may reflect the clinical status and/or treatment modality. In addition, the molecular characterization highlighted multiple differential genes and pathways, which are potentially more sensitive or specific than histologic assessment for pathotype or Krenn scoring. Similarly, the discrepancy between clinical DAS28 scores and the higher inflammatory pathways based on gene expression in the synovium further support other reported findings that clinical remission is not the same as histologic remission (44).

In an effort to determine whether blood markers can reflect synovial gene changes, we performed circulating protein analyses based on synovial gene differences or changes, predicated on the assumption that soluble and secreted proteins will diffuse from the joint and be elevated in the blood. This is in contrast to blood gene expression analysis, which relies on the presence of disease-associated cells to be present in the blood. Although we can identify the predictive signature from synovial tissue gene expression data, we were unable to detect any significant differences at baseline in any of the proteins evaluated (even those in which the synovial gene differences were significant), which is

consistent with previously published studies, including blood gene expression studies (5,10) and a proteomic analysis (45). There was little overlap between the signatures in these studies, and none have been incorporated into clinical practice. Interestingly, one study using iTRAQ labeling found proteins that predicted response to adalimumab or infliximab, but there was no correlation of markers between the 2 treatments (45). In contrast to the lack of association between baseline synovial gene and peripheral proteins, changes in circulating proteins post-anti-TNF treatment were highly consistent with gene changes in the synovium of good responders. The robust difference of blood protein markers between pre- and posttreatment could be due to inpatient comparisons that normalize the responses.

While pretreatment PCA analysis of total gene expression distinguished good responders from moderate responders and nonresponders, treatment lessened these gene expression differences. This suggests that the gene expression differences before treatment were modulated by anti-TNF therapy in good responders. Given that the inflammatory pathways were reduced posttreatment, we believe that this reflects the dominance of inflammatory pathways driving disease in good responders, and upon reduction of these overriding pathways by anti-TNF therapy, the patient populations become more similar. Conversely, there were fewer elevated pathways in moderate/nonresponders compared to good responders, suggesting that the inflammatory responses in good responders exceed other pathways active in moderate or nonresponders. Collectively, these results suggest that the primary difference between good responders and moderate/nonresponders are the robust inflammatory pathways which overshadow other pathways that are more active in nonresponders.

A limitation of this study is that we only explored a single therapeutic mechanism (i.e., anti-TNF). While other therapies such as costimulatory blockade, IL-6, or B cell-directed therapy might have impacted similar inflammatory pathways, it is possible the results of treatment with these alternative therapies could have been different. However, the inflammatory mechanisms engaged by all the biologic therapies may account for why the combination of these therapies did not increase efficacy and only led to more side effects (46,47). As an extension of these studies, we plan to use the Stratification of Biologic Therapies for RA by Pathobiology (STRAP) trial included in the Maximising Therapeutic Utility for RA (MATURA) consortium (<http://www.matura-mrc.whri.qmul.ac.uk/>) to explore responder and nonresponder mechanisms with anti-TNF and other therapeutic agents (IL-6 and B cell-targeted agents).

In conclusion, our data demonstrate that inflammatory pathways are elevated in RA patients who robustly respond to anti-TNF therapy. With greater patient numbers, we confirmed previous reports suggesting elevations in inflammation in anti-TNF responder patients and extended the investigation to define multiple pathways and synovial cell signatures elevated in good responders, which decreased following anti-TNF treatment. Although peripheral proteins could not replicate the synovial gene

prediction at baseline, decreases in inflammatory genes in the synovium within individual patients following anti-TNF treatment were observed at the protein level in blood and identified potential markers that can reflect the inflammatory changes occurring due to treatment. These results provide additional evidence for the key mechanistic activities of anti-TNF treatment on inflammatory pathways in robustly responding RA patients and on the cell populations contributing to RA pathogenesis.

## ACKNOWLEDGMENTS

We thank AbbVie employees Valerie Pivoruskas and former AbbVie employee Laura Wong for assistance with RNA isolation, the Genome Technology Access Center of Washington University in St. Louis for RNA sequencing (funded by AbbVie), Gerri Dooner (AbbVie) for sample cataloging and distribution, and Feng Hong (AbbVie) for multivariate statistical analyses.

## AUTHOR CONTRIBUTIONS

All authors were involved in drafting the article or revising it critically for important intellectual content, and all authors approved the final version to be published. Dr. Ruzek had full access to all of the data in the study and takes responsibility for the integrity of the data and the accuracy of the data analysis.

**Study conception and design.** Levesque, Cuff, Long, Pitzalis, Ruzek.

**Acquisition of data.** Conlon, Nerviani, Lewis, Pitzalis, Ruzek.

**Analysis and interpretation of data.** Wang, Rivellese, Lewis, Housley, Levesque, Cao, Cuff, Long, Pitzalis, Ruzek.

## ROLE OF THE STUDY SPONSOR

AbbVie funded this work, and in collaboration with the authors, participated in the study design, research, analysis, data collection, interpretation of data, review, and approval of the manuscript. All authors had access to relevant data and participated in the drafting, review, and approval of this publication. No honoraria or payments were made for authorship. Publication of this article was contingent upon approval by AbbVie.

## REFERENCES

1. Harre U, Schett G. Cellular and molecular pathways of structural damage in rheumatoid arthritis. *Semin Immunopathol* 2017;39:355.
2. Rubbert-Roth A, Szabó MZ, Kedves M, et al. Failure of anti-TNF treatment in patients with rheumatoid arthritis: the pros and cons of the early use of alternative biological agents. *Autoimmun Rev* 2019;18:102398.
3. McInnes IB, Schett G. Pathogenic insights from the treatment of rheumatoid arthritis. *Lancet* 2017;389:2328.
4. Mulhearn B, Barton A, Viatte S. Using the immunophenotype to predict response to biologic drugs in rheumatoid arthritis [review]. *J Pers Med* 2019;9:46.
5. Farutin V, Prod'homme T, McConnell K, et al. Molecular profiling of rheumatoid arthritis patients reveals an association between innate and adaptive cell populations and response to anti-tumor necrosis factor. *Arth Res Ther* 2019;21:216.
6. Dennis G JR, Holweg CT, Kummerfeld SK, et al. Synovial phenotypes in rheumatoid arthritis correlate with response to biologic therapeutics. *Arth Res Ther* 2014;16:R90.

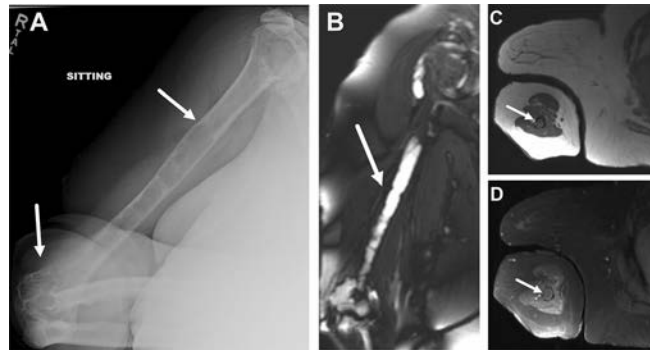
7. Hyrich KL, Watson KD, Silman AJ, et al. Predictors of response to anti-TNF- $\alpha$  therapy among patients with rheumatoid arthritis: results from the British Society for Rheumatology Biologics Register. *Rheumatology (Oxford)* 2006;45:1558–65.
8. Van Baarsen LG, Wijbrandts CA, Timmer TC, et al. Synovial tissue heterogeneity in rheumatoid arthritis in relation to disease activity and biomarkers in peripheral blood. *Arthritis Rheum* 2010;62:1602–7.
9. Lewis MJ, Barnes MR, Blighe K, et al. Molecular portraits of early rheumatoid arthritis identify clinical and treatment response phenotypes. *Cell Rep* 2019;28:2455–70.
10. Toonen EJ, Gilissen C, Franke B, et al. Validation study of existing gene expression signatures for anti-TNF treatment in patients with rheumatoid arthritis. *PLoS ONE* 2012;7:e33199.
11. Badot V, Galant C, Toukap AN, et al. Gene expression profiling in the synovium identifies a predictive signature of absence of response to adalimumab therapy in rheumatoid arthritis. *Arth Res Ther* 2009;11:R57.
12. Lindberg J, Klint EA, Catrina AI, et al. Effects of infliximab on mRNA expression profiles in synovial tissue of rheumatoid arthritis patients. *Arth Res Ther* 2006;8:R179.
13. Alivernini S, MacDonald L, Elmesmari A, et al. Distinct synovial tissue macrophage subsets regulate inflammation and remission in rheumatoid arthritis. *Nat Med* 2020;26:1295–306.
14. Yu X, Chen YA, Conejo-Garcia JR, et al. Estimation of immune cell content in tumor using single-cell RNA-seq reference data. *BMC Cancer* 2019;19:715.
15. Karman J, Wang J, Bodea C, et al. Lung gene expression and single cell analyses reveal two subsets of idiopathic pulmonary fibrosis (IPF) patients associated with different pathogenic mechanisms. *PLoS One* 2021;16:e0248889.
16. Newman A, Steen CB, Liu CL, et al. Determining cell type abundance and expression from bulk tissues with digital cytometry. *Nat Biotechnol* 2019;37:773–82.
17. Aletaha D, Neogi T, Silman AJ, et al. 2010 rheumatoid arthritis classification criteria: an American College of Rheumatology/European League Against Rheumatism collaborative initiative. *Arthritis Rheum* 2010;62:2569–81.
18. Prevoo ML, van't Hof MA, Kuper HH, et al. Modified disease activity scores that include twenty-eight-joint counts: development and validation in a prospective longitudinal study of patients with rheumatoid arthritis. *Arthritis Rheum* 1995;38:44–8.
19. Kelly S, Humby F, Filer A, et al. Ultrasound-guided synovial biopsy: a safe, well-tolerated and reliable technique for obtaining high-quality synovial tissue from both large and small joints in early arthritis patients. *Ann Rheum Dis* 2015;74:611–7.
20. Van Riel PL, Renskers L. The Disease Activity Score (DAS) and the Disease Activity Score using 28 joint counts (DAS28) in the management of rheumatoid arthritis. *Clin Exp Rheumatology* 2016;34 Suppl: S40–4.
21. Dobin A, Davis CA, Schlesinger F, et al. STAR: Ultrafast Universal RNA-seq Aligner. *Bioinformatics* 2013;29:15–21.
22. Liao Y, Smyth GK, Shi W. featureCounts: an efficient general purpose program for assigning sequence reads to genomic. *Bioinformatics* 2014;30:923–30.
23. Wang L, Wang S, Li W. RSeQC: quality control of RNA-seq experiments. *Bioinformatics* 2012;28:2184–5.
24. Barrett T, Wilhite SE, Ledoux P, et al. NCBI GEO: archive for functional genomics data sets—update. *Nucleic Acids Res* 2013;41:D991–5.
25. Robinson MD, Oshlack A. A scaling normalization method for differential expression analysis of RNA-seq data. *Genome Biol* 2010;11:R25.
26. Law CW, Chen Y, Shi W, et al. Voom: precision weights unlock linear model analysis tools for RNA-seq read counts. *Genome Biol* 2014;15:R29.
27. Wang J, Vasaikar S, Shi Z, et al. WebGestalt 2017: a more comprehensive, powerful, flexible and interactive gene set enrichment analysis toolkit. *Nucleic Acids Res* 2017;3:W130–7.
28. Wang J, Duncan D, Shi Z, et al. WEB-based GENE SeT Analysis Toolkit (WebGestalt): update 2013. *Nucleic Acids Res* 2013;41: W77–83.
29. Kanehisa M, Goto S. KEGG: kyoto encyclopedia of genes and genomes. *Nucleic Acids Res* 2000;28:27–30.
30. Hänzelmann S, Castelo R, Guinney J. GSEA: gene set variation analysis for microarray and RNA-seq data. *BMC Bioinformatics* 2013;14:7.
31. Zhang F, Wei F, Slowikowski K, et al. Defining inflammatory cell states in rheumatoid arthritis joint synovial tissues by integrating single-cell transcriptomics and mass cytometry. *Nat Immunol* 2019;2:928–42.
32. Stephenson W, Donlin LT, Butler A, et al. Single-cell RNA-seq of rheumatoid arthritis synovial tissue using low-cost microfluidic instrumentation. *Nat Commun* 2018;9:791.
33. Lindberg J, Wijbrandts CA, van Baarsen LG, et al. The gene expression profile in the synovium as a predictor of the clinical response to infliximab treatment in rheumatoid arthritis. *PLoS ONE* 2010;5: e11310.
34. Aterido A, Cañete JD, Tornero J, et al. A combined transcriptomic and genomic analysis identifies a gene signature associated with the response to anti-TNF therapy in rheumatoid arthritis. *Front Immunol* 2019;10:1459.
35. Vastesaeger N, Kutzbach AG, Amital H, et al. Prediction of remission and low disease activity in disease-modifying anti-rheumatic drug-refractory patients with rheumatoid arthritis treated with golimumab. *Rheumatology* 2016;55:1466–76.
36. Klaasen R, Thurlings RM, Wijbrandts CA, et al. The relationship between synovial lymphocyte aggregates and the clinical response to infliximab in rheumatoid arthritis: a prospective study. *Arthritis Rheum* 2009;60:3217–32.
37. Van der Pouw Kraan TC, Wijbrandts CA, van Baarsen LG, et al. Responsiveness to anti-tumor necrosis factor  $\alpha$  therapy is related to pre-treatment tissue inflammation levels in rheumatoid arthritis patients. *Ann Rheum Dis* 2008;67:563–6.
38. Ferrer I, Garcia-Esparcia P, Carmona M, et al. Olfactory receptors in non-chemosensory organs: the nervous system in health and disease. *Front Aging Neurosci* 2016;8:163.
39. Flegel C, Mantziotis S, Osthold S, et al. Expression profile of ectopic olfactory receptors determined by deep sequencing. *PLOS One* 2013;8:e55368.
40. Feldmesser E, Olender T, Khen M, et al. Widespread ectopic expression of olfactory receptor genes. *BMC Genomics* 2006;7:121.
41. Chen DY, Chen YM, Chen HH, et al. Increasing levels of circulating Th17 cells and interleukin-17 in rheumatoid arthritis patients with an inadequate response to anti-TNF- $\alpha$  therapy. *Arth Res Ther* 2011;13: R126.
42. Hull DN, Williams RO, Pathan E, et al. Anti-tumor necrosis factor treatment increases circulating T helper type 17 cells similarly in different types of inflammatory arthritis. *Clin Exp Immunol* 2015;181:401.
43. Talotta R, Berzi A, Atzeni F, et al. Paradoxical expansion of Th1 and Th17 lymphocytes in rheumatoid arthritis following infliximab treatment: a possible explanation for a lack of clinical response. *J Clin Immunol* 2015;35:550.
44. Orange DE, Agius P, DiCarlo EF, et al. Histologic and transcriptional evidence of subclinical synovial inflammation in rheumatoid arthritis patients in clinical remission. *Arthritis Rheum* 2019;71:1034–41.
45. Ortea I, Roschitzki B, Lopez-Rodriguez R, et al. Independent candidate serum protein biomarkers of response to adalimumab and to infliximab in rheumatoid arthritis: an exploratory study. *PLoS ONE* 2016;11:e0153140.

46. Genovese MC, Cohen S, Moreland L, et al. Combination therapy with etanercept and anakinra in the treatment of patients with rheumatoid arthritis who have been treated unsuccessfully with methotrexate. *Arthritis Rheum* 2004;50:1412–9.

47. Weinblatt M, Combe B, Covucci A, et al. Safety of the selective costimulation modulator abatacept in rheumatoid arthritis patients receiving background biologic and nonbiologic disease-modifying antirheumatic drugs: a one-year randomized, placebo-controlled study. *Arthritis Rheum* 2006;54:2807–16.

DOI 10.1002/art.42312


**Clinical images: Giant intraosseous synovial cyst with intraarticular connection at the elbow in rheumatoid arthritis**




The patient, a 74-year-old woman with longstanding seronegative, erosive rheumatoid arthritis (RA) who had been taking leflunomide and etanercept, presented with worsening arthralgias in her right elbow. Initial radiographs revealed a large lytic lesion in the distal humerus. Further radiographs of the humerus, obtained to evaluate the full extent of the lesion, showed an expansile cystic lesion replacing the distal two-thirds of the humerus, arising from the elbow articular surface (**arrows in A**). The lesion had indolent features of smooth endosteal scalloping, slight bone expansion, a nonsclerotic border, and no matrix. A sagittal STIR magnetic resonance image (MRI) demonstrated a corresponding T2-hyperintense marrow-replacing lesion (**arrow in B**). A T1-weighted transverse MRI through the midportion of the humeral shaft showed the marrow-replacing lesion to be isointense to fluid (**arrow in C**). A T1-weighted, fat-suppressed, postcontrast MRI at the same level demonstrated a thin rim of enhancement at the lesion's periphery, which was isointense to fluid on T1- and fluid-sensitive sequences (**arrow in D**), indicative of a cystic cavity lesion with no solid material or nodular enhancement. Lesion biopsy showed a paucicellular-type cyst with few fibrotic stroma fragments and no evidence of malignancy. Treatment was switched from etanercept to abatacept, resulting in significant improvements of RA symptoms and stable imaging results in the patient at the 3-month follow-up. Extraarticular synovial cysts as a rare complication of severe RA have been reported in only a few cases (1–3), with presence of an intraarticular connection even more unique. Identifying the described key features will help with diagnosis and with ruling out malignancy.

Author disclosures are available at <https://onlinelibrary.wiley.com/action/downloadSupplement?doi=10.1002%2Fart.42312&file=art42312-sup-0001-Disclosureform.pdf>.

1. Lohse A, Carbillet JP, Onimus M, et al. Giant intraosseous cyst-like lesions in rheumatoid arthritis: report of a case. *Joint Bone Spine* 2003;70:67–70.
2. Amin YE, Ragab Y, El-Shaarawy N, et al. Giant intraosseous synovial cyst with intraarticular communication with the ankle joint in longstanding rheumatoid arthritis. *J Rheumatol* 2012;39:180–1.
3. Kirino Y, Ihata A, Shizukuishi K, et al. Multiple extra-articular synovial cysts complicated with rheumatoid arthritis. *Mod Rheumatol* 2009;19:563–6.

Can M. Sungur, MD, PhD   
[cmsungur@wustl.edu](mailto:cmsungur@wustl.edu)  
 Department of Internal Medicine  
 Division of Rheumatology  
 Washington University  
 Jonathan C. Baker, MD   
 Mallinckrodt Institute of Radiology  
 Musculoskeletal Section  
 Washington University  
 St. Louis, MO

# Contribution of MicroRNA-27b-3p to Synovial Fibrotic Responses in Knee Osteoarthritis

Ghazaleh Tavallaei,<sup>1</sup> Starlee Lively,<sup>2</sup> Jason S. Rockel,<sup>2</sup> Shabana Amanda Ali,<sup>3</sup> Michelle Im,<sup>4</sup> Clementine Sarda,<sup>2</sup> Greniqueca M. Mitchell,<sup>2</sup> Evgeny Rossomacha,<sup>2</sup> Sayaka Nakamura,<sup>2</sup> Pratibha Potla,<sup>2</sup> Sarah Gabrial,<sup>2</sup> John Matelski,<sup>2</sup> Anusha Ratneswaran,<sup>2</sup> Kim Perry,<sup>2</sup> Boris Hinz,<sup>5</sup> Rajiv Gandhi,<sup>6</sup> Igor Jurisica,<sup>7</sup> and Mohit Kapoor<sup>8</sup> 

**Objective.** Synovial fibrosis contributes to osteoarthritis (OA) pathology, but the underlying mechanisms remain unknown. We have observed increased microRNA-27b-3p (miR-27b-3p) levels in synovial fluid of patients with late-stage radiographic knee OA. Here, we investigated the contribution of miR-27b-3p to synovial fibrosis in patients with severe knee OA and in a mouse model of knee OA.

**Methods.** We stained synovium sections obtained from patients with radiographic knee OA scored according to the Kellgren/Lawrence scale and mice that underwent destabilization of the medial meniscus (DMM) for miR-27b-3p using in situ hybridization. We examined the effects of intraarticular injection of miR-27b-3p mimic into naive mouse knee joints and intraarticular injection of a miR-27b-3p inhibitor into mouse knee joints after DMM. We performed transfection with miR-27b-3p mimic and miR-27b-3p inhibitor in human OA fibroblast-like synoviocytes (FLS) using reverse transcriptase–quantitative polymerase chain reaction (RT-qPCR) array, RNA sequencing, RT-qPCR, Western blotting, immunofluorescence, and migration assays.

**Results.** We observed increased miR-27b-3p expression in the synovium from patients with knee OA and in mice with DMM-induced arthritis. Injection of the miR-27b-3p mimic in mouse knee joints induced a synovial fibrosis-like phenotype, increased synovitis scores, and increased COL1A1 and  $\alpha$ -smooth muscle actin ( $\alpha$ -SMA) expression. In the mouse model of DMM-induced arthritis, injection of the miR-27b-3p inhibitor decreased  $\alpha$ -SMA but did not change COL1A1 expression levels or synovitis scores. Transfection with the miR-27b-3p mimic in human OA FLS induced profibrotic responses, including increased migration and expression of key extracellular matrix (ECM) genes, but transfection with the miR-27b-3p inhibitor had the opposite effects. RNA sequencing identified a PPARG/ADAMTS8 signaling axis regulated by miR-27b-3p in OA FLS. Human OA FLS transfected with miR-27b-3p mimic and then treated with the PPARG agonist rosiglitazone or with ADAMTS8 small interfering RNA exhibited altered expression of select ECM genes.

**Conclusion.** Our findings demonstrate that miR-27b-3p has a key role in ECM regulation associated with synovial fibrosis during OA.

## INTRODUCTION

Osteoarthritis (OA), the most common form of arthritis, is a leading cause of disability worldwide (1). Research on OA has

frequently focused on articular cartilage degradation and subchondral bone sclerosis, but the synovium also undergoes pathologic changes (2). The synovium, a thin connective tissue layer consisting largely of 2 types of cells (fibroblast-like

Dr. Tavallaei was recipient of a PhD scholarship from the Arthritis Society and a Queen Elizabeth II/Canadian Arthritis Network Graduate Scholarship in Science and Technology. Dr. Ali's work was supported by an Arthritis Society Postdoctoral Fellowship. Dr. Ratneswaran's work was supported by Canadian Institute of Health Research and Krembil Research Institute postdoctoral fellowships. Dr. Hinz's work was supported by the Canadian Institutes of Health Research (foundation grant 375597) and the John R. Evans Leadership Fund (awards 36050, 38861), as well as innovation funds (Fibrosis Network, award 36349) from the Canada Foundation for Innovation and the Ontario Research Fund. Dr. Jurisica's computational analysis was supported in part by the Natural Sciences Research Council (award 203475), the Canada Foundation for Innovation (awards 225404, 30865), the Ontario Research Fund (award 34876), IBM, and the Ian Lawson van Toch Fund. Dr. Kapoor's work was

supported by grants from the Natural Sciences and Engineering Research Council of Canada (NSERC) and the Schroeder Arthritis Institute via the Toronto General and Western Hospital Foundation; Dr. Kapoor was also recipient of a Tier 1 Canada Research Chair and the Tony and Shari Fell Chair in Arthritis Research.

<sup>1</sup>Ghazaleh Tavallaei, PhD: Osteoarthritis Research Program, Division of Orthopaedics, Schroeder Arthritis Institute, University Health Network, Krembil Research Institute, University Health Network, and Department of Laboratory Medicine and Pathobiology, University of Toronto, Toronto, Ontario, Canada; <sup>2</sup>Starlee Lively, PhD, Jason S. Rockel, PhD, Clementine Sarda, BSc, Greniqueca M. Mitchell, BSc, Evgeny Rossomacha, PhD, Sayaka Nakamura, MD, Pratibha Potla, MTech, Sarah Gabrial, BSc, John Matelski, MSc, Anusha Ratneswaran, PhD, Kim Perry, BSc: Osteoarthritis Research Program, Division



synoviocytes [FLS] and tissue-resident macrophages), produces synovial fluid, which nourishes articular chondrocytes and removes products of tissue metabolism (3). As OA progresses, the synovium becomes inflamed (synovitis) and hypertrophies as a result of increased vascularization, infiltration of inflammatory cells, aberrant OA FLS proliferation, and accumulation of excessive extracellular matrix (ECM) (3,4). These changes contribute to synovial fibrosis and promote joint stiffness and pain (5). Although synovial pathology was originally thought to be a secondary reaction to evolving damage in neighboring cartilage and bone tissues, it is now recognized as an active participant of OA pathogenesis (6); however, little is known about the underlying regulatory signaling networks, particularly those responsible for the altered ECM regulation contributing to synovial fibrosis.

As potent regulators of gene expression, microRNAs (miRNAs) in knee OA have been studied but mainly for their roles in cartilage homeostasis (7,8). Less is known about the contribution of these important transcriptional regulators to synovitis, particularly fibrotic responses (5,9,10). We previously reported that miRNA-27b-3p (miR-27b-3p) levels are higher in the synovial fluid of patients with advanced radiographic knee OA and identified the synovium as the major source of miR-27b-3p, as stimulation of synovial explants with interleukin-1 $\beta$  (IL-1 $\beta$ ) elicited its secretion (11). However, the specific role of miR-27b-3p to OA synovial pathology is not known. We hypothesized that miR-27b-3p helps modulate synovial ECM regulatory networks involved in synovial fibrosis during OA. In this study, we used in vivo and in vitro models, RNA sequencing analysis, and computational analysis to determine, for the first time to our knowledge, the role and mechanisms of miR-27b-3p in ECM regulation and synovial fibrotic responses during OA.

## PATIENTS AND METHODS

**Study design and OA patients.** All patients provided written informed consent for inclusion in the University Health Network Research Ethics Board–approved biomarker exploration

studies (16-5969-AE and 14-7592-AE). All animal studies were approved by the University Health Network's Animal Care Committee (animal use protocol 3729) and were conducted in accordance with relevant guidelines and regulations. A minimum of 6 animals were needed to detect a 25% difference by histology with 80% power (sigma = 0.15, alpha level of 0.05). Full sequencing data sets are available through Gene Expression Omnibus (GEO accession no. GSE152638).

We obtained synovial tissue samples from patients with radiographic knee OA (Kellgren/Lawrence [K/L] grades 3 and 4) who were undergoing total knee replacement and from patients who were undergoing knee arthroscopy (K/L grades 1 and 2) at the Toronto Western Hospital (Toronto, Canada). Synovial tissue samples were either used fresh for retrieval of FLS for culture studies or were fixed and processed for histology or for in situ hybridization (ISH). Patient anthropometric and demographic data and the patient's experimental group are listed in Supplementary Table 1, available on the *Arthritis & Rheumatology* website at <https://onlinelibrary.wiley.com/doi/10.1002/art.42285>.

### Mouse model of surgical destabilization of the medial meniscus (DMM) and intraarticular injections.

We housed 10- to 12-week-old C57BL/6J male mice (The Jackson Laboratory) in the Krembil Research Institute (Toronto, Ontario, Canada) vivarium on a 12-hour light/dark cycle in a temperature-controlled room (21°C  $\pm$  1°C) with food provided ad libitum for 1 week before we performed DMM or sham surgery (12). Knee joints (n = 6–10 for each group [DMM and sham]) were collected at 2, 5, or 10 weeks after surgery and processed for ISH, immunohistochemistry (IHC), or histology.

For the miR-27b-3p mimic injection experiments, naive 12-week-old C57BL/6J male mice were intraarticularly injected twice, 2 weeks apart, under isoflurane anesthesia with 5  $\mu$ g of mirVana miR-27b-3p mimic (ThermoFisher catalog no. 4464066) in the right knee or mirVana miRNA mimic negative control 1 (ThermoFisher catalog no. 4464061) in the left knee. Knee joints

of Orthopaedics, Schroeder Arthritis Institute, University Health Network, and Krembil Research Institute, University Health Network, Toronto, Ontario, Canada; <sup>3</sup>Shabana Amanda Ali, PhD: Osteoarthritis Research Program, Division of Orthopaedics, Schroeder Arthritis Institute, University Health Network, Krembil Research Institute, University Health Network, Toronto, Ontario, Canada, and Bone & Joint Center, Department of Orthopaedic Surgery, Henry Ford Health System, Detroit, Michigan; <sup>4</sup>Michelle Im, MSc: Faculty of Dentistry, University of Toronto, Toronto, Ontario, Canada; <sup>5</sup>Boris Hinz, PhD: Faculty of Dentistry, University of Toronto, and Laboratory of Tissue Repair and Regeneration, Keenan Research Centre for Biomedical Science of the St. Michael's Hospital, Toronto, Ontario, Canada; <sup>6</sup>Rajiv Gandhi, MD, FRCS(C): Osteoarthritis Research Program, Division of Orthopaedics, Schroeder Arthritis Institute, University Health Network, Krembil Research Institute, University Health Network, and Departments of Medical Biophysics and Computer Science, University of Toronto, Toronto, Ontario, Canada; <sup>7</sup>Igor Jurisica, PhD, DrSc: Osteoarthritis Research Program, Division of Orthopaedics, Schroeder Arthritis Institute, University Health Network, Krembil Research

Institute, University Health Network, Toronto, Departments of Medical Biophysics and Computer Science, University of Toronto, Toronto, Ontario, Canada, and Institute of Neuroimmunology, Slovak Academy of Sciences, Bratislava, Slovakia; <sup>8</sup>Mohit Kapoor, PhD: Osteoarthritis Research Program, Division of Orthopaedics, Schroeder Arthritis Institute, University Health Network, Krembil Research Institute, University Health Network, Department of Laboratory Medicine and Pathobiology, University of Toronto, and Division of Orthopaedic Surgery, Department of Surgery, University of Toronto, Toronto, Ontario, Canada.

Drs. Tavallaei and Lively contributed equally to this work.

Author disclosures are available at <https://onlinelibrary.wiley.com/action/downloadSupplement?doi=10.1002%2Fart.42285&file=art42285-sup-0001-Disclosureform.pdf>.

Address correspondence via email to Mohit Kapoor, PhD, at [mohit.kapoor@uhnresearch.ca](mailto:mohit.kapoor@uhnresearch.ca).

Submitted for publication June 9, 2021; accepted in revised form June 23, 2022.

were retrieved 5 weeks after injection ( $n = 6$  knee joints per each treatment group) and processed for IHC and histology.

For the miR-27b-3p inhibitor injection experiments, 12-week-old C57BL/6J male mice were subjected to DMM or sham surgery (right knee) and intraarticularly injected with 5  $\mu\text{g}$  of custom in vivo-grade miRCURY locked nucleic acid (LNA) mmu-miR-27b-3p inhibitor (Qiagen catalog no. 339204-YCI201647-FZA) at 1 week and 3 weeks after surgery, with knee joints retrieved at 5 weeks after surgery ( $n = 10$ ). Control animals (9 animals that had sham surgery and received control inhibitor or 10 animals that had DMM surgery and received control inhibitor) underwent the same procedure but received injections of a scrambled negative control inhibitor (Qiagen catalog no. 339204-YCI0201821-FZA).

**Histology and IHC analyses of synovium.** Human synovial samples and mouse knee joints were processed, sectioned, and stained with Safranin O (Sigma-Aldrich catalog no. S2255) and fast green (Bio Basic catalog no. FB0452), Masson's trichrome for connective tissue (Electron Microscopy Sciences catalog series no. 26367), or hematoxylin and eosin (Vector catalog no. H-3404), all in accordance with manufacturers' recommendations. Articular cartilage and synovial samples were scored in a blinded manner by 2 observers who used the Osteoarthritis Research Society International (OARSI) grading for cartilage damage and degree of synovitis (13). For IHC, sections were stained for ADAMTS8 (5  $\mu\text{g}/\text{ml}$ ; Novus Biologicals catalog no. NBP2-46494), type V collagen (COL5A1; 0.5  $\mu\text{g}/\text{ml}$ ; Abcam catalog no. ab7046), type XIV collagen alpha 1 chain (COL14A1; 1:200; Novus Biologicals catalog no. NBP2-15940), COL1A1 (1:200; Abcam catalog no. ab34710),  $\alpha$ -smooth muscle actin ( $\alpha$ -SMA; 1:400; Sigma-Aldrich catalog no. A2547), or PPARG (1:750; Novus Biologicals catalog no. NBP2-22106SS). After sections were stained, we used 3,3'-diaminobenzidine substrate (Vector catalog no. SK-4105) for visualization. We determined percentage of stained area or percentage of positive cells using ImageJ version 1.53c (14).

**In situ hybridization.** After samples were subjected to proteinase K digestion (with 7.5  $\mu\text{g}/\text{ml}$  for 10 minutes for mouse knee joints and 20  $\mu\text{g}/\text{ml}$  for 30 minutes for human synovium), sections were incubated for 1 hour at 55°C with denatured LNA-modified and 5'-end and 3'-end digoxigenin-labeled anti-sense oligonucleotides, which included the miR-27b-3p probe (80 nM for mouse and 160 nM for human; Qiagen catalog no. YD00619142), U6 small nuclear RNA (1 nM; positive control), or scrambled control probe (40 nM; negative control). Nuclei were counterstained with nuclear fast red (Sigma-Aldrich catalog no. N3020-100ML). We allowed coverslipped sections to dry overnight before visualization under brightfield illumination (Leica catalog no. ICC50W5021). We counted a minimum of 3 random fields to measure the percentage of positive cells in each section.

**FLS cultures.** We isolated FLS by enzymatic digestion of human OA synovium obtained at time of surgery (total knee replacement or knee arthroscopy). Cells were cultured at 37°C and at 5%  $\text{CO}_2$  in Dulbecco's modified Eagle's medium (DMEM; Gibco catalog no. 11995073) supplemented with 10% fetal bovine serum (Wisent catalog no. 080-150) and 100 units/ml penicillin and 100  $\mu\text{g}/\text{ml}$  streptomycin. Cells were passaged when they reached 85% confluency. Passages 3–5 were used for all culture experiments. OA FLS cultures were serum-starved (0.5% fetal bovine serum) for 3 hours before addition of 3  $\mu\text{g}/\text{ml}$  Lipofectamine RNAiMAX transfection reagent (Life Technologies, ThermoFisher catalog no. 13778-075) with either 5 nM *Homo sapiens* (hsa)-miR-27b-3p miRCURY LNA miRNA mimic (Qiagen catalog no. 339173 YM00470553) or the corresponding control mimic (Cel-miR-39-3p; Qiagen catalog no. YM00479902) or 50 nM hsa-miR-27b-3p miRCURY LNA Power inhibitor (Qiagen catalog no. 339131) or the corresponding control inhibitor (negative control A; Qiagen catalog no. 339136), after which cultures remained for 48 hours in serum-starved media. For some experiments, OA FLS culture medium was replaced 24 hours later with fresh serum-starved DMEM containing either 1) 20  $\mu\text{M}$  rosiglitazone (Tocris catalog no. 5325) or vehicle (dimethyl sulfoxide; Sigma-Aldrich catalog no. D2650) or 2) 10 nM ADAMTS8 small interfering RNA (siRNA; Sigma-Aldrich catalog no. EHU129241-20UG) or MISSION siRNA universal negative control (Sigma-Aldrich catalog no. SIC001) in 3  $\mu\text{g}/\text{ml}$  Lipofectamine and then incubated for an additional 24 hours before cells were harvested. Cells were either fixed and stained with 0.3% crystal violet (Transwell migration assay) or for immunofluorescence, or extracts were collected for protein (Western blot) or RNA analysis. For RNA analysis, we used the 834-well RT<sup>2</sup> Profiler and polymerase chain reaction (PCR) arrays for human ECM and adhesion molecules (Qiagen catalog no. PAHS-013ZE-1), conventional reverse transcriptase-quantitative PCR (RT-qPCR) (primers listed in Supplementary Table 2, available on the *Arthritis & Rheumatology* website at <https://onlinelibrary.wiley.com/doi/10.1002/art.42285>) and RT-qPCR for detection of mmu-miR-27b-3p and U6 (Qiagen catalog no. 339306), and RNA sequencing (Truseq stranded total RNA; Illumina catalog no. 20020596).

**RNA sequencing and pathway analysis.** RNA was extracted from 48-hour mimic- or control-transfected OA FLS, and libraries were prepared (Truseq stranded total RNA). We used the Illumina NextSeq 550 system (2 × 75 bp) at the Centre for Arthritis Diagnostic and Therapeutic Innovation (Schroeder Arthritis Institute, Toronto, Ontario, Canada) for sequencing analysis, followed by bioinformatics analysis to determine gene expression levels per sample (15). Genes with  $\geq 10$  counts per million in  $\geq 2$  samples were retained for the analysis. We identified differentially expressed genes (DEGs) by using the negative binomial generalized linear model with trended dispersion and trimmed means normalization. Dispersion and treatment

effect estimates were adjusted for sample pairs and genes. Significance was set at unadjusted  $P < 0.05$ , as no significant differences in gene expression remained after multiple testing correction (false discovery rate). We used R (version 3.6.0) and the edgeR (version 3.25.8) package for analysis.

We obtained putative gene targets of hsa-miR-27b-3p from mirDIP version 4.1 (<http://ophid.utoronto.ca/mirDIP>) (16) and retrieved physical protein–protein interactions from the Integrated Interactions Database version 2020-05 (<http://ophid.utoronto.ca/iid>) (17). We obtained pathway annotations from pathDIP version 4 (<http://ophid.utoronto.ca/pathDIP>) (18). The transcription regulatory network was downloaded from Catalogue of Transcriptional Regulatory Interactions, Catrin version 1 (<http://ophid.utoronto.ca/Catrin>). All networks were integrated, annotated, visualized, and analyzed using NAViGaTOR version 3.0.16 (19). The final networks were exported in an SVG format, and the final images (300 dpi in PNG format) with legends were prepared with Adobe Illustrator version 26.0.2. Gene nodes were color coded by top Gene Ontology molecular function terms identified using Uniprot and Gene Ontology slim.

**Statistical analysis.** Data analyses were completed in Excel 2010 and R 3.1.0. With the exception of RNA sequencing, we conducted all statistical analyses using GraphPad PRISM 9 software.  $P$  or  $q$  values (FDR-adjusted  $P$ ) less than 0.05 were considered significant for analysis between groups.

Additional details of methodology can be found in Supplementary Methods, available on the *Arthritis & Rheumatology* website at <https://onlinelibrary.wiley.com/doi/10.1002/art.42285>.

## RESULTS

### Association between synovial expression of miR-27b-3p and human and mouse knee OA severity.

We previously showed that miR-27b-3p expression levels were higher in synovial fluid of patients with radiographic knee OA and K/L grades 3 and 4 compared with patients with K/L grades 1 and 2 and that ex vivo human OA synovium treated with the proinflammatory mediator IL-1 $\beta$  had increased secretion of miR-27b-3p (11). Because the synovium is a major contributor to synovial fluid, we first examined expression of miR-27b-3p in synovium of patients with varying K/L grades of knee OA, with the small nuclear RNA U6 used as a positive control (Supplementary Figure 1A, available on the *Arthritis & Rheumatology* website at <https://onlinelibrary.wiley.com/doi/10.1002/art.42285>). With increased radiographic knee OA severity, we observed increased collagen fiber density under a more stratified synovial lining in patients with knee OA and K/L grades 3 and 4 relative to patients with K/L grades 1 and 2 (Figure 1A). Concomitantly, the proportion of miR-27b-3p–positive cells relative to the total number of cells quantified in the synovial

lining increased with K/L grade (Figure 1A). Thus, consistent with expression levels of miR-27b-3p in synovial fluid (11), the proportion of synovial lining cells expressing miR-27b-3p increased with radiographic knee OA severity.

To determine whether similar expression differences could be detected in an animal model of knee OA, we examined miR-27b-3p expression by ISH at 2 weeks and 10 weeks after DMM-induced OA in C57BL/6 male mice (Figure 1B). Similar to our findings in human knee OA, we observed increased collagen deposition using Masson's trichrome stain in synovium from mice with DMM-induced OA, which coincided with increased synovitis scores compared with that shown in control mice that received sham surgery (Figure 1C). DMM surgery also induced cartilage degeneration that increased in severity from 2 weeks to 10 weeks, as reflected by the increases in OARSI scores of the medial femoral condyle and medial tibial plateau (Supplementary Figure 1B). These changes in matrix organization were accompanied by increased miR-27b-3p staining in the synovium as early as 2 weeks and persisted through 10 weeks after surgery (Figure 1D). In contrast, the mouse cartilage tissue showed a decrease in miR-27b-3p expression in tibial articular chondrocytes at both time points, similar to the decreases in miR-27b-3p observed in human OA cartilage cultured with IL-1 $\beta$  (11) or as reported in fresh cartilage from patients with either OA or rheumatoid arthritis compared with that obtained from trauma patients without a history of disease (20,21). In sham-operated animals, miR-27b-3p was primarily detected in tibial articular chondrocytes, with minimal cells labeled in the synovium. In both human and mouse knee OA, synovial miR-27b-3p expression coincided with increased ECM deposition.

### Induction of a synovial fibrosis-like phenotype after intraarticular injection of miR-27b-3p mimic into the mouse knee joint.

The increases in miR-27b-3p expression observed in human and mouse OA synovium suggested a causal relationship with disease severity and prompted us to examine the effect of modifying miR-27b-3p expression in the knee joints of naive mice (Figure 2A) and of mice with DMM-induced OA using miR-27b-3p mimic and inhibitor, respectively. In synovium from miR-27b-3p mimic-injected naive knee joints, we observed consistently higher synovitis scores, as reflected by synovial thickening, increased collagen deposition, and cell infiltration (Figure 2B). These changes were paralleled by a miR-27b-3p mimic-mediated increase in the percentage of synovial cells labeled with COL1A1, a major structural collagen component of synovial ECM (22), and  $\alpha$ -SMA, a marker of activated fibroblasts (23,24). Of note, cartilage integrity remained mostly unchanged in both the miR-27b-3p mimic- and control mimic-injected mouse knee joints (Supplementary Figure 2, available on the *Arthritis & Rheumatology* website at <https://onlinelibrary.wiley.com/doi/10.1002/art.42285>). Thus, intraarticular injection of



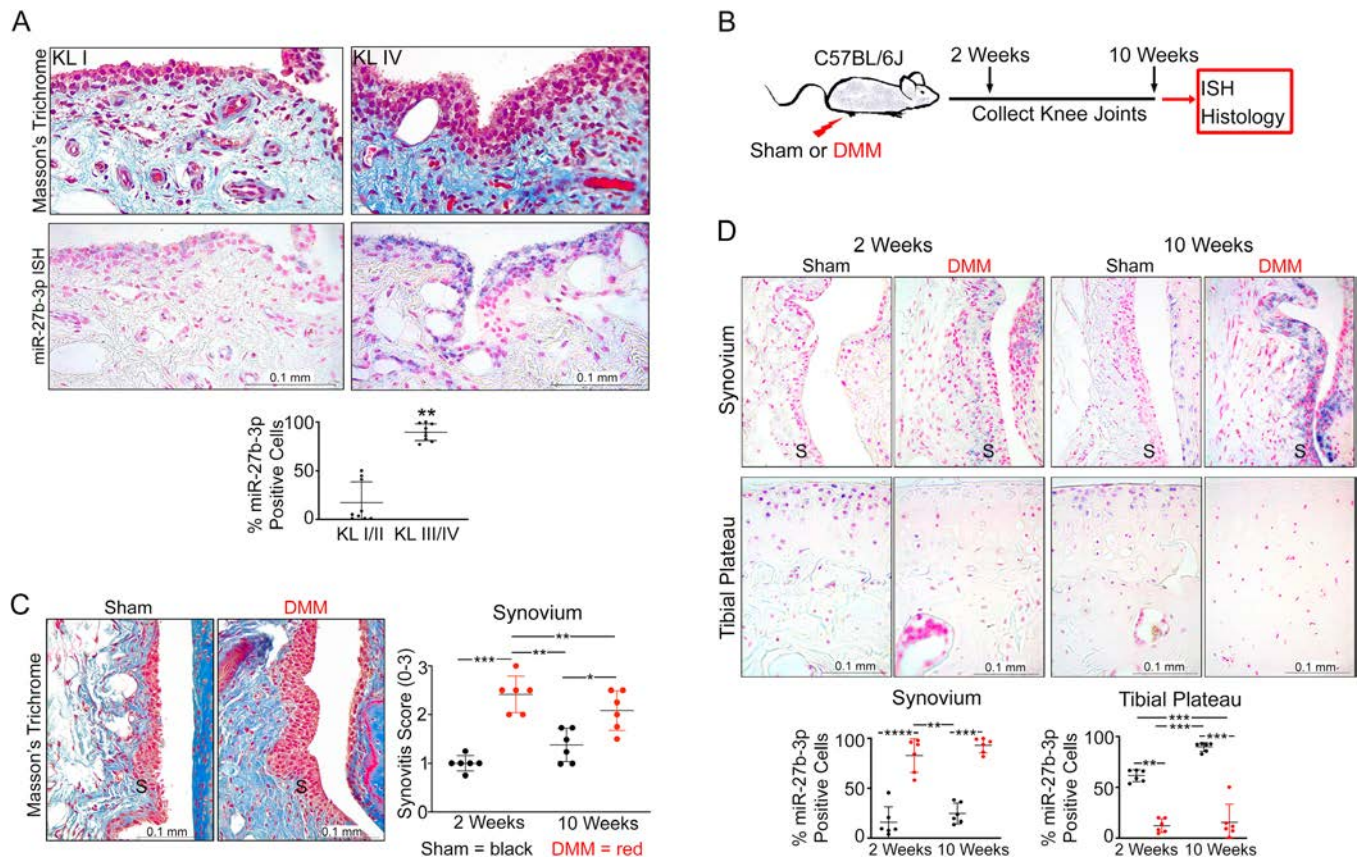


**Figure 1.** Expression of microRNA-27b-3p (miR-27b-3p) in samples obtained from human and mouse knee osteoarthritis (OA) synovium. **A**, Top, Representative images of synovium (original magnification  $\times 40$ ) stained with Masson's trichrome or miR-27b-3p in situ hybridization (ISH; purple regions) in samples from radiographic knee OA patients with Kellgren/Lawrence (K/L) radiographic severity grades 1 and 2 or K/L grades 3 and 4. Bottom, Scatter plot showing mean  $\pm$  SD proportion of miR-27b-3p-labeled cells in synovium from patients with K/L grade 1 or 2 radiographic knee OA or K/L grade 3 or 4 radiographic knee OA ( $n = 9$ /group). **B**, Destabilization of the medial meniscus (DMM) was conducted on right knees of 10- to 12-week-old C57BL/6 mice and knee joints were collected at 2 weeks or 10 weeks after surgery. **C**, Left, Representative images of synovium at 10 weeks after sham or DMM surgery; collagen accumulation in DMM model is shown in blue (Masson's trichrome). Right, Scatter plot showing mean  $\pm$  SD synovitis severity scores of mouse synovium 2 weeks or 10 weeks after sham or DMM surgery ( $n = 6$ /group). **D**, Top, ISH images of the synovium (S) or tibial plateau (original magnification  $\times 40$ ) (miR-27b-3p indicated in purple, nuclei indicated in pink [nuclear fast red]). Bottom, Scatter plots of mean  $\pm$  SD percentage of miR-27b-3p-labeled cells in the synovium or tibial chondrocytes at 2 weeks and 10 weeks after surgery. Relative data were log-transformed before analyses using Student's unpaired  $t$ -test (**A**), Kruskal-Wallis test followed by 2-stage linear step-up procedure of Benjamini, Krieger, and Yekutieli (**C**), or 2-way analysis of variance with Tukey's post hoc test (**D**). \* =  $P/q < 0.05$ ; \*\* =  $P/q < 0.01$ ; \*\*\* =  $P/q < 0.001$ ; \*\*\*\* =  $P < 0.0001$ .

miR-27b-3p mimic elicited a fibrosis-like phenotype in the synovium of healthy mouse knee joints.

In mice that received intraarticular injection of miRCURY LNA miR-27b-3p inhibitor at 1 week and 3 weeks after DMM surgery (Figure 2C), we observed no obvious differences in the histologic changes in cartilage or in synovial pathology (OARSI and synovitis scores) compared with results shown with the control inhibitor at 5 weeks after surgery (Figure 2D and Supplementary Figure 3, available on the *Arthritis & Rheumatology* website at <https://onlinelibrary.wiley.com/doi/10.1002/art.42285>) or in the percentage of synovial cells expressing COL1A1. However, the percentage of synovial cells expressing  $\alpha$ -SMA decreased in the miR-27b-3p inhibitor-treated group compared with the group that received the control inhibitor.

#### Increased expression of ECM markers and migration of human OA FLS with miR-27b-3p overexpression.

Given that intraarticular injection of miR-27b-3p mimic induced a synovial fibrosis-like phenotype with increased expression of COL1A1 in the synovium in vivo, we next examined the effect of miR-27b-3p overexpression on the production of COL1A1 in cultures of FLS, the major cell type isolated from human OA synovium obtained during total knee replacement surgeries. Transfection of OA FLS with miR-27b-3p mimic resulted in a mean  $\pm$  SD  $199 \pm 53$ -fold increase in miR-27b-3p expression (Supplementary Figure 4A, available on the *Arthritis & Rheumatology* website at <https://onlinelibrary.wiley.com/doi/10.1002/art.42285>). In addition, transfection with miR-27b-3p mimic in OA FLS resulted in an increased change of COL1A1 transcript levels of mean  $\pm$  SD

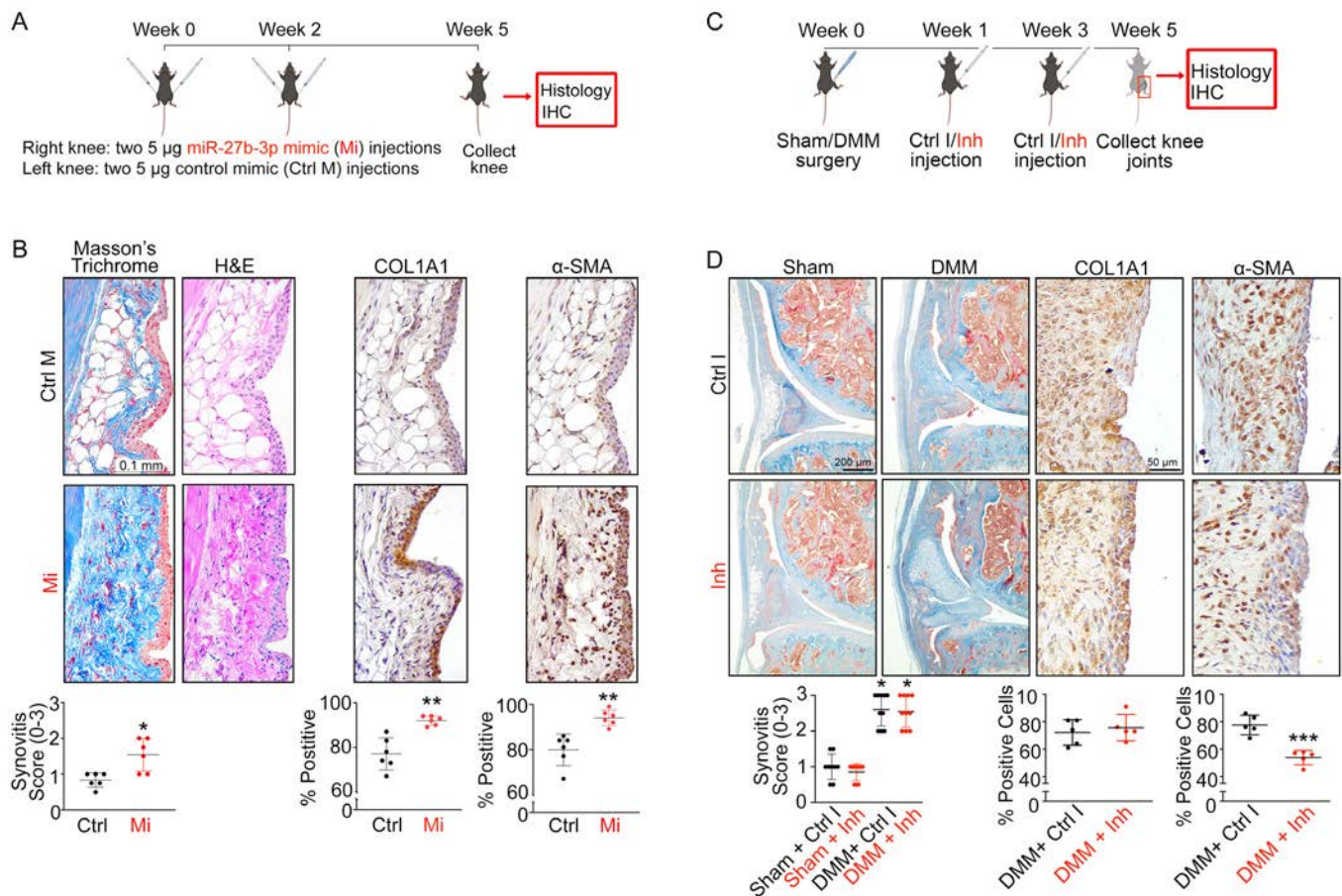


**Figure 2.** Overexpression of microRNA-27b-3p (miR-27b-3p) promotes synovial fibrosis-like responses in vivo. **A**, Schematic of miR-27b-3p mimic or control mimic injections in mouse knees. **B**, Images of synovia (original magnification  $\times 40$ ) from mouse knee joints ( $n = 6$ ) injected with miR-27b-3p mimic or with control mimic and stained with Masson's trichrome or hematoxylin and eosin (H&E) for immunohistochemical (IHC) analysis or immunolabeled with COL1A1 or  $\alpha$ -smooth muscle actin ( $\alpha$ -SMA) (shown in brown, with nuclei counterstained in blue). **C**, Schematic of injection of miR-27b-3p inhibitor (Inh) or control inhibitor (Ctrl Inh) in mouse knees (destabilization of the medial meniscus [DMM] vs. sham surgery). **D**, Top, Images of synovia (original magnification  $\times 10$ ) from sham-operated or DMM-operated mouse knee joints injected with miR-27b-3p inhibitor or with control inhibitor and stained with Masson's trichrome or DMM-operated knee joint immunolabeled with COL1A1 or  $\alpha$ -SMA (shown in brown, with nuclei counterstained in blue). Bottom, Results quantified as synovitis severity scores, and percentage of cells staining positive for COL1A1 or  $\alpha$ -SMA. Symbols represent individual samples; bars show the mean  $\pm$  SD. \* $P < 0.05$ ; \*\* $P < 0.01$ ; \*\*\* $P < 0.001$ , by Mann-Whitney unpaired U test. Color figure can be viewed in the online issue, which is available at <http://onlinelibrary.wiley.com/doi/10.1002/art.42285/abstract>.

$4.43 \pm 1.73$ -fold (Figure 4B) and protein levels of  $1.27 \pm 0.22$ -fold (Figure 3A). We observed opposite effects when cells were transfected with miR-27b-3p inhibitor, with a mean  $\pm$  SD  $0.73 \pm 0.14$ -fold change in transcript levels (Supplementary Figure 4B) and a mean  $\pm$  SD  $0.47 \pm 0.19$ -fold change in protein levels (Figure 3B). Immunofluorescence experiments demonstrated that the number of cultured OA FLS transfected with miR-27b-3p mimic expressing COL1A1 also increased (Figure 3C and Supplementary Figure 5, available on the *Arthritis & Rheumatology* website at <https://onlinelibrary.wiley.com/doi/10.1002/art.42285>), with cell numbers comparable in OA FLS that were transfected with either miR-27b-3p mimic (mean  $\pm$  SD  $53.0 \pm 11.1$ ) or control mimic (mean  $\pm$  SD  $52.5 \pm 7.9$ ). Overall, miR-27b-3p mimic transfection increased COL1A1 expression in human OA FLS, while inhibition of miR-27b-3p had the opposite effect.

Because increased migration is a key process associated with a profibrotic response of OA FLS (25,26), we next investigated whether miR-27b-3p influenced OA FLS migration using a Transwell migration assay. We found that transfection of cells with miR-27b-3p mimic increased the number of OA FLS that migrated to the underside of Transwell membranes relative to cells transfected with control mimic (Figure 3D). As with COL1A1 expression, transfection with the miR-27b-3p inhibitor had the inverse effect, reducing OA FLS migration (Figure 3E). These data suggested that miR-27b-3p influences migration in OA FLS. However, when we examined the effect of miR-27b-3p overexpression on talin and vinculin, cytoskeletal mediators of cell adhesion (27), and the cytoskeletal component vimentin, we detected no differences in the protein levels of these molecules (Supplementary Figure 6A, available on the *Arthritis &*



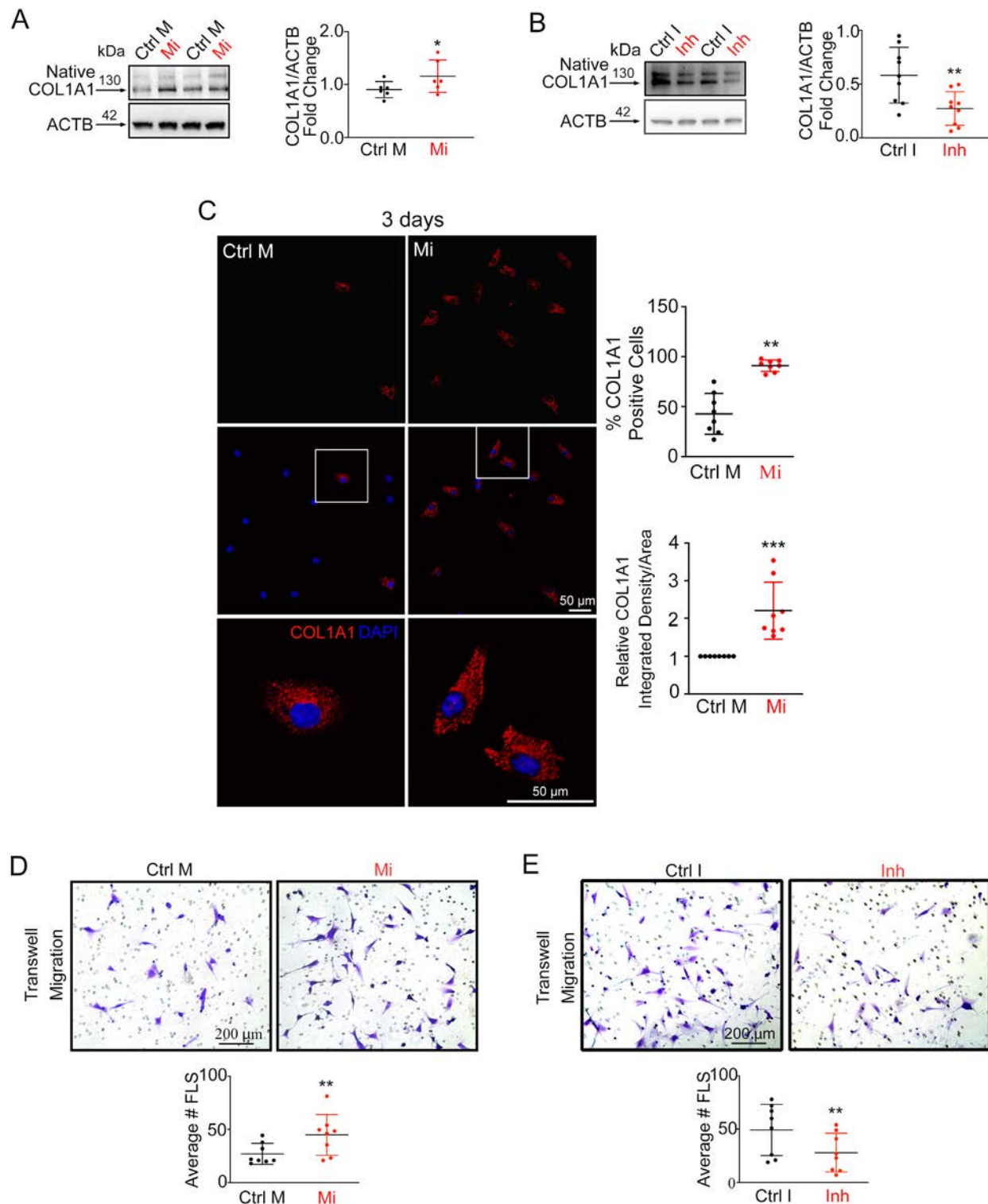


**Figure 3.** MicroRNA-27b-3p (miR-27b-3p) promotes synovial fibrosis-like responses in vitro. **A** and **B**, Left, Western blots of COL1A1 expression (compared to  $\beta$ -actin) in osteoarthritis (OA) fibroblast-like synoviocytes (FLS) transfected with miR-27b-3p mimic (Mi) or control mimic (Ctrl M) (**A**) or with miRCURY locked nucleic acid (LNA) miR-27b-3p inhibitor (Inh) or a control inhibitor (Ctrl I) (**B**) and cultured for 48 hours ( $n = 6-9$ ). Right, Log-transformed data plotted as the mean  $\pm$  SD fold change in relative expression. **C**, Left, Immunofluorescent images of COL1A1 expression in OA FLS transfected with miR-27b-3p mimic or control mimic and cultured for 3 days. Boxed areas in middle panels are shown at higher magnification in bottom panels (original magnification  $\times 20$ ). Right, Results plotted as the mean  $\pm$  SD percentage of COL1A1-positive cells and as relative COL1A1 integrated density per area ( $n = 8$  paired cultures). **D** and **E**, Top, Crystal violet-stained images of Transwell-migrated OA FLS 24 hours after transfection with miR-27b-3p mimic or control mimic (**D**) or with miR-27b-3p inhibitor (Inh) or control inhibitor (Ctrl I) (**E**). Bottom, Results plotted as the mean  $\pm$  SD number of OA FLS migrating in the Transwells ( $n = 8$  paired cultures). Data were analyzed with Student's paired 2-tailed  $t$ -tests (**A-C**) or Wilcoxon's tests (**D** and **E**). \* =  $P < 0.05$ ; \*\* =  $P < 0.01$ ; \*\*\* =  $P < 0.001$ . Color figure can be viewed in the online issue, which is available at <http://onlinelibrary.wiley.com/doi/10.1002/art.42285/abstract>.

*Rheumatology* website at <https://onlinelibrary.wiley.com/doi/10.1002/art.42285>) or in the organization of F-actin filaments or vinculin (Supplementary Figure 6B).

The effect of miR-27b-3p mimic on OA FLS COL1A1 expression prompted us to investigate whether miR-27b-3p regulated the expression of other ECM genes. Among the 84 matrix-related genes (listed in Supplementary Table 3, available on the *Arthritis & Rheumatology* website at <https://onlinelibrary.wiley.com/doi/10.1002/art.42285>) that we investigated in OA FLS using ECM-specific qPCR array, 17 genes had responses to the miR-27b-3p mimic that were below the assay's detection limits and were excluded from further analysis. Of the remaining genes, when compared to transfection with control mimic, transfection with miR-27b-3p mimic significantly increased the expression of 7 genes (*COL1A1*, *COL5A1*, *COL14A1*, thrombospondin 1 [*THBS1*], *ADAMTS8*, tenascin C [*TNC*], and fibronectin [*FN1*]) and decreased the expression of 3 genes (catenin delta 1 [*CTNND1*], hyaluronan synthase 1 [*HAS1*], and integrin alpha 2 [*ITGA2*]) (Figures 4A and B, screening phase). Validation of the array screening by RT-qPCR using mimic-transfected FLS from 4 additional patients with advanced radiographic knee OA confirmed increases in *COL1A1*, *COL14A1*, *COL5A1*, *FN1*, *ADAMTS8*, and *THBS1* (Figure 4B, validation phase). No marked differences were observed for *TNC*, *ITGA2*, *HAS1*, and *CTNND1* (Supplementary Figure 4C, available at <https://onlinelibrary.wiley.com/doi/10.1002/art.42285>). Two genes confirmed to be modified by miR-27b-3p mimic transfection in OA FLS, *ADAMTS8* and *COL5A1*, showed increased staining in cells in the synovium and reduced staining in articular chondrocytes of DMM-operated mouse knee joints (Figures 4C and D). Similar results were observed with *COL14A1* staining (Supplementary Figure 4D). Together, miR-27b-3p overexpression promoted OA FLS expression of key ECM genes and increased migration capacity, both important events associated with synovial fibrosis pathology during OA.

**Identification of ECM-related putative target genes of miR-27b-3p using RNA sequencing and computational analyses.** To better understand the complex regulatory effects of miR-27b-3p in OA FLS, we performed RNA sequencing and computational analysis to create a comprehensive signaling network of miR-27b-3p gene targets in OA FLS (Figure 5A). RNA sequencing data showed that transfection with miR-27b-3p mimic elicited significant ( $P < 0.05$ ) expression changes in 2,295 DEGs compared with that shown in OA FLS transfected with control mimic, with increased expression in 1,428 DEGs and decreased expression in 867 DEGs (Figure 5B; see Supplementary Table 4, available on the *Arthritis & Rheumatology* website at <https://onlinelibrary.wiley.com/doi/10.1002/art.42285>, for the full list and segregated up-/down-regulated DEGs). Using computational approaches, we compared predicted gene targets of miR-27b-3p using mirDIP (16) with the list of DEGs identified by RNA sequencing (Supplementary Figure 7, available on the *Arthritis & Rheumatology*

website at <https://onlinelibrary.wiley.com/doi/10.1002/art.42285>). Of the 2,295 DEGs identified by RNA sequencing in miR-27b-3p mimic-treated OA FLS, 1,862 genes (81%) overlapped with miR-27b-3p putative gene targets: 1,203 genes were up-regulated (red edges), and 659 were down-regulated (green edges). Of note, many of the miR-27b-3p-modulated DEGs were related to ECM pathways (reactome ECM-related pathway nodes outlined in purple in Supplementary Figure 7, as obtained from pathDIP) (18).

To better understand and visualize the ECM-specific signaling network of miR-27b-3p in OA FLS, we used the Gene Ontology cellular component annotations to extract the ECM-related miR-27b-3p putative gene targets from all potential targets (Supplementary Figures 7 and 8, available on the *Arthritis & Rheumatology* website at <https://onlinelibrary.wiley.com/doi/10.1002/art.42285>). The association of DEGs identified by RNA sequencing to the ECM are highlighted by blue, green, and purple gene names. Of note, several of the ECM-related target genes down-regulated by miR-27b-3p transfection were involved in vascular health, including the genes for aspartate beta-hydroxylase (*ASPH*) (28), cadherin EGF LAG seven-pass G-type receptor 1 (*CELSR1*) (29), heart development protein with EGF-like domain 1 (*HEG1*) (30), laminin subunit alpha 1 (*LAMA1*) and laminin subunit beta 1 (*LAMB1*) (31), nidogen 2 (*NID2*) (32), neuropilin 2 (*NRP2*) (33), plexin domain containing 1 (*PLXDC1*) (34), syndecan binding protein (*SDCBP*) (35), secreted protein acidic and cysteine rich (SPARC) modular calcium-binding protein 1 (*SMOC1*) (36), and vascular endothelial growth factor c (*VEGFC*) (37) or bone remodeling gene, including oncostatin M receptor (*OSMR*) (38), *SMOC1* (39), and *SMOC2* (40). In contrast, expression of many structurally related ECM miR-27b-3p target genes, including collagen genes (*COL1A2*, *COL3A1*, *COL5A2*, *COL5A3*, *COL8A2*, *COL11A1*, *COL15A1*, *COL21A1*) and peptidylprolyl isomerase B gene (*PPIB*), an important regulator of collagen folding (41), members of the ADAMTS family (*ADAMTS1*, *ADAMTS8*, *ADAMTS9*), and matricellular proteins (*SPARC*, secreted phosphoprotein 1 [*SPP1*]) were up-regulated in miR-27b-3p-transfected OA FLS. Overall, RNA sequencing coupled with computational analysis identified multiple ECM-related miR-27b-3p gene targets in OA FLS.

### Identification of a miR-27b-3p/PPARG/ADAMTS8 signaling axis regulating select ECM genes in OA FLS.

To identify the gene(s) consistently differentially expressed across all 3 investigations (qPCR array, RT-qPCR, and RNA sequencing), we took a focused approach to specifically compare the DEGs identified by qPCR array and RT-qPCR with the ECM-related putative targets identified through RNA sequencing. Although most of the genes identified by qPCR array and RT-qPCR followed similar trends in RNA sequencing (e.g., *COL1A1* showed a 2-fold increase), only *ADAMTS8* (3.4-fold increase) was significantly up-regulated ( $P < 0.05$ ) in miR-27b-3p-transfected OA FLS compared with control across all 3 investigations.

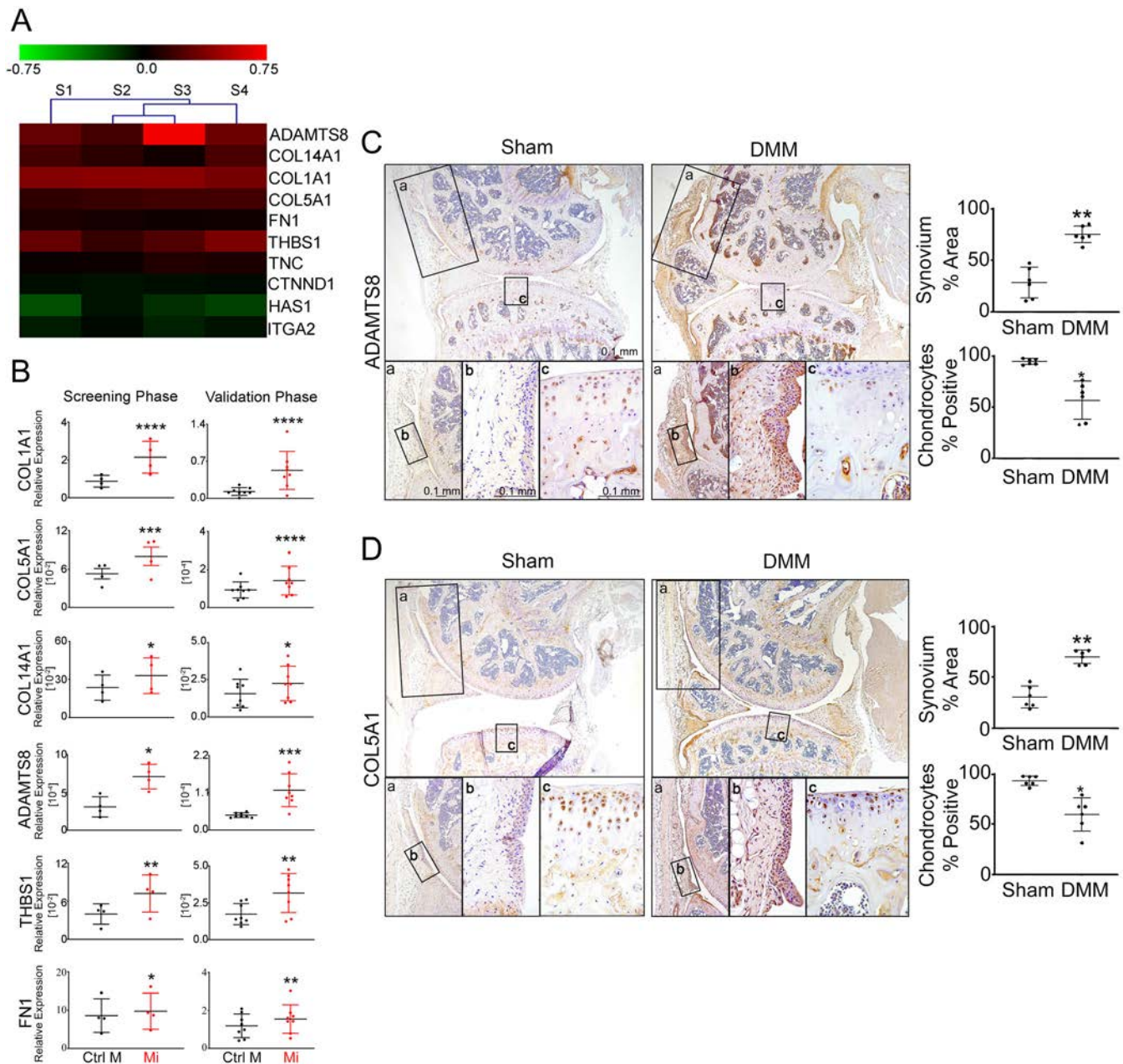


**Figure 4.** MicroRNA-27b-3p (miR-27b-3p) regulates the expression of multiple extracellular matrix (ECM)-related genes. **A**, Heatmap of genes differentially expressed in reverse transcriptase-quantitative polymerase chain reaction (RT-qPCR) array among 84 ECM-related genes found in fibroblast-like synoviocytes (FLS) isolated from osteoarthritis (OA) synovium that were transfected with miR-27b-3p mimic or with control mimic and cultured for 48 hours ( $n = 4$ ). **B**, Scatter plots obtained by RT-qPCR array (screening phase ( $n = 4$ ) and RT-qPCR (validation phase,  $n = 8$ ) comparing relative expression (mean  $\pm$  SD) of ECM-related genes (normalized to *GAPDH*) in OA FLS transfected with miR-27b-3p mimic (Mi) or control mimic (Ctrl M) and cultured for 48 hours. Data were log-transformed before analysis by Student's paired 2-tailed *t*-test. **C** and **D**, Left, Immunohistochemical analysis (DAB, brown) of ADAMTS8 (**C**) and type V collagen (COL5A1) (**D**) expression in mouse knee joints 10 weeks after destabilization of the medial meniscus (DMM) or sham surgery. Nuclei are counterstained in blue (original magnification  $\times 10$ ). Bottom panels a–c are higher-magnification views of the boxed areas, with panels a and b showing synovium (original magnification  $\times 20$  and  $\times 40$ ) and panel c showing medial tibial plateau cartilage (original magnification  $\times 40$ ). Right, Results plotted as the mean  $\pm$  SD percentage of synovium or chondrocytes staining positive for ADAMTS8 or COL5A1 in 3 digital images of  $\times 40$  fields of view ( $n = 6$  samples/group). \* =  $P < 0.05$ ; \*\* =  $P < 0.01$ ; \*\*\* =  $P < 0.001$ ; \*\*\*\* =  $P < 0.0001$ , by Student's unpaired 2-tailed *t*-test with Welch's correction. Color figure can be viewed in the online issue, which is available at <http://onlinelibrary.wiley.com/doi/10.1002/art.42285/abstract>.

Because ADAMTS8 is reported to regulate signal transduction, ECM remodeling, and fibrosis (42,43), we focused on the contribution of ADAMTS8 in miR-27b-3p signaling in OA

FLS. To examine the relationship of miR-27b-3p and ADAMTS8 in further detail, we assembled an integrated predictive network combining miR-27b-3p putative gene targets,



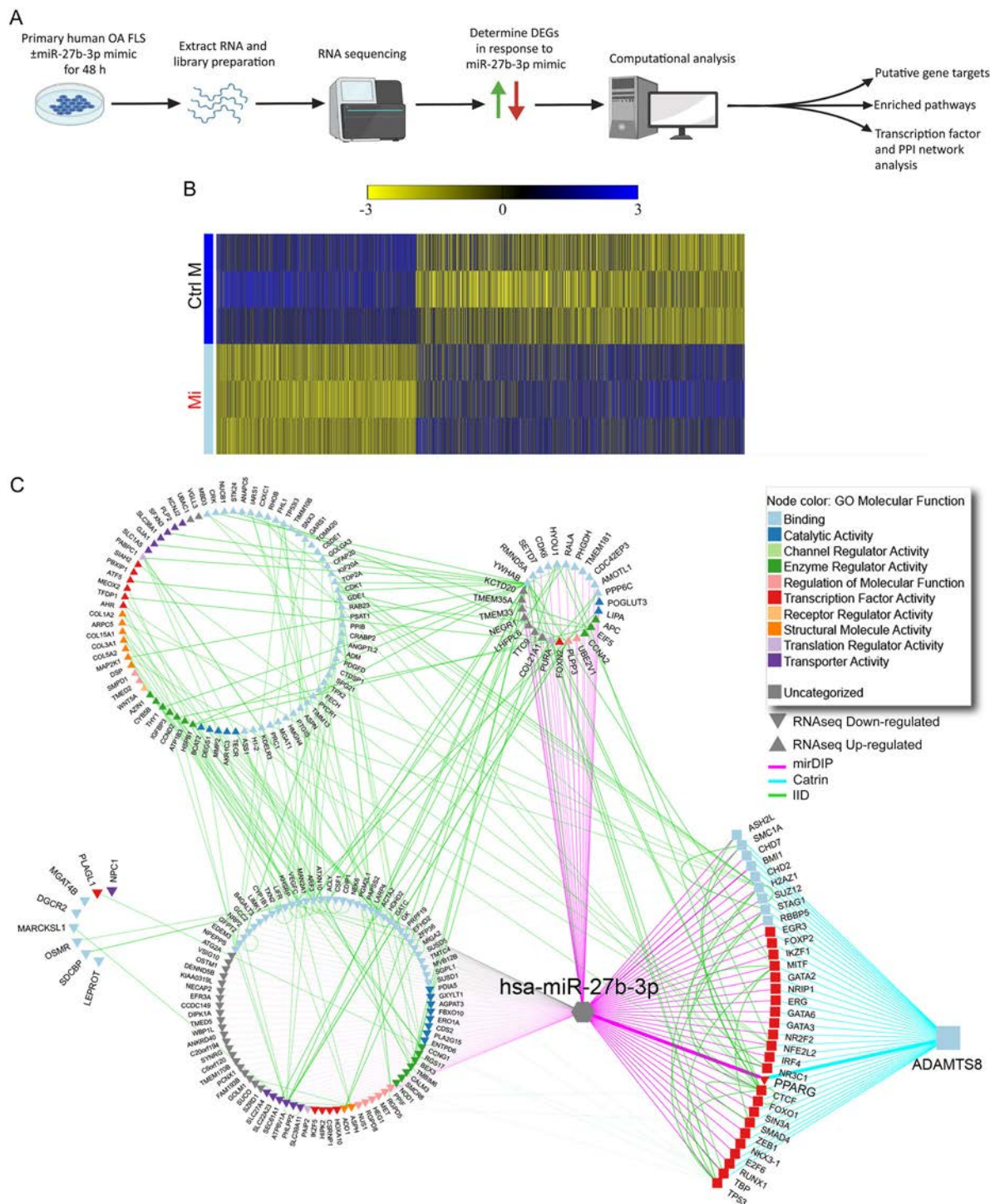


**Figure 5.** Expression profile and extracellular matrix-related network analysis of fibroblast-like synoviocytes (FLS) isolated from osteoarthritis synovium overexpressing microRNA-27b-3p (miR-27b-3p). **A**, Schematic of workflow for determination of differentially expressed genes (DEGs) and putative networks regulated by miR-27b-3p mimic treatment of human OA FLS in vitro using RNA sequencing and computational analyses. PPI = protein–protein interactions. **B**, Heatmap of the DEGs (unadjusted  $P < 0.05$ ) determined by RNA sequencing of OA FLS transfected with miR-27b-3p mimic (Mi) or control mimic (Ctrl M) and cultured for 48 hours. Columns indicate treatment-paired replicates ( $n = 3$ ). Genes are ordered based on log fold change (largest to smallest), and values are scaled by row (mean centered and divided by SD). **C**, Integrated network analysis of miR-27b-3p putative gene targets predicted to modulate ADAMTS8. The assembled network contains previously predicted *Homo sapiens* (hsa)-miR-27b-3p gene targets (microRNA Data Integration Portal [mirDIP], purple edges), ADAMTS8-associated transcription factors (Catalogue of Transcriptional Regulatory Interactions [Catrin], turquoise edges), and physical PPIs (Integrated Interactions Database [IID], green edges) of DEGs identified by RNA sequencing (RNAseq) of OA FLS transfected with miR-27b-3p (direction of expression change relative to control mimic-transfected cells is indicated by up and down triangles). Node color indicates associated Gene Ontology (GO) molecular functions. Color figure can be found in the online issue, which is available at <http://onlinelibrary.wiley.com/doi/10.1002/art.42285/abstract>.

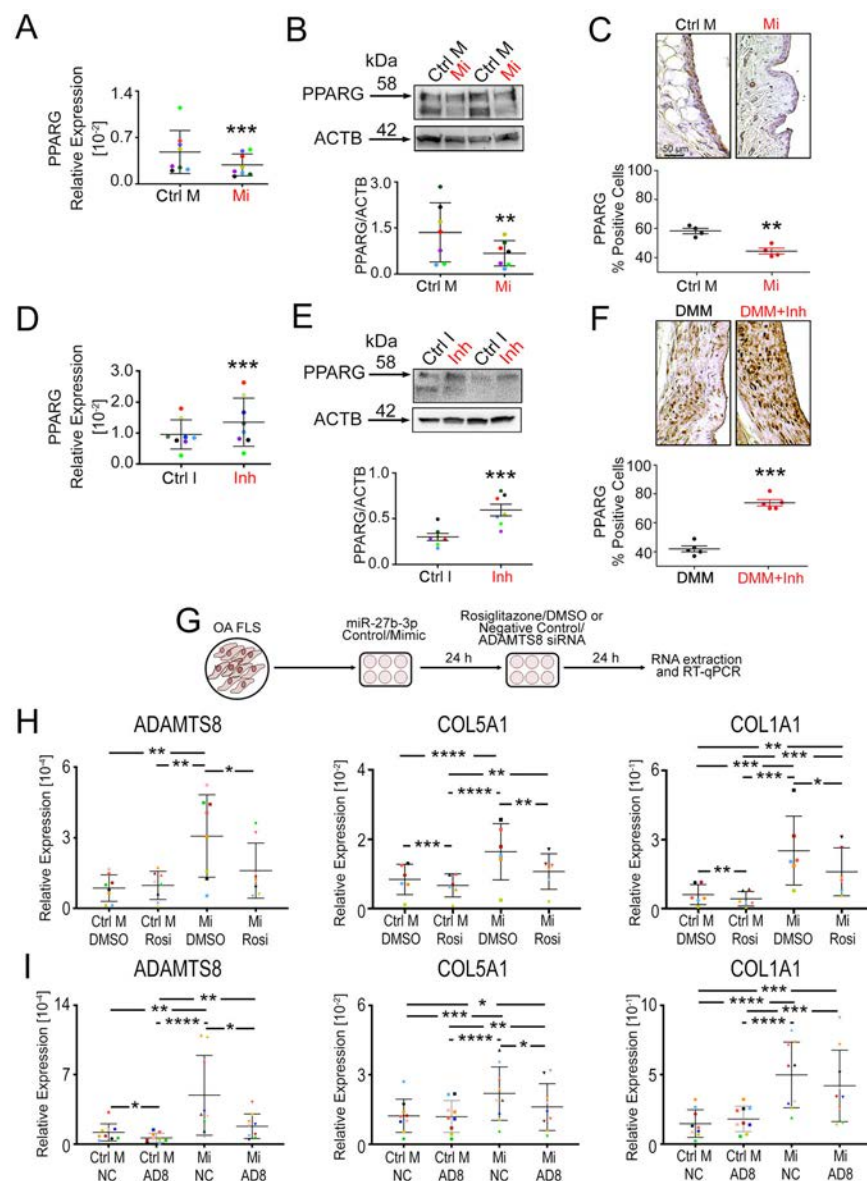


**Figure 6.** Regulation of select extracellular matrix (ECM) genes through a microRNA-27b-3p (miR-27b-3p)/PPARG/ADAMTS8 signaling axis. PPARG transcript levels (**A**, **D**) and protein levels (**B**, **E**) were determined in fibroblast-like synoviocytes (FLS) isolated from osteoarthritis (OA) synovium transfected with either miR-27b-3p mimic (Mi) or control mimic (Ctrl M) or transfected with miR-27b-3p inhibitor (Inh) or control inhibitor (Ctrl I) and cultured for 48 hours. Results were determined by reverse transcriptase–quantitative polymerase chain reaction (RT–qPCR) normalized to GAPDH ( $n = 8$ ) or by Western blot densitometry measured from upper bands appearing at ~58 kD ( $n = 7$ ). PPARG expression was determined in the synovium of naive mice injected intraarticularly with Mi or Ctrl M (**C**) or in mice that underwent destabilization of the medial meniscus (DMM) surgery and injected intraarticularly with Inh or Ctrl I (**F**), as determined by immunohistochemistry. See negative controls in Supplementary Figure 11 (available on the *Arthritis & Rheumatology* website at <https://onlinelibrary.wiley.com/doi/10.1002/art.42285>). **G**, Schematic showing transfection of OA FLS with control mimic (Ctrl M) or miR-27b-3p mimic (Mi), followed by treatment with rosiglitazone (Rosi) or DMSO as vehicle control or with small interfering RNA (siRNA) targeting ADAMTS8 (AD8) or a negative control siRNA (NC). **H** and **I**, OA FLS were transfected with control mimic or miR-27b-3p and treated with Rosi/DMSO (**H**) or ADAMTS8 siRNA/NC siRNA (**I**). RNA were extracted and assessed by RT–qPCR for expression of ADAMTS8, COL5A1, and COL1A1. Colored data points in **A**, **D**, **H**, and **I** highlight biologic replicates ( $n = 6–9$ ). Scatter plots show mean  $\pm$  SD, with relative data log-transformed before analysis by Student's paired 2-tailed  $t$ -test (**A–F**) or repeated measures 2-way analysis of variance followed by Tukey's multiple comparisons post hoc test (**H**, **I**). \* =  $P < 0.05$ ; \*\* =  $P < 0.01$ ; \*\*\* =  $P < 0.001$ ; \*\*\*\* =  $P < 0.0001$ . Color figure can be viewed in the online issue, which is available at <http://onlinelibrary.wiley.com/doi/10.1002/art.42285/abstract>.

ADAMTS8-associated transcription factors, and physical protein–protein interactions (Figure 5C). From this analysis, multiple putative miR-27b-3p-regulated transcription factors were predicted to

modulate ADAMTS8. When we applied a more stringent approach by restricting miR-27b-3p putative gene targets and ADAMTS8-associated transcription factors to the top 1% of the



prediction scores in the network analysis, we identified 14 predicted miR-27b-3p-regulated transcription factors of ADAMTS8, with only PPARG down-regulated in our RNA sequencing data.

To investigate whether PPARG was indeed involved in miR-27b-3p regulation of ADAMTS8, we first used OA FLS to determine whether modification of miR-27b-3p levels by mimic and inhibitor transfection alters PPARG expression. Our results showed that miR-27b-3p overexpression reduced the expression of PPARG (Figure 6A), while inhibition of miR-27b-3p had the reverse effect, increasing PPARG expression (Figure 6D). We found that miR-27b-3p mimic reduced and miR-27b-3p inhibitor increased protein levels of PPARG in OA FLS in vitro (Figures 6B and 6E).

We next examined whether injection of miR-27b-3p mimic or inhibitor had any effect on the expression of PPARG in the synovium in vivo. The number of PPARG-labeled cells was reduced in the synovium of naive mouse joints treated with intraarticular injection of miR-27b-3p mimic, whereas PPARG-labeled cells in the synovium of DMM-operated mice were increased with injection of miR-27b-3p inhibitor, as shown by IHC (Figures 6C and 6F). However, no significant changes in PPARG staining were observed in the articular cartilage in response to the miR-27b-3p inhibitor (Supplementary Figure 9, available on the *Arthritis & Rheumatology* website at <https://onlinelibrary.wiley.com/doi/10.1002/art.42285>).

We next used the PPARG agonist, rosiglitazone, in miR-27b-3p-transfected OA FLS to investigate the role of PPARG in miR-27b-3p-regulated expression of ADAMTS8 (Figures 6G and 6H). In support of our predictive network analysis, treatment with rosiglitazone counteracted the miR-27b-3p mimic-mediated up-regulation of ADAMTS8 (Figure 6H). We also investigated whether some of the ECM genes that we identified by qPCR array and RT-qPCR were also regulated by PPARG. Increases in *COL5A1*, *COL1A1*, and *THBS1* mediated by miR-27b-3p mimic were inhibited by rosiglitazone, whereas *COL14A1* and *FN1* were not (Figure 6H, Supplementary Figure 10A, available on the *Arthritis & Rheumatology* website at <https://onlinelibrary.wiley.com/doi/10.1002/art.42285>), suggesting a link between miR-27b-3p and PPARG activity in regulation of select ECM genes.

To further investigate the involvement of ADAMTS8 in miR-27b-3p-mediated ECM regulation, we also examined the effect of ADAMTS8 knockdown on the expression of key ECM genes in miR-27b-3p mimic-transfected cells (Figures 6G and 6I). ADAMTS8 siRNA treatment effectively reduced ADAMTS8 transcript levels by mean  $\pm$  SD 58  $\pm$  38% in OA FLS transfected with miR-27b-3p mimic and by mean  $\pm$  SD 65  $\pm$  18% in OA FLS transfected with control. Of note, the miR-27b-3p mimic-induced expression of *COL5A1* but not *COL1A1* was reduced (Figure 6I). Similarly, miR-27b-3p mimic-mediated *COL14A1* expression was also decreased by ADAMTS8 siRNA, but *THBS1* or *FN1* were not (Supplementary Figure 10B). Together, these findings suggest

that, in OA FLS, miR-27b-3p regulates a subset of ECM genes, in part, through a PPARG/ADAMTS8 signaling axis.

## DISCUSSION

This study showed that miR-27b-3p expression is elevated in human knee OA and mouse knee OA synovia and plays a crucial role in the regulation of key synovial ECM components. Injection of miR-27b-3p mimic in naive mouse knee joints induced a fibrosis-like phenotype, and the transfection of human OA FLS with miR-27b-3p mimic increased the migratory capacity of FLS and up-regulated the expression of multiple ECM genes, including *COL1A1*, *COL5A1*, and *FN1*, which are among the top 10 genes expressed in human synovium most closely related to OA (44). RNA sequencing coupled with computational analysis identified a complex ECM-specific signaling network with multiple targets of miR-27b-3p in OA FLS. Furthermore, this study identified one of the signaling arms of miR-27b-3p involving a PPARG/ADAMTS8 signaling axis that, in part, regulates the expression of select ECM components in OA FLS.

The fibrosis-modifying effects of miR-27b-3p have been demonstrated in other pathologic conditions. For instance, miR-27b-3p was found to promote cardiac fibrosis, in part through up-regulation of profibrotic ECM genes in atrial fibroblasts (45). In contrast, miR-27b-3p has been found to negatively regulate lung fibrosis (46). Thus, it is possible that the effects of miR-27b-3p on fibrotic responses may be tissue- and/or disease-specific. We observed that miR-27b-3p increased in the synovium and decreased in the cartilage in mice after DMM surgery, similar to our previous observations of miR-27b-3p expression changes in cultured human synovium and in cartilage explants in response to IL-1 $\beta$  (11). Although our study did not focus on changes in cartilage, further studies that examine the role of miR-27b-3p in cartilage homeostasis are warranted. It is intriguing that miR-27b-3p levels have been shown to be lower in cartilage tissue of patients with OA and patients with rheumatoid arthritis than in control tissues without these diseases (20,21). We also showed that intraarticular injection of miR-27b-3p mimic into healthy mouse knee joints largely spared cartilage from degeneration while promoting a fibrosis-like phenotype in the synovium with increased percentages of COL1A1- and  $\alpha$ -SMA-expressing cells. We did not observe the inverse, that is, a reduced severity of synovial pathology in the mouse model of DMM that was treated with a miR-27b-3p inhibitor. However, of note, the number of cells in the synovium expressing  $\alpha$ -SMA was reduced. Although the number of activated fibroblasts ( $\alpha$ -SMA-positive cells) was reduced in response to the miR-27b-3p inhibitor, the persistence of DMM-induced synovitis and the observation of no significant differences in the COL1A1 expression suggested that other compensatory mechanisms may be sufficient to sustain synovial pathology.

Although we did not focus on cartilage degradation, one surprising observation was the overt expression of COL5A1 in

chondrocytes of sham-operated animals. *COL5A1* is a minor component of healthy cartilage (47), with expression of *COL5A1* increased after cartilage damage; recently, *COL5A1* has been identified as a hub gene elevated in damaged knee cartilage (48). Knee surgery itself, even without meniscus destabilization (sham surgery), poses risks to the joint (e.g., during incision) and could explain the *COL5A1* expression detected in chondrocytes of sham-operated animals. Given that *COL5A1* expression declined in chondrocytes of mice subjected to DMM surgery, it is likely that meniscus destabilization elicits additional changes in the joint.

Because miR-27b-3p appeared to be an important mediator of synovial fibrosis in our study, we used RNA sequencing to examine the effects of its overexpression on OA FLS transcription profiles. A large proportion (81%) of DEGs identified overlapped with mirDIP-predicted putative gene targets. In addition, many of the up-regulated DEGs were associated with the ECM; however, many of the down-regulated DEGs were associated with vascular health and bone remodeling. Intriguingly, *ADAMTS8* was the only gene consistently and significantly increased in OA FLS with qPCR array, RT-qPCR, and RNA sequencing in response to the miR-27b-3p mimic. Its knockdown in OA FLS inhibited the miR-27b-3p-mediated induction of *COL5A1*, but not *COL1A1*, suggesting that *ADAMTS8* contributes to the miR-27b-3p regulation of select ECM genes. When the top predicted transcription factors of *ADAMTS8* and miR-27b-3p targets were examined and cross-referenced, PPARG was the only one identified by RNA sequencing to be down-regulated by miR-27b-3p transfection of OA FLS.

PPARG, a previously identified target of miR-27b-3p (49,50) with a miR-27b-targeted sequence in its 3' UTR (51), helps regulate fibroblast ECM production (52). Consistent with these previous observations, we showed that the number of PPARG-positive cells was reduced in the synovium of naive mouse joints treated with miR-27b-3p mimic, whereas the number of PPARG-positive cells in the synovium of mice subjected to DMM surgery was increased with injection of miR-27b-3p inhibitor in vivo. Similarly, we showed that miR-27b-3p mimic decreased and miR-27b-3p inhibitor increased PPARG expression in human OA FLS in vitro. Intriguingly, we showed that rosiglitazone, a PPARG agonist, inhibited miR-27b-3p-induced *ADAMTS8* as well as *COL5A1* and *COL1A1* expression in OA FLS. These data further suggest that regulation of select ECM genes occurs in part through a miR-27b-3p/PPARG/ADAMTS8 signaling axis in OA FLS.

One limitation of the present study was that we did not have access to synovial samples from healthy individuals with no musculoskeletal disease; thus, we do not know whether miR-27b-3p is expressed or whether it has an influence on ECM production in human synovium under homeostatic conditions. Obtaining synovial specimens continues to be challenging, especially from those with early stages of OA. Consequently, we are limited in our ability to investigate the influence

of demographic and anthropometric variables, like sex, on the miR-27b-3p effects reported in our present study. Furthermore, our cultures of OA FLS are enriched for FLS but are likely not pure. Even after a minimum of 3 passages used in our study, it is possible that some macrophages remained and contributed to the observed effects, although their contribution is likely minimal (53–55).

In summary, we showed for the first time a key role of miR-27b-3p and its downstream signaling mediators in ECM regulation associated with synovial fibrosis during OA.

## ACKNOWLEDGMENTS

We acknowledge the Schroeder Arthritis Institute's Division of Orthopedics clinical research team for help with patient consent and collecting clinical data. We thank Brian Wu for help with tissue histology scoring. We thank Dr. Khalid Syed for help with the clinical data. We thank the staff of the Collaborative Advanced Microscopy Labs of Dentistry (Faculty of Dentistry, University of Toronto) for training and help with image acquisition and data analysis. Figures 2A and 2C and Figure 5A were created, in part, with BioRender.com.

## AUTHOR CONTRIBUTIONS

All authors were involved in drafting the article or revising it critically for important intellectual content, and all authors approved the final version to be published. Dr. Kapoor had full access to all of the data in the study and takes responsibility for the integrity of the data and the accuracy of the data analysis.

**Study conception and design.** Tavallae, Lively, Rockel, Ali, Hinz, Jurisica, Kapoor.

**Acquisition of data.** Tavallae, Lively, Im, Sarda, Mitchell, Rossomacha, Nakamura, Gabrial, Ratneswaran, Perry.

**Analysis and interpretation of data.** Tavallae, Lively, Rockel, Potla, Matelski, Hinz, Gandhi, Jurisica, Kapoor.

## REFERENCES

1. Neogi T. The epidemiology and impact of pain in osteoarthritis. *Osteoarthritis Cartilage* 2013;21:1145–53.
2. Felson DT, Niu J, Neogi T, et al. Synovitis and the risk of knee osteoarthritis: the MOST study. *Osteoarthritis Cartilage* 2016;24:458–64.
3. Scanzello CR, Goldring SR. The role of synovitis in osteoarthritis pathogenesis. *Bone* 2012;51:249–57.
4. Maglaviceanu A, Wu B, Kapoor M. Fibroblast-like synoviocytes: role in synovial fibrosis associated with osteoarthritis. *Wound Repair Regen* 2021;29:642–9.
5. Rim YA, Ju JH. The role of fibrosis in osteoarthritis progression. *Life (Basel)* 2020;11.
6. Mathiessen A, Conaghan PG. Synovitis in osteoarthritis: current understanding with therapeutic implications. *Arthritis Res Ther* 2017;19:18.
7. Endisha H, Rockel J, Jurisica I, et al. The complex landscape of microRNAs in articular cartilage: biology, pathology, and therapeutic targets. *JCI Insight* 2018;3:e121630.
8. Malemud CJ. MicroRNAs and osteoarthritis. *Cells* 2018;7:92.
9. Tavallae G, Rockel JS, Lively S, et al. MicroRNAs in synovial pathology associated with osteoarthritis. *Front Med (Lausanne)* 2020;7:376.
10. Zhang L, Xing R, Huang Z, et al. Synovial fibrosis involvement in osteoarthritis. *Front Med (Lausanne)* 2021;8:684389.

11. Li YH, Tavalalee G, Tokar T, et al. Identification of synovial fluid micro-RNA signature in knee osteoarthritis: differentiating early- and late-stage knee osteoarthritis. *Osteoarthritis Cartilage* 2016;24:1577–86.
12. Glasson SS, Blanchet TJ, Morris EA. The surgical destabilization of the medial meniscus (DMM) model of osteoarthritis in the 129/SvEv mouse. *Osteoarthritis Cartilage* 2007;15:1061–9.
13. Glasson SS, Chambers MG, Van Den Berg WB, Little CB. The OARSI histopathology initiative—recommendations for histological assessments of osteoarthritis in the mouse. *Osteoarthritis Cartilage* 2010;18 Suppl 3:S17–23.
14. Schneider CA, Rasband WS, Eliceiri KW. NIH Image to imageJ: 25 years of image analysis. *Nat Methods* 2012;9:671–5.
15. Potla P, Ali SA, Kapoor M. A bioinformatics approach to microRNA-sequencing analysis. *Osteoarthr Cartil Open* 2021;3:100131.
16. Tokar T, Pastrello C, Rossos AE, et al. mirDIP 4.1-integrative database of human microRNA target predictions. *Nucleic Acids Res* 2018;46:D360–70.
17. Kotlyar M, Pastrello C, Malik Z, et al. IID 2018 update: context-specific physical protein-protein interactions in human, model organisms and domesticated species. *Nucleic Acids Res* 2019;47:D581–9.
18. Rahmati S, Abovsky M, Pastrello C, et al. pathDIP 4: an extended pathway annotations and enrichment analysis resource for human, model organisms and domesticated species. *Nucleic Acids Res* 2020;48:D479–88.
19. Brown KR, Otasek D, Ali M, et al. NAViGaTOR: Network analysis, visualization and graphing Toronto. *Bioinformatics* 2009;25:3327–9.
20. Zhou Y, Li S, Chen P, et al. MicroRNA-27b-3p inhibits apoptosis of chondrocyte in rheumatoid arthritis by targeting HIPK2. *Artif Cells Nanomed Biotechnol* 2019;47:1766–71.
21. Akhtar N, Rasheed Z, Ramamurthy S, et al. MicroRNA-27b regulates the expression of matrix metalloproteinase 13 in human osteoarthritis chondrocytes. *Arthritis Rheum* 2010;62:1361–71.
22. Kapoor M, McCann M, Liu S, et al. Loss of peroxisome proliferator-activated receptor  $\gamma$  in mouse fibroblasts results in increased susceptibility to bleomycin-induced skin fibrosis. *Arthritis Rheum* 2009;60:2822–9.
23. Hinz B, Celetta G, Tomasek JJ, et al. Alpha-smooth muscle actin expression upregulates fibroblast contractile activity. *Mol Biol Cell* 2001;12:2730–41.
24. Schuster R, Rockel JS, Kapoor M, et al. The inflammatory speech of fibroblasts. *Immunol Rev* 2021;302:126–46.
25. Vaamonde-Garcia C, Malaise O, Charlier E, et al. 15-Deoxy- $\delta$ -12, 14-prostaglandin J2 acts cooperatively with prednisolone to reduce TGF- $\beta$ -induced pro-fibrotic pathways in human osteoarthritis fibroblasts. *Biochem Pharmacol* 2019;165:66–78.
26. Qadri M, Jay GD, Zhang LX, et al. Proteoglycan-4 regulates fibroblast to myofibroblast transition and expression of fibrotic genes in the synovium. *Arthritis Res Ther* 2020;22:113.
27. De Pascalis C, Etienne-Manneville S. Single and collective cell migration: the mechanics of adhesions. *Mol Biol Cell* 2017;28:1833–46.
28. Kanwal M, Smahel M, Olsen M, et al. Aspartate  $\beta$ -hydroxylase as a target for cancer therapy. *J Exp Clin Cancer Res* 2020;39:163.
29. Zhan YH, Luo QC, Zhang XR, et al. CELSR1 Is a positive regulator of endothelial cell migration and angiogenesis. *Biochemistry (Mosc)* 2016;81:591–9.
30. De Kreuk BJ, Gingras AR, Knight JD, et al. Heart of glass anchors Rasip1 at endothelial cell-cell junctions to support vascular integrity. *Elife* 2016;5:e11394.
31. Aumailley M, Krieg T. Laminins: a family of diverse multifunctional molecules of basement membranes. *J Invest Dermatol* 1996;106:209–14.
32. Mokkapati S, Bechtel M, Reibetanz M, et al. Absence of the basement membrane component nidogen 2, but not of nidogen 1, results in increased lung metastasis in mice. *J Histochem Cytochem* 2012;60:280–9.
33. Harman JL, Sayers J, Chapman C, et al. Emerging roles for neuropilin-2 in cardiovascular disease. *Int J Mol Sci* 2020;21:5154.
34. Yamaji Y, Yoshida S, Ishikawa K, et al. TEM7 (PLXDC1) in neovascular endothelial cells of fibrovascular membranes from patients with proliferative diabetic retinopathy. *Invest Ophthalmol Vis Sci* 2008;49:3151–7.
35. Pradhan AK, Maji S, Das SK, et al. MDA-9/Syntenin/SDCBP: new insights into a unique multifunctional scaffold protein. *Cancer Metastasis Rev* 2020;39:769–81.
36. Awwad K, Hu J, Shi L, et al. Role of secreted modular calcium-binding protein 1 (SMOC1) in transforming growth factor  $\beta$  signalling and angiogenesis. *Cardiovasc Res* 2015;106:284–94.
37. Gonzalez-Loyola A, Petrova TV. Development and aging of the lymphatic vascular system. *Adv Drug Deliv Rev* 2021;169:63–78.
38. Walker EC, McGregor NE, Poulton IJ, et al. Oncostatin M promotes bone formation independently of resorption when signaling through leukemia inhibitory factor receptor in mice. *J Clin Invest* 2010;120:582–92.
39. Takahata Y, Hagino H, Kimura A, et al. Smoc1 and Smoc2 regulate bone formation as downstream molecules of Runx2. *Commun Biol* 2021;4:1199.
40. Morkmued S, Clauss F, Schuhbaur B, et al. Deficiency of the SMOC2 matricellular protein impairs bone healing and produces age-dependent bone loss. *Sci Rep* 2020;10:14817.
41. Pyott SM, Schwarze U, Christiansen HE, et al. Mutations in PPIB (cyclophilin B) delay type I procollagen chain association and result in perinatal lethal to moderate osteogenesis imperfecta phenotypes. *Hum Mol Genet* 2011;20:1595–609.
42. Badshah, II, Brown S, Weibel L, et al. Differential expression of secreted factors SOSTDC1 and ADAMTS8 cause profibrotic changes in linear morphoea fibroblasts. *Br J Dermatol* 2019;180:1135–49.
43. Omura J, Satoh K, Kikuchi N, et al. ADAMTS8 promotes the development of pulmonary arterial hypertension and right ventricular failure: a possible novel therapeutic target. *Circ Res* 2019;125:884–906.
44. Zhu Z, Zhong L, Li R, et al. Study of osteoarthritis-related hub genes based on bioinformatics analysis. *Biomed Res Int* 2020;2020:2379280.
45. Yang Z, Xiao Z, Guo H, et al. Novel role of the clustered miR-23b-3p and miR-27b-3p in enhanced expression of fibrosis-associated genes by targeting TGFB3 in atrial fibroblasts. *J Cell Mol Med* 2019;23:3246–56.
46. Cui H, Banerjee S, Xie N, et al. MicroRNA-27a-3p is a negative regulator of lung fibrosis by targeting myofibroblast differentiation. *Am J Respir Cell Mol Biol* 2016;54:843–52.
47. Bielajew BJ, Hu JC, Athanasiou KA. Collagen: quantification, biomechanics, and role of minor subtypes in cartilage. *Nat Rev Mater* 2020;5:730–47.
48. Aqoierbatu, Luo A, Shi Y, et al. Microarray analysis of hub genes and pathways in damaged cartilage tissues of knee. *Medicine (Baltimore)* 2021;100:e27183.
49. Xu Y, Han YF, Ye B, et al. miR-27b-3p is involved in doxorubicin resistance of human anaplastic thyroid cancer cells via targeting peroxisome proliferator-activated receptor  $\gamma$ . *Basic Clin Pharmacol Toxicol* 2018;123:670–7.
50. Shen SJ, Song Y, Ren XY, et al. MicroRNA-27b-3p promotes tumor progression and metastasis by inhibiting peroxisome proliferator-activated receptor  $\gamma$  in triple-negative breast cancer. *Front Oncol* 2020;10:1371.
51. Jennewein C, von Knethen A, Schmid T, et al. MicroRNA-27b contributes to lipopolysaccharide-mediated peroxisome proliferator-activated receptor  $\gamma$  (PPAR $\gamma$ ) mRNA destabilization. *J Biol Chem* 2010;285:11846–53.

52. Zhu HY, Bai WD, Wang HT, et al. Peroxisome proliferator-activated receptor- $\gamma$  agonist inhibits collagen synthesis in human keloid fibroblasts by suppression of early growth response-1 expression through upregulation of miR-543 expression. *Am J Cancer Res* 2016;6:1358–70.
53. Zhao J, Ouyang Q, Hu Z, et al. A protocol for the culture and isolation of murine synovial fibroblasts. *Biomed Rep* 2016;5:171–5.
54. Rosengren S, Boyle DL, Firestein GS. Acquisition, culture, and phenotyping of synovial fibroblasts. *Methods Mol Med* 2007;135:365–75.
55. Seidel MF, Koch FW, Vetter H. Macrophage-like synoviocytes display phenotypic polymorphisms in a serum-free tissue-culture medium. *Rheumatol Int* 2006;26:244–51.

# Safety and Efficacy of Bimekizumab in Patients With Active Ankylosing Spondylitis: Three-Year Results From a Phase IIb Randomized Controlled Trial and Its Open-Label Extension Study

Xenofon Baraliakos,<sup>1</sup> Atul Deodhar,<sup>2</sup> Maxime Dougados,<sup>3</sup> Lianne S. Gensler,<sup>4</sup> Anna Molto,<sup>3</sup> Sofia Ramiro,<sup>5</sup> Alan J. Kivitz,<sup>6</sup> Denis Poddubnyy,<sup>7</sup> Marga Oortgiesen,<sup>8</sup> Thomas Vaux,<sup>9</sup> Carmen Fleurinck,<sup>10</sup> Julie Shepherd-Smith,<sup>9</sup> Christine de la Loge,<sup>10</sup> Natasha de Peyrecave,<sup>10</sup> and Désirée van der Heijde<sup>11</sup>

**Objective.** To assess the long-term safety, tolerability, and efficacy of bimekizumab in patients with active ankylosing spondylitis (AS).

**Methods.** Patients with active AS who completed the dose-ranging, 48-week BE AGILE randomized controlled trial were eligible to participate in an open-label extension (OLE) study, in which patients received 160 mg of bimekizumab every 4 weeks. We present the safety and efficacy results through 156 weeks. Missing efficacy data were imputed using nonresponder imputation analysis for binary outcomes and multiple imputation for continuous outcomes.

**Results.** From weeks 0–156, 280 of 303 patients (exposure-adjusted incidence rate 141.0 per 100 patient-years) experienced  $\geq 1$  treatment-emergent adverse event; the most frequent adverse events were nasopharyngitis (8.1 per 100 patient-years) and upper respiratory tract infection (5.0 per 100 patient-years). Additionally, 67 of 303 patients (9.8 per 100 patient-years) had mild to moderate localized fungal infections (28 of 303 patients had *Candida* infections [3.7 per 100 patient-years] and 23 of 303 patients had oral candidiasis [3.0 per 100 patient-years]), 10 patients had serious infections (1.3 per 100 patient-years), and no cases of active tuberculosis were reported. Active inflammatory bowel disease (1.1 per 100 patient-years), anterior uveitis (0.7 per 100 patient-years), and adjudicated major adverse cardiovascular events (0.3 per 100 patient-years) were infrequent. The efficacy of bimekizumab treatment demonstrated at week 48 was sustained in the OLE study. At week 156, nonresponder imputation analysis showed that 53.7% of patients (72.6% of observed cases) met the Assessment of SpondyloArthritis international Society criteria for 40% improvement and 28.0% of patients (37.9% of observed cases) achieved partial remission; Ankylosing Spondylitis Disease Activity Scores were reduced from baseline (mean  $\pm$  SEM 3.9  $\pm$  0.1) to week 48 (2.1  $\pm$  0.1) and week 156 (1.9  $\pm$  0.1) (multiple imputation). Patients showed sustained improvements in pain, fatigue, physical function, and health-related quality of life.

**Conclusion.** The safety profile of bimekizumab was found to be consistent with previously demonstrated findings, and no new safety signals were identified. The efficacy of bimekizumab in patients with AS was sustained through 3 years of treatment.

## INTRODUCTION

Ankylosing spondylitis (AS) is a chronic, immune-mediated inflammatory disease that mainly affects the axial skeleton (1).

Falling within the axial spondyloarthritis (SpA) spectrum, patients with AS (also known as radiographic axial SpA) show definitive structural damage of the sacroiliac joints on pelvic radiographs (2). Due to the significant and lasting impact of AS on patients

A video abstract of this article can be found at: [https://players.brightcove.net/3806881048001/default\\_index.html?videoId=6309214489112](https://players.brightcove.net/3806881048001/default_index.html?videoId=6309214489112)

Clinicaltrials.gov identifiers: NCT02963506 and NCT03355573.

Supported by UCB Pharma.

<sup>1</sup>Xenofon Baraliakos, MD: Rheumazentrum Ruhrgebiet Herne, Ruhr-University Bochum, Bochum, Germany; <sup>2</sup>Atul Deodhar, MD: Oregon Health & Science University, Portland; <sup>3</sup>Maxime Dougados, MD, Anna Molto, MD, PhD: Université de Paris, Department of Rheumatology, Hôpital Cochin, Assistance Publique–Hôpitaux de Paris, INSERM U1153, Clinical Epidemiology and Biostatistics, PRES Sorbonne Paris-Cité, Paris, France; <sup>4</sup>Lianne S. Gensler,

MD: Department of Rheumatology, University of California, San Francisco; <sup>5</sup>Sofia Ramiro, MD, MSc, PhD: Department of Rheumatology, Leiden University Medical Center, Leiden, The Netherlands, and Department of Rheumatology, Zuyderland Medical Center, Heerlen, The Netherlands; <sup>6</sup>Alan J. Kivitz, MD: Altoona Center for Clinical Research, Duncansville, Pennsylvania; <sup>7</sup>Denis Poddubnyy, MD: Department of Gastroenterology, Infectious Diseases and Rheumatology, Charité–Universitätsmedizin Berlin, Berlin, Germany; <sup>8</sup>Marga Oortgiesen, PhD: UCB Pharma, Raleigh, North Carolina; <sup>9</sup>Thomas Vaux, MSc, Julie Shepherd-Smith, BPharm, PGDipPV: UCB Pharma, Slough, UK; <sup>10</sup>Carmen Fleurinck, MD, Christine de la Loge, MSc, Natasha de



(3–7), it is crucial to assess the long-term safety and efficacy of treatments.

Interleukin-17 (IL-17) cytokines are key mediators of inflammation in SpA and have been targeted by new monoclonal antibody therapies (8,9), including the currently approved IL-17A inhibitors secukinumab and ixekizumab (9–11). In AS patients, safety and efficacy have been reported for up to 5 years for secukinumab, up to 2 years for ixekizumab (12–15), and up to 16 weeks for brodalumab, an anti-IL-17 receptor antibody (16).

Bimekizumab is a monoclonal IgG1 antibody that inhibits IL-17F in addition to IL-17A. These 2 cytokines, which have ~50% structural homology, form homodimers and heterodimers that signal via the same receptor complex (17,18). Despite similarities, IL-17A and IL-17F have distinct proinflammatory features and can independently synergize with tumor necrosis factor (TNF) to drive and amplify the inflammatory response (18–20). Preclinical evidence has demonstrated that inhibition of both cytokines suppresses gene expression and cytokine production to a greater extent than inhibition of IL-17A alone (11,12). The independent roles of IL-17A and IL-17F in pathological bone formation have also been identified in preclinical studies, indicating that dual inhibition of these cytokines may modulate osteoblast activity to a greater extent than only IL-17A inhibition (21,22).

Clinical studies have shown that the dual inhibition of IL-17A and IL-17F with bimekizumab results in rapid and lasting clinical improvements in patients with plaque psoriasis (with superiority demonstrated against secukinumab, ustekinumab, and adalimumab), psoriatic arthritis (PsA), and AS (23–29). In summary, the body of preclinical and clinical evidence suggests that the additional inhibition of IL-17F with bimekizumab may provide an improved therapeutic approach with further potential benefits relative to existing IL-17A inhibitors.

In the phase IIb dose-ranging BE AGILE study of bimekizumab in adults with active AS, a rapid and significant reduction in disease activity was demonstrated at week 12, which was sustained through week 48 (29). Bimekizumab was well tolerated and provided substantial improvements across various domains, including patient-reported symptoms, physical function, and health-related quality of life, as well as objective signs of inflammation such as C-reactive protein (CRP) levels and features of inflammation visible on magnetic resonance imaging (MRI) (29).

Here, we report the safety and efficacy of treatment with bimekizumab for up to 156 weeks in adult patients with active AS. The primary objective of this study was to assess the long-term safety and tolerability of bimekizumab in patients with active AS, and secondarily to assess its long-term efficacy.

## PATIENTS AND METHODS

**Study design and participants.** The BE AGILE study (ClinicalTrials.gov identifier NCT02963506) was a 48-week randomized, parallel-group, phase IIb, dose-ranging study that was double-blind to week 12 and then dose-blind to week 48. From the beginning of the trial to week 48, it was conducted at 74 sites across 10 countries in Europe and the US (29). Patients who completed 48 weeks of treatment were eligible to enroll in the open-label extension (OLE) study (ClinicalTrials.gov identifier NCT03355573) for an additional 204 weeks of treatment, with a subsequent safety visit 20 weeks after the last dose (see Supplementary Figure 1, available on the *Arthritis & Rheumatology* website at <http://onlinelibrary.wiley.com/doi/10.1002/art.42282>). The OLE study was conducted at 50 sites across the same 10 countries in Europe and the US that participated in the BE AGILE study. Inclusion and exclusion criteria have been reported previously (29). All study timepoints are reported relative to baseline (week 0) of the initial randomized controlled study. We report here results up to week 156 (up to 3 years total treatment duration).

**Randomization and blinding.** At baseline of the double-blind period, patients were randomized 1:1:1:1 to receive subcutaneous injection of bimekizumab at a dose of 16 mg, 64 mg, 160 mg, or 320 mg, or placebo every 4 weeks. At week 12 of the BE AGILE study, patients initially randomized to receive 16 mg or 64 mg of bimekizumab or placebo were rerandomized 1:1 to receive 160 mg or 320 mg of bimekizumab every 4 weeks through week 48, while patients initially randomized to receive 160 mg or 320 mg of bimekizumab continued their dosing to week 48. All patients in the OLE study received 160 mg of open-label bimekizumab every 4 weeks, regardless of prior dosing regimen (Supplementary Figure 1, <http://onlinelibrary.wiley.com/doi/10.1002/art.42282>).

The BE AGILE study and the affiliated OLE study were conducted in accordance with the Declaration of Helsinki and the International Conference for Harmonisation Guidelines for

Peyrecave, DPhil: UCB Pharma, Brussels, Belgium; <sup>11</sup>Désirée van der Heijde, MD, PhD: Department of Rheumatology, Leiden University Medical Center, Leiden, The Netherlands.

Data may be requested by qualified researchers 6 months after product approval in the US and/or Europe, or global development is discontinued, and 18 months after trial completion. Investigators may request access to anonymized IPD and redacted study documents which may include raw datasets, analysis-ready datasets, study protocol, blank case report form, annotated case report form, statistical analysis plan, dataset specifications, and clinical study report. Prior to use of the data, proposals need to be approved by an

independent review panel at [www.vivli.org](http://www.vivli.org) and a signed data sharing agreement will need to be executed. All documents are available in English only, for a prespecified time, typically 12 months, on a password protected portal.

Author disclosures are available at <https://onlinelibrary.wiley.com/action/downloadSupplement?doi=10.1002%2Fart.42282&file=art42282-sup-0001-Disclosureform.pdf>.

Address correspondence via email to Xenofon Baraliakos, MD, at [xenofon.baraliakos@elisabethgruppe.de](mailto:xenofon.baraliakos@elisabethgruppe.de).

Submitted for publication January 12, 2022; accepted in revised form June 23, 2022.

Good Clinical Practice. Ethical approval was obtained from the relevant institutional review boards at participating sites. The results presented in this article are in aggregate form, and no personally identifiable information was used for this study. All patients provided written informed consent in accordance with local requirements, with additional written informed consent required for enrollment in the OLE study.

**Study procedures and outcomes.** During the OLE study, safety was assessed on study entry (week 48), then every 4 weeks up to week 60, then every 12 weeks up to week 156. Most efficacy outcomes were assessed at OLE study entry, then every 12 weeks up to week 156. The Ankylosing Spondylitis Quality of Life (ASQoL) questionnaire (30) and the Short Form 36 (SF-36) health survey (31) were assessed at the same time-points but were not assessed at week 156. The Bath Ankylosing Spondylitis Metrology Index (BASMI) (32) was assessed on OLE study entry and then every 48 weeks. The Maastricht Ankylosing Spondylitis Enthesitis Score (MASES) (33) was assessed every 12 weeks from entry to the OLE study, then every 24 weeks after week 96.

Safety outcomes (Medical Dictionary for Regulatory Activities [MedDRA] version 19.0) of the OLE study (primary objective) included incidence of treatment-emergent adverse events (TEAEs), serious TEAEs (primary safety variables), study withdrawals due to TEAEs (secondary safety variable), and prespecified adverse events of interest. Adverse events of interest included infections (serious, opportunistic, or fungal infections [including *Candida*] and tuberculosis), neutropenia, hypersensitivity, suicidal ideation and behavior, depression, major cardiovascular events, liver function test changes/enzyme elevations, and malignancies. TEAEs of inflammatory bowel disease (IBD) including ulcerative colitis, Crohn's disease, and IBD not otherwise specified as well as anterior uveitis were also reported as extra-musculoskeletal manifestations and are presented by the patient's history of the event.

The efficacy of treatment with bimekizumab in AS patients in the OLE study (secondary objective) was evaluated using the Assessment of SpondyloArthritis international Society (ASAS) criteria for 20% improvement (ASAS20) (34) and ASAS criteria for 40% improvement (ASAS40) (35), the ASAS5/6 criteria (35), the ASAS criteria for partial remission (35), the Ankylosing Spondylitis Disease Activity Score using CRP (ASDAS-CRP) (36), the ASDAS showing major improvement (36), the ASDAS showing clinically important improvement (ASDAS-CII) (36), the Bath Ankylosing Spondylitis Disease Activity Index (BASDAI) (37), the BASDAI criteria for 50% improvement (BASDAI50) (37), the Bath Ankylosing Spondylitis Functional Index (BASFI) (38), the BASMI, the MASES, and the total resolution of the MASES. Efficacy of treatment with bimekizumab was also evaluated by assessment of high-sensitivity CRP, elevated high-sensitivity CRP (>5 mg/liter), BASDAI questions 1 (fatigue) and 2 (total spine,

neck, back, or hip pain), the ASQoL, the SF-36 physical component summary (PCS) and mental component summary (MCS) scores, morning stiffness (mean of BASDAI question 5 + question 6), and the Patient Global Assessment of Disease Activity (PGADA).

**Statistical analysis.** Safety analyses are presented for exposure to bimekizumab across the total treatment period (weeks 0–156), as well as separately (weeks 0–48 and weeks 48–156) for the respective BE AGILE and OLE safety sets (patients who had  $\geq 1$  dose of bimekizumab in the relevant study period). To account for long-term, cumulative patient exposure to bimekizumab, exposure-adjusted incidence rates (EAIRs) per 100 patient-years are presented for TEAEs. EAIRs were calculated by dividing the number of patients with the specified TEAE by (i) the sum of each of those patients' time at risk (in years) at the onset of the (first, if they had >1) specified TEAE, plus (ii) the sum of time at risk for patients who did not experience that TEAE; the result was scaled to 100 patient-years.

Unless stated otherwise, efficacy variables are reported for the dose-blind set, comprising all patients who started the dose-blind period at week 12 of the BE AGILE study and who received at least 1 dose of bimekizumab during the dose-blind period, including the dose at week 12. This was to ensure that a full treatment sequence was available for each patient. For efficacy data reported by initial randomization group (baseline to week 12), outcomes are reported for the full analysis set, comprising all randomized patients who received at least 1 dose of the study drug and had a valid measurement of the ASAS components at baseline. Outcomes are summarized descriptively by visit and treatment group. Responses and change from baseline were derived relative to efficacy measurements at the double-blind period at baseline (week 0).

For binary outcomes, missing data were imputed in the most conservative manner, using the nonresponder imputation (NRI) method relative to week 0. For a given outcome and timepoint, a patient was classed as a nonresponder if data (or baseline values) were missing or if they had discontinued from the study; patients who did not enter the OLE study were considered nonresponders from week 48 onward. For continuous outcomes, missing data were imputed using multiple imputation (MI) based on the assumption that data were missing at random. Observed case data are also reported. All statistical analyses were conducted in SAS version 9.3 or later.

**Ethics approval.** This study was conducted in accordance with the principles of the Declaration of Helsinki and the International Conference on Harmonisation Guidance for Good Clinical Practice. Independent institutional review board approvals were obtained, and all patients provided written informed consent in accordance with local requirements.

## RESULTS

### Patient disposition and baseline characteristics.

Of the 303 patients randomized to receive treatment with bimekizumab or placebo at baseline (full analysis set and BE AGILE safety set), 297 patients (98.0%) completed the double-blind period, and 296 patients (97.7%) started the dose-blind period at week 12 (dose-blind set). The dose-blind period was completed at week 48 by 265 of 303 patients (87.5%), at which point 256 of 303 patients (84.5%) entered the OLE study; the remaining 9 patients did not enroll in the OLE study. Of those 256 patients, 255 were included in the OLE safety set, since 1 patient was enrolled in the OLE study but did not subsequently receive bimekizumab (Supplementary Figure 1, <http://onlinelibrary.wiley.com/doi/10.1002/art.42282>). Patient retention was high during the OLE study, with 224 of 256 patients (87.5%; 224 of 303 patients [73.9%]) remaining in the study up to week 156 (Supplementary Figures 2–3, <http://onlinelibrary.wiley.com/doi/10.1002/art.42282>). There were 32 discontinuations during the OLE study: 15 due to adverse events, 12 due to withdrawn consent, 2 due to lack of efficacy, 1 lost to follow-up, and 2 due to other reasons.

At baseline of the double-blind period, there were no notable differences in patient demographics and disease characteristics between the randomized population and the subset of patients who received bimekizumab in the OLE study (Table 1). In the latter group ( $n = 255$ ), 217 patients (85.1%) were male, 232 patients (91.0%) were positive for HLA-B27, and 29 patients (11.4%) had received prior tumor necrosis factor inhibitor (TNFi) therapy. At baseline of the double-blind period in the OLE study safety set, the median duration of AS from diagnosis was 4.6 years (range 0.0–37.3 years), and the median duration of symptoms was 12.1 years (range 0.2–47.2 years). The mean  $\pm$  SD ASDAS and BASDAI scores were  $3.9 \pm 0.8$  and  $6.4 \pm 1.4$ , respectively, and the median high-sensitivity CRP level was 12.1 mg/liter (range 0.3–130.1 mg/liter).

**Safety.** Exposure to bimekizumab over 156 weeks among all patients randomized at baseline was 815.6 patient-years, including 554.7 patient-years during the OLE study (weeks 48–156). For the total treatment period,  $\geq 1$  TEAE was observed in 280 of 303 patients (92.4%; EAIR 141.0 per 100 patient-years);  $\geq 1$  serious TEAE was observed in 43 of 303 patients (14.2%; EAIR

**Table 1.** Demographics and disease characteristics of patients with ankylosing spondylitis at baseline\*

	BE AGILE safety set (N = 303)	OLE safety set (N = 255)
Age, mean $\pm$ SD years	42.2 $\pm$ 11.8	41.8 $\pm$ 11.4
Male	256 (84.5)	217 (85.1)
HLA-B27, positive†	270 (89.1)	232 (91.0)
Age at first diagnosis, mean $\pm$ SD years	34.8 $\pm$ 10.4	34.5 $\pm$ 10.2
Symptom duration, median (min–max) years	12.3 (0.2–47.2)	12.1 (0.2–47.2)
Disease duration, median (min–max) years	4.6 (0.0–37.3)	4.6 (0.0–37.3)
ASDAS-CRP, mean $\pm$ SD	3.9 $\pm$ 0.8	3.9 $\pm$ 0.8
BASDAI, mean $\pm$ SD (0–10)	6.5 $\pm$ 1.4	6.4 $\pm$ 1.4
BASFI, mean $\pm$ SD (0–10)	5.8 $\pm$ 2.0	5.7 $\pm$ 1.9
Total spinal pain score, mean $\pm$ SD (0–10)	7.1 $\pm$ 1.7	7.0 $\pm$ 1.8
PGADA, mean $\pm$ SD (0–10)	7.0 $\pm$ 1.7	6.9 $\pm$ 1.7
hsCRP, mg/liter‡		
Mean $\pm$ SD	19.0 $\pm$ 20.9	19.5 $\pm$ 21.5
Median (min–max)	12.1 (0.3–130.1)	12.1 (0.3–130.1)
History of IBD		
Crohn's disease	2 (0.7)	1 (0.4)
Ulcerative colitis	5 (1.7)	4 (1.6)
History of anterior uveitis	46 (15.2)	39 (15.3)
History of psoriasis	9 (3.0)	7 (2.7)
Prior TNFi therapy	34 (11.2)	29 (11.4)
Concomitant treatment		
NSAIDs	272 (89.8)	232 (91.0)
csDMARDs	79 (26.1)	67 (26.3)
Corticosteroids	26 (8.6)	23 (9.0)

\* Except where indicated otherwise, values are the number (%) of patients. All data are reported for baseline of the double-blind period (week 0), not the start of the open-label extension (OLE) study (week 48). ASDAS-CRP = Ankylosing Spondylitis Disease Activity Score using C-reactive protein; BASDAI = Bath Ankylosing Spondylitis Disease Activity Index; BASFI = Bath Ankylosing Spondylitis Function Index; PGADA = Patient Global Assessment of Disease Activity; hsCRP = high-sensitivity CRP; IBD = inflammatory bowel disease; TNFi = tumor necrosis factor inhibitor; NSAIDs = nonsteroidal antiinflammatory drugs; csDMARDs = conventional synthetic disease-modifying antirheumatic drugs.

† Including 6 patients with missing results in the BE AGILE safety set and 5 patients with missing results in the OLE safety set.

‡ For hsCRP level in the BE AGILE safety set  $n = 300$  patients, and  $n = 254$  patients in the OLE safety set.

5.6 per 100 patient-years) (Table 2). TEAEs that occurred during weeks 0–48 and weeks 48–156 are shown in Table 2. For TEAEs that presented in >1 patient, EAIRs did not increase from weeks 0–48 to weeks 48–156 for the vast majority of reported TEAEs. EAIRs for serious TEAEs were 5.1 per 100 patient-years during weeks 0–48 and 5.9 during weeks 48–156; EAIRs for psoriasis were 0 during weeks 0–48 and 1.5 during weeks 48–156 (Table 2). Study discontinuations due to TEAEs were infrequent: 37 patients (12.2%) discontinued during the 156-week study period due to a TEAE, including 14 patients who discontinued during the OLE study. Study discontinuation due to TEAEs during the OLE study were most commonly due to infections and elevated liver enzymes. However, elevated liver enzymes were generally mild to moderate, and none met Hy's Law criteria. The most frequently reported TEAEs by MedDRA preferred term ( $\geq 5\%$  of patients) are shown in Table 2.

One death was reported during weeks 0–48 (cardiac arrest in a patient with cardiovascular risk factors) and 1 death was reported during the OLE study (road traffic accident); neither was considered treatment-related by the study investigators. EAIRs during weeks 0–156 were 1.3 per 100 patient-years for serious infections and 0.3 per 100 patient-years for opportunistic infections. There were no cases of active tuberculosis during the study.

A total of 67 of 303 patients (EAIR 9.8 per 100 patient-years) had a fungal infection during weeks 0–156 (Table 2). All fungal infections were assessed as mild to moderate in intensity by the study investigator and the vast majority did not lead to discontinuation (1 patient discontinued due to oral candidiasis during weeks 0–48). There were no patients with serious or systemic fungal infections. Of patients with  $\geq 1$  infection, 28 had *Candida* infections (EAIR 3.7 per 100 patient-years), with the majority of these (23 of 28; EAIR 3.0 per 100 patient-years) being oral candidiasis. Thirty-seven patients (12.2%) had fungal infections not elsewhere classified (EAIR 5.0 per 100 patient-years), with 16 of 37 patients experiencing oral infections (EAIR 2.1 per 100 patient-years). Infections at other sites were low, including oropharyngeal candidiasis in 1 patient (0.3%) and vulvovaginal infections in 3 patients (2 *Candida* infections [0.7%] and 1 fungal infection [0.3%]). In total, 8 patients (2.6%) had a *Tinea* infection (EAIR 1.0 per 100 patient-years). Sex, smoking status, and presence of diabetes mellitus were not clear risk factors for susceptibility to *Candida* infections. A total of 10 of 303 patients (3.3%) had more than 1 *Candida* infection over 156 weeks. All fungal infections, including *Candida* infections, were localized, none were systemic, and the vast majority resolved without sequelae and were easily treated with systemic or topical antifungal treatments such as clotrimazole, fluconazole, itraconazole, and nystatin (Supplementary Table 1, <http://onlinelibrary.wiley.com/doi/10.1002/art.42282>).

Across weeks 0–156, 1 patient had adjudicated suicidal ideation and behavior, 2 had depression, 2 had adjudicated major adverse cardiovascular events (including the aforementioned

cardiac arrest leading to death), and 1 patient had a malignancy (testicular seminoma) (Table 2); all of these events were considered unrelated to treatment by the study investigators. Two patients had neutropenia (both treatment-related), and 4 patients had injection site reactions, with treatment-related events in 3 patients. The most commonly reported skin disorders were dermatitis and eczema (high-level term), which occurred in 30 patients (9.9%; EAIR 3.9 per 100 patient-years); in 22 of these patients, cases of skin disorders were considered unrelated to treatment. Urticaria occurred in 1 patient and led to the patient discontinuing the study. No cases of serious hypersensitivity reactions were reported (Table 2).

**Extramusculoskeletal manifestations.** Of the 303 patients included in the BE AGILE safety set (none of whom had active/symptomatic IBD at screening and baseline), 2 (0.7%) had a history of Crohn's disease and 5 (1.7%) had a history of ulcerative colitis prior to entry in the BE AGILE study. Across weeks 0–156, 9 patients (3.0%) presented with active IBD (EAIR 1.1 per 100 patient-years), including 4 patients (1.3%) with ulcerative colitis, 4 patients (1.3%) with Crohn's disease, and 1 patient (0.3%) with unspecified IBD. Two of those 9 patients, both with ulcerative colitis, had a history of ulcerative colitis prior to entry in the BE AGILE study (Table 2). No patients presenting with active IBD had diabetes mellitus. Among the 9 patients with IBD, 3 patients experienced temporary interruption of bimekizumab treatment, and 1 patient discontinued participation in the study (due to ulcerative colitis). One patient was diagnosed as having Crohn's disease after discontinuing from the study due to a perirectal abscess; another patient was diagnosed as having Crohn's disease after withdrawing consent and discontinuing from the study to father a child.

Of the 303 patients, 46 (15.2%) had a history of anterior uveitis (which was not an exclusion criterion). Across weeks 0–156, 6 patients (2.0%) had an anterior uveitis flare (EAIR 0.7 per 100 patient-years). All cases were mild to moderate, and none were serious or led to study discontinuation. Of the 6 patients who experienced flares of anterior uveitis, 3 patients had a history of anterior uveitis, but the other 3 patients did not (Table 2 and Supplementary Table 2, <http://onlinelibrary.wiley.com/doi/10.1002/art.42282>). Across weeks 0–156, psoriasis occurred in 8 patients (2.6%; EAIR 1.0 per 100 patient-years); most cases were mild to moderate, and none led to study discontinuation.

**Efficacy.** The efficacy of bimekizumab treatment at weeks 12 and 48 of the BE AGILE study has been reported previously (29). At week 48, over half of the bimekizumab-treated patients achieved an ASAS40 response (51.7% of patients by NRI and 59.8% of observed cases); this response rate was sustained to week 156 (53.7% of patients by NRI and 72.6% of observed cases) (Figure 1A). ASAS20 and ASAS partial remission

**Table 2.** Safety outcomes for exposure to bimekizumab (BKZ) in patients with ankylosing spondylitis over 156 weeks\*

	Weeks 0–48†			Weeks 48–156		Weeks 0–156†
	160 mg BKZ every 4 weeks (n = 149; 114.2 patient-years)‡	320 mg BKZ every 4 weeks (n = 150; 119.6 patient-years)‡	Total BKZ (N = 303; 261.3 patient-years)§	Total BKZ (N = 255; 554.7 patient-years)	Total BKZ (N = 303; 815.6 patient-years)§	
Any TEAE	103 (69.1) (168.7)	122 (81.3) (221.1)	235 (77.6) (186.2)	215 (84.3) (110.8)	280 (92.4) (141.0)	
Most frequently reported TEAEs (≥5%) by preferred term						
Nasopharyngitis	13 (8.7) (12.0)	19 (12.7) (16.6)	34 (11.2) (13.7)	34 (13.3) (6.7)	57 (18.8) (8.1)	
Upper respiratory tract infection	5 (3.4) (4.5)	11 (7.3) (9.5)	17 (5.6) (6.7)	24 (9.4) (4.6)	37 (12.2) (5.0)	
Bronchitis	4 (2.7) (3.6)	12 (8.0) (10.4)	18 (5.9) (7.1)	15 (5.9) (2.8)	33 (10.9) (4.4)	
Pharyngitis	11 (7.4) (10.0)	7 (4.7) (6.1)	18 (5.9) (7.1)	15 (5.9) (2.8)	29 (9.6) (3.8)	
ALT increased	5 (3.4) (4.5)	6 (4.0) (5.1)	13 (4.3) (5.1)	15 (5.9) (2.8)	23 (7.6) (3.0)	
Oral candidiasis	8 (5.4) (7.2)	8 (5.3) (7.0)	16 (5.3) (6.3)	13 (5.1) (2.4)	23 (7.6) (3.0)	
Hypercholesterolemia	6 (4.0) (5.4)	6 (4.0) (5.2)	12 (4.0) (4.7)	11 (4.3) (2.0)	20 (6.6) (2.6)	
Hypertension	4 (2.7) (3.6)	5 (3.3) (4.3)	10 (3.3) (3.9)	11 (4.3) (2.0)	20 (6.6) (2.6)	
Rhinitis	7 (4.7) (6.3)	6 (4.0) (5.1)	14 (4.6) (5.5)	6 (2.4) (1.1)	20 (6.6) (2.6)	
Tonsillitis	4 (2.7) (3.6)	3 (2.0) (2.5)	8 (2.6) (3.1)	13 (5.1) (2.4)	19 (6.3) (2.4)	
Arthralgia	2 (1.3) (1.8)	5 (3.3) (4.3)	8 (2.6) (3.1)	11 (4.3) (2.0)	18 (5.9) (2.3)	
Conjunctivitis	3 (2.0) (2.7)	7 (4.7) (6.0)	10 (3.3) (3.9)	10 (3.9) (1.8)	18 (5.9) (2.3)	
Headache	6 (4.0) (5.4)	4 (2.7) (3.4)	13 (4.3) (5.1)	6 (2.4) (1.1)	18 (5.9) (2.3)	
Respiratory tract infection	4 (2.7) (3.6)	6 (4.0) (5.1)	11 (3.6) (4.3)	8 (3.1) (1.5)	18 (5.9) (2.3)	
GGT increased	6 (4.0) (5.4)	4 (2.7) (3.4)	13 (4.3) (5.1)	5 (2.0) (0.9)	17 (5.6) (2.2)	
Oral fungal infection	8 (5.4) (7.2)	6 (4.0) (5.1)	14 (4.6) (5.5)	8 (3.1) (1.5)	16 (5.3) (2.1)	
AST increased	3 (2.0) (2.7)	5 (3.3) (4.3)	9 (3.0) (3.5)	9 (3.5) (1.6)	16 (5.3) (2.0)	
Serious TEAEs	5 (3.4) (4.4)	6 (4.0) (5.1)	13 (4.3) (5.1)	31 (12.2) (5.9)	43 (14.2) (5.6)	
Study discontinuations due to TEAEs	7 (4.7)	10 (6.7)	20 (6.6)	14 (5.5)	37 (12.2)	
Drug-related TEAEs	48 (32.2)	54 (36.0)	110 (36.3)	90 (35.3)	149 (49.2)	
Deaths	1 (0.7)	0	1 (0.3)	1 (0.4)	2 (0.7)	
Adverse events of interest						
Serious infections	3 (2.0) (2.7)	1 (0.7) (0.8)	4 (1.3) (1.5)	6 (2.4) (1.1)	10 (3.3) (1.3)	
Opportunistic infections	0	0	1 (0.3) (0.4)	1 (0.4) (0.2)	2 (0.7) (0.3)	
Active tuberculosis	0	0	0	0	0	
Fungal infections	19 (12.8) (17.8)	23 (15.3) (20.9)	44 (14.5) (18.1)	39 (15.3) (8.0)	67 (22.1) (9.8)	
Candida infections	10 (6.7) (9.1)	9 (6.0) (7.9)	19 (6.3) (7.5)	15 (5.9) (2.8)	28 (9.2) (3.7)	
Oral candidiasis	8 (5.4) (7.2)	8 (5.3) (7.0)	16 (5.3) (6.3)	13 (5.1) (2.4)	23 (7.6) (3.0)	
Skin candidiasis	0	1 (0.7) (0.8)	1 (0.3) (0.4)	3 (1.2) (0.5)	4 (1.3) (0.5)	
Vulvovaginal candidiasis	2 (1.3) (1.8)	0	2 (0.7) (0.8)	0	2 (0.7) (0.3)	
Oropharyngeal candidiasis	0	0	0	1 (0.4) (0.2)	1 (0.3) (0.1)	
Candida infection (unspecified)	0	0	0	1 (0.4) (0.2)	1 (0.3) (0.1)	
Fungal infections NEC	9 (6.0) (8.1)	13 (8.7) (11.3)	24 (7.9) (9.5)	22 (8.6) (4.3)	37 (12.2) (5.0)	
Oral fungal infection	8 (5.4) (7.2)	6 (4.0) (5.1)	14 (4.6) (5.5)	8 (3.1) (1.5)	16 (5.3) (2.1)	
Fungal skin infection	0	5 (3.3) (4.2)	7 (2.3) (2.7)	6 (2.4) (1.1)	13 (4.3) (1.6)	
Tongue fungal infection	0	3 (2.0) (2.5)	3 (1.0) (1.2)	5 (2.0) (0.9)	7 (2.3) (0.9)	
Onychomycosis	0	0	0	4 (1.6) (0.7)	4 (1.3) (0.5)	
Ear infection fungal	1 (0.7) (0.9)	0	1 (0.3) (0.4)	0	1 (0.3) (0.1)	
Vulvovaginal mycotic infection	0	1 (0.7) (0.8)	1 (0.3) (0.4)	0	1 (0.3) (0.1)	
Otitis externa fungal	0	0	0	1 (0.4) (0.2)	1 (0.3) (0.1)	

(Continued)



Table 2. (Cont'd)

	Weeks 0–48†		Total BKZ (N = 303; 261.3 patient-years)§	Weeks 48–156	Total BKZ (N = 255; 554.7 patient-years)§	Weeks 0–156†
	160 mg BKZ every 4 weeks (n = 149; 114.2 patient-years)‡	320 mg BKZ every 4 weeks (n = 150; 119.6 patient-years)‡				
<i>Tinea</i> infections	1 (0.7) (0.9)	2 (1.3) (1.7)	3 (1.0) (1.2)	4 (1.6) (0.7)	8 (2.6) (1.0)	
<i>Tinea</i> pedis	1 (0.7) (0.9)	2 (1.3) (1.7)	3 (1.0) (1.2)	3 (1.2) (0.5)	6 (2.0) (0.8)	
Body <i>tinea</i>	0	0	0	1 (0.4) (0.2)	1 (0.3) (0.1)	
<i>Tinea</i> capitis	0	0	0	0	1 (0.3) (0.1)	
Serious hypersensitivity reactions	0	0	0	0	0	
Adjudicated SIB	0	0	0	1 (0.4) (0.2)	1 (0.3) (0.1)	
Depression	0	0	1 (0.3) (0.4)	1 (0.4) (0.2)	2 (0.7) (0.3)	
Adjudicated MACE	2 (1.3) (1.8)	0	2 (0.7) (0.8)	0	2 (0.7) (0.3)	
Liver enzyme elevation						
ALT increased	5 (3.4) (4.5)	6 (4.0) (5.1)	13 (4.3) (5.1)	15 (5.9) (2.8)	23 (7.6) (3.0)	
AST increased	3 (2.0) (2.7)	5 (3.3) (4.3)	9 (3.0) (3.5)	9 (3.5) (1.6)	16 (5.3) (2.0)	
GGT increased	6 (4.0) (5.4)	4 (2.7) (3.4)	13 (4.3) (5.1)	5 (2.0) (0.9)	17 (5.6) (2.2)	
Hepatic enzyme increased	0	3 (2.0) (2.5)	6 (2.0) (2.3)	7 (2.7) (1.3)	12 (4.0) (1.5)	
Malignancies	0	0	0	1 (0.4) (0.2)	1 (0.3) (0.1)	
IBD	1 (0.7) (0.9)	2 (1.3) (1.7)	4 (1.3) (1.5)	6 (2.4) (1.1)	9 (3.0) (1.1)	
Ulcerative colitis	0	1 (0.7) (0.8)	2 (0.7) (0.8)	3 (1.2) (0.5)	4 (1.3) (0.5)	
With prior history	0	1 (0.7)	1 (0.3)	1 (0.4)	2 (0.7)	
No prior history	0	0	1 (0.3)	2 (0.8)	2 (0.7)	
Crohn's disease	1 (0.7) (0.9)	1 (0.7) (0.8)	2 (0.7) (0.8)	2 (0.8) (0.4)	4 (1.3) (0.5)	
With prior history	0	0	0	0	0	
No prior history	1 (0.7)	1 (0.7)	2 (0.7)	2 (0.8)	4 (1.3)	
IBD not otherwise specified	0	0	0	1 (0.4) (0.2)	1 (0.3) (0.1)	
Anterior uveitis	1 (0.7) (0.9)	1 (0.7) (0.8)	2 (0.7) (0.8)	4 (1.6) (0.7)	6 (2.0) (0.7)	
With prior history	1 (0.7)	1 (0.7)	2 (0.7)	1 (0.4)	3 (1.0)	
No prior history	0	0	0	3 (1.2)	3 (1.0)	
Psoriasis	0	0	0	8 (3.1) (1.5)	8 (2.6) (1.0)	
Injection site reactions	0	3 (2.0) (2.6)	3 (1.0) (1.2)	1 (0.4) (0.2)	4 (1.3) (0.5)	

\* Values are the number (%) of patients (exposure-adjusted incidence rate). 8 patients discontinued due to infections across weeks 0–156 (1 for each of the following: perirectal abscess, oral bacterial infection, oral candidiasis, conjunctivitis, herpes zoster, impetigo, *Tinea* capitis, and nasopharyngitis). 3 patients discontinued during weeks 48–156 due to a treatment-emergent adverse event (TEAE) that initiated in weeks 0–48 are not counted within weeks 48–156. 1 death occurred in weeks 0–48 (cardiac arrest in a patient with cardiovascular risk factors) and 1 occurred during the open-label extension study (road traffic accident), but neither was considered treatment-related. 1 case of recurrent herpes zoster occurred in weeks 0–48 and 1 case of oropharyngeal candidiasis occurred in weeks 48–156. All fungal infections were mild to moderate, and none were systemic. All oral candidiasis events were mild to moderate (none were serious). Liver enzyme elevations were not associated with clinical symptoms and no cases of Hy's Law were reported. 1 case of testicular seminoma was reported. Inflammatory bowel disease (IBD), anterior uveitis, and psoriasis are extramusculoskeletal manifestations of ankylosing spondylitis. IBD not otherwise specified occurred in 1 patient with no medical history of IBD. Psoriasis occurred in 8 patients with no prior history of psoriasis. ALT = alanine aminotransferase; GGT = gamma-glutamyltransferase; AST = aspartate aminotransferase; NEC = not elsewhere classified; SIB = suicidal ideation and behavior; MACE = major adverse cardiovascular events.

† TEAEs that occurred before week 12 are reported only for patients receiving the indicated dose.

‡ TEAEs reported from the time the patient started the indicated dose.

§ TEAEs while receiving BKZ at any dose.

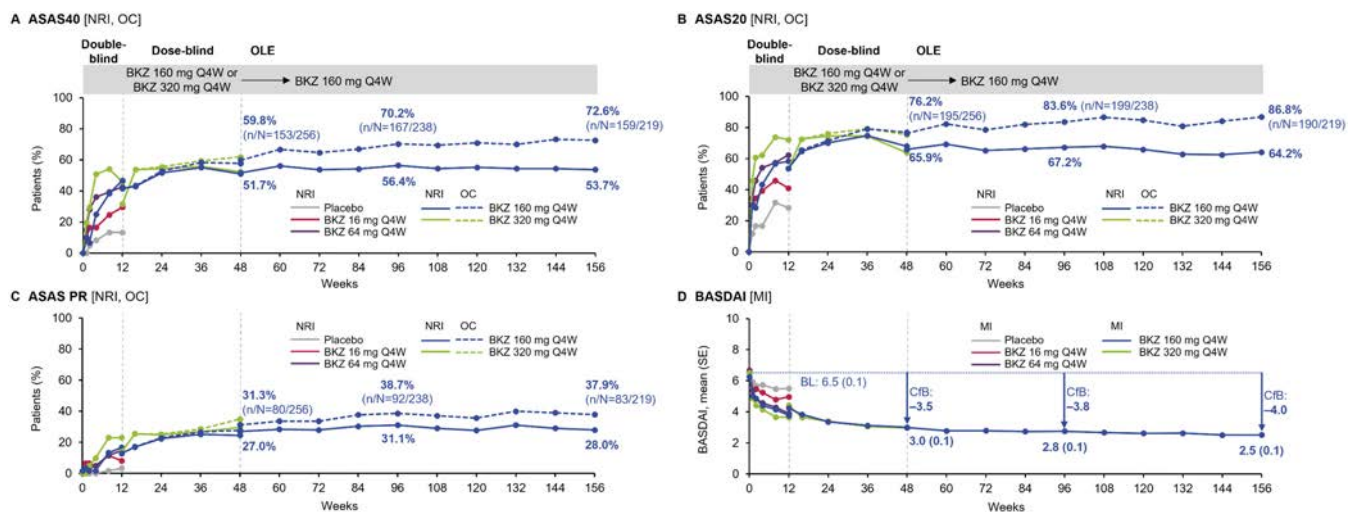


**Figure 1.** Assessment of SpondyloArthritis international Society (ASAS) criteria and Bath Ankylosing Spondylitis Disease Activity Index (BASDAI) outcomes in ankylosing spondylitis (AS) patients receiving bimekizumab (BKZ) or placebo during weeks 0–12 (full analysis set;  $n = 303$ ) and patients receiving BKZ during weeks 12–156 (dose-blind set;  $n = 296$ ). Data are shown for 299 patients (297 patients for the BASDAI) at week 12 for the double-blind groups, and data are shown for 296 patients (295 patients for the BASDAI) at week 12 for the dose-blind groups. In **A–C**, proportions of patients achieving a response on the ASAS criteria for 40% improvement (**A**), the ASAS criteria for 20% improvement (**B**), and the ASAS criteria for partial remission (PR) (**C**) were determined using nonresponder imputation (NRI) analysis and observed case (OC) analysis. In the NRI analyses, patients who did not enter the open-label extension (OLE) study were considered nonresponders from week 48 onwards. In **D**, proportions of patients achieving improvement in BASDAI score were determined using multiple imputation (MI) analysis. For BASDAI, baseline (BL) mean (blue dotted line) is shown for the total dose-blind set. Q4W = every 4 weeks; CfB = change from baseline.

responses were similarly sustained from week 48 to week 156 in the NRI analysis, with 65.9% of patients (76.2% of observed cases) achieving ASAS20 and 27.0% of patients (31.3% of observed cases) achieving ASAS partial remission responses at week 48, compared to 64.2% (86.8% of observed cases) and 28.0% (37.9% of observed cases) at week 156 (Figures 1B and C). Sustained ASAS responses through week 156 were comparable across patients who received 160 mg and patients who received 320 mg of bimekizumab every 4 weeks during the dose-blind period (Table 3).

The mean  $\pm$  SEM ASDAS at baseline was  $3.9 \pm 0.1$ ; in the MI analysis, mean  $\pm$  SEM ASDAS improved to week 48 ( $2.1 \pm 0.1$ ) and to week 156 ( $1.9 \pm 0.1$ ) (Figure 2A). In NRI analysis, major improvement in the ASDAS was achieved by 38.9% of patients at week 48, and major improvement in ASDAS was maintained by 39.9% of patients at week 156. In the observed case analysis, percentages of patients achieving major improvement in ASDAS increased from 44.9% of patients at week 48 to 54.9% of patients at week 156 (Figure 2B). ASDAS  $<2.1$  and ASDAS showing inactive disease were also sustained in weeks 48–156 in the NRI analysis: 49.3% of patients (57.0% of observed cases) had achieved ASDAS  $<2.1$  and 19.6% of patients (22.7% of observed cases) had achieved ASDAS showing inactive disease at week 48, compared to 49.0% (67.4% of observed cases) and 24.0% (33.0% of observed cases) at week 156, respectively (Figures 2D and 3).

Among patients who received bimekizumab 160 mg every 4 weeks through 156 weeks ( $n = 60$ ), individual patient-level

improvements in ASDAS were largely maintained through successive study visits (Supplementary Figure 4, <http://onlinelibrary.wiley.com/doi/10.1002/art.42282>). Most patients who achieved low disease activity or inactive disease at week 48 remained in these states at week 156. Additionally, patients who had ASDAS high disease activity at baseline tended to achieve ASDAS low disease activity earlier than those who had very high disease activity at baseline.

As with ASDAS, high baseline high-sensitivity CRP levels (mean 10.6 mg/liter [median 12.0 mg/liter]) improved substantially at week 48 (mean 3.0 mg/liter [median 3.6 mg/liter]) in the MI analysis and were sustained at week 156 (mean 2.5 mg/liter [median 2.9 mg/liter]). The mean  $\pm$  SEM BASDAI score at baseline was  $6.5 \pm 0.1$ ; in the MI analysis, BASDAI scores improved rapidly by week 48 (mean  $\pm$  SEM  $3.0 \pm 0.1$ ) and further improved by week 156 (mean  $\pm$  SEM  $2.5 \pm 0.1$ ) (Figure 1D). Following improvement in the mean  $\pm$  SEM BASMI score from  $4.7 \pm 0.1$  at baseline to  $3.9 \pm 0.1$  at week 48 (MI), spinal mobility was maintained at week 144 (mean  $\pm$  SEM BASMI score  $4.0 \pm 0.1$ ). Similar improvements occurred in mean  $\pm$  SEM MASES scores (MI) from baseline (mean  $\pm$  SEM  $4.4 \pm 0.2$ ) to week 48 (mean  $\pm$  SEM  $1.0 \pm 0.1$ ); this improvement was maintained at week 144 (mean  $\pm$  SEM MASES score  $0.7 \pm 0.1$ ) (Table 3 and Supplementary Figure 5, <http://onlinelibrary.wiley.com/doi/10.1002/art.42282>).

Improvements in physical function and health-related quality of life (HRQoL) seen at week 48 were similarly sustained with up to 3 years of bimekizumab treatment (Table 3). The mean  $\pm$  SEM BASFI score improved from  $5.7 \pm 0.1$  at baseline to  $3.1 \pm 0.1$  at

**Table 3.** Efficacy outcomes of bimekizumab (BKZ) treatment in ankylosing spondylitis patients to week 156\*

	BKZ 160 mg Q4W (dose-blind period) (n = 147) <sup>†</sup>		BKZ 320 mg Q4W (dose-blind period) (n = 149) <sup>†</sup>		Total (dose-blind period) (N = 296)	
	Imputed	OC	Imputed	OC	Imputed	OC
ASAS20 by NRI, no. (%)						
Week 48	100 (68.0)	100/130 (76.9)	95 (63.8)	95/126 (75.4)	195 (65.9)	195/256 (76.2)
Week 96	100 (68.0)	100/121 (82.6)	99 (66.4)	99/117 (84.6)	199 (67.2)	199/238 (83.6)
Week 156	97 (66.0)	97/114 (85.1)	93 (62.4)	93/105 (88.6)	190 (64.2)	190/219 (86.8)
ASAS40 by NRI, no. (%)						
Week 48	75 (51.0)	75/130 (57.7)	78 (52.3)	78/126 (61.9)	153 (51.7)	153/256 (59.8)
Week 96	84 (57.1)	84/121 (69.4)	83 (55.7)	83/117 (70.9)	167 (56.4)	167/238 (70.2)
Week 156	84 (57.1)	84/114 (73.7)	75 (50.3)	75/105 (71.4)	159 (53.7)	159/219 (72.6)
ASAS 5/6 by NRI, no. (%)						
Week 48	79 (53.7)	79/130 (60.8)	77 (51.7)	77/126 (61.1)	156 (52.7)	156/256 (60.9)
Week 96	75 (51.0)	75/121 (62.0)	79 (53.0)	79/116 (68.1)	154 (52.0)	154/237 (65.0)
Week 144	82 (55.8)	82/114 (71.9)	75 (50.3)	75/106 (70.8)	157 (53.0)	157/220 (71.4)
ASAS PR by NRI, no. (%)						
Week 48	36 (24.5)	36/130 (27.7)	44 (29.5)	44/126 (34.9)	80 (27.0)	80/256 (31.3)
Week 96	47 (32.0)	47/121 (38.8)	45 (30.2)	45/117 (38.5)	92 (31.1)	92/238 (38.7)
Week 156	46 (31.3)	46/114 (40.4)	37 (24.8)	37/105 (35.2)	83 (28.0)	83/219 (37.9)
ASDAS-CRP by MI, mean ± SEM/SD						
Baseline	3.9 ± 0.1	3.9 ± 0.8	4.0 ± 0.1	4.0 ± 0.8	3.9 ± 0.1	3.9 ± 0.8
Week 48	2.1 ± 0.1	2.1 ± 0.9	2.1 ± 0.1	2.0 ± 0.9	2.1 ± 0.1	2.0 ± 0.9
Week 96	2.0 ± 0.1	1.9 ± 0.9	2.0 ± 0.1	1.9 ± 0.8	2.0 ± 0.1	1.9 ± 0.9
Week 156	1.9 ± 0.1	1.8 ± 0.8	1.9 ± 0.1	1.8 ± 0.7	1.9 ± 0.1	1.8 ± 0.8
ASDAS-ID by NRI, no. (%)						
Week 48	28 (19.0)	28/130 (21.5)	30 (20.1)	30/126 (23.8)	58 (19.6)	58/256 (22.7)
Week 96	36 (24.5)	36/121 (29.8)	36 (24.2)	36/116 (31.0)	72 (24.3)	72/237 (30.4)
Week 156	43 (29.3)	43/113 (38.1)	28 (18.8)	28/102 (27.5)	71 (24.0)	71/215 (33.0)
ASDAS <2.1 by NRI, no. (%)						
Week 48	73 (49.7)	73/130 (56.2)	73 (49.0)	73/126 (57.9)	146 (49.3)	146/256 (57.0)
Week 96	80 (54.4)	80/121 (66.1)	73 (49.0)	73/116 (62.9)	153 (51.7)	153/237 (64.6)
Week 156	79 (53.7)	79/113 (69.9)	66 (44.3)	66/102 (64.7)	145 (49.0)	145/215 (67.4)
ASDAS major improvement by NRI, no. (%)						
Week 48	59 (40.1)	59/130 (45.4)	56 (37.6)	56/126 (44.4)	115 (38.9)	115/256 (44.9)
Week 96	65 (44.2)	65/121 (53.7)	60 (40.3)	60/116 (51.7)	125 (42.2)	125/237 (52.7)
Week 156	63 (42.9)	63/113 (55.8)	55 (36.9)	55/102 (53.9)	118 (39.9)	118/215 (54.9)
ASDAS-CII by NRI, no. (%)						
Week 48	99 (67.3)	99/130 (76.2)	101 (67.8)	101/126 (80.2)	200 (67.6)	200/256 (78.1)
Week 96	99 (67.3)	99/121 (81.8)	95 (63.8)	95/116 (81.9)	194 (65.5)	194/237 (81.9)
Week 156	92 (62.6)	92/113 (81.4)	88 (59.1)	88/102 (86.3)	180 (60.8)	180/215 (83.7)
BASDAI by MI, mean ± SEM/SD						
Baseline	6.4 ± 0.1	6.4 ± 1.4	6.6 ± 0.1	6.6 ± 1.5	6.5 ± 0.1	6.5 ± 1.4
Week 48	3.0 ± 0.2	2.8 ± 1.8	3.0 ± 0.2	2.9 ± 2.1	3.0 ± 0.1	2.8 ± 2.0
Week 96	2.7 ± 0.2	2.5 ± 1.8	2.8 ± 0.2	2.6 ± 2.0	2.8 ± 0.1	2.5 ± 1.9
Week 156	2.5 ± 0.2	2.3 ± 1.8	2.5 ± 0.2	2.3 ± 1.6	2.5 ± 0.1	2.3 ± 1.7

(Continued)

**Table 3.** (Cont'd)

	BKZ 160 mg Q4W (dose-blind period) (n = 147) <sup>†</sup>		BKZ 320 mg Q4W (dose-blind period) (n = 149) <sup>†</sup>		Total (dose-blind period) (N = 296)	
	Imputed	OC	Imputed	OC	Imputed	OC
BASDAI50 by NRI, no. (%)						
Week 48	72 (49.0)	72/130 (55.4)	77 (51.7)	77/126 (61.1)	149 (50.3)	149/256 (58.2)
Week 96	84 (57.1)	84/121 (69.4)	76 (51.0)	76/117 (65.0)	160 (54.1)	160/238 (67.2)
Week 156	79 (53.7)	79/114 (69.3)	77 (51.7)	77/105 (73.3)	156 (52.7)	156/219 (71.2)
BASFI by MI, mean ± SEM/SD						
Baseline	5.6 ± 0.2	5.6 ± 1.9	5.8 ± 0.2	5.8 ± 2.0	5.7 ± 0.1	5.7 ± 2.0
Week 48	3.1 ± 0.2	3.0 ± 2.0	3.2 ± 0.2	3.1 ± 2.4	3.1 ± 0.1	3.0 ± 2.2
Week 96	2.8 ± 0.2	2.7 ± 2.1	2.9 ± 0.2	2.8 ± 2.4	2.8 ± 0.1	2.7 ± 2.2
Week 156	2.7 ± 0.2	2.5 ± 2.0	2.9 ± 0.2	2.8 ± 2.2	2.8 ± 0.1	2.6 ± 2.1
BASMI by MI, mean ± SEM/SD						
Baseline	4.5 ± 0.1	4.5 ± 1.7	4.8 ± 0.1	4.8 ± 1.7	4.7 ± 0.1	4.7 ± 1.7
Week 48	3.9 ± 0.2	4.0 ± 1.8	3.9 ± 0.2	3.9 ± 1.8	3.9 ± 0.1	4.0 ± 1.8
Week 96	3.9 ± 0.1	4.0 ± 1.7	3.9 ± 0.2	4.0 ± 1.9	3.9 ± 0.1	4.0 ± 1.8
Week 144	4.0 ± 0.2	4.0 ± 1.7	4.0 ± 0.2	4.1 ± 2.0	4.0 ± 0.1	4.1 ± 1.8
MASES by MI, mean ± SEM/SD <sup>‡</sup>						
Baseline	4.0 ± 0.3	4.0 ± 2.7	4.9 ± 0.3	4.9 ± 3.2	4.4 ± 0.2	4.4 ± 3.0
Week 48	0.8 ± 0.2	0.7 ± 1.5	1.1 ± 0.2	1.0 ± 1.9	1.0 ± 0.1	0.8 ± 1.7
Week 96	0.7 ± 0.2	0.5 ± 1.4	1.0 ± 0.2	0.9 ± 2.3	0.8 ± 0.1	0.6 ± 1.9
Week 144	0.5 ± 0.1	0.4 ± 1.0	0.9 ± 0.2	0.7 ± 1.8	0.7 ± 0.1	0.5 ± 1.4
hsCRP by MI, geometric mean (median)						
Baseline	11.1 (13.1)	11.1 (13.1) <sup>S</sup>	10.2 (11.5)	10.2 (11.4) <sup>S</sup>	10.6 (12.0)	10.6 (12.0) <sup>S</sup>
Week 48	3.3 (3.8)	3.3 (3.5)	2.8 (3.4)	3.0 (3.5)	3.0 (3.6)	3.1 (3.5)
Week 96	2.8 (3.0)	2.8 (2.8)	2.3 (2.7)	2.5 (2.6)	2.5 (2.8)	2.7 (2.7)
Week 156	2.5 (2.7)	2.4 (2.3)	2.5 (3.0)	2.7 (2.7)	2.5 (2.9)	2.5 (2.5)
Total spinal pain by MI, mean ± SEM/SD						
Baseline	6.9 ± 0.2	6.9 ± 1.9	7.3 ± 0.1	7.3 ± 1.6	7.1 ± 0.1	7.1 ± 1.8
Week 48	3.2 ± 0.2	3.0 ± 2.1	3.1 ± 0.2	3.1 ± 2.3	3.1 ± 0.1	3.0 ± 2.2
Week 96	2.7 ± 0.2	2.5 ± 2.1	2.6 ± 0.2	2.5 ± 2.1	2.7 ± 0.1	2.5 ± 2.1
Week 156	2.6 ± 0.2	2.5 ± 2.0	2.5 ± 0.2	2.3 ± 1.8	2.5 ± 0.1	2.4 ± 1.9
Neck, back or hip pain (BASDAI question 2) by MI, mean ± SEM/SD						
Baseline	7.4 ± 0.1	7.4 ± 1.4	7.6 ± 0.1	7.6 ± 1.5	7.5 ± 0.1	7.5 ± 1.4
Week 48	3.5 ± 0.2	3.4 ± 2.3	3.4 ± 0.2	3.3 ± 2.4	3.4 ± 0.2	3.3 ± 2.4
Week 96	3.1 ± 0.2	2.9 ± 2.2	3.2 ± 0.2	3.0 ± 2.5	3.1 ± 0.2	3.0 ± 2.3
Week 156	2.8 ± 0.2	2.6 ± 2.1	2.8 ± 0.2	2.5 ± 1.9	2.8 ± 0.1	2.6 ± 2.0
Fatigue (BASDAI question 1) by MI, mean ± SEM/SD						
Baseline	6.6 ± 0.1	6.6 ± 1.6	6.7 ± 0.1	6.7 ± 1.7	6.7 ± 0.1	6.7 ± 1.7
Week 48	3.6 ± 0.2	3.5 ± 2.2	3.6 ± 0.2	3.5 ± 2.4	3.6 ± 0.1	3.5 ± 2.3
Week 96	3.0 ± 0.2	2.8 ± 2.0	3.5 ± 0.2	3.2 ± 2.3	3.3 ± 0.2	3.0 ± 2.1
Week 156	2.9 ± 0.2	2.7 ± 2.0	2.9 ± 0.2	2.7 ± 2.0	2.9 ± 0.1	2.7 ± 2.0
ASQoL by MI, mean ± SEM/SD						
Baseline	8.3 ± 0.4	8.3 ± 4.3	9.1 ± 0.4	9.1 ± 4.3	8.7 ± 0.3	8.7 ± 4.3
Week 48	3.7 ± 0.3	3.5 ± 3.9	3.6 ± 0.3	3.4 ± 4.0	3.7 ± 0.2	3.4 ± 3.9
Week 96	3.4 ± 0.3	3.0 ± 3.7	3.3 ± 0.3	2.7 ± 3.3	3.3 ± 0.2	2.9 ± 3.5
Week 144	3.1 ± 0.3	2.8 ± 3.7	3.1 ± 0.3	2.5 ± 3.0	3.1 ± 0.2	2.7 ± 3.4

(Continued)

**Table 3.** (Cont'd)

	BKZ 160 mg Q4W (dose-blind period) (n = 147) <sup>†</sup>		BKZ 320 mg Q4W (dose-blind period) (n = 149) <sup>†</sup>		Total (dose-blind period) (N = 296)	
	Imputed	OC	Imputed	OC	Imputed	OC
SF-36 PCS by MI, mean ± SEM/SD						
Baseline	32.6 ± 0.7	32.6 ± 7.9	31.9 ± 0.6	31.9 ± 7.4	32.3 ± 0.5	32.3 ± 7.7
Week 48	44.3 ± 0.8	44.8 ± 9.1	44.0 ± 0.7	44.5 ± 8.6	44.1 ± 0.5	44.6 ± 8.8
Week 96	45.4 ± 0.8	46.3 ± 9.0	44.6 ± 0.8	45.1 ± 9.0	45.0 ± 0.6	45.8 ± 9.0
Week 144	45.8 ± 0.8	46.6 ± 8.6	44.9 ± 0.8	45.4 ± 8.5	45.3 ± 0.6	46.1 ± 8.6
SF-36 MCS by MI, mean ± SEM/SD						
Baseline	54.5 ± 0.7	54.5 ± 8.4	53.8 ± 0.7	53.8 ± 8.2	54.1 ± 0.5	54.1 ± 8.3
Week 48	56.0 ± 0.6	56.3 ± 7.3	57.1 ± 0.6	57.4 ± 6.7	56.6 ± 0.4	56.8 ± 7.0
Week 96	56.3 ± 0.7	56.6 ± 8.0	57.0 ± 0.6	57.1 ± 6.7	56.6 ± 0.4	56.9 ± 7.4
Week 144	56.5 ± 0.7	57.2 ± 7.6	57.3 ± 0.6	57.5 ± 6.7	56.9 ± 0.4	57.4 ± 7.2

\* Data are reported as either imputed (multiple imputation [MI]) based on the missing at random assumption or nonresponder imputation [NRI] or as observed case (OC). For continuous variables, mean ± SEM is reported for MI analyses and mean ± SD is reported for OC analyses. ASAS20 = Assessment of SpondyloArthritis international Society criteria for 20% improvement; ASAS40 = ASAS criteria for 40% improvement; ASAS PR = ASAS partial remission; ASDAS = Ankylosing Spondylitis Disease Activity Score; ASDAS-CII = ASDAS clinically important improvement; ASDAS-CRP = ASDAS using C-reactive protein; ASDAS-ID = ASDAS inactive disease; ASQoL = Ankylosing Spondylitis Quality of Life; BASDAI = Bath Ankylosing Spondylitis Disease Activity Index; BASDAI50 = BASDAI 50% response; BASFI = Bath Ankylosing Spondylitis Function Index; BASMI = Bath Ankylosing Spondylitis Metrology Index; SF-36 = Short Form-36; PCS = physical component summary; MCS = mental component summary.

<sup>†</sup> Patients received BKZ 16 mg, 64 mg, 160 mg, or 320 mg, or placebo, every 4 weeks (Q4W) up to week 12, at which point patients receiving BKZ 16 mg or 64 mg, or placebo, were re-randomized to receive BKZ 160 mg or 320 mg Q4W from week 12 to week 48 (dose-blind period). Thereafter, during the open-label extension (OLE) period up to week 156, all patients received 160 mg Q4W, regardless of prior dosing regimen before the OLE.

<sup>‡</sup> Among patients who had Maastricht Ankylosing Spondylitis Enthesitis Score (MASES) >0 at baseline, data were available as follows: n = 100 in the dose-blind BKZ 160 mg group, n = 94 in the dose-blind BKZ 320 mg group, and n = 194 in the total dose-blind group.

<sup>§</sup> Among patients with high-sensitivity C-reactive protein (hsCRP) values in the OC analysis at baseline, data were available as follows: n = 146 in the dose-blind BKZ 160 mg group, n = 148 in the dose-blind BKZ 320 mg group, and n = 294 in the total dose-blind group.



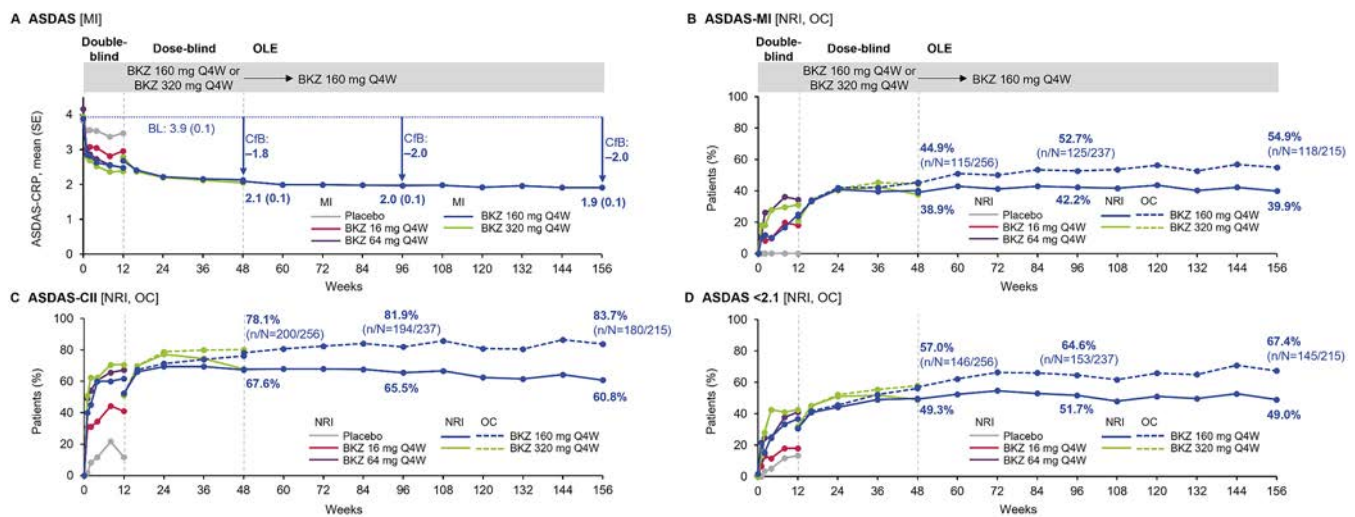


**Figure 2.** Ankylosing Spondylitis Disease Activity Score (ASDAS) outcomes to week 156. ASDAS outcomes in AS patients receiving BKZ or placebo during weeks 0–12 (full analysis set;  $n = 303$ ) and patients receiving BKZ during weeks 12–156 (dose-blind set;  $n = 296$ ). In **A**, improvements in the mean  $\pm$  SEM ASDAS using C-reactive protein were determined using multiple imputation analysis. Baseline mean score (blue dotted line) is shown for the total dose-blind set. In **B–D**, proportions of patients achieving major improvement in ASDAS (ASDAS-MI) (**B**), proportions of patients achieving clinically important improvement in ASDAS (ASDAS-CII) (**C**), and proportions of patients achieving ASDAS scores  $<2.1$  (**D**) were determined using NRI and OC analyses. In the NRI analyses, patients who did not enter the OLE study were considered nonresponders from week 48 onward. See Figure 1 for other definitions. Q4W = every 4 weeks; C/FB = change from baseline. Color figure can be viewed in the online issue, which is available at <http://onlinelibrary.wiley.com/doi/10.1002/art.42282/abstract>.

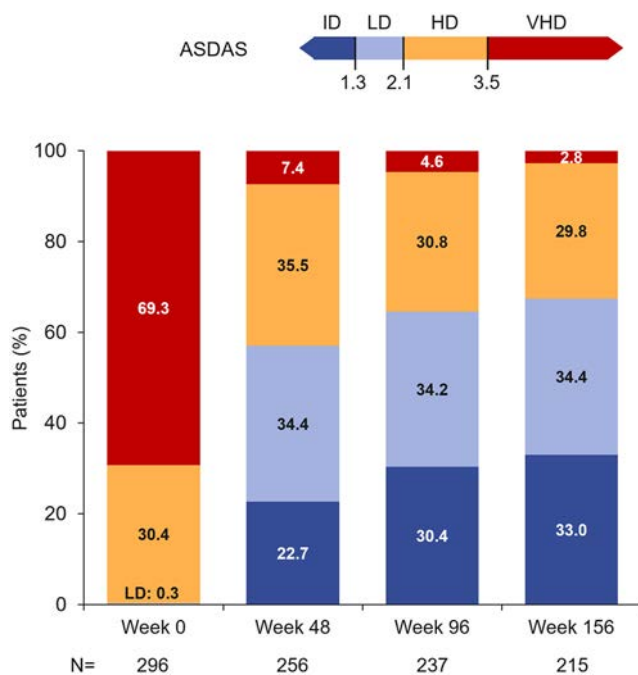


**Figure 3.** ASDAS disease states over time up to week 156. Proportions of AS patients in the dose-blind set ( $n = 296$ ) showing inactive disease (ID), low disease (LD) activity, high disease (HD) activity, and very high disease (VHD) activity. Data are reported as observed case (OC). See Figure 1 for other definitions. Color figure can be viewed in the online issue, which is available at <http://onlinelibrary.wiley.com/doi/10.1002/art.42282/abstract>.

week 48 and was sustained at  $2.8 \pm 0.1$  at week 156. Mean  $\pm$  SEM baseline scores for the SF-36 PCS (mean  $\pm$  SEM  $32.3 \pm 0.5$ ) and the ASQoL (mean  $\pm$  SEM  $8.7 \pm 0.3$ ) were indicative of impaired physical function and reduced HRQoL in this patient population with longstanding disease. At week 48 in the MI analysis, mean  $\pm$  SEM SF-36 PCS scores had improved to  $44.1 \pm 0.5$  and mean  $\pm$  SEM ASQoL scores had improved to  $3.7 \pm 0.2$ ; these improvements were maintained up to week 144, where the mean  $\pm$  SEM scores were  $45.3 \pm 0.6$  and  $3.1 \pm 0.2$ , respectively. In contrast, the mean baseline SF-36 MCS score (mean  $\pm$  SEM  $54.1 \pm 0.5$ ) was suggestive of nonimpaired psychological function (as it was greater than the US general population mean value of 50) and was maintained over 144 weeks of bimekizumab treatment (39).

## DISCUSSION

In this first report of the BE AGILE OLE study, inhibition of IL-17F in addition to IL-17A with bimekizumab treatment for up to 3 years in patients with active AS was found to be well tolerated, with efficacy sustained in the long term. The safety profile of bimekizumab was found to be in line with previous observations, with no new safety signals or increased risk identified following up to 3 years of cumulative exposure to bimekizumab (29). These long-term results support and extend previous 1-year findings that demonstrated the efficacy and tolerability of bimekizumab in patients with AS (29).

Across weeks 0–156, study discontinuations due to TEAEs were infrequent, with only 2 patients discontinuing due to lack of efficacy; incidence rates of serious infections and injection site reactions remained low. The most frequently reported TEAEs over 3 years, which included nasopharyngitis, upper respiratory tract infections, and bronchitis, were consistent with previous 1-year studies of bimekizumab in AS and PsA patients (28,29).

A recent meta-analysis of IL-17A inhibitor trials in AS patients found that the risk of serious adverse events and serious infections did not differ significantly between active treatment and placebo (40). However, inhibition of IL-17 is known to increase susceptibility to mucosal infections by *Candida* species, which reflects the role of type 17 immunity at the oral mucosa (41–44). Indeed, increased rates of infections and candidiasis have been associated with IL-17A inhibitor treatment in patients with AS and other chronic inflammatory diseases (45,46). Here, we report data which indicate that *Candida* infections were among the most commonly reported TEAEs. While the EAIR of *Candida* infections (3.7 per 100 patient-years) in this phase IIb study was higher than those in phase III studies of IL-17A inhibitors in AS patients (12–14,47,48), the majority of cases in this study were oral candidiasis and only 1 case led to study discontinuation. Furthermore, all fungal infections were of mild or moderate intensity, localized (none were systemic), and easily managed, and none were serious. Overall, findings on safety suggest that there are no new safety concerns with increased cumulative bimekizumab exposure in patients with AS over a time period of 3 years.

IBD is a known extramusculoskeletal manifestation of axial SpA, and is also thought to be associated with exposure to IL-17A inhibitors (49). The exact mechanism by which IL-17 inhibition may exacerbate IBD has not been elucidated, with contradictory findings regarding the absolute risk reported in some epidemiologic studies (50). Of the 303 patients in the study, 7 had a history of IBD. Active IBD was infrequent with bimekizumab treatment across this 156-week study (occurring in 9 patients, including 2 with a history of IBD), and most patients who experienced IBD continued in the study. EAIRs of 0.5 cases of ulcerative colitis per 100 patient-years and 0.5 cases of Crohn's disease per 100 patient-years with bimekizumab treatment were comparable to those reported in the pooled analysis of the MEASURE 1–4 studies for patients receiving secukinumab for up to 4 years (EAIR 0.2 cases of ulcerative colitis per 100 patient-years and EAIR 0.4 cases of Crohn's disease per 100 patient-years) (51). EAIRs of ulcerative colitis and Crohn's disease with bimekizumab treatment were also comparable to those reported in a pooled analysis of the COAST-V and COAST-W studies for patients receiving ixekizumab for over 1 year (EAIR 0.4 cases of ulcerative colitis per 100 patient-years and EAIR 0.8 cases of Crohn's disease per 100 patient-years) (14). These results suggest that dual inhibition of IL-17F and IL-17A does not impact IBD flares relative to IL-17A inhibition

alone; however, results from phase III studies are needed to confirm these findings.

Anterior uveitis is another extramusculoskeletal manifestation of axial SpA. Incidence of anterior uveitis across 156 weeks was low, with only 6 patients presenting with a flare, 3 of whom had histories of anterior uveitis prior to entry in the BE AGILE study. The EAIR of 0.7 cases of anterior uveitis per 100 patient-years for treatment with bimekizumab was lower than the EAIR of 1.4 cases of anterior uveitis per 100 patient-years reported in the pooled analysis of the MEASURE 1, MEASURE 2, and MEASURE 3 studies for up to 4 years of treatment with secukinumab (52), as well as a 1-year EAIR of 3.9 cases of anterior uveitis per 100 patient-years reported in a pooled analysis of the COAST-V and COAST-W studies for treatment with ixekizumab (14). The recent elucidation of a feedback loop through which the inhibition of IL-17A up-regulates IL-17F suggests that the dual inhibition of both cytokines could potentially confer additional benefits in the control of AS and its manifestations, including anterior uveitis (53). However, this prediction would need to be confirmed in subsequent studies of bimekizumab.

Efficacy analyses demonstrated that clinical outcomes were sustained over the 3-year OLE study following the rapid and clinically meaningful improvements occurring within the first year of bimekizumab treatment. Under the strictest method for handling missing data (NRI), the proportion of patients having achieved ASAS40 was >50% at all timepoints through weeks 48–156. At the time of enrolment, all patients enrolled had high or very high disease activity. By week 156, approximately half of the patient population had achieved ASDAS disease activity scores of <2.1, and approximately a quarter of the patient population had achieved ASDAS scores showing inactive disease and ASAS scores showing partial remission, demonstrating the stringent disease control attained with bimekizumab. Rapid and sustained reductions in the severity of inflammation were observed, with substantial reductions in high-sensitivity CRP levels from baseline to week 48, and low levels sustained at week 156. Additionally, BASDAI scores were sustained at very low levels with long-term bimekizumab treatment, reflecting substantial reductions, relative to baseline, across disease symptoms including spinal pain, fatigue, and stiffness. Mobility, physical function, and improvements in HRQoL achieved at week 48 were also sustained during the following 2 years of treatment with bimekizumab in this study.

The demonstrated long-term tolerability and efficacy of treatment with bimekizumab were further supported by the high rate of patient retention, with week 156 completed by nearly three-quarters of the patients randomized at baseline, or ~88% of those who enrolled in the OLE study. Efficacy at week 48 was similar among patients receiving 160 mg or 320 mg of bimekizumab every 4 weeks, and no appreciable decrease in efficacy was observed in patients who reduced their dosage from 320 mg to 160 mg every 4 weeks at the start of the OLE study.

A limitation of this analysis is the lack of an active or placebo comparator for bimekizumab during the OLE study. Placebo was only administered up to week 12, after which all patients received 160 mg or 320 mg of bimekizumab every 4 weeks. Study discontinuations also presented a limitation by potentially biasing observed results. However, patient retention was high through 3 years and imputation methods were implemented to combat potential bias, notably through NRI, the most conservative imputation approach for analyzing binary variables which may even underestimate true efficacy. We note that the underlying assumption of the MI analyses for continuous variables—that data were missing at random—may not have been met, and therefore the possibility of bias in the MI analysis cannot be eliminated. Another limitation was the absence of MRI assessment after week 48 to evaluate the long-term impact of bimekizumab on active inflammation of the spine and sacroiliac joint. In addition, as with most phase II studies of AS, no spinal radiographs were obtained during the study, and hence the impact of bimekizumab on spinal progression could not be evaluated. This will be an important area of focus in future studies.

A key strength of this phase IIb study is its 5-year duration and relatively large sample size of patients, which allows the long-term systematic monitoring of adverse events and significantly contributes to the growing evidence base for the safety and tolerability of bimekizumab in patients with AS (29,54). This study also provides the most comprehensive and long-term evidence to date of the efficacy of bimekizumab in patients with AS. The BE AGILE study and its OLE study demonstrate the sustainability of treatment effect with this first-in-class dual inhibitor of IL-17A and IL-17F. The OLE study is currently ongoing and will allow assessment of 5-year safety and efficacy outcomes upon completion. This will supplement phase III trials that are currently underway to assess bimekizumab dosages of 160 mg every 4 weeks in axial SpA patients with active nonradiographic axial SpA (ClinicalTrials.gov identifier: NCT03928704), and in patients with active AS (ClinicalTrials.gov identifier: NCT03928743). These trials will further evaluate the clinical benefits that may result from dual inhibition of IL-17A and IL-17F.

In conclusion, the safety of bimekizumab over 3 years of treatment was consistent with previous 48-week results (29). Bimekizumab delivered sustained, long-term efficacy in patients with AS, including reduced disease activity and improved patient function and quality of life. Overall, these results support bimekizumab as a promising potential treatment option in AS.

## ACKNOWLEDGMENTS

We thank the patients and the investigators and their teams who took part in this study. We also acknowledge Heather Edens, PhD (UCB Pharma), for publication coordination and James Evry, MSc, and Alexandra Quinn-Savory, MPH (Costello Medical, UK), for medical writing and editorial assistance based on the authors' input and direction.

This article was based on the original BE AGILE study (ClinicalTrials.gov identifier: NCT02963506) and its open-label extension study (ClinicalTrials.gov identifier: NCT03355573) sponsored by UCB Pharma. Support for third-party writing assistance for this article was funded by UCB Pharma in accordance with Good Publication Practice (GPP3) guidelines (<http://www.ismpp.org/gpp3>). Open Access funding enabled and organized by Projekt DEAL.

## ROLE OF THE STUDY SPONSOR

UCB Pharma facilitated the study design, funded writing assistance for the manuscript, and reviewed and approved the manuscript prior to submission. The authors independently collected the data, interpreted the results, and had the final decision to submit the manuscript for publication. Publication of this article was contingent upon approval by UCB Pharma.

## AUTHOR CONTRIBUTIONS

All authors were involved in drafting the article or revising it critically for important intellectual content, and all authors approved the final version to be published. Dr. Baraliakos had full access to all of the data in the study and takes responsibility for the integrity of the data and the accuracy of the data analysis.

**Study conception and design.** Baraliakos, Deodhar, Dougados, Gensler, Molto, Ramiro, Kivitz, Poddubnyy, Oortgiesen, Vaux, Fleurinck, Shepherd-Smith, de la Loge, de Peyrecave, van der Heijde.

**Acquisition of data.** Oortgiesen, Vaux.

**Analysis and interpretation of data.** Baraliakos, Deodhar, Dougados, Gensler, Molto, Ramiro, Kivitz, Poddubnyy, Oortgiesen, Vaux, Fleurinck, Shepherd-Smith, de la Loge, de Peyrecave, van der Heijde.

## REFERENCES





1. Sieper J, Poddubnyy D. Axial spondyloarthritis. *Lancet* 2017;390:73–84.
2. Robinson PC, van der Linden S, Khan MA, Taylor WJ. Axial spondyloarthritis: concept, construct, classification, and implications for therapy [review]. *Nat Rev Rheumatol* 2021;17:109–18.
3. Landewé R, Dougados M, Mielants H, van der Tempel H, van der Heijde D. Physical function in ankylosing spondylitis is independently determined by both disease activity and radiographic damage of the spine. *Ann Rheum Dis* 2009;68:863–7.
4. Law L, Rehnman JB, Deminger A, Klingberg E, Jacobsson LT, Forsblad-d'Elia H. Factors related to health-related quality of life in ankylosing spondylitis, overall and stratified by sex. *Arthritis Res Ther* 2018;20:284.
5. Li Y, Zhang S, Zhu J, Du X, Huang F. Sleep disturbances are associated with increased pain, disease activity, depression, and anxiety in ankylosing spondylitis: a case-control study. *Arthritis Res Ther* 2012;14:R215.
6. Machado P, Landewé R, Braun J, Hermann KG, Baraliakos X, Baker D, et al. A stratified model for health outcomes in ankylosing spondylitis. *Ann Rheum Dis* 2011;70:1758–64.
7. Sari I, Haroon N. Radiographic progression in ankylosing spondylitis: from prognostication to disease modification [review]. *Curr Rheumatol Rep* 2018;20:82.
8. Sieper J, Poddubnyy D, Miossec P. The IL-23–IL-17 pathway as a therapeutic target in axial spondyloarthritis [review]. *Nat Rev Rheumatol* 2019;15:747–57.
9. Torgutalp M, Poddubnyy D. IL-17 inhibition in axial spondyloarthritis: current and future perspectives [review]. *Expert Opin Biol Ther* 2019;19:631–41.

10. Ward MM, Deodhar A, Gensler LS, Dubreuil M, Yu D, Khan MA, et al. 2019 Update of the American College of Rheumatology/Spondylitis Association of America/Spondyloarthritis Research and Treatment Network recommendations for the treatment of ankylosing spondylitis and nonradiographic axial spondyloarthritis. *Arthritis Rheumatol* 2019;71:1599–613.
11. Van der Heijde D, Ramiro S, Landewé R, Baraliakos X, Van den Bosch F, Sepriano A, et al. 2016 update of the ASAS-EULAR management recommendations for axial spondyloarthritis. *Ann Rheum Dis* 2017;76:978–91.
12. Baraliakos X, Braun J, Deodhar A, Poddubnyy D, Kivitz A, Tahir H, et al. Long-term efficacy and safety of secukinumab 150 mg in ankylosing spondylitis: 5-year results from the phase III MEASURE 1 extension study. *RMD Open* 2019;5:e001005.
13. Marzo-Ortega H, Sieper J, Kivitz AJ, Blanco R, Cohen M, Pavelka K, et al. 5-year efficacy and safety of secukinumab in patients with ankylosing spondylitis: end-of-study results from the phase 3 MEASURE 2 trial. *Lancet Rheumatol* 2020;2:e339–46.
14. Dougados M, Wei JC, Landewé R, Sieper J, Baraliakos X, Van den Bosch F, et al. Efficacy and safety of ixekizumab through 52 weeks in two phase 3, randomised, controlled clinical trials in patients with active radiographic axial spondyloarthritis (COAST-V and COAST-W). *Ann Rheum Dis* 2020;79:176–85.
15. Braun J, Kiltz U, Deodhar A, Tomita T, Dougados M, Bolce R, et al. POS0912 Long-term treatment with ixekizumab in patients with axial spondyloarthritis: two-year results from COAST-Y. *Ann Rheum Dis* 2021;80 Suppl:716–7.
16. Wei JC, Kim TH, Kishimoto M, Ogusu N, Jeong H, Kobayashi S, et al. Efficacy and safety of brodalumab, an anti-IL17RA monoclonal antibody, in patients with axial spondyloarthritis: 16-week results from a randomised, placebo-controlled, phase 3 trial. *Ann Rheum Dis* 2021;80:1014–21.
17. Hymowitz SG, Filvaroff EH, Yin JP, Lee J, Cai L, Risser P, et al. IL-17s adopt a cystine knot fold: structure and activity of a novel cytokine, IL-17F, and implications for receptor binding. *Embo J* 2001;20:5332–41.
18. Yang XO, Chang SH, Park H, Nurieva R, Shah B, Acero L, et al. Regulation of inflammatory responses by IL-17F. *J Exp Med* 2008;205:1063–75.
19. Glatt S, Baeten D, Baker T, Griffiths M, Ionescu L, Lawson AD, et al. Dual IL-17A and IL-17F neutralisation by bimekizumab in psoriatic arthritis: evidence from preclinical experiments and a randomised placebo-controlled clinical trial that IL-17F contributes to human chronic tissue inflammation. *Ann Rheum Dis* 2018;77:523–32.
20. Yermenko N. Out of the shadow of interleukin-17A: the role of interleukin-17F and other interleukin-17 family cytokines in spondyloarthritis. *Curr Opin Rheumatol* 2021;33:333–40.
21. Bridgwood C, Russell T, Watad A, Rowe H, Zhou Q, Khan A, et al. IL-17A and IL-17F are secreted by enthesis T cells and synergize with TNF to induce CCL20 from entheseal stromal cells. *Ann Rheum Dis* 2019;78 Suppl:274.
22. Shah M, Maroof A, Gikas P, Mittal G, Keen R, Baeten D, et al. Dual neutralisation of IL-17F and IL-17A with bimekizumab blocks inflammation-driven osteogenic differentiation of human periosteal cells. *RMD Open* 2020;6:e001306.
23. Papp KA, Merola JF, Gottlieb AB, Griffiths CE, Cross N, Peterson L, et al. Dual neutralization of both interleukin 17A and interleukin 17F with bimekizumab in patients with psoriasis: results from BE ABLE 1, a 12-week randomized, double-blinded, placebo-controlled phase 2b trial. *J Am Acad Dermatol* 2018;79:277–86.
24. Gordon KB, Foley P, Krueger JG, Pinter A, Reich K, Vender R, et al. Bimekizumab efficacy and safety in moderate to severe plaque psoriasis (BE READY): a multicentre, double-blind, placebo-controlled, randomised withdrawal phase 3 trial. *Lancet* 2021;397:475–86.
25. Reich K, Warren RB, Lebwohl M, Gooderham M, Strober B, Langley RG, et al. Bimekizumab versus secukinumab in plaque psoriasis. *N Engl J Med* 2021;385:142–52.
26. Reich K, Papp KA, Blauvelt A, Langley RG, Armstrong A, Warren RB, et al. Bimekizumab versus ustekinumab for the treatment of moderate to severe plaque psoriasis (BE VIVID): efficacy and safety from a 52-week, multicentre, double-blind, active comparator and placebo controlled phase 3 trial. *Lancet* 2021;397:487–98.
27. Warren RB, Blauvelt A, Bagel J, Papp KA, Yamauchi P, Armstrong A, et al. Bimekizumab versus adalimumab in plaque psoriasis. *N Engl J Med* 2021;385:130–41.
28. Ritchlin CT, Kavanaugh A, Merola JF, Schett G, Scher JU, Warren RB, et al. Bimekizumab in patients with active psoriatic arthritis: results from a 48-week, randomised, double-blind, placebo-controlled, dose-ranging phase 2b trial. *Lancet* 2020;395:427–40.
29. Van der Heijde D, Gensler LS, Deodhar A, Baraliakos X, Poddubnyy D, Kivitz A, et al. Dual neutralisation of interleukin-17A and interleukin-17F with bimekizumab in patients with active ankylosing spondylitis: results from a 48-week phase IIb, randomised, double-blind, placebo-controlled, dose-ranging study. *Ann Rheum Dis* 2020;79:595–604.
30. Helliwell PS, Doward L, Whalley D, et al. Psychometric and scaline properties of a new quality of life instrument specific to ankylosing spondylitis [abstract]. *Arthritis Rheum* 1999;42 Suppl:S72.
31. Ware JE Jr, Snow KK, Kosinski M, et al. SF-36 health survey: manual and interpretation guide. Boston: The Health Institute, New England Medical Center; 1993.
32. Jenkinson TR, Mallorie PA, Whitelock HC, et al. Defining spinal mobility in ankylosing spondylitis (AS): the Bath AS Metrology Index. *J Rheumatol* 1994;21:1694–8.
33. Heuft-Dorenbosch L, Spoorenberg A, van Tubergen A, et al. Assessment of enthesitis in ankylosing spondylitis. *Ann Rheum Dis* 2003;62:127–32.
34. Anderson JJ, Baron G, van der Heijde D, et al. Ankylosing spondylitis assessment group preliminary definition of short-term improvement in ankylosing spondylitis. *Arthritis Rheum* 2001;44:1876–86.
35. Brandt J, Listing J, Sieper J, et al. Development and preselection of criteria for short term improvement after anti-TNF alpha treatment in ankylosing spondylitis. *Ann Rheum Dis* 2004;63:1438–44.
36. Lukas C, Landewé R, Sieper J, et al. Development of an ASAS-endorsed disease activity score (ASDAS) in patients with ankylosing spondylitis. *Ann Rheum Dis* 2009;68:18–24.
37. Garrett S, Jenkinson T, Kennedy LG, et al. A new approach to defining disease status in ankylosing spondylitis: the Bath Ankylosing Spondylitis Disease Activity Index. *J Rheumatol* 1994;21:2286–91.
38. Calin A, Garrett S, Whitelock H, et al. A new approach to defining functional ability in ankylosing spondylitis: the development of the Bath Ankylosing Spondylitis Functional Index. *J Rheumatol* 1994;21:2281–5.
39. Ware J. SF-36 health survey: manual and interpretation guide. Boston, MA: The Health Institute, New England Medical Center; 1993.
40. Wang P, Zhang S, Hu B, Liu W, Lv X, Chen S, et al. Efficacy and safety of interleukin-17A inhibitors in patients with ankylosing spondylitis: a systematic review and meta-analysis of randomized controlled trials. *Clin Rheumatol* 2021;40:3053–65.
41. Blauvelt A, Lebwohl MG, Bissonnette R. IL-23/IL-17A dysfunction phenotypes inform possible clinical effects from anti-IL-17A therapies. *J Invest Dermatol* 2015;135:1946–53.
42. Conti HR, Gaffen SL. IL-17-mediated immunity to the opportunistic fungal pathogen *Candida albicans*. *J Immunol* 2015;195:780–8.

43. Gaffen SL, Moutsopoulos NM. Regulation of host-microbe interactions at oral mucosal barriers by type 17 immunity. *Sci Immunol* 2020;5.
44. Ishigame H, Kakuta S, Nagai T, Kadoki M, Nambu A, Komiyama Y, et al. Differential roles of interleukin-17A and -17F in host defense against mucocutaneous bacterial infection and allergic responses. *Immunity* 2009;30:108–19.
45. Saunte DM, Mrowietz U, Puig L, Zachariae C. Candida infections in patients with psoriasis and psoriatic arthritis treated with interleukin-17 inhibitors and their practical management. *Brit J Dermatol* 2017; 177:47–62.
46. Yin Y, Wang M, Liu M, Zhou E, Ren T, Chang X, et al. Efficacy and safety of IL-17 inhibitors for the treatment of ankylosing spondylitis: a systematic review and meta-analysis. *Arthritis Res Ther* 2020; 22:111.
47. Kivitz AJ, Wagner U, Dokoupilova E, Supronik J, Martin R, Tallozy Z, et al. Efficacy and safety of secukinumab 150mg with and without loading regimen in ankylosing spondylitis: 104-week results from MEASURE 4 study. *Rheumatol Ther* 2018;5:447–62.
48. Pavelka K, Kivitz AJ, Dokoupilova E, Blanco R, Maradiaga M, Tahir H, et al. Secukinumab 150/300 mg provides sustained improvements in the signs and symptoms of active ankylosing spondylitis: 3-year results from the phase 3 MEASURE 3 study. *ACR Open Rheumatol* 2020;2:119–27.
49. Fragoulis GE, Liava C, Daoussis D, Akriviadis E, Garyfallos A, Dimitroulas T. Inflammatory bowel diseases and spondyloarthropathies: from pathogenesis to treatment. *World J Gastroenterol* 2019;25:2162–76.
50. Penso L, Bergqvist C, Meyer A, Herlemont P, Weill A, Zureik M, et al. Risk of inflammatory bowel disease in patients with psoriasis and psoriatic arthritis/ankylosing spondylitis initiating interleukin-17 inhibitors: a nationwide population-based study using the French National Health Data System. *Arthritis Rheumatol* 2022;74:244–52.
51. Schreiber S, Colombel JF, Feagan BG, Reich K, Deodhar AA, McInnes IB, et al. Incidence rates of inflammatory bowel disease in patients with psoriasis, psoriatic arthritis and ankylosing spondylitis treated with secukinumab: a retrospective analysis of pooled data from 21 clinical trials. *Ann Rheum Dis* 2019;78:473–9.
52. Deodhar A, Mease PJ, McInnes IB, Baraliakos X, Reich K, Blauvelt A, et al. Long-term safety of secukinumab in patients with moderate-to-severe plaque psoriasis, psoriatic arthritis, and ankylosing spondylitis: integrated pooled clinical trial and post-marketing surveillance data. *Arthritis Res Ther* 2019;21:111.
53. Chong WP, Mattapallil MJ, Raychaudhuri K, Bing SJ, Wu S, Zhong Y, et al. The cytokine IL-17A limits Th17 pathogenicity via a negative feedback loop driven by autocrine induction of IL-24. *Immunity* 2020;53:384–97.
54. Buch MH, Silva-Fernandez L, Carmona L, Aletaha D, Christensen R, Combe B, et al. Development of EULAR recommendations for the reporting of clinical trial extension studies in rheumatology. *Ann Rheum Dis* 2015;74:963–9.



# Safety and Efficacy of Bimekizumab in Patients With Active Psoriatic Arthritis: Three-Year Results From a Phase IIb Randomized Controlled Trial and Its Open-Label Extension Study

Laura C. Coates,<sup>1</sup>  Iain B. McInnes,<sup>2</sup>  Joseph F. Merola,<sup>3</sup> Richard B. Warren,<sup>4</sup> Arthur Kavanaugh,<sup>5</sup> Alice B. Gottlieb,<sup>6</sup> Laure Gossec,<sup>7</sup>  Deepak Assudani,<sup>8</sup> Rajan Bajracharya,<sup>8</sup> Jason Coarse,<sup>9</sup> Barbara Ink,<sup>8</sup> and Christopher T. Ritchlin<sup>10</sup> 

**Objective.** To assess the long-term safety, tolerability, and efficacy of bimekizumab in active psoriatic arthritis (PsA).

**Methods.** Adult patients with active PsA who completed the double- and dose-blind periods of the BE ACTIVE randomized controlled trial were eligible to enroll in the open-label extension (OLE) study at week 48, after which patients received 160 mg of bimekizumab every 4 weeks. Safety and efficacy results are presented through 152 weeks.

**Results.** At week 152, 161 of 206 patients (78.2%) remained in the study. From weeks 0–152, 184 of 206 patients experienced  $\geq 1$  treatment-emergent adverse event (126.4 per 100 patient-years). The most frequent events were nasopharyngitis (7.6 per 100 patient-years), upper respiratory tract infection (6.8 per 100 patient-years), bronchitis (3.5 per 100 patient-years), and oral candidiasis (3.5 per 100 patient-years). Additionally, 47 of 206 patients had mild to moderate localized fungal infections (9.7 per 100 patient-years), including 24 of 206 patients who had *Candida* infections (4.6 per 100 patient-years) and 19 of 206 patients who had oral candidiasis (3.5 per 100 patient-years). Four patients had serious infections (0.7 per 100 patient-years); there were no reported cases of active tuberculosis, adjudicated major adverse cardiac events, or deaths. Efficacy demonstrated at week 48 was sustained in the OLE study. At week 152, nonresponder imputation analysis showed that 52.9% of patients (69.4% of observed cases) achieved the American College of Rheumatology criteria for 50% improvement, 57.7% (73.8% of observed cases) achieved 100% skin clearance per the Psoriasis Area and Severity Index, and 51.5% (67.5% of observed cases) achieved minimal disease activity. Patients also maintained improvements in pain, physical function, and health-related quality of life.

**Conclusion.** The safety profile of bimekizumab was consistent with previous reports, with no new safety signals identified. Sustained joint and efficacy responses were observed over 3 years.

## INTRODUCTION

Psoriatic arthritis (PsA) is a chronic, immune-mediated inflammatory disease with varied musculoskeletal and dermatological manifestations, including joint inflammation, enthesitis,

dactylitis, and skin disease (1). Due to the substantial and enduring impact of psoriatic disease on patients (2,3), it is critical to evaluate the long-term safety and efficacy of treatments. In recent years, the interleukin (IL)-17 cytokine superfamily has emerged as a target of new monoclonal antibody therapies for a range of

A video abstract of this article can be found at: [https://players.brightcove.net/3806881048001/default\\_index.html?videoId=6309214290112](https://players.brightcove.net/3806881048001/default_index.html?videoId=6309214290112)

Clinicaltrials.gov identifiers: NCT02969525 and NCT03347110.

The views expressed herein are those of the authors and not necessarily those of the NHS, the NIHR, or the Department of Health.

Supported by UCB Pharma. Dr. Coates' work was supported by an NIHR Clinician Scientist award and the NIHR Oxford Biomedical Research Centre. Dr. Warren is supported by the NIHR Manchester Biomedical Research Centre.

<sup>1</sup>Laura C. Coates, PhD: Nuffield Department of Orthopaedics, Rheumatology and Musculoskeletal Diseases, University of Oxford and Oxford Biomedical Research Centre, Oxford University Hospitals NHS Trust, Oxford, UK; <sup>2</sup>Iain B. McInnes, PhD: University of Glasgow, Glasgow, UK; <sup>3</sup>Joseph F. Merola, MD: Harvard Medical School, Brigham and Women's Hospital, Boston, Massachusetts; <sup>4</sup>Richard B. Warren, PhD: Dermatology Centre, Salford Royal NHS

Foundation Trust, Manchester NIHR Biomedical Research Centre, The University of Manchester, Manchester, UK; <sup>5</sup>Arthur Kavanaugh, MD: Division of Rheumatology, Allergy, and Immunology, UC San Diego School of Medicine, La Jolla, California; <sup>6</sup>Alice B. Gottlieb, MD, PhD: Department of Dermatology, The Icahn School of Medicine at Mount Sinai, New York, New York; <sup>7</sup>Laure Gossec, MD, PhD: Sorbonne Université, INSERM, Institut Pierre Louis d'Epidémiologie et de Santé Publique, and Rheumatology Department, Pitié-Salpêtrière Hospital, AP-HP, Paris, France; <sup>8</sup>Deepak Assudani, PhD, Rajan Bajracharya, MBBS, MPH, MFPM, Barbara Ink, PhD: UCB Pharma, Slough, UK; <sup>9</sup>Jason Coarse, MS: UCB Pharma, Raleigh, North Carolina; <sup>10</sup>Christopher T. Ritchlin, MD: Department of Medicine, University of Rochester, New York, New York.

Data may be requested by qualified researchers 6 months after product approval in the US and/or Europe, or global development is discontinued, and 18 months after trial completion. Investigators may request access to

inflammatory diseases. Currently approved therapies for PsA that target IL-17 cytokines include secukinumab and ixekizumab, both of which inhibit IL-17A, one of the 6 isoforms of IL-17 (4). The safety of IL-17A inhibitor treatment has been reported up to 5 years in patients with PsA (5).

Bimekizumab is a humanized monoclonal IgG1 antibody that selectively inhibits IL-17F in addition to IL-17A. Previous studies have shown that the dual neutralization of IL-17A and IL-17F results in rapid clinical improvements in patients with PsA (phase IIb) and ankylosing spondylitis (AS) (phase IIb), sustained up to 48 weeks, and plaque psoriasis (phase III), sustained up to 56 weeks (6–8). Given that PsA is a chronic disease with the potential for lasting complications, including irreversible joint damage, an increased risk of comorbidities, impaired quality of life, and substantial psychosocial burden (9,10), it is important to establish the long-term safety and efficacy of treatments in this patient population. While studies have examined the safety and efficacy of IL-17A inhibitors in PsA patients receiving treatment for up to 5 years (5), the BE ACTIVE trial and its open-label extension (OLE) study provide the first long-term safety and efficacy data specific to the mechanism of dual neutralization of IL-17A and IL-17F in PsA patients.

In the BE ACTIVE trial, treatment with 160 mg or 320 mg of bimekizumab every 4 weeks for up to 48 weeks was shown to be well tolerated, with demonstrated efficacy in joint and skin outcomes (6). Here, we describe the long-term safety, tolerability, and efficacy of up to 3 years of treatment with bimekizumab in adult patients with PsA.

## PATIENTS AND METHODS

**Study design and participants.** The BE ACTIVE trial (ClinicalTrials.gov identifier: NCT02969525) was a 48-week randomized phase IIb dose-ranging study, double-blind and placebo-controlled from the beginning of the study to week 12, then dose-blind to week 48. It was conducted at 41 sites across 5 countries in Europe and the US (6). Patients who completed 48 weeks of treatment in the double- and dose-blind periods and gave separate informed consent were eligible to enter the OLE study (ClinicalTrials.gov identifier: NCT03347110) for a further 104 weeks of treatment, up to a total of 152 weeks. A safety follow-up visit took place at week 168, 20 weeks after the last dose of bimekizumab (see Supplementary Figure 1, available on the *Arthritis & Rheumatology* website at <http://onlinelibrary.wiley.com/doi/10.1002/art.42280>). For patients who did not complete treatment to week 152, the safety follow-up visit occurred 20 weeks

after their last dose of bimekizumab. Key inclusion and exclusion criteria have been reported previously (6).

**Randomization and blinding.** At baseline of the double-blind period, 206 patients were randomized 1:1:1:1 to receive subcutaneous bimekizumab at a dose of 16 mg every 4 weeks, 160 mg every 4 weeks with a 320 mg loading dose, 160 mg every 4 weeks, 320 mg every 4 weeks, or placebo. At week 12, patients initially randomized to receive 16 mg of bimekizumab every 4 weeks or placebo were re-randomized 1:1 to receive bimekizumab at 160 mg or 320 mg every 4 weeks through week 48, while patients initially randomized to receive bimekizumab at 160 mg or 320 mg every 4 weeks continued their dosing to week 48 (6). At week 48, patients completing the dose-blind period on bimekizumab were eligible to enroll in the OLE study. All patients in the OLE study received 160 mg of bimekizumab every 4 weeks, regardless of prior dosing regimen (Supplementary Figure 1). All study timepoints are hereafter reported relative to baseline (week 0) of the initial randomized controlled study.

**Study procedures and outcomes.** During the OLE study, safety was assessed at study entry (week 48), then every 4 weeks through week 60, followed by every 12 weeks through week 144, then every 4 weeks through week 152 and subsequently at the safety follow-up (week 168). Efficacy was assessed at OLE study entry, then every 12 weeks through week 144, and then every 4 weeks through week 152.

The prespecified primary objective of the OLE study was the long-term safety of bimekizumab treatment over 152 weeks, measured by the incidence of treatment-emergent adverse events (TEAEs) and serious TEAEs. All TEAEs were classified using the Medical Dictionary for Regulatory Activities (MedDRA) version 19.0. Prespecified safety topics of interest included serious, fungal, and opportunistic infections, including tuberculosis (TB). Prespecified safety topics of interest also included liver enzyme elevation, major adverse cardiac events (MACE), malignancies, inflammatory bowel disease (IBD), neutropenia, hypersensitivity, suicidal ideation and behavior (SIB), and depression. MACE, IBD, and SIB events were adjudicated by independent committees. TEAEs leading to withdrawal from the study were a secondary safety endpoint.

Efficacy endpoints were prespecified via protocol as secondary and included the following: the proportion of patients achieving  $\geq 20\%$ ,  $\geq 50\%$ , or  $\geq 70\%$  improvement in disease activity based on the American College of Rheumatology criteria (ACR20, ACR50, ACR70) at week 96 (11); the proportion of patients (among those

anonymized IPD and redacted study documents which may include raw datasets, analysis-ready datasets, study protocol, blank case report form, annotated case report form, statistical analysis plan, dataset specifications, and clinical study report. Prior to use of the data, proposals need to be approved by an independent review panel at [www.vivli.org](http://www.vivli.org) and a signed data sharing agreement will need to be executed. All documents are available in English only, for a prespecified time, typically 12 months, on a password protected portal.

Author disclosures are available at <https://onlinelibrary.wiley.com/action/downloadSupplement?doi=10.1002%2Fart.42280&file=art42280-sup-0001-Disclosureform.pdf>.

Address correspondence via email to Laura C. Coates, PhD, at [laura.coates@ndorms.ox.ac.uk](mailto:laura.coates@ndorms.ox.ac.uk).

Submitted for publication January 11, 2022; accepted in revised form June 23, 2022.

with  $\geq 3\%$  body surface area [BSA] affected by psoriasis at baseline of the double-blind period) achieving  $\geq 75\%$  or  $\geq 90\%$  improvement in the Psoriasis Area and Severity Index (PASI75, PASI90) at week 96 (12); and the change from baseline of the double-blind period in the Leeds Dactylitis Index (LDI, among those with LDI scores  $>0$  at baseline) (13) and the Maastricht Ankylosing Spondylitis Enthesitis Score (MASES, among those with a MASES  $>0$  at baseline) (14) at week 96. Due to a data collection error and lack of patient data for skin outcomes at the week 96 visit, data are not reported at this timepoint for PASI75/PASI90, nor for 100% improvement in the PASI.

Other efficacy endpoints included the following: the proportion of patients over time achieving ACR20, ACR50, ACR70, PASI75, PASI90, PASI100, and minimal disease activity (MDA) (15); change from baseline in LDI, MASES, Disease Activity Score in 28 joints using the C-reactive protein level (DAS28-CRP) (16), Psoriatic Arthritis Impact of Disease in 9 domains (PsAID-9) (17) total score, and Short Form 36-item health survey (SF-36) physical component summary (PCS) and mental component summary (MCS) scores (18); and the proportion of patients achieving depression and anxiety status “normal” (score  $< 8$ ) as defined by the Hospital Anxiety and Depression Scale (HADS) anxiety and HADS depression subscales (19). The classification criteria for MDA and very low disease activity (VLDA) have been reported previously (15,20).

Post hoc analyses included assessment of the proportion of patients achieving a response based on the ACR50 + PASI100 composite outcome, the proportion of patients over time achieving VLDA, and the proportion of patients over time achieving remission as defined by the Disease Activity Index for Psoriatic Arthritis (DAPSA) score (21). While not prespecified endpoints, change from baseline in Health Assessment Questionnaire disability index (HAQ DI) (22) and Patient’s Assessment of Arthritis Pain (PtAAP) total scores are also reported to show the effects of treatment on patient health-related quality of life (HRQoL) and pain.

**Statistical analysis.** In the OLE study, the safety set consisted of all randomized study participants who received  $\geq 1$  dose of bimekizumab in weeks 48–152. The full analysis set consisted of all randomized study participants who received  $\geq 1$  dose of bimekizumab in weeks 48–152 and had a valid measurement of  $\geq 1$  efficacy variable after OLE study entry. The full analysis and safety sets for the double- and dose-blind periods have been described previously (6). Of the 206 patients included in the safety set, only 204 received bimekizumab due to the withdrawal of 2 patients originally allocated to the placebo group; both patients completed the double-blind period and discontinued before receiving bimekizumab.

Primary and secondary safety analyses are presented for the safety sets. The summary of TEAEs from weeks 48–152 included all patients who received bimekizumab during the OLE study. Exposure-adjusted incidence rates (EAIRs) per 100 patient-years are reported for the BE ACTIVE (6) and OLE safety sets.

Secondary and other efficacy variables were summarized for all subjects in the BE ACTIVE full analysis set. Responder variables were derived relative to baseline of the double-blind period and were summarized descriptively. Missing binary efficacy variables were imputed in the most conservative manner, using nonresponder imputation (NRI), with patients who did not enter the OLE study considered nonresponders from week 48 onwards. Missing continuous efficacy variables were imputed using multiple imputation based on the assumption that data were missing at random. Nonmonotone missing data were imputed with the Markov chain Monte Carlo (MCMC) method; monotone missing data were imputed with a monotone regression model. All computations and generation of outputs were done in SAS version 9.3 or later.

**Ethics approval.** The BE ACTIVE trial and its OLE study were conducted in accordance with the Declaration of Helsinki and the International Conference for Harmonisation Guidelines for Good Clinical Practice. Ethical approval was obtained from the relevant institutional review boards at all participating sites. All patients provided written informed consent in accordance with local requirements, with additional written informed consent required for enrollment in the OLE study. All the results presented in this article are in aggregate form, and no personally identifiable information was used for this study.

## RESULTS

### Patient disposition and baseline characteristics.

At the end of the dose-blind period (week 48), 184 of 206 patients (89.3%) enrolled in the OLE study and 183 received  $\geq 1$  dose of bimekizumab (Supplementary Figure 1, <http://onlinelibrary.wiley.com/doi/10.1002/art.42280>). Patient retention during the OLE study comprised 161 of 184 patients (87.5%) who completed treatment to week 152. Thus, 78.2% of all patients who started at week 0 completed the full 152 weeks of treatment. Kaplan-Meier curves of patient retention rates are provided in Supplementary Figure 2 (<http://onlinelibrary.wiley.com/doi/10.1002/art.42280>).

There were 12 discontinuations during the double- and dose-blind periods: 5 due to adverse events, 5 due to withdrawn consent, and 2 due to other reasons. An additional 4 patients discontinued due to adverse events after completing the double-blind period but prior to re-randomization in the dose-blind period. A total of 184 patients entered the OLE study; however, 1 patient discontinued from the study prior to any dosing in the OLE study. There were 22 discontinuations during the OLE study: 9 due to adverse events, 2 due to loss of efficacy, 9 due to withdrawn consent (not due to adverse events), 1 due to loss to follow-up, and 1 due to other reasons (Supplementary Figure 3, <http://onlinelibrary.wiley.com/doi/10.1002/art.42280>). Patient demographics and characteristics at baseline of the double-blind period are reported in Table 1.

**Table 1.** Demographics and baseline characteristics of psoriatic arthritis patients\*

	Group A (n = 124)†	Group B (n = 82)‡	Total BKZ (N = 206)
Age, mean ± SD years	50.5 ± 12.6	47.4 ± 12.0	49.3 ± 12.4
Male	55 (44.4)	50 (61.0)	105 (51.0)
Weight, mean ± SD kg	83.8 ± 18.4	88.5 ± 18.5	85.7 ± 18.5
BMI, mean ± SD kg/m <sup>2</sup>	29.3 ± 5.9	30.1 ± 6.2	29.6 ± 6.0
Time since first diagnosis of PsA, mean ± SD years	7.9 ± 9.1	6.0 ± 6.3	7.1 ± 8.2
TJC, mean ± SD	20.6 ± 14.3	23.3 ± 15.9	21.7 ± 15.0
SJC, mean ± SD	10.9 ± 7.5	12.5 ± 9.5	11.5 ± 8.4
hsCRP, median (range) mg/liter	5.7 (0.1–99.9)	5.9 (0.3–85.2)	5.9 (0.1–99.9)
HAQ DI score, mean ± SD	1.0 ± 0.6	1.0 ± 0.6	1.0 ± 0.6
PsAID-9 total score, mean ± SD	4.5 ± 1.9	4.9 ± 2.0	4.6 ± 1.9
PtAAP score, mean ± SD	50.8 ± 22.7	54.3 ± 23.4	52.2 ± 23.0
SF-36 score, mean ± SD			
PCS	37.0 ± 9.1	36.0 ± 9.0	36.6 ± 9.1
MCS	56.0 ± 8.6	55.4 ± 9.1	55.8 ± 8.7
Psoriasis			
BSA <3%	45 (36.3)	22 (26.8)	67 (32.5)
BSA ≥3–<10%	45 (36.3)	33 (40.2)	78 (37.9)
BSA ≥10%	34 (27.4)	25 (30.5)	59 (28.6)
Dactylitis	34 (27.4)	25 (30.5)	59 (28.6)
Enthesitis	65 (52.4)	42 (51.2)	107 (51.9)
Prior TNFi therapy	23 (18.5)	16 (19.5)	39 (18.9)
Concomitant therapies			
NSAIDs	81 (65.3)	52 (63.4)	133 (64.6)
Methotrexate	75 (60.5)	56 (68.3)	131 (63.6)
Steroids	23 (18.5)	23 (28.0)	46 (22.3)

\* Except where indicated otherwise, values are the number (%) of patients. Patients were randomized to receive bimekizumab (BKZ) or placebo at any dose at the beginning of the double-blind period (weeks 0–12) of the phase IIb randomized controlled trial BE ACTIVE. In the dose-blind period, patients initially randomized to receive 16 mg of BKZ or placebo every 4 weeks were rerandomized to receive BKZ at 160 mg or 320 mg every 4 weeks, and patients initially randomized to receive BKZ at 160 mg or 320 mg every 4 weeks continued their dosing (weeks 12–48). BMI = body mass index; PsA = psoriatic arthritis; TJC = tender joint count; SJC = swollen joint count; hsCRP = high sensitivity C-reactive protein; HAQ DI = Health Assessment Questionnaire Disability Index; PsAID-9 = Psoriatic Arthritis Impact of Disease in 9 domains; PtAAP = Patient's Assessment of Arthritis Pain; SF-36 = Short Form 36-item health survey; PCS = physical component summary; MCS = mental component summary; BSA = body surface area; TNFi = tumor necrosis factor inhibitor; NSAID = nonsteroidal antiinflammatory drug.

† Patients received 160 mg of BKZ every 4 weeks continuously from week 12 to week 152 (includes those originally assigned to BKZ 160 mg every 4 weeks with a loading dose).

‡ Patients were dose-reduced from 320 mg of BKZ every 4 weeks to 160 mg every 4 weeks at OLE study entry (week 48).

Among all patients randomized at week 0 (N = 206), the mean ± SD time since first diagnosis of PsA was 7.1 ± 8.2 years. The mean ± SD tender joint count (TJC) and swollen joint count (SJC) were 21.7 ± 15.0 and 11.5 ± 8.3, respectively, and the median serum high-sensitivity C-reactive protein level was 5.9 mg/liter (range 0.1–99.9 mg/liter). At the double-blind period baseline, patients had a mean SF-36 PCS score of 36.6 (compromised physical function, increased bodily pain, and decreased general health) and a mean SF-36 MCS score of 55.8 (unimpaired mental function) (18). At the end of the dose-blind period, the mean TJC and mean SJC among the randomized patients had decreased to 5.3 and 1.9, respectively, and the mean SF-36 PCS score had increased to 45.7. At baseline, approximately two-thirds of patients (66.5%) had ≥3% BSA with psoriasis involvement, approximately one-quarter (28.6%) had dactylitis, and slightly more than one-half (51.9%) had enthesitis. Resolution of dactylitis and enthesitis at the end of the dose-blind period are reported as part of the efficacy results (see below).

**Safety.** Exposure to bimekizumab over 152 weeks among all patients randomized at baseline was 570.1 patient-years, including 392.7 patient-years of exposure during the OLE study. From the double-blind period baseline through 152 weeks of therapy, 184 of 206 patients (89.3%) experienced ≥1 TEAE (EAIR 126.4 per 100 patient-years), and 22 of 206 patients (10.7%) experienced ≥1 serious TEAE (EAIR 4.1 per 100 patient-years) (Table 2). Seventeen patients (8.3%) permanently discontinued bimekizumab due to adverse events during the double- or dose-blind periods or during the OLE study. Cellulitis and oral fungal infection resulted in discontinuation of 2 patients each, and all other TEAEs leading to discontinuation were reported for a single patient. There were no deaths reported throughout the double- and dose-blind periods or throughout the OLE study (weeks 0–152).

The most frequently reported TEAEs (incidence ≥5%) by MedDRA preferred term in the double- and dose-blind periods and the OLE study included nasopharyngitis (18.0%), upper respiratory tract infection (16.5%), bronchitis (9.2%), oral

**Table 2.** Safety of bimekizumab treatment in psoriatic arthritis patients across the BE ACTIVE randomized controlled trial and the OLE study (safety set)\*

	Weeks 0–48†		Weeks 48–152	Weeks 0–152‡
	160 mg BKZ every 4 weeks (n = 126; 113.2 patient-years)	320 mg BKZ every 4 weeks (n = 80; 72.9 patient-years)	Total BKZ (N = 183; 392.7 patient-years)	Total BKZ (N = 206; 570.1 patient-years)
Any TEAE	94 (74.6) (177.6)	57 (71.3) (165.9)	148 (80.9) (94.3)	184 (89.3) (126.4)
Serious TEAEs	8 (6.3) (7.9)	0	14 (7.7) (3.8)	22 (10.7) (4.1)
Severe TEAEs	5 (4.0) (4.6)	2 (2.5) (2.9)	8 (4.4) (2.1)	14 (6.8) (2.5)
Withdrawal due to TEAEs	6 (4.8) (5.9)	2 (2.5) (3.1)	9 (4.9) (2.3)	17 (8.3) (3.0)
Drug-related TEAEs	43 (34.1) (52.7)	29 (36.3) (57.0)	60 (32.8) (20.0)	97 (47.1) (26.4)
Deaths	0	0	0	0
Most frequently reported TEAEs (≥5%)				
by MedDRA preferred term				
Nasopharyngitis	12 (9.5) (12.0)	11 (13.8) (18.4)	19 (10.4) (5.2)	37 (18.0) (7.6)
Upper respiratory tract infection	12 (9.5) (12.0)	8 (10.0) (13.2)	20 (10.9) (5.5)	34 (16.5) (6.8)
Bronchitis	7 (5.6) (6.9)	3 (3.8) (4.8)	11 (6.0) (2.9)	19 (9.2) (3.5)
Oral candidiasis	6 (4.8) (6.0)	4 (5.0) (6.4)	13 (7.1) (3.5)	19 (9.2) (3.5)
Pharyngitis	4 (3.2) (3.9)	7 (8.8) (11.6)	10 (5.5) (2.7)	17 (8.3) (3.2)
Sinusitis	6 (4.8) (5.9)	4 (5.0) (6.5)	10 (5.5) (2.6)	17 (8.3) (3.2)
Psoriasis	2 (1.6) (1.9)	2 (2.5) (3.1)	14 (7.7) (3.7)	16 (7.8) (2.9)
Psoriatic arthropathy	2 (1.6) (1.9)	1 (1.3) (1.6)	12 (6.6) (3.1)	16 (7.8) (2.9)
Respiratory tract infection	8 (6.3) (8.0)	2 (2.5) (3.2)	4 (2.2) (1.0)	15 (7.3) (2.8)
Oral fungal infection	3 (2.4) (2.9)	3 (3.8) (4.7)	9 (4.9) (2.4)	14 (6.8) (2.6)
Tonsillitis	6 (4.8) (5.9)	2 (2.5) (3.2)	6 (3.3) (1.6)	14 (6.8) (2.6)
ALT increased	6 (4.8) (6.0)	3 (3.8) (4.7)	6 (3.3) (1.6)	13 (6.3) (2.4)
Safety topics of interest				
Serious infections	3 (2.4) (2.9)	0	1 (0.5) (0.3)	4 (1.9) (0.7)
Fungal infections	17 (13.5) (17.8)	10 (12.5) (16.7)	32 (17.5) (9.2)	47 (22.8) (9.7)
<i>Candida</i> infections	9 (7.1) (9.1)	5 (6.3) (8.1)	16 (8.7) (4.3)	24 (11.7) (4.6)
Oral candidiasis	6 (4.8) (6.0)	4 (5.0) (6.4)	13 (7.1) (3.5)	19 (9.2) (3.5)
Skin candidiasis	1 (0.8) (1.0)	0	1 (0.5) (0.3)	2 (1.0) (0.4)
Vulvovaginal candidiasis	0	0	1 (0.5) (0.3)	1 (0.5) (0.2)
Genital candidiasis	1 (0.8) (1.0)	0	1 (0.5) (0.3)	1 (0.5) (0.2)
Oropharyngeal candidiasis	1 (0.8) (1.0)	0	0	1 (0.5) (0.2)
Fungal infections NEC	9 (7.1) (9.0)	4 (5.0) (6.3)	17 (9.3) (4.6)	25 (12.1) (4.7)
Oral fungal infection	3 (2.4) (2.9)	3 (3.8) (4.7)	9 (4.9) (2.4)	14 (6.8) (2.6)
Tongue fungal infection	3 (2.4) (2.9)	0	4 (2.2) (1.0)	5 (2.4) (0.9)
Fungal skin infection	0	1 (1.3) (1.6)	3 (1.6) (0.8)	4 (1.9) (0.7)
Fungal esophagitis	1 (0.8) (1.0)	1 (1.3) (1.6)	1 (0.5) (0.3)	3 (1.5) (0.5)
Vulvovaginal mycotic infection	2 (1.6) (1.9)	0	0	2 (1.0) (0.4)
Onychomycosis	0	0	2 (1.1) (0.5)	2 (1.0) (0.4)
Fungal pharyngitis	0	0	1 (0.5) (0.3)	1 (0.5) (0.2)
<i>Tinea</i> infections	0	1 (1.3) (1.6)	1 (0.5) (0.3)	2 (1.0) (0.4)
<i>Tinea pedis</i>	0	1 (1.3) (1.6)	0	1 (0.5) (0.2)
<i>Tinea cruris</i>	0	0	1 (0.5) (0.3)	1 (0.5) (0.2)
Serious hypersensitivity reactions	0	0	0	0
Opportunistic infections	1 (0.8) (1.0)	1 (1.3) (1.6)	1 (0.5) (0.3)	3 (1.5) (0.5)
Active tuberculosis	0	0	0	0
Liver enzyme elevation				
ALT increased	6 (4.8) (6.0)	3 (3.8) (4.7)	6 (3.3) (1.6)	13 (6.3) (2.4)
AST increased	4 (3.2) (4.0)	2 (2.5) (3.1)	6 (3.3) (1.6)	10 (4.9) (1.8)
Hepatic enzymes increased	2 (1.6) (1.9)	1 (1.3) (1.6)	1 (0.5) (0.3)	4 (1.9) (0.7)
MACE	0	0	0	0
Malignancies	1 (0.8) (1.0)	0	0	1 (0.5) (0.2)
IBD	0	0	1 (0.5) (0.3)	1 (0.5) (0.2)
Microscopic colitis	0	0	1 (0.5) (0.3)	1 (0.5) (0.2)
Anterior uveitis	0	0	0	0
Neutropenia	0	1 (1.3) (1.6)	5 (2.7) (1.3)	6 (2.9) (1.1)
Drug hypersensitivity	2 (1.6) (1.9)	0	1 (0.5) (0.3)	3 (1.5) (0.5)

(Table 2 continues on next page)



**Table 2.** (Cont'd)

	Weeks 0–48†		Weeks 48–152	Weeks 0–152‡
	160 mg BKZ every 4 weeks (n = 126; 113.2 patient-years)	320 mg BKZ every 4 weeks (n = 80; 72.9 patient-years)	Total BKZ (N = 183; 392.7 patient-years)	Total BKZ (N = 206; 570.1 patient-years)
Injection site reactions	0	3 (3.8) (4.9)	0	3 (1.5) (0.5)
SIB	1 (0.8) (1.0)	0	0	1 (0.5) (0.2)
Depression	1 (0.8) (1.0)	1 (1.3) (1.6)	2 (1.1) (0.5)	4 (1.9) (0.7)

\* Values are the number (%) of patients (exposure-adjusted incidence rate per 100 patient-years). The safety set consisted of all randomized study participants who received  $\geq 1$  dose of BKZ in weeks 48–152 of the OLE study. After week 48, all patients received 160 mg of BKZ every 4 weeks, regardless of prior dosing regimen. All oral candidiasis treatment-emergent adverse events (TEAEs) were mild to moderate (no serious cases), and all fungal infections were mild to moderate and localized, not systemic. Two patients reported 3 opportunistic events (2 fungal esophagitis, 1 oropharyngeal candidiasis) in weeks 0–48, 1 patient reported 2 events (fungal pharyngitis, fungal esophagitis) in weeks 48–152. No Hy's law cases reported. Suicidal ideation and behavior (SIB) events were adjudicated by an independent committee. One malignant melanoma in situ case was reported. No drug hypersensitivity reactions were anaphylactic. OLE = open-label extension; MedDRA = Medical Dictionary for Regulatory Activities; ALT = alanine aminotransferase; AST = aspartate aminotransferase; MACE = major adverse cardiac events; IBD = inflammatory bowel disease. See Table 1 for other definitions.

† Patients re-randomized 1:1 at week 12 from placebo or 16 mg of BKZ every 4 weeks to 160 mg BKZ every 4 weeks or 320 mg BKZ every 4 weeks; 2 patients completing the double-blind period on placebo were re-randomized but did not receive BKZ. Two patients were included in both groups due to a dosing error, allocation done per actual treatment.

‡ Includes safety follow-up to possible 168 weeks total for some patients.

candidiasis (9.2%), pharyngitis (8.3%), sinusitis (8.3%), psoriasis (7.8%), psoriatic arthropathy (7.8%), respiratory tract infection (7.3%), oral fungal infection (6.8%), tonsillitis (6.8%), and alanine aminotransferase (ALT) increased (6.3%) (Table 2).

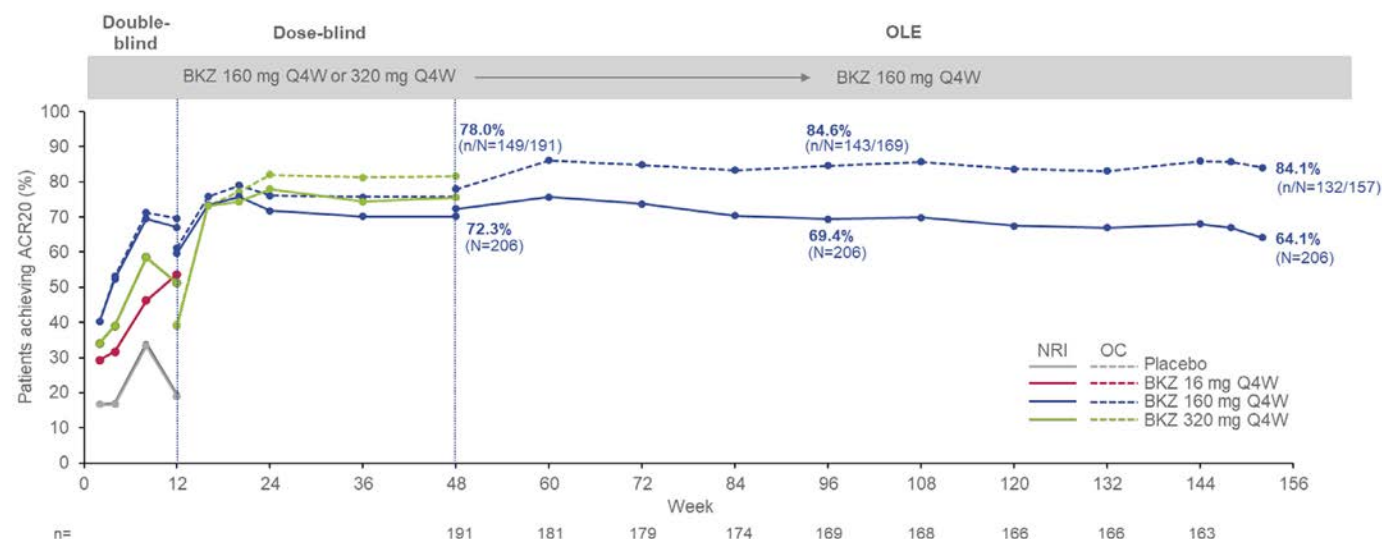
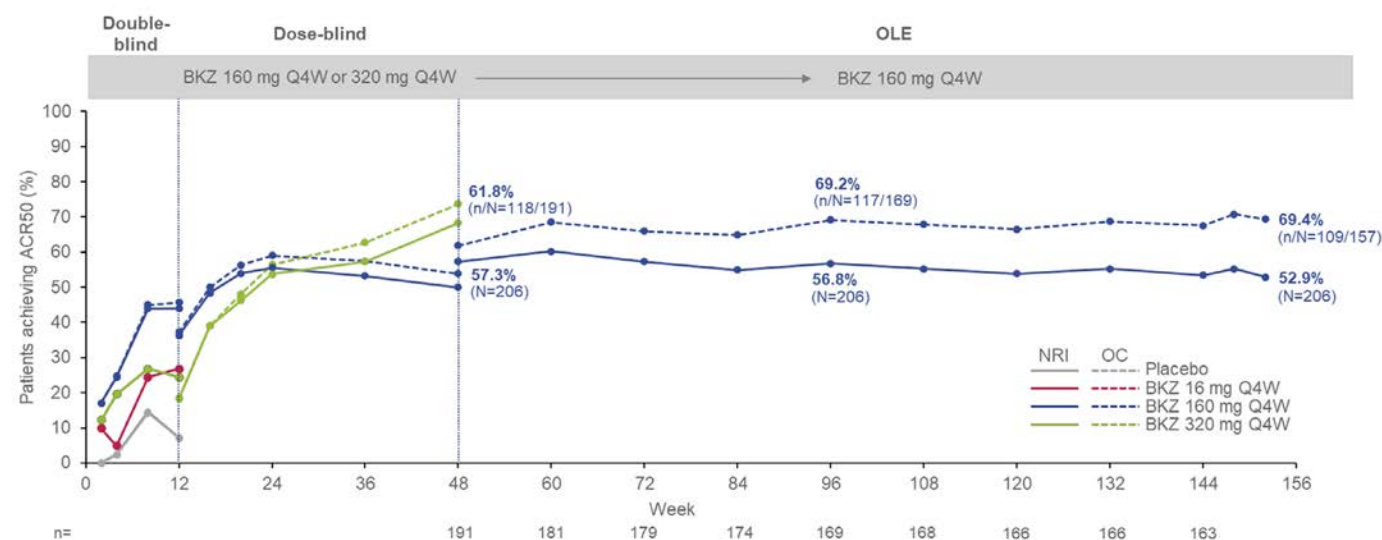
**Safety topics of interest.** Four patients (1.9%) experienced TEAEs of serious infections (1 case each of cellulitis, chronic otitis media, hepatitis E, and chronic sinusitis) during the double- and dose-blind periods and the OLE study. There was 1 case of microscopic colitis reported during the OLE study in a patient without prior history of IBD, which was adjudicated as IBD by an independent committee; the event was classified as moderate in intensity and was unrelated to treatment with bimekizumab. Throughout the double- and dose-blind periods and the OLE study, no reported events were adjudicated as MACE, and there were no reported cases of anterior uveitis. No further cases of malignancies or injection site reactions were reported during the OLE study; 1 case of malignant melanoma in situ and 3 cases of injection site reactions had been reported previously (6).

During the OLE study, 12 patients (6.6%) had reports of elevated liver enzymes, including increases in ALT, aspartate aminotransferase (AST), gamma glutamyltransferase (GGT), and blood bilirubin. Four patients (2.2%) reported elevations of ALT or AST  $>3$  times the upper limit of normal during the OLE study. None of these patients had a history of fatty liver or other hepatic dysfunction, and 2 of the 4 patients had concomitant methotrexate use. Three patients had confirmed normalization of laboratory values by the study conclusion. One patient did not complete final study assessments due to fear of COVID-19 infection, and therefore, no laboratory values were available for this patient. No patients discontinued bimekizumab due to

elevated liver enzymes in the OLE study; 2 discontinuations occurred during weeks 0–48. No Hy's Law cases were reported.

A total of 47 of 206 patients (EAIR 9.7 per 100 patient-years) had fungal infections over 152 weeks (Table 2). All fungal infections were assessed as mild to moderate in intensity by the study investigator and none were serious. Of these, 24 patients with  $\geq 1$  infection had *Candida* infections (EAIR 4.6 per 100 patient-years), with the majority of these (19 of 24; EAIR 3.5 per 100 patient-years) being oral candidiasis. Twenty-five patients had fungal infections not elsewhere classified (EAIR 4.7 per 100 patient-years), and the majority (14 of 25; EAIR 2.6 per 100 patient-years) were oral infections. Infections at other sites were low in frequency, including vulvovaginal infections (1 *Candida* infection [0.5%] and 2 fungal infections [1.0%]) and skin infections (2 *Candida* infections [1.0%] and 4 fungal infections [1.9%]) (Table 2). Two patients discontinued due to oral fungal infections. Baseline steroid use, sex, and presence of diabetes mellitus were not clear risk factors for susceptibility to *Candida* infections. All fungal infections, including *Candida* infections, were localized, not systemic, and the majority resolved and were easily treatable with systemic or topical antifungal treatments such as fluconazole, nystatin, itraconazole, and miconazole (Supplementary Table 2, <http://onlinelibrary.wiley.com/doi/10.1002/art.42280>). A total of 23 of 206 patients (11.2%) had  $>1$  episode of a fungal infection over 152 weeks, of which 12 of 206 (5.8%) had  $>1$  episode of a *Candida* infection. All *Candida* infections resolved without sequelae. No opportunistic infections were reported, except localized fungal events consisting of one case each of fungal pharyngitis and fungal esophagitis. There were no reported cases of active TB.

No cases of SIB were reported during the OLE study; 1 case was previously reported during the dose-blind period (6). Among

**A ACR20 (NRI, OC)****B ACR50 (NRI, OC)**

(Figure 1 continues on next page.)

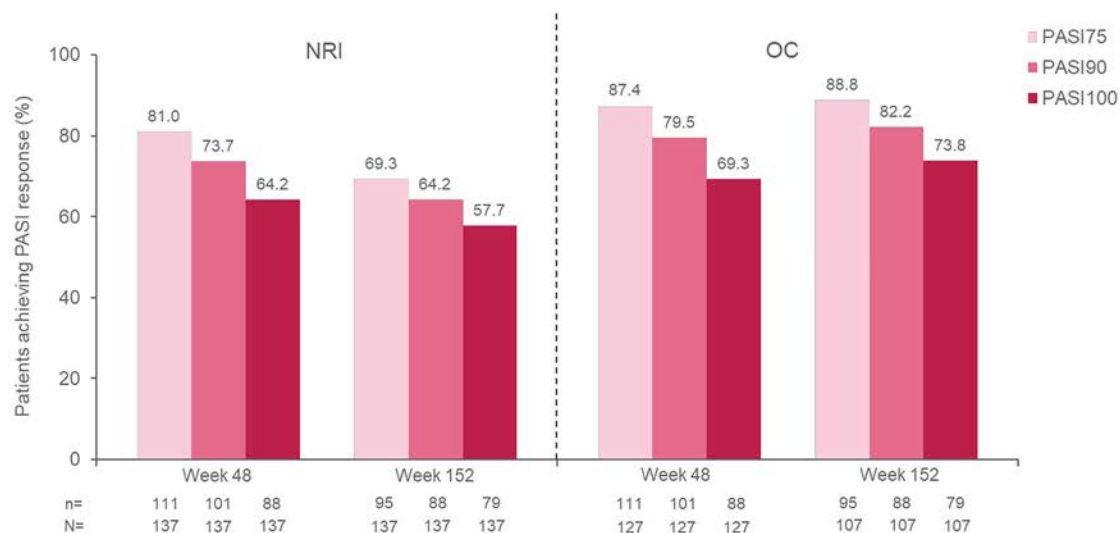
patients in the OLE study with available data ( $N = 181$ ), 92.3% had HADS anxiety and HADS depression scores of  $<8$  ("normal") at baseline of the double-blind period, which was sustained through week 48 to 92.1% at week 152. Prespecified safety topics of interest and other events across weeks 0–152 by randomized dose at baseline are provided in Supplementary Table 1 (<http://onlinelibrary.wiley.com/doi/10.1002/art.42280>).

**Efficacy.** Efficacy at weeks 12 and 48 of the BE ACTIVE trial has been reported previously (6). There was no worsening of disease in patients whose dose of bimekizumab was decreased from 320 mg to 160 mg in the OLE.

NRI analysis of joint efficacy outcomes showed that ACR20, ACR50, and ACR70 response rates were sustained, with 64.1%, 52.9%, and 39.3% of patients, respectively, meeting criteria at week 152, compared to 72.3%, 57.3%, and 39.8% of patients, respectively, meeting criteria at week 48 (Figures 1A–C). For skin efficacy outcomes, NRI analysis showed that PASI75, PASI90, and PASI100 responder rates were sustained, with 69.3%, 64.2%, and 57.7% of patients, respectively, meeting criteria at week 152, compared to 81.0%, 73.7%, and 64.2% of patients meeting criteria at week 48 (Figure 1D).

In the NRI analysis, 51.0% and 26.2% of bimekizumab-treated patients reached MDA and VLDA responses, respectively,

(Figure 1 Cont'd)

**C ACR70 (NRI, OC)****D PASI75, PASI90, PASI100 (NRI, OC)**

**Figure 1.** Key efficacy outcomes in psoriatic arthritis patients from baseline (week 0) of the double-blind period of the BE ACTIVE randomized controlled trial to week 152 (full analysis set). Nonresponder imputation (NRI; solid lines) and observed case (OC; dashed lines) data are shown for the percentages of patients achieving  $\geq 20\%$ ,  $\geq 50\%$ , and  $\geq 70\%$  improvement in disease activity based on the American College of Rheumatology criteria for all timepoints from weeks 0–152 (A–C), as well as for the percentages of patients achieving 75%, 90%, and 100% improvement in disease activity based on the Psoriasis Area and Severity Index (PASI) (D). Patients randomized to receive placebo (gray lines), 16 mg of bimekizumab (BKZ; red lines) every 4 weeks, or 320 mg of BKZ (green lines) every 4 weeks through the double-blind period are shown, and patients assigned to 160 mg of BKZ every 4 weeks with a 320 mg loading dose or 160 mg of BKZ every 4 weeks at double-blind period entry are combined for weeks 0–12 (blue lines). Percentages in the dose-blind period include those assigned to 160 mg of BKZ every 4 weeks, 160 mg of BKZ every 4 weeks with a 320 mg loading dose, or 320 mg of BKZ every 4 weeks at double-blind period entry, as well as those assigned to placebo or 16 mg of BKZ every 4 weeks who were re-randomized to 160 mg or 320 mg of BKZ every 4 weeks. All open-label extension (OLE) study patients received 160 mg of BKZ every 4 weeks regardless of prior dosing regimen; 157 patients had an efficacy assessment at week 152. At baseline of the double-blind period, 137 patients had  $\geq 3\%$  body surface area affected by psoriasis; due to a data collection error and lack of data from the study visit, week 96 data are not reported for PASI. Circles represent timepoints at which patients were assessed.

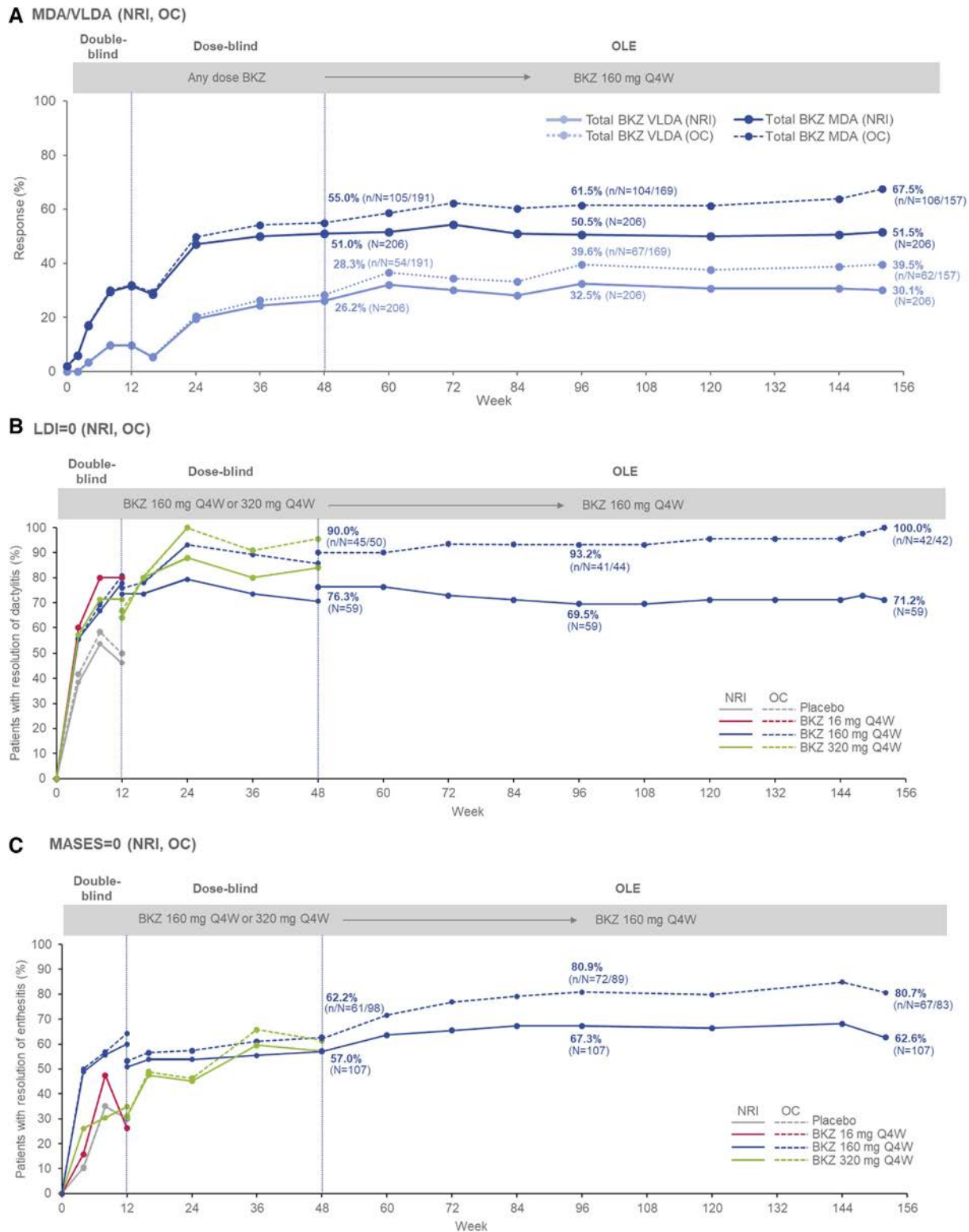


**Figure 2.** Additional efficacy outcomes in psoriatic arthritis patients from baseline (week 0) of the double-blind period of the BE ACTIVE randomized controlled trial to week 152 (full analysis set). NRI and OC data are shown for the percentages of patients achieving minimal disease activity (MDA) or very low disease activity (VLDA) (A), percentages of patients achieving resolution of dactylitis based on Leeds Dactylitis Index (LDI) score (includes patients with LDI score >0 at baseline [ $n = 59$ ]) (B), and percentages of patients achieving resolution of enthesitis based on the Maastricht Ankylosing Spondylitis Enthesitis Index (MASES) (includes patients with MASES score >0 at baseline [ $n = 107$ ]) (C). Patients were classified as having MDA or VLDA when they met 5 of 7 or 7 of 7, respectively, of the following criteria: tender joint count score  $\leq 1$ , swollen joint count score  $\leq 1$ , PASI  $\leq 1$  or  $\leq 3\%$  body surface area affected by psoriasis, visual analog scale (VAS) score  $\leq 15$  for pain, VAS score  $\leq 20$  for patient global activity, Health Assessment Questionnaire disability index score  $\leq 0.5$ , and tender entheses points score  $\leq 1$ . See Figure 1 for other definitions. Color figure can be viewed in the online issue, which is available at <http://onlinelibrary.wiley.com/doi/10.1002/art.42280/abstract>.



at week 48, with the proportions increasing to 51.5% and 30.1% at week 152 (Figure 2A). Among patients with dactylitis at baseline (LDI score > 0), 45 of 59 patients (76.3%) had resolution at week 48 in the NRI analysis, and 42 of 59 patients (71.2%) were dactylitis-free at week 152 (Figure 2B). Due to lack of convergence in the analytical model, only observed case data were generated for change from baseline in LDI over 152 weeks. The analysis showed that the mean  $\pm$  SD change from baseline (SD) in LDI score following treatment with bimekizumab was  $-8.0 \pm 69.5$  at week 48, with even greater improvement in LDI score at week 152 (mean  $\pm$  SD  $-16.2 \pm 45.5$ ) (Supplementary Table 3). Among patients with enthesitis at baseline (MASES > 0), 61 of 107 patients (57.0%) had achieved resolution at week 48 in the NRI analysis, and 67 of 107 patients (62.6%) were enthesitis-free at week 152 (Figure 2C). Multiple imputation analysis showed that the mean  $\pm$  SEM change from baseline in MASES following treatment with bimekizumab was  $-2.6 \pm 0.3$  at week 48, with even greater improvement in MASES at week 152 (mean  $\pm$  SEM  $-3.3 \pm 0.3$ ) (Supplementary Table 3, <http://onlinelibrary.wiley.com/doi/10.1002/art.42280>).

In addition, 35.0% of patients achieved remission based on the DAPSA score at week 48, increasing to 38.8% at week 152. In NRI analysis, 46.0% of bimekizumab-treated patients who had  $\geq 3\%$  BSA with psoriasis involvement at baseline of the double-blind period achieved a response based on the ACR50 + PASI100 composite outcome at week 48 and week 152 (Supplementary Table 3, <http://onlinelibrary.wiley.com/doi/10.1002/art.42280>). Patients also maintained improvements in pain, physical function, and HRQoL from week 48 to week 152, as measured by PtAAP, SF-36 PCS, PsAID-9, and HAQ DI scores (Supplementary Table 3).

## DISCUSSION

Patients with PsA require effective long-term treatment of both joint and skin symptoms. The proportion of patients with PsA who achieve an ACR50 response during treatment with currently licensed IL-17A inhibitors is ~30–50% at 16–24 weeks, while the proportion achieving PASI90 with IL-17A inhibitors is ~30–70% at 16–24 weeks, demonstrating the need for more effective treatments (23,24). Furthermore, sustaining this efficacy over the long-term is important, as patients may lose clinical benefits of treatment over time (2). In patients with PsA, 3-year extension data from studies of IL-17A inhibitors showed similar or slightly lower ACR50 and PASI90 response rates at 156 weeks compared to ACR50 and PASI90 response rates at 24 weeks (25,26). Similar trends have been observed out to 5 years with IL-17A inhibitor therapy (27).

In the phase IIb BE ACTIVE trial and its OLE study, bimekizumab was found to be well tolerated in PsA patients up to 3 years of treatment, with no new safety signals identified compared to the first 48 weeks of treatment (6). Findings from the BE ACTIVE

trial showed that both joint and skin outcomes improved from baseline of the double-blind period through week 12 to week 24, after which responses were sustained through the dose-blind period to week 48. Here, we show that efficacy outcomes were sustained at 3 years.

Patient retention supported long-term tolerability of bimekizumab, with treatment completed up to week 48 by 91.7% of patients, and up to week 152 by 78.2% of patients (87.5% of those who enrolled in the OLE study). This finding supports the long-term tolerability and efficacy of treatment with bimekizumab in adult patients with PsA.

The frequencies of TEAEs and serious TEAEs were not increased with further exposure to bimekizumab and were aligned with prior reporting for the double- and dose-blind periods from this phase IIb study in PsA patients (6). The 3 most frequently reported TEAEs over 3 years by MedDRA preferred term (nasopharyngitis, upper respiratory tract infection, and bronchitis) were consistent with previous 48-week data from the double- and dose-blind periods, as well as a study of bimekizumab in AS patients (6,7).

Given the role of the IL-23/IL-17 pathway in mucocutaneous protection against a variety of pathogens, in particular extracellular fungal infections, the inhibition of IL-17A was predicted to increase susceptibility to oral candidiasis (28–30). In addition, due to the involvement of both IL-17A and IL-17F in CD4+ T helper 17 (Th17) cell-mediated mucocutaneous immunity (31), dual inhibition of these cytokines is theoretically expected to further increase the risk of fungal infection compared with inhibition of IL-17A alone. In the OLE study, EAIIRs of *Candida* infection remained stable compared with the first 48 weeks of treatment. No clear risk factors for *Candida* infection were identified in the BE ACTIVE trial or its OLE study; however, further analyses in phase III studies of bimekizumab in PsA with larger patient populations are needed to confirm whether any potential risk factors for *Candida* infection can be distinguished. Just over one-tenth of patients with fungal infections, including *Candida* infections, reported recurrence of infection at any time during the double- and dose-blind periods or the OLE study, whereas among patients who reported *Candida* infections, one-half experienced a recurrence of infection. However, the majority of *Candida* cases over the course of the study were easily managed and resolved with topical or systemic antifungal treatment.

There were no MACE or cases of SIB during the OLE study. There was 1 moderate case of microscopic colitis adjudicated as IBD in a patient without prior history of IBD; this event was unrelated to treatment with bimekizumab. No cases of uveitis, additional injection site reactions, or nonfungal opportunistic infections were reported in the OLE study. However, results from phase III studies, including larger patient groups, are needed to further establish the long-term safety profile of bimekizumab in PsA patients.



The improvements in key joint (articular) and skin efficacy outcomes observed in patients receiving bimekizumab over 48 weeks were generally maintained through 3 years of treatment. MDA has been previously identified as a desirable target in treat-to-target strategies for PsA, defining a satisfactory state of disease activity that encompasses all aspects of the disease (15). At week 152, more than one-half of patients achieved MDA, including with NRI. Furthermore, over one-half of patients achieved ACR50 or PASI100 for those with  $\geq 3\%$  BSA with psoriasis involvement at the double-blind period baseline responses individually, and the proportion achieving both ACR50 and PASI100 responses remained stable at just under one-half of bimekizumab-treated patients between week 48 and week 152.

Notwithstanding the improvements seen in clinically assessed PsA disease outcomes, patients receiving bimekizumab also reported improvements in selected patient-reported outcome measures that were maintained over 3 years of treatment, including reduced pain, increased physical function, lower disease impact, and improved quality of life.

The 3-year duration of this phase IIb study provides the most comprehensive evidence to date of the long-term safety and efficacy of bimekizumab in patients with PsA. A limitation of the present analysis relates to the lack of an active comparator, or placebo comparator beyond week 12. After week 12, all patients received bimekizumab at 160 mg or 320 mg every 4 weeks. Efficacy was similar at week 48 among patients receiving bimekizumab at 160 mg or 320 mg, and no appreciable decrease in efficacy was observed in patients who reduced their dose from 320 mg to 160 mg at the start of the OLE study. Additionally, as a phase IIb study, the limited sample size of ~200 patients restricts the interpretation of the results. There was also no evaluation of structural inhibition in the present study. Results from phase III studies in larger patient populations are therefore awaited to further investigate the safety, tolerability, and efficacy of bimekizumab in PsA patients during long-term treatment, including structural inhibition. There are currently 2 phase III studies underway, the BE OPTIMAL trial ([ClinicalTrials.gov](https://clinicaltrials.gov/ct2/show/study/NCT03895203) identifier: NCT03895203) and the BE COMPLETE trial ([ClinicalTrials.gov](https://clinicaltrials.gov/ct2/show/study/NCT03896581) identifier: NCT03896581), as well as their combined OLE study, BE VITAL ([ClinicalTrials.gov](https://clinicaltrials.gov/ct2/show/study/NCT04009499) identifier: NCT04009499), after which more robust conclusions will likely be possible.

In conclusion, the safety of bimekizumab in patients with PsA over 3 years of treatment was consistent with the previous 48-week results, as well as other recently published studies of IL-17 inhibitors in PsA patients. High thresholds of disease control were achieved within the first year of treatment and sustained through 3 years. Despite the limited sample size, the present study supports the further development of bimekizumab to address an unmet need for improved and sustained efficacy on skin and joint disease in patients with PsA.

## ACKNOWLEDGMENTS

The authors thank the patients and the investigators and their teams who took part in this study. The authors also acknowledge Heather Edens, PhD (UCB Pharma, Smyrna, GA) for publication coordination and Aaron Keeling, BA (Costello Medical, Boston, MA) and Hannah Brechka, PhD (Costello Medical, Cambridge, UK), for medical writing and editorial assistance based on the authors' input and direction. Support for third-party writing assistance for this article, provided by Aaron Keeling, BA, and Hannah Brechka, PhD, was funded by UCB Pharma in accordance with Good Publication Practice (GPP3) guidelines (<http://www.ismpp.org/gpp3>).

## AUTHOR CONTRIBUTIONS

All authors were involved in drafting the article or revising it critically for important intellectual content, and all authors approved the final version to be published. Dr. Coates had full access to all of the data in the study and takes responsibility for the integrity of the data and the accuracy of the data analysis.

**Study conception and design.** Coates, McInnes, Merola, Warren, Kavanaugh, Gottlieb, Assudani, Bajracharya, Coarse, Ink, Ritchlin.

**Acquisition of data.** Coarse, Ink.

**Analysis and interpretation of data.** Coates, McInnes, Merola, Warren, Kavanaugh, Gottlieb, Gossec, Assudani, Bajracharya, Coarse, Ink, Ritchlin.

## ROLE OF THE STUDY SPONSOR

UCB Pharma facilitated the study design, funded writing assistance for the manuscript, and reviewed and approved the manuscript prior to submission. The authors independently collected the data, interpreted the results, and had the final decision to submit the manuscript for publication. Publication of this article was contingent upon approval by UCB Pharma.

## REFERENCES

- Coates LC, Helliwell PS. Psoriatic arthritis: state of the art review. *Clin Med (Lond)* 2017;17:65–70.
- Boehncke WH, Menter A. Burden of disease: psoriasis and psoriatic arthritis. *Am J Clin Dermatol* 2013;14:377–88.
- Gudu T, Gossec L. Quality of life in psoriatic arthritis [review]. *Expert Rev Clin Immunol* 2018;14:405–17.
- Kurschus FC, Moos S. IL-17 for therapy. *J Dermatol Sci* 2017;87:221–7.
- Deodhar A, Mease PJ, McInnes IB, Baraliakos X, Reich K, Blauvelt A, et al. Long-term safety of secukinumab in patients with moderate-to-severe plaque psoriasis, psoriatic arthritis, and ankylosing spondylitis: integrated pooled clinical trial and post-marketing surveillance data. *Arthritis Res Ther* 2019;21:111.
- Ritchlin CT, Kavanaugh A, Merola JF, Schett G, Scher JU, Warren RB, et al. Bimekizumab in patients with active psoriatic arthritis: results from a 48-week, randomised, double-blind, placebo-controlled, dose-ranging phase 2b trial. *Lancet* 2020;395:427–40.
- Van der Heijde D, Gensler LS, Deodhar A, Baraliakos X, Poddubnyy D, Kivitz A, et al. Dual neutralisation of interleukin-17A and interleukin-17F with bimekizumab in patients with active ankylosing spondylitis: results from a 48-week phase IIb, randomised, double-blind, placebo-controlled, dose-ranging study. *Ann Rheum Dis* 2020;79:595–604.
- Gordon KB, Foley P, Krueger JG, Pinter A, Reich K, Vender R, et al. Bimekizumab efficacy and safety in moderate to severe plaque psoriasis (BE READY): a multicentre, double-blind, placebo-controlled, randomised withdrawal phase 3 trial. *Lancet* 2021;397:475–86.

9. McArdle A, Pennington S, FitzGerald O. Clinical features of psoriatic arthritis: a comprehensive review of unmet clinical needs [review]. *Clin Rev Allergy Immunol* 2018;55:271–94.
10. Visalli E, Crispino N, Foti R. Multidisciplinary management of psoriatic arthritis: the benefits of a comprehensive approach. *Adv Ther* 2019; 36:806–16.
11. Mease PJ, Antoni CE, Gladman DD, et al. Psoriatic arthritis assessment tools in clinical trials. *Ann Rheum Dis* 2005;64(Suppl 2):ii49–54.
12. Fredriksson T, Pettersson U. Severe psoriasis—oral therapy with a new retinoid. *Dermatologica* 1978;157:238–44.
13. Helliwell PS, FitzGerald O, Fransen J, et al. Development of an assessment tool for dactylitis in patients with psoriatic arthritis. *J Rheumatol* 2005; 32:1745–50.
14. Heuft-Dorenbosch L, Spoorenberg A, van Tubergen A, et al. Assessment of enthesitis in ankylosing spondylitis. *Ann Rheum Dis* 2003; 62: 127–32.
15. Coates LC, Fransen J, Helliwell PS. Defining minimal disease activity in psoriatic arthritis: a proposed objective target for treatment. *Ann Rheum Dis* 2010;69:48–53.
16. Baker JF, Conaghan PG, Smolen JS, et al. Development and validation of modified disease activity scores in rheumatoid arthritis: superior correlation with magnetic resonance imaging–detected synovitis and radiographic progression. *Arthritis Rheumatol* 2014; 66:794–802.
17. Gossec L, de Wit M, Kiltz U, et al. A patient-derived and patient-reported outcome measure for assessing psoriatic arthritis: elaboration and preliminary validation of the Psoriatic Arthritis Impact of Disease (PsAID) questionnaire, a 13-country EULAR initiative. *Ann Rheum Dis* 2014;73:1012–9.
18. Ware JE Jr, Snow KK, Kosinski M, et al. SF-36 health survey: manual and interpretation guide. Boston: The Health Institute, New England Medical Center; 1993.
19. Zigmond AS, Snaith RP. The Hospital Anxiety and Depression Scale. *Acta Psychiatr Scand* 1983;67:361–70.
20. Lubrano E, Perrotta FM, Sciffignano S, Coates LC, Helliwell P. Sustained very low disease activity and remission in psoriatic arthritis patients. *Rheumatol Ther* 2019;6:521–8.
21. Schoels M, Aletaha D, Funovits J, et al. Application of the DAREA/DAPSA score for assessment of disease activity in psoriatic arthritis. *Ann Rheum Dis* 2010;69:1441–7.
22. Fries JF, Spitz P, Kraines RG, et al. Measurement of patient outcome in arthritis. *Arthritis Rheum* 1980;23:137–45.
23. Mease P, van der Heijde D, Landewe R, Mpofu S, Rahman P, Tahir H, et al. Secukinumab improves active psoriatic arthritis symptoms and inhibits radiographic progression: primary results from the randomised, double-blind, phase III FUTURE 5 study. *Ann Rheum Dis* 2018;77:890–7.
24. Mease PJ, van der Heijde D, Ritchlin CT, Okada M, Cuchacovich RS, Shuler CL, et al. Ixekizumab, an interleukin-17A specific monoclonal antibody, for the treatment of biologic-naïve patients with active psoriatic arthritis: results from the 24-week randomised, double-blind, placebo-controlled and active (adalimumab)-controlled period of the phase III trial SPIRIT-P1. *Ann Rheum Dis* 2017;76:79–87.
25. Chandran V, van der Heijde D, Fleischmann RM, Lespessailles E, Helliwell PS, Kameda H, et al. Ixekizumab treatment of biologic-naïve patients with active psoriatic arthritis: 3-year results from a phase III clinical trial (SPIRIT-P1). *Rheumatology (Oxford)* 2020;59:2774–84.
26. Mease PJ, Kavanaugh A, Reimold A, Tahir H, Rech J, Hall S, et al. Secukinumab in the treatment of psoriatic arthritis: efficacy and safety results through 3 years from the year 1 extension of the randomised phase III FUTURE 1 trial. *RMD Open* 2018;4:e000723.
27. Reich K, Warren RB, Coates LC, Di Comite G. Long-term efficacy and safety of secukinumab in the treatment of the multiple manifestations of psoriatic disease. *J Eur Acad Dermatol Venereol* 2020;34:1161–73.
28. Conti HR, Gaffen SL. IL-17-mediated immunity to the opportunistic fungal pathogen *Candida albicans*. *J Immunol* 2015;195:780–8.
29. Blauvelt A, Lebwohl MG, Bissonnette R. IL-23/IL-17A dysfunction phenotypes inform possible clinical effects from anti-IL-17A therapies. *J Invest Dermatol* 2015;135:1946–53.
30. Ishigame H, Kakuta S, Nagai T, Kadoki M, Nambu A, Komiyama Y, et al. Differential roles of interleukin-17A and -17F in host defense against mucocutaneous bacterial infection and allergic responses. *Immunity* 2009;30:108–19.
31. Mengesha BG, Conti HR. The role of IL-17 in protection against mucosal candida infections. *J Fungi (Basel)* 2017;3.

# Modulation of the Itaconate Pathway Attenuates Murine Lupus

Luz P. Blanco,<sup>1</sup> Eduardo Patino-Martinez,<sup>1</sup> Shuichiro Nakabo,<sup>1</sup> Mingzeng Zhang,<sup>1</sup> Hege L. Pedersen,<sup>1</sup> Xinghao Wang,<sup>1</sup> Carmelo Carmona-Rivera,<sup>1</sup> Dillon Claybaugh,<sup>1</sup> Zu-Xi Yu,<sup>2</sup> Equar Desta,<sup>3</sup> and Mariana J. Kaplan<sup>1</sup>

**Objective.** Itaconic acid, a Krebs cycle–derived immunometabolite, is synthesized by myeloid cells in response to danger signals to control inflammasome activation, type I interferon (IFN) responses, and oxidative stress. As these pathways are dysregulated in systemic lupus erythematosus (SLE), we investigated the role of an itaconic acid derivative in the treatment of established murine lupus.

**Methods.** Female (NZW × NZB)F<sub>1</sub> lupus-prone mice were administered 4-octyl itaconate (4-OI) or vehicle starting after clinical onset of disease (30 weeks of age) for 4 weeks (n = 10 mice /group). At 34 weeks of age (peak disease activity), animals were euthanized, organs and serum were collected, and clinical, metabolic, and immunologic parameters were evaluated.

**Results.** Proteinuria, kidney immune complex deposition, renal scores of severity and inflammation, and anti-RNP autoantibodies were significantly reduced in the 4-OI treatment group compared to the vehicle group. Splenomegaly decreased in the 4-OI group compared to vehicle, with decreases in activation markers in innate and adaptive immune cells, increases in CD8+ T cell numbers, and inhibition of JAK1 activation. Gene expression analysis in splenocytes showed significant decreases in type I IFN and proinflammatory cytokine genes and increased Treg cell–associated markers in the 4-OI group compared to the vehicle group. In human control and lupus myeloid cells, 4-OI in vitro treatment decreased proinflammatory responses and B cell responses.

**Conclusions.** These results support targeting immunometabolism as a potentially viable approach in autoimmune disease treatment, with 4-OI displaying beneficial roles attenuating immune dysregulation and organ damage in lupus.

## INTRODUCTION

Systemic lupus erythematosus (SLE) is a complex autoimmune syndrome in which multi-organ damage leads to enhanced morbidity and mortality (1,2). Many individuals affected by SLE require immunosuppression, and there is need for additional effective immunomodulatory drugs with fewer side effects (3).

Among some of the innate immune abnormalities characteristic of SLE, dysregulated type I interferon (IFN) responses, inflammasome activation, and enhanced oxidative stress are prevalent (4,5). In addition, our group and others have described a role for

mitochondrial dysfunction in SLE pathogenesis (6–9). Itaconic acid is a mitochondrial-derived immunometabolite that modulates several of these dysregulated pathways (10). Itaconic acid is synthesized by macrophages following lipopolysaccharide (LPS) challenge and, more broadly, in cells expressing the aconitate decarboxylase 1 (ACOD1) gene (also known as *IRG1*). This gene codifies for an enzyme which acts via decarboxylation of *cis*-aconitate to produce itaconic acid from the tricarboxylic acid cycle in response to proinflammatory stimuli (11). Itaconic acid effects are broad and pleiotropic, modulating not only metabolism but also inflammatory and oxidative stress–related responses (12).

Supported by the Intramural Research Program at National Institute of Arthritis and Musculoskeletal and Skin Diseases, NIH (grant ZIA-AR-041199 03-05). Dr. Pedersen's work was supported by the Northern Norway Regional Health Authority (grant HNF1343-17).

<sup>1</sup>Luz P. Blanco, PhD, Eduardo Patino-Martinez, PhD, Shuichiro Nakabo, MD, PhD, Mingzeng Zhang, MD, PhD, Hege L. Pedersen, PhD (current address: RNA and Molecular Pathology Research Group, Department of Medical Biology, Faculty of Health Sciences, UTI The Arctic University of Norway, Tromsø, Norway, and Center for Clinical Research and Education University Hospital of North Norway, Tromsø, Norway), Xinghao Wang, BS, Carmelo Carmona-Rivera, PhD, Dillon Claybaugh, BS, Mariana J. Kaplan, MD: Systemic Autoimmunity Branch, National Institute of

Arthritis and Musculoskeletal and Skin Diseases NIH, Bethesda, Maryland; <sup>2</sup>Zu-Xi Yu, MD: Pathology Core, National Heart, Lung, and Blood Institute, NIH, Bethesda, Maryland; <sup>3</sup>Equear Desta, BS: Laboratory of Animal Science Section, National Institute of Allergy and Infectious Diseases, NIH, Bethesda, Maryland;

Author disclosures are available at <https://onlinelibrary.wiley.com/action/downloadSupplement?doi=10.1002%2Fart.42284&file=art42284-sup-0001-Disclosureform.pdf>.

Address correspondence via email to Mariana J. Kaplan, MD, at [mariana.kaplan@nih.gov](mailto:mariana.kaplan@nih.gov).

Submitted for publication January 11, 2022; accepted in revised form June 23, 2022.

Because of these antiinflammatory activities, itaconic acid-improved derivatives have been isolated. In particular, 4-octyl itaconate (4-OI) is a cell-soluble electrophilic small molecule that alkylates proteins and inhibits inflammasome activation (10). Among several key targets for alkylation are Kelch-like ECH-associated protein 1 (KEAP1) and GAPDH, whose modifications lead to activation of the Nrf2 transcription factor and inhibition of aerobic glycolysis, respectively (13,14). As such, Nrf2 is considered a master regulator of cellular antioxidative and detoxification responses, while GAPDH inhibition reduces the aerobic glycolysis or Warburg effect that predominates in activated immune cells under inflammatory conditions. Furthermore, Nrf2 activation by 4-OI down-regulates type I IFN synthesis by the cyclic GMP-AMP synthase/stimulator of IFN genes pathway (15). In some in vivo animal models, 4-OI can attenuate tissue injury by reducing inflammation and oxidative stress (16–21). Moreover, the 4-OI/Nrf2 antiinflammatory axis effectively reduces proinflammatory cytokine expression in vitro in SLE peripheral blood mononuclear cells (PBMCs) (22). Given these observations, we assessed whether therapy with 4-OI would ameliorate clinical and immunologic parameters of established murine lupus.

## MATERIALS AND METHODS

**Animals and in vivo treatment.** Female (NZW × NZB) F<sub>1</sub>/J mice (stock no. 100008) were purchased from The Jackson Laboratory (Bar Harbor, ME). The National Institute of Arthritis and Musculoskeletal and Skin Diseases Animal Care and Use Committee approved animal procedures (protocol no. A019-05-03) without randomization, and all researchers were unblinded with regard to animal treatment (≥4 mice/cage). NZW × NZB mice received subcutaneous 4-OI (14 µg/kg/minute) (no. 25374; Cayman Chemical) or vehicle control (2-hydroxypropyl-beta cyclodextrin 40%) (no. 332607; Sigma-Aldrich) in phosphate buffered saline (PBS) via osmotic pump delivery (no. 2006; Alzet), which was surgically inserted into the dorsum of the animals at 30 weeks old (n = 9 mice/group). The number, age, and sex of animals were determined based on our previous experimental designs that showed that 9–10 female lupus-prone mice per group provided sufficient power when comparing various active treatments to controls. At 34 weeks of age (expected peak disease activity), mice were euthanized, and tissues and blood were collected for analysis.

**Complete blood count.** This study was performed in the National Institutes of Health (NIH) Department of Laboratory Medicine using murine blood diluted 1:3 in PBS with an Advia 120 device.

**Splenocyte gene expression.** Messenger RNA (mRNA) was purified from frozen spleens in RNeasy lysis solution, stored at –80°C, and quantification of proinflammatory mRNAs was performed as previously described (23,24). Briefly, tissue was

homogenized in RLT lysis buffer and RNA were isolated using an RNA Easy kit (Qiagen); complementary DNA was synthesized using 1 µg of RNA, a Bio-Rad iScript kit, and an ABI thermocycler. Real-time polymerase chain reaction was performed using Bio-Rad reagents and instructions, and a CFX96 Bio-Rad real-time thermocycler. Fold gene expression for each gene was calculated using the  $\beta_2$ -microglobulin housekeeping gene in mouse tissue for the 4-OI or control vehicle conditions for  $\Delta\Delta C_t$  calculations. The following primers were used: *Ifna1* (5'-AAGGACAGGCAGGACTTTGGATTC-3' [forward] and 5'-GATCTCGCAGCACAGGGATGG-3' [reverse]), *Ifnb* (5'-AAGAGTTA-CACTGCCTTTGCCATC-3' [forward] and 5'-CACTGTCTGCTGGTGGAGTTCATC-3' [reverse]), *Il6* (5'-TGGCTAAGGACCAAGACCATCCAA-3' [forward] and 5'-AACGCACTAGGTTTGCCGAGTAGA-3' [reverse]), *Tnf* (5'-CCCTCACACTCAGATCATCTCT-3' [forward] and 5'-GCTACGACGTGGGCTACAG-3' [reverse]), *Il1b* (5'-CCCTGCAGCTGGAGAGTGTGGA-3' [forward] and 5'-CTGAGCGACCTGTCTTGCCG-3' [reverse]), *Ebi3* (5'-GTTCTCCACGGTGCCCTAC-3' [forward] and 5'-CGGCTTGATGATTCGCTC-3' [reverse]), *Il12a* (5'-CCACCCCTTGCCCTCCTAAA-3' [forward] and 5'-GCCGTCTTCACCATGTCATCT-3' [reverse]), *Foxp3* (5'-CTGCC-TTGGTACATTCGTGA-3' [forward] and 5'-CCAGATGTTGTGGGTGAGTG-3' [reverse]), *Ikzf2* (5'-TAAGCTCAGCTTATTCTCAGGTCATCA-3' [forward] and 5'-ATGTTGTTTTCTGACTATCAGATGTT-3' [reverse]), *p40* (5'-CGTGCACTGAGGCTCAGAAATGTTTC-3' [forward] and 5'-TTTCTTTGCACCAGCCATGAGC-3' [reverse]). The mitochondrial:nuclear splenocyte transcription ratio was calculated using the following primers: 16S or *Mmr2* (5'-CTAGAAACCCCGAAACCAA-3' [forward] and 5'-CCAGCTATCACCAAGCTCGT-3' [reverse]), and the  $\beta_2$ -microglobulin gene was also used as housekeeping gene (5'-ATGGGAAGCCGAACATACTG-3' [forward] and 5'-CAGTCTCAGTGGGGGTGAAT-3' [reverse]). All primers were purchased from IDT Integrated DNA Technologies.

### Splenocyte immunophenotyping by flow cytometry.

Splenocytes ( $1 \times 10^6$ ) were suspended in 100 µl of fluorescence-activated cell sorting (FACS) buffer, incubated with 1 µl of TruStain FcX (no. 422302; BioLegend) at 4°C for 15 minutes, followed by incubation with various fluorochrome-conjugated antibodies (all from BioLegend) at 4°C for 30 minutes. Cells were washed twice and immediately analyzed on a BD FACS Celesta flow cytometer (BD Biosciences) followed by FlowJo software. The following anti-mouse, fluorochrome-labeled antibodies were used: panel 1: APC\_CD86 (no. 105012), APC-Cy7\_CD11b (no. 101226), BV421\_CD19 (no. 124608), PE\_CD80 (no. 104708), PE-Cy7\_CD11c (no. 117318), Percp-Cy5.5\_MHCII (no. 116416); panel 2: APC\_Ly-6C (no. 128016), APC-Cy7\_CD86 (no. 105030), BV421\_Ly-6G (no. 127628), FITC\_CD40 (no. 124608), PE\_CD11b (no. 101208), PE-Cy7\_CD45 (no. 103114), Percp-Cy5.5\_MHCII (no. 116416); panel 3: APC\_CD23 (no. 101620), APC-Cy7\_CD21 (no. 123418), BV421\_CD19 (no. 115538), FITC\_CD45 (no. 103108), PE\_IgD (no. 405706), PE-Cy7\_IgM (no. 406514), Percp-

Cy5.5\_CD138 (no. 142510); panel 4: APC\_CD8 (no. 100712), APC-Cy7\_CD44 (no. 103028), BV421\_CD4 (no. 100438), FITC\_CD19 (no. 115506), PE\_CD62L (no. 104408), PE-Cy7\_CD3 (no. 100220), PerCP-Cy5.5\_CD45 (no. 103132); panel 5: APC\_CD11c (no. 117310), PB\_B220 (no. 103227), FITC\_CD45 (no. 103108), PE\_PDCA-1 (no. 127104).

**JAK1 activation in splenocytes.** JAK1 activation was quantified by dual enzyme-linked immunosorbent assay (ELISA) to detect phosphorylated and total JAK1 simultaneously in splenic tissue samples preserved at  $-80^{\circ}\text{C}$  and lysed according to instructions of the manufacturer (no. PEL-JAK1-Y1022-T-1; RayBiotech). Spleen tissue lysates contained  $753\text{ }\mu\text{g/ml}$  protein. Optical density at  $450\text{ nm}$  was measured using a FLUOstar Omega BMG Labtech plate reader.

**Endothelium-dependent vasorelaxation.** Vasorelaxation assessments of murine aortic rings were performed as previously described (25), with reagents purchased from Sigma-Aldrich. Briefly, aortic rings ( $\sim 2\text{ mm}$ ) were excised and maintained in physiologic salt solution (PSS) with aeration ( $95\%\text{ O}_2/5\%\text{ CO}_2$ ). After equilibration for 1 hour, contraction was achieved with PSS containing  $100\text{ mM}$  potassium chloride. Relaxed aortic rings were contracted with phenylephrine. Vasorelaxation was assessed by addition of a gradient of acetylcholine ( $1 \times 10^{-9}\text{ M}$  to  $1 \times 10^{-5}\text{ M}$ ). Results were reported as the percentage of phenylephrine contraction.

**Kidney histology analysis and immune complex (IC) deposition quantification.** Kidney slides were evaluated in a blinded manner by a veterinary pathologist (ZXY) for scoring of glomerular, tubulointerstitial, vascular, and lymphoproliferative lesions, as previously described (26). Histologic evaluations were made from paraffin-embedded slides stained with hematoxylin and eosin (H&E), Masson's trichrome, and periodic acid-Schiff (PAS) using semiquantitative analysis (0 = no changes; 1 = mild changes; 2 = moderate changes; and 3 = severe changes).

Renal IC deposition was quantified as previously described (23) using Alexa Fluor 594/F(ab')<sub>2</sub> goat anti-mouse IgG (no. A11020; ThermoFisher Scientific) and fluorescein isothiocyanate anti-murine C3 antibody (no. GC3-90F-Z; Immunology Consultants Laboratories). Three random images were obtained from each stained frozen section and were analyzed with Image J software, selecting the glomerular compartment to quantify mean pixels for each fluorescence channel used.

**Quantification of serum autoantibodies.** Serum anti-double-stranded DNA (anti-dsDNA) and anti-RNP quantification were performed as previously described (23), using commercially available ELISA kits (no. 5110 and no. 5410, respectively, from Alpha Diagnostic International). Serum samples

were diluted 1:125 in the low-nonspecific binding buffer, and the assay was performed following the manufacturer's instructions.

**Proteinuria determination.** The urine albumin:creatinine ratio was determined as previously described (23), using ELISA kits for creatinine and mouse albumin (no. 1012 and no. 1011, respectively) according to instructions of the manufacturer (Exocell).

**Bone marrow (BM) isolation and differentiation of murine macrophages.** NZB  $\times$  NZW BM precursors were treated in vivo with 4-OI or vehicle, purified and cultured for 24 hours in Dulbecco's modified Eagle's medium (DMEM) (no. 11995-065; ThermoFisher Scientific), supplemented with 10% fetal bovine serum (FBS) and 1% penicillin/streptomycin. After 24 hours, medium was replaced, and BM-derived macrophages were cultured ( $1.0 \times 10^6$  cells/ml) in 96-well Seahorse plates for 6 days in DMEM medium containing macrophage colony-stimulating factor (M-CSF)  $50\text{ ng/ml}$  (no. 216-MC; R&D Systems). M-CSF was replaced every 2 days.

**Quantification of neutrophil extracellular traps (NETs) and mitochondrial reactive oxygen species (mROS).** Isolation of mouse BM-derived neutrophils and human peripheral blood neutrophils, quantification of NET formation, and mROS were performed as previously described (23). Briefly, BM neutrophils were purified with Percoll gradient, and human neutrophils were purified using sedimentation with 2% Dextran, following a Ficoll gradient. Cells were seeded in 96-well plates ( $200,000\text{ cells}/100\text{ }\mu\text{l/well}$  in triplicates for each dye) and allowed to form NETs in the presence of Sytox (to quantify extracellular DNA;  $1\text{ }\mu\text{M}$  final concentration), Quant-It PicoGreen (to quantify total DNA; stock solution diluted 1:250), and MitoSOX (to quantify mROS; final concentration  $200\text{ ng/ml}$ ). All dyes were from ThermoFisher Scientific. At baseline, 1 hour, and 2 hours, fluorescence was measured for PicoGreen ( $485$  of  $520\text{ nm}$ ), MitoSOX ( $510$  of  $580\text{ nm}$ ), and Sytox ( $485$  of  $520\text{ nm}$ ), respectively, using a FluoStar Omega BMG Labtech plate reader. Cells without dye were used as blanks.

**Seahorse analysis.** This analysis was performed as previously described (27). The following reagents were used: glucose (no. G8769), oligomycin (no. 75351), carbonyl cyanide-4-(tri-fluoro-methoxy) phenylhydrazone (FCCP; no. C2910), 2-deoxy-D-glucose (2-DG; no. D1634), rotenone (no. R8875), antimycin A (no. A8674), sodium pyruvate (no. S8636), L-glutamine (no. 103579-100), XF calibrant (pH 7.4; no. 10084-000), and XF RPMI medium (pH 7.4; no. 103576-100) (all from Sigma-Aldrich). Seahorse plates and cartridges were from Agilent. BM-derived macrophages or splenocytes were plated on Corning Cell-Tak-coated Seahorse culture plates ( $300,000\text{ cells/well}$ ) (no. 354240; ThermoFisher Scientific) in XF RPMI medium. Seahorse XF



analysis was performed at 37°C with no CO<sub>2</sub>, using an XF-96 analyzer according to instructions of the manufacturer (Agilent). Mitochondrial stress test assay was performed using Seahorse XF RPMI medium with 25 mM glucose, 1 mM sodium pyruvate, and 2 mM L-glutamine. For mitochondrial stress tests, cells were treated serially with oligomycin (5  $\mu$ M), FCCP (1  $\mu$ M), rotenone (100 nM), and antimycin A (1  $\mu$ M), and oxygen consumption rates were quantified. For glycolysis stress tests, 300,000 cells/well were suspended in Seahorse XF RPMI medium with 2 mM L-glutamine; cells were treated serially with glucose (25 mM), oligomycin (5  $\mu$ M), and 2-DG (100 mM), and extracellular acidification rates were measured over time. Cell numbers at assay completion were normalized to DNA content using CyQuant dye (ThermoFisher Scientific; no. C7026). Wave, Excel, and Graph-Pad Prism software were used to analyze and graph the data.

**Western blot analysis.** Splenocyte extracts were prepared using Pierce RIPA Buffer (no. 8990; ThermoFisher

Scientific) with protease and phosphatase cocktail inhibitors. Protein concentration was determined using BCA Protein Assay Reagent (no. 23227; Pierce). Protein was resolved on NuPAGE 4–12% Bis-Tris gel, transferred to a nitrocellulose membrane, and then blocked for 1 hour with 10% bovine serum albumin (BSA). Antibody against mitochondrial antiviral signaling protein (MAVS) (no. sc-365334; Santa Cruz Biotechnology) was diluted 1:1,000 in 5% BSA and added and incubated overnight at 4°C. Monoclonal antibody against GAPDH (no. MA1-16757; Invitrogen) was used as a loading control and incubated for 1 hour at room temperature. After incubation with primary antibodies, membranes were washed 3 times and incubated with secondary antibodies coupled to IRDye 800CW. Membranes were developed using a Li-Cor Odyssey Clx scanner.

**Isolation of human primary monocyte-derived macrophages and cytokine measurements.** Subjects provided informed consent to participate in an NIH institutional review

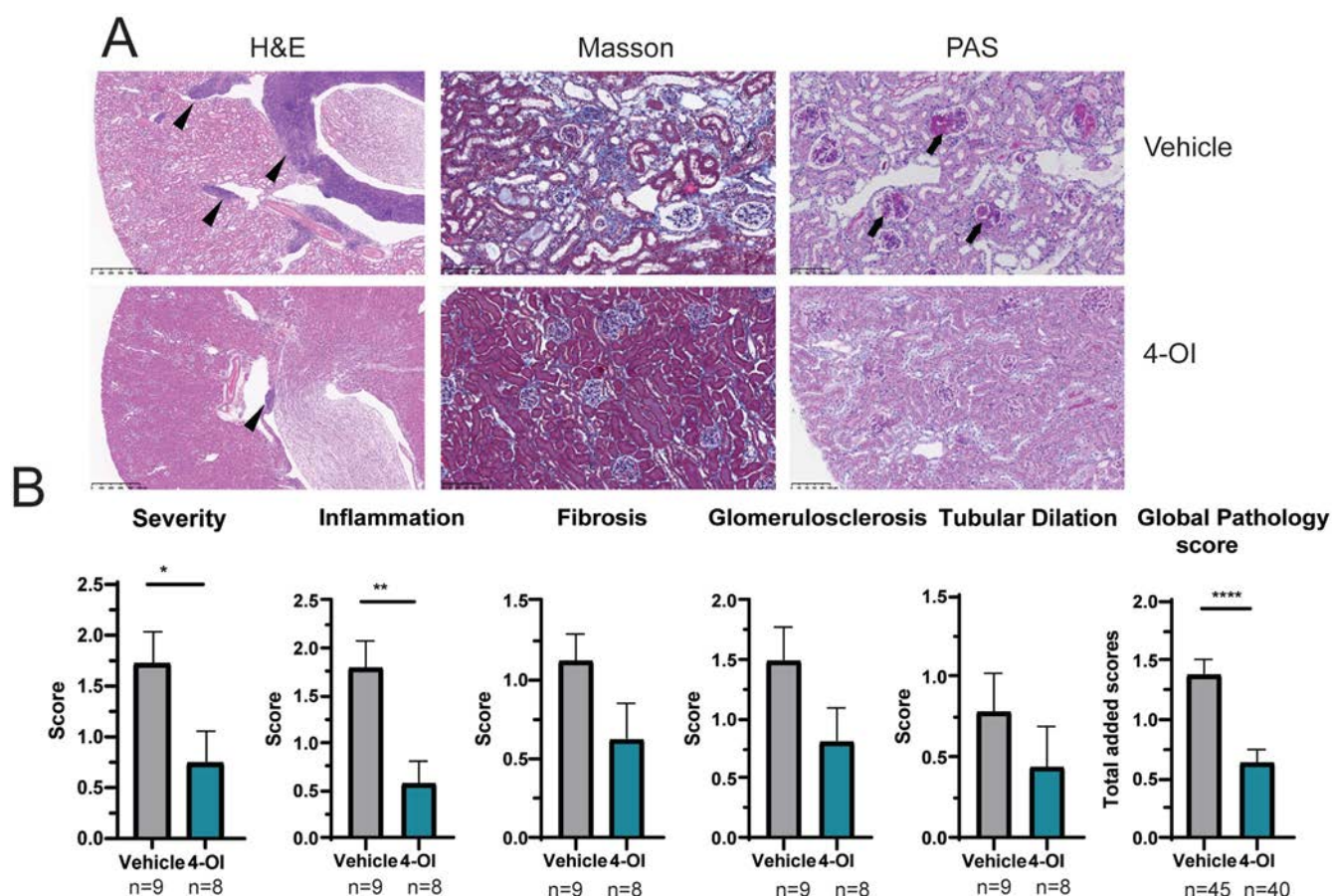


**Figure 1.** Attenuation of lupus pathologic features in the kidneys of mice with 4-octyl itaconate (4-OI) treatment. **A**, Representative kidney tissue images stained with hematoxylin and eosin (H&E) (original magnification  $\times 40$ ), Masson's trichrome (original magnification  $\times 200$ ), and periodic acid–Schiff (PAS). In H&E-stained images, **arrowheads** show inflammation. In PAS-stained images, **arrows** show glomerulosclerosis. **B**, Kidney pathology scores. Mice were treated with 4-OI or vehicle control. The number of animals per group is shown for each score; the global pathology score is the sum of all individual scores (severity, inflammation, fibrosis, glomerulosclerosis, and tubular dilation). Bars show the mean  $\pm$  SEM. \* =  $P < 0.05$ ; \*\* =  $P < 0.01$ ; \*\*\*\* =  $P < 0.001$ , by Mann-Whitney test.

board-approved protocol (no. 94-AR-0066). Human PBMCs were obtained using Ficoll density gradient Lymphoprep (StemCell Technologies; no. 07801) on whole blood from healthy donors or lupus patients. CD14<sup>+</sup> monocytes were purified by

positive selection using magnetic separation systems (MACS, no. 130-050-201; Miltenyi Biotec). Cells were cultured at  $0.5 \times 10^6$  cells/ml for 6 days in RPMI 1640 medium (Gibco, no. 11875093; ThermoFisher Scientific), with 10% FBS

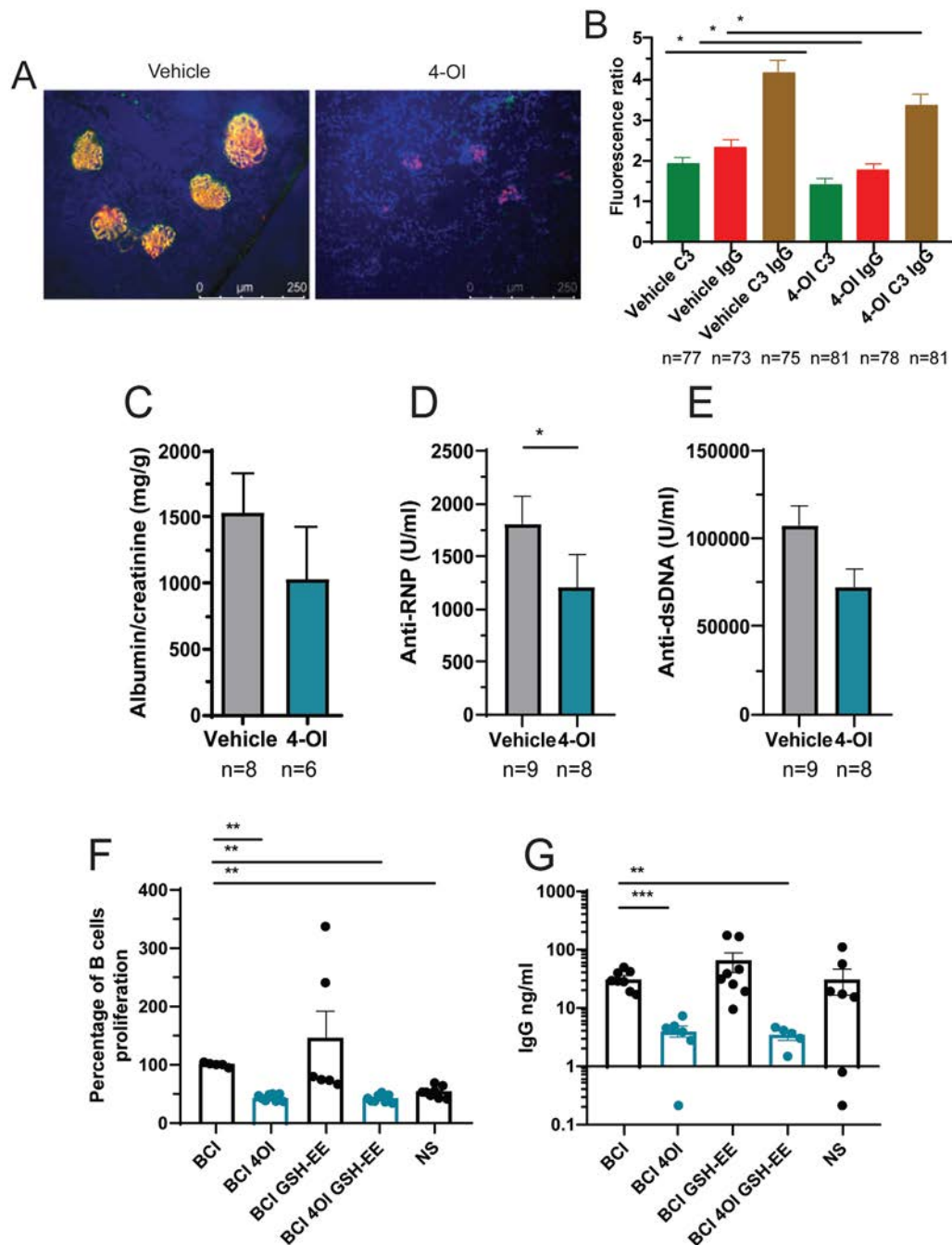


**Figure 2.** Attenuation of kidney damage and serum autoantibody levels in mice, and human B cell responses with 4-octyl itaconate (4-OI) treatment. **A**, Representative immunofluorescence photomicrographs displaying immune complex deposition. IgG is depicted in red, C3 in green, and nuclei in blue. Original magnification  $\times 40$ . **B**, Quantification of the results of pixel analysis of glomeruli in 3 different images from panel **A**, using ImageJ. **C**, Analysis of proteinuria in mice at the time of euthanasia. **D** and **E**, Serum levels of antibodies against RNP (**D**) and double-stranded DNA (dsDNA) (**E**). The number of mice per group is shown; any discrepancy in numbers is due to failure to collect urine in some of the mice in **C**. **F** and **G**, Human B cell proliferation (**F**) and total IgG secretion (**G**) after stimulation with BCI alone or stimulation with BCI followed by treatment with 4-OI, glutathione ethyl ester (GSH-EE), or 4-OI plus GSH-EE, or in conditions of nonstimulation (NS) in samples from 3 different healthy human donors (with technical duplicates for B cell proliferation and technical triplicates for enzyme-linked immunosorbent assay). Bars show the mean  $\pm$  SEM. \* =  $P < 0.05$ ; \*\* =  $P < 0.01$ ; \*\*\* =  $P < 0.001$ , by Mann-Whitney test.

containing granulocyte-M-CSF 25 ng/ml (no. 300-03; Pepro-Tech) or M-CSF 10 ng/ml (no. 216-MC; R&D Systems) to generate GM macrophages (M1) and M macrophages (M2), respectively. Cytokines were replaced every 2 days.

Six day-cultured macrophages were preincubated with 4-OI (0.5 mM or 1.0 mM) for 3 hours and then cultured in the presence or absence of 100 ng/ml *Escherichia coli* 0111:B4 LPS (no. L2630; Sigma-Aldrich) for 24 hours. Macrophage supernatants were harvested and stored at  $-80^{\circ}\text{C}$  until tested by ELISA (BD Biosciences) to quantify secreted human tumor necrosis factor (TNF; no. 555212), interleukin-6 (IL-6; no. 555220), IL-10 (no. 555157), IL-1 $\beta$  (no. 557953), and IL-8 (no. 555244).

**Isolation, culture, and stimulation of B cells.** Healthy control PBMCs were isolated with Ficoll gradient and treated using a MojoSort Human Pan B Cell Isolation Kit (no. 480081; BioLegend). CD19+ B cell purity was >90%. Purified CD19+ B cells (50,000 cells/200  $\mu\text{l}$ ) were cultured alone or with 1,000 units/ml IFN $\alpha$  (no. ab285741; Abcam), 0.5  $\mu\text{M}$  CpG-containing oligonucleotide (no. tlr-2216; Invivogen), or 1  $\mu\text{g}/\text{ml}$  anti-IgM B cell receptor (no. 109-006-129; Jackson ImmunoResearch) in 96-well plates. The 4-OI (1  $\mu\text{M}$ ) and glutathione ethyl ester (GSH-EE; 0.5  $\mu\text{M}$ ) (no. 14953; Cayman Chemical) were added on day 0 and remained in the culture for the duration of the assay. Culture medium was RPMI 1640 supplemented with 10% FCS, 100 units/ml penicillin, and 100 units/ml streptomycin.

**B cell proliferation analysis.** B cells were stained with BD Horizon CFSE (1  $\mu\text{M}$ ; no. 565082) following instructions of the manufacturer (BD Biosciences). Cells were washed twice and cultured (5 days for the first 2 donors and 7 days for the third donor). Analysis was performed using an Attune NxT Flow Cytometer, then using the FlowJo software and the proliferation modeling tool to obtain the percentage of divided B cells.

**IgG ELISA.** For quantification of in vitro IgG secretion, B cells were cultured alone or with in vitro stimulation in 96-well plates, as described above. IgG levels in the medium were determined using a Total Human IgG ELISA kit (no. 88-50550-22) following instructions of the manufacturer (ThermoFisher Scientific).

**Statistical analysis.** Statistical analysis was performed using GraphPad Prism software.

## RESULTS

**Decrease in lupus nephritis severity and autoantibody levels with 4-OI treatment.** Use of 4-OI led to histopathologic improvements in severity, inflammation, and global scores when compared with vehicle-treated mice (Figures 1A and B). Morphologically, there was noticeable kidney histology improvement upon treatment with 4-OI. Specifically, in the

4-OI-treated group, kidneys showed remarkable reduced inflammation compared to the vehicle-treated group. In addition, glomerulosclerosis and fibrosis were also less severe in the group

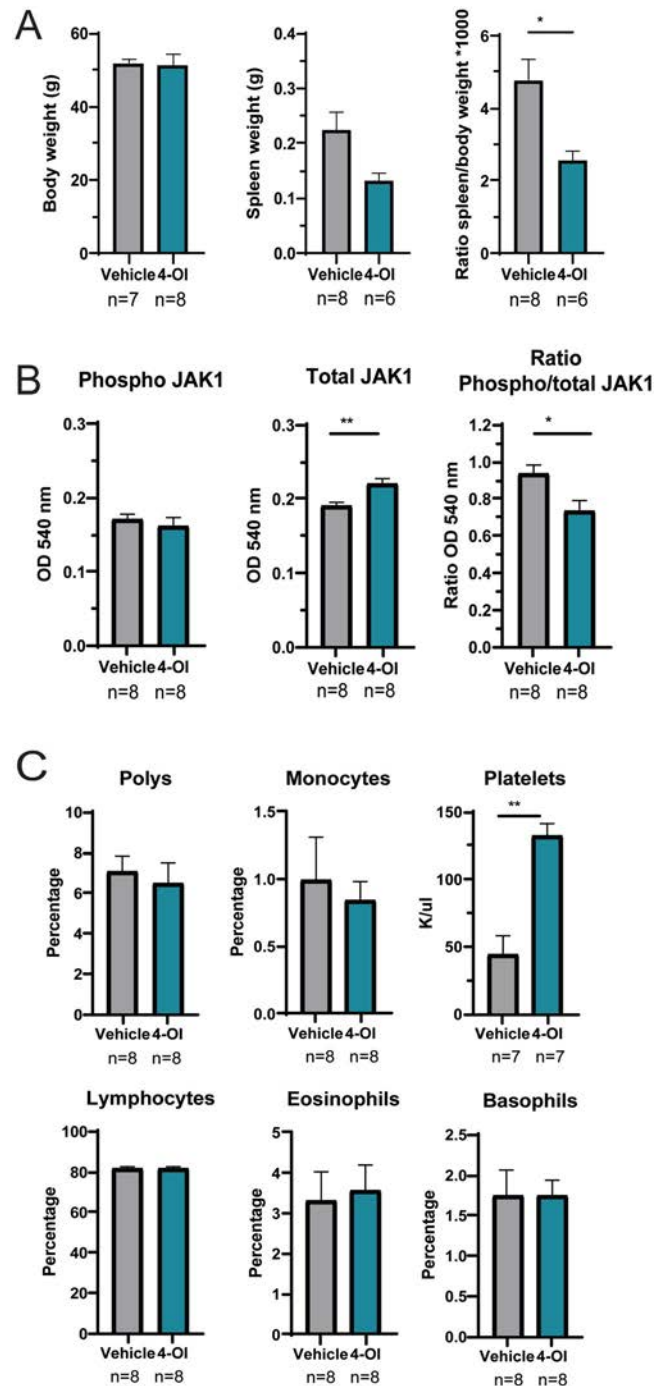


**Figure 3.** Modulation of splenomegaly, JAK1 activation, and platelet counts by 4-octyl itaconate (4-OI) in mice. **A**, Body and spleen weights with their ratio are displayed. **B**, Spleen tissue was homogenized, and phospho-JAK1 and total JAK1 proteins were detected by enzyme-linked immunosorbent assay. **C**, Complete blood cell counts are shown. Outlier data points were detected using the GraphPad ROUT method ( $Q = 10\%$ ) and excluded from the analysis. Bars show the mean  $\pm$  SEM. \* =  $P < 0.05$ ; \*\* =  $P < 0.01$ , by Mann-Whitney test. Polys = neutrophils.



treated with 4-OI. The total renal severity score was lower in 4-OI-treated mice than in vehicle treated (Figure 1B). Furthermore, IC deposition was significantly reduced in the 4-OI group compared to vehicle alone (Figures 2A and B). These histologic changes were associated with decreases in the albumin:creatinine ratio in the 4-OI group (Figure 2C), compared to the vehicle group, indicating improvement in kidney function. One of the mice in the 4-OI treatment spontaneously succumbed to kidney failure on day 26.

Serum autoantibodies against RNP were significantly decreased while anti-dsDNA also decreased, albeit not significantly, in the 4-OI group, compared to the vehicle group (Figures 2D and E). Consistent with these findings, *in vitro* incubation of human B cells with 4-OI inhibited proliferation and total IgG secretion, even in the presence of the GSH-EE cell-permeant glutathione compound that prevents 4-OI protein alkylation

(Figures 2F and G). Overall, *in vivo* 4-OI treatment led to improvement in murine lupus glomerulonephritis and decreased *in vivo* autoantibody levels, while *in vitro* 4-OI decreased human B cell proliferation and IgG synthesis.

**Improvement of thrombocytopenia and modulation of lymphoid organ responses in murine lupus with 4-OI treatment.** Body weight remained similar between the 2 treatment groups, while the spleen:body weight ratio in 4-OI-treated mice was significantly reduced compared to mice treated with vehicle alone (Figure 3A). A recent report suggested that 4-OI can inhibit JAK1 kinase activity (28). Supporting these findings, JAK1 activation (ratio of phospho-JAK1:total JAK1) in murine lupus splenocytes was significantly reduced in the *in vivo*-treated 4-OI group compared to vehicle (Figure 3B).

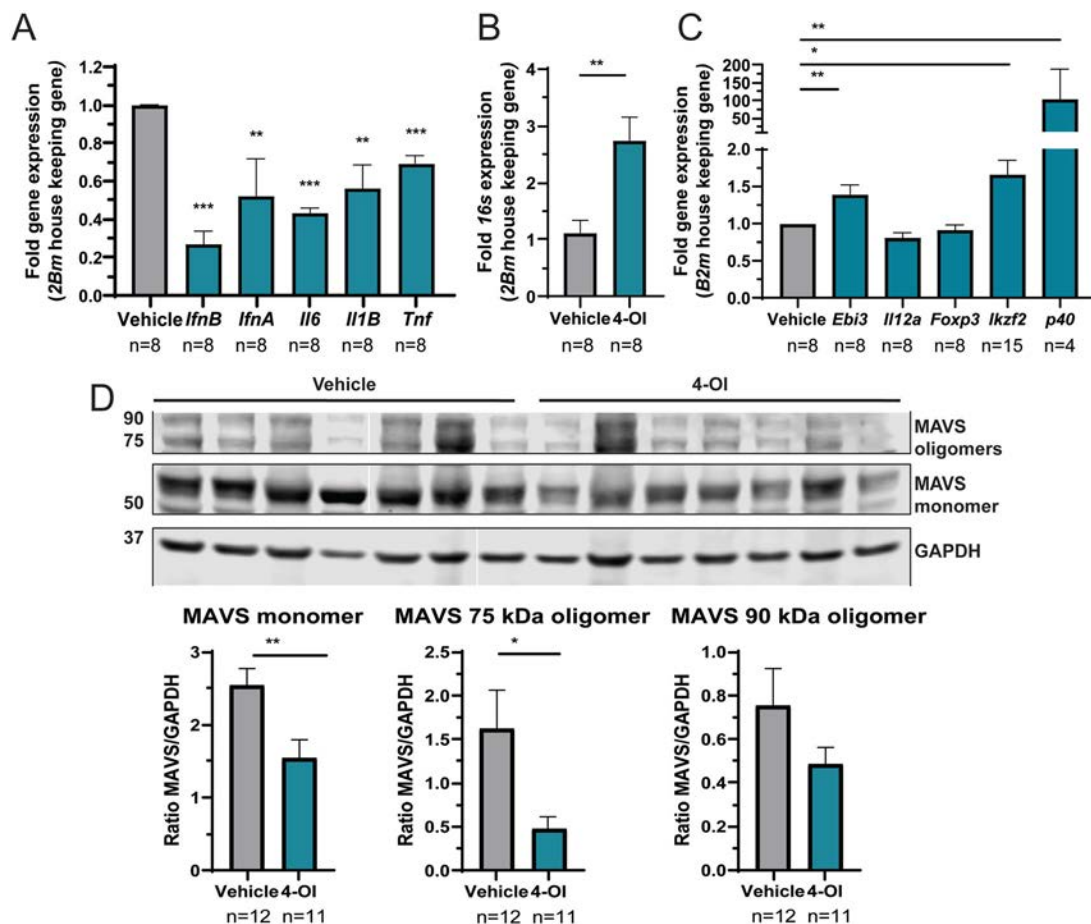


**Figure 4.** Effect of 4-octyl itaconate (4-OI) on gene expression and inflammasome protein expression in spleen cells in mice. **A**, Gene expression in splenocytes was analyzed by quantitative real-time polymerase chain reaction (qRT-PCR) normalized against *B2m* (housekeeping gene). **B**, The 16S mitochondrial gene expression in splenocytes was determined by qRT-PCR as a surrogate of mitochondrial transcriptional activity. **C**, Gene expression of associated Treg cell markers is shown. Mice were treated with 4-OI or vehicle control ( $n = 4$  mice/group with 2 technical duplicates, except for *Ikzf2*, which was performed in quadruplicate). Missing values are samples with no amplification. Bars show the mean  $\pm$  SEM. **D**, The expression of mitochondrial antiviral signaling protein (MAVS) monomer, MAVS 75 kDa oligomer, MAVS 90 kDa oligomer, and GAPDH was quantified by Western blotting in lysates of splenocytes from vehicle- or 4-OI-treated mice. The first Western blot was performed with 5 vehicle-treated animals and 4 4-OI-treated animals, and the second blot was performed with 7 animals in each group. Bars show the mean  $\pm$  SEM ratio of protein to GAPDH loading control expression. \* =  $P < 0.05$ ; \*\* =  $P < 0.01$ ; \*\*\* =  $P < 0.001$ , by Mann-Whitney test.

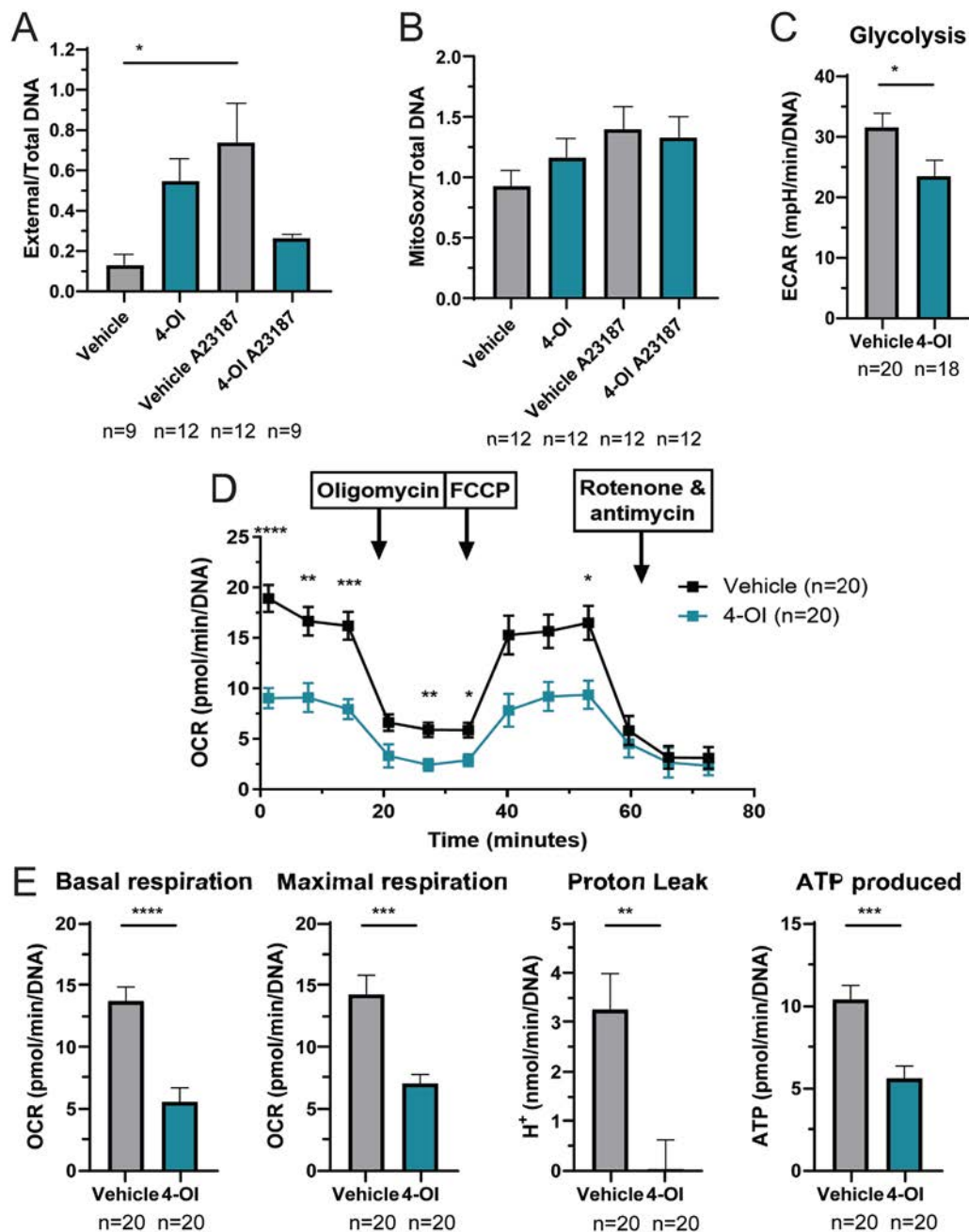


**Figure 5.** Modulation of neutrophil extracellular trap (NET) formation and immunometabolism with 4-octyl itaconate (4-OI) treatment in mice. **A**, NETs were quantified in bone marrow (BM)-derived neutrophils, 2 hours post-plating, by Sytox and PicoGreen plate assay to measure external and total DNA, respectively. **B**, Mitochondrial reactive oxygen species (mROS) were quantified in BM-derived neutrophils, 1 hour post-plating, using MitoSox by plate assay. In **A** and **B**, mice were treated with 4-OI or vehicle control ( $n = 4$  mice per group and 3 technical repeats). Neutrophils were stimulated with the A23187 calcium ionophore ( $250 \mu\text{M}$ ) to induce NETs and mROS. **C**, Glycolysis of murine BM-differentiated macrophages was measured by Seahorse ( $n = 4$  mice/group with 5 technical repeats). **D**, Mitochondrial stress test analysis of splenocytes was performed by Seahorse. Statistical analysis used 2-way analysis of variance. **E**, Parameters for Seahorse analysis of splenocytes were calculated using the values from **D**. Seahorse studies included mice treated with 4-OI or vehicle ( $n = 4$  mice/group with 5 technical repeats). Outlier data points were detected using the GraphPad ROUT method ( $Q = 10\%$ ) and excluded from the analysis. Bars show the mean  $\pm$  SEM. \* =  $P < 0.05$ ; \*\* =  $P < 0.01$ ; \*\*\* =  $P < 0.001$ ; \*\*\*\* =  $P < 0.0001$ , by Mann-Whitney test. ECAR = extracellular acidification rate; OCR = oxygen consumption rate; FCCP = carbonyl cyanide-4-(trifluoro-methoxy) phenylhydrazone.

NZB  $\times$  NZW mice develop thrombocytopenia and vascular dysfunction as part of immune-mediated dysregulation. Mice treated with 4-OI had significant improvements in platelet counts (Figure 3C) and endothelium-dependent

vasorelaxation compared to those treated with vehicle (see Supplementary Figure 1, available on the *Arthritis & Rheumatology* website at <http://onlinelibrary.wiley.com/doi/10.1002/art.42284>).



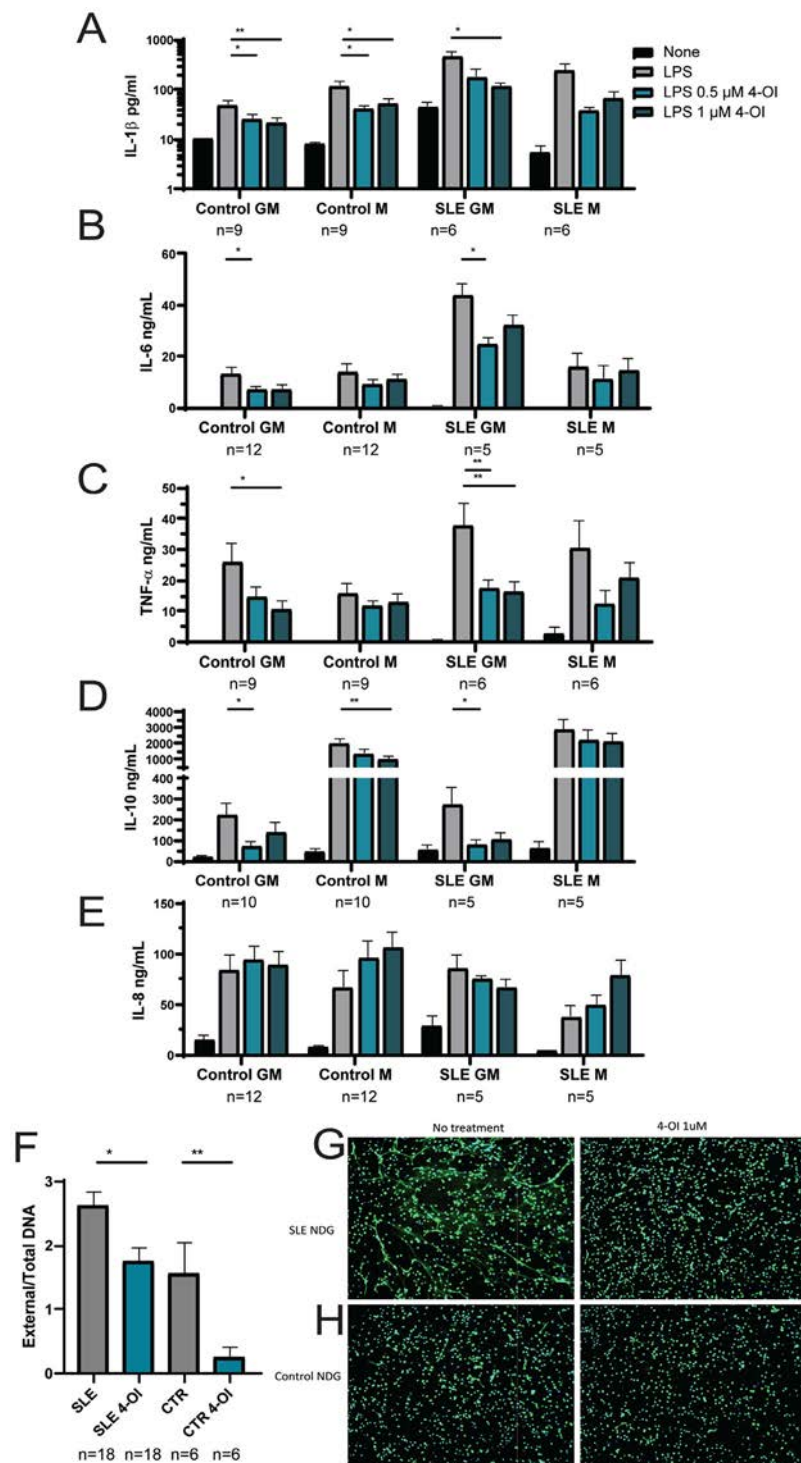


**Figure 6.** In vitro effect of 4-octyl itaconate (4-OI) on cytokine release by human monocyte-derived primary macrophages and neutrophil extracellular trap (NET) formation. **A–E**, Human primary monocyte-derived macrophages ( $n \geq 6$  from different donors) were obtained from circulating monocytes from healthy controls or patients with systemic lupus erythematosus (SLE) by differentiating between either granulocyte-macrophage colony-stimulating factor (GM-CSF) (proinflammatory) or M-CSF (antiinflammatory) (M) macrophages for 7 days. Cytokines in supernatants were measured by enzyme-linked immunosorbent assay after 24 hours of treatment with 4-OI or vehicle. Measured cytokines included interleukin-1 $\beta$  (**A**), IL-6 (**B**), tumor necrosis factor (TNF) (**C**), IL-10 (**D**), and IL-8 (**E**). **F**, NET formation in normal dense granulocytes (NDGs) was measured by fluorometry plate assay. **G** and **H**, Fluorescence microscopy imaging shows merged immunofluorescence staining with primary antibody against neutrophil elastase (green) and DNA (nuclei and NET fibers; Hoechst blue) in NDGs from SLE patients (**G**) and healthy controls (**H**). Original magnification  $\times 10$ . In **A–F**, experiments were performed with technical duplicates in 9 SLE patients and 3 healthy controls (CTR). Bars show the mean  $\pm$  SEM. \* =  $P < 0.05$ ; \*\* =  $P < 0.01$ , by Mann-Whitney test.

Splenocyte gene expression analysis revealed significant decreases in *Ifna*, *Ifnb*, *Il6*, *Il1b*, and *Tnf* with 4-OI treatment compared to vehicle (Figure 4A). As itaconic acid is a mitochondrial immunometabolite that reduces oxidative stress, we quantified 16S gene expression as a surrogate of mitochondrial transcription and found it significantly increased in the 4-OI group compared to the vehicle group (Figure 4B), suggesting a beneficial effect in mitochondrial physiology. With regard to immune cell composition in the spleen, the effects of 4-OI were mild and included significant increases in the mean fluorescent intensity of CD80, but not CD86, in dendritic cells (DCs) and B cells (Supplementary Figure 2, <http://onlinelibrary.wiley.com/doi/10.1002/art.42284>). The percentage of splenic CD8 T cells was significantly increased by 4-OI treatment compared to vehicle, with a significant reduction in the CD4:CD8 ratio (mean  $\pm$  SEM  $4.1 \pm 0.6$  for vehicle versus  $2.6 \pm 0.2$  for 4-OI;  $P < 0.03$  by Student's *t*-test). As a surrogate for assessing Treg cells, we quantified splenocyte gene expression of cytokine-associated genes and Treg cell differentiation gene markers. Gene transcription of transcription factor Helios (*Iikzf2*) and components of suppressive cytokines *Ebi3* (IL-35) and *p40* (29) were significantly enhanced, supporting the notion that 4-OI induces immunoregulatory effects (Figure 4C).

MAVS is an essential adaptor for retinoic acid-inducible gene 1/melanoma differentiation-associated protein 5 signaling and sensing of RNA; it plays pathogenic roles in some murine lupus models. Because MAVS forms oligomers in lupus cells in high-oxidative stress conditions (30), we measured MAVS protein expression by Western blot. MAVS monomers and oligomers were decreased in the 4-OI group compared to vehicle (Figure 4D). Overall, these results indicate that 4-OI attenuates oxidative damage and immune dysregulation in lymphoid organs in murine lupus.

**Modulation of neutrophil responses with 4-OI treatment.** Neutrophils contribute to oxidative stress during inflammatory responses. To analyze the effect of 4-OI in neutrophil phenotype and function, we tested the ability of BM-derived neutrophils to form NETs, a feature that is dysregulated in murine and human lupus in association with aberrant mROS synthesis (23). Mice treated with 4-OI showed a trend toward enhanced basal NET formation and mROS synthesis; however, they displayed unresponsiveness to calcium ionophore-induced NET formation and enhanced mROS (Figures 5A and B). These data suggest that 4-OI attenuates neutrophil activation and NET formation in response to stimulation.

As the itaconate pathway is involved in the regulation of metabolism, we analyzed the effect of 4-OI in the bioenergetics of BM-derived macrophages and splenocytes. While oxidative phosphorylation (OXPHOS) was not significantly modulated in macrophages after in vivo 4-OI administration, glycolysis was significantly inhibited (Figure 5C). Splenocytes, which in lupus have

been described to exhibit enhanced mitochondrial OXPHOS (31), displayed significant OXPHOS reduction after 4-OI exposure when compared to vehicle-treated mice (Figures 5D and E), including reductions in basal and maximal respiration, proton leak, and ATP production. Overall, 4-OI modulated immunometabolic parameters in murine lupus.

**Modulation of inflammatory responses in human myeloid cells with in vitro 4-OI treatment.** To further assess the effects of 4-OI in human lupus, we assessed whether it could modulate proinflammatory responses of human monocyte-derived macrophages and NET formation in human neutrophils. Healthy control or SLE peripheral blood monocytes were differentiated into GM (M1, proinflammatory) or M (M2, anti-inflammatory) macrophages and treated with 4-OI, stimulated with 100 ng/ml LPS for 24 hours, and cytokine secretion was quantified. In vitro, both 0.5- and 1- $\mu$ M 4-OI concentrations significantly reduced the levels of secreted IL-1 $\beta$ , IL-6, TNF, and IL-10, particularly in the GM macrophages (Figures 6A–D). Furthermore, 4-OI inhibited secretion of IL-1 $\beta$  and IL-10 by healthy control macrophages (Figures 6A and D). In contrast, there was no modulation of IL-8 secretion by 4-OI in control- or SLE patient-derived macrophages (Figure 6E). Additionally, NET formation in controls or SLE patients was inhibited with 1  $\mu$ M 4-OI (Figures 6F–H). These data support an immunoregulatory role of 4-OI in human myeloid cells.

## DISCUSSION

We found that subcutaneous administration of 4-OI improves features of murine lupus when treatment is initiated after clinical disease is already established. The beneficial effects were observed in renal function, histopathology and IC deposition, platelet counts, vascular dysfunction, and in the levels of circulating autoantibodies. Furthermore, the drug inhibited inflammatory responses in immune cells and changed immunometabolic parameters. These effects might be related, with the previously documented ability of itaconate to attenuate proinflammatory pathways in other inflammatory models. Given that most immune cell subsets in lymphoid organs did not significantly change, it remains to be further determined the mechanisms by which autoimmune responses were hampered in murine lupus, but it could be related to modulation of myeloid cell dysregulation with downstream effects on other innate and adaptive immune cells, including Treg cells and B cells.

Levels of various antinuclear antibodies as well as type I IFN pathway dysregulation were reduced by 4-OI administration. The mechanisms leading to down-modulation of these autoimmune responses are likely multifactorial. As autoantigen/autoantibody ICs can trigger type I IFN production (32), it is possible that modulation of IC formation (via 4-OI decreasing autoantigen generation by inhibiting NET formation or other types of

inflammatory cell death) may decrease immune dysregulation. Decreases in synthesis and release of other inflammatory cytokines by immune cells observed with 4-OI may also hamper autoantibody generation, as previously reported (33,34). Among the effects that 4-OI had on various cytokines, it reduced the ability of human macrophages to secrete IL-10. This cytokine may play pathogenic roles in SLE, including autoantibody synthesis (35–37). It is therefore possible that decreases in autoantibodies and improvement in platelet numbers following 4-OI treatment could be due in part to effects on IL-10 synthesis, in addition to the direct inhibition of B cell function that was observed by *in vitro* human studies. Given that inhibition of B cell proliferation and IgG secretion by human B cells after 4-OI treatment was not alkylation-dependent, it is possible that the immunomodulation might occur through other effects in immunometabolism, such as inhibition of succinate dehydrogenase (38), which should be explored in future studies.

Recently described attenuation of specific allergic inflammatory responses in mice by 4-OI intranasal treatment was accomplished via reduction of DC priming activity (39). A similar phenomenon might take effect here, in which 4-OI treatment could partially reduce DC priming responses to lupus autoantigens. Other possible effects of 4-OI to explain the elevated numbers of CD8<sup>+</sup> T cells in 4-OI-treated animals is the observed inhibition of glycolysis and mechanistic target of rapamycin (mTOR) pathways. This is supported by previous findings that rapamycin, an inhibitor of mTOR, can increase both CD8<sup>+</sup> T cells and Treg cell function in SLE patients with concomitant improvement in disease activity (40,41).

While FoxP3 levels were not transcriptionally regulated by treatment, future studies should assess whether survival of memory CD8<sup>+</sup> T cells and CD8-specific FoxP3 expression or Treg cell suppressor function are affected by this treatment. Another important aspect is the regulation of perturbed metabolic responses with 4-OI. Proinflammatory (M1) macrophages rely on glycolysis and exhibit impairment of the T cell-attracting chemokine cycle and OXPHOS, whereas antiinflammatory (M2) macrophages are more dependent on mitochondrial OXPHOS (42). In our study, 4-OI treatment attenuated glycolysis in BM-derived macrophages, and this may have significant relevance for lupus-prone mice, as enhanced glycolysis is associated with the elevated proinflammatory environment characteristic of SLE. Indeed, blunting glycolysis in macrophages has been shown to improve lupus nephritis in mice (43). In addition, 4-OI treatment enhanced the mitochondrial gene transcription, suggesting a potential improvement in mitochondrial function (24,44). Furthermore, the reduction of MAVS oligomerization with 4-OI suggests that the oxidative stress status was reduced, most probably through the Nrf2 pathway, given that ROS play a role in inducing MAVS-

dependent responses in SLE (30). This in turn may help decrease aberrant responses to nucleic acids in lupus cells. In addition, 4-OI promoted a decreased ability of murine and human neutrophils to synthesize NETs.

Part of the mechanism that may be involved in blunting inflammatory responses is through the recently described role of 4-OI in modulating JAK1-mediated pathways. The JAK/STAT pathway plays fundamental roles in SLE (45). We observed that 4-OI blunted activation of JAK1 in murine lupus, as recently described (28). Overall, these results indicate that 4-OI exerts pleiotropic antiinflammatory effects on myeloid cells and adaptive immune cells.

Limitations of this study include the use of a single mouse model of lupus, indicating that effects on other potential lupus manifestations (such as skin involvement) were therefore not addressed. It is important to mention that the beneficial effects were observed when therapy was started only after immune dysregulation and organ damage were well established. Serum concentrations of itaconic acid have been previously reported to be significantly reduced in SLE patients with active disease compared to healthy controls (46). As we observed amelioration of established murine lupus, our findings add new evidence to the existing literature which suggests that modulation of immunometabolism may be a viable therapeutic strategy in SLE and other systemic autoimmune disorders. This was strengthened by the beneficial effects observed in human cells *in vitro*. These findings support the possibility of further exploring the role of itaconate-derived medications in autoimmune disorders such as SLE.

## ACKNOWLEDGMENTS

We thank the Office of Science and Technology, Intramural Research Program, National Institute of Arthritis and Musculoskeletal and Skin Diseases (NIAMS)/NIH for technical support.

## AUTHOR CONTRIBUTIONS

All authors were involved in drafting the article or revising it critically for important intellectual content, and all authors approved the final version to be published. Dr. Kaplan had full access to all of the data in the study and takes responsibility for the integrity of the data and the accuracy of the data analysis.

**Study conception and design.** Blanco, Kaplan.

**Acquisition of data.** Blanco, Patino-Martinez, Nakabo, Zhang, Pedersen, Wang, Carmona-Rivera, Claybaugh, Desta.

**Analysis and interpretation of data.** Blanco, Patino-Martinez, Nakabo, Carmona-Rivera, Yu, Kaplan.

## REFERENCES

1. Kaplan MJ. Role of neutrophils in systemic autoimmune diseases. *Arthritis Res Ther* 2013;15:219.
2. Mohan C, Putterman C. Genetics and pathogenesis of systemic lupus erythematosus and lupus nephritis [review]. *Nat Rev Nephrol* 2015; 11:329–41.




3. Kiriakidou M, Chin KL. Systemic lupus erythematosus. *Ann Intern Med* 2020;172:ITC81–96.
4. Crow MK, Olfieriev M, Kirou KA. Type I interferons in autoimmune disease [review]. *Annu Rev Pathol* 2019;14:369–93.
5. Li Z, Guo J, Bi L. Role of the NLRP3 inflammasome in autoimmune diseases. *Biomed Pharmacother* 2020;130:110542.
6. Perl A. Oxidative stress in the pathology and treatment of systemic lupus erythematosus [review]. *Nat Rev Rheumatol* 2013;9:674–86.
7. Lightfoot YL, Blanco LP, Kaplan MJ. Metabolic abnormalities and oxidative stress in lupus. *Curr Opin Rheumatol* 2017;29.
8. Romo-Tena J, Kaplan MJ. Immunometabolism in the pathogenesis of systemic lupus erythematosus: an update. *Curr Opin Rheumatol* 2020;32.
9. Kim J, Gupta R, Blanco LP, et al. VDAC oligomers form mitochondrial pores to release mtDNA fragments and promote lupus-like disease. *Science* 2019;366:1531–6.
10. Hooftman A, O'Neill LA. The immunomodulatory potential of the metabolite itaconate. *Trends Immunol* 2019;40:687–98.
11. Diskin C, Ryan TA, O'Neill LA. Modification of proteins by metabolites in immunity. *Immunity* 2021;54:19–31.
12. Luan HH, Medzhitov R. Food fight: role of itaconate and other metabolites in antimicrobial defense [review]. *Cell Metab* 2016;24:379–87.
13. Mills EL, Ryan DG, Prag HA, et al. Itaconate is an anti-inflammatory metabolite that activates Nrf2 via alkylation of KEAP1. *Nature* 2018;556:113–7.
14. Liao ST, Han C, Xu DQ, et al. 4-Octyl itaconate inhibits aerobic glycolysis by targeting GAPDH to exert anti-inflammatory effects. *Nat Commun* 2019;10:5091.
15. Olagnier D, Brandt AM, Gunderstofte C, et al. Nrf2 negatively regulates STING indicating a link between antiviral sensing and metabolic reprogramming. *Nat Commun* 2018;9:3506.
16. Li R, Yang W, Yin Y, et al. 4-OI attenuates carbon tetrachloride-induced hepatic injury via regulating oxidative stress and the inflammatory response. *Front Pharmacol* 2021;12:651444.
17. Li Y, Chen X, Zhang H, et al. 4-octyl itaconate alleviates lipopolysaccharide-induced acute lung injury in mice by inhibiting oxidative stress and inflammation. *Drug Des Devel Ther* 2020;14:5547–58.
18. Liu G, Wu Y, Jin S, et al. Itaconate ameliorates methicillin-resistant *Staphylococcus aureus*-induced acute lung injury through the Nrf2/ARE pathway. *Ann Transl Med* 2021;9:712.
19. Tian F, Wang Z, He J, et al. 4-Octyl itaconate protects against renal fibrosis via inhibiting TGF- $\beta$ /Smad pathway, autophagy and reducing generation of reactive oxygen species. *Eur J Pharmacol* 2020;873:172989.
20. Xin Y, Zou L, Lang S. 4-Octyl itaconate (4-OI) attenuates lipopolysaccharide-induced acute lung injury by suppressing PI3K/Akt/NF- $\kappa$ B signaling pathways in mice. *Exp Ther Med* 2021;21:141.
21. Li R, Yang W, Yin Y, et al. Protective role of 4-octyl itaconate in murine LPS/D-GalN-induced acute liver failure via inhibiting inflammation, oxidative stress, and apoptosis. *Oxid Med Cell Longev* 2021;2021:9932099.
22. Tang C, Wang X, Xie Y, et al. 4-octyl itaconate activates Nrf2 signaling to inhibit pro-inflammatory cytokine production in peripheral blood mononuclear cells of systemic lupus erythematosus patients. *Cell Physiol Biochem* 2018;51:979–90.
23. Lood C, Blanco LP, Purmalek MM, et al. Neutrophil extracellular traps enriched in oxidized mitochondrial DNA are interferogenic and contribute to lupus-like disease. *Nat Med* 2016;22:146–53.
24. Blanco LP, Pedersen HL, Wang X, et al. Improved mitochondrial metabolism and reduced inflammation following attenuation of murine lupus with coenzyme Q10 analog idebenone. *Arthritis Rheumatol* 2020;72:454–64.
25. Carmona-Rivera C, Purmalek MM, Moore E, et al. A role for muscarinic receptors in neutrophil extracellular trap formation and levamisole-induced autoimmunity. *JCI Insight* 2017;2:e89780.
26. Furumoto Y, Smith CK, Blanco L, et al. Tofacitinib ameliorates murine lupus and its associated vascular dysfunction. *Arthritis Rheumatol* 2017;69:148–60.
27. Gupta S, Nakabo S, Blanco LP, et al. Sex differences in neutrophil biology modulate response to type I interferons and immunometabolism. *Proc Natl Acad Sci USA* 2020;117:16481–91.
28. Runtsch MC, Angiari S, Hooftman A, et al. Itaconate and itaconate derivatives target JAK1 to suppress alternative activation of macrophages. *Cell Metab* 2022;34:487–501.
29. Lee SY, Moon SJ, Moon YM, et al. A novel cytokine consisting of the p40 and EBI3 subunits suppresses experimental autoimmune arthritis via reciprocal regulation of Th17 and Treg cells. *Cell Mol Immunol* 2022;19:79–91.
30. Buskiewicz IA, Montgomery T, Yasewicz EC, et al. Reactive oxygen species induce virus-independent MAVS oligomerization in systemic lupus erythematosus. *Sci Signal* 2016;9:ra115.
31. Wahl DR, Petersen B, Warner R, et al. Characterization of the metabolic phenotype of chronically activated lymphocytes. *Lupus* 2010;19:1492–501.
32. Lövgren T, Eloranta ML, Båve U, et al. Induction of interferon- $\alpha$  production in plasmacytoid dendritic cells by immune complexes containing nucleic acid released by necrotic or late apoptotic cells and lupus IgG. *Arthritis Rheum* 2004;50:1861–72.
33. Dienz O, Eaton SM, Bond JP, et al. The induction of antibody production by IL-6 is indirectly mediated by IL-21 produced by CD4+ T cells. *J Exp Med* 2009;206:69–78.
34. Nakae S, Asano M, Horai R, et al. Interleukin-1  $\beta$ , but not interleukin-1  $\alpha$ , is required for T-cell-dependent antibody production. *Immunology* 2001;104:402–9.
35. Baglaenko Y, Manion KP, Chang NH, et al. IL-10 production is critical for sustaining the expansion of CD5+ B and NKT cells and restraining autoantibody production in congenic lupus-prone mice. *PLoS One* 2016;11:e0150515.
36. Teichmann LL, Kashgarian M, Weaver CT, et al. B cell-derived IL-10 does not regulate spontaneous systemic autoimmunity in MRL.Fas (lpr) mice. *J Immunol (Baltimore)* 2012;188:678–85.
37. Xu L, Wang L, Shi Y, et al. Up-Regulated Interleukin-10 Induced by E2F Transcription Factor 2–MicroRNA-17-5p Circuitry in Extrafollicular Effector B Cells Contributes to Autoantibody Production in Systemic Lupus Erythematosus Arthritis Rheumatol 2021;74:496–507.
38. Domínguez-Andrés J, Novakovic B, Li Y, et al. The itaconate pathway is a central regulatory node linking innate immune tolerance and trained immunity. *Cell Metab* 2019;29:211–20.
39. Jaiswal AK, Yadav J, Makhija S, et al. Irg1/itaconate metabolic pathway is a crucial determinant of dendritic cells immune-priming function and contributes to resolute allergen-induced airway inflammation. *Mucosal Immunology* 2022;15:301–13.
40. Lai ZW, Kelly R, Winans T, et al. Sirolimus in patients with clinically active systemic lupus erythematosus resistant to, or intolerant of, conventional medications: a single-arm, open-label, phase 1/2 trial. *Lancet* 2018;391:1186–96.
41. Kato H, Perl A. Blockade of Treg cell differentiation and function by the interleukin-21–mechanistic target of rapamycin axis via suppression of autophagy in patients with systemic lupus erythematosus. *Arthritis Rheumatol* 2018;70:427–38.
42. Viola A, Munari F, Sánchez-Rodríguez R, et al. The metabolic signature of macrophage responses [review]. *Front Immunol* 2019;10:1462.

43. Jing C, Castro-Dopico T, Richoz N, et al. Macrophage metabolic reprogramming presents a therapeutic target in lupus nephritis. *Proc Natl Acad Sci USA* 2020;117:15160–71.
44. Reyes A, Rusecka J, Tońska K, et al. RNase H1 regulates mitochondrial transcription and translation via the degradation of 7S RNA. *Front Genet* 2020;10:1393.
45. Hedrich CM, Rauen T, Apostolidis SA, et al. Stat3 promotes IL-10 expression in lupus T cells through trans-activation and chromatin remodeling. *Proc Natl Acad Sci USA* 2014;111:13457–62.
46. Li Y, Liang L, Deng X, et al. Lipidomic and metabolomic profiling reveals novel candidate biomarkers in active systemic lupus erythematosus. *Int J Clin Exp Pathol* 2019;12:857–66.



**BRIEF REPORT**

# Telomere Length and Development of Systemic Lupus Erythematosus: A Mendelian Randomization Study

Xu-Fan Wang,<sup>1</sup> Wen-Jing Xu,<sup>1</sup> Fei-Fei Wang,<sup>1</sup> Rui Leng,<sup>1</sup> Xiao-Ke Yang,<sup>2</sup> Hua-Zhi Ling,<sup>3</sup> Yin-Guang Fan,<sup>1</sup> Jin-Hui Tao,<sup>4</sup>  Zong-Wen Shuai,<sup>2</sup> Li Zhang,<sup>5</sup> Dong-Qing Ye,<sup>1</sup>  and Rui-Xue Leng,<sup>1</sup> 

**Objective.** Previous observational studies demonstrated that a subset of patients with systemic lupus erythematosus (SLE) have markedly short telomere length in leukocytes. This study was undertaken to test whether leukocyte telomere length is causally associated with risk of SLE.

**Methods.** A 2-sample Mendelian randomization (MR) analysis was conducted to estimate causality of telomere length on SLE in European populations. A replication 2-sample MR study using Asian genetic data was also conducted. A reverse MR analysis was then performed to test the effects of SLE on telomere length. The autoantibodies targeting telomere-associated protein (telomeric repeat-binding factor 1 [TERF1] autoantibodies) were detected in patients with SLE, healthy controls, and patients with rheumatoid arthritis.

**Results.** The results of the inverse variance-weighted method (odds ratio [OR] 2.96 [95% confidence interval (95% CI) 1.58–5.55],  $P < 0.001$ ) showed strong evidence for a causal relationship between longer telomere length and risk of SLE in people with European ancestry. The outcomes of MR-Egger regression analysis (OR 29.46 [95% CI 3.02–287.60],  $P = 0.033$ ) and MR pleiotropy residual sum and outlier analysis (OR 3.62 [95% CI 2.03–6.46],  $P = 0.002$ ) also showed that longer telomere length was significantly associated with increased risk of SLE in a European population. Sensitivity analyses using different methods and summary data sets showed that the results were still broadly consistent. A replication MR study using Asian genetic data yielded similar findings. However, the reverse MR analysis showed that genetically predicted SLE was not causally associated with telomere length. In addition, we found that TERF1 autoantibodies were present in 2 of 40 SLE patients (5.0%).

**Conclusion.** In contrast with previous observational studies, MR analyses show that longer telomere length is significantly associated with increased risk of SLE.

## INTRODUCTION

Systemic lupus erythematosus (SLE) is a common systemic autoimmune disease characterized by the production of autoantibodies and a complex genetic inheritance. There is not any single factor that could fully explain the etiology of SLE; interaction between genetic and environmental factors may contribute to SLE.

Available data have suggested that telomere length is associated with inflammation and immunity (1), which indicated that there might be potential linkage between telomere length and risk of SLE. To date, considerable observational studies have compared telomere length in SLE patients with that of healthy controls. In the majority of these studies (2–4), telomere length was found to become shorter in SLE patients compared to healthy controls. A previous meta-analysis tried to combine these

Supported by the National Natural Science Foundation of China (82073652), the Research Fund of Anhui Institute of Translational Medicine (award 2021zhyc-C22) and the Chinese National High Level Personnel Special Support Plan.

Mr. X. Wang, Ms. Xu, and Ms. F. Wang contributed equally to this work.

<sup>1</sup>Xu-Fan Wang, BS, Wen-Jing Xu, BPA, Fei-Fei Wang, BMed, Rui Leng, BMed, Yin-Guang Fan, MD, Dong-Qing Ye, MD, Rui-Xue Leng, MD: Department of Epidemiology and Biostatistics, School of Public Health, Anhui Medical University, and Inflammation and Immune Mediated Diseases Laboratory of Anhui Province, Hefei, China; <sup>2</sup>Xiao-Ke Yang, MD, Zong-Wen Shuai, MD: Department of Rheumatology and Immunology, the First Affiliated Hospital of Anhui Medical University, Hefei, China; <sup>3</sup>Hua-Zhi Ling, MMed: Department of Clinical Laboratory, the First Affiliated Hospital of Anhui Medical University, Hefei, China; <sup>4</sup>Jin-Hui Tao, MD: Department of Rheumatology and

Immunology, the First Affiliated Hospital of University of Science and Technology of China, Hefei, China; <sup>5</sup>Li Zhang, MD: National Health Commission of the People's Republic of China, Key Laboratory of Enteric Pathogenic Microbiology (Jiangsu Provincial Center for Disease Control and Prevention), Nanjing, China.

Author disclosures are available at <https://onlinelibrary.wiley.com/action/downloadSupplement?doi=10.1002%2Fart.42304&file=art42304-sup-0001-Disclosureform.pdf>.

Address correspondence via email to Li Zhang, MD, at [zhangli411@yeah.net](mailto:zhangli411@yeah.net); to Dong-Qing Ye, MD, at [ydq@ahmu.edu.cn](mailto:ydq@ahmu.edu.cn); or to Rui-Xue Leng, MD, at [lengruixue@ahmu.edu.cn](mailto:lengruixue@ahmu.edu.cn).

Submitted for publication December 18, 2021; accepted in revised form July 7, 2022.

epidemiologic data and found that telomere length is significantly shorter in SLE patients, regardless of ethnicity, sample type, or assay method evaluated (5).

Given the presence of potential unadjusted confounding factors and reverse causation, achieving a reasonable conclusion is a troublesome challenge in traditional case-control or cross-sectional studies. In order to overcome these limitations, the Mendelian randomization (MR) method using instrumental variables can be employed as an alternative approach to determine the causality of the exposure on the outcome. The present study was designed to employ a 2-sample MR approach to explore the causal relationship between telomere length and SLE. In addition, we also screened autoantibodies targeting telomere-associated protein (telomeric repeat-binding factor 1 [TERF1] autoantibodies) in SLE patients.

## MATERIALS AND METHODS

**Genetic data sources of SLE.** SLE summary data was collected from a genome-wide association study (GWAS) that included 5,201 SLE cases and 9,066 healthy controls of European descent, accessed using MR-Base platform (6,7). For Asian SLE data, we extracted single-nucleotide polymorphism (SNP) information from a new GWAS in China. All the cases in the Chinese SLE GWAS were recruited from Anhui Province of China. Diagnosis was determined according to the 1997 update to the American College of Rheumatology revised criteria for SLE (8). The methods of genotyping (see Supplementary Methods, available on the *Arthritis & Rheumatology* website at <http://onlinelibrary.wiley.com/doi/10.1002/art.42304>), quality control, and analyses for the SLE GWAS followed the procedures used in our previous rheumatoid arthritis (RA) GWAS (9). Briefly, an association analysis of autosomes in the Chinese SLE GWAS was performed with adjustment for age, sex, and 10 principal components, by using an additive model. Imputed SNPs were restricted based on minor allele frequency of  $>0.005$  and INFO scores of  $>0.70$ , which indicates a high degree of imputation accuracy. Finally, 1,548 SLE cases and 2,879 healthy controls passed rigorous quality control filtering and were included in this study. The  $\lambda_{GC}$  estimated in the Chinese SLE GWAS was 1.040 after excluding SNPs within the HLA region (chromosome 6, 25–35 Mb), indicating a subtle inflation of  $P$  values.

**Selection of telomere length-associated SNPs.** We directly extracted summarized statistics of significant verified SNPs related to telomere length ( $P < 5.00 \times 10^{-8}$ ) from a GWAS meta-analysis involving 37,684 participants of European ancestry (10). To avoid the effect of strong linkage disequilibrium (LD), we set an LD threshold for extracted SNPs ( $r^2 < 0.001$ ). Finally, 7 SNPs were collected as instrumental variables. We also extracted summary data (10 independent SNPs) related to telomere length in an independent Asian population including 23,096 samples from Singaporean Chinese subjects (11).

**MR analysis.** We harmonized both the exposure and outcome data sets to correctly align the effect alleles. The inverse variance-weighted method (IVW) with random effects, MR-Egger regression method, and MR pleiotropy residual sum and outlier (MR-PRESSO) test were used to assess the causal effect of exposure on outcome, which were the most common MR methods (12) and were performed using the R package TwoSampleMR (version 0.5.5) (7). The F statistic was used to assess the impact of weak instrumental variables bias on the present MR research, the formula of which is  $r^2(n - k - 1)/(k[1 - r^2])$ . In this equation,  $r^2$  represents the cumulative explained variance of collected SNPs on telomere length. Here “ $n$ ” is the sample size, and “ $k$ ” refers to the counts of the extracted SNPs. When the F statistic is  $>10$ , the chosen SNPs were considered to be strong instrumental variables (7,12,13).  $P$  values were determined by 2-tailed test, and  $P$  values of less than 0.05 were considered significant. All statistical analyses were performed using R (version 3.6.0).

### Heterogeneity, pleiotropy, and sensitivity analysis.

We performed MR-Egger regression test and IVW approaches to test the heterogeneity between chosen SNPs, and Cochran's Q statistic was applied to respectively assess the effect of heterogeneity. In addition, the MR-Egger regression method was used to examine potential horizontal pleiotropy (7). To further verify MR model assumptions, we performed additional analyses. To check that the instrumental variables were not just associated with the exposure (telomere length) but that they were most likely causal, we reviewed the function information of potential causal genes at loci of the instrumental variables. For each index SNP, we also searched for potential associations with multiple traits in the GWAS catalog (URL: <https://www.ebi.ac.uk/gwas/>) using LDtrait (setting:  $P$  for traits-associated SNPs  $<5.00 \times 10^{-8}$ ,  $r^2$  for an LD of  $>0.20$  in Europeans [EUR] or East Asians [EAS], and a  $\pm 500$ -kbp window of the queried SNPs) (14). In order to further relax the exclusion restriction assumption, we performed median- and mode-based methods (7), serving as sensitivity analyses. The median-based method is more resistant to pleiotropy; it takes the median instrumental variable from all instrumental variables included and is therefore robust when  $<50\%$  of the SNPs are invalid. The mode-based method returns an unbiased causal effect if the SNPs within the largest cluster are valid instruments (7). To ascertain whether our estimations were driven by any individual SNP with a large effect, we carried out leave-one-out analysis where we removed 1 SNP at a time and performed IVW on the remaining SNPs (7,12). To test whether these estimations change when using a large number of instrumental variables, we obtained full summary statistics of leukocyte telomere length from the latest GWAS analysis (15). The details of the selection of instrumental variables in the GWAS are described in Supplementary Methods (<http://onlinelibrary.wiley.com/doi/10.1002/art.42304>).

**TERF1 autoantibody measurements.** TERF1 autoantibodies were the most common of the shelterin autoantibodies and were associated with short lymphocyte telomere length in other autoimmune diseases (16); we thus developed an enzyme-linked immunosorbent assay (ELISA) to screen for TERF1 autoantibodies. First, 96-well ELISA plates (Corning) were coated with purified TERF1 protein (Sino Biological) and incubated overnight at 4°C. The plates were blocked with 200 µl of 5% milk for 1 hour at 37°C and were washed 3 times with phosphate buffered saline (PBST). Then 1:100 diluted plasma samples were added and incubated at 37°C for 1 hour. Following 3 washes with PBST, 100 µl of a 1:10,000 dilution of horseradish peroxidase-conjugated anti-human IgG (Sigma) was added and plates were incubated for 1 hour at 37°C. After 3 washes with PBST, 100 µl of 3,3',5,5'-tetramethylbenzidine substrate (Thermo Scientific) was added and incubated at room temperature for 10 minutes, following which the color change was monitored at 450 nm by adding 50 µl of 2M H<sub>2</sub>SO<sub>4</sub> to stop the reaction. The cutoff for autoantibody positivity was set as the mean + 4 SD of healthy control values (16). To confirm the presence of autoantibodies among patients found to be positive by ELISA, we further used 2 other methods (Indirect ELISA with dilution gradient and magnetic beads-based antibody pull-down) to detect TERF1 autoantibodies (see Supplementary Methods, <http://onlinelibrary.wiley.com/doi/10.1002/art.42304>).

**Ethics approval.** The GWAS summary data for European and Asian populations used in this study were obtained from publicly available data sets. The Anhui Chinese study and the overall protocols were approved by the medical ethics committee of Anhui Medical University, and written informed consent was

obtained from all participants. All procedures were performed in accordance with the Declaration of Helsinki.

## RESULTS

We selected 7 SNPs as instrumental variables from summary data of telomere length in the European population. The characteristics of the 7 extracted SNPs in the European population are shown in Table 1. The F statistic of these SNPs was 67.54, indicating that the selected instrumental variables were robust to ensure the reliability of 2-sample MR results. Among these SNPs, 4 SNPs (rs10936599, rs7675998, rs2736100, and rs755017) were nominally associated with risk of SLE ( $P \leq 0.005$ ).

The results of the IVW (odds ratio [OR] 2.96 [95% confidence interval (95% CI) 1.58–5.55],  $P < 0.001$ ) showed strong evidence for a causal relationship between longer telomere length and risk of SLE in people with European ancestry. Significant findings were observed using the MR-Egger method (OR 29.46 [95% CI 3.02–287.60],  $P = 0.033$ ). Moreover, the MR-PRESSO test (OR 3.62 [95% CI 2.03–6.46],  $P = 0.002$ ) suggested that the effect was not altered after removing 1 outlier variant (Table 2). The outcomes of heterogeneity analyses employing the MR-Egger method (Cochrane's  $Q = 9.53$ ;  $P = 0.090$ ) and IVW (Cochrane's  $Q = 17.37$ ;  $P = 0.008$ ) demonstrated that there was heterogeneity among selected SNPs. We used MR-Egger regression approaches to test the horizontal pleiotropy among extracted SNPs, none of which showed evidence that pleiotropy would affect the results of 2-sample MR analyses ( $\beta$  intercept  $-0.17$ ; SE = 0.08;  $P = 0.098$ ).

We further reviewed the functional involvement of potential causal genes at loci of instrumental variables and found that 5 of

**Table 1.** Associations of instrumental SNPs with telomere length and SLE in European and Asian populations\*

SNP	Chromosome	Effect alleles	Other alleles	Telomere length			SLE		
				$\beta$	SE	<i>P</i>	$\beta$	SE	<i>P</i>
European population									
rs11125529	2	C	A	−0.056	0.010	$4.48 \times 10^{-8}$	0.010	0.059	0.865
rs10936599	3	T	C	−0.097	0.008	$2.54 \times 10^{-31}$	−0.139	0.033	<0.001
rs7675998	4	A	G	−0.074	0.009	$4.35 \times 10^{-16}$	−0.105	0.036	0.003
rs2736100	5	A	C	−0.078	0.009	$4.38 \times 10^{-19}$	−0.083	0.030	0.005
rs9420907	10	A	C	−0.069	0.010	$6.90 \times 10^{-11}$	−0.049	0.042	0.250
rs8105767	19	A	G	−0.048	0.008	$1.11 \times 10^{-9}$	0.041	0.030	0.167
rs755017	20	A	G	−0.062	0.011	$6.71 \times 10^{-9}$	−0.157	0.044	<0.001
Asian population									
rs3219104	1	C	A	0.074	0.009	$2.23 \times 10^{-16}$	−0.017	0.047	0.715
rs2293607	3	C	T	−0.120	0.009	$7.57 \times 10^{-39}$	−0.071	0.046	0.125
rs10857352	4	G	A	0.064	0.011	$4.85 \times 10^{-9}$	0.094	0.054	0.081
rs7705526	5	A	C	0.118	0.009	$2.61 \times 10^{-38}$	0.103	0.048	0.032
rs7776744	7	G	A	−0.058	0.009	$2.51 \times 10^{-10}$	0.103	0.047	0.028
rs28365964	8	C	T	0.270	0.035	$6.96 \times 10^{-15}$	0.036	0.195	0.854
rs12415148	10	C	T	0.204	0.020	$2.78 \times 10^{-25}$	0.207	0.092	0.025
rs227080	11	G	A	−0.060	0.009	$1.87 \times 10^{-10}$	0.062	0.047	0.186
rs41293836	14	T	C	0.233	0.017	$2.47 \times 10^{-42}$	0.214	0.079	0.007
rs41309367	20	T	C	−0.058	0.010	$1.16 \times 10^{-8}$	−0.053	0.053	0.318

\* SNPs = single-nucleotide polymorphisms; SLE = systemic lupus erythematosus.

**Table 2.** Associations between genetically predicted telomere length and risk of SLE in European and Asian populations\*

	MR analyses of TL and risk of SLE			MR analyses excluding SNPs associated with confounding traits		
	No. of SNPs	OR (95% CI)	P	No. of SNPs	OR (95% CI)	P
European population						
IVW with random effects	7	2.96 (1.58–5.55)	<0.001	6	2.66 (1.43–4.93)	0.002
MR-Egger	7	29.46 (3.02–287.60)	0.033	6	44.76 (8.38–239.15)	0.011
MR-PRESSO	6	3.62 (2.03–6.46)	0.002	5	3.26 (1.96–5.44)	0.003
Simple median	7	2.91 (1.64–5.18)	<0.001	6	2.43 (1.35–4.37)	0.003
Weighted median	7	3.75 (2.28–6.15)	<0.001	6	3.56 (2.17–5.85)	<0.001
Simple mode	7	3.51 (1.73–7.13)	0.013	6	3.26 (1.77–6.00)	0.013
Weighted mode	7	3.66 (2.22–6.05)	0.002	6	3.51 (2.10–5.87)	0.005
Asian population						
IVW with random effects	10	1.76 (1.11–2.79)	0.017	9	1.74 (1.06–2.86)	0.030
MR-Egger	10	3.85 (1.64–9.06)	0.015	9	4.38 (1.85–10.40)	0.012
MR-PRESSO	10	1.76 (1.03–3.00)	0.041	8	1.93 (1.20–3.11)	0.014
Simple median	10	2.08 (1.29–3.36)	0.003	9	1.81 (1.09–2.99)	0.021
Weighted median	10	2.41 (1.56–3.72)	<0.001	9	2.39 (1.54–3.71)	<0.001
Simple mode	10	2.43 (1.35–4.37)	0.016	9	2.39 (1.36–4.21)	0.017
Weighted mode	10	2.35 (1.54–3.59)	0.003	9	2.34 (1.52–3.59)	0.005

\* SLE = systemic lupus erythematosus; MR = Mendelian randomization; TL = telomere length; SNP = single-nucleotide polymorphism; OR = odds ratio; 95% CI = 95% confidence interval; IVW = inverse variance-weighted method; MR-PRESSO = MR pleiotropy residual sum and outlier.

7 instrumental SNPs identified in European ancestry lie in or near genes that are functionally associated with telomere length (see Supplementary Table 1, <http://onlinelibrary.wiley.com/doi/10.1002/art.42304>). An MR analysis including the 5 causal instrumental variables in European ancestry showed that the MR results were broadly significant (see Supplementary Table 2, <http://onlinelibrary.wiley.com/doi/10.1002/art.42304>). A traits-association analysis (see Supplementary Table 3, <http://onlinelibrary.wiley.com/doi/10.1002/art.42304>) showed that the SNP rs755017 at the *RTEL1* gene region is associated with multiple autoimmune conditions and several potential confounders (inflammatory bowel disease, RA, C-reactive protein levels, serum 25-hydroxyvitamin D levels, age of smoking initiation, body mass index [BMI], and type 2 diabetes mellitus). A sensitivity analysis removing the SNP demonstrated similar results (Table 2).

To further relax exclusion restriction assumption, we performed median- and mode-based MR methods. We did not observe substantial changes in results using the 2 methods (Table 2). In addition, the results of sensitivity analysis using the leave-one-out method indicated no single SNP significantly influenced the results of the analysis (Figure 1A). Furthermore, to ascertain whether these estimations were changed by using a large number of instrumental variables (>90 instrumental variables), we conducted MR analysis using summary statistics of leukocyte telomere length from the latest GWAS analysis (15). Using 2 different instrumental variable sets, the replication MR study showed that the results were still broadly consistent (see Supplementary Table 4, <http://onlinelibrary.wiley.com/doi/10.1002/art.42304>).

In order to investigate whether the conclusion reached in European patients also applies to Asian patients, a replication

2-sample MR research was implemented. We extracted summary data of 10 significant SNPs (Table 1) related to telomere length from a GWAS meta-analysis involving 23,096 samples from Singaporean Chinese subjects. Then these SNPs were reviewed in an independent Chinese SLE GWAS. No high LD was found between selected SNPs and no weak instrumental variables bias was found in the 2-sample MR findings ( $F = 94.07$ ). Almost all instrumental SNPs used in our study lie in or near genes that perform prominent roles in regulating telomere length (see Supplementary Table 1, <http://onlinelibrary.wiley.com/doi/10.1002/art.42304>). The results of the IVW demonstrated the causality of telomere length on SLE (OR 1.76 [95% CI 1.11–2.79],  $P = 0.017$ ), and the other approaches obtained similar outcomes (Table 2). There was slight heterogeneity between chosen SNPs when employing the MR-Egger regression method (Cochrane's  $Q = 12.14$ ;  $P = 0.145$ ) and IVW (Cochrane's  $Q = 18.40$ ;  $P = 0.031$ ). The outcomes of the MR-Egger regression method indicated no obvious sign of horizontal pleiotropy ( $\beta$  intercept  $-0.09$ ; SE = 0.05;  $P = 0.077$ ). A sensitivity analysis additionally removing 1 SNP (rs41309367 at the *RTEL1* gene region) had consistent findings (Table 2). For the leave-one-out sensitivity analysis, several SNPs might slightly affect the results of analyses (Figure 1B).

We then performed a reverse MR analysis using SLE SNPs as instrumental variables to test their effects on telomere length (see Supplementary Methods, <http://onlinelibrary.wiley.com/doi/10.1002/art.42304>). We directly extracted summarized statistics of 41 verified SNPs ( $P < 5.00 \times 10^{-08}$ ) related to SLE from a GWAS meta-analysis involving participants with European ancestry (6). By using multiple methods, the MR analysis showed that genetically predicted SLE was not causally associated with

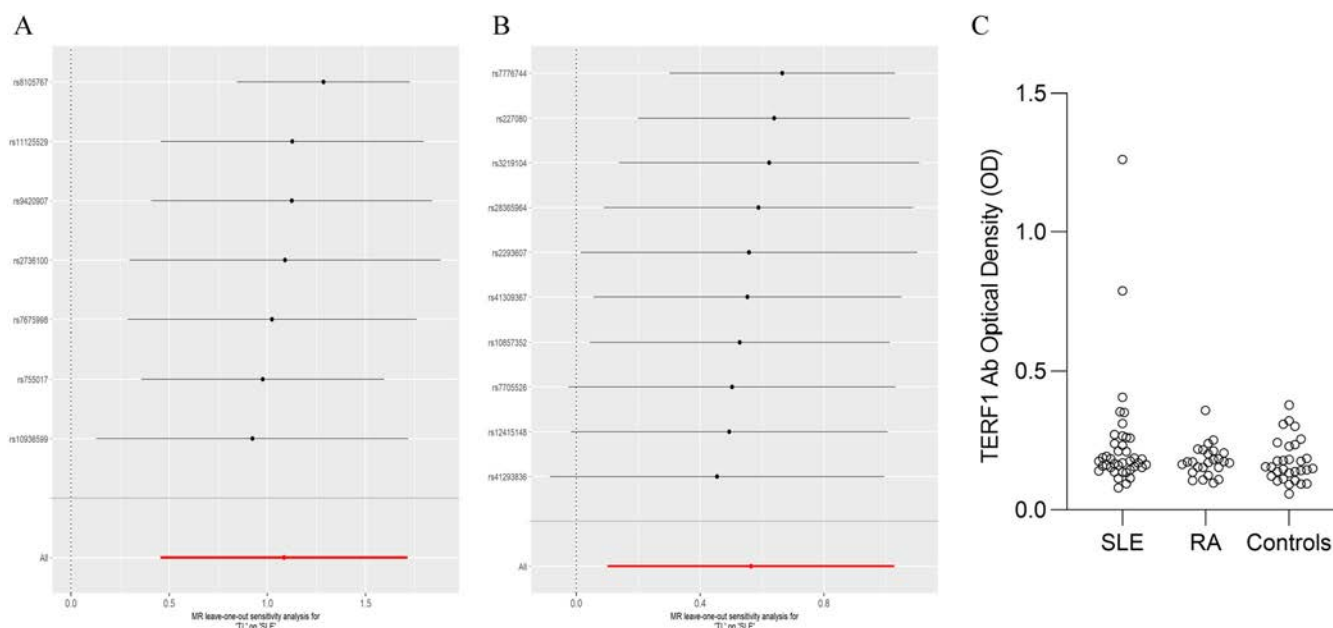


**Figure 1.** Sensitivity analyses and telomeric repeat-binding factor 1 (TERF1) enzyme-linked immunosorbent assay (ELISA). **A**, Leave-one-out Mendelian randomization (MR) analysis in a European population. **B**, Leave-one-out MR analysis in an Asian population. **C**, TERF1 autoantibodies detected using ELISA in patients with systemic lupus erythematosus (SLE) ( $n = 40$ ), those with rheumatoid arthritis (RA) ( $n = 25$ ), and healthy controls ( $n = 30$ ). TL = telomere length; Ab = antibody.

telomere length (see Supplementary Table 5, <http://onlinelibrary.wiley.com/doi/10.1002/art.42304>).

We also screened plasma from 40 SLE patients, 25 RA patients, and 30 healthy controls for TERF1 autoantibodies by ELISA. TERF1 autoantibodies were present in 2 of 40 SLE patients (5.0%). However, the TERF1 autoantibodies were not found in RA patients and healthy controls (Figure 1C). Using 2 additional methods, we confirmed the presence of TERF1 autoantibodies among patients who were positive by ELISA. Using ELISA with dilution gradient, we observed that optical density values were decreased when the dilution ratio was increased in the 2 SLE patients who were positive by ELISA (see Supplementary Figure 1, <http://onlinelibrary.wiley.com/doi/10.1002/art.42304>). Magnetic beads-based antibody pull-down also confirmed that TERF1 binding autoantibodies were present in the same SLE samples but not in samples from RA patients and healthy controls (see Supplementary Figure 2, <http://onlinelibrary.wiley.com/doi/10.1002/art.42304>).

## DISCUSSION

In the present study, we performed an MR analysis using European genetic data to investigate the association of telomere length with risk of SLE. Our results indicate that genetically predicted telomere length is positively associated with risk of SLE. A replication study using Asian genetic data also yielded similar findings, suggesting the robustness of the causal association. The reverse MR analysis showed that

genetically predicted SLE is not causally associated with telomere length.

Although the precise mechanism for how longer telomere length confers increased risk of SLE remains unclear, there are several possible explanations. It has been reported that children and adults who are telomerase mutation carriers with short telomere length develop a T cell immunodeficiency that can manifest in the absence of bone marrow failure and causes life-threatening opportunistic infections. Furthermore, telomerase-null mice with short telomere length have defects throughout T cell development. The loss of telomere sequences from the ends of chromosomes is associated with cell cycle arrest and T cell apoptosis and immunosenescence, which may further lead to a decline in adaptive immune response (17). Recently, using an MRL/lpr lupus mouse model, it has been shown that human umbilical cord-derived mesenchymal stem cell transplantation ameliorates lupus symptoms through increasing CD4+ T cell senescence via the MiR-199a-5p/Sirt1/p53 axis (18), suggesting that longer telomere length may increase risk of SLE by maintaining T cell proliferation capability. Except for T cells, other immune cell function may also be associated with telomere length maintenance. For example, Zhdanov et al showed that regulatory T cells, which play a fundamental role in the maintenance of immunologic tolerance by suppressing effector-target lymphocytes, can cause in vitro telomere-dependent apoptosis and senescence in target T cells, B cells, and natural killer cells in a contact-independent manner (19). Although these explanations are biologically



plausible, there remains a paucity of direct functional data regarding the role of telomerase/telomere length in SLE. Therefore, future studies are warranted to investigate the overall net effect of telomere length maintenance in the development of SLE using mice models.

Previous observational studies (2–5) demonstrated that a subset of SLE patients have markedly short telomere length in leukocytes. We further summarized the characteristics of the previous studies (see Supplementary Table 6, <http://onlinelibrary.wiley.com/doi/10.1002/art.42304>) and found that the common confounders adjusted for in these studies were age and sex. However, other potential confounders such as BMI or smoking (2) were not adjusted for when telomere length was compared between SLE cases and healthy controls. Furthermore, the summary data showed that most SLE cases in these studies received treatments which may lead to telomere shortening. For example, Lee et al showed that exposure to glucocorticoids is associated with a significant reduction of telomere length in both mice and humans (20).

We also note that the findings from previous studies might be prone to reverse causation. First, telomere shortening could result from exposure to oxidative stress, which is an important feature of SLE pathology (21,22). Second, telomere shortening in lymphocytes may be partially caused by excessive lymphocyte proliferation that in turn leads to telomere shortening (23). Finally, Adler et al found that autoantibodies targeting telomere-associated proteins in a subset of patients with systemic sclerosis (SSc) are associated with short lymphocyte telomere length. They found that TERF1 autoantibodies were present in 40 of 442 SSc patients (9.0%) (16). Consistent with this, we found that TERF1 autoantibodies were present in 2 of 40 SLE patients (5%). Unexpectedly, using a reverse MR analysis, we found that that genetically predicted SLE was not causally associated with telomere length. Sensitivity analyses using different methods (see Supplementary Table 5, <http://onlinelibrary.wiley.com/doi/10.1002/art.42304>) showed that the results were still consistent, suggesting SLE disease progression itself may not substantially affect leukocyte telomere length. However, we noted that there is still a lack of longitudinal studies considering different treatment drugs to examine the dynamic changes and clinical significance of telomere length in SLE.

Though we obtained significant results using the 2-sample MR method, several limitations of the present study should be noted. First, telomere length GWAS data were measured in blood leukocytes (10,11,15), and leukocyte telomere length might be not enough to represent telomere length in other cell or tissue subgroups associated with SLE. Second, we tested MR assumptions using the different methods and, although the results were found to be broadly consistent, some residual uncertainty inevitably remains. Finally, the sample size for detecting TERF1 autoantibodies was small in this study. The statistical power can be increased further in future studies with larger sample sizes. In

spite of this, our research shows that telomere length is positively associated with risk of SLE.

## ACKNOWLEDGMENTS

We like to thank all the participants for their involvement in this study and researchers for sharing relevant summary data.

## AUTHOR CONTRIBUTIONS

All authors were involved in drafting the article or revising it critically for important intellectual content, and all authors approved the final version to be published. Dr. Rui-Xue Leng had full access to all of the data in the study and takes responsibility for the integrity of the data and the accuracy of the data analysis.

**Study conception and design.** X. Wang, Rui-Xue Leng.

**Acquisition of data.** X. Wang, Xu, F. Wang, Rui Leng, Yang, Ling, Tao, Shuai, Zhang, Ye, Rui-Xue Leng.


**Analysis and interpretation of data.** X. Wang, Xu, F. Wang, Fan, Zhang, Ye, Rui-Xue Leng.

## REFERENCES

1. Heba AC, Toupance S, Arnone D, et al. Telomeres: new players in immune-mediated inflammatory diseases? *J Autoimmun* 2021;123: 102699.
2. Haque S, Rakieh C, Marriage F, et al. Shortened telomere length in patients with systemic lupus erythematosus. *Arthritis Rheum* 2013; 65:1319–23.
3. Skamra C, Romero-Diaz J, Sandhu A, et al. Telomere length in patients with systemic lupus erythematosus and its associations with carotid plaque. *Rheumatology (Oxford)* 2013;52:1101–8.
4. Kurosaka D, Yasuda J, Yoshida K, et al. Abnormal telomerase activity and telomere length in T and B cells from patients with systemic lupus erythematosus. *J Rheumatol* 2006;33:1102–7.
5. Lee YH, Jung JH, Seo YH, et al. Association between shortened telomere length and systemic lupus erythematosus: a meta-analysis. *Lupus* 2017;26:282–8.
6. Bentham J, Morris DL, Graham DS, et al. Genetic association analyses implicate aberrant regulation of innate and adaptive immunity genes in the pathogenesis of systemic lupus erythematosus. *Nat Genet* 2015;47:1457–64.
7. Hemani G, Zheng J, Elsworth B, et al. The MR-Base platform supports systematic causal inference across the human phenome. *Elife* 2018;7:e34408.
8. Hochberg MC, for the Diagnostic and Therapeutic Criteria Committee of the American College of Rheumatology. Updating the American College of Rheumatology revised criteria for the classification of systemic lupus erythematosus [letter]. *Arthritis Rheum* 1997; 40:1725.
9. Leng RX, Di DS, Ni J, et al. Identification of new susceptibility loci associated with rheumatoid arthritis. *Ann Rheum Dis* 2020;79: 1565–71.
10. Codd V, Nelson CP, Albrecht E, et al. Identification of seven loci affecting mean telomere length and their association with disease. *Nat Genet* 2013;45:422–7.
11. Dorajoo R, Chang X, Gurung RL, et al. Loci for human leukocyte telomere length in the Singaporean Chinese population and trans-ethnic genetic studies. *Nat Commun* 2019;10:2491.
12. Tang B, Shi H, Alfredsson L, et al. Obesity-related traits and the development of rheumatoid arthritis: evidence from genetic data. *Arthritis Rheumatol* 2021;73:203–11.

13. Pierce BL, Burgess S. Efficient design for Mendelian randomization studies: subsample and 2-sample instrumental variable estimators. *Am J Epidemiol* 2013;178:1177–84.
14. Lin SH, Brown DW, Machiela MJ. LDtrait: An online tool for identifying published phenotype associations in linkage disequilibrium. *Cancer Res* 2020;80:3443–6.
15. Codd V, Wang Q, Allara E, et al. Polygenic basis and biomedical consequences of telomere length variation. *Nat Genet* 2021;53:1425–33.
16. Adler BL, Boin F, Wolters PJ, et al. Autoantibodies targeting telomere-associated proteins in systemic sclerosis. *Ann Rheum Dis* 2021;80:912–9.
17. Wagner CL, Hanumanthu VS, Talbot CC Jr, et al. Short telomere syndromes cause a primary T cell immunodeficiency. *J Clin Invest* 2018;128:5222–34.
18. Cheng T, Ding S, Liu S, et al. Human umbilical cord-derived mesenchymal stem cell therapy ameliorates lupus through increasing CD4+ T cell senescence via MiR-199a-5p/Sirt1/p53 axis. *Theranostics* 2021;11:893–905.
19. Zhdanov DD, Gladilina YA, Grishin DV, et al. Contact-independent suppressive activity of regulatory T cells is associated with telomerase inhibition, telomere shortening and target lymphocyte apoptosis. *Mol Immunol* 2018;101:229–44.
20. Lee RS, Zandi PP, Santos A, et al. Cross-species association between telomere length and glucocorticoid exposure. *J Clin Endocrinol Metab* 2021;106:e5124–35.
21. Saretzki G, Von Zglinicki T. Replicative aging, telomeres, and oxidative stress. *Ann N Y Acad Sci* 2002;959:24–9.
22. Perl A. Oxidative stress in the pathology and treatment of systemic lupus erythematosus [review]. *Nat Rev Rheumatol* 2013;9:674–86.
23. Lakota K, Hanumanthu VS, Agrawal R, et al. Short lymphocyte, but not granulocyte, telomere length in a subset of patients with systemic sclerosis. *Ann Rheum Dis* 2019;78:1142–4.

# Variability of Primary Sjögren's Syndrome Is Driven by Interferon- $\alpha$ and Interferon- $\alpha$ Blood Levels Are Associated With the Class II HLA-DQ Locus

Diana Trutschel,<sup>1</sup> Pierre Bost,<sup>2</sup> Xavier Mariette,<sup>3</sup> Vincent Bondet,<sup>4</sup> Alba Llibre,<sup>4</sup> Celine Posseme,<sup>4</sup> Bruno Charbit,<sup>5</sup> Christian W. Thorball,<sup>6</sup> Roland Jonsson,<sup>7</sup> Christopher J. Lessard,<sup>8</sup> Renaud Felten,<sup>9</sup> Wan Fai Ng,<sup>10</sup> Lucienne Chatenoud,<sup>11</sup> Hélène Dumortier,<sup>12</sup> Jean Sibilia,<sup>13</sup> Jacques Fellay,<sup>14</sup> Karl A. Brokstad,<sup>15</sup> Silke Appel,<sup>15</sup> Jessica R. Tarn,<sup>16</sup> Lluís Quintana-Murci,<sup>17</sup> Michael Mingueneau,<sup>18</sup> Nicolas Meyer,<sup>19</sup> Darragh Duffy,<sup>4</sup> Benno Schwikowski,<sup>1</sup> and Jacques Eric Gottenberg,<sup>9</sup>  on behalf of The Milieu Intérieur Consortium, ASSESS study investigators, and NECESSITY Consortium

**Objective.** Primary Sjögren's syndrome (SS) is the second most frequent systemic autoimmune disease, affecting 0.1% of the general population. To characterize the molecular and clinical variabilities among patients with primary SS, we integrated transcriptomic, proteomic, cellular, and genetic data with clinical phenotypes in a cohort of 351 patients with primary SS.

**Methods.** We analyzed blood transcriptomes and genotypes of 351 patients with primary SS who were participants in a multicenter prospective clinical cohort. We replicated the transcriptome analysis in 3 independent cohorts ( $n = 462$  patients). We determined circulating interferon- $\alpha$  (IFN $\alpha$ ) and IFN $\gamma$  protein concentrations using digital single molecular arrays (Simoa).

**Results.** Transcriptome analysis of the prospective cohort showed a strong IFN gene signature in more than half of the patients; this finding was replicated in the 3 independent cohorts. Because gene expression analysis did not discriminate between type I IFN and type II IFN, we used Simoa to demonstrate that the IFN transcriptomic signature was driven by circulating IFN $\alpha$  and not by IFN $\gamma$  protein levels. IFN $\alpha$  protein levels, detectable in 75% of patients, were significantly associated with clinical and immunologic features of primary SS disease activity at enrollment and with increased frequency of systemic complications over the 5-year follow-up. Genetic analysis revealed a significant association between IFN $\alpha$  protein levels, a major histocompatibility (MHC) class II haplotype, and anti-SSA antibody. Additional cellular analysis revealed that an MHC class II HLA-DQ locus acts through up-regulation of HLA class II molecules on conventional dendritic cells.

**Conclusion.** We identified the predominance of IFN $\alpha$  as a driver of primary SS variability, with IFN $\alpha$  demonstrating an association with HLA gene polymorphisms.

Supported by the Innovative Medicines Initiative 2 Joint Undertaking (JU) (grant 806975). The JU receives support from the European Union's Horizon 2020 research and innovation program and the European Union and the European Federation of Pharmaceutical Industries and Associations. This work was also supported by the National Institutes of Health (National Institute of Arthritis and Musculoskeletal Skin Disease grant R01-AR-065953). The Assessment of Systemic Signs and Evolution in Sjögren's Syndrome (ASSESS) national multicenter prospective cohort was formed in 2006 with a French Ministry of Health grant (Programme Hospitalier de Recherche Clinique 2005 P060228). The ASSESS cohort is promoted by the French Society of Rheumatology and receives research grants from the French Society of Rheumatology. Dr. Gottenberg's work was supported by Bristol Myers Squibb for transcriptomic analysis of the ASSESS and Norwegian cohorts and by Geneviève Garnier (Association Française du Syndrome de Gougerot-Sjögren et des syndromes secs). Drs. Trutschel's and Schwikowski's work was supported by Geneviève Garnier (Association Française du Syndrome de Gougerot-Sjögren et des syndromes secs).

The present article reflects only the authors' view, and the contents are the sole responsibility of the authors; the JU is not responsible for any use that may be made of the information it contains, and the contents do not necessarily reflect the official views of the National Institutes of Health.

<sup>1</sup>Diana Trutschel, Dr, Benno Schwikowski, PhD: Computational Systems Biomedicine Lab, Institut Pasteur, Université Paris Cité, Paris, France; <sup>2</sup>Pierre Bost, PhD: Computational Systems Biomedicine Lab, Institut Pasteur, Université Paris Cité, Paris, France, Department of Quantitative Biomedicine, University of Zurich, and ETH Zurich, Institute for Molecular Health Sciences, Zurich, Switzerland; <sup>3</sup>Xavier Mariette, MD, PhD: Department of Rheumatology, Hôpital Bichat, Assistance Publique-Hôpitaux de Paris, Université Paris-Saclay, INSERM UMR1184—Immunology of viral infections and autoimmune diseases, Le Kremlin-Bicêtre, France; <sup>4</sup>Vincent Bondet, PhD, Alba Llibre, PhD, Celine Posseme, PhD: Department of Immunology, Translational Immunology Unit, Institut Pasteur, Université Cité Paris, Paris, France; <sup>5</sup>Bruno Charbit, MSc, Darragh Duffy, PhD: Cytometry and Biomarkers UTEchS, CRT, Institut Pasteur, Université Cité Paris, Institut Pasteur, Paris, France; <sup>6</sup>Christian

## INTRODUCTION

Primary Sjögren's syndrome (SS) is a systemic autoimmune disease affecting 0.1% of the general population (1) that mainly targets the exocrine system, such as the salivary and lacrimal glands. The clinical presentation of primary SS is highly heterogeneous. Fatigue, dryness, and pain are hallmarks of the disease, but one-third to one-half of patients develop systemic complications (notably, articular involvement, lung involvement, peripheral neuropathy, vasculitis), and 5–10% develop mucosa-associated lymphoid tissue-type lymphoma (2). No clinical biomarker is currently available to identify the patients with primary SS at risk of systemic complications.

To date, no specific immunomodulatory drug has demonstrated efficacy for primary SS. Disappointing results from randomized clinical trials (3–5) can be attributed to our current lack of understanding of the pathogenesis and molecular basis of this disease and to the clinical and biologic heterogeneity of the patients.

In this study, we aimed to 1) identify molecular endotypes of the disease associated with clinical phenotypes and serum biomarkers that might provide therapeutic guidance in a precision medicine approach, 2) identify major physiologic correlates of the molecular endotypes, and 3) determine possible genetic associations with the molecular endotypes.

## PATIENTS AND METHODS

### Description of cohorts of patients with primary SS.

The Assessment of Systemic Signs and Evolution in Sjögren's Syndrome (ASSESS) cohort is a multicenter prospective French clinical cohort (6) (Supplementary Figure 1A, available on the *Arthritis & Rheumatology* website at <https://onlinelibrary.wiley.com/doi/10.1002/art.42265>). ASSESS enrolled 395 patients (see Appendix A for a list of the study investigators) (see

Supplementary Methods, available on the *Arthritis & Rheumatology* website at <https://onlinelibrary.wiley.com/doi/10.1002/art.42265>).

We performed molecular stratification of patients from the ASSESS cohort, based on transcriptomics. To replicate our findings, we repeated our transcriptome analysis in an independent cohort of patients with primary SS and in 2 public data sets. The independent cohort enrolled 141 consecutive patients with primary SS who were referred for specialist consultation at the Department of Rheumatology, Haukeland University Hospital, Bergen, Norway. The 2 public data sets included 190 patients with primary SS from Oklahoma (7) and 131 patients with primary SS from the UK (8), with both cohorts included in Gene Expression Omnibus (GEO) (a database at the National Center for Biotechnology Information; accession no. GSE51092 and accession no. GSE66795, respectively).

To analyze HLA-DR expression in blood cells among population subsets, we reanalyzed data from a mass cytometry study of blood cells from 49 patients with primary SS performed in the Paris-Sud University Hospital (9).

**Unsupervised transcriptome analysis.** Results of the transcriptome analysis were stratified using a robust consensus clustering algorithm based on the PhenoGraph method (10) (Supplementary Methods). The number of clusters was determined using 2 criteria. First, we aimed our analysis on clusters with a high total number of cluster-associated markers, i.e., those genes whose high expression would be specific to one of the clusters. Second, for robustness, we aimed to examine a smaller set of larger clusters. Without attempting to formally combine these 2 criteria (in a necessarily ad hoc manner), we selected solutions directly from plots representing the different possible tradeoffs between the 2 criteria (Supplementary Figures 1F and 2B, available on the *Arthritis & Rheumatology*

W. Thorball, PhD: School of Life Sciences, École Polytechnique Fédérale de Lausanne, and Precision Medicine Unit, Biomedical Data Science Center, Lausanne University Hospital and University of Lausanne, Lausanne, Switzerland; <sup>7</sup>Roland Jonsson, Prof DMD, PhD: Department of Rheumatology, Haukeland University Hospital, and Broegemann Research Laboratory, Department of Clinical Science, University of Bergen, Bergen, Norway; <sup>8</sup>Christopher J. Lessard, PhD: Genes and Human Disease Research Program, Oklahoma Medical Research Foundation, and Department of Pathology, University of Oklahoma Health Sciences Center, Oklahoma City, Oklahoma; <sup>9</sup>Renaud Felten, MD, Jacques Eric Gottenberg, MD, PhD: Department of Rheumatology, Strasbourg University Hospital, National Centre For Rare Systemic Autoimmune Diseases, and Immunology, Immunopathology and Therapeutic Chemistry, Institute of Molecular and Cellular Biology, Strasbourg University, Strasbourg, France; <sup>10</sup>Wan Fai Ng, PhD: Translational and Clinical Research Institute, Newcastle University, NIHR Newcastle Biomedical Centre, and NIHR Newcastle Clinical Research Facility, Newcastle upon Tyne Hospitals NHS Foundation Trust, Newcastle upon Tyne, UK; <sup>11</sup>Lucienne Chatenoud, MD, PhD: Université Paris Descartes, Sorbonne Paris Cité, INEM, CNRS UMR8253, Hôpital Necker-Enfants Malades, Paris, France; <sup>12</sup>Hélène Dumortier, PhD: Immunology, Immunopathology and Therapeutic Chemistry, Institute of Molecular and Cellular Biology, Strasbourg University, Strasbourg, France; <sup>13</sup>Jean Sibilia, MD: Department of Rheumatology, Strasbourg University Hospital, National Centre For Rare Systemic Autoimmune Diseases, CNRS

UPR3572, Immunology, Immunopathology and Therapeutic Chemistry, Institute of Molecular and Cellular Biology, Strasbourg University, Strasbourg, France; <sup>14</sup>Jacques Fellay, MD, PhD: School of Life Sciences, École Polytechnique Fédérale de Lausanne, and Precision Medicine Unit, Biomedical Data Science Center, Lausanne University Hospital and University of Lausanne, Lausanne, Switzerland; <sup>15</sup>Karl A. Brokstad, PhD, Silke Appel, PhD: Broegemann Research Laboratory, Department of Clinical Science, University of Bergen, Bergen, Norway; <sup>16</sup>Jessica R. Tarn, Dr: Translational and Clinical Research Institute, Newcastle University, Newcastle upon Tyne, UK; <sup>17</sup>Lluís Quintana Murci, Prof, Dr: Department of Genomes & Genetics, Human Evolutionary Genetics, Institut Pasteur, CNRS URA3012, Paris, France; <sup>18</sup>Michael Mingueneau, PhD: Multiple Sclerosis and Neurorepair Research Unit, Biogen, Cambridge, Massachusetts; <sup>19</sup>Nicolas Meyer, MD, PhD: CHU de Strasbourg, Service de Santé Publique, GMRC, Strasbourg, France, and CNRS, iCUBE, UMR7357, Illkirch, France.

Author disclosures are available at <https://onlinelibrary.wiley.com/action/downloadSupplement?doi=10.1002%2Fart.42265&file=art42265-sup-0001-Disclosureform.pdf>.

Address correspondence via email to Jacques-Eric Gottenberg, MD, PhD, at [jacques-eric.gottenberg@chru-strasbourg.fr](mailto:jacques-eric.gottenberg@chru-strasbourg.fr) or via email to Benno Schwikowski, PhD, at [benno@pasteur.fr](mailto:benno@pasteur.fr).

Submitted for publication August 25, 2021; accepted in revised form June 10, 2022.

website at <https://onlinelibrary.wiley.com/doi/10.1002/art.42265>). Cluster-associated marker genes were identified using the Limma R package (11). For the detection of significant enrichment of biologic pathways, we performed gene set enrichment analysis (12) against “hallmark” gene sets that are available in the Molecular Signatures Database (13).

For further analysis, we computed an interferon (IFN) score that represented the aggregate expression of 5 key IFN genes (IFI44, IFI44L, IFIT1, IFIT3, MxA) (14) that were standardized (see Supplementary Methods).

#### IFN $\alpha$ and IFN $\gamma$ quantification in the ASSESS cohort.

Simoa assays were developed using a Quanterix Homebrew Simoa assay kit in accordance with the manufacturer's instructions (15,16) (see Supplementary Methods).

**Statistical analysis of clinical data.** All statistical analyses were performed using the R statistical software package (version 3.5.0). Because of the non-Gaussian distribution of several continuous variables (even if log-transformed), we used the Kruskal-Wallis rank test to detect the significant differences of continuous clinical variables across clusters. We then applied the Bonferroni method for adjustment of *P* values involving multiple comparisons. Application of different linear model analyses is explained in the Supplementary Methods.

**HLA imputation and fine mapping.** The patient data from the ASSESS cohort had been previously genotyped using ImmunoChip (17) (see Supplementary Methods for imputation methods) (18–21).

The imputed single-nucleotide polymorphisms (SNPs) and classic HLA alleles were tested for associations with IFN $\alpha$  concentrations using linear regression and SSA status with logistic regression, with both analyses corrected for the first 10 principal components. We tested multiallelic amino acid positions for associations using the multiple degree of freedom omnibus test, which included the same covariates as used for the regression analyses.

For performance of HLA fine mapping, we only included samples of European descent (*N* = 246), as determined by principal components analysis, with EigenStrat (22) and HapMap3 (from the International HapMap Consortium, 2010) used as references.

Manhattan plots (23) and the online LocusZoom tool (24) were used to determine the results of the association tests on the SNPs related to their location within the genome.

We calculated the posterior probabilities and frequency of HLA-DR/DQ haplotypes using the R package Haplo.Stats, as the phases of these HLA alleles cannot be resolved from genotyping data. To analyze the associations between haplotypes and circulating IFN, we used the Haplo.glm method within Haplo.Stats and HLA-DRB1\*11:01;DQA1\*01:02;DQB1\*06:02 as the baseline.

## RESULTS

**Patient stratification using unsupervised transcriptome analysis of 4 primary SS cohorts.** We analyzed whole blood transcriptome and genotype results in patients with primary SS from the multicenter prospective French clinical cohort (6) (Supplementary Figure 1A [<https://onlinelibrary.wiley.com/doi/10.1002/art.42265>]). Implementation of strict quality control over clinical, serologic, genetic, and transcriptome data resulted in a high-quality database of 351 patients with primary SS. Clinical descriptions of the cohort and quality controls of the data are shown in Supplementary Figures 1B–D.

The use of a clustering approach for transcriptome data allowed us to identify 4 patient clusters of different sizes (comprising a total of 63 patients, 110 patients, 91 patients, and 87 patients per cluster), which we named clusters 1, 2, 3, and 4, respectively (Figure 1A, as well as Supplementary Figures 1E and 1F). Data projection with low-dimensional embedding validated the consistency of our approach (Supplementary Figures 1G–I).

To understand the biology underlying each of these 4 clusters, we considered the genes that were significantly differentially expressed among clusters of patients with primary SS as cluster-associated marker genes (Supplementary Table 1, available on the *Arthritis & Rheumatology* website at <https://onlinelibrary.wiley.com/doi/10.1002/art.42265>). We identified 131 gene markers differentially expressed between the 4 clusters (Supplementary Methods). Among these genes, IFN-stimulated genes (ISGs) were strongly enriched in cluster 3 and cluster 4, with 45 genes for the IFN $\gamma$  response signature ( $P = 2.90 \times 10^{-72}$ ) and 38 genes for the IFN $\alpha$  response signature ( $P = 1.49 \times 10^{-71}$ ) in the hallmark gene sets. ISGs such as RSAD2 and OAS2 were overexpressed specifically in clusters 3 and 4 (i.e., in 52% of patients) compared with presence in clusters 1 and 2 (Figure 1B). Because hierarchical clustering revealed a strong correlation between ISG expression, those genes were grouped in a gene module that we named the ISG module.

We also detected a significant enrichment of genes related to heme metabolism (8 genes,  $P = 1.53 \times 10^{-6}$ ), which included AHSP and FECH, 2 hemoglobin-related genes that were overexpressed in clusters 3 and 1 but not in clusters 2 and 4 (Figure 1B). In further analysis using the Human Tissue Compendium database (25), we observed that these genes were specifically expressed by erythroid and erythroid progenitor cells but not by immune cells (Supplementary Figure 1J). These genes were highly coexpressed and clustered together in a specific gene module that we named the erythroid module (Figure 1A).

**Molecular stratification strategy replicates in 3 independent primary SS cohorts.** To probe the robustness of our findings, we repeated our analysis in an independent cohort of patients with primary SS and in 2 public transcriptome data



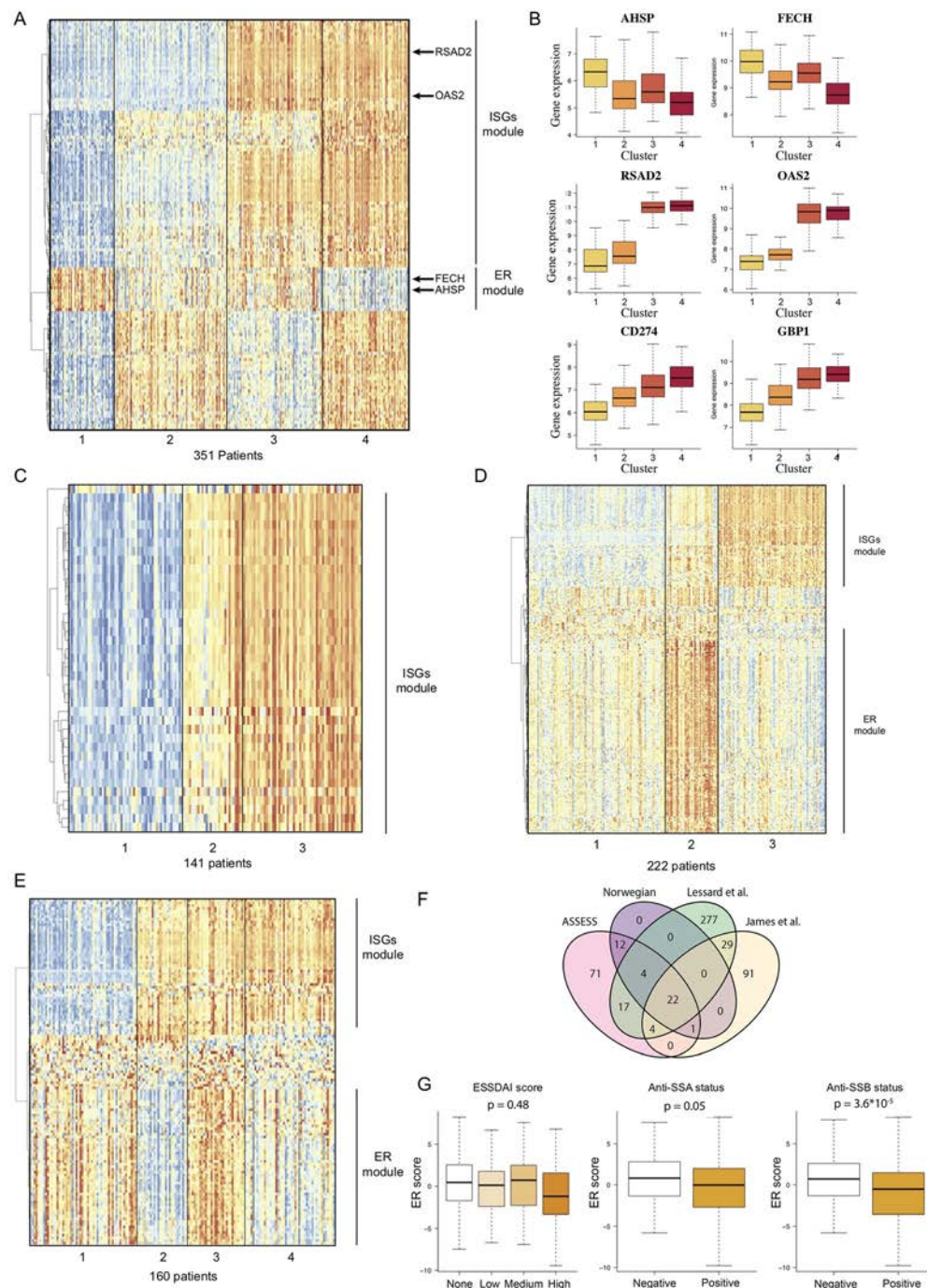


**Figure 1.** Unsupervised transcriptomic analysis enables robust stratification of patients with primary Sjögren's syndrome (SS) in 4 different cohorts. **A**, Expression of marker genes across the 4 clusters of patients from the Assessment of Systemic Signs and Evolution in Sjögren's Syndrome (ASSESS) cohort, normalized by row, and annotation of the identified gene modules based on hierarchical clustering. **B**, Expression of 6 genes identified as marker genes across the patients from the ASSESS cohort. Values are shown as box plots, where the line inside the box represents the median, the box represents the interquartile range, and the whiskers represent the 10th and 90th percentiles. **C**, Expression of marker genes across the 3 clusters of patients identified in the Norwegian cohort and annotation of the identified gene modules based on hierarchical clustering. **D**, Expression of marker genes across the 4 clusters of patients identified in the cohort from Lessard et al (7) and annotation of the identified gene modules based on hierarchical clustering. **E**, Expression of marker genes across the 4 clusters of patients identified in the cohort from James et al (8) and annotation of the identified gene modules based on hierarchical clustering. **F**, Intersection between the sets of marker genes identified in the 4 different primary SS cohorts. **G**, Association between erythroid (ER) transcriptomic score and EULAR Sjögren's Syndrome Disease Activity Index (ESSDAI) score, anti-SSA status, and anti-SSB status. ISG = interferon-stimulated gene.

sets of patients with primary SS (Supplementary Table 2, available on the *Arthritis & Rheumatology* website at <https://onlinelibrary.wiley.com/doi/10.1002/art.42265>).

For the independent cohort (141 consecutive patients with primary SS referred for specialist consultation in Norway), the whole blood transcriptome data were generated with the same microarray and hybridization techniques that were used for the ASSESS cohort, with data analysis performed in an identical manner. Our analysis revealed 3 clusters with 39 differentially expressed cluster-associated markers (Supplementary Table 3, available on the *Arthritis & Rheumatology* website at <https://onlinelibrary.wiley.com/doi/10.1002/art.42265>). We found that ISGs were strongly enriched among these markers, with 22 genes ( $P = 1.22 \times 10^{-48}$ ) shown for the IFN $\alpha$  signature and 29 genes ( $P = 1.30 \times 10^{-59}$ ) shown for the IFN $\gamma$  signature in the hallmark gene sets (Figure 1C, as well as Supplementary Figures 2A and 2B, available on the *Arthritis & Rheumatology* website at <https://onlinelibrary.wiley.com/doi/10.1002/art.42265>). Consistency of the clustering was successfully verified with low-dimensional embedding (Supplementary Figures 2D and 2E). In this cohort, we did not detect any significant enrichment in genes linked to erythroid cell and heme metabolism.

For the 2 public transcriptome data sets, which included 190 patients (7) and 131 patients (8) with primary SS, the whole blood transcriptome analysis was performed using different microarray technologies (HumanWG-6 version 3.0 Illumina BeadChip kit and HumanHT-12 version 4 Illumina BeadChip kit, respectively). Our analysis of the 2 cohorts revealed clusters identified as clusters 3 and 4, as defined by differential expression of 353 and 147 genes, respectively (Figures 1D and 1E, as well as Supplementary Figures 2B and 2C and Supplementary Tables 4 and 5, available on the *Arthritis & Rheumatology* website at <https://onlinelibrary.wiley.com/doi/10.1002/art.42265>). In both of the public cohorts, an IFN gene signature was identified through gene set enrichment analysis, with 27 and 31 genes ( $P = 8.77 \times 10^{-47}$  and  $P = 2.55 \times 10^{-53}$ ), respectively, belonging to the IFN $\alpha$  predicted signature and 46 and 35 genes ( $P = 5.17 \times 10^{-57}$  and  $P = 1.13 \times 10^{-52}$ ), respectively, belonging to the IFN $\gamma$  predicted signature, according to the hallmark database. In addition, we detected an erythroid signature in both data sets (38 and 30 genes [ $P = 4.9 \times 10^{-57}$  and  $P = 6.23 \times 10^{-53}$ ], respectively) (Figures 1D and 1E).

We then studied the overlap between the different markers identified in the ASSESS cohort and the 3 other primary SS cohorts (Figure 1F). Of the 22 genes that were validated as marker genes across all 4 cohorts, nearly all were ISGs, with 20 genes belonging to the IFN $\gamma$  predicted signature ( $P = 2.56 \times 10^{-44}$ ) and 17 genes belonging to the IFN $\alpha$  predicted signature ( $P = 4.84 \times 10^{-41}$ ), thus strongly supporting the critical role of IFN signaling in primary SS.

Lastly, we investigated the potential role of the erythroid gene module. We therefore computed an erythroid expression score

for each patient of the ASSESS cohort and looked for associations with clinical and biologic parameters. We did not observe a significant association with the EULAR Sjögren's Syndrome Disease Activity Index (ESSDAI, the international score of systemic disease activity) (26) ( $P = .48$ ) but observed associations with anti-SSA ( $P = .045$ ) and anti-SSB status ( $P = 3.63 \times 10^{-5}$ ) (Figure 1G).

Thus, our results demonstrated that the stratification of patients with primary SS by whole blood transcriptome data and through our analytic pipeline was highly reproducible for determination of ISG signatures across different independent cohorts and microarray technologies.

### Association of IFN $\alpha$ but not IFN $\gamma$ with the transcriptome signature and with disease activity.

IFN $\alpha$  and IFN $\gamma$ , antiviral cytokines that trigger similar transcriptional changes in immune cells, are challenging to discriminate using gene expression data. To assess whether the transcriptional changes underlying the molecular stratification were regulated by IFN $\alpha$  and/or by IFN $\gamma$ , we measured baseline circulating IFN $\alpha$  and IFN $\gamma$  protein concentrations. Detectable concentrations of IFN $\alpha$  were observed in 277 (74.9%) of the 370 patients assessed, and detectable concentrations of IFN $\gamma$  were observed in 364 (96.8%) of the 376 patients assessed. Significant differences in IFN $\alpha$  concentrations between clusters were observed, with IFN $\alpha$  levels in patients from clusters 1 and 2 close to the lower limit of detection (0.6 fg/ml) and with IFN $\alpha$  levels in patients from clusters 3 and 4 detected at high concentrations (median 60 fg/ml) (Figure 2A). Similarly, IFN $\gamma$  concentrations significantly differed across clusters, with cluster 3 having the highest levels (median IFN $\gamma$  concentration of 192, 430, 567, and 475 fg/ml in clusters 1, 2, 3 and 4, respectively) (Figure 2A).

When we applied linear function modeling to the whole transcriptome data of ASSESS patients, 95% of the IFN-inducible genes (1,552 genes) were specifically correlated with serum IFN $\alpha$  concentration, whereas only 7 genes were specifically correlated with serum IFN $\gamma$  concentration. We also found that 70 genes, including CD274 and GBP1/4/5, were correlated with both IFN $\alpha$  and IFN $\gamma$  concentrations (Figure 2B). Among the 82 cluster-associated markers of the ASSESS cohort, 14 were solely correlated with serum IFN $\alpha$  concentration, 38 were correlated with serum concentrations of both IFN $\alpha$  and IFN $\gamma$ , and none of the markers were correlated solely with serum IFN $\gamma$  concentrations.

We observed a strong association between IFN $\alpha$  concentration and antibody status, including anti-SSA status ( $P = 5.09 \times 10^{-28}$ ), anti-SSB serum positivity ( $P = 2.45 \times 10^{-14}$ ), and increased serum concentrations of rheumatoid factor (RF) ( $r^2 = 0.662$ ,  $P = 1.19 \times 10^{-41}$ ) (Figures 2C and 2D). This association with the autoantibodies was considerably weaker when we examined IFN $\gamma$ , especially for RF ( $r^2 = 0.172$ ) (Figures 2C and 2D). Significant associations between IFN $\alpha$  concentrations and the B cell activation markers (B2M, BAFF), immunoglobulin free light chains, and CCL19 were observed; however, for IFN $\gamma$ , associations with

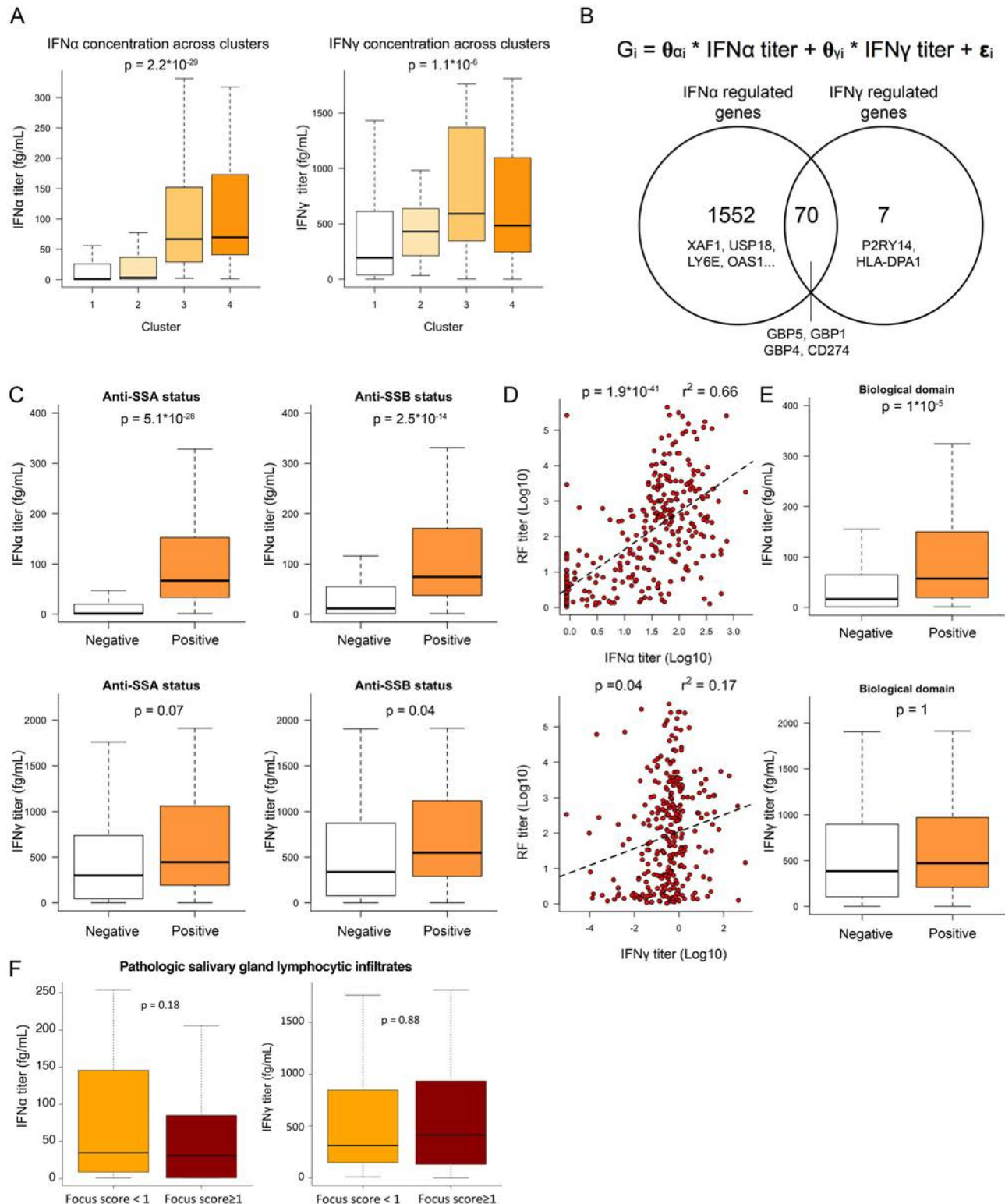


**Figure 2.** Quantification of interferon- $\alpha$  (IFN $\alpha$ ) and IFN $\gamma$  protein serum concentrations by digital enzyme-linked immunosorbent assay reveals the pivotal role of IFN $\alpha$  in patients with primary Sjögren's syndrome (SS). **A**, IFN $\alpha$  (left) and IFN $\gamma$  (right) serum titers across clusters. **B**, Description of the linear model used to describe gene expression (top) and Venn diagram showing the number of genes transcriptionally controlled by IFN $\alpha$ , IFN $\gamma$ , or both (bottom). **C**, IFN $\alpha$  (top) and IFN $\gamma$  (bottom) concentrations based on anti-SSA (left) and anti-SSB (right) status. **D**, Correlations between IFN $\alpha$  and rheumatoid factor (RF) concentrations (top) and between IFN $\gamma$  and RF concentrations (bottom). Dashed lines are based on the linear regression between the 2 variables. **E**, IFN $\alpha$  (top) and IFN $\gamma$  (bottom) concentrations based on presence versus absence of an active biologic domain according to components of the EULAR Sjögren's Syndrome Disease Activity Index (ESSDAI). **F**, Concentrations of IFN $\alpha$  (left) and IFN $\gamma$  (right) according to focus score of inflammatory infiltrates in the salivary glands of patients with primary SS. For box plots, the line inside the box represents the median, the box represents the interquartile range, and the whiskers extend to the most extreme data point that is no more than 1.5 times the interquartile range from the box. Color figure can be viewed in the online issue, which is available at <http://onlinelibrary.wiley.com/doi/10.1002/art.42265/abstract>.



these markers were weaker and barely significant (Supplementary Figures 3A and 3B, available on the *Arthritis & Rheumatology* website at <https://onlinelibrary.wiley.com/doi/10.1002/art.42265>).

The low  $r^2$  values indicated that not much variance can be explained by single predictors, such as blood biomarkers, suggesting more complex relationships between IFN $\alpha$  and blood serum markers. Significant differences were observed in IFN $\alpha$  concentrations but not in IFN $\gamma$  concentrations between patients with or without an active biologic domain of the ESSDAI (the domain is considered active when complement components are low, gamma globulin or IgG levels are high, and/or a cryoglobulinemia is detected) (Figure 2E). We found that, within the biologic domain, IgG and gamma globulins were the main drivers of the correlation to IFN $\alpha$ , showing a positive correlation to the IFN $\alpha$  concentration in the blood (for correlation with IgG, Spearman's  $r = 0.5$ ,  $P \leq 0.01$ ; for correlation with total gamma globulins, Spearman's  $r = 0.47$ ,  $P \leq 0.01$ ); however, C3 and C4 showed only small, negative correlations (for correlation with C3, Spearman's  $r = -0.16$ ,  $P = 0.003$ ; for correlation with C4, Spearman's  $r = -0.27$ ,  $P = 0.02$ ), with no difference visible for the patients having or not having cryoglobulins ( $P = 0.5$ ) (see Supplementary Figures 3B–E). Together, our results suggested a dominant role of IFN $\alpha$ , compared with IFN $\gamma$ , for inducing B cell activation and systemic activity of the disease.

We also analyzed IFN $\alpha$  and IFN $\gamma$  concentrations in patient salivary gland lymphocytic infiltrates but could not detect differences in blood IFN $\alpha$  or IFN $\gamma$  concentrations between patients with focus score of  $\geq 1$  and those with a focus score of  $<1$  according to the results of a minor salivary gland biopsy done any time prior to enrollment (Figure 2F).

We then analyzed associations between IFN $\alpha$  and IFN $\gamma$  concentrations and clinical involvement at enrollment and during follow-up. At enrollment, systemic complications were more frequent in patients with detectable IFN $\alpha$  serum concentrations. The mean ESSDAI at enrollment was higher (mean score 4 [range 0–31] versus mean score 2 [range 1–18],  $P = 0.0004$ ) in patients with detectable IFN $\alpha$  serum concentrations. The proportions of patients with active disease on the ESSDAI, according to the cutaneous domain (22.8% versus 0%,  $P = 0.028$ ), hematologic domain (24.6% versus 8.1%,  $P = 0.0038$ ), and biologic domain (28.5% versus 11.4%,  $P < 0.0001$ ) of the ESSDAI were also higher in patients with detectable IFN $\alpha$  serum concentrations.

We next analyzed the course of systemic complications that occurred in these patients prospectively over 5 years according to baseline IFN $\alpha$  serum concentrations. The ESSDAI values repeated across times were therefore modeled using a beta mixed regression analysis. During the 5-year prospective follow-up, patients with baseline detectable IFN $\alpha$  developed significantly more frequent systemic complications (odds ratio [OR] 1.54 [95% confidence interval 1.14–2.13]), with a similar, but nonsignificant, trend for anti-SSA positivity and type I IFN gene score at

enrollment (OR 1.24 [95% confidence interval 0.92–1.69] and OR 0.97 [95% confidence interval 0.95–0.99], respectively).

No association was observed between 1) blood IFN $\alpha$  concentration and patient symptoms, as assessed according to the EULAR Sjögren's Syndrome Patient Reported Index (ESSPRI) (27), 2) blood IFN $\gamma$  concentrations and systemic clinical complications (according to the ESSDAI), and 3) IFN $\gamma$  concentrations and patient symptoms (according to the ESSPRI) at enrollment and during follow-up.

**Genetic determinant for IFN $\alpha$  serum concentration by genetic analysis.** We also investigated any indications of genetic contributions to stratification of patients with primary SS. When we investigated any statistical associations between circulating levels of IFN $\alpha$  protein and 102,744 SNPs among 307 patients from the ASSESS cohort who were previously genotyped, we observed a quantitative trait locus in the major histocompatibility complex (MHC) locus (top SNP was rs9273012,  $P = 4.64 \times 10^{-9}$ ) and a suggestive association with the KIF3A locus in chromosome 5 (top SNP was rs7732667,  $P = 3.37 \times 10^{-5}$ ) (Figure 3A). A detailed analysis of the MHC locus revealed that the SNP with the strongest association with circulating levels of IFN $\alpha$ , rs9273012, was located in the HLA-DQA1 gene, a member of the HLA class II gene family (Figures 3B and 3C). A conditioning analysis on rs9273012 (i.e., including this SNP as a covariate in the regression model) revealed no further independent associations (Supplementary Figure 4D, available on the *Arthritis & Rheumatology* website at <https://onlinelibrary.wiley.com/doi/10.1002/art.42265>). Interestingly, more than 13% of the variance observed in IFN $\alpha$  concentration was solely explained by this SNP.

To obtain a more detailed view of the MHC class II locus, we performed a detailed fine mapping of the MHC region using the SNP2HLA v1.0 software and the Type 1 Diabetes Genetics Consortium reference panel (21) (Supplementary Figure 4A) among the 291 patients from the European HapMap Consortium samples with clustering data. Our analysis revealed a significant and specific association between IFN $\alpha$  concentrations and the HLA-DQA1\*05:01 allele, an allele previously identified as strongly associated with primary SS (7) and also as part of a larger HLA-DR/DQ haplotype. The DRB1\*03:01;DQA1\*05:01;DQB1\*02:01 haplotype was the most frequent in our cohort (Supplementary Figure 4D). Furthermore, the DRB1\*03:01;DQA1\*05:01;DQB1\*02:01 haplotype was the only one significantly associated with IFN $\alpha$  levels (data not shown).

To investigate the possibility that this HLA haplotype could directly regulate IFN $\alpha$  gene expression, we looked for possible associations between IFN $\alpha$  gene expression in whole blood of the ASSESS patients and rs9273012 status. No significant difference in IFN $\alpha$  gene expression was observed in the presence of the rs9273012 polymorphism (Supplementary Figure 4B). Because IFN $\alpha$  gene expression is highly transient in nature, we utilized the

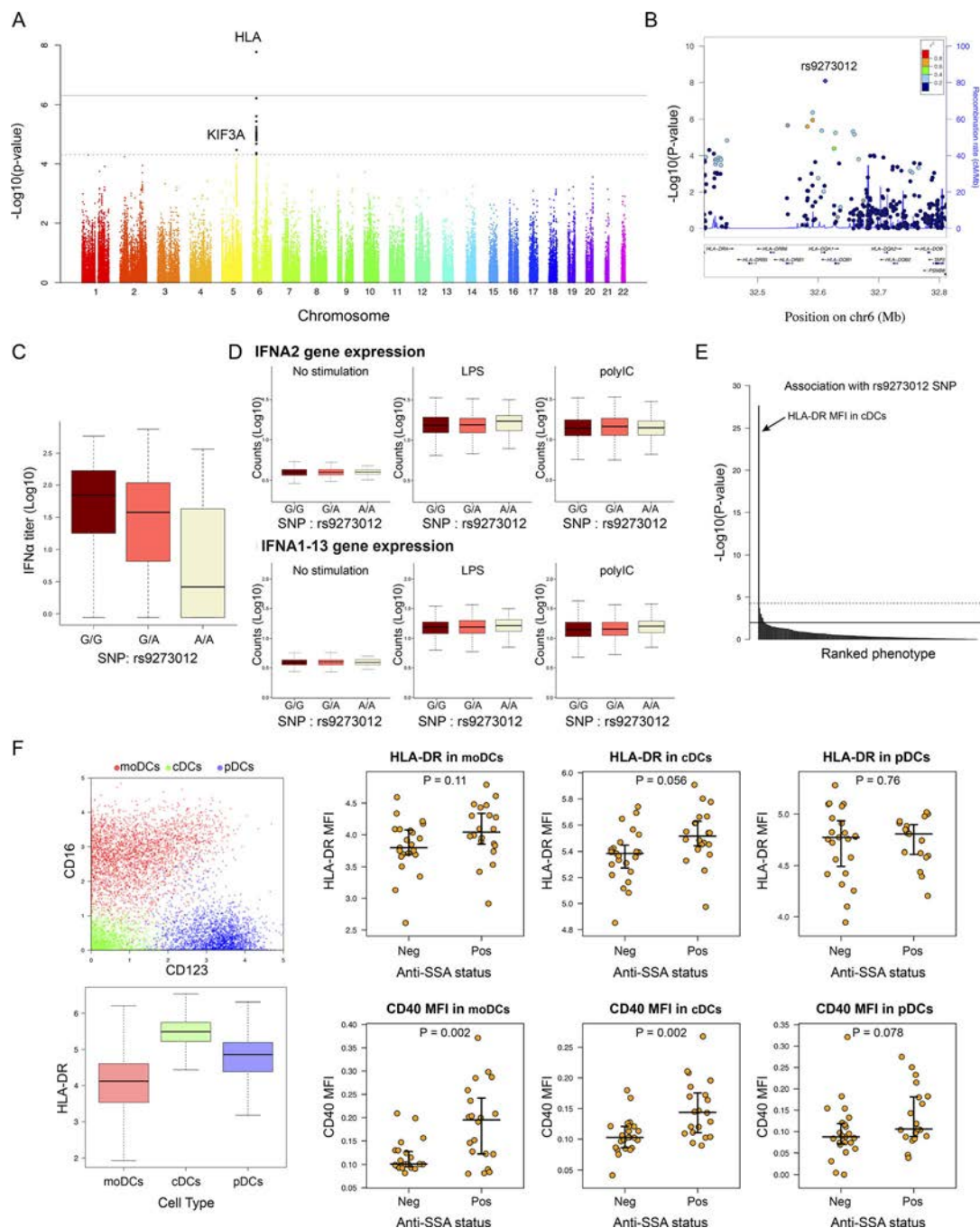


**Figure 3.** Genome-wide association study reveals a genetic determinant in patient stratification and interferon- $\alpha$  (IFN $\alpha$ ) blood concentration in patients with primary Sjögren's syndrome. **A**, Genome-wide association between single-nucleotide polymorphisms (SNPs) and IFN $\alpha$  concentration. Dashed line corresponds to the threshold for a suggested genome-wide association, and solid line corresponds to a significant genome-wide association. **B**, LocusZoom plot of the HLA region. **C**, IFN $\alpha$  concentration according to the rs9273012 SNP status. **D**, IFN $\alpha$  gene expression in whole blood from 1,000 healthy donors from the Milieu Intérieur cohort, under conditions of no stimulation versus stimulation with lipopolysaccharide (LPS) versus stimulation with poly(I-C). **E**,  $P$  values indicating possible statistical significance of associations between the rs9273012 SNP and the 166 immunophenotypes measured in the Milieu Intérieur study from Patin et al (30). The top horizontal line represents the threshold after Bonferroni correction for multiple testing at  $P = 0.05$ . **F**, Mass cytometry analysis of data from Mingueneau et al (9). Panels show the 3 dendritic cell (DC) populations defined using unsupervised analysis (top left) and HLA-DR expression in the 3 DC populations (bottom left), as well as mean fluorescence intensity (MFI) results for HLA-DR (top right) and CD40 (bottom right) in the 3 DC populations based on anti-SSA status. For box plots, the line inside the box represents the median, the box represents the interquartile range, and the whiskers extend to the most extreme data point that is no more than 1.5 times the interquartile range from the box. moDCs = monocyte-derived DCs; cDCs = conventional DCs; pDCs = plasmacytoid DCs; Neg = negative; Pos = positive. Color figure can be viewed in the online issue, which is available at <http://onlinelibrary.wiley.com/doi/10.1002/art.42265/abstract>.



Milieu Intérieur cohort of healthy donors (28) to examine possible genetic associations between the rs9273012 polymorphism and induced IFN gene expression following whole blood stimulation with the poly(I-C) (synthetic analog of double-stranded RNA recognized by the Toll-like receptor 3) (29) (see Appendix A for a list of the study investigators). No associations were observed between the different alleles and induced gene expression of IFNA2 as measured by Nanostring array analysis (Figure 3D).

We also took advantage of extensive cellular phenotypes previously described in the same healthy donors and observed that the rs9273012 G allele was significantly and specifically associated with higher protein expression levels of HLA-DR in conventional dendritic cells (cDCs) (30) ( $P = 2.14 \times 10^{-28}$ ) (Figure 3E). Because a mix of 166 distinct immunophenotypes (for details, see Supplementary Table S3 in ref. 31) had been analyzed, the second-lowest  $P$  value of HLA-DR in conventional dendritic cell subset 3 cells (cDC3s) was below the global significance threshold. HLA-DR expression by cDCs in primary SS was then investigated by reanalysis of data from a mass cytometry study of primary SS blood cells (9). Unsupervised analysis of these data revealed 3 cellular clusters corresponding to DCs: monocyte-derived DCs (CD16 + CD123-), cDCs (CD16 - CD123-), and plasmacytoid DCs (CD16 - CD123+). Both the monocyte-derived DCs and the cDCs exhibited higher expression of CD40 in anti-SSA-positive patients compared with anti-SSA-negative patients ( $P = 2.01 \times 10^{-3}$  and  $P = 2.01 \times 10^{-3}$ , respectively); however, only cDCs exhibited higher expression of HLA-DR in anti-SSA-positive patients compared with anti-SSA-negative patients ( $P = 0.056$ ) (Figure 3F). Thus, we observed that the rs9273012 polymorphism was associated with increased HLA class II expression in cDCs from healthy controls and that HLA class II expression was increased in cDCs from patients with anti-SSA autoantibodies.

In our investigation of the relationship between HLA gene polymorphisms and anti-SSA status in the ASSESS cohort, we observed a consistent signal in the HLA-DQA1 locus (Supplementary Figure 4C). The SNP that had the strongest association with IFN $\alpha$  levels, rs9273012, also had the strongest association with anti-SSA autoantibody positivity ( $P = 4.31 \times 10^{-12}$ ).

## DISCUSSION

Our unsupervised gene expression analytic pipeline, newly applied to blood transcriptome data from 813 patients with primary SS, identified a consistent stratification with clusters associated with IFN and erythroid signatures across different cohorts and microarray technologies. Combining this approach with digital enzyme-linked immunosorbent assay in a well-characterized cohort revealed the key role of circulating IFN $\alpha$  protein, as opposed to IFN $\gamma$ , through its association with clinical and immunologic phenotypes, highlighting its relevance as a therapeutic target. Furthermore, our analysis revealed a

significant association between a specific HLA class II gene polymorphism, anti-SSA antibody, and circulating IFN $\alpha$ . The use of well-defined healthy donor data from the Milieu Intérieur cohort and the confirmation in anti-SSA-positive patients with primary SS strongly suggested that this HLA gene polymorphism affects HLA expression on cDCs, thus likely leading to increased autoantigen presentation, autoantibody secretion, and immune complex formation, which can subsequently trigger IFN $\alpha$  secretion.

Limitations of our study are mostly related to the observational design, its focus on peripheral blood only, and the absence of longitudinal biologic assessments.

A strength of our study is the innovative use of an unsupervised clustering method, which has been only previously reported for single cell analysis, to analyze the transcriptome data across different primary SS cohorts. Most previous transcriptomic analyses in primary SS compared limited population samples (31–33) with healthy controls and used bioinformatics prediction, resulting in the description of an IFN signature that did not discriminate between contributions of IFN $\alpha$  and contributions of IFN $\gamma$  to primary SS. The new bioinformatic pipeline in our study, which involved a much larger data set, confirmed the presence of an IFN module but also identified an erythroid module that was previously reported in patients with systemic lupus erythematosus (34). Further analysis may shed light on the potential pathogenic mechanisms associated with the action of this erythroid module.

Both type I and type II IFNs are relevant pathogenic suspects in primary SS, based on genetic predisposition to the disease (involving IFN regulatory factor 5 in the IFN $\alpha$  pathway and interleukin-12A and STAT4 in the IFN $\gamma$  pathway) and the pathogenic cell populations involved (plasmacytoid DCs, the major IFN $\alpha$ -producing cells, and natural killer and CD8 T cells, which secrete IFN $\gamma$ ) (32,35,36). A deeper understanding of the respective contributions of IFN $\alpha$  and IFN $\gamma$  is therefore crucial for selective therapeutic targeting.

Of note, most of the genes induced by IFN $\alpha$  are also induced by IFN $\gamma$ , making such a “signature” actually a broader marker of both IFN $\alpha$  and IFN $\gamma$  activity (37). To our knowledge, our study is the first to measure circulating IFN proteins in a large prospective cohort of patients with primary SS concomitantly with their transcriptomic signature. The quantification of both IFN proteins in the circulation at attomolar concentrations allowed us to determine that 95% of the IFN-inducible genes are correlated with serum IFN $\alpha$  but not with IFN $\gamma$ . A recent multiomic profiling study in a cross-sectional cohort of patients with primary SS also showed a correlation between serum IFN $\alpha$  concentration and type I IFN signature (38) but did not assess serum IFN $\gamma$  concentration. Of note, our study, which focused on peripheral blood, did not exclude a possible role of IFN $\beta$  (another type I IFN), IFN $\gamma$  (type II IFN), or type III IFNs in salivary glands (39–41).

Our multiomic study also allowed us to analyze the relationship between IFN protein concentrations and patient genotypes,

whole blood transcriptome results, and clinical phenotypes. A highly significant association between HLA class II gene polymorphisms and circulating IFN $\alpha$  protein concentrations was identified. Specifically, in primary SS, we demonstrated an association between an HLA allele, HLA-DQA1\*05:01, and both anti-SSA antibody and blood IFN $\alpha$  concentrations. The associations between HLA class II polymorphisms and autoantibodies and between autoantibodies and the IFN signature have long been known (42–44), as well as the associations between anti-SSA antibodies, cutaneous involvement, and hematologic and biologic domains (45,46). SNPs associated with HLA class II genes were also associated with the IFN signature and autoantibodies in a recent multiomic study of patients with primary SS (38). Our present results add mechanistic explanations underlying this association. In healthy donors, HLA expression and this specific polymorphism were not associated with IFN $\alpha$  induction upon stimulation, indicating that they do not directly influence IFN $\alpha$  secretion. However, in the same healthy donors, this HLA allele was associated with HLA-DR protein up-regulation in conventional DCs, but not in plasmacytoid DCs. In addition, HLA-DR was up-regulated in cDCs from patients with primary SS who were anti-SSA positive compared with patients with primary SS who were anti-SSA negative. This suggests that HLA-DQA1\*05:01, as part of the HLA DRB1\*03:01;DQA1\*05:01;DQB1\*02:01/DQB1\*03:01 haplotype, promotes HLA class II molecule expression at the cDC surface, and thus SSA antigen presentation by cDCs, resulting in anti-SSA secretion and immune complex formation, which in turn increases IFN $\alpha$  secretion.

In primary SS, and perhaps in other autoimmune diseases, HLA might therefore predispose to IFN $\alpha$  secretion indirectly, by favoring classic presentation by cDCs of SSA peptides to T cells, leading to anti-SSA antibodies and immune complexes stimulating IFN $\alpha$  secretion. This analysis on DCs and the expression of HLA-DR on B cells, which are also pivotal antigen-presenting cells, deserves further investigation.

Our results also revealed the potential of circulating IFN $\alpha$  as a biomarker in primary SS. Previous studies have suggested the use of quantitative IFN $\alpha$  and IFN $\gamma$  signatures as biomarkers on the basis of messenger RNA expression by quantitative polymerase chain reaction of IFN-inducible genes; however, these studies were mainly cross-sectional and had limited sample sizes (39,41,47). The strength of our present study was the direct quantification of IFN $\alpha$  and IFN $\gamma$  protein using a highly sensitive method in a cohort prospectively observed for 5 years. The fact that the proportion of patients with detectable circulating IFN $\alpha$  was higher than the proportion of patients with detectable IFN signature suggests that the detection of circulating IFN $\alpha$  protein is a more sensitive measure of IFN $\alpha$  activity than is a transcriptomic signature. In agreement with previous studies of IFN signatures (8,38,39), fatigue, pain, and dryness were not associated with either circulating IFN $\alpha$  or circulating IFN $\gamma$  levels. However, in contrast to IFN $\gamma$ , we found that circulating IFN $\alpha$  was highly

significantly associated with autoantibodies and markers of B cell activation. In addition, in contrast to IFN $\gamma$ , circulating IFN $\alpha$  was significantly associated with systemic complications at enrollment. Baseline detectable IFN $\alpha$  was also associated with more frequent systemic complications during the 5-year prospective follow-up. Further studies that assess IFN $\alpha$  longitudinally at different time points are necessary to confirm the potential predictive role of IFN $\alpha$ .

Although hydroxychloroquine treatment has been shown to decrease the strength of IFN $\alpha$  signatures (14), we observed that circulating IFN $\alpha$  levels were not significantly different among 113 of 352 patients in our analyses who were prescribed hydroxychloroquine at enrollment (see Supplementary Figure 3F). This might be related to nonadherence of some patients to hydroxychloroquine (blood levels of hydroxychloroquine were not assessed).

In conclusion, the strong transcriptomic stratification of patients with primary SS in our analysis was clinically relevant, supported by our observation that it was driven by IFN $\alpha$  rather than by IFN $\gamma$ , and was associated with HLA gene polymorphisms. Beyond the specific implications for primary SS, this gene analysis approach may also be useful to move to precision therapy in other complex autoimmune diseases.

## AUTHOR CONTRIBUTIONS

All authors were involved in drafting the article or revising it critically for important intellectual content, and all authors approved the final version to be published. Dr. Gottenberg had full access to all of the data in the study and takes responsibility for the integrity of the data and the accuracy of the data analysis.

**Study conception and design.** Trutschel, Bost, Mariette, Duffy, Schwikowski, Gottenberg.

**Acquisition of data.** Trutschel, Bost, Mariette, Bondet, Llibre, Posseme, Charbit, Thorball, Jonsson, Lessard, Felten, Ng, Chatenoud, Dumortier, Sibilia, Fellay, Brokstad, Appel, Tarn, Murci, Mingueneau, Meyer, Duffy, Schwikowski, Gottenberg.

**Analysis and interpretation of data.** Trutschel, Bost, Mariette, Bondet, Llibre, Posseme, Charbit, Thorball, Jonsson, Lessard, Felten, Ng, Chatenoud, Dumortier, Sibilia, Fellay, Brokstad, Appel, Tarn, Murci, Mingueneau, Meyer, Duffy, Schwikowski, Gottenberg.




## REFERENCES

- Mariette X, Criswell LA. Primary Sjögren's syndrome. *N Engl J Med* 2018;378:931–9.
- Nocturne G, Pontarini E, Bombardieri M, et al. Lymphomas complicating primary Sjögren's syndrome: from autoimmunity to lymphoma. *Rheumatology (Oxford)* 2019;60:3513–21.
- Gottenberg JE, Ravaud P, Puéchal X, et al. Effects of hydroxychloroquine on symptomatic improvement in primary Sjögren syndrome: the JOQUER randomized clinical trial. *JAMA* 2014;312:249–58.
- Devauchelle-Pensec V, Mariette X, Jousse-Joulin S, et al. Treatment of primary Sjögren syndrome with rituximab. *Ann Intern Med* 2018;160:233–42.
- Bowman SJ, Everett CC, O'Dwyer JL, et al. Randomized controlled trial of rituximab and cost-effectiveness analysis in treating fatigue

- and oral dryness in primary Sjögren's syndrome. *Arthritis Rheumatol* 2017;69:1440–50.
6. Gottenberg JE, Seror R, Miceli-Richard C, et al. Serum levels of beta2-microglobulin and free light chains of immunoglobulins are associated with systemic disease activity in primary Sjögren's syndrome. Data at enrollment in the prospective ASSESS cohort. *PLoS One* 2013;8:e59868.
  7. Lessard CJ, Li H, Adrianto I, et al. Variants at multiple loci implicated in both innate and adaptive immune responses are associated with Sjögren's syndrome. *Nat Genet* 2013;45:1284–92.
  8. James K, Al-Ali S, Tarn J, et al. A transcriptional signature of fatigue derived from patients with primary Sjögren's syndrome. *PLoS One* 2015;10:e0143970.
  9. Mingueneau M, Boudaoud S, Haskett S, et al. Cytometry by time-of-flight immunophenotyping identifies a blood Sjögren's signature correlating with disease activity and glandular inflammation. *J Allergy Clin Immunol* 2016;137:1809–21.
  10. Levine JH, Simonds EF, Bendall SC, et al. Data-driven phenotypic dissection of AML reveals progenitor-like cells that correlate with prognosis. *Cell* 2015;162:184–97.
  11. Ritchie ME, Phipson B, Wu D, et al. Limma powers differential expression analyses for RNA-sequencing and microarray studies. *Nucleic Acids Res* 2015;43:e47.
  12. Subramanian A, Tamayo P, Mootha VK, et al. Gene set enrichment analysis: a knowledge-based approach for interpreting genome-wide expression profiles. *Proc Natl Acad Sci U S A* 2005;102:15545–50.
  13. Liberzon A, Birger C, Thorvaldsdóttir H, et al. The Molecular Signatures Database hallmark gene set collection. *Cell Syst* 2015;1:417–25.
  14. Bodewes IL, Al-Ali S, van Helden-Meeuwsen CG, et al. Systemic interferon type I and type II signatures in primary Sjögren's syndrome reveal differences in biological disease activity. *Rheumatology (Oxford)* 2018;57:921–30.
  15. Rodero MP, Decalf J, Bondet V, et al. Detection of interferon  $\alpha$  protein reveals differential levels and cellular sources in disease. *J Exp Med* 2017;214:1547–55.
  16. Meyer S, Woodward M, Hertel C, et al. AIRE-deficient patients harbor unique high-affinity disease-ameliorating autoantibodies. *Cell* 2016;166:582–95.
  17. Cortes A, Brown MA. Promise and pitfalls of the Immunochip. *Arthritis Res Ther* 2011;13:101.
  18. McCarthy S, Das S, Kretzschmar W, et al. A reference panel of 64,976 haplotypes for genotype imputation. *Nat Genet* 2016;48:1279–83.
  19. Durbin R. Efficient haplotype matching and storage using the positional Burrows-Wheeler transform (PBWT). *Bioinformatics* 2014;30:1266–72.
  20. Loh PR, Danecek P, Palamara PF, et al. Reference-based phasing using the Haplotype Reference Consortium panel. *Nat Genet* 2016;48:1443–8.
  21. Jia X, Han B, Onengut-Gumuscu S, et al. Imputing amino acid polymorphisms in human leukocyte antigens. *PLoS One* 2013;8:e64683.
  22. Price AL, Patterson NJ, Plenge RM, et al. Principal components analysis corrects for stratification in genome-wide association studies. *Nat Genet* 2006;38:904–9.
  23. Gibson G. Hints of hidden heritability in GWAS. *Nat Genet* 2010;42:558–60.
  24. Pruim RJ, Welch RP, Sanna S, et al. LocusZoom: regional visualization of genome-wide association scan results. *Bioinformatics* 2010;26:2336–7.
  25. Su AI, Wiltshire T, Batalov S, et al. A gene atlas of the mouse and human protein-encoding transcriptomes. *Proc Natl Acad Sci U S A* 2004;101:6062–7.
  26. Seror R, Ravaud P, Bowman SJ, et al, on behalf of the EULAR Sjögren's Task Force. EULAR Sjögren's Syndrome Disease Activity Index: development of a consensus systemic disease activity index for primary Sjögren's syndrome. *Ann Rheum Dis* 2010;69:1103–9.
  27. Seror R, Ravaud P, Mariette X, et al, on behalf of the EULAR Sjögren's Task Force. EULAR Sjögren's Syndrome Patient Reported Index (ESSPRI): development of a consensus patient index for primary Sjögren's syndrome. *Ann Rheum Dis* 2011;70:968–72.
  28. Thomas S, Rouilly V, Patin E, et al. The Milieu Intérieur study: an integrative approach for study of human immunological variance. *Clin Immunol* 2015;157:277–93.
  29. Urrutia A, Duffy D, Rouilly V, et al. Standardized whole-blood transcriptional profiling enables the deconvolution of complex induced immune responses. *Cell Rep* 2016;16:2777–91.
  30. Patin E, Hasan M, Bergstedt J, et al. Natural variation in the parameters of innate immune cells is preferentially driven by genetic factors. *Nat Immunol* 2018;19:302–14.
  31. Emamian ES, Leon JM, Lessard CJ, et al. Peripheral blood gene expression profiling in Sjögren's syndrome. *Genes Immun* 2009;10:285–96.
  32. Gottenberg JE, Cagnard N, Lucchesi C, et al. Activation of IFN pathways and plasmacytoid dendritic cell recruitment in target organs of primary Sjögren's syndrome. *Proc Natl Acad Sci U S A* 2006;103:2770–5.
  33. Hjelmervik TO, Petersen K, Jonassen I, et al. Gene expression profiling of minor salivary glands clearly distinguishes primary Sjögren's syndrome patients from healthy control subjects. *Arthritis Rheum* 2005;52:1534–44.
  34. Banchereau R, Hong S, Cantarel B, et al. Personalized immunomonitoring uncovers molecular networks that stratify lupus patients. *Cell* 2016;165:551–65.
  35. Rusakiewicz S, Nocturne G, Lazure T, et al. NCR3/NKp30 contributes to pathogenesis in primary Sjögren's syndrome. *Sci Transl Med* 2013;5:195ra96.
  36. Tasaki S, Suzuki K, Nishikawa A, et al. Multiomic disease signatures converge to cytotoxic CD8 T cells in primary Sjögren's syndrome. *Ann Rheum Dis* 2017;76:1458–66.
  37. Hall JC, Casciola-Rosen L, Berger AE, et al. Precise probes of type II interferon activity define the origin of interferon signatures in target tissues in rheumatic diseases. *Proc Natl Acad Sci U S A* 2012;109:17609–14.
  38. Soret P, Le Dantec C, Desvaux E, et al. A new molecular classification to drive precision treatment strategies in primary Sjögren's syndrome. *Nat Commun* 2021;12:3523.
  39. Bodewes IL, Huijser E, van Helden-Meeuwsen CG, et al. TBK1: a key regulator and potential treatment target for interferon positive Sjögren's syndrome, systemic lupus erythematosus and systemic sclerosis. *J Autoimmun* 2018;91:97–102.
  40. Hall JC, Baer AN, Shah AA, et al. Molecular subsetting of interferon pathways in Sjögren's syndrome. *Arthritis Rheumatol*;67:2437–46.
  41. Nezos A, Gravani F, Tassidou A, et al. Type I and II interferon signatures in Sjögren's syndrome pathogenesis: contributions in distinct clinical phenotypes and Sjögren's related lymphomagenesis. *J Autoimmun* 2015;63:47–58.
  42. Gottenberg JE, Busson M, Loiseau P, et al. In primary Sjögren's syndrome, HLA class II is associated exclusively with autoantibody production and spreading of the autoimmune response. *Arthritis Rheum* 2003;48:2240–5.
  43. Harley JB, Reichlin M, Arnett FC, et al. Gene interaction at HLA-DQ enhances autoantibody production in primary Sjögren's syndrome. *Science* 1986;232:1145–7.

44. Lovgren T, Eloranta ML, Bave U, et al. Induction of interferon- $\alpha$  production in plasmacytoid dendritic cells by immune complexes containing nucleic acid released by necrotic or late apoptotic cells and lupus IgG. *Arthritis Rheum* 2004;50:1861–72.
45. Brito-Zerón P, Acar-Denizli N, Ng WF, et al. How immunological profile drives clinical phenotype of primary Sjögren's syndrome at diagnosis: analysis of 10,500 patients (Sjögren Big Data Project). *Clin Exp Rheumatol* 2018;36 Suppl:102–12.
46. Kyriakidis NC, Kapsogeorgou EK, Tzioufas AG. A comprehensive review of autoantibodies in primary Sjögren's syndrome: clinical phenotypes and regulatory mechanisms. *J Autoimmun* 2014;51: 67–74.
47. Brkic Z, Maria NI, van Helden-Meeuwsen CG, et al. Prevalence of interferon type I signature in CD14 monocytes of patients with Sjögren's syndrome and association with disease activity and BAFF gene expression. *Ann Rheum Dis* 2013;72:728–35.

# Epigenetic Regulation of Profibrotic Macrophages in Systemic Sclerosis–Associated Interstitial Lung Disease

Anna Papazoglou,<sup>1</sup>  Mengqi Huang,<sup>1</sup> Melissa Bulik,<sup>2</sup> Annika Lafyatis,<sup>2</sup> Tracy Tabib,<sup>1</sup> Christina Morse,<sup>1</sup> John Sembrat,<sup>3</sup> Mauricio Rojas,<sup>4</sup> Eleanor Valenzi,<sup>3</sup>  and Robert Lafyatis<sup>1</sup> 

**Objective.** Systemic sclerosis–associated interstitial lung disease (SSc-ILD) is the leading cause of death in patients with SSc with unclear pathogenesis and limited treatment options. Evidence strongly supports an important role for profibrotic secreted phosphoprotein 1 (SPP1)–expressing macrophages in SSc-ILD. This study was undertaken to define the transcriptome and chromatin structural changes of SPP1 SSc-ILD macrophages in order to better understand their role in promoting fibrosis and to identify transcription factors associated with open chromatin driving their altered phenotype.

**Methods.** We performed single-cell RNA sequencing (scRNA-Seq) on 11 explanted SSc-ILD and healthy control lung samples, as well as single-cell assay for transposase-accessible chromatin sequencing on 5 lung samples to define altered chromatin accessibility of SPP1 macrophages. We predicted transcription factors regulating SPP1 macrophages using single-cell regulatory network inference and clustering (SCENIC) and determined transcription factor binding sites associated with global alterations in SPP1 chromatin accessibility using Signac/Seurat.

**Results.** We identified distinct macrophage subpopulations using scRNA-Seq analysis in healthy and SSc-ILD lungs and assessed gene expression changes during the change of healthy control macrophages into SPP1 macrophages. Analysis of open chromatin validated SCENIC predictions, indicating that microphthalmia-associated transcription factor, transcription factor EB, activating transcription factor 6, sterol regulatory element binding transcription factor 1, basic helix-loop-helix family member E40, Kruppel-like factor 6, ETS variant transcription factor 5, and/or members of the activator protein 1 family of transcription factors regulate SPP1 macrophage differentiation.

**Conclusion.** Our findings shed light on the underlying changes in chromatin structure and transcription factor regulation of profibrotic SPP1 macrophages in SSc-ILD. Similar alterations in SPP1 macrophages may underpin fibrosis in other organs involved in SSc and point to novel targets for the treatment of SSc-ILD, specifically targeting profibrotic macrophages.

## INTRODUCTION

Systemic sclerosis (SSc) is a multisystem, autoimmune, fibrotic disease of unknown etiology with life-threatening fibrotic complications, including SSc-associated interstitial lung disease (SSc-ILD) (1,2). Despite advances in new SSc-ILD treatment options, such as nintedanib (3), tocilizumab (4,5), and myeloablative autologous stem cell transplantation (6), SSc-ILD remains

difficult to treat. The consequences for survival and quality of life are important, as ~50% of SSc patients develop SSc-ILD (2), and 33% of SSc patients die of SSc-ILD fibrotic complications (7).

Increasing evidence supports important roles for macrophages in SSc-ILD. Specifically, macrophage-associated gene expression on lung biopsies correlates with progressive SSc-ILD, worsening lung fibrosis on high-resolution computed tomography, and reduced performance on pulmonary function

Dr. Papazoglou's work was supported by the National Heart, Lung, and Blood Institute, NIH (5T32-AI-89443-10) and a Physician-Scientist Institutional Award from the Burroughs Wellcome Fund. Dr. R. Lafyatis' work was supported by the National Institute of Arthritis and Musculoskeletal and Skin Diseases, NIH (award 2P50-AR-060780) and the National Heart, Lung, and Blood Institute, NIH (award R01-HL-123766). The context is solely responsibility of the authors and does not necessarily represent the official views of the NIH.

<sup>1</sup>Anna Papazoglou, MD, Mengqi Huang, PhD, Tracy Tabib, MS, Christina Morse, BS, Robert Lafyatis, MD: Division of Rheumatology and Clinical Immunology, University of Pittsburgh, Pittsburgh, Pennsylvania; <sup>2</sup>Melissa Bulik, MS, Annika Lafyatis, BS: Department of Human Genetics, University of Pittsburgh, Pittsburgh,

Pennsylvania; <sup>3</sup>John Sembrat, MS, Eleanor Valenzi, MD: Division of Pulmonary, Allergy and Critical Care Medicine, University of Pittsburgh, Pittsburgh, Pennsylvania; <sup>4</sup>Mauricio Rojas, MD: Division of Pulmonary, Critical Care and Sleep Medicine, Ohio State University, Columbus.

Author disclosures are available at <https://onlinelibrary.wiley.com/action/downloadSupplement?doi=10.1002%2Fart.42286&file=act42286-sup-0001-Disclosureform.pdf>.

Address correspondence via email to Anna Papazoglou, MD, at [papazogloua@upmc.edu](mailto:papazogloua@upmc.edu).

Submitted for publication May 11, 2021; accepted in revised form June 23, 2022.



tests (8). SSc-ILD lungs show strongly up-regulated expression of *CCL18*, which is expressed primarily by macrophages (9) and has been found to play a key role in pulmonary fibrotic disease by attracting immune cells and stimulating collagen overproduction (10,11). Strikingly, elevated *CCL18* levels in SSc sera are completely blocked by the anti-interleukin-6 (IL-6) receptor antagonist tocilizumab (4,5), indicating that serum *CCL18* is a biomarker for IL-6 activity in SSc. The distinct gene expression signature of SSc-ILD compared to healthy lungs also shows up-regulation of macrophage gene markers *AIF1*, *CD163*, *MS4A4A*, as well as *SPP1* (8,12), a marker of profibrotic macrophages in idiopathic pulmonary fibrosis (IPF) (13,14). Lower lung lobes of IPF patients, where fibrosis is typically more advanced, demonstrated an increased number of macrophages expressing *SPP1* compared to upper lung lobes in IPF patients and controls (14). Additionally, in murine bleomycin-induced lung fibrosis, intravenous administration of Ly6C<sup>high</sup> inflammatory monocyte progenitor cells facilitates the progression of fibrosis through an increase of alternatively activated lung macrophages, whereas macrophage depletion during fibrinogenesis is associated with less fibrosis (15).

In order to study the pathophysiology of SSc-ILD and define the role of profibrotic macrophages, we analyzed gene expression and altered chromatin structure of pulmonary macrophages from control and SSc-ILD lungs using single-cell RNA sequencing (scRNA-Seq) and single-cell assay for transposase accessible chromatin sequencing (scATAC-Seq). The conceptual basis for our work is that chromatin structure indicates the underlying transcriptional regulation. Chromatin structural changes or remodeling, during which chromatin is open or accessible to transcription factors, is associated with regulated gene expression, affecting the transcriptome and consequently the cell phenotype (16). In this study, we sought to identify key transcription factors driving the altered transcriptome and differentiation of profibrotic lung macrophages, as well as to gain insight on signals, including cytokines, that contribute to profibrotic macrophage differentiation.

## METHODS

Single-cell RNA-Seq using 3' v3 and 5' v1 chemistries (10X Genomics) was performed on 11 explanted lung tissue samples, including lungs from both SSc-ILD patients and healthy control (Supplementary Table 1, available on the *Arthritis & Rheumatology* website at <https://onlinelibrary.wiley.com/doi/10.1002/art.42286>). Single-cell reagent kits (3' v3 or 5' v1 chemistries; 10X Genomics) were used for the library preparation samples after digestion, as described by Valenzi et al (13). Library quantification and sequencing of the scRNA-Seq complementary DNA (cDNA) libraries were carried out by the UPMC Genome Center, using an Illumina NextSeq-500 (14).

Lung samples from healthy controls and SSc-ILD patients were also analyzed using scATAC-Seq (single-cell ATAC reagent

kits [v1 chemistry]; 10X Genomics). Data were analyzed using the R packages Seurat version 4.0 (17) and Signac version 1.0.9004 (18), Loupe Browser 3.1.1 (10X Genomics), and single-cell regulatory network inference and clustering (SCENIC) (19). More details are available in the Supplementary Methods (<https://onlinelibrary.wiley.com/doi/10.1002/art.42286>).

## RESULTS

**Profibrotic macrophages show discrete changes in transcriptomes.** We analyzed lungs from 6 healthy controls and 5 SSc-ILD patients using scRNA-Seq (Supplementary Table 1, <https://onlinelibrary.wiley.com/doi/10.1002/art.42286>). We conducted bioinformatics analyses of samples in 2 groups because 2 different scRNA-Seq chemistries were used, with different numbers of SSc-ILD and healthy control lungs analyzed with each chemistry. Given the uneven number of sample types, batch correction between chemistries was problematic and might have obscured changes in macrophage transcriptomes associated with SSc-ILD. We first describe 5 lung samples from 1 healthy control and 4 SSc-ILD patients, in which single-cell cDNA libraries were prepared using the 3' v3 chemistry. After dimensional reduction and visualization using Uniform Manifold Approximation and Projection (UMAP) (20), we identified cell types in each cluster, as we have previously described (13), using characteristic gene markers for each cell population (Figure 1A and Supplementary Figures 1–3, <https://onlinelibrary.wiley.com/doi/10.1002/art.42286>). Myeloid cells were identified by markers *CD163*, *AIF1*, and *MARCO*. Three macrophage subpopulations were identified by highly differentially expressed gene markers, similar to those seen in patients with IPF (13), which included secreted phosphoprotein 1 (*SPP1*) macrophages, fatty acid binding protein 4 (*FABP4*) macrophages, and ficolin-1 (*FCN1*) macrophages. The vast majority of the *SPP1* macrophage cluster consisted of macrophages from the SSc-ILD patients, with few *SPP1* macrophages from lungs of the controls (Figures 1B and C). Notably, *SPP1* was up-regulated in the SSc macrophages compared to normal macrophages within the same cluster (Supplementary Figures 1–4). Dendritic cells (DCs) were rare and clustered together with the *FCN1*-expressing macrophages (14) (Figure 1 and Supplementary Figure 4).

Comparing *SPP1* macrophages to the *FABP4* and *FCN1* macrophages revealed multiple differentially expressed genes (Supplementary Table 1), including *SPP1*, *LGMN*, seen coregulated in our previous analyses (14), and *PLA2G7*, a target of transcriptional regulation discussed below (Supplementary Figure 4, <https://onlinelibrary.wiley.com/doi/10.1002/art.42286>). Differentially expressed genes associated with each macrophage subpopulation compared to the other 2 subpopulations were determined and queried for enriched gene ontology pathways. Up-regulated genes in *SPP1* macrophages compared to *FABP4* macrophages and *FCN1* macrophages revealed enrichment of

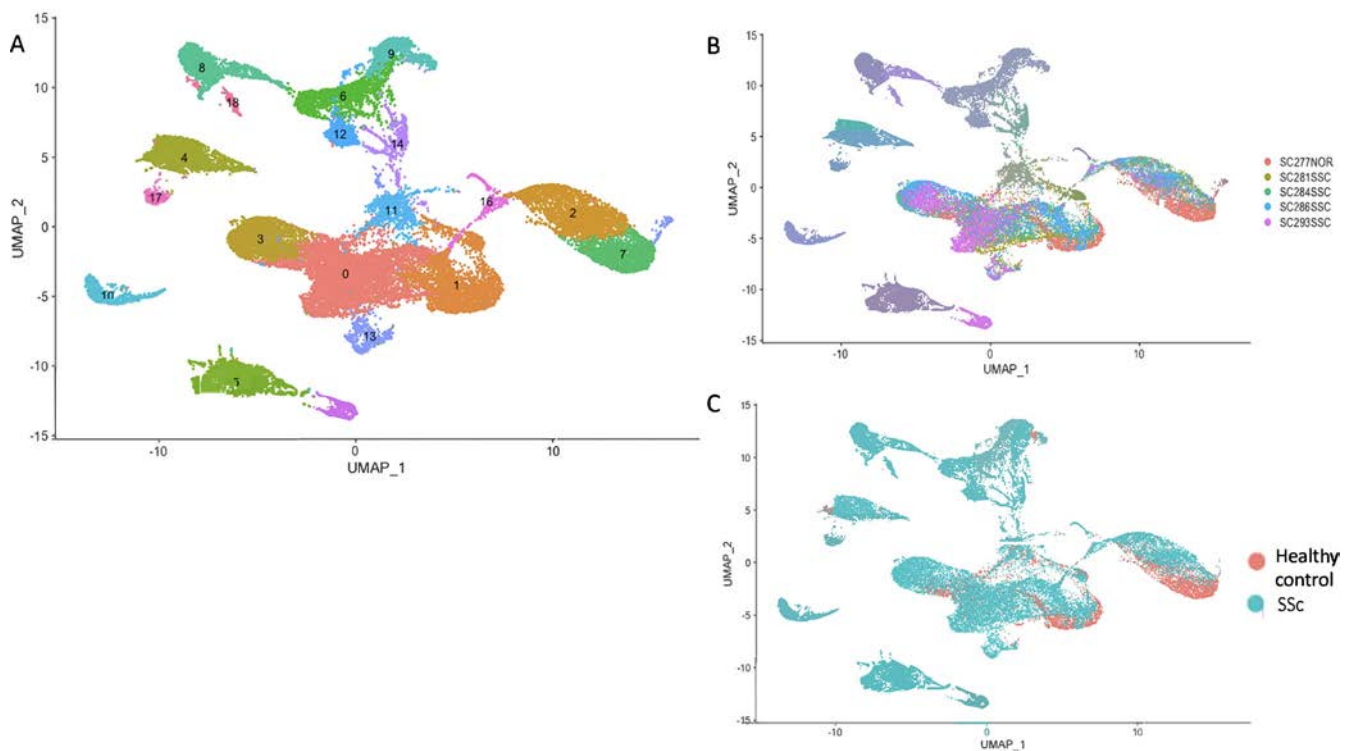


**Figure 1.** Single-cell RNA-sequencing analysis of lung samples in 3' v3 chemistry. Analyses were conducted using 5 lung samples ( $n = 1$  healthy control and 4 patients with systemic sclerosis-associated interstitial lung disease [SSc-ILD]). **A**, Cell clustering identified by Uniform Manifold Approximation and Projection (UMAP) according to cell type. 0 = secreted phosphoprotein 1 (SPP1) macrophages; 1 = ficolin-1 macrophages and dendritic cells (DCs); 2 = T cells; 3 = fatty acid binding protein 4 macrophages; 4 = endothelial cells; 5 = fibroblasts; 6 = goblet cells and alveolar type 1 cells; 7 = natural killer cells; 8 = ciliated cells and goblet cells; 9 = alveolar type 2 cells; 10 = mast cells; 11 = low-quality cells; 12 = basal cells; 13 = proliferating cells; 14 = goblet cells; 15 = pericytes and smooth muscle cells; 16 = B cells; 17 = lymphatic endothelial cells; 18 = ciliated cells. Macrophage subpopulations, DCs, and proliferating cells are located along the center of the UMAPs. **B**, Cell clustering identified by UMAP according to individual identity. **C**, Cell clustering identified by UMAP according to health status. SPP1 macrophage cluster 0 is formed primarily of macrophages from the patients with SSc-ILD.

genes implicated in lipid metabolism and myeloid cell activation (Supplementary Figures 5 and 6 and Supplementary Table 2, <https://onlinelibrary.wiley.com/doi/10.1002/art.42286>). Lipid metabolism plays a key role in macrophage activation by fatty acid synthesis, in which fatty acids can be utilized as precursors for inflammatory mediators synthesis, with significant effect on the course of many metabolic diseases (21,22). Up-regulated differentially expressed genes in FABP4 macrophages compared to SPP1 and FCN1 macrophages demonstrated enrichment for negative regulation of macrophage differentiation and regulation of cholesterol storage and myeloid leukocyte activation pathways (23–25) (Supplementary Table 3).

**Lung myeloid cell subpopulations.** We reclustered the myeloid cells from these samples, including macrophages, DCs, and proliferating macrophages, guided by Clustree (Supplementary Figure 7, <https://onlinelibrary.wiley.com/doi/10.1002/art.42286>). This subclustering segregated most cells from the SSc-ILD and healthy samples into different clusters (Figure 2). The largest cluster, SSc-ILD SPP1 macrophages, selectively expressed *MERTK* and *LGMN*, and SSc FABP4

macrophages selectively expressed *INHBA*. Control and SSc-ILD FCN1 macrophages selectively expressed *IL1B* as well as *SIGLEC10* markers (Figure 2). These and other gene markers defined these macrophage subpopulations (Supplementary Figure 4 and Supplementary Table 4).

These findings are mainly consistent with our previous work examining macrophages in IPF (14). *IFI27*, an interferon-regulated gene, and *CCL18*, a strong serum pharmacodynamic biomarker for tocilizumab (4,5), were both more highly expressed in SSc SPP1 and FABP4 macrophages and in the proliferating macrophage clusters, compared to SPP1 and FABP4 macrophages from healthy controls (Figure 2). Although *IFI27* was also expressed by other lung cell populations, *CCL18* was almost exclusively expressed by lung macrophages. The proliferating macrophage cluster included both SPP1 and FABP4 macrophages, as this cluster showed a group of cells expressing *SPP1* (Figure 2C) and other markers of SPP1 cells (*MERTK* and *LGMN*; Figure 2D), as well as another group of cells expressing *FABP4* (Figure 2C) and other markers of FABP4 cells (*INHBA*; Figure 2D). These proliferating macrophages originated almost exclusively from the SSc-ILD patient lungs (Figure 2B), indicating

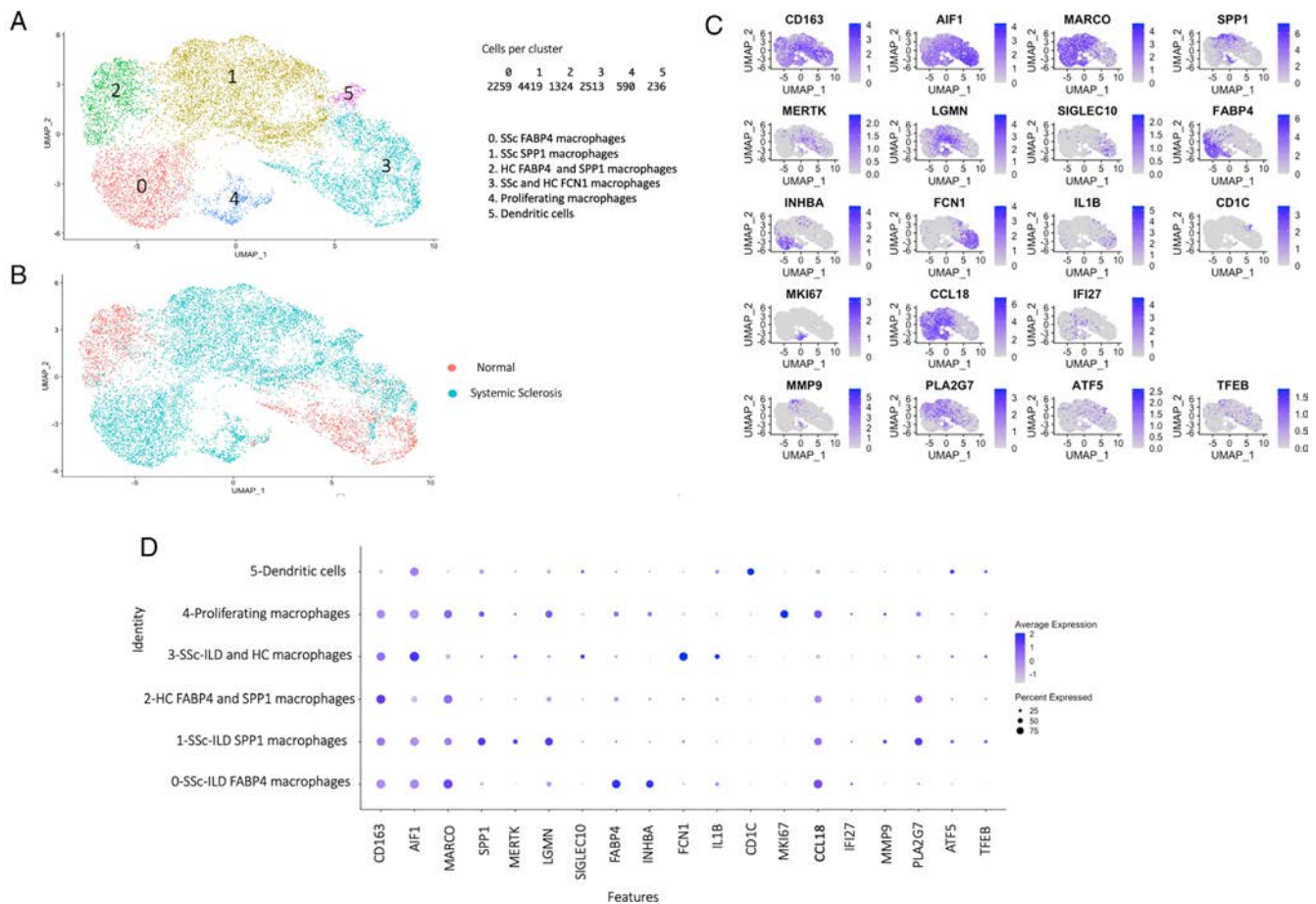


**Figure 2.** Single-cell RNA-sequencing (scRNA-Seq) analysis of macrophage subpopulations, DCs, and proliferating macrophages in 3' v3 chemistry. Analyses were conducted using 5 lung samples ( $n = 1$  healthy control [HC] and 4 SSC-ILD patients). **A**, Cell clustering identified by UMAP according to cell type. **B**, Cell clustering identified by UMAP according to health status. **C**, Feature plot showing gene expression by macrophage subpopulations, DCs, and proliferating macrophages, and by other lung cell subtypes. **D**, Dot plot showing gene expression by macrophages, DCs, and proliferating macrophages. The dot plot shows up-regulation of *SPP1*, *MERTK*, and *LGMN* in SSC-ILD SPP1 macrophages and proliferating macrophages. *MMP9* and *PLA2G7* gene markers were up-regulated in SSC-ILD SPP1 macrophages compared to all other macrophages. FABP4 = fatty acid binding protein 4 (see Figure 1 for other definitions). Color figure can be viewed in the online issue, which is available at <http://onlinelibrary.wiley.com/doi/10.1002/art.42286/abstract>.

that proliferating macrophages potentially differentiate into the profibrotic SPP1 macrophage phenotype. The DCs, which also originated almost entirely from the SSC-ILD lungs, clustered into a discrete cluster expressing *CD1C* (Figure 2C) and other markers of type 2 conventional dendritic cells (not shown) (26).

**Validation of macrophage subsets in SSC-ILD 5' v1 chemistry.** We extended the above results by analyzing scRNA-Seq data from an additional 5 control lung samples and 1 SSC-ILD lung sample, in which single-cell cDNA libraries were prepared using 5' v1 chemistry. Myeloid subpopulations reflected those found in the analogous 3' v3 subclustering (Figure 3 and Supplementary Figures 8–11, <https://onlinelibrary.wiley.com/doi/10.1002/art.42286>). Of note, most of the macrophages in the SPP1 macrophage cluster originated from the SSC-ILD patient, consistent with the 3' v3 chemistry clustering. The proliferating macrophage population was relatively small, as there was only

1 SSC-ILD lung and 5 control lungs, but both *SPP1* and *FABP4* expression were noted (Supplementary Figure 9). The proliferating cell cluster also included some control natural killer cells.

*CCL18* (4,5), *IFI27*, *MMP9*, and *PLA2G7* (27) were up-regulated in the SPP1 macrophages from SSC-ILD lungs compared to SPP1 macrophages from healthy lungs (Supplementary Figure 9, <https://onlinelibrary.wiley.com/doi/10.1002/art.42286>). Notably, *IFI27* gene expression in the serum of SSC patients is associated with digital ulcers (28). *MMP9* is also elevated in the serum of SSC patients and correlates with the modified Rodnan skin score (29). In addition to *SPP1*, *PLA2G7*, which is discussed further below, differentiated SPP1 macrophages compared to FABP4 and FCN1 macrophages (Supplementary Figures 12 and 13).

**Combined batch-corrected data sets.** In order to examine a larger data set including both SSC-ILD and controls,

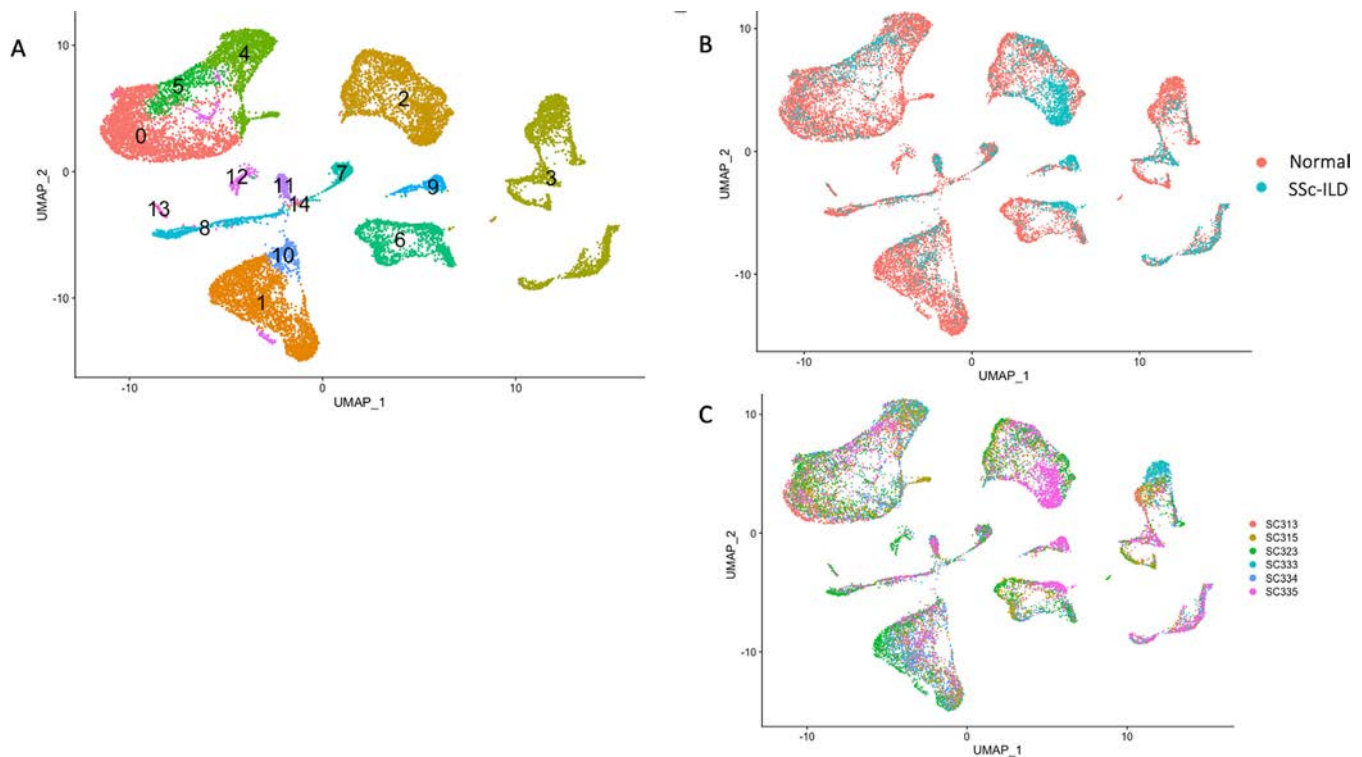


**Figure 3.** Single-cell RNA-sequencing analysis of lung samples in 5' v1 chemistry. Analyses were conducted using 6 lung samples ( $n = 5$  healthy controls and 1 SSc-ILD patient). **A**, Cell clustering identified by UMAP according to cell type. Macrophage subpopulations, DCs, and proliferating cells are located along the upper-left part of the UMAPs. 0 = ficolin-1 macrophages and DCs; 1 = T cells and natural killer cells; 2 = endothelial cells; 3 = epithelial cells; 4 = fatty acid binding protein 4 macrophages; 5 = SPP1 macrophages; 6 = fibroblasts; 7 = lymphatic endothelial cells; 8 = B cells; 9 = pericytes and smooth muscle cells; 10 = mitochondrial related genes; 11 = mast cells; 12 = proliferating cells; 13 = DCs; 14 = hemoglobin-related cells. **B**, Cell clustering identified by UMAP according to health status. SPP1 macrophage cluster 5 is formed primarily of macrophages from the SSc-ILD patient SC335. **C**, Cell clustering identified by UMAP according to individual identity. See Figure 1 for other definitions. Color figure can be viewed in the online issue, which is available at <http://onlinelibrary.wiley.com/doi/10.1002/art.42286/abstract>.

we Harmony batch-corrected and combined our 2 data sets (Supplementary Figures 14–20, <https://onlinelibrary.wiley.com/doi/10.1002/art.42286>). Similar to our previous analyses, we identified the same cell types including myeloid cells after dimensional reduction and visualization by UMAP. Consistent with our previous results, the SPP1 macrophage cluster was formed mainly by macrophages from SSc-ILD patients. We subsequently reclustered the myeloid cells. As above, SPP1 macrophages, also expressing gene markers *MERTK*, *LGMN*, *CCL18*, *MMP9*, *TFEB*, *PLA2G7*, were almost exclusively from SSc-ILD samples. Thus, the results of this combined analysis are consistent with analyses of the uncombined data sets.

**Pathway analysis of upstream regulators of SPP1 macrophages.** To address upstream drivers of macrophage differentiation in SSc-ILD, we analyzed genes differentially up-regulated in SPP1 macrophages using Ingenuity Pathway Analysis. This analysis supported several different mediators as potential upstream drivers of the SSc-ILD phenotype, including lipopolysaccharide and other Toll-like receptor activators, IL-6 and transforming growth factor  $\beta$  (TGF $\beta$ ), all of which have been implicated in previous studies, as well as IL-33 and other

cytokines (Supplementary Table 5, <https://onlinelibrary.wiley.com/doi/10.1002/art.42286>).

**Similar pathologic changes in other SSc organs suggested by skin microarray data.** Our data examining the epigenetics of the profibrotic macrophages in SSc-ILD may also be relevant for skin fibrosis and other target organs in SSc. IL-6 inhibition with tocilizumab in the faSScinat (safety and efficacy of subcutaneous tocilizumab in adults with systemic sclerosis) clinical trial, while just missing a statistically significant  $P$  value in both phase 2 and phase 3 trials, down-regulated genes associated with M2 macrophages (30) and decreased expression of TGF $\beta$ -regulated genes in explant fibroblast cultures (31). In order to better understand whether SPP1 macrophages contribute to fibrosis in other SSc organs, we examined gene expression in SSc skin. *SPP1* and *CCL18* expression was markedly increased in bulk RNA in SSc skin. Previously described skin scRNA-Seq data indicated that the expression of these genes comes primarily from myeloid cells in the skin (Supplementary Figures 21–23, <https://onlinelibrary.wiley.com/doi/10.1002/art.42286>).



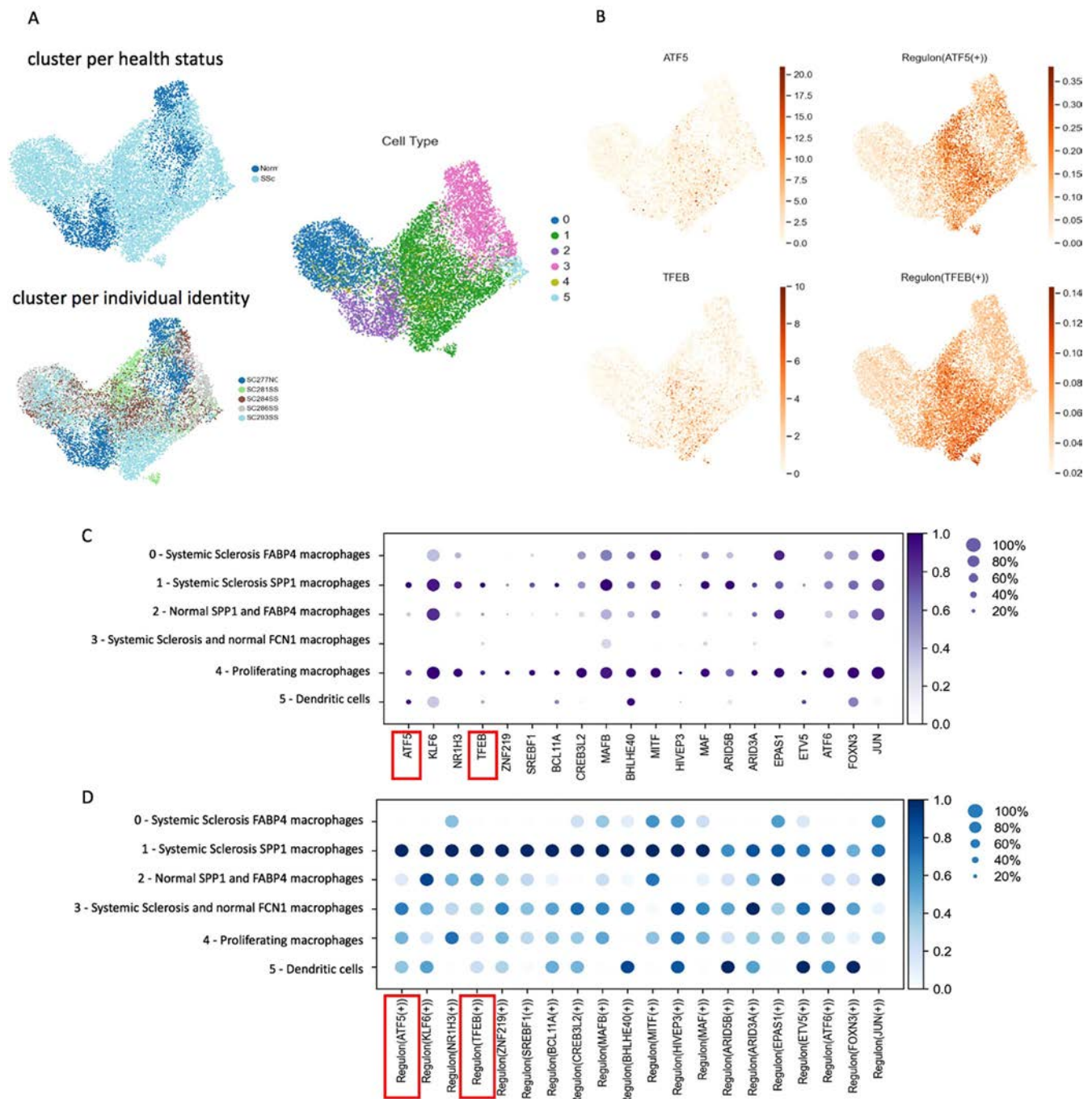


**Figure 4.** Single-cell regulatory network inference and clustering (SCENIC) showing regulons and transcription factors predicted to be important in regulating SPP1 macrophages. Analyses of macrophages, DCs, and proliferating macrophages were conducted using 5 lung samples ( $n = 1$  healthy control and 4 SSc-ILD patients) in 3' v3 chemistry. **A**, Cell clusters according to health status, individual identity, and cell type. 0 = SSc-ILD fatty acid binding protein 4 (FABP4) macrophages; 1 = SSc-ILD SPP1 macrophages; 2 = healthy control SPP1 and FABP4 macrophages; 3 = SSc-ILD and healthy control FCN1 macrophages; 4 = proliferating macrophages; 5 = DCs. **B**, Analyses showing *SPP1* as a target gene for activating transcription factor 5 (ATF5) and transcription factor EB (TFEB) transcription factors and regulons. **C**, Dot plot showing transcription factors, including ATF5 and TFEB (red boxes), predicted to be important in regulating SPP1 macrophages. **D**, Dot plot showing regulons, including ATF5 and TFEB regulons (red boxes), predicted to be important in regulating SPP1 macrophages. KLF6 = Kruppel-like factor 6; NR1H3 = nuclear receptor subfamily 1 group H member 3; ZNF219 = zinc finger protein 219; SREBF1 = sterol regulatory element binding protein factor 1; CREB3L2 = CREB protein 3-like 2; MafB = Maf basic leucine zipper transcription factor B; bHLHE40 = basic helix-loop-helix family member E40; MITF = microphthalmia-associated transcription factor; HIVEP3 = HIVEP zinc finger 3; ARID5B = AT-rich interaction domain 5B; EPAS1 = endothelial PAS domain protein 1; ETV5 = ETS variant transcription factor 5 (see Figure 1 for other definitions). Color figure can be viewed in the online issue, which is available at <http://onlinelibrary.wiley.com/doi/10.1002/art.42286/abstract>.



Motif Name	Fold enrichment	P
SSc-ILD sample SC336		
FOS	3.19010822	6.86E-145
FOSL1::JUNB	3.4413536	1.02E-143
BATF3	2.9786597	2.52E-140
FOSL2::JUN	3.32140474	5.48E-131
JUN(var.2)	3.04331528	1.07E-128
FOSL1::JUND	3.26643938	1.59E-127
FOSL2::JUNB	3.23793531	9.57E-126
MAF::NFE2	2.66199575	5.99E-56
MITF	1.82166811	1.01E-05
TFEB	1.73941338	3.75E-05
ATF6	1.70764316	0.00072468
SREBF1	1.43184691	0.0011076
BHLHE40	1.09720706	0.36788806
KLF6	0.90018323	0.88278759
ETV5	0.71966307	0.99424075
SSc-ILD sample SC294		
NFKB2	3.01107011	0.00589081
RELA	2.74533414	0.00589081
NFKB1	2.70067517	0.00589081
FOSB::JUNB	2.65102267	0.00589081
FOSL2::JUND	2.63504611	0.00589081
JDP2	2.61442107	0.00589081
NFE2	2.52034217	0.00589081
JUN(var.2)	2.42862887	0.00589081
MITF	2.19428571	0.00589081
SREBF1	1.58342582	0.00589081
TFEB	1.81588903	0.00589081
BHLHE40	1.65048544	0.00589081
ETV5	0.62227754	0.00589081

**Figure 5.** Accessible motifs associated with transcription factors in regulating secreted phosphoprotein 1 (SPP1) macrophages, as determined by single-cell accessible chromatin sequencing analysis of systemic sclerosis-associated interstitial lung disease (SSc-ILD) lung samples. The list shows enriched transcription factor-accessible motifs important in the regulation of SPP1 macrophages compared to FABP4 macrophages, as predicted by Signac and single-cell regulatory network inference and clustering software in analyses of SSc-ILD lung samples SC336 and SC294, included the following enriched motifs (indicated by red boxes): MITF, TFEB, ATF6, SREBF1, bHLHE40, KLF6, and ETV5 for sample SC336; and MITF, SREBF1, TFEB, bHLHE40, and ETV5 for sample SC294. Also indicated are activator protein 1 transcription family members including Fos, FOSL1, JunD, JunB, BATF3, FOSL2, Jun, Maf, and nuclear factor erythroid 2 (NFE2). See Figure 4 for other definitions. Color figure can be viewed in the online issue, which is available at <http://onlinelibrary.wiley.com/doi/10.1002/art.42286/abstract>.

### Prediction of transcription factors activating transcription factor 5 (ATF5) and transcription factor EB (TFEB) regulating SPP1 macrophage differentiation.

SCENIC provides a bioinformatics method for reconstructing gene regulatory networks, as well as identifying cell states, providing insights into the transcription factors leading to cellular heterogeneity (19). SCENIC identifies regulons (a transcription factor) and its associated downstream target genes, by examining coregulated gene expression in a single-cell data set and using Rcis-Target to confirm transcription factor binding sites in downstream target genes. We used SCENIC to predict regulons and transcription factors regulating SPP1 macrophage differentiation, comparing the transcriptomes of SSc-ILD SPP1 macrophages to all FABP4 macrophages, all FCN1 macrophages, and proliferating macrophages. These cells were then clustered by their regulon activity score and labeled according to cell population, patient individual identity, and health status (Figure 4A).

Notably, SPP1 macrophages formed the biggest cluster, composed almost entirely of cells from SSc-ILD lungs and including cells from each SSc-ILD sample. SPP1 macrophages were further examined by SCENIC for regulons predicted to selectively regulate the SSc SPP1 macrophage transcriptome (Figures 4B–D). Multiple regulons (Figure 4D) and their associated transcription factors (Figure 4C) were selectively up-regulated in SPP1 macrophages compared to the other macrophage populations.

Most of these regulons were also up-regulated in the proliferating macrophage population, of which most of the cells expressed *SPP1* and were thus likely contributing to the SSc SPP1 macrophage population. The regulons for ATF5 and TFEB both have *SPP1* and *MMP9* as target genes (Supplementary Figures 24 and 25, <https://onlinelibrary.wiley.com/doi/10.1002/art.42286>). *SPP1* and *MMP9* are not only gene markers of the SPP1 macrophage population but also have profibrotic

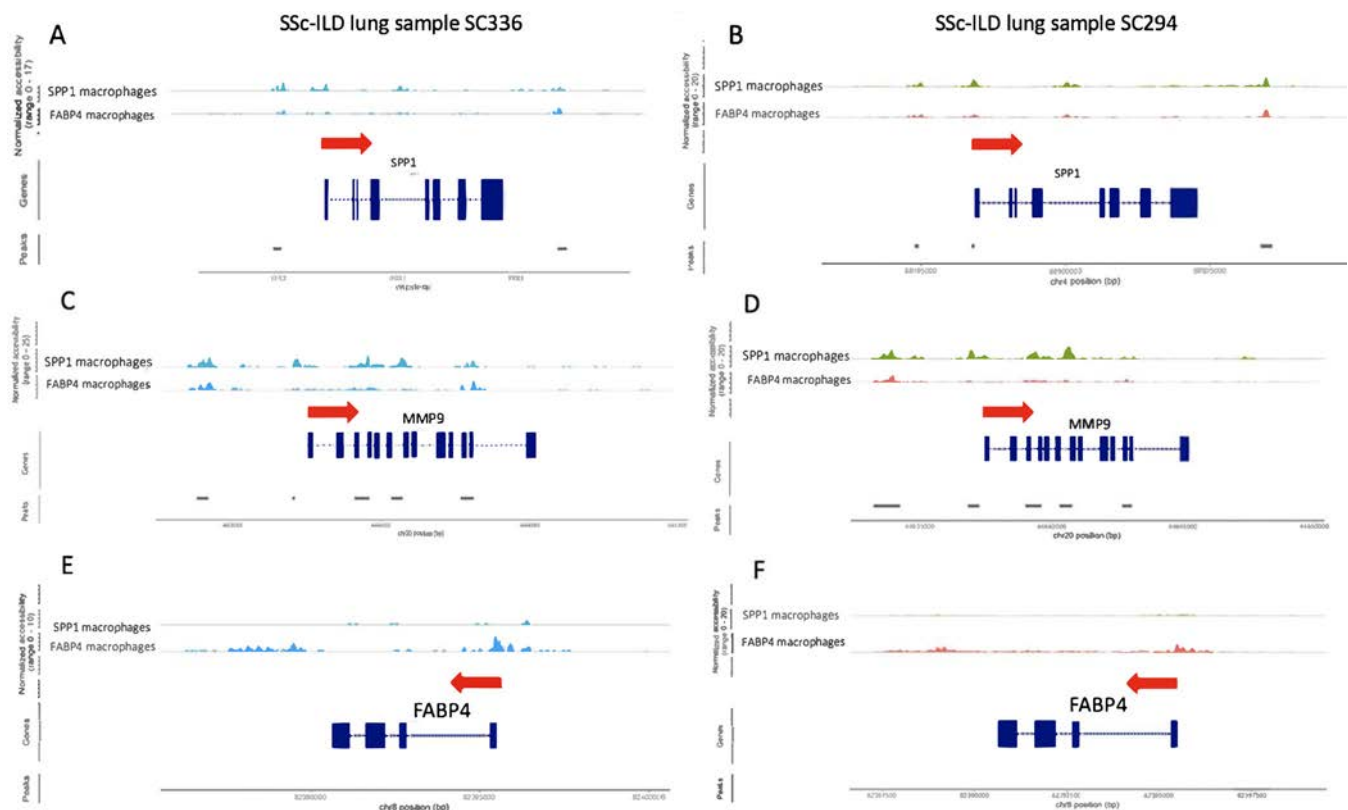


**Figure 6.** Chromatin pattern changes for SPP1 macrophages compared to fatty acid binding protein 4 (FABP4) macrophages. Analyses were conducted with single-cell assay for transposase accessible chromatin sequencing of 2 SSc-ILD lung samples, using Signac. Red **arrows** indicate the direction of transcription. Exons are shown in blocks, and introns flank exons. **A** and **B**, *SPP1* showed more accessible chromatin for the SSc-ILD SPP1 macrophages compared to FABP4 macrophages in the region proximal to the transcriptional start site for SSc-ILD lungs, as well as regions further 5' of the promoter and in intron 4. **C** and **D**, *MMP9* also showed more accessible chromatin in SPP1 macrophages, but in this case increased accessibility was not seen around the promoter but rather in regions around exon 6, exons 9–12, and introns. **E** and **F**, *FABP4* showed strikingly more accessible chromatin in a region proximal to the transcriptional start site and in a broad second region 3' from the gene in FABP4 macrophages compared to SPP1 macrophages. See Figure 1 for other definitions. Color figure can be viewed in the online issue, which is available at <http://onlinelibrary.wiley.com/doi/10.1002/art.42286/abstract>.

activity (12,14,29). *SPP1* gene expression is up-regulated in SSc-ILD and IPF lungs compared to control lungs based on previous findings (12,14). *SPP1* is included in the differentiating genes between SSc-ILD and IPF lungs, in contrast to control lungs (12). Increased serum matrix metalloproteinase 9 (MMP9) correlates with the degree of skin fibrosis in SSc patients through fibroblast activation and acceleration of fibrosis under the effect of proinflammatory cytokines such as TGF $\beta$  and IL-1 $\beta$  (29). Thus, SCENIC particularly implicates TFEB and ATF5 as key transcription factors regulating SPP1 macrophage cell differentiation, likely promoting the profibrotic activity of these cells.

**Altered chromatin structure implicates transcription factors regulating profibrotic SSc-ILD SPP1 macrophage differentiation.** In order to better understand the transcription factors regulating differentiation of SSc-ILD SPP1 macrophages and using an orthogonal technology to SCENIC predictions, we analyzed lung samples with scATAC-Seq in parallel with scRNA-Seq (Supplementary Table 1).

scATAC-Seq examines the chromatin structure of nuclei from each cell by cleaving open chromatin with a Tn5 transposase and then partitioning cells and ligating cell-specific barcodes to the DNA fragments. The resulting fragments indicate open chromatin structure on a cell-by-cell basis. We analyzed scATAC-Seq data by clustering nuclei for both SSc-ILD samples using 2 bioinformatics approaches: Loupe software (10X Genomics) and Signac (18) (Supplementary Figures 26–28, <https://onlinelibrary.wiley.com/doi/10.1002/art.42286>).

For Loupe, the cell types in each cluster were identified by examining the accessibility of promoters of gene markers for each cell type. Macrophages were identified as having open chromatin for the promoters of *CD163*, *AIF1*, and *MARCO*, and FABP4 and SPP1 macrophage populations were identified by open chromatin in the respective 5' promoters (Supplementary Figure 27). In a complementary analysis, we identified nuclei clusters by integrating with the paired scRNA-Seq data to predict cell types (Signac) (18). Signac software maps the cells by examining open chromatin in promoters of differentially expressed genes defined

by scRNA-Seq cell clusters (Supplementary Figures 27 and 28). We used both Loupe and Signac to determine enriched, accessible motifs for transcription factors, reflecting open chromatin across the genome, and comparing SPP1 macrophages to FABP4 macrophages for each SSc-ILD sample (Supplementary Figures 25 and 29 and Supplementary Table 1). Both of these programs use the Jasp database to identify transcription factor binding motifs (32).

Strikingly, many of the transcription factors binding motifs enriched in open chromatin of SPP1 macrophages were the same transcription factor-associated regulons predicted by SCENIC to regulate the differentiation of profibrotic SPP1 macrophages: TFEB, ATF6, microphthalmia-associated transcription factor (MITF), basic helix-loop-helix family member E40 (bHLHE40), Kruppel-like factor 6, ETS variant transcription factor 5 (ETV5), nuclear receptor subfamily 1 group H member 3, CREB protein 3-like 2, Maf basic leucine zipper transcription factor B (MafB), and AT-rich-interactive domain 3A (Figure 5 and Figure 4C). In addition, multiple members of the activator protein 1 (AP-1) transcription factor family, binding as homo- and heterodimers, were identified across both software outputs. AP-1 proteins include the Jun, Fos, ATF, and musculoaponeurotic fibrosarcoma (Maf) protein families (33). Specifically, the Jun family proteins c-Jun, JunB, JunD, Fos family proteins c-Fos (FOS), FosB, Fra-1 (FOSL1), Fra-2 (FOSL2), and Maf family proteins c-Maf (MAF), MafA, MafB, MafF, MafG, and MafK were enriched. Of these, the Maf regulon was also predicted by SCENIC to regulate SPP1 macrophage differentiation (Figure 4D).

As examples of the epigenetic modifications associated with differentiation into SPP1 macrophages, we examined accessible chromatin of the following gene markers: *SPP1*, *MMP9*, and *FABP4*, comparing SPP1 macrophages and FABP4 macrophages in SSc-ILD (Figure 6 and Supplementary Figures 30–32, <https://onlinelibrary.wiley.com/doi/10.1002/art.42286>). *SPP1* showed more accessible chromatin for the SSc-ILD SPP1 macrophages compared to FABP4 macrophages in the promoter region immediately proximal to the transcriptional start site, as well as regions further upstream of the promoter and the fourth intronic region. *MMP9* also showed more accessible chromatin in SPP1 macrophages, but in this case, increased accessibility was not seen at the promoter but rather in regions around exon 6, exons 9–12, and introns (Figure 6). In contrast, *FABP4* showed strikingly more accessible chromatin in a region proximal to the transcriptional start site and in a broad second region 3' from the gene in FABP4 macrophages compared to SPP1 macrophages.

Although we also examined scATAC-Seq data from several control lungs, technical variability, and the inability to clearly distinguish, in the scATAC-Seq assay, between macrophage populations precluded direct comparison of SSc-ILD and control macrophages (Supplementary Figures 33–37).

**Increased SPP1/MERTK macrophages and TFEB expression in SSc-ILD.** Finally, in order to show increased

SPP1 macrophage expression in SSc-ILD, we identified these cells by staining the coexpressed surface marker MERTK (Supplementary Figure 38, <https://onlinelibrary.wiley.com/doi/10.1002/art.42286>). In addition, we found that a subpopulation of these cells strongly coexpressed TFEB (Supplementary Figures 39 and 40). Available antibodies did not allow us to detect ATF5.

## DISCUSSION

The mechanisms driving fibrosis in SSc-ILD are currently uncertain; however, the association of macrophage gene expression, particularly of *SPP1*, with progressive fibrosis makes these cells likely mediators of profibrotic signals to fibroblasts (8). This study confirms the highly increased numbers of a subpopulation of macrophages, characterized by up-regulated expression of *SPP1* and *MMP9*, as well as a broader transcriptome in SSc-ILD, which is consistent with previous studies both from our group and others (9–16). Analysis of the differentially expressed genes between SPP1 macrophages compared to all other macrophage subpopulations linked SPP1 macrophages to lipid metabolism pathways. Lipid metabolism plays an important role in macrophage function (21). Several transcription factors, including peroxisome proliferator-activated family of receptors and CCAAT enhancer binding proteins (sterol regulatory element binding proteins [SREBPs]), have been implicated in lipid metabolism in macrophages (21). Further investigation of the effect of lipid metabolism on the development of macrophage phenotype would be important, in view of drugs targeting metabolic pathways (21–25).

*SPP1* and *MMP9* were selectively up-regulated by SSc SPP1 macrophages. Osteopontin, the product of *SPP1*, is increased in the serum of patients with SSc (34,35) and has been implicated in IPF (36), as well as in renal and bone marrow fibrosis (37,38), suggesting that SPP1 macrophages may have a more general role in promoting fibrosis. *MMP9* expression is also elevated in IPF (39). Additionally, *MMP9* activity is increased in bronchoalveolar lavage fluid of rapidly progressive IPF and in SSc-ILD (40). *MMP9* expression in SSc-ILD lungs uniquely by SPP1 macrophages and proliferating SPP1 macrophages suggests that increased levels in serum and bronchoalveolar lavage (BAL) in SSc-ILD patients may reflect the activity and/or degree of lung infiltration by these cells, and thus might serve as a biomarker for their activity (35).

We used 2 approaches to define likely transcription factors controlling the differentiation of SPP1 macrophages: SCENIC analysis of the SPP1 macrophage transcriptome and scATAC-Seq analysis of open chromatin in SPP1 macrophages. SCENIC analyzes gene regulatory networks (i.e., it looks at genes coregulated with transcription factors of each cell). Several approaches exist for identifying target genes directly regulated by transcription factors (41), including the following: 1) direct transcription factor–DNA binding assays; 2) computational predictions of transcription

factor–target interactions (i.e., position weight matrices); and 3) gene regulatory networks that assume transcription factor expression levels regulate targeted genes. SCENIC uses the third approach in its initial screening, with the resulting gene regulatory network then filtered with CisTarget, a database incorporating results used in methods 1 and 2 (42). The concordance between the predictions from SCENIC and our scATAC-Seq data are mutually reinforcing but, in particular, strongly reinforce the value of SCENIC in analyzing scRNA-Seq transcriptomes.

Our scATAC-Seq data show characteristic chromatin pattern changes for SPP1 macrophages with increased accessibility of SPP1 and MMP9 and decreased accessibility of FABP4, reflecting the altered binding of transcription factors and enhancers comparing SPP1 macrophages to FABP4 macrophages. These observations provided confidence in our scATAC-Seq data. However, altered open chromatin peaks are too broad to implicate specific transcription factors on the basis of individual genes; therefore, Signac bioinformatics, examining transcription factor binding sites in open chromatin across the genome, provided a more robust method for detecting the likely role of specific transcription factors regulating the phenotype of SPP1 macrophages. This identified numerous transcription factors, including ATF5, TFEB, BCL11A, ETV5, Jun, and others, requiring further experimental validation for their specific roles in regulating SPP1 macrophage differentiation.

Several of the transcription factors identified to participate in SPP1 macrophage differentiation have been implicated in profibrotic phenotypes in other settings. TFEB potentially plays a role in silicosis, an occupational irreversible fibrotic lung disease, through disruption of lysosomal autophagy in alveolar macrophages (43). In particular, pulmonary fibrosis in silicosis is promoted with phagocytosis of crystalline silica particles by alveolar macrophages, resulting in apoptosis and inflammation. There is increasing evidence of TFEB interplay with TGF $\beta$  (44). TGF $\beta$  inhibition associated with blockade of BRAF (B-Raf proto-oncogene, serine/threonine kinase) inhibition and TFEB phosphorylation contributes to malignant cells responsiveness to chemotherapy in melanoma (45). Thus, the effect of TFEB on profibrotic SPP1 macrophage differentiation requires further study. ATF6 and its role in macrophage endoplasmic reticulum stress has also been implicated in the pathophysiology of lung fibrosis (46). Similarly, SREB factor 1 was implicated in progression of murine pulmonary fibrosis (47), and bHLHE40 has been identified as an important homeostatic regulator of macrophages in lungs through pulmonary surfactant turnover (48).

Members of the AP-1 transcription factor family, predicted in our analysis to play an important role in the profibrotic phenotype of SPP1 macrophages, have been investigated in the pathophysiology of many fibrotic diseases. As the binding sites for these family members are similar, our data do not clearly discriminate which family member is most important in SPP1 macrophage differentiation. Overexpression of Jun, a prototype AP-1 family

member, is associated with severe multiorgan fibrosis in murine models (49). Fos-related antigen-2 transcription factor (Fra-2 or FOSL2) overexpression has been associated with murine SSc-like lung fibrosis (50). Myofibroblasts are activated in vitro by macrophages in a Fra-2–dependent manner, consequently promoting fibrosis. In addition, both myeloid cell inactivation of Fra-2 and Fra-2/AP-1 inhibitors attenuate pulmonary fibrosis in murine bleomycin models (50). Thus, our data strongly support the findings of these murine studies, indicating a critical role for AP-1 transcription factors in the development of profibrotic SPP1 macrophages in human SSc-ILD. Defining the specific AP-1 family member(s) that are most important in regulating SSc-ILD SPP1 macrophage will be key for the potential targeting of Fra-2 or other AP-1 family members in SSc-ILD.

Proliferating cells in our data set were largely composed of proliferating SPP1 and FABP4 macrophages from SSc-ILD lungs, consistent with our previous work showing proliferating macrophages in IPF (14). While the stimulus for proliferation of these cells is uncertain, regeneration of tissue-resident macrophages through macrophage colony-stimulating factor and granulocyte–macrophage colony-stimulating factor is known to occur in repopulation of inflamed tissues following resolution of inflammation (51). IPF scRNA-Seq data also indicate increased *CSF1* expression in lung mast cells and up-regulation of *LGMN* and other genes regulated by IL-4 (14,52). *CSF1* is up-regulated by SSc-ILD SPP1 macrophages and mast cells, as well as by control pericytes, smooth muscle cells, and fibroblasts. These findings support proliferating macrophages as the primary source for profibrotic SPP1, suggesting that antiproliferative agents or drugs blocking macrophage cytokines might have efficacy in treating SSc-ILD.

There is increasing evidence linking chemokine CCL18 with pulmonary inflammation, supporting its potential future use as early marker of SSc-ILD (9,30,35,53). Our data reflected up-regulation of *CCL18* in SPP1 macrophages from the SSc-ILD lungs compared to healthy controls. Elevated CCL18 in the serum and supernatants of cultured BAL from SSc patients is associated with more advanced ILD based on pulmonary function testing (53). CCL18 concentration in the serum of SSc patients was strikingly decreased following treatment with tocilizumab, and *CCL18* expression in skin biopsies of SSc patients was down-regulated following tocilizumab treatment, along with other macrophage markers (30). In light of the recent US Food and Drug Administration approval of tocilizumab for decreasing progression of SSc-ILD, *CCL18* has emerged as a marker of IL-6 in SSc-ILD. By extension, the up-regulation of *CCL18* in SSc-ILD SPP1 macrophages compared to controls observed in our results supports the role of SPP1 macrophages as drivers of fibrosis in SSc-ILD. Possibly, *CCL18* and *SPP1* expression characterizes macrophages with common functional background and profibrotic potential (35).

The limitations of this study include the preclusion of direct comparison of SSc-ILD and control macrophages to

scATAC-Seq due to technical variability and bioinformatics challenges to clearly distinguish macrophage subpopulations after scATAC-Seq in normal lungs. Additionally, since the lung explants were obtained at the time of lung transplant, indicating advanced stage of SSc-ILD, they may reflect later stages of SSc-ILD. It is possible that earlier stages of SSc-ILD might have different mechanisms driving disease. Furthermore, we note that the sample size is small, scRNA-Seq analysis groups 3' and 5' are skewed respectively toward SSc-ILD lungs (compared to those of controls), and single-cell analyses, including data integration, are parameterizable.

In summary, our transcriptomal analysis demonstrates the transcriptome of profibrotic SPP1 macrophages in SSc-ILD and reveals critical transcription factors in the profibrotic phenotype through changes in chromatin accessibility. These findings support further investigation of key transcription factors, particularly of ATF5 and TFEB, which activate SPP1 macrophage signature genes.

## ACKNOWLEDGMENTS

The authors would like to acknowledge the University of Pittsburgh Medical Center Lung Transplantation team for procurement of lungs, the Center for Organ Research and Education (CORE), and the organ donors and their families for the generous lung tissue donation used in the study.

## AUTHOR CONTRIBUTIONS

All authors were involved in drafting the article or revising it critically for important intellectual content, and all authors approved the final version to be published. Dr. Papazoglou had full access to all of the data in the study and takes responsibility for the integrity of the data and the accuracy of the data analysis.

**Study conception and design.** Papazoglou, Huang, Bulik, A. Lafyatis, Tabib, Morse, Sembrat, Rojas, Valenzi, R. Lafyatis.

**Acquisition of data.** Papazoglou, Huang, Bulik, A. Lafyatis, Tabib, Morse, Sembrat, Rojas, Valenzi, R. Lafyatis.

**Analysis and interpretation of data.** Papazoglou, Huang, Bulik, A. Lafyatis, Tabib, Morse, Sembrat, Rojas, Valenzi, R. Lafyatis.

## REFERENCES

1. Abraham DJ, Varga J. Scleroderma: from cell and molecular mechanisms to disease models. *Trends Immunol* 2005;26:587–95.
2. Steele R, Hudson M, Lo E, et al, on behalf of the Canadian Scleroderma Research Group. Clinical decision rule to predict the presence of interstitial lung disease in systemic sclerosis. *Arthritis Care Res (Hoboken)* 2012;64:519–24.
3. Distler O, Highland KB, Gahlemann M, et al. Nintedanib for systemic sclerosis-associated interstitial lung disease. *N Engl J Med* 2019;380:2518–28.
4. Khanna D, Lin CJ, Furst DE, et al. Tocilizumab in systemic sclerosis: a randomised, double-blind, placebo-controlled, phase 3 trial. *Lancet Respir Med* 2020;8:963–74.
5. Khanna D, Denton CP, Lin CJ, et al. Safety and efficacy of subcutaneous tocilizumab in systemic sclerosis: results from the open-label period of a phase II randomised controlled trial (faSScinate). *Ann Rheum Dis* 2018;77:212–20.
6. Sullivan KM, Goldmuntz EA, Keyes-Elstein L, et al. Myeloablative autologous stem-cell transplantation for severe scleroderma. *N Engl J Med* 2018;378:35–47.
7. Steen VD, Medsger TA. Changes in causes of death in systemic sclerosis, 1972–2002. *Ann Rheum Dis* 2007;66:940–4.
8. Christmann RB, Sampaio-Barros P, Stifano G, et al. Association of interferon- and transforming growth factor  $\beta$ -regulated genes and macrophage activation with systemic sclerosis-related progressive lung fibrosis. *Arthritis Rheumatol* 2014;66:714–25.
9. Schutyser E, Richmond A, Van Damme J. Involvement of CC chemokine ligand 18 (CCL18) in normal and pathological processes. *J Leukoc Biol* 2005;78:14–26.
10. Atamas SP, Luzina IG, Choi J, et al. Pulmonary and activation-regulated chemokine stimulates collagen production in lung fibroblasts. *Am J Respir Cell Mol Biol* 2003;29:743–9.
11. Prasse A, Pechkovsky DV, Toews GB, et al. A vicious circle of alveolar macrophages and fibroblasts perpetuates pulmonary fibrosis via CCL18. *Am J Respir Crit Care Med* 2006;173:781–92.
12. Hsu E, Shi H, Jordan RM, et al. Lung tissues in patients with systemic sclerosis have gene expression patterns unique to pulmonary fibrosis and pulmonary hypertension. *Arthritis Rheum* 2011;63:783–94.
13. Valenzi E, Bulik M, Tabib T, et al. Single-cell analysis reveals fibroblast heterogeneity and myofibroblasts in systemic sclerosis-associated interstitial lung disease. *Ann Rheum Dis* 2019;78:1379–87.
14. Morse C, Tabib T, Sembrat J, et al. Proliferating SPP1/MERTK-expressing macrophages in idiopathic pulmonary fibrosis. *Eur Respir J* 2019;54.
15. Gibbons MA, MacKinnon AC, Ramachandran P, et al. Ly6Chi monocytes direct alternatively activated profibrotic macrophage regulation of lung fibrosis. *Am J Respir Crit Care Med* 2011;184:569–81.
16. Voss TC, Hager GL. Dynamic regulation of transcriptional states by chromatin and transcription factors [review]. *Nat Rev Genet* 2014;15:69–81.
17. Butler A, Hoffman P, Smibert P, et al. Integrating single-cell transcriptomic data across different conditions, technologies, and species. *Nat Biotechnol* 2018;36:411–20.
18. Stuart T, Srivastava A, Madad S, et al. Single-cell chromatin state analysis with Signac. *Nat Methods* 2021;18:1333–41.
19. Aibar S, Gonzalez-Blas CB, Moerman T, et al. SCENIC: single-cell regulatory network inference and clustering. *Nat Methods* 2017;14:1083–6.
20. Becht E, McInnes L, Healy J, et al. Dimensionality reduction for visualizing single-cell data using UMAP. *Nat Biotechnol* 2018. E-pub ahead of print.
21. Remmerie A, Scott CL. Macrophages and lipid metabolism. *Cell Immunol* 2018;330:27–42.
22. Batista-Gonzalez A, Vidal R, Criollo A, et al. New insights on the role of lipid metabolism in the metabolic reprogramming of macrophages. *Front Immunol* 2019;10:2993.
23. Hume DA, Summers KM, Rehli M. Transcriptional regulation and macrophage differentiation [review]. *Microbiol Spectr* 2016;4.
24. Consortium F, Suzuki H, Forrest AR, et al. The transcriptional network that controls growth arrest and differentiation in a human myeloid leukemia cell line. *Nat Genet* 2009;41:553–62.
25. Cuchel M, Rader DJ. Macrophage reverse cholesterol transport: key to the regression of atherosclerosis? *Circulation* 2006;113:2548–55.
26. Collin M, Bigley V. Human dendritic cell subsets: an update. *Immunology* 2018;154:3–20.
27. Bauer Y, Tedrow J, de Bernard S, et al. A novel genomic signature with translational significance for human idiopathic pulmonary fibrosis. *Am J Respir Cell Mol Biol* 2015;52:217–31.



28. Bos CL, van Baarsen LG, Timmer TC, et al. Molecular subtypes of systemic sclerosis in association with anti-centromere antibodies and digital ulcers. *Genes Immun* 2009;10:210–8.
29. Kim WU, Min SY, Cho ML, et al. Elevated matrix metalloproteinase-9 in patients with systemic sclerosis. *Arthritis Res Ther* 2005;7:R71–9.
30. Khanna D, Denton CP, Jhreis A, et al. Safety and efficacy of subcutaneous tocilizumab in adults with systemic sclerosis (faSScinate): a phase 2, randomised, controlled trial. *Lancet* 2016;387:2630–40.
31. Denton CP, Ong VH, Xu S, et al. Therapeutic interleukin-6 blockade reverses transforming growth factor- $\beta$  pathway activation in dermal fibroblasts: insights from the faSScinate clinical trial in systemic sclerosis. *Ann Rheum Dis* 2018;77:1362–71.
32. Fomes O, Castro-Mondragon JA, Khan A, et al. JASPAR 2020: update of the open-access database of transcription factor binding profiles. *Nucleic Acids Res* 2020;48:D87–92.
33. Gazon H, Barbeau B, Mesnard JM, et al. Hijacking of the AP-1 signaling pathway during development of ATL. *Front Microbiol* 2017;8:2686.
34. Wu M, Schneider DJ, Mayes MD, et al. Osteopontin in systemic sclerosis and its role in dermal fibrosis. *J Invest Dermatol* 2012;132:1605–14.
35. Gao X, Jia G, Guttman A, et al. Osteopontin links myeloid activation and disease progression in systemic sclerosis. *Cell Rep Med* 2020;1:100140.
36. Pardo A, Gibson K, Cisneros J, et al. Up-regulation and profibrotic role of osteopontin in human idiopathic pulmonary fibrosis. *PLoS Med* 2005;2:e251.
37. Merszei J, Wu J, Torres L, et al. Osteopontin overproduction is associated with progression of glomerular fibrosis in a rat model of anti-glomerular basement membrane glomerulonephritis. *Am J Nephrol* 2010;32:262–71.
38. Ruberti S, Bianchi E, Guglielmelli P, et al. Involvement of MAF/SPP1 axis in the development of bone marrow fibrosis in PMF patients. *Leukemia* 2018;32:438–49.
39. Dancer RC, Wood AM, Thickett DR. Metalloproteinases in idiopathic pulmonary fibrosis. *Eur Respir J* 2011;38:1461–7.
40. Andersen GN, Nilsson K, Pourazar J, et al. Bronchoalveolar matrix metalloproteinase 9 relates to restrictive lung function impairment in systemic sclerosis. *Respir Med* 2007;101:2199–206.
41. Garcia-Alonso L, Holland CH, Ibrahim MM, et al. Benchmark and integration of resources for the estimation of human transcription factor activities. *Genome Res* 2019;29:1363–75.
42. Herrmann C, Van de Sande B, Potier D, et al. i-cisTarget: an integrative genomics method for the prediction of regulatory features and cis-regulatory modules. *Nucleic Acids Res* 2012;40:e114.
43. He X, Chen S, Li C, et al. Trehalose alleviates crystalline silica-induced pulmonary fibrosis via activation of the TFEB-mediated autophagy-lysosomal system in alveolar macrophages. *Cells* 2020;9.
44. Lafyatis R. Transforming growth factor  $\beta$ —at the centre of systemic sclerosis [review]. *Nat Rev Rheumatol* 2014;10:706–19.
45. Li S, Song Y, Quach C, et al. Transcriptional regulation of autophagy-lysosomal function in BRAF-driven melanoma progression and chemoresistance. *Nat Commun* 2019;10:1693.
46. Burman A, Tanjore H, Blackwell TS. Endoplasmic reticulum stress in pulmonary fibrosis. *Matrix Biol* 2018;68–69:355–65.
47. Shichino S, Ueha S, Hashimoto S, et al. Transcriptome network analysis identifies protective role of the LXR/SREBP-1c axis in murine pulmonary fibrosis. *JCI Insight* 2019;4.
48. Rauschmeier R, Gustafsson C, Reinhardt A, et al. Bhlhe40 and Bhlhe41 transcription factors regulate alveolar macrophage self-renewal and identity. *EMBO J* 2019;38:e101233.
49. Wernig G, Chen SY, Cui L, et al. Unifying mechanism for different fibrotic diseases. *Proc Natl Acad Sci U S A* 2017;114:4757–62.
50. Ucer AC, Bakiri L, Roediger B, et al. Fra-2-expressing macrophages promote lung fibrosis in mice. *J Clin Invest* 2019;129:3293–309.
51. Davies LC, Jenkins SJ, Allen JE, et al. Tissue-resident macrophages. *Nat Immunol* 2013;14:986–95.
52. Birnhuber A, Biasin V, Schnoegl D, et al. Transcription factor Fra-2 and its emerging role in matrix deposition, proliferation and inflammation in chronic lung diseases. *Cell Signal* 2019;64:109408.
53. Prasse A, Pechkovsky DV, Toews GB, et al. CCL18 as an indicator of pulmonary fibrotic activity in idiopathic interstitial pneumonias and systemic sclerosis. *Arthritis Rheum* 2007;56:1685–93.

# Superiority of Low-Dose Benzbromarone to Low-Dose Febuxostat in a Prospective, Randomized Comparative Effectiveness Trial in Gout Patients With Renal Uric Acid Underexcretion

Fei Yan,<sup>1</sup> Xiaomei Xue,<sup>1</sup> Jie Lu,<sup>1</sup> Nicola Dalbeth,<sup>2</sup> Han Qi,<sup>1</sup> Qing Yu,<sup>3</sup> Can Wang,<sup>4</sup> Mingshu Sun,<sup>5</sup> Lingling Cui,<sup>4</sup> Zhen Liu,<sup>4</sup> Yuwei He,<sup>4</sup> Xuan Yuan,<sup>6</sup> Ying Chen,<sup>4</sup> Xiaoyu Cheng,<sup>4</sup> Lidan Ma,<sup>1</sup> Hailong Li,<sup>6</sup> Aichang Ji,<sup>6</sup> Shuhui Hu,<sup>1</sup> Zijiang Ran,<sup>1</sup> Robert Terkeltaub,<sup>7</sup> and Changgui Li<sup>1</sup>

**Objective.** The predominant mechanism driving hyperuricemia in gout is renal uric acid underexcretion; however, the standard urate-lowering therapy (ULT) recommendation is first-line xanthine oxidase inhibitor (XOI), irrespective of the cause of hyperuricemia. This comparative effectiveness clinical trial was undertaken to compare first-line nontitrated low-dose benzbromarone (LDBen) uricosuric therapy to XOI ULT with low-dose febuxostat (LDFeb) in gout patients with renal uric acid underexcretion.

**Methods.** We conducted a prospective, randomized, single-center, open-label trial in men with gout and renal uric acid underexcretion (defined as fractional excretion of urate <5.5% and uric acid excretion ≤600 mg/day/1.73 m<sup>2</sup>). A total of 196 participants were randomly assigned to receive LDBen 25 mg daily or LDFeb 20 mg daily for 12 weeks. All participants received daily urine alkalization with oral sodium bicarbonate. The primary end point was the rate of achieving the serum urate target of <6 mg/dl.

**Results.** More participants in the LDBen group achieved the serum urate target than those in the LDFeb group (61% compared to 32%,  $P < 0.001$ ). Rates of adverse events, including gout flares and urolithiasis, did not differ between groups, with the exception of greater transaminase elevation in the LDFeb group (4% for LDBen compared to 15% for LDFeb,  $P = 0.008$ ).

**Conclusion.** Compared to LDFeb, LDBen has superior urate-lowering efficacy and similar safety in treating relatively young and healthy patients with renal uric acid underexcretion-type gout.

## INTRODUCTION

In gout, increased serum urate, called hyperuricemia, promotes crystal deposition of monosodium urate monohydrate

crystals in articular and periarticular structures, which can trigger acute episodes of very painful inflammatory arthritis (gout flare) (1,2). Longstanding hyperuricemia and gout can also lead to palpable tophi, joint damage, and urolithiasis (1). Urate-lowering

Supported by the National Key Research and Development Program (award 2022YFE0107600), Shandong Provincial Key Research and Development Plan Major Scientific and Technological Innovation Project (award 2021CXGC011103), the National Natural Science Foundation of China (awards 31900413, 81770869, and 81900636), and Shandong Provincial Science Foundation for Outstanding Youth Scholars (award ZR2021YQ56). Dr. Terkeltaub's work was supported by the NIH (grants AR-060772 and AR-075990) and the VA Research Service.

Drs. Yan, Xue, and Lu contributed equally to this work.

<sup>1</sup>Fei Yan, MD, Xiaomei Xue, MD, Jie Lu, MD, Han Qi, MS, Shuhui Hu, MS, Zijiang Ran, MS, Changgui Li, MD: Shandong Provincial Key Laboratory of Metabolic Diseases and Qingdao Key Laboratory of Gout and Department of Endocrinology and Metabolism, the Affiliated Hospital of Qingdao University, Shandong Provincial Clinical Research Center for Immune Diseases and Gout, Qingdao, Institute of Metabolic Diseases, Qingdao University, and China Shandong Provincial Clinical Research Center for Immune Diseases and Gout, Qingdao, China; <sup>2</sup>Nicola Dalbeth, MD: Department of Medicine, University of Auckland, Auckland, New Zealand; <sup>3</sup>Qing Yu, MS: Department of Endocrinology

and Metabolism, the Affiliated Hospital of Qingdao University, Qingdao, China; <sup>4</sup>Can Wang, MD, Lingling Cui, PhD, Zhen Liu, PhD, Yuwei He, PhD, Ying Chen, MD, Xiaoyu Cheng, MD: Shandong Provincial Key Laboratory of Metabolic Diseases and Qingdao Key Laboratory of Gout and the Department of Endocrinology and Metabolism, the Affiliated Hospital of Qingdao University, and Shandong Provincial Clinical Research Center for Immune Diseases and Gout, Qingdao, China; <sup>5</sup>Mingshu Sun, MD: Department of Rheumatology and Immunology, the Affiliated Hospital of Qingdao University, Qingdao, China; <sup>6</sup>Xuan Yuan, MD, Hailong Li, PhD, Aichang Ji, PhD: Institute of Metabolic Diseases, Qingdao University, Qingdao, China; <sup>7</sup>Robert Terkeltaub, PhD: VA San Diego VA Healthcare Center, University of California San Diego.

Author disclosures are available at <https://onlinelibrary.wiley.com/action/downloadSupplement?doi=10.1002%2Fart.42266&file=art42266-sup-0001-Disclosureform.pdf>.

Address correspondence via email to Robert Terkeltaub, PhD, at [rterkeltaub@ucsd.edu](mailto:rterkeltaub@ucsd.edu) or to Changgui Li, MD, at [lichanggui@medmail.com.cn](mailto:lichanggui@medmail.com.cn).

Submitted for publication January 5, 2022; accepted in revised form June 10, 2022.

therapy (ULT) is the central strategy for effectively controlling hyperuricemia and gout (3–5). However, the pathophysiology of hyperuricemia is heterogeneous in gout patients (6–10).

Renal uric acid underexcretion is the predominant cause of hyperuricemia (~70–90% of gout patients) (7). However, uric acid overproduction and intestinal uric acid underexcretion with renal uric acid overload can also drive hyperuricemia alone or in combination with renal uric acid underexcretion in gout (6,8–10). Ichida et al (9) developed criteria to classify hyperuricemia in gout into uric acid overproduction, renal uric acid underexcretion, extrarenal uric acid underexcretion, and combined mechanism types, via clinical and genetic test results and via fractional excretion of urate and uric acid excretion under low-purine diet conditions. As such, fractional excretion of urate <5.5% and uric acid excretion  $\leq 600$  mg/day/1.73 m<sup>2</sup> is used as criteria to define renal uric acid underexcretion-type gout (9).

The principal oral ULT agents are the xanthine oxidase inhibitors (XOIs) allopurinol and febuxostat, and uricosuric agents that all act as inhibitors of the renal urate transporter 1 (URAT1) (benzbromarone and probenecid) (11–14). Based on available evidence to date, the 2020 American College of Rheumatology (ACR) gout management guidelines and 2016 EULAR gout management guidelines recommend XOI using allopurinol as the first-line ULT approach (12,13). Whereas the 2016 EULAR guidelines recommend uricosuric therapy as a second-line ULT option in gout, the 2020 ACR guidelines only provide conditional recommendation for probenecid use as a second-line agent after treatment failure with allopurinol, and benzbromarone is not part of this clinical guideline, since the drug is not approved for use in the US (12,13). Allopurinol, febuxostat, and benzbromarone are all broadly used in Asia and are comparably effective in achieving serum urate target and gout flare burden reduction in ULT treatment-to-target dose titration studies in Asian populations; however, the prevalence of HLA-B\*5801 that is associated with allopurinol hypersensitivity is higher in those of Han Chinese, Korean, and Thai descent (7.4%) (11,12,15–18). Notably, febuxostat is a recommended ULT in China, though at a dose of only 20–40 mg daily (13,19).

Moreover, a randomized controlled trial in Chinese gout patients that did not separate patients according to pathophysiology driving hyperuricemia used a 20-mg daily febuxostat dose, which is a quarter of the maximum approved in the US (and a sixth of the maximum dose prescribed outside the US), and used benzbromarone 25 mg daily (a quarter of the typical maximum dose used in clinical practice and an eighth of the maximum advised dose most often used in moderate-to-severe renal impairment); the rate of achieving the serum urate target was similar compared to these low-dose regimens (15) (low-dose febuxostat [LDFeb] and low-dose benzbromarone [LDBen]).

We hypothesized that LDBen would have superior urate-lowering ability and similar safety compared to first-line LDFeb in patients with renal uric acid underexcretion-type gout. The aim

of this randomized comparative trial was to compare efficacy and safety of LDFeb and LDBen to treat renal uric acid underexcretion-type gout.

## PATIENTS AND METHODS

**Study design and participants.** This open-label, prospective, randomized study was conducted at the Gout Clinic of the Affiliated Hospital of Qingdao University. We compared the efficacy and safety of LDBen and LDFeb in men with renal underexcretion-type gout who were treated with 12 weeks of ULT. Inclusion criteria included the following: gout according to the 2015 ACR/EULAR gout classification criteria (19), male sex, age ranging from 18 years to 70 years, serum urate levels between 7.0 mg/dl and 10.0 mg/dl, and renal uric acid underexcretion. Renal underexcretion-type gout is defined as fractional excretion of urate of <5.5% and uric acid excretion of  $\leq 600$  mg/day/1.73 m<sup>2</sup> (9). Participants were excluded if 1 of the following criteria was met: fractional excretion of urate of  $\geq 5.5\%$  or uric acid excretion of  $>600$  mg/day/1.73 m<sup>2</sup>, gout flare within 2 weeks before enrollment, urinary calculi, elevated transaminases ( $>2.0$  times the upper limit of normal [ULN]), estimated glomerular filtration rate (eGFR) of  $<60$  ml/minute/1.73 m<sup>2</sup>, or the need to take any urate-lowering drug or other medicine affecting serum urate levels (Supplementary Table 1, available on the *Arthritis & Rheumatology* website at <http://onlinelibrary.wiley.com/doi/10.1002/art.42266>). The ethics committee at the Affiliated Hospital of Qingdao University approved the trial. It was registered in the Chinese Clinical Trial Registration Center (identifier: ChiCTR1900022981). Written informed consent was obtained from all participants.

**Treatment and procedures.** As described in the previous study (16), all participants enrolled in the trial underwent a 14-day washout period, which indicated that they stopped receiving urate-lowering drugs and adhered to a low-purine diet. During the study, other urate-lowering drugs or drugs that are known to affect the serum urate level were prohibited. A randomization list was created using a random number generator. Participants were assigned a random code and were randomized in a 1:1 ratio to receive either LDBen or LDFeb. Participants received oral febuxostat or benzbromarone once daily in the morning. All participants received daily urine alkalization with oral sodium bicarbonate, 1 gm/3 times daily. During treatment with the study drug, colchicine and/or nonsteroidal antiinflammatory drugs were prescribed to participants if they experienced a gout flare. In participants with serum transaminase elevation that more than doubled from baseline values, hepatoprotective treatment (diammonium glycyrrhizinate, silybinin, or polyene phosphatidylcholine) was prescribed.

The clinician did not know which treatment option a participant would receive before randomization. Both the participant and the treating clinician knew the treatment allocation after

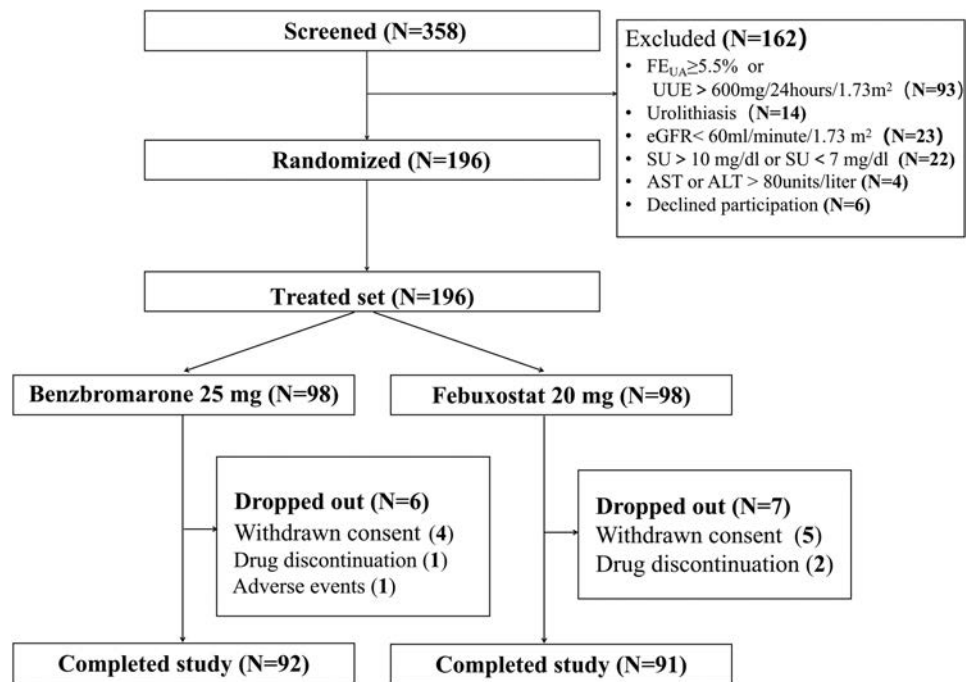


**Figure 1.** Flow chart of the study design showing how patients with renal underexcretion-type gout were organized into the benzbromarone and febuxostat treatment groups.  $FE_{UA}$  = fractional excretion of urate;  $UUE$  = uric acid excretion;  $eGFR$  = estimated glomerular filtration rate;  $SU$  = serum urate;  $ALT$  = alanine aminotransferase;  $AST$  = aspartate aminotransferase.

randomization. Participants were given advice on nondrug treatment approaches, including diet and exercise.

Information collected at baseline included age, age at disease onset, disease duration, lifestyle, body weight, height, body mass index (BMI) (weight [kg]/height [ $\text{m}^2$ ]), disease history (tophus, hypertension, fatty liver, hyperlipidemia, diabetes, cardiovascular disease [CVD]), and family history of gout. Serum biochemical data that were collected included serum urate levels, alanine aminotransferase (ALT) level, aspartate aminotransferase (AST) level, fasting glucose values, triglycerides, total cholesterol, and creatinine levels. Renal function was assessed as the  $eGFR$ , determined using Chronic Kidney Disease Epidemiology Collaboration design formulas: for creatinine  $\leq 80\text{ }\mu\text{moles}/\text{liter}$  (0.9 mg/dl),  $eGFR$  (in  $\text{ml}/\text{minute}/1.73\text{ m}^2$ ) =  $141 \times (\text{creatinine} [\text{mg}/\text{dl}]/0.9)^{-0.411} \times 0.993^{\text{age}(\text{years})}$ ; for creatinine  $> 80\text{ }\mu\text{moles}/\text{liter}$  (0.9 mg/dl),  $eGFR$  (in  $\text{ml}/\text{minute}/1.73\text{ m}^2$ ) =  $141 \times (\text{creatinine} [\text{mg}/\text{dl}]/0.9)^{-1.209} \times 0.993^{\text{age}(\text{years})}$ . Clinical obesity was defined as a BMI of  $\geq 28\text{ kg}/\text{m}^2$ , based on criteria in Asian populations (20,21). We measured the biochemical parameters at every visit. Participants were considered withdrawn cases after 3 consecutive days without medication.

**Outcomes.** The primary efficacy outcome was the rate of achieving the target serum urate level of  $< 6.0\text{ mg}/\text{dl}$  at week 12 of treatment. Secondary efficacy outcomes included the rate of achieving the target serum urate level of  $< 5.0\text{ mg}/\text{dl}$ , the change in serum urate (serum urate  $\Delta\%$  [baseline serum urate

level–visit serum urate level]/baseline serum urate level), and changes in other laboratory parameters including serum urate level, fasting glucose values, total cholesterol, triglycerides, AST level, ALT level, creatinine level, and  $eGFR$ . Safety outcomes included the incidence of gout flares and the percentage of participants with treatment-emergent adverse events (AEs). Changes in renal function, changes in liver function, and urolithiasis were AEs of particular interest in this study.

**Sample size.** Sample size was determined based on the primary end point (rate of achieving the target serum urate level  $< 6.0\text{ mg}/\text{dl}$  at week 12 of treatment). Based on findings from the previous study and the preliminary study, we estimated that the rate of achieving the serum urate target would be 60% in the LDBen group and 38% in the LDFeb group (15,16). We calculated that a sample size of 78 patients per group would be required according to a 5% 2-sided significance level and 80% power to detect a difference between the LDBen group and LDFeb group (in a 1:1 allocation). A sample size of 98 was calculated for each group to account for an estimated 20% dropout rate.

**Statistical analysis.** Statistical analyses were performed using SPSS version 22.0 (IBM). All continuous variables are shown as the mean  $\pm$  SD or the median (interquartile range) and categorical variables are shown as percentages. Continuous variables were compared using  $t$ -test for independent

samples or Mann-Whitney U test, and categorical variables between the 2 groups were compared using chi-square test. Within-group variables from each visit were compared to baseline values using paired-sample *t*-test or Wilcoxon signed rank test. *P* values less than 0.05 were considered statistically significant.

## RESULTS

**Study flow and clinical characteristics.** The clinical trial was initiated on May 3, 2019 and completed on January 26, 2021. In this trial, 196 participants were randomized to receive ULT with LDBen (N = 98) or LDFeb (N = 98) (Figure 1). Overall, 183 participants (93.4%) completed the trial, and 13 participants dropped out before the end of the study (6 in the LDBen group, 7 in the LDFeb group). The reasons cited for discontinuation included voluntarily withdrawal (4 in the LDBen group, 5 in the LDFeb group) and drug discontinuation (1 in the LDBen group, 2 in the LDFeb group). One participant in the LDBen group

dropped out of the trial because of gout flare at week 4 (Figure 1). Patients in both groups received medication according to the regimen, as confirmed by pill counts.

Clinical characteristics at baseline were similar between the 2 groups (Table 1). Participants receiving either LDBen or LDFeb were a mean age of 43.89 years and 43.29 years, respectively. The mean  $\pm$  SD duration of gout was similar in the 2 groups (LDBen 5.2  $\pm$  4.6 years versus LDFeb 5.6  $\pm$  4.8 years). More than 75% of study participants had not received prior ULT. Baseline serum urate levels were 8.72  $\pm$  0.73 mg/dl in the LDBen group and 8.59  $\pm$  0.70 mg/dl in the LDFeb group. Laboratory parameters and coexisting conditions (obesity, hypertension, fatty liver, hyperlipidemia, diabetes, and CVD) were similar at baseline between the groups (Table 1).

**Efficacy.** The primary efficacy outcome was the proportion of participants with serum urate levels of <6 mg/dl during the treatment period. The proportion of participants who achieved the treatment urate target was significantly higher in the LDBen

**Table 1.** Baseline demographic and clinical characteristics of patients with renal underexcretion-type gout receiving either LDBen or LDFeb\*

	LDBen (n = 98)	LDFeb (n = 98)
Demographic and clinical characteristics		
Age, mean $\pm$ SD years	43.89 $\pm$ 13.10	43.29 $\pm$ 12.22
Male, no. (%) of patients	98 (100)	98 (100)
Height, mean $\pm$ SD cm	174.01 $\pm$ 5.84	175.37 $\pm$ 5.73
Body weight, mean $\pm$ SD kg	81.07 $\pm$ 9.82	82.98 $\pm$ 11.27
Body mass index, mean $\pm$ SD kg/m <sup>2</sup>	26.77 $\pm$ 2.85	26.97 $\pm$ 3.21
SBP, mean $\pm$ SD mm Hg	133.19 $\pm$ 16.23	134.18 $\pm$ 15.32
DBP, mean $\pm$ SD mm Hg	84.21 $\pm$ 10.80	85.84 $\pm$ 12.09
Gout feature		
Serum urate, median (IQR) mg/dl	8.70 (7.91–9.06)	8.77 (8.10–9.27)
Age at onset, mean $\pm$ SD years	39 $\pm$ 12	38 $\pm$ 10
Duration of gout, mean $\pm$ SD years	5.2 $\pm$ 4.6	5.6 $\pm$ 4.8
Gout flare frequency, no. (%) of patients		
Less than twice a year	48 (49)	45 (46)
Twice or more than twice a year	50 (51)	53 (54)
Tophus, no. (%) of patients	18 (18)	18 (18)
Family history of gout, no. (%) of patients	16 (16)	21 (21)
ULT naive, no. (%) of patients	75 (77)	79 (81)
Coexisting conditions, no. (%) of patients		
Obesity	40 (41)	32 (33)
Hypertension	16 (16)	20 (20)
Cardiovascular disease	2 (2)	0 (0)
Fatty liver	17 (17)	24 (24)
Hyperlipidemia	20 (20)	17 (17)
Diabetes	15 (15)	14 (14)
Blood chemistry parameters		
Serum creatinine, median (IQR) $\mu$ moles/liter	82 (76–93)	85 (76–95)
Fasting glucose, mean $\pm$ SD mmoles/liter	5.52 $\pm$ 0.68	5.56 $\pm$ 0.63
Cholesterol, mean $\pm$ SD mmoles/liter	4.84 $\pm$ 0.82	4.76 $\pm$ 1.17
Triglyceride, median (IQR) mmoles/liter	1.69 (1.17–2.34)	1.67 (1.25–2.53)
AST, median (IQR) units/liter	21.00 (18.00–24.25)	19 (17–24)
ALT, median (IQR) units/liter	26.0 (18.0–37.5)	23.50 (16.75, 36.00)
eGFR, mean $\pm$ SD ml/minute/1.73 m <sup>2</sup>	96.30 $\pm$ 15.51	94.60 $\pm$ 15.09

\* LDBen = low-dose benzbromarone; LDFeb = low-dose febuxostat; SBP = systolic blood pressure; DBP = diastolic blood pressure; IQR = interquartile range; ULT = urate-lowering therapy; AST = aspartate aminotransferase; ALT = alanine aminotransferase; eGFR = estimated glomerular filtration rate.



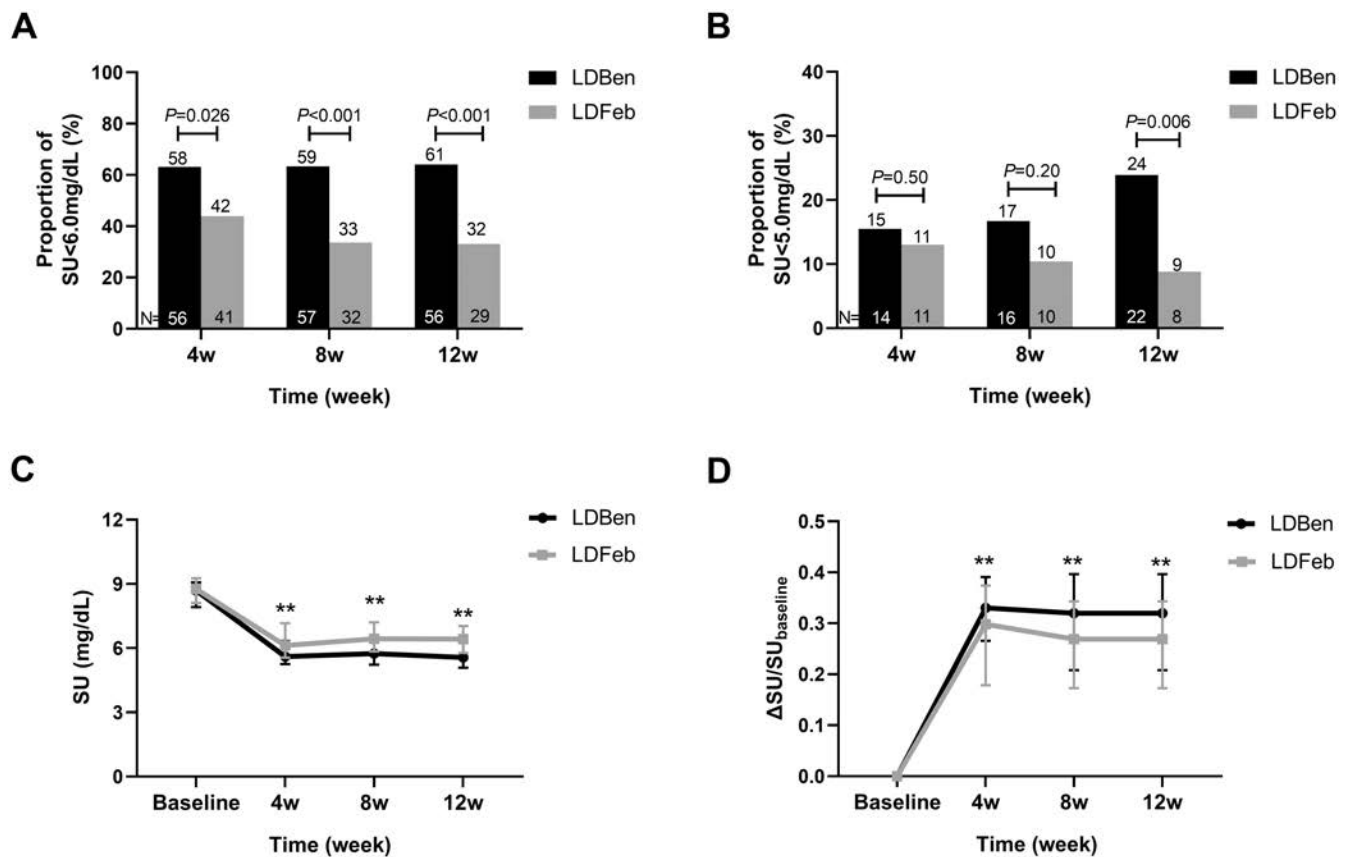


**Figure 2.** Efficacy of low-dose benzbromarone (LDBen) and low-dose febuxostat (LDFeb) in patients with renal underexcretion-type gout. **A** and **B**, Proportion of participants with serum urate levels of <6.0 mg/dl (**A**) and <5.0 mg/dl (**B**) at weeks 4, 8, and 12 after the initiation of treatment. Values at the bottom of the bars show the number of participants and values at the top of the bars show the percentage of participants. **C**, Trend of serum urate level in the 2 groups at weeks 4, 8, and 12. **D**, Change in serum urate levels in the 2 groups at weeks 4, 8, and 12, calculated as  $\Delta = (\text{baseline serum urate level} - \text{visit serum urate level})/\text{baseline serum urate level}$ . Results at each timepoint in **C** and **D** are the mean  $\pm$  SD. \*\* =  $P < 0.01$ .

group than in the LDFeb group at week 4 (58% versus 42%,  $P = 0.03$ ), week 8 (59% versus 33%,  $P < 0.001$ ), and week 12 (61% versus 32%,  $P < 0.001$ ) (Figure 2A).

The proportion of participants who achieved a serum urate level of <5.0 mg/dl in the 2 groups was similar at weeks 4 and 8, but more participants in the LDBen group achieved this lower serum urate level after 12 weeks (LDBen 24% versus LDFeb 9%,  $P = 0.006$ ) (Figure 2B). The mean serum urate concentration during the entire study period in the LDBen group was significantly lower than in the LDFeb group ( $P < 0.001$ ). At week 12, the mean  $\pm$  SD serum urate level decreased from  $8.59 \pm 0.70$  mg/dl to  $5.81 \pm 1.19$  mg/dl in the LDBen group and from  $8.72 \pm 0.73$  mg/dl to  $6.39 \pm 0.94$  mg/dl in the LDFeb group, respectively (Figure 2C). The mean  $\pm$  SD percentage change in serum urate level (serum urate  $\Delta = [\text{baseline serum urate level} - \text{visit serum urate level}]/\text{baseline serum urate level}$ ) at week 12 was 32.0% in the LDBen group and 26.5% in the LDFeb group ( $P < 0.001$ ) (Figure 2D).

No differences were detected in terms of glucose and lipid metabolic markers between the 2 groups at week 12 (Table 2).

However, the mean fasting glucose concentration in the LDBen group was significantly lower than in the LDFeb group at weeks 4 and 8 ( $P < 0.001$  at both time points) (Table 2).

**Safety.** Over the 12-week study period, the incidence rates of AEs were similar between the 2 groups (60% in the LDBen group and 65% in the LDFeb group). There were no serious AEs (Table 3). There were no skin reactions, gastrointestinal AEs, fulminant hepatitis, or major adverse cardiac events in either group (data not shown). No between-group differences were observed in terms of the proportion of participants with gout flare (LDBen 30% versus LDFeb 36%,  $P = 0.36$ ) (Table 3).

Liver and kidney function were monitored throughout the trial. An increase from baseline AST level was observed at each follow-up visit in patients in the LDFeb group ( $P < 0.001$ ). In contrast, AST levels in the LDBen group did not increase over time and were lower than the LDFeb group at weeks 4 and 12 ( $P < 0.01$  at both time points). The percentage of participants with AST elevation was significantly lower in the LDBen group than in the LDFeb group (1% versus 9%,  $P = 0.02$ ).

**Table 2.** Major clinical parameters during the trial in 98 participants receiving LDBen and 98 participants receiving LDFeb\*

	Baseline	Week 4	Week 8	Week 12
Completed follow-up, no. (%) of patients				
LDBen	98 (100)	97 (99)	96 (98)	92 (94)
LDFeb	98 (100)	98 (100)	96 (98)	91 (93)
Serum urate, median (IQR) mg/dl				
LDBen	8.70 (7.91–9.06)	5.60 (5.26–6.34) <sup>†‡</sup>	5.74 (5.22–6.60) <sup>†‡</sup>	5.57 (5.08–6.46) <sup>†‡</sup>
LDFeb	8.77 (8.10–9.27)	6.12 (5.55–7.16) <sup>‡</sup>	6.44 (5.84–7.21) <sup>‡</sup>	6.42 (5.77–7.03) <sup>‡</sup>
Fasting glucose, mean ± SD mmol/liter				
LDBen	5.52 ± 0.68	5.35 ± 0.54 <sup>†‡</sup>	5.34 ± 0.44 <sup>†‡</sup>	5.39 ± 0.51
LDFeb	5.56 ± 0.63	5.65 ± 0.58	5.69 ± 0.59 <sup>§</sup>	5.54 ± 0.58
Cholesterol, mean ± SD mmol/liter				
LDBen	4.84 ± 0.82	4.80 ± 0.84	4.84 ± 0.86	4.80 ± 0.85
LDFeb	4.76 ± 1.17	4.77 ± 0.99	4.83 ± 0.93	4.85 ± 1.01
Triglycerides, median (IQR) mmol/liter				
LDBen	1.69 (1.17–2.34)	1.57 (1.19–1.99)	1.56 (1.14–2.00) <sup>§</sup>	1.50 (1.19–2.11) <sup>‡</sup>
LDFeb	1.67 (1.25–2.52)	1.74 (1.22–2.67)	1.65 (1.17–2.44)	1.77 (1.17–2.50)
AST, median (IQR) units/liter				
LDBen	21.00 (18.00–24.25)	20 (17–23) <sup>†§</sup>	21.00 (17.25–23.75)	20.00 (16.25–23.00) <sup>†</sup>
LDFeb	19 (17–24)	22 (18–27) <sup>‡</sup>	21 (18–28) <sup>‡</sup>	22 (18–28) <sup>‡</sup>
ALT, median (IQR) units/liter				
LDBen	26.0 (20.0–37.5)	24 (18–33) <sup>‡</sup>	25.00 (19.00–33.75)	24 (17–33) <sup>†¶</sup>
LDFeb	23.50 (16.75–36.00)	27 (18–37) <sup>§</sup>	27.00 (18.00–40.75) <sup>§</sup>	28 (19–40)
Creatinine, median (IQR) μmol/liter				
LDBen	82 (76–93)	79.5 (72.0–88.0) <sup>‡</sup>	84 (76–91)	81 (75–89)
LDFeb	85.00 (76.00–95.25)	81.0 (74.0–90.5) <sup>‡</sup>	82.5 (75.0–90.0) <sup>§</sup>	83 (74–91)
eGFR, mean ± SD ml/minute/1.73 m <sup>2</sup>				
LDBen	96.30 ± 15.51	100.57 ± 19.96 <sup>§</sup>	96.86 ± 15.00	98.39 ± 15.42
LDFeb	94.60 ± 15.09	97.33 ± 16.71 <sup>‡</sup>	97.85 ± 15.58 <sup>§</sup>	97.40 ± 15.87

\* IQR = interquartile range; AST = aspartate aminotransferase; ALT = alanine aminotransferase; eGFR = estimated glomerular filtration rate.

†  $P < 0.01$  for low-dose benzbromarone (LDBen) compared to low-dose febuxostat (LDFeb).

‡  $P < 0.01$  for baseline values compared to weeks 4, 8, and 12 in the LDBen group or LDFeb group.

§  $P < 0.05$  for baseline values compared to weeks 4, 8, and 12 in the LDBen group or LDFeb group.

¶  $P < 0.05$  for LDBen compared to LDFeb.

(Table 3). Furthermore, fewer participants in the LDBen group had a 1–2-times elevation from baseline in their AST level compared to participants in the LDFeb group (1% versus 8%,  $P = 0.03$ ). The ALT level decreased in the LDBen group but increased in the LDFeb group at weeks 4 and 8, and at week

12, the ALT level remained lower in the LDBen group compared to the LDFeb group ( $P = 0.03$ ). Overall, the percentage of participants with transaminase elevation above the ULN was lower in the LDBen group than in the LDFeb group (4% versus 15%,  $P = 0.008$ ) (Table 3).

**Table 3.** Frequency of adverse events in patients with renal underexcretion-type gout during the trial of LDBen and LDFeb\*

	LDBen (n = 98)	LDFeb (n = 98)	P
Urolithiasis	5 (5)	2 (2)	0.25
Gout flare	30 (31)	36 (37)	0.36
Once	18 (18)	16 (16)	0.71
Twice	9 (9)	14 (14)	0.27
More than twice	3 (3)	6 (6)	0.50
New-onset AST level elevation <sup>†</sup>	1 (1)	9 (9)	0.009 <sup>‡</sup>
1–2-times elevation	1 (1)	8 (8)	0.035 <sup>‡</sup>
2–3-times elevation	0 (0)	1 (1)	1.00
New-onset ALT level elevation <sup>†</sup>	4 (4)	10 (10)	0.10
1–2-times elevation	3 (3)	8 (8)	0.12
2–3-times elevation	1 (1)	2 (2)	1.00
eGFR <60 ml/minute/1.73 m <sup>2</sup>	0 (0)	0 (0)	1.00
Other level of eGFR	0 (0)	0 (0)	1.00

\* Values are the number (%) of patients. LDBen = low-dose benzbromarone; LDFeb = low-dose febuxostat; AST = aspartate aminotransferase; ALT = alanine aminotransferase; eGFR = estimated glomerular filtration rate.

† New-onset elevation indicates an elevation above the upper limit of normal from baseline to week 12.

‡  $P$  value was statistically significant.

There were no significant differences between the 2 groups in terms of serum creatinine levels and eGFR during the treatment period (Table 2). No participant in either group developed an eGFR of  $<60$  mL/minute/1.73 m<sup>2</sup>. Urolithiasis was observed in 5 participants in the LDBen group and 2 participants in the LDFeb group (5% versus 2%,  $P = 0.25$ ) (Table 3).

## DISCUSSION

The findings from this randomized clinical trial provide important new insights into gout management. Specifically, despite advanced understanding of the pathophysiologic basis of hyperuricemia and gout, prescribing ULT according to the hyperuricemia classification type is not generally recommended and is rarely done in Western clinical practice (12,13,19). Earlier findings from observational studies suggested that benzbromarone may be more effective than allopurinol in the reduction of serum urate levels in hyperuricemia caused by renal uric acid underexcretion (22). This Chinese gout study population-based trial was unique, not only by comparing the efficiency and safety of benzbromarone and febuxostat in randomized clinical trial participants with renal underexcretion-type gout, but also by comparing low-dose regimens. LDBen (25 mg/day) had greater urate-lowering efficacy and an excellent safety profile compared to LDFeb (20 mg/day) over 12 weeks of therapy. Low-dose benzbromarone had significantly greater serum urate-lowering treatment success than LDFeb in patients with renal underexcretion-type gout.

Importantly, the trial was designed to test a hypothesis by comparing uricosuric ULT to XOI ULT in patients with gout with a single predominant cause of hyperuricemia. This design promoted the enrollment of a relatively healthy population of younger participants with disease onset particularly common in the 30–40-year-old age group. It is well recognized that the capacity to renally excrete uric acid is partly modulated by the functional capacity for glomerular filtration of urate. In this context, stage 3 chronic kidney disease, which is very prevalent in gout patients (23,24), was an exclusion criterion in this study. In addition, this Chinese gout study population had substantially lower prevalence of hypertension, dyslipidemia, and CVD than typical Western gout clinical trial populations (25). Furthermore, all participants received 1 gm/3 times daily oral sodium bicarbonate for the purpose of alkalinizing the urine, which likely limited urolithiasis (16) and may have enhanced urate-lowering efficacy (26).

Moreover, use of ULTs differed from that in Western clinical trials and typical Western medical practice patterns and recommendations for gout, where allopurinol is the recommended first-line ULT (12,13,27). In this context, US Food and Drug Administration–approved dosing of febuxostat is 40 mg/day and 80 mg/day, and benzbromarone is not approved in the US and is only recommended as a second-line ULT drug in Europe due to potentially lethal hepatotoxicity reactions not believed to be due to modulation of URAT1 activity (12). Furthermore, in

countries where benzbromarone is approved, the starting dosages of benzbromarone range from 12.5 mg to 50 mg daily (28–31). Hence, as emerging URAT1 inhibitor uricosuric therapies are developed as potential monotherapies in clinical trials among Western patient populations (27), careful consideration will likely be needed in clinical trial patient selection for the pathophysiologic type of hyperuricemia, comorbidities, and use of urine alkalization with agents such as potassium citrate (16).

The comparison of results in distinctly designed clinical trials is clearly imperfect. However, in the current low-dose ULT trial in this selective cohort of renal uric acid underexcretion-type gout, the percentage of participants achieving the serum urate target of  $<6.0$  mg/dL was 61% in the LDBen group, which was approximately double that observed in the LDFeb group. In contrast, Naoyuki et al (28) found that the percentage of patients who achieved the serum urate target ( $<6.0$  mg/dL) was 45.7% in the 20 mg/day febuxostat treatment group. Liang et al (15) indicated that, similar to our results, the frequency of achieving the serum urate target was 39.5% among 105 gout patients who were not selected for primary uric acid underexcretion and who received febuxostat 20 mg/day, whereas the frequency of achieving the serum urate target was only 35.7% among 109 patients receiving benzbromarone 25 mg/day.

In this study, the urate-lowering effect of benzbromarone appeared to be steadier than febuxostat over the trial period. Importantly, febuxostat does lead to a sustained reduction at the final time point compared to baseline values. While we did not observe differences in terms of medication adherence using pill counts between groups, it is possible that these differences might be attributed to the following: differences in adherence behavior; differences in the mechanisms of the ULT; a decline in fractional excretion of urate as serum urate levels were reduced by treatment with febuxostat (32); or differences due to chance. There were no differences in reported medication adherence between the LDBen group and LDFeb group. Some variation in urate levels over time is often observed in ULT trials (15,33).

Not surprisingly, lack of clinical trial evidence to date has been accompanied by lack of consensus regarding use of assays for renal uric acid underexcretion in clinical practice for promoting precision in gout management. For example, the 2006 EULAR gout management guidelines recommended that renal uric acid excretion should be determined in selected gout patients, especially those with a family history of early-onset gout, those with gout onset at age  $<25$  years, or those with renal calculi (strength of recommendation 72 [95% confidence interval 62–81]) (18). The 2012 ACR Guidelines for the Management of Gout recommended that clinicians consider causes of hyperuricemia in gout patients (evidence grade C) (34). However, the most recent update of the ACR guidelines for management of gout conditionally recommended against using urinary uric acid levels to determine the precision of therapy choice and strategy in ULT (34,35).

We did not observe severe hepatotoxicity associated with LDBen, but ethnic background may affect drug responses, and severe hepatotoxicity with benzbromarone has rarely been reported in Asia (11). Notably, elevated transaminases and the rare occurrence of severe liver injury have been reported in patients receiving febuxostat (14,36). In our study, the proportion of participants with liver damage in the LDFeb group was higher than that in the LDBen group, most clearly demonstrated by the increase in AST level. No significant change in triglyceride levels was reported in this study, though a previous study suggested that febuxostat could cause elevated triglycerides (15). In this study, the incidence of urolithiasis in the LDBen group (5%) was numerically but not significantly higher than that in the LDFeb group (2%). Incidence rates of urolithiasis of ~3% have been reported with benzbromarone 75–120 mg/day (37,38), including in a trial in China using benzbromarone 25 mg/day (16), similar to our results.

Several other study limitations should be noted, such as the single center, open-label design and relatively short treatment period, which did not allow for the assessment of long-term safety. We only included patients who were relatively young, had few comorbidities, and had a baseline serum urate level ranging from 8.0 mg/dl to 10 mg/dl; therefore, study results may not be generalizable to patients with higher serum urate levels or impaired kidney function, and may also not be generalizable to patients from other geographic regions, age groups, and ethnic groups. Only men were recruited in this study, and the findings may not be generalizable to women with gout. Furthermore, the scope to more widely implement this treatment strategy is currently limited because the availability of benzbromarone and other uricosurics varies across the globe and in many countries is very limited. The efficacy of benzbromarone and febuxostat in gout patients with normal renal uric acid excretion was not compared in this study. Last, the serum urate-lowering efficacy of both benzbromarone and febuxostat was not maximal at doses of the ULT used here.

In conclusion, this study demonstrates that LDBen has greater serum urate-lowering efficacy than LDFeb in relatively young and healthy patients with renal underexcretion-type gout. Further investigation is warranted to test precision in the model for use of an URAT1 inhibitor in selecting first-line ULT according to primary renal uric acid underexcretion, as opposed to decreased renal function. However, the results suggest that LDBen may warrant stronger consideration as a safe and effective therapy to achieve serum urate target in gout patients without moderate chronic kidney disease.

## AUTHOR CONTRIBUTIONS

All authors were involved in drafting the article or revising it critically for important intellectual content, and all authors approved the final version to be published. Drs. C. Li and Terkeltaub had full access to all of

the data in the study and takes responsibility for the integrity of the data and the accuracy of the data analysis.

**Study conception and design.** C. Li.

**Acquisition of data.** Yan, Xue, Lu, Qi, Yu, Wang, Sun, Cui, Liu, He, Yuan, Chen, Cheng, Ma, H. Li, Ji, Hu, Ran.

**Analysis and interpretation of data.** Yan, Xue, Lu, Dalbeth, Terkeltaub.

## REFERENCES



1. Dalbeth N, Gosling AL, Gaffo A, et al. Gout. *Lancet* 2021;397:1843–55.
2. Dalbeth N, Merriman TR, Stamp LK. Gout. *Lancet* 2016;388:2039–52.
3. Perez-Ruiz F. Treating to target: a strategy to cure gout. *Rheumatology (Oxford)* 2009;48 Suppl:ii9–14.
4. Liu X, Zhai T, Ma R, et al. Effects of uric acid-lowering therapy on the progression of chronic kidney disease: a systematic review and meta-analysis. *Ren Fail* 2018;40:289–97.
5. Shoji A, Yamanaka H, Kamatani N. A retrospective study of the relationship between serum urate level and recurrent attacks of gouty arthritis: evidence for reduction of recurrent gouty arthritis with antihyperuricemic therapy. *Arthritis Rheum* 2004;51:321–5.
6. Mandal AK, Mount DB. The molecular physiology of uric acid homeostasis. *Annu Rev Physiol* 2015;77:323–45.
7. Vitart V, Rudan I, Hayward C, et al. SLC2A9 is a newly identified urate transporter influencing serum urate concentration, urate excretion and gout. *Nat Genet* 2008;40:437–42.
8. Dalbeth N, Merriman T. Crystal ball gazing: new therapeutic targets for hyperuricaemia and gout. *Rheumatology (Oxford)* 2009;48:222–6.
9. Ichida K, Matsuo H, Takada T, et al. Decreased extra-renal urate excretion is a common cause of hyperuricemia. *Nat Commun* 2012;3:764.
10. Woodward OM, Kottgen A, Coresh J, et al. Identification of a urate transporter, ABCG2, with a common functional polymorphism causing gout. *Proc Natl Acad Sci U S A* 2009;106:10338–42.
11. Azevedo VF, Kos IA, Vargas-Santos AB, et al. Benzbromarone in the treatment of gout. *Adv Rheumatol* 2019;59:37.
12. FitzGerald JD, Dalbeth N, Mikuls T, et al. 2020 American College of Rheumatology guideline for the management of gout. *Arthritis Rheumatol* 2020;72:879–95.
13. Richette P, Doherty M, Pascual E, et al. 2016 updated EULAR evidence-based recommendations for the management of gout. *Ann Rheum Dis* 2017;76:29–42.
14. Frampton JE. Febuxostat: a review of its use in the treatment of hyperuricaemia in patients with gout. *Drugs* 2015;75:427–38.
15. Liang N, Sun M, Sun R, et al. Baseline urate level and renal function predict outcomes of urate-lowering therapy using low doses of febuxostat and benzbromarone: a prospective, randomized controlled study in a Chinese primary gout cohort. *Arthritis Res Ther* 2019;21:200.
16. Xue X, Liu Z, Li X, et al. The efficacy and safety of citrate mixture vs sodium bicarbonate on urine alkalization in Chinese primary gout patients with benzbromarone: a prospective, randomized controlled study. *Rheumatology (Oxford)* 2021;60:2661–71.
17. Yamanaka H, Tamaki S, Ide Y, et al. Stepwise dose increase of febuxostat is comparable with colchicine prophylaxis for the prevention of gout flares during the initial phase of urate-lowering therapy: results from FORTUNE-1, a prospective, multicentre randomised study. *Ann Rheum Dis* 2018;77:270–6.
18. Zhang W, Doherty M, Pascual E, et al. EULAR evidence based recommendations for gout. Part I: Diagnosis. Report of a task force of the Standing Committee for International Clinical Studies Including Therapeutics (ESCISIT). *Ann Rheum Dis* 2006;65:1301–11.

19. Neogi T, Jansen TL, Dalbeth N, et al. 2015 Gout classification criteria: an American College of Rheumatology/European League Against Rheumatism collaborative initiative. *Arthritis Rheumatol* 2015;67:2557–68.
20. Zhou BF, Cooperative Meta-Analysis Group of the Working Group on Obesity in China. Predictive values of body mass index and waist circumference for risk factors of certain related diseases in Chinese adults—study on optimal cut-off points of body mass index and waist circumference in Chinese adults. *Biomed Environ Sci* 2002;15:83–96.
21. WHO Expert Consultation. Appropriate body-mass index for Asian populations and its implications for policy and intervention strategies [review]. *Lancet* 2004;363:157–63.
22. Perez-Ruiz F, Alonso-Ruiz A, Calabozo M, et al. Efficacy of allopurinol and benzbromarone for the control of hyperuricaemia. A pathogenic approach to the treatment of primary chronic gout. *Ann Rheum Dis* 1998;57:545–9.
23. Roughley MJ, Belcher J, Mallen CD, et al. Gout and risk of chronic kidney disease and nephrolithiasis: meta-analysis of observational studies. *Arthritis Res Ther* 2015;17:90.
24. Roughley M, Sultan AA, Clarkson L, et al. Risk of chronic kidney disease in patients with gout and the impact of urate lowering therapy: a population-based cohort study. *Arthritis Res Ther* 2018;20:243.
25. Mackenzie IS, Ford I, Nuki G, et al. Long-term cardiovascular safety of febuxostat compared with allopurinol in patients with gout (FAST): a multicentre, prospective, randomised, open-label, non-inferiority trial. *Lancet* 2020;396:1745–57.
26. Wiederkehr MR, Moe OW. Uric acid nephrolithiasis: a systemic metabolic disorder. *Clin Rev Bone Miner Metab* 2011;9:207–17.
27. Benn CL, Dua P, Gurrell R, et al. Physiology of hyperuricemia and urate-lowering treatments. *Front Med (Lausanne)* 2018;5:160.
28. Kamatani N, Fujimori S, Hada T, et al. An allopurinol-controlled, multicenter, randomized, open-label, parallel between-group, comparative study of febuxostat (TMX-67), a non-purine-selective inhibitor of xanthine oxidase, in patients with hyperuricemia including those with gout in Japan: phase 2 exploratory clinical study. *J Clin Rheumatol* 2011;17:S44–9.
29. Multidisciplinary Expert Task Force on Hyperuricemia and Related Diseases. Chinese multidisciplinary expert consensus on the diagnosis and treatment of hyperuricemia and related diseases. *Chin Med J (Engl)* 2017;130:2473–88.
30. Yamanaka H, Japanese Society of Gout and Nucleic Acid Metabolism. Japanese guideline for the management of hyperuricemia and gout: second edition. *Nucleosides Nucleotides Nucleic Acids* 2011;30:1018–29.
31. Yu KH, Chen DY, Chen JH, et al. Management of gout and hyperuricemia: multidisciplinary consensus in Taiwan. *Int J Rheum Dis* 2018;21:772–87.
32. Liu S, Perez-Ruiz F, Miner JN. Patients with gout differ from healthy subjects in renal response to changes in serum uric acid. *Joint Bone Spine* 2017;84:183–8.
33. Lin Y, Chen X, Ding H, et al. Efficacy and safety of a selective URAT1 inhibitor SHR4640 in Chinese subjects with hyperuricaemia: a randomized controlled phase II study. *Rheumatology (Oxford)* 2021;60:5089–97.
34. Khanna D, Fitzgerald JD, Khanna PP, et al. 2012 American College of Rheumatology guidelines for management of gout. Part 1: systematic nonpharmacologic and pharmacologic therapeutic approaches to hyperuricemia. *Arthritis Care Res (Hoboken)* 2012;64:1431–46.
35. Jansen TL. Rational pharmacotherapy (RPT) in goutology: define the serum uric acid target & treat-to-target patient cohort and review on urate lowering therapy (ULT) applying synthetic drugs. *Joint Bone Spine* 2015;82:225–9.
36. Bohm M, Vuppalanchi R, Chalasani N, et al. Febuxostat-induced acute liver injury. *Hepatology* 2016;63:1047–9.
37. Masbernard A, Giudicelli CP. Ten years' experience with benzbromarone in the management of gout and hyperuricaemia. *S Afr Med J* 1981;59:701–6.
38. Stamp LK, Haslett J, Frampton C, et al. The safety and efficacy of benzbromarone in gout in Aotearoa New Zealand. *Intern Med J* 2016;46:1075–80.



**BRIEF REPORT**

# Imaging Mass Cytometry Reveals Predominant Innate Immune Signature and Endothelial–Immune Cell Interaction in Juvenile Myositis Compared to Lupus Skin

Jessica L. Turnier,<sup>1</sup>  Christine M. Yee,<sup>2</sup> Jacqueline A. Madison,<sup>3</sup> Syed M. Rizvi,<sup>2</sup> Celine C. Berthier,<sup>4</sup> Fei Wen,<sup>2</sup> and J. Michelle Kahlenberg<sup>5</sup> 

**Objective.** Cutaneous inflammation can signal disease in juvenile dermatomyositis (DM) and childhood-onset systemic lupus erythematosus (cSLE), but we do not fully understand cellular mechanisms of cutaneous inflammation. In this study, we used imaging mass cytometry to characterize cutaneous inflammatory cell populations and cell–cell interactions in juvenile DM as compared to cSLE.

**Methods.** We performed imaging mass cytometry analysis on skin biopsy samples from juvenile DM patients (n = 6) and cSLE patients (n = 4). Tissue slides were processed and incubated with metal-tagged antibodies for CD14, CD15, CD16, CD56, CD68, CD11c, HLA–DR, blood dendritic cell antigen 2, CD20, CD27, CD138, CD4, CD8, E-cadherin, CD31, pan-keratin, and type I collagen. Stained tissue was ablated, and raw data were acquired using the Hyperion imaging system. We utilized the Phenograph unsupervised clustering algorithm to determine cell marker expression and permutation test by histoCAT to perform neighborhood analysis.

**Results.** We identified 14 cell populations in juvenile DM and cSLE skin, including CD14+ and CD68+ macrophages, myeloid and plasmacytoid dendritic cells (pDCs), CD4+ and CD8+ T cells, and B cells. Overall, cSLE skin had a higher inflammatory cell infiltrate, with increased CD14+ macrophages, pDCs, and CD8+ T cells and immune cell–immune cell interactions. Juvenile DM skin displayed a stronger innate immune signature, with a higher overall percentage of CD14+ macrophages and prominent endothelial cell–immune cell interaction.

**Conclusion.** Our findings identify immune cell population differences, including CD14+ macrophages, pDCs, and CD8+ T cells, in juvenile DM skin compared to cSLE skin, and highlight a predominant innate immune signature and endothelial cell–immune cell interaction in juvenile DM, providing insight into candidate cell populations and interactions to better understand disease-specific pathophysiology.

## INTRODUCTION

Juvenile dermatomyositis (DM) and childhood-onset systemic lupus erythematosus (cSLE) are multisystem inflammatory diseases with overlapping yet distinct clinical phenotypes and unique tropism for major organ involvement. Cutaneous

inflammation is often the first recognized symptom at disease onset, and substantial clinical and histopathologic overlap exists between skin lesions (1). Both juvenile DM and cSLE skin lesions demonstrate interface dermatitis, characterized by lymphocytic infiltrate and apoptotic keratinocytes at the dermoepidermal junction and also share an association with type I interferon (IFN)

Dr. Turnier's work was supported by a Cure JM Foundation Research Grant, Rheumatology Research Foundation Investigator Award, an NIH LRP Pediatric Research Renewal Award (award 2L40-AR-070531-04), and a Michigan Institute for Clinical & Health Research (MICH) Pilot Grant (UL1-TR-002240). Dr. Wen's work was supported by the NIH (awards S10-OD-020053 and P30-CA-046592), the Taubman Institute Innovative Program, and the National Science Foundation (award 1653611). Dr. Kahlenberg's work was supported by the NIH (awards R01-AR-071384 and K24-AR-076975), and the Taubman Institute Innovative Program.

<sup>1</sup>Jessica L. Turnier, MD: Division of Pediatric Rheumatology, Department of Pediatrics, University of Michigan, Ann Arbor; <sup>2</sup>Christine M. Yee Auy, BS, Syed M. Rizvi, PhD, Fei Wen, PhD: Department of Chemical Engineering, University of Michigan, Ann Arbor; <sup>3</sup>Jacqueline A. Madison, MD: Division of

Pediatric Rheumatology, Department of Pediatrics, and Division of Rheumatology, Department of Internal Medicine, University of Michigan, Ann Arbor; <sup>4</sup>Celine C. Berthier, PhD: Division of Nephrology, Department of Internal Medicine, University of Michigan, Ann Arbor; <sup>5</sup>J. Michelle Kahlenberg, MD, PhD: Division of Rheumatology, Department of Internal Medicine, University of Michigan, Ann Arbor.

Author disclosures are available at <https://onlinelibrary.wiley.com/action/downloadSupplement?doi=10.1002%2Fart.42283&file=art42283-sup-0001-Disclosureform.pdf>.

Address correspondence via email to Jessica Turnier, MD, at [turnierj@med.umich.edu](mailto:turnierj@med.umich.edu).

Submitted for publication March 11, 2022; accepted in revised form June 23, 2022.

activation (2). Cutaneous inflammation has further been demonstrated to associate with systemic disease activity and chronicity in juvenile DM and cSLE (3); however, we are limited in our understanding of pathogenic mechanisms and immune cells that drive cutaneous inflammation and disease-specific phenotypes.

Imaging mass cytometry (IMC) is a powerful tool to study disease phenotypes through simultaneous analysis of multiple protein targets while preserving tissue architecture and lending insights into cellular microenvironment and interactions (4). A recent publication harnessing IMC for adult DM skin immunophenotyping identified 13 unique immune cell populations and described a predominant myeloid signature, with abundant CD14<sup>+</sup> macrophages and CD11c<sup>+</sup> myeloid dendritic cells (mDCs), in addition to lymphoid cells (5). Prior use of mass cytometry to characterize cSLE blood defined a CD14<sup>high</sup> monocyte cytokine signature that was inducible in peripheral blood from healthy controls after treatment with cSLE plasma (6). Improving our understanding of immune cell populations and cell-cell interactions central to tissue inflammation is key to informing the development of targeted treatment for juvenile DM and cSLE patients.

In the present study, we use IMC to characterize similarities and differences in inflammatory cells and cell-cell interactions at a single-cell level within juvenile DM lesional skin compared to cSLE lesional skin. Our findings identify differences in cell populations, including CD14<sup>+</sup> macrophages, plasmacytoid DCs (pDCs), and CD8<sup>+</sup> T cells, in juvenile DM versus cSLE, and highlight a predominance of innate immune cells and endothelial cell-immune cell interactions in juvenile DM skin, providing insight into immune cell populations and cellular interactions as candidates for further study.

## PATIENTS AND METHODS

**Human subjects, skin biopsy samples, and clinical data acquisition.** Formalin-fixed paraffin-embedded (FFPE) skin biopsy samples previously obtained for clinical care at the University of Michigan were obtained after institutional review board approval. Diagnoses at the time of biopsy for juvenile DM or cSLE were made by a pediatric rheumatologist and were verified by chart review of clinical findings, laboratory data, imaging, and histopathology. All juvenile DM patients ( $n = 6$ ) met the 2017 EULAR/American College of Rheumatology (ACR) classification criteria (7), with 1 patient having skin-predominant disease. All cSLE patients ( $n = 4$ ) met the 1997 ACR classification criteria for SLE (8) at time of biopsy, with the exception of 1 patient with isolated cutaneous lupus at diagnosis who later developed features of systemic disease 3 years after biopsy. Lesional skin was from varied locations, including the elbow ( $n = 3$ ), finger ( $n = 2$ ), arm ( $n = 2$ ), cheek, scalp, and thigh (all  $n = 1$ ). Clinical data were collected retrospectively by chart review (Supplementary Table 1, available on the *Arthritis & Rheumatology* website at <https://onlinelibrary.wiley.com/doi/10.1002/art.42283>).

**IMC sample preparation and image processing.** We performed IMC on all skin biopsy samples to identify and quantify immune cell populations that were present. FFPE tissue slides were heated for 2 hours at 60°C, deparaffinized, and rehydrated. Slides were placed in Tris-EDTA (pH 9) antigen retrieval buffer and heated at 96°C for 30 minutes. After cooling, slides were blocked in 3% bovine serum albumin and incubated with metal-tagged antibodies. Our antibody panel included the following markers: CD14, CD15, CD16, CD56, CD68, CD11c, HLA-DR, blood dendritic cell antigen 2, CD20, CD27, CD138, CD4, CD8, E-cadherin, CD31, pan-keratin, and type I collagen. Stained tissue was ablated, and raw data were acquired using the Hyperion imaging system (Fluidigm). Multiplexed cytometry by time-of-flight mass spectrometry imaging data were preprocessed using commercial acquisition software (Fluidigm), converted to TIFF images, and then segmented into individual cells using CellProfiler version 3.1.8.

**IMC data analysis.** For dimensionality reduction, we used visualization of t-distributed stochastic neighbor embedding (t-SNE) to determine phenotypic diversity of cell populations. The Phenograph unsupervised clustering algorithm was used to determine cell marker expression (9). A heatmap was generated to demonstrate median Z score marker expression of cells in each cluster. Neighborhood analysis was performed by permutation test using histoCAT (10) with a permutation number of 999 and a  $P$  value threshold of 0.01.

**Microarray data analysis to evaluate innate and adaptive signatures.** We previously performed microarray gene expression analysis on all lesional skin samples (11). Using the xCell webtool (<http://xcell.ucsf.edu>) (12), we generated innate and adaptive transcriptional immune signatures from samples. Each patient signature was generated for innate immune signatures by adding xCell enrichment scores from DCs, pDCs, macrophages, and monocytes (94, 38, 259, and 303 genes, respectively) and for adaptive immune signatures by adding scores from B cells, CD4<sup>+</sup> T cells, and CD8<sup>+</sup> T cells (135, 158, and 116 genes, respectively).

**Statistical analysis.** Cell populations were quantified by number of cells per mm<sup>2</sup> of tissue and translated into percentage of total immune cells identified in each patient sample. Differences in cell populations between juvenile DM and cSLE were assessed in GraphPad Prism 8 software using Student's 2-tailed  $t$ -test, with  $P$  values less than 0.05 considered significant.

## RESULTS

**Key differences in absolute number of immune cell populations within skin lesions in juvenile DM and cSLE.** Childhood-onset SLE skin lesions had an overall higher inflammatory cell infiltrate compared to juvenile DM (Figure 1A).

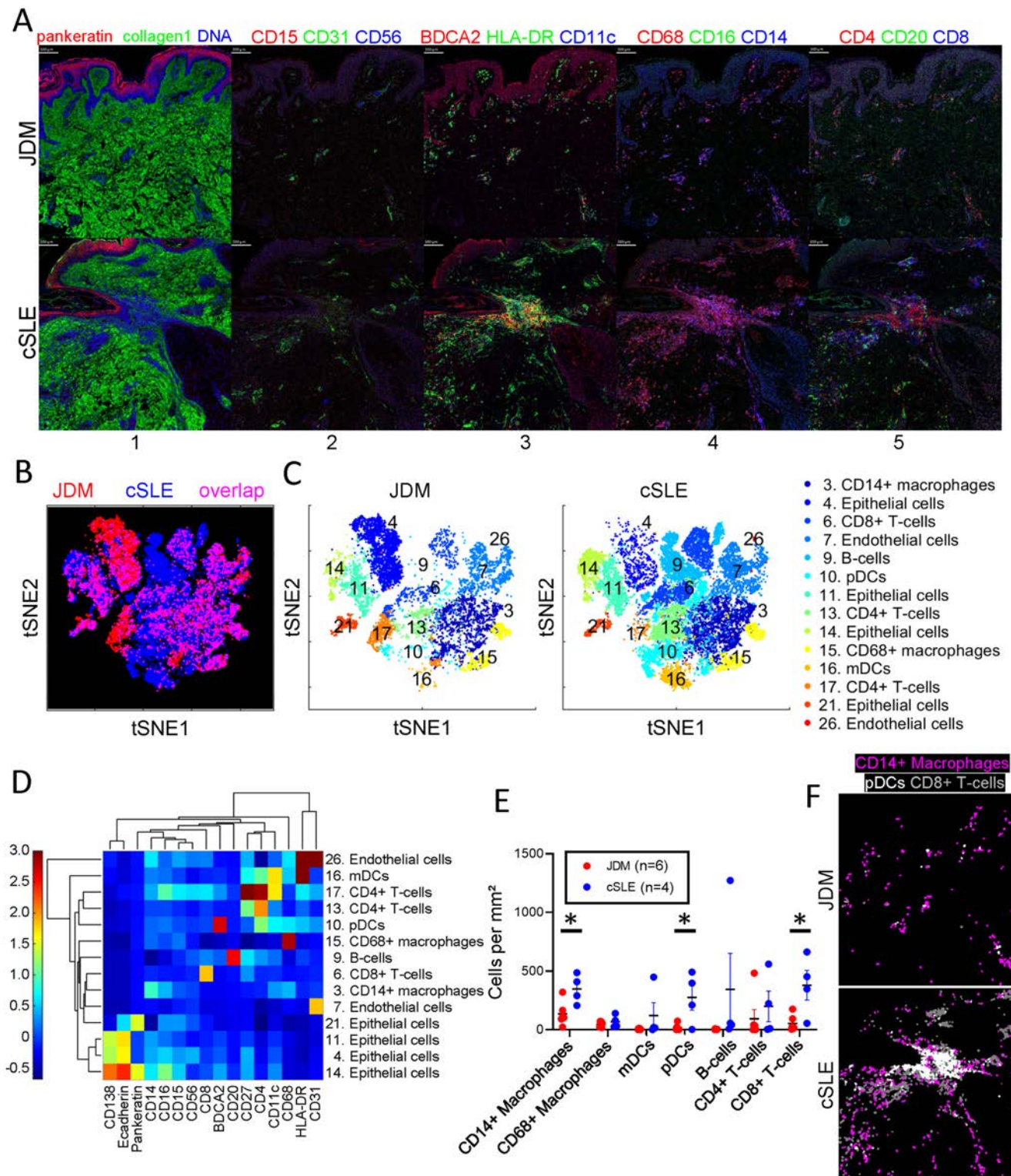


**Figure 1.** CD14+ macrophages, plasmacytoid dendritic cells (pDCs), and CD8+ T cells were increased in childhood-onset systemic lupus erythematosus (cSLE) compared to juvenile dermatomyositis (JDM) lesional skin. **A**, Multiplexed images demonstrating staining for cellular markers in JDM and cSLE skin samples, represented by different colors in panels 1–5. Bars = 100  $\mu$ m. **B** and **C**, Analysis by t-distributed stochastic neighbor embedding (t-SNE) dimensionality reduction demonstrating overlay of identified JDM and cSLE cell clusters (**B**) and individual t-SNE plots by disease (**C**). **D**, Phenograph clustergram and heatmap showing marker expression by cell cluster. **E**, Quantification of immune cell types per disease based on marker expression. Bars show the mean  $\pm$  SEM. \* =  $P < 0.05$ . **F**, Representative images demonstrating higher quantities of CD14+ macrophages, pDCs, and CD8+ T cells in cSLE compared to JDM. Magnification is the same as in **A**. BDCA2 = blood dendritic cell antigen 2; mDCs = myeloid DCs.



Using the t-SNE dimensionality reduction tool, we visualized cell clusters that overlapped between diseases and those more predominant in either juvenile DM or cSLE (Figures 1B and 1C and Supplementary Figure 1, <https://onlinelibrary.wiley.com/doi/10.1002/art.42283>). Overall, we identified 26 unique cell clusters in juvenile DM and cSLE skin (Supplementary Figure 1), of which we were able to definitively identify 14 cell populations using marker expression patterns (Figure 1D), including 8 immune cell populations: CD14+ macrophages (cluster 3), CD68+ macrophages (cluster 15), mDCs (cluster 16), pDCs (cluster 10), B cells (cluster 9), CD4+ T cells (clusters 13 and 17), and CD8+ T cells (cluster 6).

While all immune cell populations were present in both diseases, there were differences in cell numbers per cluster according to disease. Notably, cSLE skin showed increased CD14+ macrophages, pDCs, and CD8+ T cells (Figure 1E). This is demonstrated visually by the spatial distribution of labeled cells in juvenile DM compared to cSLE skin (Figure 1F). Interestingly, we noted 2 CD4+ T cell populations, with cluster 17 additionally displaying CD11c and CD27 coexpression (Figure 1D). CD4+ T cells from cluster 17 were more concentrated in juvenile

DM skin (Figures 1B and C) and could potentially represent a more highly activated, migratory T cell population (13).

### Overall immune cell composition differs in juvenile DM skin lesions compared to cSLE skin lesions.

While CD14+ macrophages were the predominant immune cell population in both juvenile DM and cSLE, juvenile DM had an overall higher percentage of CD14+ macrophages relative to total immune cell composition (46.1% versus 30%) (Figure 2A and Supplementary Table 2A, <https://onlinelibrary.wiley.com/doi/10.1002/art.42283>). In contrast, cSLE exhibited a higher overall percentage of pDCs and CD8+ T cells than juvenile DM (13.5% versus 3.9%, and 21% versus 13%, respectively). In juvenile DM, the composition of identified immune cells from highest to lowest percentage included CD14+ macrophages (46.1%) followed by CD68+ macrophages (24%), CD8+ T cells (13%), CD4+ T cells (11.7%), pDCs (3.9%), mDCs (0.9%), and B cells (0.5%) (Figure 2A and Supplementary Table 2A). Of note, B cells were scarce in all juvenile DM samples. In cSLE, the most populous immune cells were also CD14+ macrophages (30%),

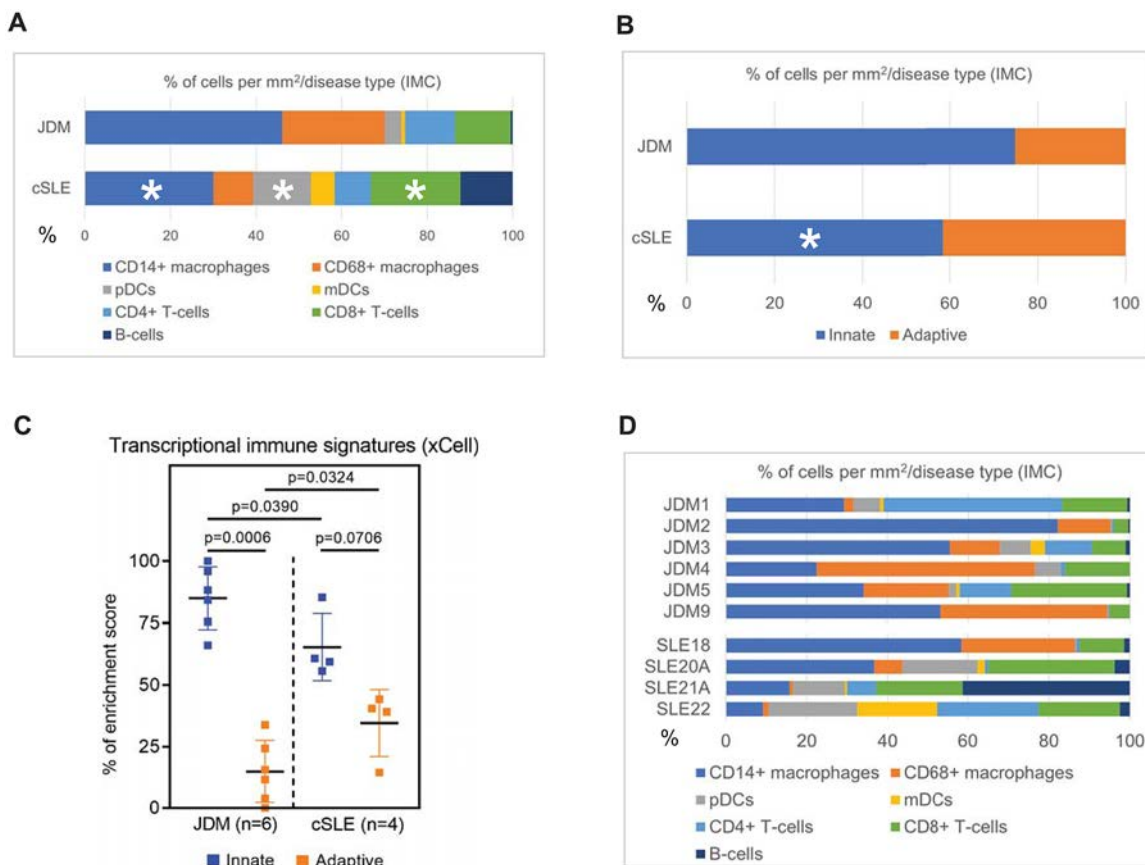


**Figure 2.** Overall immune cell composition in JDM compared to cSLE skin was predominantly innate immune cells. **A** and **B**, Bar graphs showing percent composition of immune cell types by disease (**A**) and innate versus adaptive immune cell categorization, with CD14+ and CD68+ macrophages, pDCs, and mDCs categorized as innate, and CD4+ and CD8+ T cells and B cells as adaptive (**B**). \* =  $P < 0.05$  versus JDM. **C**, Innate versus adaptive immune cell enrichment from skin microarrays of the same patients. Bars show the mean  $\pm$  SD. **D**, Bar graph showing individual patient sample immune cell composition. IMC = imaging mass cytometry (see Figure 1 for other definitions).

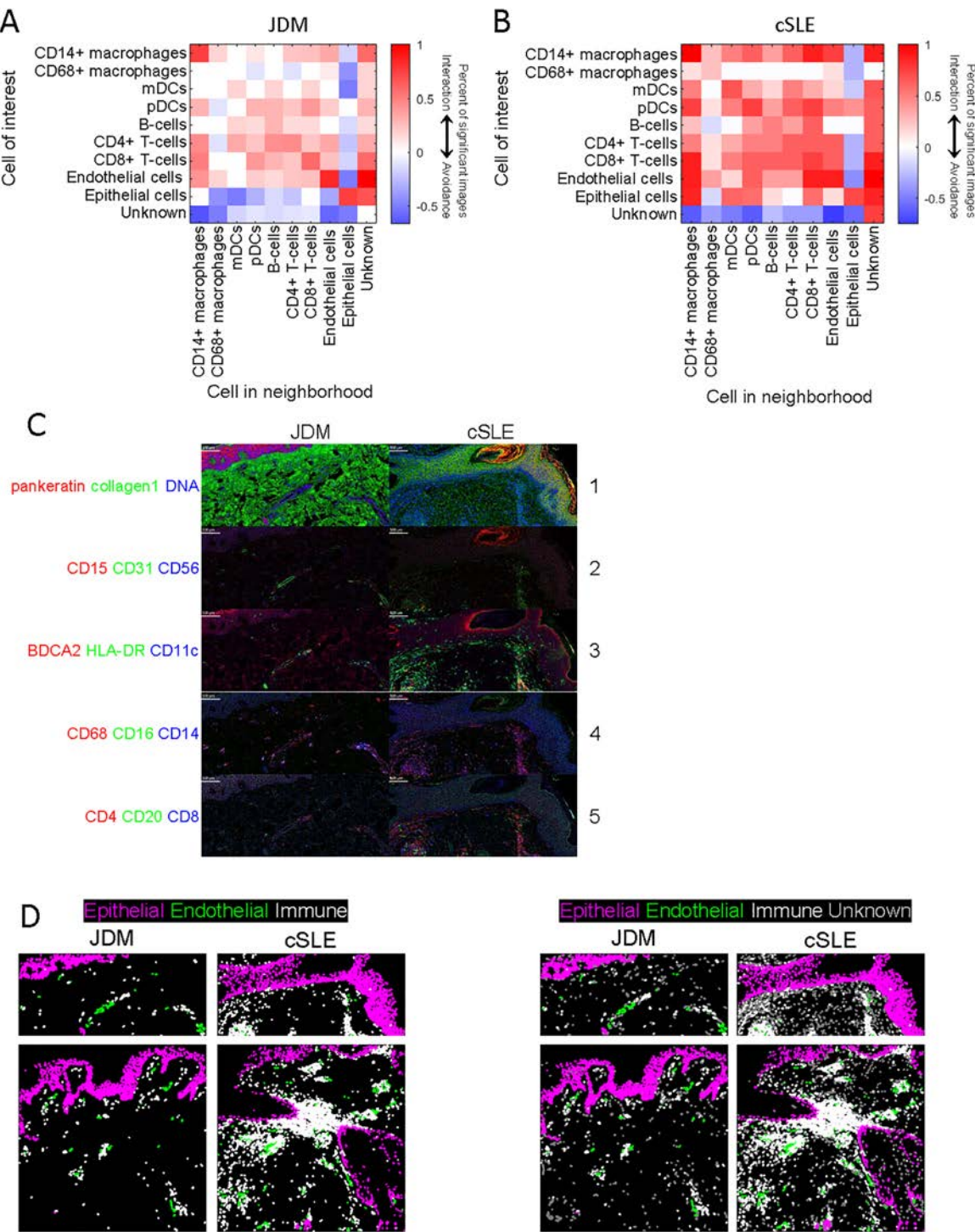


**Figure 3.** Cell–cell interactions in JDM and cSLE lesional skin using neighborhood analysis. **A** and **B**, Heatmaps highlighting differences in cell–cell interactions in JDM (**A**) and cSLE (**B**) lesional skin using permutation tests for neighborhood analysis. Red represents a positive association ( $P < 0.01$ ), white represents an insignificant association, and blue represents a negative association ( $P < 0.01$ ). **C**, Multiplexed images demonstrating staining for cellular markers in JDM and cSLE skin samples, represented by different colors in panels 1–5. Bars = 100 μm. **D**, Demonstration of increased epithelial cell–immune cell interaction in cSLE compared to JDM lesional skin, and an overall more prominent endothelial cell–immune cell interaction in JDM. Magnification is the same as in **C**. See Figure 1 for definitions.

followed by CD8+ T cells (21%), pDCs (13.5%), B cells (12.2%), CD68+ macrophages (9.3%), CD4+ T cells (8.4%), and mDCs (5.6%).

**Higher innate immune signature, relative to adaptive immune signature, demonstrated by juvenile DM skin lesions compared to cSLE skin lesions.** Upon grouping



cells into an innate immune (macrophages and DCs) and adaptive immune (T cells and B cells) categorization, juvenile DM demonstrated a stronger innate immune signature compared to cSLE (74.9% versus 58.4%) (Figure 2B and Supplementary Table 2B, <https://onlinelibrary.wiley.com/doi/10.1002/art.42283>). The increased innate immune signature in juvenile DM skin lesions observed using IMC was also seen at the transcriptional level using xCell cell types enrichment analysis (see Patients and Methods) (11) (Figure 2C).

**Clinical cohort characteristics and inflammatory heterogeneity within individual skin lesions.** A high degree of variability existed in immune cell composition within individual patient skin lesions (Figure 2D), and these cellular data are accompanied by clinical and histopathologic data in Supplementary Table 1 (<https://onlinelibrary.wiley.com/doi/10.1002/art.42283>). While all juvenile DM skin lesions consistently had macrophages composing  $\geq 30\%$  of inflammatory infiltrate, the degree of T cell infiltrate varied (Figure 2D). The 2 juvenile DM patients (referred to in Figure 2 as JDM1 and JDM5) with skin-predominant disease at diagnosis had more T cell infiltrate, although these patients were also treatment-naïve. The 2 juvenile DM patients (JDM2 and JDM9) with prolonged disease duration at biopsy (5–6 versus 0 years for the rest of the juvenile DM cohort) demonstrated predominant innate immune signatures, although both were also receiving immunosuppressive therapy with at least methotrexate (Figure 2D). In the cSLE patient with isolated cutaneous lupus at biopsy and discoid lupus phenotype (referred to in Figure 2 as SLE21A), B cells predominated in the skin lesion (14) (Figure 2D and Supplementary Table 1).

**Endothelial cell-immune cell interactions characterize juvenile DM skin lesions.** Using neighborhood analysis to examine immune cell–immune cell interactions, juvenile DM demonstrated fewer overall interactions between immune cells (Figures 3A–C). In cSLE, pDCs and mDCs exhibited more interaction with other immune cells compared to juvenile DM. In both juvenile DM and cSLE, CD68+ macrophages had the least interaction with other cells. Both CD4+ and CD8+ T cells demonstrated interaction with most immune cells in both juvenile DM and cSLE (Figures 3A–C).

We then examined predicted cell–cell interactions with 2 important skin populations within both diseases: endothelial and epithelial cells. Intriguingly, cSLE skin displayed a higher number of positive cell–cell interactions for our identified immune cell populations with both epithelial and endothelial cells (Figures 3A and B). In contrast, juvenile DM skin demonstrated a striking contrast between endothelial and epithelial cell–immune cell interactions, with positive endothelial cell–immune cell interaction and epithelial cell–immune cell avoidance (Figure 3A). Of note, in juvenile DM, CD14+ macrophages displayed the strongest interaction with endothelial cells. This finding of endothelial cell–immune cell

interaction and epithelial cell–immune cell avoidance in juvenile DM was confirmed by visualizing spatial distribution of labeled cells, with a lack of noted proximity between immune and epithelial cells near the dermoepidermal junction but the presence of immune cells surrounding vasculature (Figure 3D). These data suggest that pathologic immune education in skin may involve not only immune cell–immune cell interactions, but that the epidermis may play a stronger role in pathogenic responses in cSLE compared to juvenile DM.

## DISCUSSION

In this study, we provide the first characterization of immune cell populations and cell–cell interactions within pediatric dermatomyositis and lupus lesional skin using IMC. We identified a more prominent innate immune signature in juvenile DM as compared to cSLE skin. While CD14+ and CD68+ macrophages were the most numerous immune cells composing juvenile DM skin lesions, cSLE had a more even distribution of innate and adaptive immune cells. Skin lesions in cSLE demonstrated denser inflammatory cell infiltrate, notably with higher absolute numbers of CD14+ macrophages, pDCs, and CD8+ T cells and an overall higher number of cell–cell interactions compared to juvenile DM. Unlike cSLE, juvenile DM patients had few B cells in skin lesions. When considering cell–cell interactions in juvenile DM, compared to cSLE, juvenile DM patients displayed a prominent endothelial cell–immune cell interaction and no significant epithelial cell–immune cell interactions with identified cell populations.

The use of IMC in this study allowed us to define immune cell populations in juvenile DM and cSLE with more granularity than previously possible. Our finding that CD14+ macrophages comprise the top immune cell population in juvenile DM skin is consistent with IMC data recently reported by Patel et al on adult DM lesional skin (5). In that study, CD14+ macrophages were also found to positively associate with skin disease activity (5). In contrast to that study, mDCs were not as prominent in juvenile DM skin within our cohort. A direct comparison of all cell populations identified between our cohort and the published adult DM cohort is challenging, given the use of different marker panels and the presence of unidentified clusters in both studies. There is likely more macrophage diversity in both juvenile DM and cSLE skin than we were able to identify using our marker panel. While we identified 2 macrophage populations, 4 populations were identified in adult DM skin, including CD14+, CD14+CD16+, phosphorylated stimulator of IFN genes–positive (p-STING+), and MAC387+ macrophages. The p-STING+ macrophage population in adult DM also displayed CD68 coexpression and may be included within our identified CD68+ macrophage population.

The finding of a stronger innate immune signature versus adaptive immune signature in juvenile DM compared to cSLE at both transcriptional and protein levels suggests differences in

pathophysiology. Consistent with this, our previously published gene expression data identified a stronger type II IFN signature in cSLE skin lesions compared to juvenile DM skin lesions (11), supporting a larger role for adaptive immunity in cSLE. While innate immunity likely plays an important role in both juvenile DM and cSLE pathogenesis, the influence of innate immune mechanisms in regulation of cutaneous inflammation in juvenile DM as compared to cSLE has not been well studied to date. In juvenile DM, skin disease as compared to muscle disease is often more resistant to treatment, and we may need to consider different treatment targets, potentially targeting the innate immune system, to improve skin disease and underlying vasculopathy.

The CD4:CD8 T cell ratio in juvenile DM skin within our study (0.9) was more equivalent than that identified in adult DM to date (5). In contrast, we identified a much lower CD4:CD8 T cell ratio in cSLE (0.4). The finding of an overall higher number of CD4+ T cells coexpressing CD11c in juvenile DM skin (cluster 17; Figures 1B and C) suggests that these cells could potentially represent invariant natural killer T (iNKT) cells or another activated T cell population (13). Invariant NKT cells represent less studied immune cells that bridge innate and adaptive immune response and serve as regulators of the immune response through secretion of cytokines, including IFN $\gamma$ , and play a role in cytotoxicity (13).

Our data suggest a striking contrast of positive endothelial cell-immune cell and avoidant epithelial cell-immune cell interactions in juvenile DM skin, supporting the notion that an underlying vasculopathic process occurs in skin, reflected clinically by pronounced nailfold capillary abnormalities that we often see in children. Previous reports that DM is characterized by marked expression of *MXA*, an IFN-inducible gene, in endothelial cells, whereas in SLE, *MXA* expression is often more prominent near areas of interface dermatitis would also align with our data (15). We do not fully understand the mechanisms connecting IFN to disease pathogenesis. Through further study of the relation of IFN to endothelial cell-immune cell interactions in juvenile DM, we may uncover disease-specific mechanisms.

It is important to emphasize that our findings should be interpreted in the context of markers present on our IMC panel. Other immune cells that potentially play important roles in juvenile DM can be included in future IMC antibody panels to further characterize immune cell subtypes and their variations in inflammatory cytokine and chemokine expression. Our study was also limited by small sample size and clinical heterogeneity within patient phenotypes and treatment status. Given retrospective data collection, we lacked the ability to collect detailed skin or systemic disease activity measures or paired fresh tissue or blood. Future analysis will include fresh tissue with paired blood to allow for in-depth clinical/mechanistic characterization.

Overall, the results of this study pave the way to better understand immunophenotypes in pediatric myositis and lupus and lend insight into the use of molecular and single-cell

signatures to target treatment based on predominant cell types in lesional tissue.

## ACKNOWLEDGMENTS

We express our many thanks to the myositis and lupus patients for generously sharing their samples for our work. We thank the Cure Juvenile Myositis and Rheumatology Research Foundation for supporting our work. We also thank the support of the University of Michigan CyTOF Core and the George M. O'Brien Michigan Kidney Translational Research Core Center (P30DK081943).

## AUTHOR CONTRIBUTIONS

All authors were involved in drafting the article or revising it critically for important intellectual content, and all authors approved the final version to be published. Dr. Turnier had full access to all of the data in the study and takes responsibility for the integrity of the data and the accuracy of the data analysis.

**Study conception and design.** Turnier, Wen, Kahlenberg.

**Acquisition of data.** Turnier, Yee, Madison, Rizvi, Wen, Kahlenberg.

**Analysis and interpretation of data.** Turnier, Yee, Berthier, Wen, Kahlenberg.

## REFERENCES

- Smith ES, Hallman JR, DeLuca AM, et al. Dermatomyositis: a clinicopathological study of 40 patients. *Am J Dermatopathol* 2009; 31:61–7.
- Wenzel J, Tuting T. An IFN-associated cytotoxic cellular immune response against viral, self-, or tumor antigens is a common pathogenic feature in "interface dermatitis." *J Invest Dermatol* 2008;128: 2392–402.
- Christen-Zaech S, Seshadri R, Sundberg J, et al. Persistent association of nailfold capillaroscopy changes and skin involvement over thirty-six months with duration of untreated disease in patients with juvenile dermatomyositis. *Arthritis Rheum* 2008;58:571–6.
- Giesen C, Wang HA, Schapiro D, et al. Highly multiplexed imaging of tumor tissues with subcellular resolution by mass cytometry. *Nat Methods* 2014;11:417–22.
- Patel J, Maddukuri S, Li Y, et al. Highly multiplexed mass cytometry identifies the immunophenotype in the skin of dermatomyositis. *J Invest Dermatol* 2021;141:2151–60.
- O'Gorman WE, Kong DS, Balboni IM, et al. Mass cytometry identifies a distinct monocyte cytokine signature shared by clinically heterogeneous pediatric SLE patients. *J Autoimmun* 2017. E-pub ahead of print.
- Lundberg IE, TjÄrnlund A, Bottai M, et al. 2017 European League Against Rheumatism/American College of Rheumatology classification criteria for adult and juvenile idiopathic inflammatory myopathies and their major subgroups. *Arthritis Rheumatol* 2017;69:2271–82.
- Hochberg MC. Updating the American College of Rheumatology revised criteria for the classification of systemic lupus erythematosus. *Arthritis Rheum* 1997;40:1725.
- Levine JH, Simonds EF, Bendall SC, et al. Data-driven phenotypic dissection of AML reveals progenitor-like cells that correlate with prognosis. *Cell* 2015;162:184–97.
- Schapiro D, Jackson HW, Raghuraman S, et al. histoCAT: analysis of cell phenotypes and interactions in multiplex image cytometry data. *Nat Methods* 2017;14:873–6.
- Turnier JL, Pachman LM, Lowe L, et al. Comparison of lesional juvenile myositis and lupus skin reveals overlapping yet

- unique disease pathophysiology. *Arthritis Rheumatol* 2021;73:1062–72.
12. Aran D, Hu Z, Butte, AJ. xCell: digitally portraying the tissue cellular heterogeneity landscape. *Genome Biol* 2017;18, 220.
13. Qualai J, Li LX, Cantero J, et al. Expression of CD11c is associated with unconventional activated T cell subsets with high migratory potential. *PLoS One* 2016;11:e0154253.
14. Abernathy-Close L, Lazar S, Stannard J, et al. B cell signatures distinguish cutaneous lupus erythematosus subtypes and the presence of systemic disease activity. *Front Immunol* 2021;12:775353.
15. Magro CM, Segal JP, Crowson AN, et al. The phenotypic profile of dermatomyositis and lupus erythematosus: a comparative analysis. *J Cutan Pathol* 2010;37:659–71.

# Increasing Prevalence of Antinuclear Antibodies in the United States

Gregg E. Dinse,<sup>1</sup> Christine G. Parks,<sup>2</sup> Clarice R. Weinberg,<sup>3</sup> Carol A. Co,<sup>1</sup> Jesse Wilkerson,<sup>1</sup> Darryl C. Zeldin,<sup>4</sup> Edward K. L. Chan,<sup>5</sup> and Frederick W. Miller<sup>6</sup>

**Objective.** Growing evidence suggests increasing frequencies of autoimmunity and autoimmune diseases, but findings are limited by the lack of systematic data and evolving approaches and definitions. This study was undertaken to investigate whether the prevalence of antinuclear antibodies (ANA), the most common biomarker of autoimmunity, changed over a recent 25-year span in the US.

**Methods.** Serum ANA were measured by standard indirect immunofluorescence assays on HEp-2 cells in 13,519 participants age  $\geq 12$  years from the National Health and Nutrition Examination Survey, with approximately one-third from each of 3 time periods: 1988–1991, 1999–2004, and 2011–2012. We used logistic regression adjusted for sex, age, race/ethnicity, and survey design variables to estimate changes in ANA prevalence across the time periods.

**Results.** The prevalence of ANA was 11.0% (95% confidence interval [95% CI] 9.7–12.6%) in 1988–1991, 11.4% (95% CI 10.2–12.8%) in 1999–2004, and 16.1% (95% CI 14.4–18.0%) in 2011–2012 ( $P$  for trend  $< 0.0001$ ), corresponding to ~22.3 million, ~26.6 million, and ~41.5 million affected individuals, respectively. Among adolescents age 12–19 years, ANA prevalence increased substantially, with odds ratios of 2.07 (95% CI 1.18–3.64) and 2.77 (95% CI 1.56–4.91) in the second and third time periods relative to the first ( $P$  for trend = 0.0004). ANA prevalence increased in both sexes (especially in men), older adults (age  $\geq 50$  years), and non-Hispanic white individuals. These increases in ANA prevalence were not explained by concurrent trends in weight (obesity/overweight), smoking exposure, or alcohol consumption.

**Conclusion.** The prevalence of ANA in the US has increased considerably in recent years. Additional studies to determine factors underlying these increases in ANA prevalence could elucidate causes of autoimmunity and enable the development of preventative measures.

## INTRODUCTION

Autoimmune diseases are a diverse group of disorders characterized by damaging immune responses to self antigens and, for the most part, are of unknown etiology (1,2). They are thought to impact 3–5% of the population, with increasing rates observed several

decades ago (3). Recent studies suggest continued increases in the rates of certain autoimmune diseases (4–6), but it is unclear whether these trends are due to changes in recognition and diagnosis, or if they are true temporal changes in incidence (7).

As the most common biomarker of autoimmunity, antinuclear antibodies (ANA) are observed in many patients with various

This article—originally published in *Arthritis & Rheumatology* 2020;72(6):1026–35 (<https://onlinelibrary.wiley.com/doi/10.1002/art.41214>)—was retracted by agreement among the authors, the journal Editor-in-Chief Daniel H. Solomon, MD, PhD, the American College of Rheumatology, and Wiley Periodicals LLC. The retraction was agreed upon due to the many corrections required because the Centers for Disease Control and Prevention removed some of the publicly released National Health and Nutrition Examination Survey (NHANES) data used in the original study and then released revised data; the retraction was not the result of any author wrongdoing or error. The corrections do not change the conclusions of the paper but are necessary for accuracy. The text, figure, and tables in <https://doi.org/10.1002/art.42330> have been updated to reflect the currently available NHANES data. The interpretation and conclusions contained herein are those of the authors and do not necessarily represent positions of any of the authors' affiliations.

Supported by the Intramural Research Program of the NIH, National Institute of Environmental Health Sciences under projects Z01-ES-025041 and Z01-ES-101074, and under contracts HHSN273201600011C and GS-00F-173CA/75N96021F00109 to Social & Scientific Systems, a DLH Holdings Corp. Company.

<sup>1</sup>Gregg E. Dinse, ScD, Carol A. Co, MS, Jesse Wilkerson, BS: Social & Scientific Systems, a DLH Holding Corp. Company, Durham, North Carolina; <sup>2</sup>Christine G. Parks, PhD: Epidemiology Branch, National Institute of Environmental Health Sciences, NIH, Durham, North Carolina; <sup>3</sup>Clarice R. Weinberg, PhD: Biostatistics and Computational Biology Branch, National Institute of Environmental Health Sciences, NIH, Durham, North Carolina; <sup>4</sup>Darryl C. Zeldin, MD: Division of Intramural Research, National Institute of Environmental Health Sciences, NIH, Durham, North Carolina; <sup>5</sup>Edward K. L. Chan, PhD: University of Florida Health Science Center, Gainesville, Florida; <sup>6</sup>Frederick W. Miller, MD, PhD: Clinical Research Branch, National Institute of Environmental Health Sciences, NIH, Durham, North Carolina.

Author disclosures are available at <https://onlinelibrary.wiley.com/action/downloadSupplement?doi=10.1002%2Fart.42330&file=art42330-sup-0001-Disclosureform.pdf>.

Address correspondence via email to Frederick W. Miller, MD, PhD, at [millerf@mail.nih.gov](mailto:millerf@mail.nih.gov).

Submitted for publication July 28, 2022; accepted in revised form August 11, 2022.

autoimmune diseases. ANA are also seen in the general population, where they have been associated with demographic factors such as older age, female sex and parity (8,9), genetic factors (10), and various environmental exposures, including chemicals, infections, and medications (11–13). To investigate whether the prevalence of autoimmunity is increasing over time in the US population, we used data from the National Health and Nutrition Examination Survey (NHANES) to estimate the prevalence of ANA over a 25-year span from 1988 to 2012.

## SUBJECTS AND METHODS

**Study population.** We measured ANA in 13,519 persons age  $\geq 12$  years sampled from 3 NHANES time periods: 1988–1991 (4,727 persons), 1999–2004 (4,527 persons), and 2011–2012 (4,265 persons). The NHANES sampled nationally representative members of the noninstitutionalized US population and provided weights to adjust for nonresponse and the probability of selection into each ANA subsample (14). All participants completed questionnaires, and most provided blood specimens. Available data included demographic characteristics, health covariates, measured factors (e.g., height and weight), and constructed variables such as body mass index (BMI). The NHANES protocol was approved by the Human Subjects Institutional Review Board of the US Centers for Disease Control and Prevention (CDC).

**Ethics committee approval.** Written informed consent was obtained from all participants. This study was approved by the US CDC research ethics board.

**ANA assessment.** Serum samples were shipped with dry ice and stored at  $-80^{\circ}\text{C}$  until evaluated by indirect immunofluorescence at a 1:80 dilution using the NOVA Lite HEp-2 ANA slide with DAPI kit (Inova Diagnostics), with a highly specific fluorescein isothiocyanate-conjugated secondary antibody (goat anti-human IgG). Images were captured using the NOVA View automated fluorescence microscope system (Inova Diagnostics) and stored digitally. Immunofluorescence staining intensities were graded using a 0–4 scale compared to standard references (8). Participants who had grades of 1–4 were positive for ANA; those with grades of 3 or 4 were further assessed by sequential ANA titers up to 1:1,280 dilution. ANA patterns, including nuclear, cytoplasmic, or mitotic, were defined according to international consensus (15). All serum samples were assayed using the same methods in a single laboratory. Readings were made independently by at least 2 experienced evaluators (who were blinded with regard to sample characteristics and time period), who agreed on  $>95\%$  of the intensities and patterns; differences were resolved by consensus or adjudicated by a third blinded rater (EKLC) who was also blinded with regard to sample characteristics. Repeat testing of random samples showed  $>98\%$  concordance.

**Participant characteristics.** We considered sex, age, and race/ethnicity as correlates of ANA and possible explanatory variables or modifiers of ANA time trends. Age was categorized by decade for covariate adjustment and categorized into 3 groups for stratification: adolescents (age 12–19 years), younger adults (age 20–49 years), or older adults (age  $\geq 50$  years). Race/ethnicity was categorized as non-Hispanic White, non-Hispanic African American, Mexican American, or other. Using previous covariate definitions (8), we also examined BMI, smoking exposure, alcohol consumption, poverty/income ratio, and education. The NHANES includes limited data on autoimmune diseases, but self-reports of physician-diagnosed thyroid disease were available for all participants age  $\geq 20$  years across the 3 time periods.

**Statistical analysis.** A dichotomous response variable was created by treating an ANA grade of 0 as negative and grades 1–4 as positive. We estimated time period-specific ANA prevalence overall and in subgroups defined by participant characteristics. Estimates and 95% confidence intervals (95% CIs) were derived from weighted logistic regression models for ANA positivity. The number of people age  $\geq 12$  years who were positive for ANA in the US population was estimated by multiplying the US Census Bureau's estimate of the time period-specific size of the NHANES target population by our time period-specific overall estimate of ANA prevalence. For each time period, we evaluated ANA associations with characteristic categories using prevalence odds ratios (ORs) and 95% CIs from weighted logistic models adjusted for sex, age, and race/ethnicity. The overall association of each characteristic with ANA was assessed by an F-test from a statistical contrast.

We investigated ANA time trends overall and in subgroups to explore trend modifiers. We fitted 2 logistic models to data from all 3 time periods and both models were adjusted for sex, age, and race/ethnicity. The first model included a categorical covariate for time period, from which ORs and 95% CIs were calculated to assess how ANA differed in the second and third time periods relative to the first. The second model included a quantitative covariate for the time between period midpoints (0, 12, or 22 years) and ANA time trends were assessed using a chi-square test. These exploratory analyses did not formally test if ANA time trends differed across subgroups. Supplemental analyses examined time trends in thyroid disease and the association between thyroid disease and ANA.

All analyses were performed using SAS version 9.4, and all analyses accounted for the survey design variables (strata, clusters, and sampling weights). The sampling weights allowed for population-representative estimates, adjusted for nonresponse and selection probabilities (14). We used the SURVEYLOGISTIC procedure to perform the logistic analyses, with domain statements to properly handle the sampling weights in subgroup analyses. Variance estimates for the 95% CIs were obtained using the Taylor series method. Reported *P* values were 2-sided and



unadjusted for multiple comparisons, though multiplying the *P* values by the number of comparisons would provide a conservative Bonferroni-type correction.

## RESULTS

### Participant characteristics and ANA prevalence.

Sample characteristics for each time period separately and combined are shown in Table 1. Certain characteristics changed over time (e.g., smoking decreased, whereas obesity and alcohol consumption increased). A total of 1,857 (13.7%) of the 13,519 participants were positive for ANA.

Adjustment for the survey design variables, but not for covariates, yielded population-representative ANA prevalence estimates of 11.0% (95% CI 9.7–12.6%) in 1988–1991, 11.4% (95% CI 10.2–12.8%) in 1999–2004, and 16.1% (95% CI 14.4–18.0%) in 2011–2012 for persons age  $\geq 12$  years (Figure 1 and

Table 2). These estimates correspond to ~22.3 million (95% CI 19.5–25.5), ~26.6 million (95% CI 23.8–29.8), and ~41.5 million (95% CI 37.2–46.4) ANA-positive persons, respectively. Time period-specific estimates of ANA prevalence in various subgroups are also shown in Figure 1 and Table 2.

**ANA correlates.** Weighted but unadjusted analyses supported several known associations, including higher ANA prevalence in women and older adults (Table 2). Among non-Hispanic participants, African American participants had a higher ANA prevalence than White participants in 1988–1991, but that difference was attenuated in 2011–2012 consequent to the greater increase over the same time period among White participants. Also, ANA prevalence was higher in nonsmokers than active smokers, and higher in participants who did not consume alcohol than in moderate/heavy alcohol consumers.

**Table 1.** Unweighted ANA positivity counts, sample sizes, and percentages of participants with indicated characteristics in each time period\*

Characteristic	Period 1 (1988–1991)		Period 2 (1999–2004)		Period 3 (2011–2012)		All periods combined	
	No. ANA positive	No. of participants (% of total)	No. ANA positive	No. of participants (% of total)	No. ANA positive	No. of participants (% of total)	No. ANA positive	No. of participants (% of total)
Overall	643	4,727 (100)	545	4,527 (100)	669	4,265 (100)	1,857	13,519 (100)
Sex								
Male	216	2,363 (50.0)	160	2,180 (48.2)	237	2,098 (49.2)	613	6,641 (49.1)
Female	427	2,364 (50.0)	385	2,347 (51.8)	432	2,167 (50.8)	1,244	6,878 (50.9)
Age, years								
Adolescent (age 12–19)	45	676 (14.3)	102	1,098 (24.3)	87	767 (18.0)	234	2,541 (18.8)
Younger adult (age 20–49)	248	2,218 (46.9)	176	1,827 (40.4)	239	1,808 (42.4)	663	5,853 (43.3)
Older adult (age $\geq 50$ )	350	1,833 (38.8)	267	1,602 (35.4)	343	1,690 (39.6)	960	5,125 (37.9)
Race/ethnicity								
Non-Hispanic White	252	2,060 (43.6)	240	2,060 (45.5)	256	1,566 (36.7)	748	5,686 (42.1)
Non-Hispanic African American	176	1,164 (24.6)	131	926 (20.5)	181	1,033 (24.2)	488	3,123 (23.1)
Mexican American	196	1,354 (28.6)	137	1,158 (25.6)	61	504 (11.8)	394	3,016 (22.3)
Other	19	149 (3.2)	37	383 (8.5)	171	1,162 (27.3)	227	1,694 (12.5)
Body mass index†								
Underweight/healthy (<25 kg/m <sup>2</sup> )	293	2,191 (46.5)	224	1,778 (39.4)	217	1,555 (37.1)	734	5,524 (41.2)
Overweight (25–<30 kg/m <sup>2</sup> )	197	1,483 (31.5)	151	1,405 (31.1)	204	1,214 (28.9)	552	4,102 (30.6)
Obese ( $\geq 30$ kg/m <sup>2</sup> )	150	1,036 (22.0)	169	1,334 (29.5)	232	1,427 (34.0)	551	3,797 (28.3)
Smoking exposure‡								
Nonsmoker (<0.05 ng/ml)	88	411 (9.1)	260	1,847 (41.1)	399	2,366 (55.5)	747	4,624 (34.8)
Secondhand (0.05–15 ng/ml)	352	2,788 (61.6)	197	1,654 (36.8)	146	1,039 (24.4)	695	5,481 (41.3)
Active (>15 ng/ml)	164	1,326 (29.3)	86	998 (22.2)	124	859 (20.2)	374	3,183 (24.0)
Alcohol consumption§								
None (<12 total)	349	2,009 (53.0)	156	1,011 (35.2)	161	814 (29.4)	666	3,834 (40.7)
Light (1–3 per week)	104	834 (22.0)	151	1,184 (41.2)	202	1,197 (43.3)	457	3,215 (34.1)
Moderate/heavy (>3 per week)	93	948 (25.0)	46	676 (23.6)	101	754 (27.3)	240	2,378 (25.2)

\* Some groups were oversampled in certain time periods (e.g., adolescents in 1999–2004 and Asian Americans [Other] in 2011–2012). ANA = antinuclear antibody.

† The categories were determined by kg/m<sup>2</sup> (as listed) for persons age  $\geq 20$  years and by US Centers for Disease Control and Prevention growth chart percentiles (<85, 85 to <95, or  $\geq 95$ ) from 2000 for persons age 12–19 years.

‡ Determined using current measured cotinine levels.

§ Data (number of drinks consumed in the past year) were available for participants age  $\geq 20$  years.

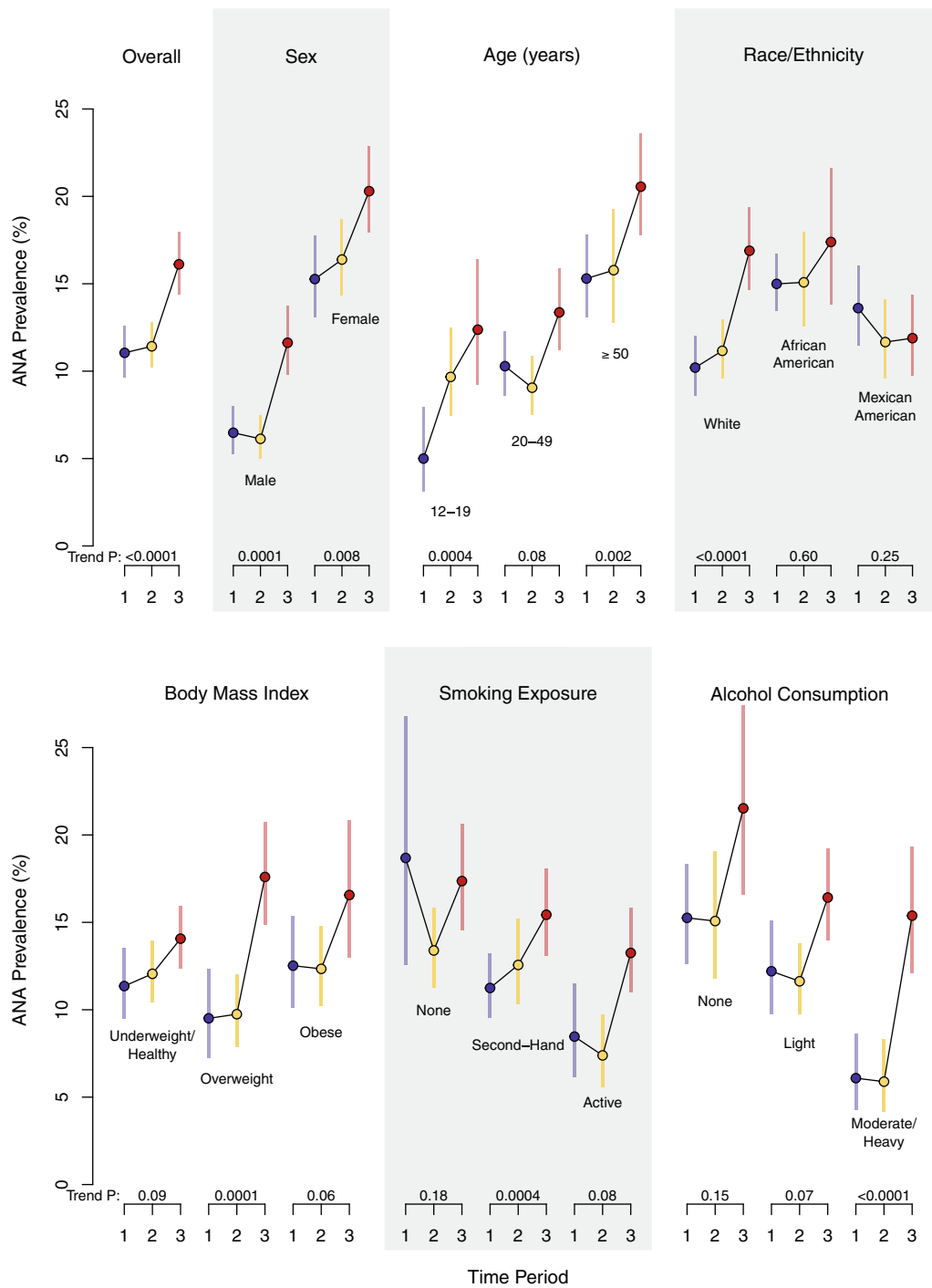


**Figure 1.** Estimated prevalence of antinuclear antibodies (ANA) by time period in the US population and selected subgroups. Circles represent weighted estimates of ANA prevalence, and vertical colored lines show the 95% confidence intervals for period 1 (1988–1991) (blue), period 2 (1999–2004) (yellow), and period 3 (2011–2012) (red). The estimates for the 3 time periods are connected by black lines to visualize time trends. For each time period, the prevalence estimate was derived from a logistic regression model for ANA positivity adjusted for the survey design variables (strata, clusters, and sampling weights) and a single categorical covariate for the characteristic defining the subgroup. Participants with missing subgroup data for body mass index, smoking exposure, or alcohol consumption were excluded from those analyses. *P* values for ANA time trends are displayed below each subgroup and were derived from a logistic regression model that was also adjusted for sex, age, and race/ethnicity.

**Table 2.** Weighted ANA prevalence estimates for participants with the indicated characteristics in each time period\*

Characteristic	Period 1 (1988–1991)	Period 2 (1999–2004)	Period 3 (2011–2012)
Overall	11.0 (9.7–12.6)	11.4 (10.2–12.8)	16.1 (14.4–18.0)
Sex			
Male	6.5 (5.2–8.0)	6.1 (5.0–7.5)	11.6 (9.8–13.7)
Female	15.3 (13.1–17.7)	16.4 (14.3–18.7)	20.3 (17.9–22.9)
Age, years			
Adolescent (age 12–19)	5.0 (3.1–7.9)	9.7 (7.5–12.5)	12.4 (9.2–16.4)
Younger adult (age 20–49)	10.3 (8.6–12.3)	9.1 (7.5–10.9)	13.4 (11.2–15.9)
Older adult (age ≥50)	15.3 (13.1–17.8)	15.8 (12.8–19.3)	20.6 (17.8–23.6)
Race/ethnicity			
Non-Hispanic White	10.2 (8.6–12.0)	11.2 (9.6–13.0)	16.9 (14.7–19.4)
Non-Hispanic African American	15.0 (13.4–16.7)	15.1 (12.6–18.0)	17.4 (13.8–21.6)
Mexican American	13.6 (11.5–16.0)	11.7 (9.6–14.1)	11.9 (9.8–14.4)
Other	12.0 (6.2–21.9)	9.3 (6.6–12.9)	14.0 (11.9–16.4)
Body mass index†			
Underweight/healthy (<25 kg/m <sup>2</sup> )	11.4 (9.5–13.5)	12.1 (10.4–13.9)	14.1 (12.4–15.9)
Overweight (25–<30 kg/m <sup>2</sup> )	9.5 (7.3–12.4)	9.7 (7.9–12.0)	17.6 (14.9–20.7)
Obese (≥30 kg/m <sup>2</sup> )	12.5 (10.1–15.4)	12.3 (10.2–14.8)	16.6 (13.0–20.9)
Smoking exposure‡			
Nonsmoker (<0.05 ng/ml)	18.7 (12.6–26.8)	13.4 (11.3–15.8)	17.4 (14.5–20.6)
Secondhand (0.05–15 ng/ml)	11.2 (9.5–13.2)	12.6 (10.3–15.2)	15.4 (13.1–18.1)
Active (>15 ng/ml)	8.5 (6.2–11.5)	7.4 (5.6–9.7)	13.3 (11.0–15.8)
Alcohol consumption§			
None (<12 total)	15.3 (12.6–18.3)	15.1 (11.8–19.1)	21.5 (16.6–27.4)
Light (1–3 per week)	12.2 (9.8–15.1)	11.6 (9.8–13.8)	16.4 (14.0–19.2)
Moderate/heavy (>3 per week)	6.1 (4.3–8.6)	5.9 (4.2–8.3)	15.4 (12.1–19.3)

\* Values are the weighted estimate of antinuclear antibody (ANA) prevalence (95% confidence interval [95% CI]) as a percentage. The weighted estimate of ANA prevalence was derived from a logistic regression model adjusted for the survey design variables (strata, clusters, and sampling weights) and a categorical covariate for the characteristic of interest but not for other covariates. The estimated numbers of persons with ANA in the US (with 95% CI) in millions are as follows: 22.3 (95% CI 19.5–25.5) for period 1, 26.6 (95% CI 23.8–29.8) for period 2, and 41.5 (95% CI 37.2–46.4) for period 3.

† The categories were determined by kg/m<sup>2</sup> (as listed) for persons age ≥20 years and by US Centers for Disease Control and Prevention growth chart percentiles (<85, 85 to <95, or ≥95) from 2000 for persons age 12–19 years.

‡ Determined using current measured cotinine levels.

§ Data (number of drinks consumed in the past year) were available for participants age ≥20 years.

Covariate-adjusted models confirmed several ANA correlates (Table 3). All 3 time periods showed an ANA association with sex ( $P < 0.0001$ ) and age ( $P \leq 0.003$ ), whereas evidence of an ANA association with other characteristics was either lacking or varied across time periods. The odds of having ANA were 2–3 times higher in women than men, with OR 2.53 (95% CI 1.90–3.36) in 1988–1991, OR 2.97 (95% CI 2.28–3.87) in 1999–2004, and OR 1.92 (95% CI 1.57–2.36) in 2011–2012. Similarly, the time period-specific ANA ORs for older adults relative to adolescents were OR 3.63 (95% CI 2.02–6.55), OR 1.75 (95% CI 1.19–2.56), and OR 1.76 (95% CI 1.20–2.56), for each respective time period. Relative to non-Hispanic White participants, the odds of having ANA were higher for non-Hispanic African American participants (OR 1.75 [CI 1.33–2.31]) and Mexican American participants (OR 1.87 [95% CI 1.40–2.50]) in 1988–1991, but racial/ethnic differences diminished in 1999–2004 and 2011–2012. Compared with being underweight/healthy, the time period-specific ANA associations with being overweight or obese transitioned from inverse to positive across the 3 time periods, though most 95% CIs included the null

value of 1.0. The ANA associations for active smokers versus nonsmokers were inverse in all 3 time periods, but most 95% CIs included 1.0. Compared with no alcohol consumption, moderate/heavy alcohol consumption was inversely associated with ANA in 1988–1991 (OR 0.56 [95% CI 0.34–0.92]) and 1999–2004 (OR 0.62 [95% CI 0.41–0.93]), but not in 2011–2012, as support for an overall ANA association with alcohol consumption decreased over time.

**ANA time trends.** There was strong evidence that ANA prevalence increased over time, primarily from the second time period to the third time period (Table 4). After adjustment for covariates, estimated ORs for the second time period and third time period relative to the first time period were 1.02 (95% CI 0.84–1.24) and 1.50 (95% CI 1.23–1.82), respectively, reflecting an overall ANA time trend ( $P < 0.0001$ ). In stratified analyses, the ANA time trend was seen in both men ( $P = 0.0001$ ) and women ( $P = 0.008$ ). Within age subgroups, the time trend was clearly apparent in adolescents ( $P = 0.0004$ ), with ORs that steadily increased across all time periods (from an OR of 1.00 to 2.07 to

**Table 3.** Covariate-adjusted ANA prevalence OR estimates among participants with indicated characteristics in each time period\*

Characteristic	Period 1 (1988–1991), OR (95% CI)	Period 2 (1999–2004), OR (95% CI)	Period 3 (2011–2012), OR (95% CI)
Sex			
Male	1.00 (reference)	1.00 (reference)	1.00 (reference)
Female	2.53 (1.90–3.36)	2.97 (2.28–3.87)	1.92 (1.57–2.36)
P†	< 0.0001	< 0.0001	< 0.0001
Age, years			
Adolescent (age 12–19)	1.00 (reference)	1.00 (reference)	1.00 (reference)
Younger adult (age 20–49)	2.27 (1.43–3.62)	0.92 (0.62–1.37)	1.07 (0.77–1.49)
Older adult (age ≥50)	3.63 (2.02–6.55)	1.75 (1.19–2.56)	1.76 (1.20–2.56)
P†	0.0007	0.002	0.003
Race/ethnicity			
Non-Hispanic White	1.00 (reference)	1.00 (reference)	1.00 (reference)
Non-Hispanic African American	1.75 (1.33–2.31)	1.52 (1.14–2.03)	1.08 (0.84–1.40)
Mexican American	1.87 (1.40–2.50)	1.31 (0.99–1.72)	0.80 (0.60–1.08)
Other	1.39 (0.62–3.13)	0.87 (0.57–1.33)	0.87 (0.67–1.11)
P†	0.0007	0.02	0.34
Body mass index‡			
Underweight/healthy (<25 kg/m <sup>2</sup> )	1.00 (reference)	1.00 (reference)	1.00 (reference)
Overweight (25–<30 kg/m <sup>2</sup> )	0.74 (0.54–1.02)	0.81 (0.60–1.10)	1.29 (1.03–1.61)
Obese (≥30 kg/m <sup>2</sup> )	0.90 (0.65–1.25)	0.99 (0.77–1.27)	1.15 (0.86–1.54)
P†	0.19	0.36	0.04
Smoking exposure§			
Nonsmoker (<0.05 ng/ml)	1.00 (reference)	1.00 (reference)	1.00 (reference)
Secondhand (0.05–15 ng/ml)	0.68 (0.44–1.05)	1.12 (0.85–1.48)	1.03 (0.80–1.33)
Active (>15 ng/ml)	0.56 (0.31–1.01)	0.69 (0.49–0.96)	0.82 (0.54–1.24)
P†	0.13	0.08	0.52
Alcohol consumption¶			
None (<12 total)	1.00 (reference)	1.00 (reference)	1.00 (reference)
Light (1–3 per week)	1.07 (0.70–1.63)	0.97 (0.67–1.41)	0.90 (0.64–1.27)
Moderate/heavy (>3 per week)	0.56 (0.34–0.92)	0.62 (0.41–0.93)	0.93 (0.62–1.38)
P†	0.03	0.05	0.82

\* The antinuclear antibody (ANA) association with each characteristic category relative to the reference category was assessed by estimating a period-specific odds ratio (OR) under a logistic regression model adjusted for the survey design variables (strata, clusters, and sampling weights) and categorical covariates for sex, age, race/ethnicity, and the characteristic of interest. 95% CI = 95% confidence interval.

† P values for assessing the ANA association with each characteristic overall were determined based on an F test from a statistical contrast.

‡ The categories were determined by kg/m<sup>2</sup> (as listed) for persons age ≥20 years and by US Centers for Disease Control and Prevention growth chart percentiles (<85, 85 to <95, or ≥95) from 2000 for persons age 12–19 years.

§ Determined using current measured cotinine levels.

¶ Data (number of drinks consumed in the past year) were available for participants age ≥20 years.

2.77). Although we observed no time trend in adults age 20–49 years, ANA prevalence increased over time in adults age ≥50 years ( $P = 0.002$ ). ANA time trends were also apparent in other subgroups (Table 4), notably non-Hispanic White participants, overweight participants, those exposed to secondhand smoke, and moderate/heavy drinkers. Further adjustment for BMI, smoking exposure, or alcohol consumption (in addition to sex, age, and race/ethnicity) had little impact on the ANA time trends.

**Supplemental analyses.** We performed supplemental analyses to assess possible ANA correlates and time trends within additional subgroups, such as those based on finer age groups (by decade), sex/age combinations, smoking history, poverty/income ratio, and education (see Supplementary Tables 1–4, available on the *Arthritis & Rheumatology* website

at <http://onlinelibrary.wiley.com/doi/10.1002/art.42330>). Though there was little indication of an overall ANA association with smoking history, poverty/income ratio, or education, we found strong evidence of increasing ANA time trends in the higher income subgroup ( $P = 0.0001$ ) and higher education subgroup ( $P = 0.0008$ ).

To further explore changes in ANA over time, we considered trends in ANA staining intensities, titers, and patterns in ANA-positive participants. None of these factors was informative, though there was weak evidence suggesting that mitotic patterns increased over time (Supplementary Table 5, <http://onlinelibrary.wiley.com/doi/10.1002/art.42330>).

We also investigated changes over time in the prevalence of thyroid disease and its association with ANA. The overall prevalence of self-reported, physician-diagnosed thyroid disease increased across the 3 time periods ( $P$  for trend <0.0001), as well as in various sex-by-age subgroups (Supplementary Table 6,

**Table 4.** Covariate-adjusted assessments of ANA time trends for participants in the indicated characteristic-based subgroups\*

Characteristic	ANA+/total no. of participants	Period (1988–1991), OR (95% CI)	Period 2 (1999–2004), OR (95% CI)	Period 3 (2011–2012), OR (95% CI)	P for trend
Overall	1,857/13,519	1.00 (reference)	1.02 (0.84–1.24)	1.50 (1.23–1.82)	<0.0001
Sex					
Male	613/6,641	1.00 (reference)	0.90 (0.67–1.22)	1.76 (1.32–2.35)	0.0001
Female	1,244/6,878	1.00 (reference)	1.07 (0.84–1.36)	1.37 (1.09–1.73)	0.008
Age, years					
Adolescent (age 12–19)	234/2,541	1.00 (reference)	2.07 (1.18–3.64)	2.77 (1.56–4.91)	0.0004
Younger adult (age 20–49)	663/5,853	1.00 (reference)	0.84 (0.63–1.13)	1.30 (0.99–1.73)	0.08
Older adult (age ≥50)	960/5,125	1.00 (reference)	1.07 (0.79–1.45)	1.52 (1.17–1.98)	0.002
Race/ethnicity					
Non-Hispanic White	748/5,686	1.00 (reference)	1.08 (0.84–1.38)	1.71 (1.34–2.18)	<0.0001
Non-Hispanic African American	488/3,123	1.00 (reference)	0.97 (0.75–1.24)	1.08 (0.81–1.45)	0.60
Mexican American	394/3,016	1.00 (reference)	0.81 (0.61–1.07)	0.82 (0.61–1.11)	0.25
Other	227/1,694	1.00 (reference)	0.73 (0.34–1.59)	1.15 (0.57–2.33)	0.45
Body mass index†					
Underweight/healthy (<25 kg/m <sup>2</sup> )	734/5,524	1.00 (reference)	1.04 (0.81–1.34)	1.24 (0.98–1.59)	0.09
Overweight (25–<30 kg/m <sup>2</sup> )	552/4,102	1.00 (reference)	1.01 (0.71–1.45)	1.98 (1.39–2.83)	0.0001
Obese (≥30 kg/m <sup>2</sup> )	551/3,797	1.00 (reference)	1.04 (0.75–1.44)	1.44 (0.97–2.12)	0.06
Smoking exposure‡					
Nonsmoker (<0.05 ng/ml)	747/4,624	1.00 (reference)	0.73 (0.45–1.18)	1.03 (0.63–1.69)	0.18
Secondhand (0.05–15 ng/ml)	695/5,481	1.00 (reference)	1.24 (0.93–1.65)	1.69 (1.30–2.20)	0.0004
Active (>15 ng/ml)	374/3,183	1.00 (reference)	0.81 (0.53–1.24)	1.43 (1.00–2.06)	0.08
Alcohol consumption§					
None (<12 total)	666/3,834	1.00 (reference)	0.96 (0.67–1.37)	1.39 (0.95–2.02)	0.15
Light (1–3 per week)	457/3,215	1.00 (reference)	0.85 (0.61–1.18)	1.29 (0.94–1.77)	0.07
Moderate/heavy (>3 per week)	240/2,378	1.00 (reference)	0.98 (0.58–1.63)	2.46 (1.58–3.84)	<0.0001

\* The antinuclear antibody (ANA) time trend assessments were based on 2 logistic regression models adjusted for the survey design variables (strata, clusters, and sampling weights) and categorical covariates for sex, age, and race/ethnicity. In one model, a categorical covariate for time period was added and the ANA prevalence odds ratio (OR) for each time period was estimated, relative to the first. In the other model, a quantitative covariate for the number of years between period midpoints, relative to the first, was added and a *P* value was determined by a chi-square test to assess an ANA time trend. 95% CI = 95% confidence interval.

† The categories were determined by kg/m<sup>2</sup> (as listed) for persons age ≥20 years and by US Centers for Disease Control and Prevention growth chart percentiles (<85, 85 to <95, or ≥95) from 2000 for persons age 12–19 years.

‡ Determined using current measured cotinine levels.

§ Data (number of drinks consumed in the past year) were available for participants age ≥20 years.

<http://onlinelibrary.wiley.com/doi/10.1002/art.42330>). In each time period, ANA rates were higher among those with thyroid disease (21–24%) compared to those without thyroid disease (12–16%).

## DISCUSSION

Most autoimmune diseases are persistent conditions, with unknown etiologies and diverse pathologic manifestations. They impact as many as 1 in 20 individuals in the adult US population, with substantial personal and societal costs. Recent studies suggest the incidence of some autoimmune diseases may be increasing (4–6). However, true temporal trends are difficult to determine due to the lack of national registries and changes in the assessment and diagnosis of specific diseases (16). We hypothesized that the prevalence of ANA, an objective and common biomarker of autoimmunity, may also have increased over time.

The NHANES databases and serum repositories provided a unique opportunity to assess this hypothesis in nationally

representative samples of the US population age ≥12 years across 3 time periods (1988–1991, 1999–2004, and 2011–2012). As expected, a considerable proportion of the population had ANA. Our novel and robust findings suggest that ANA prevalence increased substantially in the US over the 25-year timeframe examined, increasing from 11.0% in 1988–1991 to 11.4% in 1999–2004 to 16.1% in 2011–2012 for persons age ≥12 years, which corresponds to ~22.3 million, ~26.6 million, and ~41.5 million affected persons, respectively. We adjusted for sex, age, and race/ethnicity, and found positive ANA time trends overall and in certain subgroups. Further adjustment for key health characteristics, some of which have shifted in recent years (e.g., obesity, smoking exposure, and alcohol consumption), had little impact.

Increasing evidence suggests that autoantibodies precede the onset of symptomatic autoimmune disease by several years (17,18); thus, ANA may be intermediate markers on the pathway toward disease or may signal increased susceptibility to autoimmune diseases through related causal pathways. ANA have also



been associated with other factors, including chemical exposures, infections, medications, and parity (9,11–13), some of which are likely changing in frequency in the US population. Like ANA, autoimmune thyroid disease is more common in women and the likelihood of development increases with age (19). Additionally, an elevated prevalence of ANA has been seen in patients with thyroid disease (20). In exploratory analyses of the same samples of NHANES data, we observed both an increasing prevalence of self-reported thyroid disease and an association between thyroid disease and ANA. Because trends in ANA could be markers of increasing susceptibility to developing autoimmune diseases, the concurrent time trends in thyroid disease and ANA exemplify the potential clinical relevance of our broader findings.

Our previous research identified several ANA correlates (8). The present study confirmed that ANA prevalence increased with age and was relatively high in women and non-Hispanic African American participants. The numbers of individuals who are obese or overweight have increased dramatically in the US population, and though statistical support was weak, our results suggest a possibly shifting association between ANA prevalence and individuals who are overweight, from inverse associations in the first 2 time periods to a positive association in the third time period (when ANA prevalence also increased the most). Although higher BMI has been associated with risk of systemic autoimmune diseases, such as systemic lupus erythematosus (SLE) and rheumatoid arthritis (21,22), further study is needed to understand the relationship between ANA and BMI. While smoking is a risk factor for some autoimmune diseases, smoking appears to be protective for others (23). Active smoking was weakly associated with lower levels of ANA. Rates of smoking have decreased in the population, but inclusion of smoking in our models had little impact on the observed ANA time trends. The data also suggested a possible inverse association between ANA and alcohol consumption in the first 2 time periods. These findings are in part consistent with increasing evidence, including that from 2 recent prospective cohorts, of a possible protective role of moderate alcohol consumption on the risk of developing SLE (24,25). Thus, further investigation is needed to understand and expand on these concerns.

Our study had several strengths. The ANA subsamples were large, spanned 25 years, and were representative of the US population (age  $\geq 12$  years). Also, all ANA assays were performed in the same laboratory and used the same methods. In addition, our analyses accounted for sociodemographic factors and various health behaviors as potential trend modifiers.

However, our findings should be interpreted in the context of certain limitations: 1) associations were based on cross-sectional data rather than repeated measures; 2) some variables were self-reported, including the limited questionnaire data on autoimmune diseases; 3) ANA were not assessed in children age  $< 12$  years;

and 4) the NHANES excludes institutionalized participants, such as the elderly in residential care. Although some of the serum samples were 3 decades old, there were no gross differences in appearance or behavior of the samples to suggest degradation, and antibodies are known to be stable over time in frozen storage (26). Moreover, the observed time trends were not apparent in all subgroups, as might be expected if the age of the specimens influenced the measured levels of ANA.

Pisetsky and colleagues (27) reconfirmed that different ANA assay kits can give different results. They were interested in assessing variation in ANA assays and thus used 3 ANA kits, an ANA enzyme-linked immunosorbent assay, and a bead-based multiplex assay, whereas we purposely used a single assay (performed in 1 laboratory) to provide as much consistency as possible in our evaluation of ANA changes over time. We used the NOVA View system due to familiarity, previous positive experiences, and the need to improve efficiency for the large number of samples in our study by using a semiautomated system. Thus, we were restricted to the ANA assay that accompanied the system and we knew that this assay could detect some autoantibodies that others could not (e.g., autoantibodies to cytoplasmic rods and rings). Using another assay could have led to systematically higher or lower ANA prevalence estimates, but we focused on trends across the time periods. Even if time period-specific estimates shifted upward or downward with one assay versus another, presumably the same trends would be seen across time periods.

The reported  $P$  values were not adjusted for multiple comparisons, and some apparent trends and associations could be due to chance. Nevertheless, our main finding that ANA prevalence increased over time is consistent, with  $P \leq 0.0001$  for the trend overall and in many subgroups, so these  $P$  values would remain noteworthy even after making conservative Bonferroni adjustments that multiply by the number of comparisons.

The standard HEP-2 assay for ANA detects a heterogeneous group of autoantibodies and is a commonly used diagnostic tool in a clinical context (15). However, relatively little is known about the natural history of ANA in the absence of an autoimmune disease. Given that memory B cells typically persist once tolerance to self antigens is broken, currently detected ANA may reflect both past and recent exposures. Our cross-sectional data did not allow us to determine the timing of ANA development relative to aging and other factors, such as smoking; however, observed differences across demographic subgroups or covariates suggest research opportunities to better understand the determinants of autoimmunity and autoimmune diseases. The ANA staining pattern is an important consideration for understanding the relevance of ANA in symptomatic and healthy populations. A dense fine speckled pattern of staining has been associated with anti-dense fine speckled 70 autoantibodies and may be more common in healthy individuals than in those with autoimmune diseases (28,29). However, neither a dense fine speckled pattern of

staining nor other ANA patterns appeared to explain the increasing ANA time trends observed in our study. The autoantigens recognized by the mitotic staining pattern, which showed weak evidence of increasing over time, are poorly understood and have uncertain clinical implications (15,30).

Although ANA prevalence increased across the 3 periods in many subgroups, the rate and timing of this increase were not always the same, especially with respect to age. Reasons for the generation of ANA at different times across the lifespan may vary. For example, the incidence of ANA in older adults may be related to immunosenescence (31) or to exposures that increase with age, such as medications. Notably, while ANA prevalence was highest in adults age  $\geq 70$  years, it varied little over time in this age group (20.9–24.5%) (Supplementary Table 2, <http://onlinelibrary.wiley.com/doi/10.1002/art.42330>). In contrast, ANA prevalence in adolescents age 12–19 years increased dramatically from 5.0% to 9.7% to 12.4% across the 3 time periods. While investigations of ANA in healthy children are limited (32,33), potential explanations for an increase in ANA prevalence include changes in perinatal or early-life exposures, such as childhood infections or other types of exposures during developmentally sensitive periods, possibly leading to dysregulated immunity. The rising ANA time trend observed in this age group may be particularly concerning if ANA are harbingers of increased susceptibility to future autoimmune diseases.

In conclusion, the overall prevalence of ANA in the US increased from 1988 to 2012, with a greater increase in recent years. Both sex and age were consistently strong ANA correlates, while ANA associations with race/ethnicity, BMI, smoking exposure, and alcohol consumption varied over time. The positive ANA time trends were most pronounced in adolescents, men, and non-Hispanic White participants. Additional studies to complement our exploratory investigation, particularly of the aforementioned sociodemographic groups, should be the focus of future research to determine the driving forces underlying these ANA increases and to inform the development of possible preventative measures.

## ACKNOWLEDGMENTS

We thank Drs. Charles Dillon, Helen Meier, and Paivi Salo for their helpful comments, Justin Nicholas and Rodrigo Mora for technical laboratory assistance, and Dr. Geraldine McQuillan for administrative and regulatory assistance. We also thank Wayne Pereanu for technical editing and the members of the NHANES Autoimmunity Study Group (including Drs. Linda Birnbaum, Richard Cohn, Dori Germolec, Minoru Satoh, Nigel Walker, and Irene Whitt) for initiating the studies that motivated much of this research. We thank Dr. Michael Mahler (Inova Diagnostics) for providing the use of the NOVA View automated fluorescence microscope system for data collection.

## AUTHOR CONTRIBUTIONS

All authors were involved in drafting the paper or revising it critically for important intellectual content, and all authors approved the final version. Dr. Miller had full access to all of the data in the study and takes

responsibility for the integrity of the data and the accuracy of the data analysis.

**Study conception and design.** Dinse, Parks, Weinberg, Zeldin, Chan, Miller.

**Acquisition of data.** Dinse, Co, Wilkerson, Chan.

**Analysis and interpretation of data.** Dinse, Parks, Weinberg, Co, Wilkerson, Zeldin, Chan, Miller.

## REFERENCES

- Davidson A, Diamond B. Autoimmune diseases. *N Engl J Med* 2001; 345:340–50.
- Wang L, Wang FS, Gershwin ME. Human autoimmune diseases: a comprehensive update. *J Intern Med* 2015;278:369–95.
- Bach JF. The effect of infections on susceptibility to autoimmune and allergic diseases. *N Engl J Med* 2002;347:911–20.
- Lerner A, Matthias T. The world incidence and prevalence of autoimmune diseases is increasing. *Int J of Celiac Dis* 2015;3:151–5.
- Fatoye F, Gebrye T, Svenson LW. Real-world incidence and prevalence of systemic lupus erythematosus in Alberta, Canada. *Rheumatol Int* 2018;38:1721–6.
- Mayer-Davis EJ, Lawrence JM, Dabelea D, et al. Incidence trends of type 1 and type 2 diabetes among youths, 2002–2012. *N Engl J Med* 2017;376:1419–29.
- Schmidt CW. Questions persist: environmental factors in autoimmune disease. *Environ Health Perspect* 2011;119:A249–53.
- Satoh M, Chan EK, Ho LA, et al. Prevalence and sociodemographic correlates of antinuclear antibodies in the United States. *Arthritis Rheum* 2012;64:2319–27.
- Parks CG, Miller FW, Satoh M, et al. Reproductive and hormonal risk factors for antinuclear antibodies (ANA) in a representative sample of U.S. women. *Cancer Epidemiol Biomarkers Prev* 2014;23:2492–502.
- Liao KP, Kurreeman F, Li G, et al. Associations of autoantibodies, autoimmune risk alleles, and clinical diagnoses from the electronic medical records in rheumatoid arthritis cases and non-rheumatoid arthritis controls. *Arthritis Rheum* 2013;65:571–81.
- Chang C, Gershwin ME. Drugs and autoimmunity—a contemporary review and mechanistic approach. *J Autoimmun* 2010;34:J266–75.
- Miller FW, Alfredsson L, Costenbader KH, et al. Epidemiology of environmental exposures and human autoimmune diseases: findings from a National Institute of Environmental Health Sciences expert panel workshop. *J Autoimmun* 2012;39:259–71.
- Dinse GE, Jusko TA, Whitt IZ, et al. Associations between selected xenobiotics and antinuclear antibodies in the National Health and Nutrition Examination Survey, 1999–2004. *Environ Health Perspect* 2016;124:426–36.
- Johnson CL, Paulose-Ram R, Ogden CL, et al. National health and nutrition examination survey: analytic guidelines, 1999–2010. *Vital Health Stat* 2013;1–24.
- Damoiseaux J, Andrade LE, Carballo OG, et al. Clinical relevance of HEp-2 indirect immunofluorescent patterns: the International Consensus on ANA patterns (ICAP) perspective. *Ann Rheum Dis* 2019;78: 879–89.
- Ungprasert P, Sagar V, Crowson CS, et al. Incidence of systemic lupus erythematosus in a population-based cohort using revised 1997 American College of Rheumatology and the 2012 Systemic Lupus International Collaborating Clinics classification criteria. *Lupus* 2017;26:240–7.
- Arbuckle MR, McClain MT, Rubertone MV, et al. Development of autoantibodies before the clinical onset of systemic lupus erythematosus. *N Engl J Med* 2003;349:1526–33.

18. Lingampalli N, Sokolove J, Lahey LJ, et al. Combination of anti-citrullinated protein antibodies and rheumatoid factor is associated with increased systemic inflammatory mediators and more rapid progression from preclinical to clinical rheumatoid arthritis. *Clin Immunol* 2018;195:119–26.
19. Stathatos N, Daniels GH. Autoimmune thyroid disease. *Curr Opin Rheumatol* 2012;24:70–5.
20. Tektonidou MG, Anapliotou M, Vlachoyiannopoulos P, et al. Presence of systemic autoimmune disorders in patients with autoimmune thyroid diseases. *Ann Rheum Dis* 2004;63:1159–61.
21. Tedeschi SK, Barbhaiya M, Malspeis S, et al. Obesity and the risk of systemic lupus erythematosus among women in the Nurses' Health Studies. *Semin Arthritis Rheum* 2017;47:376–83.
22. Tedeschi SK, Cui J, Arkema EV, et al. Elevated BMI and antibodies to citrullinated proteins interact to increase rheumatoid arthritis risk and shorten time to diagnosis: a nested case-control study of women in the Nurses' Health Studies. *Semin Arthritis Rheum* 2017;46:692–8.
23. Perricone C, Versini M, Ben-Ami D, et al. Smoke and autoimmunity: the fire behind the disease [review]. *Autoimmun Rev* 2016;15:354–74.
24. Cozier YC, Barbhaiya M, Castro-Webb N, et al. Relationship of cigarette smoking and alcohol consumption to incidence of systemic lupus erythematosus in a prospective cohort study of Black women. *Arthritis Care Res (Hoboken)* 2019;71:671–7.
25. Barbhaiya M, Lu B, Sparks JA, et al. Influence of alcohol consumption on the risk of systemic lupus erythematosus among women in the Nurses' Health Study cohorts. *Arthritis Care Res (Hoboken)* 2017;69:384–92.
26. Argentieri MC, Pilla D, Vanzati A, et al. Antibodies are forever: a study using 12-26-year-old expired antibodies. *Histopathology* 2013;63:869–76.
27. Pisetsky DS, Spencer DM, Lipsky PE, et al. Assay variation in the detection of antinuclear antibodies in the sera of patients with established SLE. *Ann Rheum Dis* 2018;77:911–3.
28. Mariz HA, Sato EI, Barbosa SH, et al. Pattern on the antinuclear antibody–HEp-2 test is a critical parameter for discriminating antinuclear antibody–positive healthy individuals and patients with autoimmune rheumatic diseases. *Arthritis Rheum* 2011;63:191–200.
29. Mahler M, Andrade LE, Casiano CA, et al. Implications for redefining the dense fine speckled and related indirect immunofluorescence patterns [review]. *Expert Rev Clin Immunol* 2019;15:447–8.
30. Chan EK, Damoiseaux J, Carballo OG, et al. Report of the First International Consensus on standardized nomenclature of antinuclear antibody HEp-2 cell patterns 2014-2015. *Front Immunol* 2015;6:412.
31. Weyand CM, Goronzy JJ. Aging of the immune system. Mechanisms and therapeutic targets. *Ann Am Thorac Soc* 2016;13 Suppl:S422–8.
32. Sperotto F, Cuffaro G, Brachi S, et al. Prevalence of antinuclear antibodies in schoolchildren during puberty and possible relationship with musculoskeletal pain: a longitudinal study. *J Rheumatol* 2014;41:1405–8.
33. Hilario MO, Len CA, Roja SC, et al. Frequency of antinuclear antibodies in healthy children and adolescents. *Clin Pediatr (Phila)* 2004;43:637–42.

## LETTERS

DOI 10.1002/art.42303

### Systemic glucocorticoids confound SARS-CoV-2 acquisition or even clinical outcomes in patients with autoimmune disease treated with biologics: comment on the article by Simon et al

To the Editor:

We read with great interest the brief report by Dr. Simon et al (1) in which they assessed the immune responses to SARS-CoV-2 infection or vaccination against SARS-CoV-2 in 14 patients with autoimmune disease (AID) and B cell depletion. Serum samples from AID patients treated with rituximab who had SARS-CoV-2 infection and those who were vaccinated against SARS-CoV-2 had lower levels of IgG antibodies against the S1 domain of the spike protein (mean  $\pm$  SD at optical density of 450 nm,  $2.9 \pm 2.2$  and  $0.2 \pm 0.3$ , respectively) than healthy controls (mean  $\pm$  SD  $5.4 \pm 2.5$ ). These findings suggest that B cell depletion may be associated with an increased risk of COVID-19 acquisition or even adverse outcomes in AID patients.

We note that, although Simon et al stated that a large limitation was the small number of patients with B cell depletion who were exposed to SARS-CoV-2 infection or vaccination, there was no information in the article on whether biologic medications with or without concomitant glucocorticoids were given, with glucocorticoids deemed as a confounding factor. Glucocorticoids lead to broad immunosuppressive effects and are recommended by current guidelines as part of the standard care for AID (2). In a national cohort from The Netherlands (3), glucocorticoids were used alone or combined with biologics in 6% and 45% of AID patients, respectively.

Studies conducted during the COVID-19 pandemic showed that systemic glucocorticoids increased the risk of SARS-CoV-2 acquisition or even resulted in adverse outcomes. In a retrospective cohort study of 213 AID patients from Detroit, glucocorticoids were associated with a 5.48-fold increased rate of hospital admission among those who tested positive for SARS-CoV-2 (odds ratio [OR] 5.48, 95% confidence interval [95% CI] 1.28–26.1) (4). In a meta-analysis of COVID-19 susceptibility in AID patients, Fagni et al (5) stated that use of 2.5 mg or more of prednisone daily was associated with a significantly higher probability of SARS-CoV-2 acquisition (OR 2.89, 95% CI 1.26–6.62) and use of 10 mg or more of prednisone daily was associated with a doubled risk of hospitalization (OR 2.05, 95% CI 1.06–3.96). However, although the relative risk associated with glucocorticoids has been generally shown as linear to daily dosage and treatment duration (6), information on the effects of glucocorticoids plus



biologics on SARS-CoV-2 acquisition in AID patients remains scarce.

We suggest that the available data do not show that glucocorticoids on their own increase the risk of SARS-CoV-2 acquisition or even the risk of adverse outcomes. First, AID patients often receive courses of systemic glucocorticoids to reduce disease activity during the initial episode and the subsequent flares, and thus a broad overlap is found between glucocorticoid usage and disease activity (7). Thus far, studies have not yet shown which of these 2 variables is the major contributor to risk.

Second, patients with connective tissue diseases (CTDs) have a higher risk of SARS-CoV-2 acquisition than patients without CTDs. In a meta-analysis that comprised 319,025 patients from 62 studies, CTD patients had the highest prevalence of COVID-19 (3.4%) compared with other AIDs, which is likely due to the higher proportion of patients with CTDs versus other AIDs who use glucocorticoids (60.3%) (8).

Third, an increased risk of SARS-CoV-2 acquisition associated with glucocorticoid usage comes as a consequence of pandemic outcomes in low-resource settings (9,10). AID patients in low-resource settings may potentially be exposed to factors that result in adverse outcomes compared with their counterparts in high-income countries.

Author disclosures are available at <https://onlinelibrary.wiley.com/action/downloadSupplement?doi=10.1002%2Fart.42303&file=art42303-sup-0001-Disclosureform.pdf>.

Man-Man Niu, MD  
Qi Jiang, MD   
Yan-Fang Zhang, MD  
Dao-Ting Li, MD  
Qian Yang, MD  
Peng Hu, PhD   
[hupeng28@aliyun.com](mailto:hupeng28@aliyun.com)  
Department of Pediatrics  
The First Affiliated Hospital  
of Anhui Medical University  
Hefei, China

1. Simon D, Tascilar K, Schmidt K, et al. Humoral and cellular immune responses to SARS-CoV-2 infection and vaccination in autoimmune disease patients with B cell depletion. *Arthritis Rheumatol* 2022;74:33–7.
2. Fraenkel L, Bathon JM, England BR, et al. 2021 American College of Rheumatology guideline for the treatment of rheumatoid arthritis. *Arthritis Rheumatol* 2021;73:1108–23.
3. Wieske L, van Dam KP, Steenhuis M, et al. Humoral responses after second and third SARS-CoV-2 vaccination in patients with immune-mediated inflammatory disorders on immunosuppressants: a cohort study. *Lancet Rheumatol* 2022;4:e338–50.

4. Veenstra J, Buechler CR, Robinson G, et al. Antecedent immunosuppressive therapy for immune-mediated inflammatory diseases in the setting of a COVID-19 outbreak. *J Am Acad Dermatol* 2020;83:1696–703.
5. Fagni F, Simon D, Tascilar K, et al. COVID-19 and immune-mediated inflammatory diseases: effect of disease and treatment on COVID-19 outcomes and vaccine responses. *Lancet Rheumatol* 2021;3:e724–36.
6. Gianfrancesco M, Hyrich KL, Al-Adely S, et al. Characteristics associated with hospitalisation for COVID-19 in people with rheumatic disease: data from the COVID-19 Global Rheumatology Alliance physician-reported registry. *Ann Rheum Dis* 2020;79:859–66.
7. Barnes PJ, Adcock IM. Glucocorticoid resistance in inflammatory diseases. *Lancet* 2009;373:1905–17.
8. Akiyama S, Hamdeh S, Micic D, Sakuraba A. Prevalence and clinical outcomes of COVID-19 in patients with autoimmune diseases: a systematic review and meta-analysis. *Ann Rheum Dis* 2021;80:384–91.
9. Barber MR, Clarke AE. Socioeconomic consequences of systemic lupus erythematosus. *Curr Opin Rheumatol* 2017;29:480–5.
10. Águas R, Mahdi A, Shretta R, et al. Potential health and economic impacts of dexamethasone treatment for patients with COVID-19. *Nat Commun* 2021;12:915.

DOI 10.1002/art.42305

## Reply

### To the Editor:

We thank Dr. Niu and colleagues for their remark that prolonged glucocorticoid treatment increases the susceptibility to COVID-19 acquisition and decreases the response to vaccination (1). In relation to our study, the authors asked about the potential effects of concomitant glucocorticoid therapy on blunted vaccination responses in rituximab-treated patients with AID. It has been known since the 1970s that glucocorticoids reduce T cell (2,3) and B cell (4,5) activation and thereby inhibit mounting of adaptive immune responses against infections.

When interrogating whether background glucocorticoid treatment could have added to the reduced immune responses to vaccination or infection with SARS-CoV-2, we found no major exposure to glucocorticoid treatment in this cohort. Only 3 patients (1 vaccinated and 2 infected with SARS-CoV-2) were receiving glucocorticoids. Furthermore, doses of glucocorticoids were low (mean  $\pm$  SD 4.6  $\pm$  3.8 mg prednisolone/day). Hence, it is unlikely that the background glucocorticoids were responsible for the impaired immune response in the vaccinated patients or the patients with SARS-CoV-2 infection.

Another potential source of glucocorticoids in this context is their administration in combination with rituximab infusion, in which patients receive a single shot of 25 mg of prednisolone together with rituximab infusion. Previous data from patients with shock (6) and those experiencing asthma episodes (7,8), in whom systemic bolus glucocorticoids are also frequently used for short-term treatment, have not shown that such treatment affected the responses to tetanus (6) or influenza vaccines (7,8). Short-term glucocorticoid treatment also did not seem to affect the immune

response to the SARS-CoV-2 vaccine (9). Therefore, we cannot assume that the single dose of glucocorticoids significantly contributed to the observed blunted humoral immune responses to SARS-CoV-2 in rituximab-treated patients.

The observation that T cell responses are maintained, while B cell responses are severely suppressed, in rituximab-treated patients with AIDs supports a specific effect of B cell-depleting agents rather than of glucocorticoids that would also impair T cell activation. These findings and the comments raised by Niu and colleagues, however, also suggest that continuous higher doses of glucocorticoids may be problematic in B cell-depleted patients, as immune responses to infection and vaccinations largely depend on intact T cell responses if B cells are absent.

Georg Schett, MD   
[georg.schett@uk-erlangen.de](mailto:georg.schett@uk-erlangen.de)  
 David Simon, MD   
 Filippo Fagni, MD   
 Korey Tascilar, MD   
 Department of Internal Medicine 3  
 Deutsches Zentrum fuer Immuntherapie  
 Friedrich-Alexander University Erlangen-Nuremberg  
 and Universitätsklinikum Erlangen  
 Erlangen, Germany

1. Fagni F, Simon D, Tascilar K, et al. COVID-19 and immune-mediated inflammatory diseases: effect of disease and treatment on COVID-19 outcomes and vaccine responses. *Lancet Rheumatol* 2021;3:e724–36.
2. Fauci AS, Dale DC. The effect of in vivo hydrocortisone on subpopulations of human lymphocytes. *J Clin Invest* 1974;53:240–6.
3. Saxon A, Stevens RH, Ramer SJ, et al. Glucocorticoids administered in vivo inhibit human suppressor T lymphocyte function and diminish B lymphocyte responsiveness in in vitro immunoglobulin synthesis. *J Clin Invest* 1978;61:922–30.
4. Fauci AS, Pratt KR, Whalen G. Activation of human B lymphocytes. IV. Regulatory effects of corticosteroids on the triggering signal in the plaque-forming cell response of human peripheral blood B lymphocytes to polyclonal activation. *J Immunol* 1977;119:598–603.
5. Grayson J, Dooley NJ, Koski IR, et al. Immunoglobulin production induced in vitro by glucocorticoid hormones: t cell-dependent stimulation of immunoglobulin production without B cell proliferation in cultures of human peripheral blood lymphocytes. *J Clin Invest* 1981;68:1539–47.
6. Johnson JR, Denis R, Lucas CE, et al. The effect of steroids for shock on the immune response to tetanus toxoid. *Am Surg* 1987;53:389–91.
7. Fairchok MP, Tremontozzi DP, Carter PS, et al. Effect of prednisone on response to influenza virus vaccine in asthmatic children. *Arch Pediatr Adolesc Med* 1998;152:1191–5.
8. Park CL, Frank AL, Sullivan M, et al. Influenza vaccination of children during acute asthma exacerbation and concurrent prednisone therapy. *Pediatrics* 1996;98:196–200.
9. Yang J, Ko JH, Baek JY, et al. Effects of short-term corticosteroid use on reactogenicity and immunogenicity of the first dose of ChAdOx1 nCoV-19 vaccine. *Front Immunol* 2021;12:744206.



DOI 10.1002/art.42302

# Optimal bridging strategy in active early rheumatoid arthritis: a bridge falling short? Comment on the article by Krause et al

To the Editor:

We read with great interest the article by Dr. Krause et al, who reported results from the Corticoid Bridging in Rheumatoid Arthritis (CORRA) trial. The authors compared a high-dose glucocorticoid (GC) bridging strategy, a low-dose GC bridging strategy, and placebo during a 12-week intervention period in a cohort of patients with early rheumatoid arthritis (RA) and concluded that the short-term GC bridging strategy with prednisolone had no benefit in slowing the radiologic progression of RA (1). However, certain points need clarification.

First, we would like to comment on the period of GC bridging therapy used in their study. Patients in the Combinatietherapie Bij Reumatoide Artritis (COBRA) trial, an early study, who were given GC bridging (60 mg/day, tapered to 7.5 mg/day) for 28 weeks experienced a slowed rate of radiographic RA progression, which persisted in the subsequent 4–5 years of follow-up (2). The subsequent COBRA Light (30 mg/day, tapered to 7.5 mg/day) and COBRA Slim (30 mg/day, tapered to 5 mg/day) trials also showed a similar beneficial effect of GC bridging with a much lower cumulative dose of GCs (3,4). In the Computer-Assisted Management in Early Rheumatoid Arthritis II trial, patients who used 10 mg of prednisolone with methotrexate for 2 years experienced improved radiologic outcomes, which remained significantly improved, even at 4 years, without any long-term safety concerns (5,6). Thus, we suggest that the lack of benefits in radiologic outcome in the CORRA trial may have been because of the short duration of bridging GC therapy and that a longer period of bridging GC therapy may have resulted in a beneficial effect.

Second, in a similar study conducted in early RA patients with a treat-to-target strategy, Bakker et al reported that GC bridging with low-dose prednisolone significantly improved the radiologic outcomes (5). However, of note, most patients included in the study from Bakker et al had almost no radiographic erosion at baseline (at baseline, the median erosion score was 0 [range 0–1], and erosive damage was present in 17% of patients who were given prednisolone and methotrexate). On the other hand, Krause et al reported a mean erosion score of 2.1 in all of the study groups. In early RA, baseline erosion has been shown to be a predictor of further progression of erosion (7). Thus, the higher erosion score at baseline in the CORRA study may be a reason behind the lack of significant improvements in radiologic outcomes with GC bridging. It would be interesting to know whether GC bridging would affect radiologic outcomes in the subgroup of patients with no or minimal erosion at baseline.

Finally, the authors concluded that, although there were differences in disease activity and patient-reported outcomes at

12 weeks, these differences were not sustained at week 24 and week 52. However, of note, all patients received treatment per the physician's discretion during the 40-week observation period, which included use of GCs in the placebo group during that period. This was reflected by the lack of any significant differences in the cumulative GC dose between the placebo group and both of the prednisolone groups during the 40-week observation period. This liberal use of GCs may have contributed to the lack of difference in disease activity outcomes and patient-reported outcomes between the placebo and prednisolone groups at 24 and 52 weeks.

Author disclosures are available at <https://onlinelibrary.wiley.com/action/downloadSupplement?doi=10.1002%2Fart.42302&file=art42302-sup-0001-Disclosureform.pdf>.

Joydeep Samanta, MD, DM   
Alekhya Amudalapalli, MD  
Ashlesha Shukla, MD  
BV Harish, MD  
Sudhish Gadde, MD  
Rasmi R. Sahoo, MD, DM   
Pradeepta S. Patro, MD, DM  
[drpradeepta07@gmail.com](mailto:drpradeepta07@gmail.com)  
Department of Rheumatology  
Institute of Medical Sciences  
and SUM Hospital  
Bhubaneswar, India

1. Krause D, Mai A, Klaassen-Mielke R, et al. The efficacy of short-term bridging strategies with high- and low-dose prednisolone on radiographic and clinical outcomes in active early rheumatoid arthritis: a double-blind, randomized, placebo-controlled trial. *Arthritis Rheumatol* 2022;74:1628–37.
2. Landewé RB, Boers M, Verhoeven AC, et al. COBRA combination therapy in patients with early rheumatoid arthritis: long-term structural benefits of a brief intervention. *Arthritis Rheum* 2002;46:347–56.
3. Konijn NP, van Tuyl LH, Boers M, et al. Similar efficacy and safety of initial COBRA-light and COBRA therapy in rheumatoid arthritis: 4-year results from the COBRA-light trial. *Rheumatology (Oxford)* 2017;56:1586–96.
4. Verschueren P, De Cock D, Corluy L, et al. Effectiveness of methotrexate with step-down glucocorticoid remission induction (COBRA Slim) versus other intensive treatment strategies for early rheumatoid arthritis in a treat-to-target approach: 1-year results of CareRA, a randomised pragmatic open-label superiority trial. *Ann Rheum Dis* 2017;76:511–20.
5. Bakker MF, Jacobs JW, Welsing PM, et al. Low-dose prednisone inclusion in a methotrexate-based, tight control strategy for early rheumatoid arthritis: a randomized trial. *Ann Intern Med* 2012;156:329–39.
6. Safy M, Jacobs J, IJff ND, et al; Society for Rheumatology Research Utrecht (SRU). Long-term outcome is better when a methotrexate-based treatment strategy is combined with 10 mg prednisone daily: follow-up after the second Computer-Assisted Management in Early Rheumatoid Arthritis trial. *Ann Rheum Dis* 2017;76:1432–5.
7. Rydell E, Forslind K, Nilsson JÅ, et al. Predictors of radiographic erosion and joint space narrowing progression in patients with early rheumatoid arthritis: a cohort study. *Arthritis Res Ther* 2021;23:27.

DOI 10.1002/art.42300

**Reply***To the Editor:*

We thank Dr. Samanta and colleagues for their comments on our article. We surmised that Samanta et al wanted to defend the role of GCs in the treatment of RA, including its potential in disease-modifying effects. There is indeed no reasonable doubt that the landmark articles that they cited demonstrate the benefits of prolonged GC use on structural joint damage in patients with RA. However, in contrast to our trial, patients in those studies received cumulative GC doses of more than 2,000 mg of prednisolone/prednisone and up to 3,650 mg per year.

The use of high GC doses has been shown to possibly harm patients, particularly regarding cardiovascular disease and osteoporosis. For example, the recent growing concern regarding the use of GCs in RA led the European Alliance of Associations for Rheumatology to recommend that treatment with GCs be discontinued within ~3 months (1). Similarly, the 2021 American College of Rheumatology guideline for the treatment of RA included a conditional recommendation for the use of conventional synthetic disease-modifying antirheumatic drugs (csDMARDs) without short-term (<3 months) GCs in csDMARD-naïve patients who have moderate to high disease activity and a strong recommendation against longer-term GC use in this situation (2). Indeed, a recent study of patients included in the CorEvitas registry showed that cumulative GC doses >1,100 mg over the previous 6 months increased the adjusted hazard ratio for cardiovascular events to 2.05 (3).


Much of the focus of our study was on the short-term use of GCs. In this setting, our study showed no effect of GCs on structural joint damage in patients with early RA and only limited advantages of the higher GC dose on disease activity, pain, and functional capacity compared with lower GC dose. Nevertheless, we agree with our colleagues from India that a longer period of GC use may have led to different results. However, and this answer also relates to point 3 of their comments, during the long 40-week observation period in our study when treatment decisions were only based on physician discretion, the GC doses administered were comparable between the groups, although still lower than in the articles cited.

Regarding the second comment from Samanta et al, we do not think that a Sharp/van der Heijde (SvdH) score of 2.1 is very high, given that the total SvdH erosion score can be up to 280. Rather, we argue that the mean change detected in the score was rather low in all 3 treatment groups (0.7, 0.7, and 0.6, respectively). Therefore, a statistically significant difference, potentially even clinically relevant, between the groups was difficult to demonstrate.

In summary, the current situation remains a typical one in medicine: one has to weigh the advantages and disadvantages of medical treatment with GCs. When GCs are only administered

for short periods of time, they seem to show no advantage in terms of structure modification.

Author disclosures are available at <https://onlinelibrary.wiley.com/action/downloadSupplement?doi=10.1002%2Fart.42300&file=art42300-sup-0001-Disclosureform.pdf>.

Dietmar Krause, MD  
[gundi.krause@t-online.de](mailto:gundi.krause@t-online.de)  
*Rheumatology practice*  
 Gladbeck, Germany  
 and Ruhr University  
 Bochum, Germany  
 Juergen Braun, MD   
*Ruhr University*  
 Bochum, Germany  
 and Ruhr Area Rheumatism Centre  
 Herne, Germany

1. Smolen JS, Landewé RB, Bijlsma JW, et al. EULAR recommendations for the management of rheumatoid arthritis with synthetic and biological disease-modifying antirheumatic drugs: 2019 update. *Ann Rheum Dis* 2020;79:685–99.
2. Fraenkel L, Bathon JM, England BR, et al. 2021 American College of Rheumatology guideline for the treatment of rheumatoid arthritis. *Arthritis Care Res (Hoboken)* 2021;73:924–39.
3. Ocon AJ, Reed G, Pappas DA, et al. Short-term dose and duration-dependent glucocorticoid risk for cardiovascular events in glucocorticoid-naïve patients with rheumatoid arthritis. *Ann Rheum Dis* 2021;80:1522–9.

DOI 10.1002/art.42278

**Characterization of mucosal-associated invariant T cells in blood of patients with axial spondyloarthritis and in axial entheses of healthy controls: comment on the article by Rosine et al**

*To the Editor:*

We read with great interest the article by Dr. Rosine et al (1), who characterized circulating mucosal-associated invariant T (MAIT) cells in patients with axial spondyloarthritis (SpA). The authors showed that circulating MAIT cells were associated with higher interleukin-17A (IL-17A) production compared with conventional CD4+, CD8+, and  $\gamma\delta$  T cells. The authors also reported that MAIT cells displayed high *IL17A* and *IL23R* gene expression and that they may strongly express *IL17F* gene after stimulation by anti-CD3 and anti-CD28 antibodies plus IL-7 and/or IL-18. Finally, the authors reported the presence of MAIT cells in the axial entheses of healthy subjects.


Rosine et al also extended previous MAIT cell analysis in axial SpA, reporting that MAIT cells circulated in the blood of patients with axial SpA at a lower frequency than in the blood of healthy subjects. However, after activation by phorbol myristate acetate/ionomycin, they showed that MAIT cells from patients with axial SpA were able to produce IL-17A at higher levels than MAIT cells

from healthy controls and that the number of MAIT cells expressing IL-17A was higher in axial SpA patients compared with controls.

We previously evaluated a series of patients with radiographic axial SpA and found that patients with axial SpA had a higher proportion of IL-17A/interferon- $\gamma$ -producing MAIT cells and IL-22-producing MAIT cells (2). As reported in an SKG mouse model that develops an SpA-like disease, the synergistic effects of IL-22 and IL-17A are required to promote enthesitis (3). In a mouse model of arthritis, overexpression of IL-23 induced the production of IL-22 by enthesal IL-23R+CD4-CD8-CD3+ T cells, with the involvement of IL-22 in the induction of genes implicated in bone proliferation (4).

Although Rosine et al highlighted the presence of MAIT cells in enthesal structures of healthy subjects and reported that these cells expressed the vascular endothelial growth factor gene involved in angiogenesis (*VEGFA*) at high levels, we currently do not know the specific expression of MAIT cells within the sites of inflammation in axial SpA patients. Moreover, IL-22 production by resident enthesal MAIT cells was not examined by Rosine et al. Finally, MAIT cells are primarily expressed at mucosal surfaces and in the blood, but they also express chemokine receptors and can migrate to specific tissues, such as the gut. With the consideration of the involvement of the gut and joint in axial SpA, attention should also be given to the specific expression of chemokine receptors (e.g., CCR9) associated with  $\alpha 4\beta 1$  and  $\alpha 4\beta 7$  integrins by MAIT cells.

Author disclosures are available at <https://onlinelibrary.wiley.com/action/downloadSupplement?doi=10.1002%2Fart.42278&file=art42278-sup-0001-Disclosureform.pdf>.

Eric Toussiot, MD, PhD 

[etoussiot@chu-besancon.fr](mailto:etoussiot@chu-besancon.fr)

INSERM CIC-1431, Centre d'investigation clinique

Département de Rhumatologie, Pole PACTE

CHU de Besançon

Département de Thérapeutique

Université de Bourgogne Franche-Comté

and INSERM UMR 1098, Etablissement Français du Sang

Bourgogne Franche Comté

Université Bourgogne Franche-Comté

Relations Hôte Greffon Tumeurs

Ingénierie cellulaire et génique, LabEx LipSTIC

Caroline Laheurte, PhD

INSERM UMR 1098, Etablissement Français du Sang Bourgogne

Franche Comté, Université Bourgogne Franche-Comté


Relations Hôte Greffon Tumeurs

Ingénierie cellulaire et génique, LabEx LipSTIC

and Etablissement Français du Sang Bourgogne Franche-Comté

INSERM CIC-1431, Plateforme de

BioMonitoring, Centre d'investigation clinique

Philippe Saas, PharmD, PhD 

INSERM CIC-1431, Centre d'investigation clinique

INSERM UMR 1098, Etablissement Français du Sang Bourgogne

Franche Comté, Université Bourgogne Franche-Comté

Relations Hôte Greffon Tumeurs

Ingénierie cellulaire et génique, LabEx LipSTIC

and Etablissement Français du Sang Bourgogne

Franche-Comté, INSERM CIC-1431, Plateforme de

BioMonitoring, Centre d'investigation clinique

Besançon, France

1. Rosine N, Rowe H, Koturan S, et al. Characterization of blood mucosal-associated invariant T cells in patients with axial spondyloarthritis and of resident mucosal-associated invariant T cells from the axial entheses of non-axial spondyloarthritis control patients. *Arthritis Rheumatol* 2022; 74:1786–95.
2. Toussiot É, Laheurte C, Gaugler B, et al. Increased IL-22- and IL-17A-producing mucosal-associated invariant T cells in the peripheral blood of patients with ankylosing spondylitis. *Front Immunol* 2018;9:1610.
3. Benham H, Rehaume LM, Hasnain SZ, et al. Interleukin-23 mediates the intestinal response to microbial  $\beta$ -1,3-glucan and the development of spondyloarthritis pathology in SKG mice. *Arthritis Rheumatol* 2014; 66:1755–67.
4. Sherlock JP, Joyce-Shaikh B, Turner SP, et al. IL-23 induces spondyloarthropathy by acting on ROR- $\gamma$ t+CD3+CD4-CD8- enthesal resident T cells. *Nat Med* 2012;18:1069–76.

DOI 10.1002/art.42277

## Reply

To the Editor:

We thank Dr. Toussiot et al for their interest in our article and for their comments. They raised the question of cytokine secretion, especially IL-22, within the inflammation sites of patients with axial SpA, which could be of interest, considering the synergic effects of IL-22 with IL-17 (1). We agree with Toussiot et al that IL-22 may be of interest in axial SpA and that proteomic and transcriptomic analyses are of high value in the axial entheses of these patients. Nevertheless, to date, only Appel et al have analyzed facet joints of patients with ankylosing spondylitis who underwent thoracolumbar spine corrective surgery for severe advanced ankylosis, where expression in facet joints of IL-17 but not IL-22 was reported (2).

Toussiot et al noted the potential importance of IL-23 in enthesitis inflammation according to animal models, which has been reported in the SKG mouse model (3) and in the IL-23 minicircle overexpression model (4,5). Nevertheless, the precise role of IL-22 in axial enthesitis in these models has not been clearly defined. Moreover, it is not known whether these animal models reflect human pathology in the axis. In fact, although the blocking of IL-23 in the pathologic processes of human disease is effective in peripheral forms of SpA, its blocking in the axial forms has not been successful. We attempted to address this dilemma by postulating that the cells or cytokines involved in the axis were not necessarily the same as those involved in the periphery.

Finally, at least among people without SpA, IL-22 expression is low or absent in perienthesal bone and enthesal soft tissue, as shown in Figure 5 in our article. Although we did not investigate the IL-22 transcript in enthesal MAIT cells, previous studies have demonstrated elevated IL-22 transcript levels in in vitro-stimulated enthesal tissues containing other innate lymphocytes, namely, group 3 innate lymphoid cells (6). Moreover, results of previous studies have suggested that bone formation

depends more on IL-17 than on IL-22 (7,8). Thus, even if we agree on the potential importance of IL-22 as a key cytokine in the homeostasis of MAIT cells, its involvement in inflammation and in bone formation in the axis of SpA patients remains an open question.

Nicolas Rosine, MD, PhD  
Lars Rogge, PhD  
*Institut Pasteur, Immunoregulation Unit  
and Department of Immunology  
Université de Paris  
Paris, France*  
Dennis McGonagle, MD, PhD  
*Institute of Rheumatic and Musculoskeletal Medicine  
University of Leeds  
Leeds, UK*  
Corinne Miceli-Richard, MD, PhD   
[corinne.miceli@aphp.fr](mailto:corinne.miceli@aphp.fr)  
*Institut Pasteur, Immunoregulation Unit  
and Department of Immunology  
Université de Paris  
and Service de Rhumatologie  
Hôpital Cochin Port Royal, AP-HP  
Paris, France*

1. Lindahl H, Olsson T. Interleukin-22 influences the Th1/Th17 axis. *Front Immunol* 2021;12:618110.
2. Appel H, Maier R, Wu P, et al. Analysis of IL-17(+) cells in facet joints of patients with spondyloarthritis suggests that the innate immune pathway might be of greater relevance than the Th17-mediated adaptive immune response. *Arthritis Res Ther* 2011;13:R95.
3. Sherlock JP, Joyce-Shaikh B, Turner SP, et al. IL-23 induces spondyloarthropathy by acting on ROR- $\gamma$ t+ CD3+CD4-CD8- enthesal resident T cells. *Nat Med* 2012;18:1069–76.
4. Ruutu M, Thomas G, Steck R, et al.  $\beta$ -glucan triggers spondylarthritis and Crohn's disease-like ileitis in SKG mice. *Arthritis Rheum* 2012;64:2211–22.
5. Benham H, Rehaume LM, Hasnain SZ, et al. Interleukin-23 mediates the intestinal response to microbial  $\beta$ -1,3-glucan and the development of spondyloarthritis pathology in SKG mice. *Arthritis Rheumatol* 2014;66:1755–67.
6. Cuthbert RJ, Fragkakis EM, Dunsmuir R, et al. Group 3 innate lymphoid cells in human entheses. *Arthritis Rheumatol* 2017;69:1816–22.
7. Osta B, Roux JP, Lavocat F, et al. Differential effects of IL-17A and TNF- $\alpha$  on osteoblastic differentiation of isolated synoviocytes and on bone explants from arthritis patients. *Front Immunol* 2015;6:151.
8. Ono T, Okamoto K, Nakashima T, et al. IL-17-producing  $\gamma\delta$  T cells enhance bone regeneration. *Nat Commun* 2016;7:10928.

## Reviewers

The individuals who served as reviewers for *Arthritis & Rheumatology* in 2022 are listed below. The Editorial Board is very grateful to our reviewers for the time and expertise they have devoted to the journal. Through their thoughtful and insightful critiques they have provided an invaluable service to the journal, our authors, and the discipline of rheumatology.

Daniel H. Solomon, MD, MPH, Editor-in-Chief

Abu-Amer, Yousef	Behrens, Edward	Byram, Kevin	Conaghan, Philip
Adamopoulos, Iannis	Beier, Frank	Cai, Ken	Conway, Richard
Aghayev, Ayaz	Belmont, H	Cailotto, Frederic	Cook, Stuart
Ahmed, Ali	Bennett, Alexander	Calabrese, Leonard	Cornec, Divi
Ahmed, Salahuddin	Beretta, Lorenzo	Canna, Scott	Corr, Maripat
Ainsworth, Richard	Berger, Christoph	Cappelli, Laura	Craft, Joseph
Akbar, Moeed	Bermas, Bonnie	Carlesso, Lisa	Cron, Randy
Alarcón, Graciela	Beukelman, Timothy	Carrier, Michael	Crow, Mary*
Allenspach, Eric	Bhattacharyya, Swati	Casciola-Rosen, Livia	Crowson, Cynthia
Alles, Sascha	Bhutani, Nidhi	Casey, Kerry*	Cuda, Carla
Amoura, Zahir	Bijlsma, Johannes	Chakraborty, Adri	Cui, Jing
Anders, Hans-Joachim	Birmann, Brenda	Chan, Alice	Curtis, Jeffrey
Andersson, Helena	Blanco, Francisco	Chang, Margaret	Cutolo, Maurizio
Andrade, Felipe	Blom, Arjen	Chapman, Victoria	Czarny, Malwina
Ansalone, Cecilia	Bockenstedt, Linda	Charles, Julia	Dahlqvist, Johanna
Appleton, Christopher	Bogatkevich, Galina S.	Chatham, Winn	Davidson, Anne
Aringer, Martin	Boilard, Eric	Cheng, Joshua	Davis III, John
Asahara, Hiroshi	Boin, Francesco	Chighizola, Cecilia	De Benedetti, Fabrizio
Ascherman, Dana	Bolster, Marcy	Chimenti, Maria Sole	Deane, Kevin
Askanase, Anca	Bondt, Albert	Chiu, Ying-Ming	Deane, Kevin D.
Assassi, Shervin	Bossini-Castillo, Lara	Chizzolini, Carlo	Deguine, Jacques
Atkinson, John	Boumpas, Dimitri	Choi, Hyon	Del Galdo, Francesco
Attur, Mukundan	Bowman, Simon J.	Choi, May	Dell'Accio, Francesco
Bae, Sang-Cheol	Bowness, Paul	Christensen, Robin	Dellaripa, Paul
Baer, Alan	Bowness, Paul	Christopher-Stine, Lisa	Demoruelle, M
Baker, Joshua F.	Boyer, Olivier	Chu, Cong-Qiu	Denton, Christopher
Ballestar, Esteban	Brenner, Michael	Chung, Lorinda	Deodhar, Atul
Bansback, Nick	Brix, Silke	Cid, María	DeVita, Paul
Barber, Claire	Broder, Anna	Cipolletta, Edoardo	Dhaun, Neeraj
Barnabe, Cheryl	Brouwer, Elisabeth	Giurea, Adrian	Diamantopoulos, Andreas
Barnas, Jennifer	Brown, Eric	Cobos, Gabriela	Diamond, Betty
Barnes, Betsy	Brown, Matthew	Cohen, Stanley	Diaz-Torne, Cesar
Barrat, Franck	Brown, Matthew	Colbert, Robert	Diekman, Brian
Bartoloni, Elena	Brunger, Jonathan	Coleman, Mitch	Djokovic, Aleksandra
Bateman, John	Budd, Ralph	Collins, Jamie*	Donlin, Laura
Bathon, Joan	Bujor, Andreea	Collins, John	Dougados, Maxime
Becce, Fabio	Buttgereit, Frank	Collins, Kelsey	Dua, Anisha*
Beck, Lisa	Bykerk, Vivian	Comte, Denis	

\*Each of these individuals reviewed at least 4 manuscripts.



Dubreuil, Maureen	Gorelik, Mark	Jonason, Jennifer	Langford, Carol A.
Eder, Lihi	Gossec, Laure	Jones, Alexis	Lauper, Kim
Efthimiou, Petros	Gourh, Pravitt	Jones, Simon	Lee, Pui
Ehrenstein, Michael R	Grainger, Rebecca	Jonsson, A. Helena	Lessard, Christopher
Eleftheriou, Despina	Grayson, Peter	Juryne, Michael	Liao, Wilson
Elewaut, Dirk	Greenberg, Steven	Kain, Renate	Limaye, Vidya
Elkon, Keith	Griffin, Timothy	Kalunian, Kenneth	Liossis, Stamatis-Nick
Elkon, Keith B.	Guerhazi, Ali	Kang, Insoo	Lioté, Frédéric
Emery, Paul	Guma, Monica	Kang, Jae Hee	Little, Dianne
England, Bryant	Guzman, Jaime	Kapetanovic, Meliha	Liu, Chuanju
Ermann, Joerg	Haberman, Rebecca	Kaplan, Chelsea	Liu, Yong-Xin
Esdaile, John	Hachulla, Eric	Kapoor, Mohit	Liu-Bryan, Ru
Fava, Andrea	Hahn, Bevrá H.	Karabayas, Maira	Lockshin, Michael
Fearon, Ursula	Harasymowicz, Natalia	Karp, David	Loeser, Richard
Feghali-Bostwick, Carol	Haroon, Nigil	Kavanaugh, Arthur	Longobardi, Lara
Feldman, Candace	Harper, Lorraine	Kendall, Peggy	Looney, Richard J.
Ferguson, Ian	Hatemi, Gulen	Kerick, Martin	López-Isac, Elena
Ferrada, Marcela	Hawker, Gillian	Kerr, Gail S.	Lopez-Sola, Marina
Ferraz-Amaro, Ivan	Hayashi, Daichi	Killiany, Ron	Lories, Rik
Filer, Andrew	Helfgott, Simon	Kim, Alfred	Losina, Elena
Filippucci, Emilio	Henderson, Lauren	Kim, Kwangwoo	Lotz, Martin
Fiorentino, David	Henriksen, Marius	Kim, Seoyoung	Loughlin, John
Fiorentino, David F.	Herrick, Ariane	Kisselev, Alexei	Lubberts, Erik
FitzGerald, John	Hissink Muller, Petra	Klareskog, Lars	Lucas, Emma
FitzGerald, Oliver	Hoffmann-Vold,	Kloppenburger, Margreet	Lund, Merete Hetland
Fleischmann, Roy M.	Anna-Maria	Knevel, Rachel	Lundberg, Ingrid E.
Flores-Suarez, Luis	Hogan, Susan	Knight, Jason*	Lundberg, Karin
Fox, David	Holmqvist, Marie	Kochi, Yuta	Lyons, Paul
Fox, Robert	Horowitz, Diane	Kohler, Minna	Machado, Pedro
Freydin, Maxim	Houssiau, Frederic	Koralov, S.	Maerz, Tristan
Fritzler, Marvin	Howard, Timothy	Korman, Benjamin	Maher, Toby
Fujimoto, Manabu	Hsieh, Evelyn	Kottyan, Leah	Mahony, Christopher
Fujio, Keishi	Hsueh, Ming-Feng	Kozyrev, Sergey	Maksymowich, Walter
Furer, Victoria	Huang, ZeYu	Kraus, Virginia Byers	Mammen, Andrew
Fuschiotti, Patrizia	Huber, Adam	Kremer, Joel	Mankia, Kulveer
Gaffo, Angelo	Hummers, Laura	Kristensen, Lars Erik	Manske, Sarah
Galloway, James	Hunzinger, Katherine	Kronbichler, Andreas	Marahleh, Aseel
Gasparian, Armen Yuri	Hyrich, Kimme L.	Kronke, Gerhard	Mariette, Xavier
Gaston, Hill	Isenberg, David	Kuhn, Kristine*	Márquez, Ana
Genovese, Mark	Ishigaki, Kazuyoshi	Kumanogoh, Atsushi	Marston, Bethany
Georgel, Philippe	Jackson, Shaun	Kumar, Deepak	Martorana, Davide
Ghomrawi, Hassan	Jatuworapruk, Kanon	Kuwana, Masataka*	Marzo-Ortega, Helena
Giles, Ian	Jayne, David	Kvien, Tore	Massarotti, Elena
Giles, Jon	Jefferies, Caroline	Kwok, Seung-ki	Mathai, Stephen
Gilkeson, Gary	Jeffries, Matlock*	Kyttaris, Vasileios	Matson, Scott
Ginzler, Ellen	Jennette, Charles	La Cava, Antonio	Matsuo, Hirotaka
Gladman, Dafna*	Jiang, Xia	Lakhanpal, Amit	Mavragani, Clio
Goldring, Mary	Jiang, Yan-Fang	Lam, Christina	Mayes, Maureen
Gono, Takahisa	Jiemy, William	Lambert, Robert	McCarthy, Geraldine
Goodson, Nicola J.	Johnson, Sindhu	Langefeld, Carl*	McCormick, Natalie

\*Each of these individuals reviewed at least 4 manuscripts.

McGill, Neil	Pelaez-Ballestas, Ingris	Saraux, Alain	Taams, Leonie
McGonagle, Dennis	Perl, Andras	Sato, Shinichi	Takeuchi, Tsutomu
McHugh, Neil	Perlman, Harris	Satoh, Minoru	Tanaka, Yoshiya
McMahon, Maureen	Pernis, Alessandra	Savic, Sinisa	Tang, Donge
McNulty, Margaret	Pillai, Shiv	Sawalha, Amr	Tansley, Sarah
Mecoli, Christopher*	Pillinger, Michael	Scheel-Toellner, Dagmar	Taylor, Peter
Meffre, Eric	Pioli, Patricia	Scher, Jose U.	Tedeschi, Sara*
Mehta, Jay	Pisetsky, David	Scherlinger, Marc	Teng, Yoe Kie Onno
Meissner, Yvette	Plaas, Anna	Schrodi, Steven	Terrier, Benjamin
Merrill, Joan	Poddubnyy, Denis	Schulert, Grant	Thiele, Geoffrey
Merriman, Tony	Pollak, Amy	Schwarz, Edward	Thomas, Donald
Meulenbelt, Ingrid	Pugh, Dan	Sciascia, Savino	Thomas, Ranjeny
Michaud, Kaleb	Qin, Ling	Selzer, Faith	Tin, Adrienne
Micu, Mihaela	Rada, Balazs	Sepriano, Alexandre	Tomasson, Gunnar
Mielenz, Dirk	Radner, Helga	Shah, Nisarg	Toro-Dominguez, Daniel
Mikecz, Katalin	Rai, Muhammad Farooq	Shea, M. Kyla	Torralba, Karina
Mikuls, Ted	Ramanan, Athimalaipet	Shelef, Miriam	Torres, Rosa
Min, Michelle	Ramming, Andreas	Shen, Nan	Trajanoska, Katerina
Miner, Jeffrey N.	Ramsey-Goldman, Rosalind	Silverman, Gregg	Tsokos, George
Miner, Jonathan	Randi, Anna	Silverman, Gregg J.	Tsou, Pei-Suen
Mitchell, Aaron	Rao, Deepak	Simard, Julia	Tsuchiya, Naoyuki
Mócsai, Attila	Ravelli, Angelo	Singh, Ram	Turkiewicz, Aleksandra
Mohan, Chandra	Ray, John	Skaug, Brian	Vaglio, Augusto
Mok, Chi Chiu	Raychaudhuri, Siba	Smith, Judy	van der Heijde, Désirée
Morand, Eric	Raychaudhuri, Soumya	Smith, Melanie	van der Woude, Diane
Morel, Laurence	Real, Eva	Smith, Rona	van Meurs, Joyce
Morris, David	Reed, Ann	Smith, Stacy	Vassilopoulos, Dimitrios
Mukherjee, Monica	Reynolds, Gary	So, Alexander	Veale, Douglas
Mustelin, Tomas	Richmond, Jillian	Sokolove, Jeremy*	Vincent, Tonia
Myasoedova, Elena	Riddle, Daniel	Soni, Anushka	Vital, Edward
Nagafuchi, Yasuo	Robinson, Philip	Soy, Mehmet	de Vlam, Kurt
Nash, Peter	Roddy, Edward	Sparks, Jeffrey*	Vogel, Tiphane
Navarro-Millán, Iris	Rodríguez-Paredes, Manuel	Specks, Ulrich	Volkman, Elizabeth
Navid, Fatemeh	Ronnblo, Lars	Spiera, Robert	Voulgarelis, Michael
Nikolic-Paterson, David	Roseen, Eric	Sriram, Uma	Vyse, Tim
Nived, Ola	Rosenbaum, James	St. Clair, Eugene	Wagner, Denisa
Nordmark, Gunnel	Rosenberg, Alan	Stavre, Zheni	Wallace, Graham
Ogdie, Alexis	Rosenthal, Ann K.	Steen, Virginia	Walsh, David
Okada, Yukinori	Rosser, Elizabeth	Stefanik, Joshua	Wan, Hong
Okiyama, Naoko	Rubbert-Roth, Andrea	Steiner, Guenter	Wang, Guo Chun
O'Sullivan, Kim	Ruddle, Nancy	Stiburkova, Blanka	Wang, Shuang-yin
Otero, Miguel	Saevardottir, Saedis	Stone, James	Warrington, Kenneth J.
Paik, Julie	Sakaue, Saori	Stone, John H.	Weber, Brittany
Paine, Ananta	Salmon, Jane	Suh, Chang-Hee	Wedderburn, Lucy
Paley, Michael	Salvarani, Carlo	Suissa, Samy	Wei, James
Park-Min, Kyung-Hyun	Samuels, Jonathan	Sullivan, Keith	Cheng-Chung
Parks, Christine	Sanchez-Guerrero, Jorge	Svensson, Mattias	Wei, Kevin*
Pascart, Tristan	Sancho, Jaime	Sweasy, Joann	Weinans, Harrie
Paulin, Francisco		Syversen, Silje	Weinstein, Jason
Peffer, Mandy			Weisman, Michael

\*Each of these individuals reviewed at least 4 manuscripts.

---

Weiss, Pamela	Yang, Niansheng	Ytterberg, Steven	Zhang, Zhuoli
Wendling, Daniel	Yasuda, Shinsuke	Yu, Chack-Yung	Zhao, Yanfang
Werth, Victoria	Yau, Michelle	Zeb, Alam	Zhou, Wei
Wilkinson, J. Mark	Yazdany, Jinoos	Zhan, Yiqiang	Zhu, Zhaozhong
Winter, Deborah	Yelin, Edward	Zhang, Guohong	Zimmerman,
Winthrop, Kevin	Yeung, Rae	Zhang, Meixia	Zoe
Woodward, Owen	Yoshida, Kazuki	Zhang, Xuan	Zulian,
Worthing, Angus	You, Sungyong	Zhang, Yeja	Francesco
Yammani, Raghunatha	Young, David	Zhang, Yuqing	Zuo, Jian

---

\*Each of these individuals reviewed at least 4 manuscripts.